

Investigating faunal responses to climate and environmental change using ancient DNA from ursids

Alexander Theodore Salis

*Thesis submitted in fulfilment of the requirements
for the degree of Doctor of Philosophy*

in

Biological Sciences

at The University of Adelaide

Faculty of Sciences

School of Biological Sciences

Australian Centre for Ancient DNA

Table of Contents

Abstract.....	iv
Thesis Declaration.....	v
Acknowledgements	vi
Chapter 1: General Introduction.....	1
1.1 The Changing Climate and Biodiversity	2
1.1.1 Extinctions and biodiversity loss.....	2
1.1.2 Quaternary climatic and environmental change.....	3
1.1.3 Quaternary environment and megafauna.....	4
1.2 Ancient DNA and Quaternary Research.....	8
1.2.1 Ancient DNA.....	8
1.2.2 Ancient DNA and megafaunal extinction and evolutionary history.....	9
1.3 Bears as a Quaternary Model Taxon.....	12
1.3.1 Carnivora	12
1.3.2 Bears.....	12
1.3.3 Bear phylogenetics and evolutionary history.....	13
1.3.4 The brown bear (<i>Ursus arctos</i>)	15
1.3.5 Brown bear phylogeography and evolutionary history.....	15
1.4 Thesis Overview	19
1.4.1 Thesis scope and aims	19
1.4.2 Chapter 2: Lions and brown bears colonised North America in multiple synchronous waves of dispersal across the Bering Land Bridge	19
1.4.3 Chapter 3: Phylogeography of the extinct North American giant short-faced bear (<i>Arctodus simus</i>), with comments on their palaeobiology	20
1.4.4 Chapter 4: Ancient genomes reveal hybridisation between extinct short-faced bears and the extant spectacled bear (<i>Tremarctos ornatus</i>).....	20
1.4.5 Chapter 5: From Iberia to Siberia: Phylogeography and evolutionary history of Eurasian brown bears	21
1.5 References.....	22
Chapter 2: : Lions and brown bears colonised North America in multiple synchronous waves of dispersal across the Bering Land Bridge	39
2.1 Authorship Statement	39
2.2 Manuscript	45
Abstract:	46

<i>Introduction:</i>	47
<i>Materials and Methods:</i>	50
<i>Results:</i>	53
<i>Discussion:</i>	59
<i>Conclusion:</i>	64
<i>Acknowledgements:</i>	65
<i>References:</i>	66
2.3 Supplementary Information	75
Chapter 3: Phylogeography of the extinct North American giant short-faced bear (<i>Arctodus simus</i>), with comments on their palaeobiology	99
3.1 Authorship Statement	99
3.2 Manuscript.....	102
<i>Abstract:</i>	102
<i>Introduction:</i>	103
<i>Methods:</i>	105
<i>Results:</i>	110
<i>Discussion:</i>	115
<i>Acknowledgements:</i>	116
<i>References:</i>	117
3.3 Supplementary Information	124
Chapter 4: Ancient genomes reveal hybridisation between extinct short-faced bears and the extant spectacled bear (<i>Tremarctos ornatus</i>)	131
4.1 Authorship Statement.....	131
4.2 Manuscript.....	134
<i>Summary:</i>	134
<i>Results and Discussion:</i>	135
<i>Acknowledgements:</i>	142
<i>Materials and Methods:</i>	143
<i>References:</i>	147
4.3 Supplementary Information	153
Chapter 5: From Iberia to Siberia: Phylogeography and evolutionary history of Eurasian brown bears	165
5.1 Authorship statement	165
5.2 Manuscript.....	168

<i>Abstract:</i>	168
<i>Introduction:</i>	169
<i>Methods:</i>	172
<i>Results and Discussion:</i>	177
<i>Conclusion:</i>	200
<i>Acknowledgements:</i>	200
<i>References:</i>	201
5.3 Supplementary Information	214
Chapter 6: Discussion.....	239
6.1 Thesis summary	240
6.1.1 <i>Research summary</i>	240
6.1.2 <i>Chapter 2: Lions and brown bears colonised North America in multiple synchronous waves of dispersal across the Bering Land Bridge</i>	240
6.1.3 <i>Chapter 3: Phylogeography of the extinct North American giant short-faced bear (Arctodus simus), with comments on their paleobiology</i>	241
6.1.4 <i>Chapter 4: Ancient genomes reveal hybridisation between extinct short-faced bears and the extant spectacled bear (Tremarctos ornatus)</i>	241
6.1.5 <i>Chapter 5: From Iberia to Siberia: Phylogeography and evolutionary history of Eurasian brown bears</i>	242
6.2 Synthesis and General Discussion	244
6.2.1 <i>Carnivore guilds of the Pleistocene: Diversity and niche partitioning</i>	244
6.2.2 <i>Brown bear-polar bear relationship</i>	250
6.2.3 <i>Ancient DNA benefits museum collections</i>	253
6.3 Limitations and Future Directions	256
6.3.1 <i>Choice of loci</i>	256
6.3.2 <i>Limitations of different loci</i>	258
6.3.3 <i>Evolutionary history of tremarctine bears</i>	261
6.3.4 <i>Future directions for brown bear mitogenomics</i>	262
6.3.5 <i>Extending ancient mitogenomics to other animal taxa</i>	262
6.4 Conclusion	264
6.5 References	265
Appendix: Widespread male sex bias in mammal fossil and museum collections	275

Abstract

The Late Quaternary Period (the past ~1.0 million years) is characterised by cyclical growth and retraction of glaciers and polar ice caps driven by periods of cooler and warmer global temperatures. Ancient DNA has emerged as a key tool for unravelling the impacts of climate and environmental change as it enables detection of population and species level changes that would otherwise be undetectable. Ursids (bears) have shown potential as a model taxon for investigating faunal responses to climate and environmental change during the Late Quaternary, especially brown bears (*Ursus arctos*), which have an extensive subfossil record, Holarctic distribution, and well-studied mitochondrial phylogeography.

My PhD research uses ancient DNA techniques to investigate the evolutionary history of ursids during the Late Quaternary. In Chapters 2 and 5 I use analyses of new mitochondrial genome sequences from 217 ancient brown bears to investigate phylogeographic structure across their Holarctic distribution and refine their mitochondrial phylogeny, revealing striking patterns of migration and population turnover that correlate with drastic changes in the climate and environment during the Pleistocene. In Chapter 2 I also demonstrate that population changes observed in North American brown bears are paralleled by changes in lion populations, suggesting analogous drivers of phylogeographic structure and population dynamics between these two carnivorans. In Chapter 3 I use 31 mitochondrial genomes from the extinct North American giant short-faced bear, *Arctodus simus*, to investigate their phylogeography and taxonomy, revealing striking sexual dimorphism and a lack of evidence for previously described subspecies. Finally, in Chapter 4 I use whole genome data from extinct short-faced bears to investigate the evolutionary history of Tremarctinae and find evidence for extensive hybridisation resulting in phylogenetic discordance between the mitochondrial and nuclear genomes.

My research demonstrates the usefulness of ancient DNA datasets for understanding the evolutionary history of species and populations. Further, I argue that my data provide added evidence for the suitability of ursids as model taxa for studying Quaternary biogeography, as they appear to have exhibited pronounced responses to past climate and environmental change, have undergone extensive hybridisation among species within the family (including extinct lineages), and comprise species that both survived and went extinct during the Pleistocene-Holocene transition.

Thesis Declaration

I, Alexander Theodore Salis, certify that this work contains no material which has been accepted for the award of any other degree or diploma in my name, in any university or other tertiary institution and, to the best of my knowledge and belief, contains no material previously published or written by another person, except where due reference has been made in the text. In addition, I certify that no part of this work will, in the future, be used in a submission in my name, for any other degree or diploma in any university or other tertiary institution without the prior approval of the University of Adelaide and where applicable, any partner institution responsible for the joint-award of this degree.

I acknowledge that copyright of published works contained within this thesis resides with the copyright holder(s) of those works.

I also give permission for the digital version of my thesis to be made available on the web, via the University's digital research repository, the Library Search and also through web search engines, unless permission has been granted by the University to restrict access for a period of time.

I acknowledge the support I have received for my research through the provision of an Australian Government Research Training Program Scholarship.

Alexander Theodore Salis

September 10th, 2020

Acknowledgements

Firstly, this thesis would not have been possible without the excellent help and guidance of my primary supervisor Dr Kieren Mitchell, and my co-supervisor Assistant Professor Jeremy Austin. Ensuring that I had the resources, guidance, and support to complete my research in the face of adversity. Further I would like to thank Sarah Bray, for the excellent work she did during her PhD at the Australian Centre for Ancient DNA (ACAD) which made a lot of my research possible.

I would like to thank all the collaborators and institutions who allowed us to use their valuable samples and the people who collected samples and performed early analyses prior to my PhD, in particular: Blaine Schubert, Leo Soibelzon, Cristina Valdiosera, and Michael Lee. I would like to thank the many members of the ACAD megafauna group over the years, especially those who trained me in the lab and gave me support and guidance, especially: Bastien Llamas, Holly Heiniger, Pere Bover, Lindsey Fenderson, Graham Gower, Yichen Liu, and Ayla van Loenen. I would like to further thank Holly Heiniger for her amazing laboratory support and her work which made my PhD possible. Additionally, I would like to thank Kris Helgen for stepping up during difficult times and offering his much need support.

I would also like to thank Nic Rawlence and the University of Otago Palaeogenetics Laboratory who hosted me during the final months of my PhD. Lastly, I would like to thank my family for the encouragement, support, and advice.

Chapter 1

General Introduction

1.1 The Changing Climate and Biodiversity

1.1.1 Extinctions and biodiversity loss

The world is currently in the midst of what has been referred to as the sixth mass extinction, otherwise known as the Holocene/Anthropocene extinction (Ceballos and Ehrlich, 2018; Ceballos et al., 2015; Lewis and Maslin, 2015). The past few hundred years have seen a dramatic increase worldwide in species extinctions and turnovers, changes in species distributions and biodiversity (Barnosky et al., 2011; Ceballos et al., 2015), where biodiversity is the measure of genetic, species, or ecosystem-level variation. The current loss of species is estimated to be between 100 and 1000 times the natural background extinction rate throughout geological time (Ceballos and Ehrlich, 2018; Ceballos et al., 2015; De Vos et al., 2015; Pimm et al., 2014). Human exploitation, habitat loss and degradation, and human-induced climate change have been implicated as the primary drivers of this accelerating biodiversity loss. In order to understand current biodiversity trajectories and how to best conserve current and future biodiversity, it is important to understand how species and ecosystems have responded to past climatic and environmental changes. Investigating past biodiversity change may allow us to identify factors that put species at risk for extinction. By combining data from palaeontology, genetics, and ecology, species' responses to climate and environmental change can be determined, and patterns and shared drivers may be identified (Barnosky et al., 2011; Ceballos et al., 2015; Hofman et al., 2015). Ultimately, this information may reveal why some species survive while others perish and allow more effective allocation of conservation funding.

One of the most recent extinction events, which is often regarded as the start of the current Holocene extinction crisis, is the Late Quaternary extinction of terrestrial megafauna. The Quaternary Period is the most recent of the three periods of the Cenozoic Era and is divided into two epochs: the Pleistocene, 2.58 million years ago (mya) to 11.7 kya; and the Holocene, 11.7 kya to present. While the rate of extinction at the end of the Pleistocene was much less than what we are currently experiencing, the Quaternary extinction event saw the extinction of numerous megafauna species across the world, with a large proportion of extinctions clustering around the Pleistocene–Holocene transition ~11.7 thousand years ago (kya) (Barnosky et al., 2004; Cooper et al., 2015; Koch and

Barnosky, 2006). Notably this extinction event is within the limits of ancient DNA research, and therefore represents our best opportunity for understanding the patterns and processes leading to extinction or survival of species threatened by a rapidly changing environment.

1.1.2 Quaternary climatic and environmental change

The Quaternary is characterised by cyclical growth and retraction of glaciers and polar ice caps driven by periods of cooler and warmer global temperatures (Figure 1) (Denton et al., 2010; Jansson and Dynesius, 2002). These climatic changes appear to have been driven by Milankovitch cycles, which are periodic perturbations in Earth's orbit around the sun, axial tilt, and axis of rotation that alter sunlight/radiation received during the different seasons (Jansson and Dynesius, 2002). It is becoming increasingly evident that Quaternary climate fluctuations and concomitant environmental change played a significant role in shaping species distributions and evolution (Cooper et al., 2015; Jansson and Dynesius, 2002).

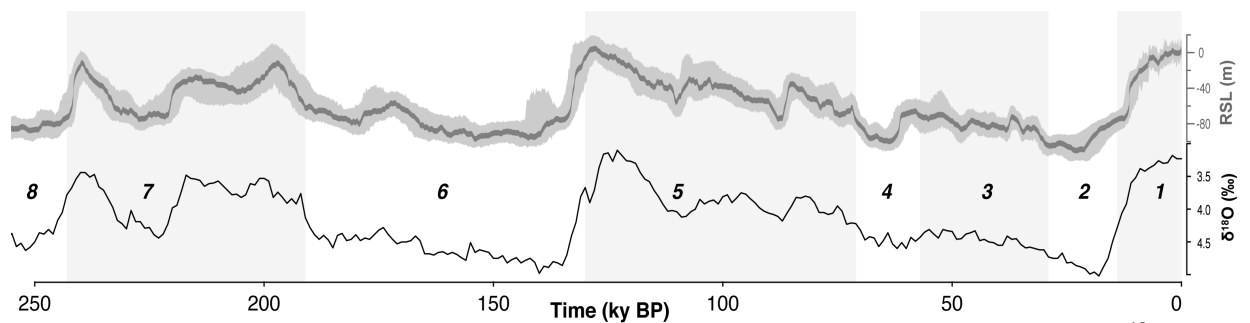


Figure 1: Relative sea level (RSL) compared to the present in metres (m) plotted above $\delta^{18}\text{O}$ measured from Greenland ice-cores. $\delta^{18}\text{O}$ is the ratio of stable isotopes oxygen-18 and oxygen-16 and is a proxy for temperature. A clear pattern of a rise in sea level with rising temperature ($\delta^{18}\text{O}$) can be observed. Numbered grey and white bars indicated different Marine Isotope Stages (MIS), where grey bars (odd numbers) are warm interglacials and white (even numbers) are cold glacials.

Climate change during the Quaternary caused drastic changes in temperature and sea level, with resulting shifts in habitat across the continents. Temperatures during glacial maxima — when the ice reached its greatest extent — were up to 21 °C colder than the current climate (Cuffey et al., 1995) and were generally followed by periods of rapid warming of 5–10 °C (but potentially up to 16 °C) known as Dansgaard-Oeschger (D-O) events (Rahmstorf, 2002; Wolff et al., 2010). With these changes in temperature came the formation and retraction of vast ice sheets in the form of glaciers and polar ice caps, with

1.1 THE CHANGING CLIMATE AND BIODIVERSITY

corresponding fluctuations in sea level (Figure 1). During glacial maxima sea level may have fallen as low as 120 m below the current level (Rahmstorf, 2002). These lower sea levels uncovered large areas of previously inundated land, resulting in the periodic formation of land bridges between previously unconnected land masses, such as the Bering Land Bridge (or Beringia) connecting Eurasia and the New World (Elias et al., 1996).

1.1.3 Quaternary environment and megafauna

It is widely believed that many animal taxa tracked Quaternary changes in climate, ice sheets, and sea levels, moving as suitable habitat became available or vanished, resulting in dynamic distributions of species through time (Eldredge, 1989; Eldredge, 1995; Hewitt, 1996, 1999). Land bridges between continents are thought to have played an important role in facilitating the movement of animal populations during periods of environmental change (Elias et al., 1996; Stehli and Webb, 1985). One widely cited model — the “Expansion/Contraction” (E/C) model — suggests that the ranges of many temperate European species contracted into southern refugia on Mediterranean peninsulas (Iberia, Italy, and the Balkans) during glacial maxima, followed by northward expansion during interglacial periods as glacial ice retracted (Figure 2) (e.g. Hewitt, 1996, 1999, 2000; Provan and Bennett, 2008). Inability to track environmental changes may have put a species at risk of extinction if they were unable to adapt to the new local environmental conditions (Dalen et al., 2007; Provan and Bennett, 2008).

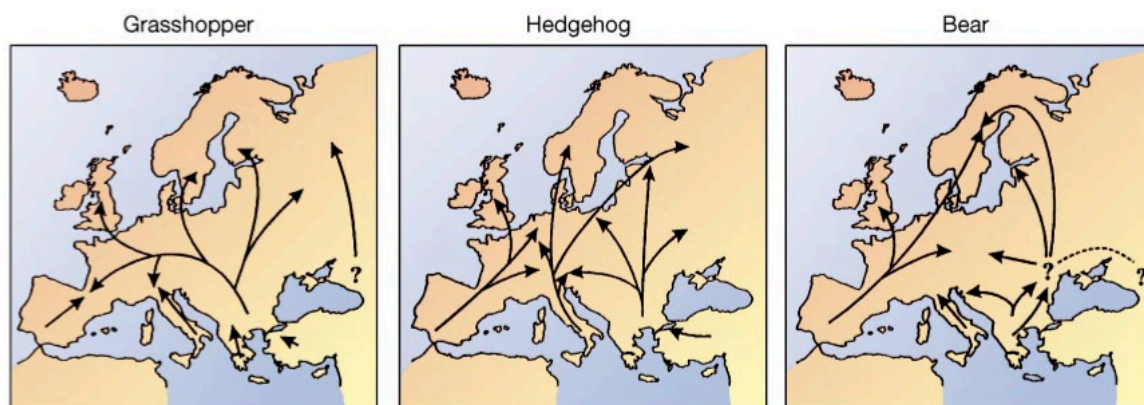


Figure 2: Post-glacial expansion of three model species used to develop the “Expansion/Contraction” model. Arrows indicate the movement of populations out of refugial areas in Iberia, Italy, the Balkans, and the Caucasus region. Figure reproduced from Hewitt (2000).

During the Late Pleistocene a wide range of megafauna taxa across most continents became extinct or experienced massive population declines (Barnosky et al., 2004). These extinctions are thought to have had major ecological consequences, with changes in plant community structure, vegetation cover, species diversity, and fire regimes (Doughty, 2013; Johnson, 2009). The cause of these extinctions has been highly controversial over the past 50 years and the contributions of various factors remain contentious today (Barnosky et al., 2004; Cooper et al., 2015; Haynes, 2013; Koch and Barnosky, 2006; Prescott et al., 2012; Sandom et al., 2014). Both climate change and human activity have been proposed to play major roles in the extinction of megafauna. Climatic changes appear to coincide with the extinction of many megafauna (Barnosky et al., 2004; Cooper et al., 2015; Guthrie, 2006; Metcalf et al., 2016), but it is undeniable that many recent Pleistocene megafauna extinctions also coincided with the local arrival of humans (Alroy, 2001; Barnosky and Lindsey, 2010). This has created much debate about whether climate or human impact is the major driving force behind these extinctions (Koch and Barnosky, 2006).

Human contributions to megafaunal population decline and/or extinction could have taken several forms, including overkill (overhunting resulting in reduced prey populations), blitzkrieg (rapid overkill completely depleting prey populations), and “sitzkrieg” (habitat destruction, modification, and fragmentation, as well as the introduction of exotic species and disease). Overkill is distinct from blitzkrieg in that under an “overkill” model extinction could occur millennia after first contact while under “blitzkrieg” extinction could occur within a single generation (Koch and Barnosky, 2006). Blitzkrieg has been suggested as the primary driver of extinction in New Zealand, with Polynesian hunting resulting in the rapid extinction of numerous bird species, including the giant flightless moa (Allentoft et al., 2014; Holdaway, 1989). More protracted models of overkill have been suggested for Australia, with extinction occurring ~13,500 years after human arrival, though blitzkrieg may have occurred on a more local scale (Johnson et al., 2016; Salter et al., 2016). In both Australia and New Zealand, sitzkrieg has also been proposed as a major cause of extinction. In New Zealand and other Pacific islands, the impact of introduced predators (pigs, dogs, rats) is thought to have been immense, as many islands lacked terrestrial predators prior to human arrival and native fauna were therefore naïve and susceptible to predation (Holdaway, 1989, 1996; Holdaway, 1999; Koch and Barnosky, 2006; Wroe et al., 2004). In Australia, habitat modification through

1.1 THE CHANGING CLIMATE AND BIODIVERSITY

human use of fire has been suggested as a major cause of extinction (Miller et al., 2005; Miller et al., 1999). It now seems more probable that increased fire frequency/intensity actually resulted from herbivore extinction rather than direct anthropogenic causes (Rule et al., 2012), where the loss of herbivore communities results in woody plant species creating a more burnable environment. Although anthropogenic causes for extinctions on small landmasses such as New Zealand seem clear, extrapolation to large continental megafaunal extinction during the Quaternary has been criticised. Major opposition to overkill explanations of Quaternary extinctions has stemmed from a lack of direct archaeological evidence of human hunting and the fact that many species known to have been hunted, such as bison, did not go extinct (Barnosky et al., 2004; Grayson and Meltzer, 2003; Koch and Barnosky, 2006).

Environmental causes of Quaternary megafaunal extinction have largely focused on climate change, although less well supported theories have been proposed, such as an extra-terrestrial impact (Firestone et al., 2007; Koch and Barnosky, 2006). However, many of the megafaunal extinctions during the Quaternary roughly coincide with climatic shifts, especially those associated with the end of the Last Glacial Maximum (LGM), suggesting that environmental change was a major driving force of Quaternary extinctions (Barnosky et al., 2004; Guthrie, 2006; Koch and Barnosky, 2006). Instead of earlier suggestions of climatic catastrophe (*e.g.*, drought, quick freeze), more recent hypotheses focus on habitat and landscape change, such that regions with conditions sufficient to support megafauna became increasingly restricted and fragmented or completely disappeared (Guthrie, 2006; Mann et al., 2015). There has also been a shift in focus from cold periods as drivers of extinction to periods of intense, rapid warming, especially those associated with D-O events (Cooper et al., 2015; Mann et al., 2015; Metcalf et al., 2016; Rozas-Davila et al., 2016). It is argued that these rapid changes in climate led to changes in plant diversity, with an increase in anti-herbivore features, in turn supporting smaller biomasses of large mammals (Guthrie, 2006; Mann et al., 2015). Indeed, pollen, lake, soil, and marine cores have been used to show an increase in temperature and moisture on the landscape at the end of the LGM (Bigelow and Edwards, 2001; Lozhkin et al., 1993), as well as the accumulation of organic material and peatland expansion associated with increased temperature throughout the Pleistocene (Mann et al., 2015; Treat et al., 2019). This would result in the landscape changing to one fragmented by lakes, bogs, forests, and low-nutrient, acidic soils, in turn, resulting in floral communities that were defended against

herbivory and concomitant smaller biomass of large animals (Guthrie, 2006; Hofreiter and Stewart, 2009; Mann et al., 2015; Treat et al., 2019).

Despite the contention surrounding the causes of megafaunal declines and extinctions, it is clear that the loss of megafaunal diversity had a profound impact on ecosystems, with knock on effects in food webs, changes in vegetation communities, and loss of co-evolutionary relationships (Johnson, 2009; Smith et al., 2016). A majority of extinctions were of megafaunal herbivores, which palaeoecological studies suggest maintained a state of vegetative openness on the landscape and helped in creating more diverse profiles of vegetation in more wooded areas (Bakker et al., 2009; Gill et al., 2012; Johnson, 2009; Smith et al., 2016). Therefore, following these extinctions and the consequent release of palatable hardwoods from herbivory pressure these habitats may have changed to a more dense and less diverse profile (Johnson, 2009). There also appears to have been a shift in the type of herbivory in ecosystems following megafaunal extinctions, with grazers replaced by frugivores and granivores (Smith et al., 2016). In addition, megafaunal extinctions and declines often appear to closely precede enhanced fire regimes, with low fire intensity prior to declines (Gill et al., 2009; Johnson, 2009). It is thought that the release of many woody plant species from herbivory pressure leads to an increase in plant biomass resulting in a more burnable environment (Gill et al., 2009; Johnson, 2009).

Understanding how and why so many megafaunal species became extinct during the Late Quaternary and the role humans and climate played is paramount for explaining not only the current distribution and status of species but also for future conservation management of extant species, especially considering current climate change (Hadly et al., 2004). Fossil assemblages and modern genetic data are of limited value for investigating the effect of climate and humans on past animal populations, as they will often fail to record genetic turnovers and bottlenecks. In contrast, ancient DNA allows researchers to sample genetic diversity from ancient populations and extinct species, revealing genetic turnovers and bottlenecks, thus allowing the investigation of demographic scenarios leading to extinction.

1.2 Ancient DNA and Quaternary Research

1.2.1 Ancient DNA

Ancient DNA (aDNA) is DNA from remains of organism, where the DNA has not been specifically preserved and may therefore be degraded. Ancient DNA can be extracted from museum specimens, archaeological or subfossil (*i.e.*, not fully fossilised) remains, or even sediment samples, and can provide insight into the evolutionary history and genetic relationships of populations or species. However, the analysis of aDNA is hampered by technical difficulties stemming from the exponential nature of DNA decay (Allentoft et al., 2012). After the death of an organism, cellular repair mechanisms no longer function and the DNA is exposed to numerous factors that threaten its stability (Dabney et al., 2013b; Hofreiter et al., 2001; Paabo et al., 1989; Paabo et al., 2004), including digestion by intracellular nucleases and microorganisms. Under certain conditions (*e.g.*, extreme cold, anoxia) the impact of these digestive mechanisms may be inhibited, however, even then the DNA is still exposed to hydrolytic and oxidative damage (Dabney et al., 2013b; Hofreiter et al., 2001; Paabo et al., 1989; Paabo et al., 2004). As a result, aDNA is highly fragmented (average fragment length often <100 bp), contains lesions that block DNA replication, and contains miscoding lesions primarily resulting from cytosine deamination (Hofreiter et al., 2001; Paabo et al., 1989; Paabo et al., 2004). Ultimately the cumulative effects of these processes will be so extensive that no useful or informative DNA molecules will remain, leaving only a relatively short window (several hundred thousand years) during which ancient DNA can be successfully sequenced (Allentoft et al., 2012; Hofreiter et al., 2001; Paabo et al., 1989; Paabo et al., 2004). Due to the degraded nature of aDNA another complicating factor is contamination with “exogenous” DNA molecules, which can eclipse the endogenous DNA in terms of concentration (Gilbert et al., 2005; Kolman and Tuross, 2000; Malmstrom et al., 2005; Noonan et al., 2005; Skoglund et al., 2014). Therefore, contamination controls are extremely important, and criteria have been proposed to validate the authenticity of a sample (Cooper and Poinar, 2000; Llamas et al., 2017).

With the development of high-throughput sequencing (HTS) techniques, the amount of data that can be extracted from ancient samples has greatly increased, overcoming many of the pitfalls of previous methods based on PCR and Sanger sequencing (Knapp and

Hofreiter, 2010; van Dijk et al., 2014). HTS allows an enormous number (millions to billions) of DNA molecules to be sequenced at a relatively low cost (Goodwin et al., 2016; van Dijk et al., 2014) and is not greatly hampered by the short fragment lengths characteristic of ancient DNA (Knapp and Hofreiter, 2010). Furthermore, as a high number of individual of whole molecules are sequenced (as opposed to fragments of molecules in traditional PCR based Sanger sequencing), HTS allows characteristic patterns of DNA damage, such as miscoding lesions, to be identified and accounted for (Ginolhac et al., 2011; Green et al., 2009; Jonsson et al., 2013). There are two main approaches to HTS: straight “shotgun” sequencing, or sequencing in combination with an enrichment/complexity-reduction technique. Shotgun HTS is where all molecules are sequenced, giving an untargeted and minimally biased view of the total DNA present. However, the amount of contaminant DNA in aDNA extracts often makes this shotgun sequencing uneconomical, and the use of enrichment techniques to increase the relative concentration of endogenous DNA is often essential (Knapp and Hofreiter, 2010). Traditional PCR-based enrichment methods often fail to take full advantage of the pool of molecules and is laborious when scaled to multiple loci, let alone full mitochondrial and nuclear genomes (Knapp and Hofreiter, 2010). Consequently, DNA-DNA or DNA-RNA hybridisation capture methods are increasingly being used as they can target many very short molecules at multiple loci across the genome using synthetic DNA or RNA baits (Carpenter et al., 2013; Knapp and Hofreiter, 2010; Richards et al., 2019). Hybridisation capture allows the targeting of a large number of short molecules from multiple loci in a single reaction, making it suitable for single-nucleotide polymorphism (SNP) analyses or sequencing of full mitogenomes (Carpenter et al., 2013; Gnrke et al., 2009).

1.2.2 Ancient DNA and megafaunal extinction and evolutionary history

Ancient DNA (aDNA) has contributed significantly to the deduction of the causes of megafauna extinctions and population turnover, whether human-induced or related to climatic changes (Campos et al., 2010; Cooper et al., 2015; Lorenzen et al., 2011; Palkopoulou et al., 2015). It is increasingly accepted that evolutionary interpretations based on modern genetic data alone can lead to misleading historic reconstructions and phylogeographic patterns. This is because contemporary DNA sequences only show the result of a modern snapshot of evolution, giving a static picture of a highly dynamic process (Paabo et al., 2004). The introduction of aDNA has provided a partial solution to

1.2 ANCIENT DNA AND QUATERNARY RESEARCH

this problem as it allows researchers to look retrospectively in order to capture the process of molecular evolution and population dynamics.

Much of the debate surrounding megafaunal extinctions has been centred on fossil assemblages and morphology. These methods are likely to fail to detect important and informative population-level processes, such as genetic turnovers and bottlenecks, especially considering the loss of genetic diversity through drift in populations that have experienced recent bottlenecks (Cooper et al., 2015; Davison et al., 2011; Paabo, 2000). Extraction of ancient DNA from Pleistocene megafauna remains is a valuable tool for inferring demographic scenarios, as it allows the detection of population bottlenecks, expansions and turnovers that can then be compared to other temporal environmental and anthropogenic events, possibly allowing the deduction of putative causative agents of these dynamic population processes (Cooper et al., 2015; Davison et al., 2011).

For example, aDNA analyses have revealed dynamic processes such as population and species level extinction recolonisation events, population declines and habitat tracking during the Pleistocene in brown bears (Barnes et al., 2002), polar bears (Miller et al., 2012), bison (Hofreiter and Stewart, 2009; Shapiro et al., 2004), musk oxen (Campos et al., 2010), and even non-megafaunal species such as lemmings (Brace et al., 2012) and arctic foxes (Dalen et al., 2007). These past demographic events would be virtually undetectable using conventional fossil-based methods and modern genetic data. Detection of these events does not assign causation, but if well resolved climate and human occupation records with calibration onto a common timescale are made available, confident inferences on possible causes can be hypothesised and tested. Therefore, it is undeniable that aDNA is paramount in the debate surrounding the decline and extinction of megafaunal species during the Quaternary, due to its ability to reveal dynamics that would otherwise go unrecognised. In addition, aDNA research can also be used to reveal patterns in extant species, allowing the testing of hypotheses based on modern distributions and phylogeography (Bray et al., 2013; Dalen et al., 2007), with the results potentially being applicable to conservation management in relation to changing climate and modern population dynamics (Boessenkool et al., 2009; Bray et al., 2013; Hofman et al., 2015; Leonard, 2008; Miller and Waits, 2003; Waters and Grosser, 2016).

The majority of early aDNA research focused on the maternally inherited, more abundant, and smaller mitochondrial genome, ignoring the more complex and more challenging to sequence nuclear genome. With advances in technological and analytic frameworks for ancient DNA, the retrieval of high-quality nuclear data for use in population-level genetic studies is now achievable. Indeed, a wealth of information surrounding demographic trajectories, taxonomic relationships, and admixture has been uncovered using nuclear genomic data, which may have been missed using mtDNA alone. For example, nuclear aDNA has revealed the demographic trajectory of mammoths leading up to their extinction (Palkopoulou et al., 2015), taxonomic relationships and admixture in ancient wolves and domestic dogs (Skoglund et al., 2015), and admixture and demography of polar bear and brown bears relative to past climate change (Miller et al., 2012). Therefore, nuclear genomic data may help further understand the evolutionary history of extinct and extant taxa.

Taxonomically speaking, a majority of megafauna aDNA research has focused on herbivores such as mammoths (Debruyne et al., 2008; Enk et al., 2016; Miller et al., 2008; Palkopoulou et al., 2013; Palkopoulou et al., 2015; Pecnerova et al., 2017), horses (Fages et al., 2019; Gaunitz et al., 2018; Heintzman et al., 2017; Librado et al., 2017; Lorenzen et al., 2011; Orlando et al., 2013; Schubert et al., 2014), and bison (Froese et al., 2017; Heintzman et al., 2016; Lorenzen et al., 2011; Massilani et al., 2016; Shapiro et al., 2004; Soubrier et al., 2016), with results showing differing impacts of climate and human activity. Many of these megafauna herbivore taxa have proven useful as model species to investigate the role of climate and environmental change on population dynamics and species turnover (Cooper et al., 2015; Lorenzen et al., 2011; Metcalf et al., 2016). However, changes in herbivore communities would ultimately have corresponding impacts on carnivore communities, including the stability, viability, and persistence of populations. However, due to the lower abundance of carnivores in the fossil record, only a relatively limited number of aDNA studies have attempted to investigate the influence of climate and environmental change on carnivore communities (Barnes et al., 2002; Barnett et al., 2016; Barnett et al., 2009; Ersmark et al., 2019; Ersmark et al., 2016; Gretzinger et al., 2019; Loog et al., 2020; Paijmans et al., 2017; Stanton et al., 2020; Stiller et al., 2010; Valdiosera et al., 2007; Valdiosera et al., 2008). Unlike many carnivorous/omnivorous megafauna, brown bears (*Ursus arctos*) represent a promising Late Quaternary model species, as they have a Holarctic distribution, abundant subfossil

1.3 BEARS AS A QUATERNARY MODEL TAXON

remains, and well-documented modern genetic diversity (Davison et al., 2011; Paabo, 2000). Furthermore, as they occupy a vastly different niche than megafauna herbivores, brown bears offer an alternative perspective on the influence of climate and humans on megafauna, which could potentially be extended to other carnivores/omnivores.

1.3 Bears as a Quaternary Model Taxon

1.3.1 Carnivora

Carnivora is an order of placental mammals, one of the few to occur naturally on all continents, including both terrestrial and aquatic species, with most species exhibiting a degree of carnivory (eating animal flesh). They represent a large range in size from the smallest representative, the least weasel (*Mustela nivalis*) weighing a mere 25 g and measuring 11 cm, to male southern elephant seals (*Mirounga leonine*) that can weigh up to 5000 kg and measure 6.7 m in length. Carnivora arose 60 million years ago (mya) in the Paleocene of North America, and most extant families of carnivorans had diversified by the Miocene (23–5.3 mya). Carnivora is divided into two clades: (1) the cat-like Feliformia, including cats (Felidae), mongooses (Herpestidae), hyenas (Hyaenidae), and civets (Nandiniidae); and (2) the dog-like Caniformia, including dogs (Canidae), bears (Ursidae), mustelids (Mustelidae), skunks, and badgers (Mephitidae), red pandas (Ailuridae), raccoons and related taxa (Procyonidae), and seals, walruses, and sea lions (Pinnipedia).

1.3.2 Bears

Bears are mammals of the family Ursidae, belonging to the order Carnivora. Their closest relatives are pinnipeds, musteloids, and canids. Bears originated in Eurasia and started to diversify during the Miocene, 11 to 12 mya. Ursidae is comprised of three subfamilies that are represented by eight extant species: the giant panda (*Ailuropoda melanoleuca*), which is the sole representative of Ailuropodinae; the spectacled bear (*Tremarctos ornatus*), which is the only living representative of Tremarctinae (the short-faced bears); and sun bears (*Helarctos malayanus*), sloth bears (*Melursus ursinus*), American black bears (*Ursus americanus*), Asiatic black bears (*Ursus thibetanus*), polar bears (*Ursus maritimus*), and brown bears (*Ursus arctos*), which comprise Ursinae. Despite there being

only eight extant species, bears are widespread, inhabiting a variety of environments throughout the Northern Hemisphere and parts of the Southern Hemisphere. During the Pleistocene a number of extinct species also existed. Extinct species of Ursinae include the cave bears (*Ursus spelaeus*, *U. ingressus*, and *U. deningeri*) in Eurasia, and the Etruscan bear (*U. eustruscus*) in Europe, Asia, and North Africa. Extinct diversity of Tremarctinae includes South American short-faced bears (*Arctotherium sp.*), North American short-faced bears (*Arctodus sp.*), and the Florida spectacled bear (*Tremarctos floridanus*) (McLellan and Reiner, 1994). This extinct ursid diversity included the largest terrestrial mammalian carnivores to exist, the North American giant short-faced bear — *Arctodus simus* — and the South American giant short-faced bear — *Arctotherium angustidens* — the largest individuals of which are estimated to have weighed upwards of 1000 kg (Christiansen, 1999; Gobetz and Martin, 2001; Soibelzon and Schubert, 2011).

1.3.3 Bear phylogenetics and evolutionary history

Disentangling ursid phylogenetics and evolutionary history has proven challenging. Evidence from the fossil record, morphology, mitochondrial data, and nuclear loci have all offered different perspectives on the evolutionary history of bears. Early mitochondrial studies failed to confidently disentangle many relationships between the different extant species. For example, within Ursinae, the placement of Asiatic and American brown bears has proven difficult, with fossil data, morphology and mitochondrial phylogenies placing them as sister taxa (Krause et al., 2008; McLellan and Reiner, 1994; Yu et al., 2004; Yu et al., 2007) (Figure 3A), while nuclear data suggest the American black bear as sister to polar and brown bears (Kutschera et al., 2014; Pages et al., 2008) (Figure 3B). Additionally, different types of data have provided conflicting placements of the sloth bear within the ursid phylogenetic tree. Mitochondrial analyses place the sloth bear as basal within Ursinae (Yu et al., 2004; Yu et al., 2007) (Figure 3A), while nuclear analyses have placed it closer to the sun bear (Kutschera et al., 2014; Pages et al., 2008) (Figure 3B). Furthermore, mitochondrial phylogenies have placed polar bears within brown bear diversity. This has long been argued to be the result of either hybridisation or incomplete lineage sorting. Not until many different nuclear loci could be analysed was the true distinct relationship between the bears able to be retrieved, with evidence supporting that polar bears carry introgressed brown bear mitochondrial genomes (Hailer et al., 2012; Miller et al., 2012). With subsequent analyses of full nuclear genomes, the degree of

1.3 BEARS AS A QUATERNARY MODEL TAXON

hybridisation could be quantified, with up to 8.8% of modern brown genomes comprising DNA of polar bear origin (Cahill et al., 2013; Cahill et al., 2015; Hailer, 2015; Liu et al., 2014).

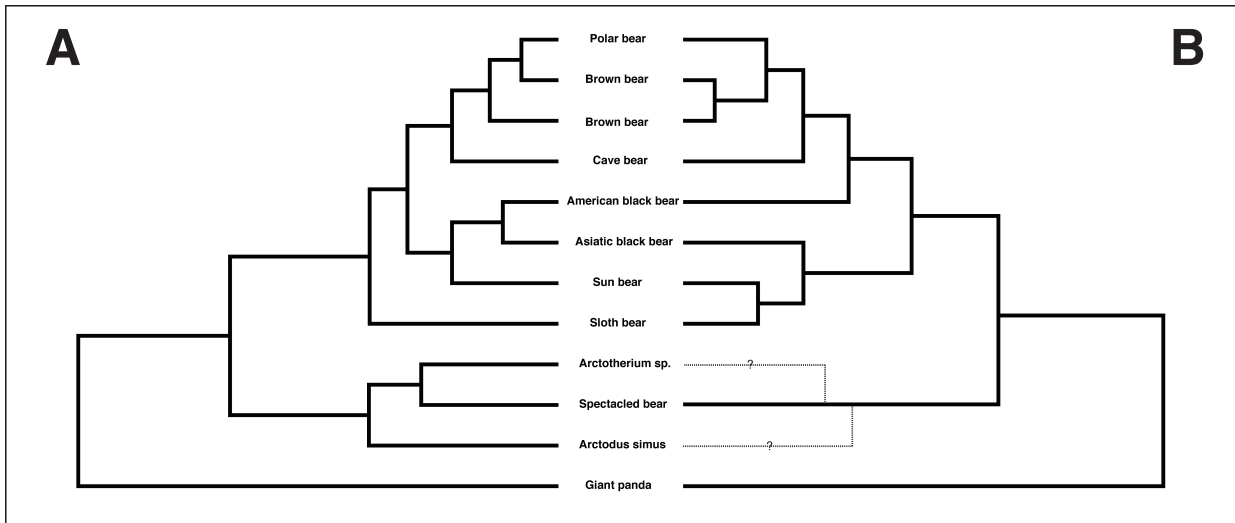


Figure 3: Schematic representation of ursid phylogeny from A) mitochondrial data and B) full nuclear genomes. Dashed lines indicate extinct species for which there are mitochondrial data but no nuclear data.

As sequencing technologies have improved, phylogenetic studies have included extinct species, including cave bears (Dabney et al., 2013a; Krause et al., 2008; Loreille et al., 2001; Noonan et al., 2005), North American short-faced bears (*A. simus*) (Krause et al., 2008), and South American short-faced bears (*Arctotherium sp.*) (Metcalf et al., 2016; Mitchell et al., 2016), but these studies have largely been based on mitochondrial data. These mitochondrial data have revealed cave bears to be sister to brown bears and polar bears ((Krause et al., 2008; Loreille et al., 2001; Noonan et al., 2005)), and *Arctotherium* to be sister to extant spectacled bears (Mitchell et al., 2016) (Figure 3A). However, with improvement of sequencing technologies and decreases to the cost of sequencing whole genomes, it has become clear that nuclear genomes are crucial to fully deduce ursid phylogenetics and evolutionary history. Indeed, whole genome sequencing has revealed a genetic landscape characterised by frequent hybridisation and introgression within ursids (Barlow et al., 2018; Cahill et al., 2013; Cahill et al., 2018; Cahill et al., 2015; Hailer, 2015; Kumar et al., 2017; Liu et al., 2014).

Analysis of full genomes have revealed more accurate relationships within ursine bears, with the sun bears and sloth bears being sister taxa and forming a clade with Asian black bears, while American black bears form a clade with polar bears and brown bears

(Kumar et al., 2017) (Figure 3B). Although the mitochondrial genomes of a number of extinct species have been analysed and have proven crucial to understanding ursid phylogenetics, nuclear data have been harder to obtain. Recently, the full genome of cave bears has been sequenced, showing extensive hybridisation with brown bears (Barlow et al., 2018; Barlow et al., 2020). However, no nuclear data from extinct tremarctine bears have been sequenced. The mitochondrial phylogeny of Tremarctinae is in conflict with morphological and fossil assemblage-based reconstructions, which suggest the genera *Arctotherium* and *Arctodus* should be sister with *Tremarctos* forming a separate clade (McLellan and Reiner, 1994; Soibelzon et al., 2005; Trajano and Ferrarezzi, 1995). In light of the conflict seen within ursine bears resulting from hybridisation, nuclear data may provide yet another different topology for Tremarctinae.

1.3.4 The brown bear (*Ursus arctos*)

The brown bear is one of the largest extant terrestrial carnivores, with a wide distribution throughout the Holarctic, from Europe, through Asia, and into North America. Brown bears have provided a useful animal model for Pleistocene biogeography, due to their wide distribution and relatively abundant subfossil remains from throughout the Holocene and Pleistocene (Sommer and Benecke, 2005). Brown bears are largely solitary and tend to exhibit a variable polygamous mating system, with plasticity in mating strategies based on geographical and environmental factors (Steyaert et al., 2012). Like most mammals, dispersal is mostly achieved while still young (Greenwood, 1980; Zedrosser et al., 2007). Natal dispersal is largely sex-biased, with males dispersing further from their mothers' home ranges and females exhibiting high philopatry, establishing home ranges adjacent or within that of their mother (Stoen et al., 2006; Zedrosser et al., 2007). There have been suggestions of competition for philopatry among females, with subdominant sisters being forced to disperse (Zedrosser et al., 2007). However, even when females do disperse, the dispersal distance is considerably less than that of males (Stoen et al., 2006). These sex-specific dispersal behaviours can have a profound influence on species' genetics, resulting in high levels of mitochondrial structuring across the landscape compared to nuclear loci.

1.3.5 Brown bear phylogeography and evolutionary history

The modern mitochondrial DNA (mtDNA) phylogeography of brown bears throughout Europe, North America, and Asia has been extensively studied, with geographically

1.3 BEARS AS A QUATERNARY MODEL TAXON

structured mtDNA clades proposed by Leonard et al. (2000) and subsequently extended to include extinct and less well characterised clades (Figure 4) (Barnes et al., 2002; Calvignac et al., 2009; Calvignac et al., 2008; Çilingir et al., 2016; Davison et al., 2011; Miller et al., 2006). Modern European bears have traditionally been divided into two distinct lineages, eastern (clade 3a) and western (clade 1) (Kohn et al., 1995; Taberlet and Bouvet, 1994). The eastern lineage is widespread, found from eastern Russia to Northern Scandinavia (Korsten et al., 2009; Saarma et al., 2007; Tammelaht et al., 2010), while the western lineage is found throughout Spain, France, Italy, and southern Scandinavia, and is further split into two groups: the Iberian lineage (clade 1a) and the Balkan/Italian lineage (clade 1b) (Kohn et al., 1995; Taberlet and Bouvet, 1994). In North America, four extant phylogeographically restricted clades have been identified: clade 2a in the Admiralty, Baranof, and Chicagof (ABC) islands of southern Alaska, clade 3a in western Alaska, 3b in eastern Alaska, and clade 4 in southern Canada and the contiguous USA (Talbot and Shields, 1996; Waits et al., 1998). The three latter North American clades (3a, 3b, and 4) are also found in Hokkaido, Japan, in a phylogeographically distinct distribution (Hirata et al., 2013; Masuda et al., 1998; Matsuhashi et al., 2001; Matsuhashi et al., 1999). Clade 3b has also been identified in bears from the Russian Far East (Gus'kov et al., 2013; Miller et al., 2006) and Altai-Sayan region (Tumendemberel et al., 2019). Furthermore, less well characterised clades have been identified in Asia: clade 5 in Tibet; clade 6 in the Gobi desert and Pakistan; and an Iranian clade recently denoted as clade 7 by Çilingir et al. (2016) (Ashrafzadeh et al., 2016; Calvignac et al., 2009; Miller et al., 2006). Clade 7 contains a strikingly high degree of haplotype diversity and the presence of three geographically restricted subclades, reminiscent of patterns seen in Hokkaido, North America, and Europe (Ashrafzadeh et al., 2016).

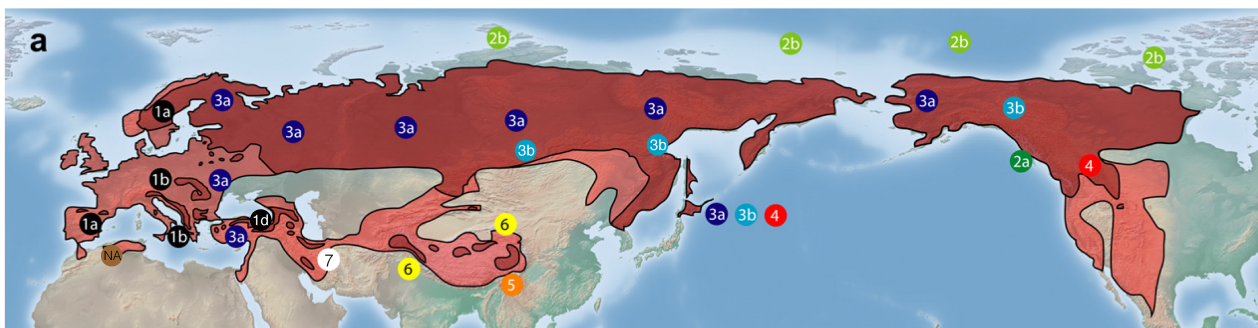


Figure 4: Current (dark red) and historic (light red) distribution of brown bears with approximate distribution of mitochondrial clades 1 to 7, and the extinct North African clade (NA). Adapted from Davison et al. (2011).

Ancient DNA (aDNA) studies have further revealed apparently extinct lineages of brown bear mtDNA lineages, as well as revealing signatures of dynamic population processes. For example, Barnes et al. (2002) observed the extinct subclades 2c and 3c in North America during the Pleistocene. Moreover, a complex temporal phylogeographic structuring was observed in North America, with a dynamic history of local extinctions and repopulation from Eurasia of distinct subclades throughout the Pleistocene apparently coincident with climatic shifts (Barnes et al., 2002). Studies of brown bear remains from Eurasia have extended the historical range of clade 3b west into the Altai-Sayan and Caucasus regions (Hirata et al., 2014), and possibly identified the presence of the extinct clade 3c in the Pleistocene Russian Far East (Rey-Iglesia et al., 2019). Meanwhile, a study of extinct “Atlas bears” revealed the recent extinction of an endemic North African mtDNA clade as well as the presence of the Iberian subclade 1a in Africa, possibly resulting from introduction of western European bears by Romans or Carthaginians for wild beast battles (Calvignac et al., 2008). Valdiosera et al. (2007) identified extinct divergent clade 1 haplotypes in France, which were later grouped as subclade 1c (Davison et al., 2011), indicative of higher diversity pre-LGM and of significant loss of variation following the end of the LGM. Calvignac et al. (2009) also identified a supposedly divergent extinct clade 1 lineage in ancient Lebanese samples, this lineage was later found to be extant in Turkish bears and was denoted as clade 1d (Çilingir et al., 2016). The abundance of lost genetic variation demonstrates the “time-trapped” nature of modern DNA alone and the necessity of aDNA for understanding current genetic variation. The study of aDNA from subfossil material can recover lost genetic variation, revealing past demographic processes, which may have been influenced by climate change or anthropogenic influences.

The phylogeographic structure seen in modern European brown bears has been considered to be largely consistent with the European “expansion/contraction” model of postglacial recolonisation. In fact, brown bears were one of the key species in developing this model (Hewitt, 1999, 2000, 2004). Under Hewitt’s model, brown bears would have been restricted to refugia on the Iberian (clade 1a) and Italian/Balkan (clade 1b) peninsulas. Following the end of the LGM, it has been proposed that clade 1a was first to expand out of its Iberian refugium and into southern Scandinavia, creating a hybrid zone with the eastern clade 3a, with the northward expansion of clade 1b in the Italian and Balkan peninsulas potentially hindered by the late deglaciation of the Alps, creating the

1.3 BEARS AS A QUATERNARY MODEL TAXON

phylogeographic pattern observed today (Hewitt, 1999; Sommer and Benecke, 2005; Taberlet and Bouvet, 1994). However, ancient DNA studies have raised doubts about the isolation, existence, and timing of expansion of these southern refugia, with suggestions of gene flow across Europe before the LGM and between refugia during and after (Ersmark et al., 2019; Hofreiter et al., 2004; Valdiosera et al., 2007; Valdiosera et al., 2008).

The timing of expansion from refugia has also come into doubt with the discovery of clade 1b in southern Scandinavia 5310 years before present (ybp) (Bray et al., 2013). Indeed, ancient DNA data suggest that the expansion of the Italian/Balkan lineage was not hindered by the glaciated alps, with evidence of expansion as early as 12,000 ybp in Germany (Bray, 2010). These results indicate that the phylogeographic pattern observed today might not be the direct result of expansion from refugia following the end of the LGM and that bears from the Italian/Balkan refugium may have been the first to expand into northern Europe, followed by a turnover event sometime between 2000 and 5000 ybp, resulting in the current phylogeographic pattern (Bray et al., 2013). Furthermore, a recent study, using the largest number of brown bear ancient sequences to date, showed high late Pleistocene diversity and refuted the confinement of bears to southern refugia during the LGM. They instead showed genetic turnover prior to the LGM and demographic decline and structuring of populations during the Holocene (Ersmark et al., 2019). Further research to elucidate the demographic scenario leading to the current phylogeography and past population dynamics in Europe would require more extensive sampling of European subfossil material immediately after and during the LGM, to allow more confident inferences of population movements. More extensive sampling of subfossil material from putative refugia, namely the Iberian and Balkan refugia, would also allow more accurate testing about refugial existence, isolation, and connectivity.

The majority of previous mtDNA studies, including those on ursids, have focused on fragments of the control region and cytochrome *b*. While these regions have proved informative for inferring phylogeographic structure, reconstructing phylogenies, and formulating/testing questions about demographic histories, it is undeniable that extension to full mitogenomes would be beneficial, allowing refinement of previous conclusions and analyses. For example, expansion to full mitogenomes could further clarify the phylogenetic relationships among and within the less well-characterised clades, such as

clade 5, 6, and 7, as well as the North African clade. Full mitogenomes from a range of clades and subclades, and from ancient specimens, would also allow more accurate and reliable estimates of mutation rates and divergence times, which could be more confidently correlated with past events (*i.e.* climatic changes) that may have been driving forces for population dynamics.

1.4 Thesis Overview

1.4.1 Thesis scope and aims

In this thesis, I explore the evolutionary history of bears using ancient mitochondrial and nuclear genomes. The drastic changes in climate and environment during the Late Quaternary have driven the evolutionary history of many megafauna species and ancient DNA allows us to learn about populations that lived in the past. With the advent of high-throughput sequencing and hybridization enrichment techniques, the scope of samples and the data that can be extracted from such samples has been expanded, with the possibility of whole genome data being obtained from well-preserved samples. In this thesis, I aim to broaden our understanding of the evolutionary history of bears, both at the species level (*e.g.* brown bears) and at higher taxonomic scales. Furthermore, a main objective of the research I present across the following chapters is to gain a better understanding of the response of megafauna to climatic and environmental change.

1.4.2 Chapter 2: Lions and brown bears colonised North America in multiple synchronous waves of dispersal across the Bering Land Bridge

During the Pleistocene, the growth and retreat of ice sheets and glaciers resulted in corresponding changes in sea level. These changes in sea level resulted in previously submerged land become subaerial and vice versa. A classic exemplar of this process is the Bering Land Bridge, connecting the Americas to Eurasia between Alaska and Far East Russia. This land bridge formed an intermittent connection between the continents throughout the Pleistocene, alternating between a submerged and subaerial state. This intermittent connection would have alternately fragmented populations and allowed migrations between Eurasia and North America. In Chapter 2 I investigate the influence of the Bering Land Bridge and Pleistocene climate change on the diversity and distribution

1.4 THESIS OVERVIEW

of two carnivoran taxa, lions (*Panthera* spp.) and brown bears (*Ursus arctos*), using whole mitogenomes from 39 lions and 103 bears.

1.4.3 Chapter 3: Phylogeography of the extinct North American giant short-faced bear (*Arctodus simus*), with comments on their palaeobiology

The North American giant short-faced bear (*Arctodus simus*) is an emblematic member of carnivore guilds of the continent, becoming extinct during the Pleistocene–Holocene transition (Kurtén, 1967; Kurtén and Anderson, 1980). A plenitude of past research has debated the ecological niche inhabited by this species (e.g. Barnes et al., 2002; Emslie and Czaplewski, 1985; Figueirido et al., 2010; Matheus, 1995; Matheus, 2003), as well as different explanations for variation in size seen across the range of *A. simus* (i.e. extreme sexual dimorphism versus taxonomic subdivisions) (e.g. Richards et al., 1996; Schubert, 2010; Schubert et al., 2010). However, despite being one of the most intensely studied megafauna species of Pleistocene North America, genetic data has been published from only a single specimen (Krause et al., 2008). In this chapter I used hybridisation enrichment techniques to obtain mitogenomic data from an additional 31 *A. simus* specimens from across their range, from Eastern Beringia to New Mexico, in order to investigate mitochondrial diversity, phylogeography, and evidence for distinct subspecies within *A. simus*. Further, I used shallow shotgun sequencing data to genetically determine the sex of specimens, which I combined with size estimates to test whether observed size variation represents sexual dimorphism. I synthesise these different data to provide insights into the palaeobiology of the taxon.

1.4.4 Chapter 4: Ancient genomes reveal hybridisation between extinct short-faced bears and the extant spectacled bear (*Tremarctos ornatus*)

Following the investigation of the phylogeography and diversity of *A. simus* in Chapter 3, I investigate the evolutionary history of short-faced bears more broadly (family: Tremarctinae). Previous work has investigated the evolutionary history and phylogenetics of short-faced bears using mitochondrial data (Mitchell et al., 2016), but no investigations of the nuclear genome have previously been undertaken. I obtained whole genomic data from the two extinct short-faced bear lineages — *Arctodus* and *Arctotherium* — using shotgun sequencing of DNA from three *A. simus* specimens from North America and a single *Arctotherium* sp. specimen from South America. I combined these new data with

published whole genomes from all extant species of bear with the objective of investigating the phylogenetic relationships among short-faced bears and testing for evidence of hybridisation both within short-faced bears and between short-faced bears and the more common bear family, Ursinae, with which tremarctine bears coexisted in North America during the Pleistocene.

1.4.5 Chapter 5: From Iberia to Siberia: Phylogeography and evolutionary history of Eurasian brown bears

Eurasia has been a major focus of Quaternary research, with special interest paid to Europe, large expanses of which were intermittently glaciated during the Pleistocene. Brown bears have been used as a model for the responses of temperate taxa to environmental changes during the Late Quaternary (Hewitt, 1999, 2000, 2004). Consequently, many ancient DNA studies have focused on European brown bears, but largely relied on short mitochondrial fragments (Ersmark et al., 2019; Fortes et al., 2016; Hofreiter et al., 2004; Valdiosera et al., 2007; Valdiosera et al., 2008; Xenikoudakis et al., 2015). North Asia has been far less represented in aDNA studies, with low mitochondrial diversity seen across Russia despite the fossil evidence suggesting the species evolved in the region (Anijalg et al., 2018; Davison et al., 2011; Korsten et al., 2009; Rey-Iglesia et al., 2019). Adding to the brown bear data produced in Chapter 2, I used hybridisation enrichment techniques to sequence a further 114 mitogenomes from ancient and historic brown bear specimens from North Asia, Europe, and North Africa, resulting in the largest dataset of ancient brown bear mitochondrial genomes to date. My objectives in this chapter were to comprehensively sample brown bear diversity and infer the evolutionary history of the species in its putative birthplace, Eurasia. Chapter 5 represents the first comprehensive aDNA study of brown bears across Eurasia (from Iberia to Western Beringia), including samples ranging in age from historic times to beyond the limits of radiocarbon dating, from ecologically and biogeographically important areas such as the Caucasus, Ural, and Altai mountains. The data I produced allowed me to propose and test a number of evolutionary scenarios for brown bear evolution in Eurasia.

1.5 References

- Allentoft, M.E., Collins, M., Harker, D., Haile, J., Oskam, C.L., Hale, M.L., Campos, P.F., Samaniego, J.A., Gilbert, M.T., Willerslev, E., Zhang, G., Scofield, R.P., Holdaway, R.N., Bunce, M., 2012. The half-life of DNA in bone: measuring decay kinetics in 158 dated fossils. *Proc. R. Soc. B.* 279, 4724-4733.
- Allentoft, M.E., Heller, R., Oskam, C.L., Lorenzen, E.D., Hale, M.L., Gilbert, M.T., Jacomb, C., Holdaway, R.N., Bunce, M., 2014. Extinct New Zealand megafauna were not in decline before human colonization. *Proc. Natl. Acad. Sci. U. S. A.* 111, 4922-4927.
- Alroy, J., 2001. A multispecies overkill simulation of the end-Pleistocene megafaunal mass extinction. *Science* 292, 1893-1896.
- Anijalg, P., Ho, S.Y.W., Davison, J., Keis, M., Tammeleht, E., Bobowik, K., Tumanov, I.L., Saveljev, A.P., Lyapunova, E.A., Vorobiev, A.A., Markov, N.I., Kryukov, A.P., Kojola, I., Swenson, J.E., Hagen, S.B., Eiken, H.G., Paule, L., Saarma, U., 2018. Large-scale migrations of brown bears in Eurasia and to North America during the Late Pleistocene. *J. Biogeogr.* 45, 394-405.
- Ashrafzadeh, M.R., Kaboli, M., Naghavi, M.R., 2016. Mitochondrial DNA analysis of Iranian brown bears (*Ursus arctos*) reveals new phylogeographic lineage. *Mamm. Biol.* 81, 1-9.
- Bakker, E.S., Olff, H., Gleichman, J.M., 2009. Contrasting effects of large herbivore grazing on smaller herbivores. *Basic Appl. Ecol.* 10, 141-150.
- Barlow, A., Cahill, J.A., Hartmann, S., Theunert, C., Xenikoudakis, G., Fortes, G.G., Paijmans, J.L.A., Rabeder, G., Frischauf, C., Grandal-d'Anglade, A., Garcia-Vazquez, A., Murtskhvaladze, M., Saarma, U., Anijalg, P., Skrbinek, T., Bertorelle, G., Gasparian, B., Bar-Oz, G., Pinhasi, R., Slatkin, M., Dalen, L., Shapiro, B., Hofreiter, M., 2018. Partial genomic survival of cave bears in living brown bears. *Nat. Ecol. Evol.* 2, 1563-1570.
- Barlow, A., Paijmans, J., Alberti, F., Gasparyan, B., Pinhasi, R., Foronova, I., Puzachenko, A., Pacher, M., Dalén, L., Baryshnikov, G., Hofreiter, M., 2020. Middle Pleistocene cave bear genome calibrates the evolutionary history of Palaeartic bears. *SSRN Electron. J.* <https://doi.org/10.2139/ssrn.3523359>.
- Barnes, I., Matheus, P., Shapiro, B., Jensen, D., Cooper, A., 2002. Dynamics of Pleistocene population extinctions in Beringian brown bears. *Science* 295, 2267-2270.
- Barnett, R., Lisandra, M., Zepeda Mendoza, M.L., Soares, A., Soares, R., Ho, S., Zazula, G., Yamaguchi, N., Shapiro, B., Kirillova, I., Larson, G., Thomas, M., Gilbert, P., 2016. Mitogenomics of the extinct cave lion, *Panthera spelaea* (Goldfuss, 1810), resolve its position within the *Panthera* cats. *Open Quat.* 2, 1-11.
- Barnett, R., Shapiro, B., Barnes, I., Ho, S.Y.W., Burger, J., Yamaguchi, N., Higham, T.F.G., Wheeler, H.T., Rosendahl, W., Sher, A.V., Sotnikova, M., Kuznetsova, T.,

- Baryshnikov, G.F., Martin, L.D., Harington, C.R., Burns, J.A., Cooper, A., 2009. Phylogeography of lions (*Panthera leo* ssp.) reveals three distinct taxa and a late Pleistocene reduction in genetic diversity. *Mol. Ecol.* 18, 1668-1677.
- Barnosky, A.D., Koch, P.L., Feranec, R.S., Wing, S.L., Shabel, A.B., 2004. Assessing the causes of late Pleistocene extinctions on the continents. *Science* 306, 70-75.
- Barnosky, A.D., Lindsey, E.L., 2010. Timing of Quaternary megafaunal extinction in South America in relation to human arrival and climate change. *Quat. Int.* 217, 10-29.
- Barnosky, A.D., Matzke, N., Tomiya, S., Wogan, G.O., Swartz, B., Quental, T.B., Marshall, C., McGuire, J.L., Lindsey, E.L., Maguire, K.C., Mersey, B., Ferrer, E.A., 2011. Has the Earth's sixth mass extinction already arrived? *Nature* 471, 51-57.
- Bigelow, N.H., Edwards, M.E., 2001. A 14,000 yr paleoenvironmental record from Windmill Lake, Central Alaska: Lateglacial and Holocene vegetation in the Alaska range. *Quat. Sci. Rev.* 20, 203-215.
- Boessenkool, S., Austin, J.J., Worthy, T.H., Scofield, P., Cooper, A., Seddon, P.J., Waters, J.M., 2009. Relict or colonizer? Extinction and range expansion of penguins in southern New Zealand. *Proc. R. Soc. B.* 276, 815-821.
- Brace, S., Palkopoulou, E., Dalen, L., Lister, A.M., Miller, R., Otte, M., Germonpre, M., Blockley, S.P.E., Stewart, J.R., Barnes, I., 2012. Serial population extinctions in a small mammal indicate Late Pleistocene ecosystem instability. *Proc. Natl. Acad. Sci. U. S. A.* 109, 20532-20536.
- Bray, S.C., 2010. Mitochondrial DNA analysis of the evolution and genetic diversity of ancient and extinct bears, School of Earth and Environmental Sciences. University of Adelaide.
- Bray, S.C.E., Austin, J.J., Metcalf, J.L., Østbye, K., Østbye, E., Lauritzen, S.-E., Aaris-Sørensen, K., Valdiosera, C., Adler, C.J., Cooper, A., 2013. Ancient DNA identifies post-glacial recolonisation, not recent bottlenecks, as the primary driver of contemporary mtDNA phylogeography and diversity in Scandinavian brown bears. *Divers. Distrib.* 19, 245-256.
- Cahill, J.A., Green, R.E., Fulton, T.L., Stiller, M., Jay, F., Ovsyanikov, N., Salamzade, R., St. John, J., Stirling, I., Slatkin, M., Shapiro, B., 2013. Genomic evidence for island population conversion resolves conflicting theories of polar bear evolution. *PLoS Genet.* 9, e1003345.
- Cahill, J.A., Heintzman, P.D., Harris, K., Teasdale, M.D., Kapp, J., Soares, A.E.R., Stirling, I., Bradley, D., Edwards, C.J., Graim, K., Kisleika, A.A., Malev, A.V., Monaghan, N., Green, R.E., Shapiro, B., 2018. Genomic evidence of widespread admixture from polar bears into brown bears during the last ice age. *Mol. Biol. Evol.* 35, 1120-1129.
- Cahill, J.A., Stirling, I., Kistler, L., Salamzade, R., Ersmark, E., Fulton, T.L., Stiller, M., Green, R.E., Shapiro, B., 2015. Genomic evidence of geographically widespread effect of gene flow from polar bears into brown bears. *Mol. Ecol.* 24, 1205-1217.

1.5 REFERENCES

- Calvignac, S., Hughes, S., Hanni, C., 2009. Genetic diversity of endangered brown bear (*Ursus arctos*) populations at the crossroads of Europe, Asia and Africa. *Divers. Distrib.* 15, 742-750.
- Calvignac, S., Hughes, S., Tougaard, C., Michaux, J., Thevenot, M., Philippe, M., Hamdine, W., Hanni, C., 2008. Ancient DNA evidence for the loss of a highly divergent brown bear clade during historical times. *Mol. Ecol.* 17, 1962-1970.
- Campos, P.F., Willerslev, E., Sher, A., Orlando, L., Axelsson, E., Tikhonov, A., Aaris-Sorensen, K., Greenwood, A.D., Kahlke, R.D., Kosintsev, P., Krakhmalnaya, T., Kuznetsova, T., Lemey, P., MacPhee, R., Norris, C.A., Shepherd, K., Suchard, M.A., Zazula, G.D., Shapiro, B., Gilbert, M.T.P., 2010. Ancient DNA analyses exclude humans as the driving force behind late Pleistocene musk ox (*Ovibos moschatus*) population dynamics. *Proc. Natl. Acad. Sci. U. S. A.* 107, 5675-5680.
- Carpenter, M.L., Buenrostro, J.D., Valdiosera, C., Schroeder, H., Allentoft, M.E., Sikora, M., Rasmussen, M., Gravel, S., Guillen, S., Nekhrizov, G., Leshtakov, K., Dimitrova, D., Theodossiev, N., Pettener, D., Luiselli, D., Sandoval, K., Moreno-Estrada, A., Li, Y.R., Wang, J., Gilbert, M.T.P., Willerslev, E., Greenleaf, W.J., Bustamante, C.D., 2013. Pulling out the 1%: Whole-Genome Capture for the Targeted Enrichment of Ancient DNA Sequencing Libraries. *Am. J. Hum. Genet.* 93, 852-864.
- Ceballos, G., Ehrlich, P.R., 2018. The misunderstood sixth mass extinction. *Science* 360, 1080-1081.
- Ceballos, G., Ehrlich, P.R., Barnosky, A.D., Garcia, A., Pringle, R.M., Palmer, T.M., 2015. Accelerated modern human-induced species losses: Entering the sixth mass extinction. *Sci. Adv.* 1, e1400253.
- Christiansen, P., 1999. What size were *Arctodus simus* and *Ursus spelaeus* (Carnivora: Ursidae)? *Ann. Zool. Fenn.* 36, 93-102.
- Çilingir, F.G., Akın Pekşen, Ç., Ambarlı, H., Beerli, P., Bilgin, C.C., 2016. Exceptional maternal lineage diversity in brown bears (*Ursus arctos*) from Turkey. *Zool. J. Linn. Soc.* 176, 463-477.
- Cooper, A., Poinar, H.N., 2000. Ancient DNA: Do it right or not at all. *Science* 289, 1139.
- Cooper, A., Turney, C., Hughen, K.A., Brook, B.W., McDonald, H.G., Bradshaw, C.J.A., 2015. Abrupt warming events drove Late Pleistocene Holarctic megafaunal turnover. *Science* 349, 602-606.
- Cuffey, K.M., Clow, G.D., Alley, R.B., Stuiver, M., Waddington, E.D., Saltus, R.W., 1995. Large Arctic Temperature-Change at the Wisconsin-Holocene Glacial Transition. *Science* 270, 455-458.
- Dabney, J., Knapp, M., Glocke, I., Gansauge, M.-T., Weihmann, A., Nickel, B., Valdiosera, C., García, N., Pääbo, S., Arsuaga, J.-L., Meyer, M., 2013a. Complete mitochondrial genome sequence of a Middle Pleistocene cave bear reconstructed from ultrashort DNA fragments. *Proc. Natl. Acad. Sci. U. S. A.* 110, 15758-15763.

- Dabney, J., Meyer, M., Paabo, S., 2013b. Ancient DNA damage. *Cold Spring Harb. Perspect. Biol.* 5, a012567.
- Dalen, L., Nystrom, V., Valdiosera, C., Germonpre, M., Sablin, M., Turner, E., Angerbjorn, A., Arsuaga, J.L., Gotherstrom, A., 2007. Ancient DNA reveals lack of postglacial habitat tracking in the arctic fox. *Proc. Natl. Acad. Sci. U. S. A.* 104, 6726-6729.
- Davison, J., Ho, S.Y.W., Bray, S.C., Korsten, M., Tammeleht, E., Hindrikson, M., Ostbye, K., Ostbye, E., Lauritzen, S.E., Austin, J., Cooper, A., Saarma, U., 2011. Late-Quaternary biogeographic scenarios for the brown bear (*Ursus arctos*), a wild mammal model species. *Quat. Sci. Rev.* 30, 418-430.
- De Vos, J.M., Joppa, L.N., Gittleman, J.L., Stephens, P.R., Pimm, S.L., 2015. Estimating the normal background rate of species extinction. *Conserv. Biol.* 29, 452-462.
- Debruyne, R., Chu, G., King, C.E., Bos, K., Kuch, M., Schwarz, C., Szpak, P., Grocke, D.R., Matheus, P., Zazula, G., Guthrie, D., Froese, D., Buigues, B., de Marliave, C., Flemming, C., Poinar, D., Fisher, D., Southon, J., Tikhonov, A.N., MacPhee, R.D.E., Poinar, H.N., 2008. Out of America: Ancient DNA evidence for a New World origin of Late Quaternary woolly mammoths. *Curr. Biol.* 18, 1320-1326.
- Denton, G.H., Anderson, R.F., Toggweiler, J.R., Edwards, R.L., Schaefer, J.M., Putnam, A.E., 2010. The last glacial termination. *Science* 328, 1652-1656.
- Doughty, C.E., 2013. Preindustrial Human Impacts on Global and Regional Environment. *Annu. Rev. Environ. Resour.* 38, 503-527.
- Eldredge, N., 1989. *Macroevolutionary Dynamics: Species, Niches, and Adaptive Peaks*. McGraw-Hill, New York.
- Eldredge, N., 1995. *Reinventing Darwin the Great Debate at the High Table of Evolutionary Theory*. Wiley Publishers, New York.
- Elias, S.A., Short, S.K., Nelson, C.H., Birks, H.H., 1996. Life and times of the Bering land bridge. *Nature* 382, 60-63.
- Emslie, S.D., Czaplewski, N.J., 1985. A new record of giant short-faced bear, *Arctodus simus*, from western North America with a re-evaluation of its paleobiology. *Contrib. Sci. (Los. Angel.)* 371, 1-12.
- Enk, J., Devault, A., Widga, C., Saunders, J., Szpak, P., Southon, J., Rouillard, J.-M., Shapiro, B., Golding, G.B., Zazula, G., Froese, D., Fisher, D.C., MacPhee, R.D.E., Poinar, H., 2016. *Mammuthus* population dynamics in Late Pleistocene North America: Divergence, phylogeography, and introgression. *Front. Ecol. Evol.* 4, 42.
- Ersmark, E., Baryshnikov, G., Higham, T., Argant, A., Castanos, P., Doppes, D., Gasparik, M., Germonpre, M., Liden, K., Lipecki, G., Marciszak, A., Miller, R., Moreno-Garcia, M., Pacher, M., Robu, M., Rodriguez-Varela, R., Rojo Guerra, M., Sabol, M., Spassov, N., Stora, J., Valdiosera, C., Villaluenga, A., Stewart, J.R., Dalen, L., 2019. Genetic turnovers and northern survival during the last glacial maximum in European brown bears. *Ecol. Evol.* 9, 5891-5905.

1.5 REFERENCES

- Ersmark, E., Klutsch, C.F.C., Chan, Y.L., Sinding, M.H.S., Fain, S.P., Illarionova, N.A., Oskarsson, M., Uhlen, M., Zhang, Y.P., Dalen, L., Savolainen, P., 2016. From the past to the present: Wolf phylogeography and demographic history based on the mitochondrial control region. *Front. Ecol. Evol.* 4.
- Fages, A., Hanghoj, K., Khan, N., Gaunitz, C., Seguin-Orlando, A., Leonardi, M., Constantz, C.M., Gamba, C., Al-Rasheid, K.A.S., Albizuri, S., Alfarhan, A.H., Allentoft, M., Alquraishi, S., Anthony, D., Baimukhanov, N., Barrett, J.H., Bayarsaikhan, J., Benecke, N., Bernaldez-Sanchez, E., Berrocal-Rangel, L., Biglari, F., Boessenkool, S., Boldgiv, B., Brem, G., Brown, D., Burger, J., Crubezy, E., Daugnora, L., Davoudi, H., Damgaard, P.D., de Villa-Ceballos, M.D.L.D.Y., Deschler-Erb, S., Detry, C., Dill, N., Oom, M.D.M., Dohr, A., Ellingvag, S., Erdenebaatar, D., Fathi, H., Felkel, S., Fernandez-Rodriguez, C., Garcia-Vinas, E., Germonpre, M., Granado, J.D., Hallsson, J.H., Hemmer, H., Hofreiter, M., Kasparov, A., Khasanov, M., Khazaeli, R., Kosintsev, P., Kristiansen, K., Kubatbek, T., Kuderna, L., Kuznetsov, P., Laleh, H., Leonard, J.A., Lhuillier, J., von Lettow-Vorbeck, C.L., Logvin, A., Lougas, L., Ludwig, A., Luis, C., Arruda, A.M., Marques-Bonet, T., Silva, R.M., Merz, V., Mijiddorj, E., Miller, B.K., Monchalov, O., Mohaseb, F.A., Morales, A., Nieto-Espinet, A., Nistelberger, H., Onar, V., Palsdottir, A.H., Pitulko, V., Pitskhelauri, K., Pruvost, M., Sikanjic, P.R., Papesa, A.R., Roslyakova, N., Sardari, A., Sauer, E., Schafberg, R., Scheu, A., Schibler, J., Schlumbaum, A., Serrand, N., Serres-Armero, A., Shapiro, B., Seno, S.S., Shevnina, I., Shidrang, S., Southon, J., Star, B., Sykes, N., Taheri, K., Taylor, W., Teegen, W.R., Vukicevic, T.T., Trixl, S., Tumen, D., Undrakhbold, S., Usmanova, E., Vahdati, A., Valenzuela-Lamas, S., Viegas, C., Wallner, B., Weinstock, J., Zaibert, V., Clavel, B., Lepetz, S., Mashkour, M., Helgason, A., Stefansson, K., Barrey, E., Willerslev, E., Outram, A.K., Librado, P., Orlando, L., 2019. Tracking Five Millennia of Horse Management with Extensive Ancient Genome Time Series. *Cell* 177, 1419-1435.
- Figueirido, B., Pérez-Claros, J.A., Torregrosa, V., Martín-Serra, A., Palmqvist, P., 2010. Demythologizing *Arctodus simus*, the 'short-faced' long-legged and predaceous bear that never was. *J. Vertebr. Paleontol.* 30, 262-275.
- Firestone, R.B., West, A., Kennett, J.P., Becker, L., Bunch, T.E., Revay, Z.S., Schultz, P.H., Belgya, T., Kennett, D.J., Erlandson, J.M., Dickenson, O.J., Goodyear, A.C., Harris, R.S., Howard, G.A., Kloosterman, J.B., Lechler, P., Mayewski, P.A., Montgomery, J., Poreda, R., Darrah, T., Hee, S.S.Q., Smitha, A.R., Stich, A., Topping, W., Wittke, J.H., Wolbach, W.S., 2007. Evidence for an extraterrestrial impact 12,900 years ago that contributed to the megafaunal extinctions and the Younger Dryas cooling. *Proc. Natl. Acad. Sci. U. S. A.* 104, 16016-16021.
- Fortes, G.G., Grandal-d'Anglade, A., Kolbe, B., Fernandes, D., Meleg, I.N., Garcia-Vazquez, A., Pinto-Llona, A.C., Constantin, S., de Torres, T.J., Ortiz, J.E., Frischauf, C., Rabeder, G., Hofreiter, M., Barlow, A., 2016. Ancient DNA reveals differences in behaviour and sociality between brown bears and extinct cave bears. *Mol. Ecol.* 25, 4907-4918.
- Froese, D., Stiller, M., Heintzman, P.D., Reyes, A.V., Zazula, G.D., Soares, A.E., Meyer, M., Hall, E., Jensen, B.J., Arnold, L.J., MacPhee, R.D., Shapiro, B., 2017. Fossil

- and genomic evidence constrains the timing of bison arrival in North America. Proc. Natl. Acad. Sci. U. S. A. 114, 3457-3462.
- Gaunitz, C., Fages, A., Hanghoj, K., Albrechtsen, A., Khan, N., Schubert, M., Seguin-Orlando, A., Owens, I.J., Felkel, S., Bignon-Lau, O., Damgaard, P.D., Mittnik, A., Mohaseb, A.F., Davoudi, H., Alquraishi, S., Alfarhan, A.H., Al-Rasheid, K.A.S., Crubezy, E., Benecke, N., Olsen, S., Brown, D., Anthony, D., Massy, K., Pitulko, V., Kasparov, A., Brem, G., Hofreiter, M., Mukhtarova, G., Baimukhanov, N., Lougas, L., Onar, V., Stockhammer, P.W., Krause, J., Boldgiv, B., Undrakhbold, S., Erdenebaatar, D., Lepetz, S., Mashkour, M., Ludwig, A., Wallner, B., Merz, V., Merz, I., Zaibert, V., Willerslev, E., Librado, P., Outram, A.K., Orlando, L., 2018. Ancient genomes revisit the ancestry of domestic and Przewalski's horses. Science 360, 111-114.
- Gilbert, M.T.P., Bandelt, H.J., Hofreiter, M., Barnes, I., 2005. Assessing ancient DNA studies. Trends Ecol. Evol. 20, 541-544.
- Gill, J.L., Williams, J.W., Jackson, S.T., Donnelly, J.P., Schellinger, G.C., 2012. Climatic and megaherbivory controls on late-glacial vegetation dynamics: a new, high-resolution, multi-proxy record from Silver Lake, Ohio. Quat. Sci. Rev. 34, 66-80.
- Gill, J.L., Williams, J.W., Jackson, S.T., Lininger, K.B., Robinson, G.S., 2009. Pleistocene megafaunal collapse, novel plant communities, and enhanced fire regimes in North America. Science 326, 1100-1103.
- Ginolhac, A., Rasmussen, M., Gilbert, M.T.P., Willerslev, E., Orlando, L., 2011. mapDamage: testing for damage patterns in ancient DNA sequences. Bioinformatics 27, 2153-2155.
- Gnirke, A., Melnikov, A., Maguire, J., Rogov, P., LeProust, E.M., Brockman, W., Fennell, T., Giannoukos, G., Fisher, S., Russ, C., Gabriel, S., Jaffe, D.B., Lander, E.S., Nusbaum, C., 2009. Solution hybrid selection with ultra-long oligonucleotides for massively parallel targeted sequencing. Nat. Biotechnol. 27, 182-189.
- Gobetz, K., Martin, L., 2001. An exceptionally large short faced bear (*Arctodus simus*) from the late Pleistocene (?)/early Holocene of Kansas. Curr. Res. Pleistocene 18, 97-99.
- Goodwin, S., McPherson, J.D., McCombie, W.R., 2016. Coming of age: ten years of next-generation sequencing technologies. Nat. Rev. Genet. 17, 333-351.
- Grayson, D.K., Meltzer, D.J., 2003. A requiem for North American overkill. J. Archaeol. Sci. 30, 585-593.
- Green, R.E., Briggs, A.W., Krause, J., Prufer, K., Burbano, H.A., Siebauer, M., Lachmann, M., Paabo, S., 2009. The Neandertal genome and ancient DNA authenticity. EMBO J. 28, 2494-2502.
- Greenwood, P.J., 1980. Mating systems, philopatry and dispersal in birds and mammals. Anim. Behav. 28, 1140-1162.

1.5 REFERENCES

- Gretzinger, J., Molak, M., Reiter, E., Pfrengle, S., Urban, C., Neukamm, J., Blant, M., Conard, N.J., Cupillard, C., Dimitrijevic, V., Drucker, D.G., Hofman-Kaminska, E., Kowalczyk, R., Krajcarz, M.T., Krajcarz, M., Munzel, S.C., Peresani, M., Romandini, M., Ruffi, I., Soler, J., Terlato, G., Krause, J., Bocherens, H., Schuenemann, V.J., 2019. Large-scale mitogenomic analysis of the phylogeography of the Late Pleistocene cave bear. *Sci. Rep.* 9.
- Gus'kov, V.Y., Sheremet'eva, I.N., Seredkin, I.V., Kryukov, A.P., 2013. Mitochondrial cytochrome *b* gene variation in brown bear (*Ursus arctos* Linnaeus, 1758) from southern part of Russian Far East. *Russ. J. Genet.* 49, 1213–1218.
- Guthrie, R.D., 2006. New carbon dates link climatic change with human colonization and Pleistocene extinctions. *Nature* 441, 207-209.
- Hadly, E.A., Ramakrishnan, U., Chan, Y.L., van Tuinen, M., O'Keefe, K., Spaeth, P.A., Conroy, C.J., 2004. Genetic response to climatic change: Insights from ancient DNA and phylochronology. *PLoS Biol.* 2, 1600-1609.
- Hailer, F., 2015. Introgressive hybridization: brown bears as vectors for polar bear alleles. *Mol. Ecol.* 24, 1161-1163.
- Hailer, F., Kutschera, V.E., Hallstrom, B.M., Klassert, D., Fain, S.R., Leonard, J.A., Arnason, U., Janke, A., 2012. Nuclear genomic sequences reveal that polar bears are an old and distinct bear lineage. *Science* 336, 344-347.
- Haynes, G., 2013. Extinctions in North America's late glacial landscapes. *Quat. Int.* 285, 89-98.
- Heintzman, P.D., Froese, D., Ives, J.W., Soares, A.E., Zazula, G.D., Letts, B., Andrews, T.D., Driver, J.C., Hall, E., Hare, P.G., Jass, C.N., MacKay, G., Southon, J.R., Stiller, M., Woywitka, R., Suchard, M.A., Shapiro, B., 2016. Bison phylogeography constrains dispersal and viability of the Ice Free Corridor in western Canada. *Proc. Natl. Acad. Sci. U. S. A.* 113, 8057-8063.
- Heintzman, P.D., Zazula, G.D., Macphee, R.D.E., Scott, E., Cahill, J.A., McHorse, B.K., Kapp, J.D., Stiller, M., Wooller, M.J., Orlando, L., Southon, J., Froese, D.G., Shapiro, B., 2017. A new genus of horse from Pleistocene North America. *Elife* 6, e29944.
- Hewitt, G.M., 1996. Some genetic consequences of ice ages, and their role in divergence and speciation. *Biol. J. Linn. Soc.* 58, 247-276.
- Hewitt, G.M., 1999. Post-glacial re-colonization of European biota. *Biol. J. Linn. Soc.* 68, 87-112.
- Hewitt, G.M., 2000. The genetic legacy of the Quaternary ice ages. *Nature* 405, 907-913.
- Hewitt, G.M., 2004. Biodiversity: A climate for colonization. *Heredity* 92, 1-2.
- Hirata, D., Abramov, A.V., Baryshnikov, G.F., Masuda, R., 2014. Mitochondrial DNA haplogrouping of the brown bear, *Ursus arctos* (Carnivora: Ursidae) in Asia, based on a newly developed APLP analysis. *Biol. J. Linn. Soc.* 111, 627-635.

- Hirata, D., Mano, T., Abramov, A.V., Baryshnikov, G.F., Kosintsev, P.A., Vorobiev, A.A., Raichev, E.G., Tsunoda, H., Kaneko, Y., Murata, K., Fukui, D., Masuda, R., 2013. Molecular phylogeography of the brown bear (*Ursus arctos*) in Northeastern Asia based on analyses of complete mitochondrial DNA sequences. *Mol. Biol. Evol.* 30, 1644-1652.
- Hofman, C.A., Rick, T.C., Fleischer, R.C., Maldonado, J.E., 2015. Conservation archaeogenomics: ancient DNA and biodiversity in the Anthropocene. *Trends Ecol. Evol.* 30, 540-549.
- Hofreiter, M., Serre, D., Poinar, H.N., Kuch, M., Paabo, S., 2001. Ancient DNA. *Nat. Rev. Genet.* 2, 353-359.
- Hofreiter, M., Serre, D., Rohland, N., Rabeder, G., Nagel, D., Conard, N., Munzel, S., Paabo, S., 2004. Lack of phylogeography in European mammals before the last glaciation. *Proc. Natl. Acad. Sci. U. S. A.* 101, 12963-12968.
- Hofreiter, M., Stewart, J., 2009. Ecological change, range fluctuations and population dynamics during the Pleistocene. *Curr. Biol.* 19, R584-R594.
- Holdaway, R.N., 1989. New Zealand's pre-human avifauna and its vulnerability. *N. Z. J. Ecol.* 12, 11-25.
- Holdaway, R.N., 1996. Arrival of rats in New Zealand. *Nature* 384, 225-226.
- Holdaway, R.N., 1999. Introduced Predators and Avifaunal Extinction in New Zealand, in: MacPhee, R.D.E. (Ed.), *Extinctions in Near Time: Causes, Contexts, and Consequences*. Springer US, Boston, MA, pp. 189-238.
- Jansson, R., Dynesius, M., 2002. The fate of clades in a world of recurrent climatic change: Milankovitch oscillations and evolution. *Annu. Rev. Ecol. Syst.* 33, 741-777.
- Johnson, C.N., 2009. Ecological consequences of Late Quaternary extinctions of megafauna. *Proc. R. Soc. B.* 276, 2509-2519.
- Johnson, C.N., Alroy, J., Beeton, N.J., Bird, M.I., Brook, B.W., Cooper, A., Gillespie, R., Herrando-Perez, S., Jacobs, Z., Miller, G.H., Prideaux, G.J., Roberts, R.G., Rodriguez-Rey, M., Salte, F., Turney, C.S.M., Bradshaw, C.J.A., 2016. What caused extinction of the Pleistocene megafauna of Sahul? *Proc. R. Soc. B.* 283, 20152399.
- Jonsson, H., Ginolhac, A., Schubert, M., Johnson, P.L.F., Orlando, L., 2013. mapDamage2.0: fast approximate Bayesian estimates of ancient DNA damage parameters. *Bioinformatics* 29, 1682-1684.
- Knapp, M., Hofreiter, M., 2010. Next generation sequencing of ancient DNA: Requirements, strategies and perspectives. *Genes* 1, 227-243.
- Koch, P.L., Barnosky, A.D., 2006. Late quaternary extinctions: State of the debate. *Annual Review of Ecology Evolution and Systematics* 37, 215-250.

1.5 REFERENCES

- Kohn, M., Knauer, F., Stoffella, A., Schroder, W., Paabo, S., 1995. Conservation genetics of the European brown bear - a study using excremental PCR of nuclear and mitochondrial sequences. *Mol. Ecol.* 4, 95-103.
- Kolman, C.J., Tuross, N., 2000. Ancient DNA analysis of human populations. *Am. J. Phys. Anthropol.* 111, 5-23.
- Korsten, M., Ho, S.Y.W., Davison, J., Pahn, B., Vulla, E., Roht, M., Tumanov, I.L., Kojola, I., Andersone-Lilley, Z., Ozolins, J., Pilot, M., Mertzanis, Y., Giannakopoulos, A., Vorobiev, A.A., Markov, N.I., Saveljev, A.P., Lyapunova, E.A., Abramov, A.V., Mannil, P., Valdmann, H., Pazetnov, S.V., Pazetnov, V.S., Rokov, A.M., Saarma, U., 2009. Sudden expansion of a single brown bear maternal lineage across northern continental Eurasia after the last ice age: a general demographic model for mammals? *Mol. Ecol.* 18, 1963-1979.
- Krause, J., Unger, T., Nocon, A., Malaspinas, A.S., Kolokotronis, S.O., Stiller, M., Soibelzon, L., Spriggs, H., Dear, P.H., Briggs, A.W., Bray, S.C., O'Brien, S.J., Rabeder, G., Matheus, P., Cooper, A., Slatkin, M., Paabo, S., Hofreiter, M., 2008. Mitochondrial genomes reveal an explosive radiation of extinct and extant bears near the Miocene-Pliocene boundary. *BMC Evol. Biol.* 8, 220.
- Kumar, V., Lammers, F., Bidon, T., Pfenninger, M., Kolter, L., Nilsson, M.A., Janke, A., 2017. The evolutionary history of bears is characterized by gene flow across species. *Sci. Rep.* 7, 46487.
- Kurtén, B., 1967. Pleistocene bears of North America. 2. Genus *Arctodus*, short-faced bears. *Acta Zool. Fenn.* 117, 1-60.
- Kurtén, B., Anderson, E., 1980. Pleistocene Mammals of North America. Columbia University Press, New York.
- Kutschera, V.E., Bidon, T., Hailer, F., Rodi, J.L., Fain, S.R., Janke, A., 2014. Bears in a forest of gene trees: Phylogenetic inference is complicated by incomplete lineage sorting and gene flow. *Mol. Biol. Evol.* 31, 2004-2017.
- Leonard, J.A., 2008. Ancient DNA applications for wildlife conservation. *Mol. Ecol.* 17, 4186-4196.
- Leonard, J.A., Wayne, R.K., Cooper, A., 2000. Population genetics of Ice age brown bears. *Proc. Natl. Acad. Sci. U. S. A.* 97, 1651-1654.
- Lewis, S.L., Maslin, M.A., 2015. Defining the anthropocene. *Nature* 519, 171-180.
- Librado, P., Gamba, C., Gaunitz, C., Sarkissian, C.D., Pruvost, M., Albrechtsen, A., Fages, A., Khan, N., Schubert, M., Jagannathan, V., Serres-Armero, A., Kuderna, L.F.K., Povolotskaya, I.S., Seguin-Orlando, A., Lepetz, S., Neuditschko, M., Theves, C., Alquraishi, S., Alfarhan, A.H., Al-Rasheid, K., Rieder, S., Samashev, Z., Francfort, H.P., Benecke, N., Hofreiter, M., Ludwig, A., Keyser, C., Marques-Bonet, T., Ludes, B., Crubezy, E., Leeb, T., Willerslev, E., Orlando, L., 2017. Ancient genomic changes associated with domestication of the horse. *Science* 356, 442-445.

- Liu, S.P., Lorenzen, E.D., Fumagalli, M., Li, B., Harris, K., Xiong, Z.J., Zhou, L., Korneliussen, T.S., Somel, M., Babbitt, C., Wray, G., Li, J.W., He, W.M., Wang, Z., Fu, W.J., Xiang, X.Y., Morgan, C.C., Doherty, A., O'Connell, M.J., McInerney, J.O., Born, E.W., Dalen, L., Dietz, R., Orlando, L., Sonne, C., Zhang, G.J., Nielsen, R., Willerslev, E., Wang, J., 2014. Population genomics reveal recent speciation and rapid evolutionary adaptation in polar bears. *Cell* 157, 785-794.
- Llamas, B., Valverde, G., Fehren-Schmitz, L., Weyrich, L.S., Cooper, A., Haak, W., 2017. From the field to the laboratory: Controlling DNA contamination in human ancient DNA research in the high-throughput sequencing era. *STAR Sci. Technol. Archaeol. Res.* 3, 1-14.
- Loog, L., Thalmann, O., Sinding, M.H.S., Schuenemann, V.J., Perri, A., Germonpré, M., Bocherens, H., Witt, K.E., Castruita, J.A.S., Velasco, M.S., Lundstrom, I.K.C., Wales, N., Sonet, G., Frantz, L., Schroeder, H., Budd, J., Jimenez, E.L., Fedorov, S., Gasparyan, B., Kandel, A.W., L'zni-kov?-Galetov, M., Napierala, H., Uerpmann, H.P., Nikolskiy, P.A., Pavlova, E.Y., Pitulko, V.V., Herzig, K.H., Malhi, R.S., Willerslev, E., Hansen, A.J., Dobney, K., Gilbert, M.T.P., Krause, J., Larson, G., Eriksson, A., Manica, A., 2020. Ancient DNA suggests modern wolves trace their origin to a Late Pleistocene expansion from Beringia. *Mol. Ecol.* 29, 1596-1610.
- Loreille, O., Orlando, L., Patou-Mathis, M., Philippe, M., Taberlet, P., Hanni, C., 2001. Ancient DNA analysis reveals divergence of the cave bear, *Ursus spelaeus*, and brown bear, *Ursus arctos*, lineages. *Curr. Biol.* 11, 200-203.
- Lorenzen, E.D., Nogues-Bravo, D., Orlando, L., Weinstock, J., Binladen, J., Marske, K.A., Ugan, A., Borregaard, M.K., Gilbert, M.T., Nielsen, R., Ho, S.Y., Goebel, T., Graf, K.E., Byers, D., Stenderup, J.T., Rasmussen, M., Campos, P.F., Leonard, J.A., Koepfli, K.P., Froese, D., Zazula, G., Stafford, T.W., Jr., Aaris-Sorensen, K., Batra, P., Haywood, A.M., Singarayer, J.S., Valdes, P.J., Boeskorov, G., Burns, J.A., Davydov, S.P., Haile, J., Jenkins, D.L., Kosintsev, P., Kuznetsova, T., Lai, X., Martin, L.D., McDonald, H.G., Mol, D., Meldgaard, M., Munch, K., Stephan, E., Sablin, M., Sommer, R.S., Sipko, T., Scott, E., Suchard, M.A., Tikhonov, A., Willerslev, R., Wayne, R.K., Cooper, A., Hofreiter, M., Sher, A., Shapiro, B., Rahbek, C., Willerslev, E., 2011. Species-specific responses of Late Quaternary megafauna to climate and humans. *Nature* 479, 359-364.
- Lozhkin, A.V., Anderson, P.M., Eisner, W.R., Ravako, L.G., Hopkins, D.M., Brubaker, L.B., Colinvaux, P.A., Miller, M.C., 1993. Late Quaternary Lacustrine Pollen Records from Southwestern Beringia. *Quat. Res.* 39, 314-324.
- Malmstrom, H., Stora, J., Dalen, L., Holmlund, G., Gotherstrom, A., 2005. Extensive human DNA contamination in extracts from ancient dog bones and teeth. *Mol. Biol. Evol.* 22, 2040-2047.
- Mann, D.H., Groves, P., Reanier, R.E., Gaglioti, B.V., Kunz, M.L., Shapiro, B., 2015. Life and extinction of megafauna in the ice-age Arctic. *Proc. Natl. Acad. Sci. U. S. A.* 112, 14301-14306.
- Massilani, D., Guimaraes, S., Brugal, J.P., Bennett, E.A., Tokarska, M., Arbogast, R.M., Baryshnikov, G., Boeskorov, G., Castel, J.C., Davydov, S., Madelaine, S., Putelat,

1.5 REFERENCES

- O., Spasskaya, N.N., Uerpmann, H.P., Grange, T., Geigl, E.M., 2016. Past climate changes, population dynamics and the origin of Bison in Europe. *BMC Biol.* 14, 93.
- Masuda, R., Murata, K., Aiurzaniin, A., Yoshida, M.C., 1998. Phylogenetic status of brown bears *Ursus arctos* of Asia: A preliminary result inferred from mitochondrial DNA control region sequences. *Hereditas* 128, 277-280.
- Matheus, P.E., 1995. Diet and co-ecology of Pleistocene short-faced bears and brown bears in eastern Beringia. *Quat. Res.* 44, 447-453.
- Matheus, P.E., 2003. Locomotor adaptations and ecomorphology of short-faced bears (*Arctodus simus*) in eastern Beringia, Occasional Papers in Earth Science No. 7. Yukon Palaeontology Program, Department of Tourism and Culture, Whitehorse.
- Matsushashi, T., Masuda, R., Mano, T., Murata, K., Aiurzaniin, A., 2001. Phylogenetic relationships among worldwide populations of the brown bear *Ursus arctos*. *Zool. Sci.* 18, 1137-1143.
- Matsushashi, T., Masuda, R., Mano, T., Yoshida, M.C., 1999. Microevolution of the mitochondrial DNA control region in the Japanese brown bear (*Ursus arctos*) population. *Mol. Biol. Evol.* 16, 676-684.
- McLellan, B., Reiner, D.C., 1994. A review of bear evolution. *Bears Their Biol. Manag.* 9, 85-96.
- Metcalf, J.L., Turney, C., Barnett, R., Martin, F., Bray, S.C., Vilstrup, J.T., Orlando, L., Salas-Gismondi, R., Loponte, D., Medina, M., De Nigris, M., Civalero, T., Fernandez, P.M., Gasco, A., Duran, V., Seymour, K.L., Otaola, C., Gil, A., Paunero, R., Prevosti, F.J., Bradshaw, C.J., Wheeler, J.C., Borrero, L., Austin, J.J., Cooper, A., 2016. Synergistic roles of climate warming and human occupation in Patagonian megafaunal extinctions during the Last Deglaciation. *Sci. Adv.* 2, e1501682.
- Miller, C.R., Waits, L.P., 2003. The history of effective population size and genetic diversity in the Yellowstone grizzly (*Ursus arctos*): Implications for conservation. *Proc. Natl. Acad. Sci. U. S. A.* 100, 4334-4339.
- Miller, C.R., Waits, L.P., Joyce, P., 2006. Phylogeography and mitochondrial diversity of extirpated brown bear (*Ursus arctos*) populations in the contiguous United States and Mexico. *Mol. Ecol.* 15, 4477-4485.
- Miller, G.H., Fogel, M.L., Magee, J.W., Gagan, M.K., Clarke, S.J., Johnson, B.J., 2005. Ecosystem collapse in pleistocene Australia and a human role in megafaunal extinction. *Science* 309, 287-290.
- Miller, G.H., Magee, J.W., Johnson, B.J., Fogel, M.L., Spooner, N.A., McCulloch, M.T., Ayliffe, L.K., 1999. Pleistocene extinction of *Genyornis newtoni*: Human impact on Australian megafauna. *Science* 283, 205-208.
- Miller, W., Drautz, D.I., Ratan, A., Pusey, B., Qi, J., Lesk, A.M., Tomsho, L.P., Packard, M.D., Zhao, F.Q., Sher, A., Tikhonov, A., Raney, B., Patterson, N., Lindblad-Toh, K., Lander, E.S., Knight, J.R., Irzyk, G.P., Fredrikson, K.M., Harkins, T.T.,

- Sheridan, S., Pringle, T., Schuster, S.C., 2008. Sequencing the nuclear genome of the extinct woolly mammoth. *Nature* 456, 387-U351.
- Miller, W., Schuster, S.C., Welch, A.J., Ratan, A., Bedoya-Reina, O.C., Zhao, F.Q., Kim, H.L., Burhans, R.C., Drautz, D.I., Wittekindt, N.E., Tomsho, L.P., Ibarra-Laclette, E., Herrera-Estrella, L., Peacock, E., Farley, S., Sage, G.K., Rode, K., Obbard, M., Montiel, R., Bachmann, L., Ingolfsson, O., Aars, J., Mailund, T., Wiig, O., Talbot, S.L., Lindqvist, C., 2012. Polar and brown bear genomes reveal ancient admixture and demographic footprints of past climate change. *Proc. Natl. Acad. Sci. U. S. A.* 109, E2382-E2390.
- Mitchell, K.J., Bray, S.C., Bover, P., Soibelzon, L., Schubert, B.W., Prevosti, F., Prieto, A., Martin, F., Austin, J.J., Cooper, A., 2016. Ancient mitochondrial DNA reveals convergent evolution of giant short-faced bears (*Tremarctinae*) in North and South America. *Biol. Lett.* 12, 20160062.
- Noonan, J.P., Hofreiter, M., Smith, D., Priest, J.R., Rohland, N., Rabeder, G., Krause, J., Dettler, J.C., Paabo, S., Rubin, E.M., 2005. Genomic sequencing of Pleistocene cave bears. *Science* 309, 597-600.
- Orlando, L., Ginolhac, A., Zhang, G.J., Froese, D., Albrechtsen, A., Stiller, M., Schubert, M., Cappellini, E., Petersen, B., Moltke, I., Johnson, P.L.F., Fumagalli, M., Vilstrup, J.T., Raghavan, M., Korneliussen, T., Malaspina, A.S., Vogt, J., Szklarczyk, D., Kelstrup, C.D., Vinther, J., Dolocan, A., Stenderup, J., Velazquez, A.M.V., Cahill, J., Rasmussen, M., Wang, X.L., Min, J.M., Zazula, G.D., Seguin-Orlando, A., Mortensen, C., Magnussen, K., Thompson, J.F., Weinstock, J., Gregersen, K., Roed, K.H., Eisenmann, V., Rubin, C.J., Miller, D.C., Antczak, D.F., Bertelsen, M.F., Brunak, S., Al-Rasheid, K.A.S., Ryder, O., Andersson, L., Mundy, J., Krogh, A., Gilbert, M.T.P., Kjaer, K., Sicheritz-Ponten, T., Jensen, L.J., Olsen, J.V., Hofreiter, M., Nielsen, R., Shapiro, B., Wang, J., Willerslev, E., 2013. Recalibrating *Equus* evolution using the genome sequence of an early Middle Pleistocene horse. *Nature* 499, 74-78.
- Paabo, S., 2000. Of bears, conservation genetics, and the value of time travel. *Proc. Natl. Acad. Sci. U. S. A.* 97, 1320-1321.
- Paabo, S., Higuchi, R.G., Wilson, A.C., 1989. Ancient DNA and the Polymerase Chain-Reaction - the Emerging Field of Molecular Archaeology. *J. Biol. Chem.* 264, 9709-9712.
- Paabo, S., Poinar, H., Serre, D., Jaenicke-Despres, V., Hebler, J., Rohland, N., Kuch, M., Krause, J., Vigilant, L., Hofreiter, M., 2004. Genetic analyses from ancient DNA. *Annu. Rev. Genet.* 38, 645-679.
- Pages, M., Calvignac, S., Klein, C., Paris, M., Hughes, S., Hanni, C., 2008. Combined analysis of fourteen nuclear genes refines the Ursidae phylogeny. *Mol. Phylogenet. Evol.* 47, 73-83.
- Pajmans, J.L.A., Barnett, R., Gilbert, M.T.P., Zepeda-Mendoza, M.L., Reumer, J.W.F., de Vos, J., Zazula, G., Nagel, D., Baryshnikov, G.F., Leonard, J.A., Rohland, N., Westbury, M.V., Barlow, A., Hofreiter, M., 2017. Evolutionary history of saber-toothed cats based on ancient mitogenomics. *Curr. Biol.* 27, 3330-3336.

1.5 REFERENCES

- Palkopoulou, E., Dalen, L., Lister, A.M., Vartanyan, S., Sablin, M., Sher, A., Edmark, V.N., Brandstrom, M.D., Germonpre, M., Barnes, I., Thomas, J.A., 2013. Holarctic genetic structure and range dynamics in the woolly mammoth. *Proc. R. Soc. B.* 280, 20131910.
- Palkopoulou, E., Mallick, S., Skoglund, P., Enk, J., Rohland, N., Li, H., Omrak, A., Vartanyan, S., Poinar, H., Gotherstrom, A., Reich, D., Dalen, L., 2015. Complete genomes reveal signatures of demographic and genetic declines in the woolly mammoth. *Curr. Biol.* 25, 1395-1400.
- Pecnerova, P., Diez-Del-Molino, D., Dussex, N., Feuerborn, T., von Seth, J., van der Plicht, J., Nikolskiy, P., Tikhonov, A., Vartanyan, S., Dalen, L., 2017. Genome-Based Sexing Provides Clues about Behavior and Social Structure in the Woolly Mammoth. *Curr. Biol.* 27, 3505-3510.e3503.
- Pimm, S.L., Jenkins, C.N., Abell, R., Brooks, T.M., Gittleman, J.L., Joppa, L.N., Raven, P.H., Roberts, C.M., Sexton, J.O., 2014. The biodiversity of species and their rates of extinction, distribution, and protection. *Science* 344, 1246752.
- Prescott, G.W., Williams, D.R., Balmford, A., Green, R.E., Manica, A., 2012. Quantitative global analysis of the role of climate and people in explaining late Quaternary megafaunal extinctions. *Proc. Natl. Acad. Sci. U. S. A.* 109, 4527-4531.
- Provan, J., Bennett, K.D., 2008. Phylogeographic insights into cryptic glacial refugia. *Trends Ecol. Evol.* 23, 564-571.
- Rahmstorf, S., 2002. Ocean circulation and climate during the past 120,000 years. *Nature* 419, 207-214.
- Rey-Iglesia, A., Garcia-Vazquez, A., Treadaway, E.C., van der Plicht, J., Baryshnikov, G.F., Szpak, P., Bocherens, H., Boeskorov, G.G., Lorenzen, E.D., 2019. Evolutionary history and palaeoecology of brown bear in North-East Siberia re-examined using ancient DNA and stable isotopes from skeletal remains. *Sci. Rep.* 9, 4462.
- Richards, R.L., Churcher, C.S., Turnbull, W.D., 1996. Distribution and size variation in North American short-faced bears, *Arctodus simus*, in: Stewart, K.M., Seymour, K.L. (Eds.), *Palaeoecology and palaeoenvironments of late Cenozoic mammals: tributes to the career of C.S. (Rufus) Churcher*. University of Toronto Press, Toronto, pp. 191-246.
- Richards, S.M., Hovhannisyanyan, N., Gilliam, M., Ingram, J., Skadhauge, B., Heiniger, H., Llamas, B., Mitchell, K.J., Meachen, J., Fincher, G.B., Austin, J.J., Cooper, A., 2019. Low-cost cross-taxon enrichment of mitochondrial DNA using in-house synthesised RNA probes. *PLoS ONE* 14, e0209499.
- Rozas-Davila, A., Valencia, B.G., Bush, M.B., 2016. The functional extinction of Andean megafauna. *Ecology* 97, 2533-2539.
- Rule, S., Brook, B.W., Haberle, S.G., Turney, C.S.M., Kershaw, A.P., Johnson, C.N., 2012. The Aftermath of Megafaunal Extinction: Ecosystem Transformation in Pleistocene Australia. *Science* 335, 1483-1486.

- Saarma, U., Ho, S.Y.W., Pybus, O.G., Kaljuste, M., Tumanov, I.L., Kojola, I., Vorobiev, A.A., Markov, N.I., Saveljev, A.P., Valdmann, H., Lyapunova, E.A., Abramov, A.V., Mannil, P., Korsten, M., Vulla, E., Pazetnov, S.V., Pazetnov, V.S., Putschkovskiy, S.V., Rokov, A.M., 2007. Mitogenetic structure of brown bears (*Ursus arctos* L.) in northeastern Europe and a new time frame for the formation of European brown bear lineages. *Mol. Ecol.* 16, 401-413.
- Saltre, F., Rodriguez-Rey, M., Brook, B.W., Johnson, C.N., Turney, C.S., Alroy, J., Cooper, A., Beeton, N., Bird, M.I., Fordham, D.A., Gillespie, R., Herrando-Perez, S., Jacobs, Z., Miller, G.H., Nogues-Bravo, D., Prideaux, G.J., Roberts, R.G., Bradshaw, C.J., 2016. Climate change not to blame for late Quaternary megafauna extinctions in Australia. *Nat. Commun.* 7, 10511.
- Sandom, C., Faurby, S., Sandel, B., Svenning, J.-C., 2014. Global late Quaternary megafauna extinctions linked to humans, not climate change. *Proc. R. Soc. B.* 281, 20133254.
- Schubert, B.W., 2010. Late Quaternary chronology and extinction of North American giant short-faced bears (*Arctodus simus*). *Quat. Int.* 217, 188-194.
- Schubert, B.W., Hulbert, R.C., MacFadden, B.J., Searle, M., Searle, S., 2010. Giant Short-Faced Bears (*Arctodus simus*) in Pleistocene Florida USA; A Substantial Range Extension. *J. Paleontol.* 84, 79-87.
- Schubert, M., Jonsson, H., Chang, D., Sarkissian, C.D., Ermini, L., Ginolhac, A., Albrechtsen, A., Dupanloup, I., Foucal, A., Petersen, B., Fumagalli, M., Raghavan, M., Seguin-Orlando, A., Korneliusson, T.S., Velazquez, A.M.V., Stenderup, J., Hoover, C.A., Rubin, C.J., Alfarhan, A.H., Alquraishi, S.A., Al-Rasheid, K.A.S., MacHugh, D.E., Kalbfleisch, T., MacLeod, J.N., Rubin, E.M., Sichevitz-Ponten, T., Andersson, L., Hofreiter, M., Marques-Bonet, T., Gilbert, M.T.P., Nielsen, R., Excoffier, L., Willerslev, E., Shapiro, B., Orlando, L., 2014. Prehistoric genomes reveal the genetic foundation and cost of horse domestication. *Proc. Natl. Acad. Sci. U. S. A.* 111, E5661-E5669.
- Shapiro, B., Drummond, A.J., Rambaut, A., Wilson, M.C., Matheus, P.E., Sher, A.V., Pybus, O.G., Gilbert, M.T.P., Barnes, I., Binladen, J., Willerslev, E., Hansen, A.J., Baryshnikov, G.F., Burns, J.A., Davydov, S., Driver, J.C., Froese, D.G., Harington, C.R., Keddle, G., Kosintsev, P., Kunz, M.L., Martin, L.D., Stephenson, R.O., Storer, J., Tedford, R., Zimov, S., Cooper, A., 2004. Rise and fall of the Beringian steppe bison. *Science* 306, 1561-1565.
- Skoglund, P., Ersmark, E., Palkopoulou, E., Dalen, L., 2015. Ancient Wolf Genome Reveals an Early Divergence of Domestic Dog Ancestors and Admixture into High-Latitude Breeds. *Curr. Biol.* 25, 1515-1519.
- Skoglund, P., Northoff, B.H., Shunkov, M.V., Derevianko, A.P., Paabo, S., Krause, J., Jakobsson, M., 2014. Separating endogenous ancient DNA from modern day contamination in a Siberian Neandertal. *Proc. Natl. Acad. Sci. U. S. A.* 111, 2229-2234.

1.5 REFERENCES

- Smith, F.A., Tome, C.P., Smith, E.A.E., Lyons, S.K., Newsome, S.D., Stafford, T.W., 2016. Unraveling the consequences of the terminal Pleistocene megafauna extinction on mammal community assembly. *Ecography* 39, 223-239.
- Soibelzon, L.H., Schubert, B.W., 2011. The largest known bear, *Arctotherium angustidens*, from the early Pleistocene Pampean region of Argentina: with a discussion of size and diet trends in bears. *J. Paleontol.* 85, 69-75, 67.
- Soibelzon, L.H., Tonni, E.P., Bond, M., 2005. The fossil record of South American short-faced bears (Ursidae, Tremarctinae). *J. South Am. Earth Sci.* 20, 105-113.
- Sommer, R.S., Benecke, N., 2005. The recolonization of Europe by brown bears *Ursus arctos* Linnaeus, 1758 after the Last Glacial Maximum. *Mammal Rev.* 35, 156-164.
- Soubrier, J., Gower, G., Chen, K., Richards, S.M., Llamas, B., Mitchell, K.J., Ho, S.Y.W., Kosintsev, P., Lee, M.S.Y., Baryshnikov, G., Bollongino, R., Bover, P., Burger, J., Chivall, D., Cregut-Bonnoure, E., Decker, J.E., Doronichev, V.B., Douka, K., Fordham, D.A., Fontana, F., Fritz, C., Glimmerveen, J., Golovanova, L.V., Groves, C., Guerreschi, A., Haak, W., Higham, T., Hofman-Kaminska, E., Immel, A., Julien, M.A., Krause, J., Krotova, O., Langbein, F., Larson, G., Rohrlach, A., Scheu, A., Schnabel, R.D., Taylor, J.F., Tokarska, M., Tosello, G., van der Plicht, J., van Loenen, A., Vigne, J.D., Wooley, O., Orlando, L., Kowalczyk, R., Shapiro, B., Cooper, A., 2016. Early cave art and ancient DNA record the origin of European bison. *Nat. Commun.* 7, 13158.
- Stanton, D.W.G., Alberti, F., Plotnikov, V., Androsov, S., Grigoriev, S., Fedorov, S., Kosintsev, P., Nagel, D., Vartanyan, S., Barnes, I., Barnett, R., Ersmark, E., Doppes, D., Germonpre, M., Hofreiter, M., Rosendahl, W., Skoglund, P., Dalen, L., 2020. Early Pleistocene origin and extensive intra-species diversity of the extinct cave lion. *Sci. Rep.* 10, 12621.
- Stehli, F.G., Webb, S.D., 1985. *The Great American Biotic Interchange*. Plenum Press, New York.
- Steyaert, S.M.J.G., Endrestol, A., Hacklander, K., Swenson, J.E., Zedrosser, A., 2012. The mating system of the brown bear *Ursus arctos*. *Mammal Rev.* 42, 12-34.
- Stiller, M., Baryshnikov, G., Bocherens, H., Grandal-d'Anglade, A., Hilpert, B., Munzel, S.C., Pinhasi, R., Rabeder, G., Rosendahl, W., Trinkaus, E., Hofreiter, M., Knapp, M., 2010. Withering Away-25,000 Years of Genetic Decline Preceded Cave Bear Extinction. *Mol. Biol. Evol.* 27, 975-978.
- Stoen, O.G., Zedrosser, A., Saebo, S., Swenson, J.E., 2006. Inversely density-dependent natal dispersal in brown bears *Ursus arctos*. *Oecologia* 148, 356-364.
- Taberlet, P., Bouvet, J., 1994. Mitochondrial DNA Polymorphism, Phylogeography, and Conservation Genetics of the Brown Bear *Ursus arctos* in Europe. *Proc. R. Soc. B.* 255, 195-200.
- Talbot, S.L., Shields, G.F., 1996. Phylogeography of brown bears (*Ursus arctos*) of Alaska and parphyly within the Ursidae. *Mol. Phylogenet. Evol.* 5, 477-494.

- Tammeleht, E., Remm, J., Korsten, M., Davison, J., Tumanov, I., Saveljev, A., Mannil, P., Kojola, I., Saarma, U., 2010. Genetic structure in large, continuous mammal populations: the example of brown bears in northwestern Eurasia. *Mol. Ecol.* 19, 5359-5370.
- Trajano, E., Ferrarezzi, H., 1995. A Fossil Bear from Northeastern Brazil, with a Phylogenetic Analysis of the South American Extinct Tremarctinae (Ursidae). *J. Vertebr. Paleontol.* 14, 552-561.
- Treat, C.C., Kleinen, T., Broothaerts, N., Dalton, A.S., Dommain, R., Douglas, T.A., Drexler, J.Z., Finkelstein, S.A., Grosse, G., Hope, G., Hutchings, J., Jones, M.C., Kuhry, P., Lacourse, T., Lahteenoja, O., Loisel, J., Notebaert, B., Payne, R.J., Peteet, D.M., Sannel, A.B.K., Stelling, J.M., Strauss, J., Swindles, G.T., Talbot, J., Tarnocai, C., Verstraeten, G., Williams, C.J., Xia, Z.Y., Yu, Z.C., Valiranta, M., Hattestrand, M., Alexanderson, H., Brovkin, V., 2019. Widespread global peatland establishment and persistence over the last 130,000 y. *Proc. Natl. Acad. Sci. U. S. A.* 116, 4822-4827.
- Tumendemberel, O., Zedrosser, A., Proctor, M.F., Reynolds, H.V., Adams, J.R., Sullivan, J.M., Jacobs, S.J., Khorloojav, T., Tserenbataa, T., Batmunkh, M., Swenson, J.E., Waits, L.P., 2019. Phylogeography, genetic diversity, and connectivity of brown bear populations in Central Asia. *PLoS ONE* 14.
- Valdiosera, C.E., Garcia, N., Anderung, C., Dalen, L., Cregut-Bonnoure, E., Kahlke, R.D., Stiller, M., Brandstrom, M., Thomas, M.G., Arsuaga, J.L., Gotherstrom, A., Barnes, I., 2007. Staying out in the cold: glacial refugia and mitochondrial DNA phylogeography in ancient European brown bears. *Mol. Ecol.* 16, 5140-5148.
- Valdiosera, C.E., Garcia-Garitagoitia, J.L., Garcia, N., Doadrio, I., Thomas, M.G., Hanni, C., Arsuaga, J.L., Barnes, I., Hofreiter, M., Orlando, L., Gotherstrom, A., 2008. Surprising migration and population size dynamics in ancient Iberian brown bears (*Ursus arctos*). *Proc. Natl. Acad. Sci. U. S. A.* 105, 5123-5128.
- van Dijk, E.L., Auger, H., Jaszczyszyn, Y., Thermes, C., 2014. Ten years of next-generation sequencing technology. *Trends Genet* 30, 418-426.
- Waits, L.P., Talbot, S.L., Ward, R.H., Shields, G.F., 1998. Mitochondrial DNA phylogeography of the North American brown bear and implications for conservation. *Conserv. Biol.* 12, 408-417.
- Waters, J.M., Grosser, S., 2016. Managing shifting species: Ancient DNA reveals conservation conundrums in a dynamic world. *Bioessays* 38, 1177-1184.
- Wolff, E.W., Chappellaz, J., Blunier, T., Rasmussen, S.O., Svensson, A., 2010. Millennial-scale variability during the last glacial: The ice core record. *Quat. Sci. Rev.* 29, 2828-2838.
- Wroe, S., Field, J., Fullagar, R., Jeremiin, L.S., 2004. Megafaunal extinction in the late Quaternary and the global overkill hypothesis. *Alcheringa* 28, 291-331.

1.5 REFERENCES

- Xenikoudakis, G., Ersmark, E., Tison, J.L., Waits, L., Kindberg, J., Swenson, J.E., Dalen, L., 2015. Consequences of a demographic bottleneck on genetic structure and variation in the Scandinavian brown bear. *Mol. Ecol.* 24, 3441-3454.
- Yu, L., Li, Q.W., Ryder, O.A., Zhang, Y.P., 2004. Phylogeny of the bears (Ursidae) based on nuclear and mitochondrial genes. *Mol. Phylogenet. Evol.* 32, 480-494.
- Yu, L., Li, Y.W., Ryder, O.A., Zhang, Y.P., 2007. Analysis of complete mitochondrial genome sequences increases phylogenetic resolution of bears (Ursidae), a mammalian family that experienced rapid speciation. *BMC Evol. Biol.* 7, 198.
- Zedrosser, A., Stoen, O.G., Saebo, S., Swenson, J.E., 2007. Should I stay or should I go? Natal dispersal in the brown bear. *Anim. Behav.* 74, 369-376.

Chapter 2

Lions and brown bears colonised North America in multiple synchronous waves of dispersal across the Bering Land Bridge

Manuscript submitted to *Molecular Ecology*
Submitted to *BioRxiv*

2.1 Authorship Statement

Statement of Authorship

Title of Paper	Lions and brown bears colonized North America in multiple synchronous waves of dispersal across the Bering Land Bridge
Publication Status	<input type="checkbox"/> Published <input type="checkbox"/> Accepted for Publication <input type="checkbox"/> Submitted for Publication <input checked="" type="checkbox"/> Unpublished and Unsubmitted work written in manuscript style
Publication Details	Submitted to the Proceedings of the National Academy of Sciences of the United States of America. Submitted to bioRxiv

Principal Author

Name of Principal Author (Candidate)	Alexander Theodore Salis			
Contribution to the Paper	Performed DNA extractions, DNA library construction and amplification, hybridisation enrichment, preparation for sequencing, and bioinformatic processing of sequencing data. Performed phylogenetic analyses, interpreted results, created figures, wrote manuscript and edited manuscript.			
Overall percentage (%)	80			
Certification:	This paper reports on original research I conducted during the period of my Higher Degree by Research candidature and is not subject to any obligations or contractual agreements with a third party that would constrain its inclusion in this thesis. I am the primary author of this paper.			
Signature	<table border="1" style="width: 100%;"> <tr> <td style="width: 60%;"></td> <td style="width: 20%;">Date</td> <td style="width: 20%;">06/08/2020</td> </tr> </table>		Date	06/08/2020
	Date	06/08/2020		

Co-Author Contributions

By signing the Statement of Authorship, each author certifies that:

- i. the candidate's stated contribution to the publication is accurate (as detailed above);
- ii. permission is granted for the candidate to include the publication in the thesis; and
- iii. the sum of all co-author contributions is equal to 100% less the candidate's stated contribution.

Name of Co-Author	Sarah Bray			
Contribution to the Paper	Performed DNA extractions, interpreted results, edited and critically evaluated the manuscript.			
Signature	<table border="1" style="width: 100%;"> <tr> <td style="width: 60%;"></td> <td style="width: 20%;">Date</td> <td style="width: 20%;">07/08/2020</td> </tr> </table>		Date	07/08/2020
	Date	07/08/2020		

Name of Co-Author	Michael S Y Lee			
Contribution to the Paper	Performed phylogeographic model testing, assisted with interpreting results, assisted with writing manuscript, edited and critically evaluated the manuscript.			
Signature	<table border="1" style="width: 100%;"> <tr> <td style="width: 60%;"></td> <td style="width: 20%;">Date</td> <td style="width: 20%;">14.8.20</td> </tr> </table>		Date	14.8.20
	Date	14.8.20		

Name of Co-Author	Holly Heiniger		
Contribution to the Paper	Performed DNA extractions, DNA library construction and amplification, hybridisation enrichment, preparation for sequencing (lion samples). Edited and critically evaluated the manuscript.		
Signature		Date	07/08/2020

Name of Co-Author	Ross Barnett		
Contribution to the Paper	Performed DNA extractions, interpreted results, edited and critically evaluated the manuscript.!		
Signature		Date	7th Aug 2020

Name of Co-Author	James A Burns		
Contribution to the Paper	Provided access to samples, edited and critically evaluated the manuscript.		
Signature		Date	7 August 2020

Name of Co-Author	Vladimir Doronichev		
Contribution to the Paper	Provided access to samples, edited and critically evaluated the manuscript.		
Signature		Date	07/08/2020

Name of Co-Author	Liubov Golovanova		
Contribution to the Paper	Provided access to samples, edited and critically evaluated the manuscript		
Signature		Date	07/08/2020

2.1 AUTHORSHIP STATEMENT

Name of Co-Author	Daryl Fedge		
Contribution to the Paper	Provided access to samples, interpreted results, edited and critically evaluated the manuscript.		
Signature		Date	7 AUG. 2020

Name of Co-Author	C Richard Harington		
Contribution to the Paper	Provided access to samples, edited and critically evaluated the manuscript.		
Signature		Date	August 20, 2020

Name of Co-Author	Bryan Hockett		
Contribution to the Paper	Provided access to samples, edited and critically evaluated the manuscript.		
Signature		Date	8/7/2020

Name of Co-Author	Pavel Kosintsev		
Contribution to the Paper	Provided access to samples, edited and critically evaluated the manuscript.		
Signature		Date	10.08.2020

Name of Co-Author	Xulong Lai		
Contribution to the Paper	Provided access to samples, edited and critically evaluated the manuscript.		
Signature		Date	August 07, 2020

Name of Co-Author	Quentin Mackie		
Contribution to the Paper	Provided access to samples, interpreted results, edited and critically evaluated the manuscript.		
Signature	<i>Quentin Mackie</i>	Date	Sept 2, 2020


Name of Co-Author	Sergei Vasilev		
Contribution to the Paper	Provided access to samples, edited and critically evaluated the manuscript.		
Signature		Date	17.08.2020


Name of Co-Author	Jacobo Weinstock		
Contribution to the Paper	Performed DNA extraction, edited and critically evaluated the manuscript.		
Signature		Date	10/8/2020

Name of Co-Author	Nobuyuki Yamaguchi		
Contribution to the Paper	Provided access to samples, edited and critically evaluated the manuscript.		
Signature		Date	09/08/2020

Name of Co-Author	Julie Meachen		
Contribution to the Paper	Provided access to samples, conception of project, edited and critically evaluated the manuscript.		
Signature		Date	August 11, 2020

2.1 AUTHORSHIP STATEMENT

Name of Co-Author	Alan Cooper		
Contribution to the Paper	Supervised work, conception of project, interpreted results, wrote and edited the manuscript.		
Signature		Date	6 Aug, 2020

Name of Co-Author	Kieren J. Mitchell		
Contribution to the Paper	Supervised work, conception of project, performed DNA extraction and library preparation (lion samples), interpreted results, wrote and edited the manuscript.		
Signature		Date	17/8/20

2.2 Manuscript

Lions and brown bears colonised North America in multiple synchronous waves of dispersal across the Bering Land Bridge

Alexander T Salis^{1#}, Sarah C E Bray^{1,2}, Michael S Y Lee^{3,4}, Holly Heiniger¹, Ross Barnett⁵, James A Burns⁶, Vladimir Doronichev⁷, Daryl Fedje⁸, Liubov Golovanova⁷, C Richard Harington⁹, Bryan Hockett¹⁰, Pavel Kosintsev^{11,12}, Xulong Lai¹³, Quentin Mackie⁸, Sergei Vasiliev¹⁴, Jacobo Weinstock¹⁵, Nobuyuki Yamaguchi¹⁶, Julie Meachen¹⁷, Alan Cooper^{4##}, Kieren J Mitchell^{1##}*

¹Australian Centre for Ancient DNA (ACAD), School of Biological Sciences, University of Adelaide, South Australia, Australia, 5005

²Registry of Senior Australians (ROSA), South Australian Health and Medical Research Institute (SAHMRI), Adelaide, South Australia, 5000

³College of Science and Engineering, Flinders University, Bedford Park, South Australia, 5042

⁴South Australian Museum, Adelaide 5000, South Australia

⁵Natural History Museum of Denmark, University of Copenhagen, Copenhagen, Denmark

⁶Curator Emeritus, Royal Alberta Museum, Edmonton, Alberta, Canada, T5J 0G2

⁷ANO Laboratory of Prehistory, St Petersburg, Russia

⁸Department of Anthropology, University of Victoria, Victoria, B.C., Canada

⁹Curator Emeritus and Research Associate, Research Division (Paleobiology), Canadian Museum of Nature, Ottawa, Canada

¹⁰US Department of Interior, Bureau of Land Management, Nevada State Office, Reno, Nevada, USA

¹¹Institute of Plant and Animal Ecology, Ural Branch of the Russian Academy of Sciences, Yekaterinburg, Russia

¹²Department of History, Ural Federal University, Yekaterinburg, Russia

¹³State Key Laboratory of Biogeology and Environmental Geology, China University of Geosciences, Wuhan, Hubei 430074, China

¹⁴Institute of Archaeology and Ethnography, Russian Academy of Sciences, Russia

¹⁵Faculty of Humanities (Archaeology), University of Southampton, UK

¹⁶Institute of Tropical Biodiversity and Sustainable Development, University Malaysia Terengganu, 21030 Kuala Nerus, Malaysia

¹⁷Anatomy Department, Des Moines University, Des Moines, IA, USA

#Corresponding author(s): A.T.S. (alexander.t.salis@gmail.com), A.C. (alanjcooper42@gmail.com), K.J.M. (kieren.mitchell@adelaide.edu.au)

*These authors contributed equally

Author Contributions

A.T.S., A.C., J.M., and K.J.M. designed research; A.T.S., S.C.E.B., H.H., R.B., J.W., and K.J.M. performed research; J.A.B., V.D., D.F., L.G., C.R.H., B.H., P.K., X.L., Q.M., S.V., N.Y., and J.M. contributed new reagents/analytic tools; A.T.S., M.S.Y.L., and K.J.M. analysed data; A.T.S., A.C., and K.J.M. wrote the paper with input from S.C.E.B., M.S.Y.L., H.H., R.B., J.A.B., D.F., B.H., P.K., X.L., Q.M., N.Y., and J.M.

Abstract:

The Bering Land Bridge connecting North America and Eurasia was periodically exposed and inundated by oscillating sea levels during the Pleistocene glacial cycles. This land connection allowed the intermittent dispersal of animals, including humans, between Western Beringia (far north-east Asia) and Eastern Beringia (north-west North America), changing the faunal community composition of both continents. The Pleistocene glacial cycles also had profound impacts on temperature, precipitation, and vegetation, impacting faunal community structure and demography. While these palaeoenvironmental impacts have been studied in many large herbivores from Beringia (*e.g.*, bison, mammoths, horses), the Pleistocene population dynamics of the diverse guild of carnivorans present in the region are less well understood, due to their lower abundances. In this study, we analyse mitochondrial genome data from ancient brown bears (*Ursus arctos*; n = 103) and lions (*Panthera* spp.; n = 39), two megafaunal carnivorans that dispersed into North America during the Pleistocene. Our results reveal striking synchronicity in the population dynamics of Beringian lions and brown bears, with multiple waves of dispersal across the Bering Land Bridge coinciding with glacial periods of low sea levels, as well as synchronous local extinctions in Eastern Beringia during Marine Isotope Stage 3. The evolutionary histories of these two taxa underscore the crucial biogeographic role of the Bering Land Bridge in the distribution, turnover, and maintenance of megafaunal populations in North America.

Keywords

Ancient DNA, brown bears, lions, phylogeography, Beringia

Main Text

Introduction:

During the Pleistocene (2.58 million to 11,700 years ago), Eastern Beringia — the area comprising Alaska and parts of Yukon Territory — was inhabited by numerous species of megafauna (Harington, Naughton, Dalby, Rose, & Dawson, 2003). Many of these taxa belonged to endemic New World lineages, such as the giant short-faced bear (*Arctodus simus*), Jefferson's ground sloth (*Megalonyx jeffersonii*), and the stilt-legged horse (*Haringtonhippus francisci*) (Harington et al., 2003; Kurtén & Anderson, 1980). However, Eastern Beringian megafaunal diversity also included non-endemic species that dispersed from Western Beringia — the area of Russia east of the Lena River — during the Pleistocene (Elias & Crocker, 2008; Elias, Short, Nelson, & Birks, 1996; Harington et al., 2003). Some of these immigrant taxa, including moose (*Alces alces*) and elk/wapiti (*Cervus canadensis*), appear to have arrived during the Last Glacial Maximum (LGM) when the Bering Land Bridge connecting Western and Eastern Beringia was most recently exposed (Guthrie, 2006; Hundertmark et al., 2002; Meiri, Lister, Kosintsev, Zazula, & Barnes, 2020; Meiri et al., 2014). Other taxa apparently invaded much earlier in the Pleistocene, for example bison (*Bison* spp.) (Froese et al., 2017; Shapiro et al., 2004), and mammoth (*Mammuthus* spp.) (Enk et al., 2016; Lister & Sher, 2015). However, the exact timeline and processes underlying early Pleistocene dispersals are currently poorly characterised, and it remains uncertain whether the arrivals of individual species represented independent chance events or more concerted waves of species responding to changes in climate and environment.

Sea level records from the Northern Pacific indicate that the Bering Land Bridge opened and closed multiple times during the Pleistocene (Hopkins, 1973; Hu et al., 2010), in glacial and interglacial periods respectively. During glacial Marine Isotope Stage 6 (MIS 6) around 185 thousand years ago (kya) to 135 kya, sea levels were low enough to allow the Bering Land Bridge to be uncovered (Colleoni, Wekerle, Näslund, Brandefelt, & Masina, 2016; Hopkins, 1973). In the subsequent MIS 5, interglacial sea levels increased to higher than present-day, flooding the Bering Land Bridge from approximately 135 to 70 kya before it re-emerged again ~70 to 60 kya during glacial MIS 4 (Hu et al., 2010). Intermittent connections may have occurred again during MIS 3, before the final

2.2 MANUSCRIPT

emergence during MIS 2/LGM starting ~34 kya and finishing at 11 kya (Hu et al., 2010; Jakobsson et al., 2017).

Repeated glacial cycles also had profound effects on vegetation, which could also influence animal dispersal. For example, increased temperature during interstadials is likely to have resulted in the landscape becoming wetter, in turn facilitating the accumulation of organic matter (“paludification”) and the expansion of peatlands (Mann et al., 2015; Treat et al., 2019). Paludification is thought to have lowered nutrient availability and favoured less palatable plant species, negatively impacting megafaunal herbivore populations. Indeed, Mann *et al.* (Mann et al., 2015) observed that during interstadials in Alaska there was an initial increase in megafaunal herbivore abundance followed by a decrease coincident with peatland expansion. In addition, bone nitrogen isotopes demonstrate that the diet of horses in Alaska changed radically coincident with an increase in peatlands during Greenland Interstadial 1 (14.7-12.9 kya) (Mann et al., 2015). Changes in herbivore communities are likely to have impacted populations of megafaunal carnivores and omnivores, potentially affecting their ability to colonise or persist in Eastern Beringia through multiple glacial cycles. However, our understanding of fine-scale carnivore responses to environmental change in Eastern Beringia has been limited by their relative rarity in the fossil record. Although several studies have used ancient DNA to examine megafaunal carnivoran population dynamics (e.g., Barnes, Matheus, Shapiro, Jensen, & Cooper, 2002; Barnett et al., 2009), sample sizes have generally been small and resolution limited.

During the Late Pleistocene, a number of megafaunal carnivorans roamed Eastern Beringia, including the giant short-faced bear (*Arctodus simus*), grey wolves (*Canis lupus*), and scimitar-toothed cats (*Homotherium serum*) (Harington et al., 2003; Kurtén & Anderson, 1980). Lions (*Panthera* spp.) and brown bears (*Ursus arctos*) appear to have dispersed into northern North America from Eurasia via the Bering Land Bridge during the Pleistocene (Kurtén & Anderson, 1980). Genetic data from North American lion and brown bear subfossils (preserved non-mineralised animal remains) have revealed a complicated history (Barnes et al., 2002; Barnett et al., 2009; Davison et al., 2011; Ersmark et al., 2015; Leonard, Wayne, & Cooper, 2000). For example, North American Pleistocene lions have been grouped into two lineages based on both fossil evidence and

mitochondrial DNA, potentially representing two distinct species (or alternatively two subspecies of the extant lion).

The cave lion, *Panthera (leo) spelaea*, is currently described as being found in both Eastern Beringia and Eurasia; while the American lion, *Panthera (leo) atrox*, is described as being found exclusively south of the North American Cordilleran and Laurentide Ice Sheets (Barnett et al., 2009; Baryshnikov & Boeskorov, 2001; Kurtén, 1985). Early research had initially described eastern Beringian lions as *P. l. atrox* (Harington, 1969; Harington, 1996; Whitmore & Foster, 1967), however, the identity of specimens across Beringia was contentious, also being described as *P. l. spelaea* (Kurtén, 1985; Sotnikova & Nikolskiy, 2006) or a completely separate subspecies, *Panthera leo vereshchagini* (Baryshnikov & Boeskorov, 2001). Later, it was widely considered that *atrox* was restricted south of the North American ice sheets, distinct from Beringian lions (Barnett et al., 2009; Christiansen & Harris, 2009; Stuart & Lister, 2011). The genetic divergence between the American lion and its relatives is estimated to have occurred ~340 kya (Barnett et al., 2009), suggesting that the ancestors of the American lion entered North America prior to MIS 6. In contrast, molecular data suggest that brown bears first colonised North America ~70 kya (around the MIS 5/MIS 4 transition), and subsequently appear to have become locally extinct in Eastern Beringia between ~35 kya and 21 kya (Barnes et al., 2002; Davison et al., 2011; Kurtén, 1985). Genetic data from ancient lions and brown bears has so far been limited to only short fragments of mitochondrial DNA and a small number of individuals. As a result, both the timeline for dispersal and the number of waves of dispersal of brown bears and lions into North America is still relatively uncertain.

To better understand the dynamics and assembly of the Eastern Beringian megafaunal carnivoran guild and their responses to climatic and environmental change, we sequenced near-complete mitochondrial genomes from 39 Pleistocene lions and 103 Pleistocene/Holocene brown bears from North America and Eurasia. In combination with new radiocarbon dates and previously published genetic data this allowed us to refine the phylogenetic and temporal histories of both groups and identify common drivers of dispersal and turnover.

Materials and Methods:

Sample preparation, DNA extraction, library preparation, and mitochondrial enrichment

We sampled 120 brown bear subfossil bone and tooth specimens from northern Asia and North America, and 47 lion subfossils from Europe, northern Asia, and North America (Supplementary tables S1 and S2). Twenty-six samples were radiocarbon dated at the Oxford Radiocarbon Accelerator Unit of the University of Oxford. Radiocarbon date of the specimens were combined with published dates from North American brown bears and lions, as well as *Arctodus simus* (Supplementary table S3). All radiocarbon dates were calibrated with the IntCal13 curve (Reimer et al., 2013) using OxCal 4.4 (Ramsey, 2009).

Sample preparation, DNA extraction and library construction were conducted in purpose-built ancient DNA (aDNA) clean-room facilities at the University of Adelaide's Australian Centre for Ancient DNA (ACAD) or the Henry Wellcome Ancient Biomolecules Centre at the University of Oxford and a number of precautions were taken to minimise contamination of samples with exogenous DNA (Cooper & Poinar, 2000).

DNA extraction was performed on bone or tooth powder using either an in-house silica-based extraction protocol adapted from Dabney *et al.* (Dabney et al., 2013) or a phenol-chloroform-based extraction protocol from Bray *et al.* (Bray et al., 2013). Double-stranded Illumina libraries were constructed following the protocol of Meyer *et al.* (Meyer et al., 2012) with truncated Illumina adapters with unique dual 7-mer internal barcodes added to allow identification and exclusion of any downstream contamination and including partial uracil-DNA glycosylase (UDG) treatment (Rohland, Harney, Mallick, Nordenfelt, & Reich, 2015) to restrict cytosine deamination to terminal nucleotides.

Brown bear libraries were enriched with home-made RNA baits following Richards *et al.* (Richards et al., 2019) produced from long-range PCR fragments amplified from modern brown bear DNA (UAM 87948 and UAM 125917 tissue samples from the University of Alaska Fairbanks Museum) using primers from Hwang *et al.* (Hwang et al., 2008). For lion libraries, commercially synthesised biotinylated 80-mer RNA baits (Arbor Biosciences, MI, USA) were used to enrich for mammalian mitochondrial DNA (Mitchell et al., 2016). DNA-RNA hybridisation enrichment was performed according to

manufacturer's recommendations (MYbaits protocol v3). Libraries were pooled and sequenced on an Illumina NextSeq using 2 x 75 bp PE (150 cycle) High Output chemistry. A more detailed description of the laboratory methods is available in the Supplementary Material.

Data processing

Sequenced reads were demultiplexed using SABRE (<https://github.com/najoshi/sabre>) and were then processed through Paleomix v1.2.12 (Schubert et al., 2014), with adapter sequences removed and pair end sequences merged using ADAPTER REMOVAL v2.1.7 (Schubert, Lindgreen, & Orlando, 2016), and merged reads mapped against either the mitochondrial genome of *Panthera spelaea* (KX258452) or *Ursus arctos* (EU497665) using BWA v0.7.15 (Li & Durbin, 2009). Reads with mapping Phred scores less than 25 were removed using SAMTOOLS 1.5 (Li et al., 2009) and PCR duplicates were removed using “paleomix rmdup_collapsed” and MARKDUPLICATES from the Picard package (<http://broadinstitute.github.io/picard/>). Data from our lion samples exhibited signals consistent with the presence of nuclear mitochondrial DNA segments (numts), which are known to be widespread in felid genomes (Kim et al., 2006). The numt sequence was identified and lion samples were remapped with the numt sequence included as an additional scaffold to allow separation of true mitochondrial sequences and numt sequences. Mapped reads were visualised in Geneious Prime v2019.0.4 (<https://www.geneious.com>) and we created a 75% majority consensus sequence, calling N at sites with less than 3x coverage. Subsequent analyses were restricted to specimens with greater than 70% of the mitochondrial genome covered, representing 103 and 39 of the brown bear and lion samples respectively. Published sequencing data from one modern brown bear (Liu et al., 2014) and two ancient cave lions (Barnett et al., 2016) were also processed through the pipeline described above (Supplementary table S4). A more detailed description of the data processing methods is available in the Supplementary Material.

Phylogenetic analyses

Brown bear consensus sequences were aligned using MUSCLE v3.8.425 (Edgar, 2004) in Geneious Prime v2019.0.4 with an additional 46 brown bear and polar bear mitogenomes downloaded from GenBank (Supplementary table S5). Lion sequences were aligned separately also using MUSCLE v3.8.425. PartitionFinder 2.1.1 (Lanfear, Frandsen,

2.2 MANUSCRIPT

Wright, Senfeld, & Calcott, 2016) was used to find the best-fitting partitioning scheme using the Bayesian information criterion, separating the data into 5 partitions for each alignment (Supplementary table S6). Bayesian tip-dating analyses were then performed on each taxon using BEAST 2.6.1 (Bouckaert et al., 2019). The temporal signal in our dataset was evaluated using leave-one-out cross-validation (e.g. Stiller et al., 2014), using only the finite-dated specimens (Supplementary Fig. S1). The ages of undated specimens were then estimated one at a time using the dated specimens as calibration for the molecular clock (Supplementary Fig. S2). Once all samples were assigned an age (either based on radiocarbon dating or Bayesian date estimation), we conducted a date-randomisation test (Ramsden, Holmes, & Charleston, 2009; Stiller et al., 2014), to test for sufficient temporal signal within the datasets (Supplementary Fig. S3). Runs described above were performed with a strict clock with a uniform prior on rate ($0-10^{-5}$ mutations per site per year), constant population coalescent tree prior with a $1/x$ distribution on population size, a uniform prior ($0-500,000$) on the age of the sequence being estimated if required, and run for 30 million steps with sampling every 3000 steps. Convergence was checked in Tracer v1.7.1 (Rambaut, Drummond, Xie, Baele, & Suchard, 2018). Final BEAST analyses were conducted using a strict clock with a uniform prior on rate ($0-10^{-5}$ mutations per site per year), and a Bayesian skyline coalescent tree prior. We ran three independent MCMC chains, each run for 50 million steps, sampling every 5,000 steps. Results from individual runs were combined using LogCombiner after discarding the first 10% of steps as burn-in. Maximum clade credibility trees were generated in TreeAnnotator using the median node age.

To test for the association of migrations between Eurasia and North America with glacial periods, phylogeographic model testing was performed in BEAST (Suchard et al., 2018). The same substitution model settings were used as described above, but the alignments were combined in a single analysis, with a separate tree estimated simultaneously for each taxon. Clade 2 brown bears were excluded from the analysis due to lack of sampling, and the introgressed nature with polar bears resulting in a complicated evolutionary history of the clade (Cahill et al., 2013; Cahill et al., 2018; Cahill et al., 2015; Edwards et al., 2011; Hailer, 2015; Hailer & Welch, 2016; Miller et al., 2012). Each tip was assigned a binary phylogeographic character (Eurasia vs North America), and the rate of evolution of this character was estimated directly from the data. Two models for the evolution of this character were tested: a strict clock, where rates of evolution were

constant through time and a two-epoch clock that had two separate rates (interglacial and glacial periods). Note, in this method, tree topology and dispersal times for the two clades are essentially estimated separately (unlinked trees), but dispersal rates for the two epochs (combined glacial and combined interglacial) are estimated based on the pooled data from both trees and have identical priors. Bayes Factors were estimated and compared using Akaike's Information Criterion for MCMC samples (Tracer). Four independent MCMC chains were run for 20 million steps each, sampling every 2,000 steps. We checked for convergence and sufficient sampling of parameters in Tracer v1.7.1 (Rambaut et al., 2018). A more detailed description of the phylogenetic analysis methods is available in the Supplementary Material.

Results:

Brown bears

We produced 103 new near-complete (i.e., >70% coverage) mitogenomes from Pleistocene/Holocene subfossil *Ursus arctos* specimens from North America (n=53) and Eurasia (n=50), which we analysed along with previously published data from 47 brown and polar bears (Hirata et al., 2013; Lindqvist et al., 2010; Liu et al., 2014; Miller et al., 2012; Rey-Iglesia et al., 2019), spanning 107 unique mitochondrial haplotypes. We used BEAST2 (Bouckaert et al., 2019) to create a time-calibrated phylogenetic tree (Fig. 1), which was largely concordant with previous studies in grouping Beringian brown bear mitochondrial diversity into four major spatio-temporally restricted clades: clade 2 (including clade 2a, 2b, and 2c, also encompassing extant polar bears), clade 3 (including 3a, 3b, and 3c), clade 4, and clade 5 (Barnes et al., 2002; Davison et al., 2011; Hirata et al., 2013; Leonard et al., 2000; Talbot & Shields, 1996; Waits, Talbot, Ward, & Shields, 1998). The temporal and geographic distributions of the different clades appear to result from dispersals into Eastern Beringia at widely different points in time.

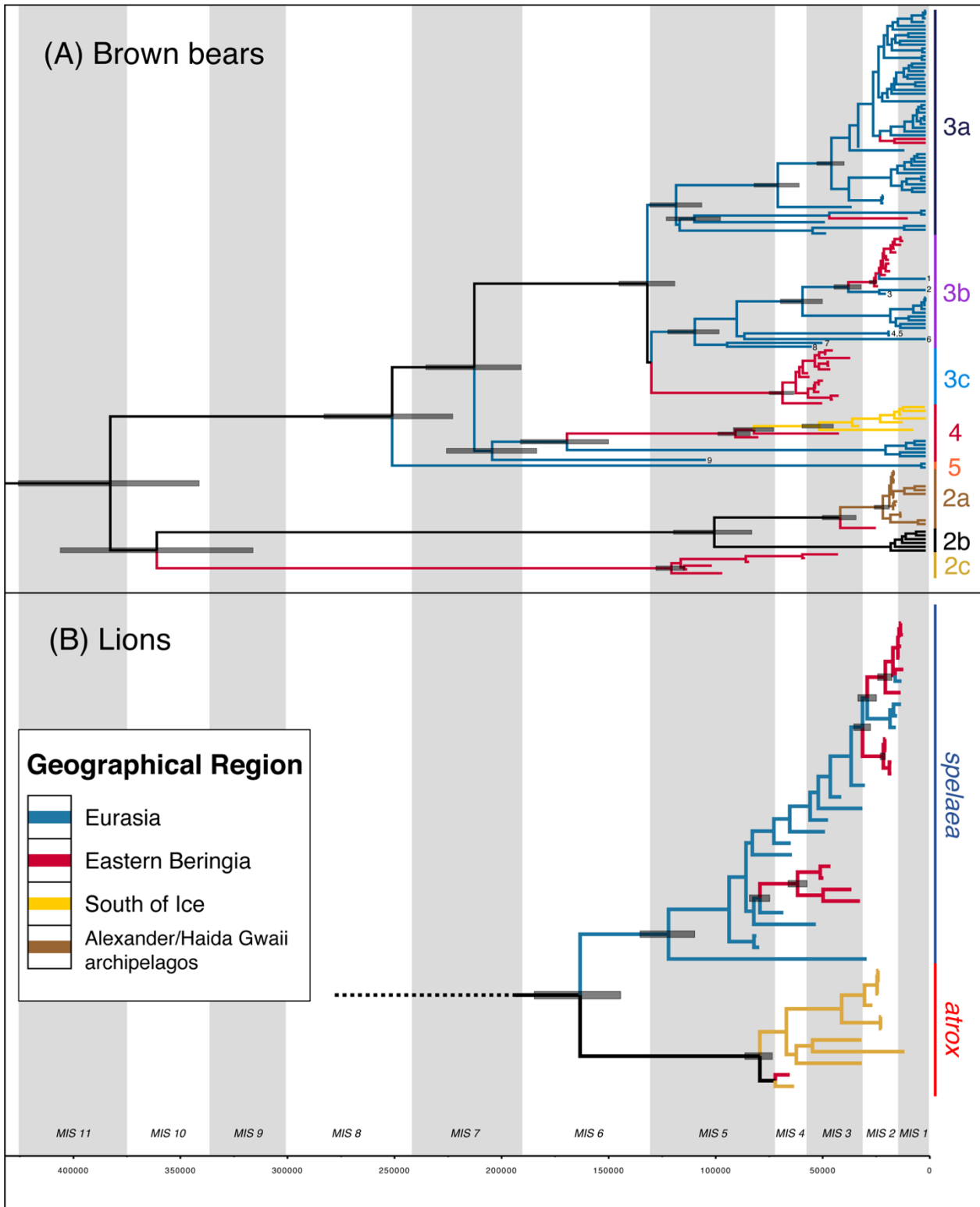


Fig. 1. Bayesian phylogenetic trees inferred from (A) brown bear and (B) lion mitogenomes. The grey vertical columns represent odd-numbered MIS stages (interglacials) and white columns even-numbered MIS stages (glacials). Bars on nodes represent 95% Highest Posterior Densities for node age estimates indicated for modes leading to major clades and those reported in main text. Numbers on tips in (A) refer to selected specimens mentioned in text: 1 = A155, 2 = A156, 3 = A1945, 4 = A1944, 5 = A1946, 6 = A138, 7 = A5889, 8 = MH255807, 9 = A5883. Clade 2b in the brown bear tree represents modern polar bear sequences. For detailed trees with tip labels, and posterior support values see Supplementary Figs S4 and S5.

Within Eurasia we identified three ancient specimens (A155, A156, and A1945) with haplotypes closely related to North American clade 3b bears, and five deeply divergent Eurasian clade 3b bears (A138, A1944, A1946, A5889, and MH255807), including a published mitogenome previously assigned to clade 3c (28) (Fig. 1; Supplementary Fig. S4). The addition of these specimens increased the estimate for the Time to Most Recent Common Ancestor (TMRCA) for Eurasian and North American clade 3b bears from 75 kya (Davison et al., 2011) to 114 kya (95% highest posterior density (HPD): 100.2–127.3 kya). We also identified a new haplotype that is sister-taxon to all clade 4 bears from an ancient specimen (A5883) from Da'an Cave in Northeast China, for which we estimated a median age of 103 kya (95% HPD: 66.7–140.6 kya).

Our time-calibrated Bayesian phylogenetic analysis returned median age estimates for five Eastern Beringian brown bear specimens that were older than the previous ~70 kya estimate for the initial colonisation of North America (Barnes et al., 2002; Davison et al., 2011; Kurtén & Anderson, 1980): A345 at 78.3 kya (95% HPD: 58.6–98.9 kya), A335 at 82.4 kya (95% HPD: 64.9–103.3 kya), A298 at 95.1 kya (95% HPD: 64.9–127.1 kya), A193 at 100 kya (95% HPD: 74.0–130.2 kya), and A318 at 111.4 kya (95% HPD: 79.0–148.8 kya) (Supplementary Fig. S2A). These older samples likely descend from the original wave of brown bears entering North America, and all belong to either mitochondrial clade 2c or 4 (Figs 1 and 2), neither of which is found in Eastern Beringia after 35 kya. Clade 4 bears are currently restricted to the contiguous 48 States and appear to have diverged from Eastern Beringian clade 4 bears ~83 kya (95% HPD: 73.4–93.8 kya), soon after the 92 kya TMRCA for all North American clade 4 brown bears (95% HPD: 83.2–101.6 kya). In turn, North American clade 4 brown bears appear to have diverged from Eurasian clade 4 bears (found today in Japan) much earlier, ~177 kya (95% HPD: 154.5–201.7 kya) during MIS 6. The other early bears, clade 2c, are currently represented by only six pre-35 kya samples from Eastern Beringia and have not been found in any modern bears, and have a TMRCA in early MIS 5, ~121 kya (95% HPD: 114.4–128.5 kya). An additional extinct clade, 3c, was also identified in Eastern Beringia between 40 and 35 kya, and the 15 specimens make up the majority of samples found in that time period. The TMRCA of the 15 clade 3c brown bears indicates that the clade arrived in Eastern Beringia during MIS 4 ~69 kya (95% HPD: 62.3–75.2 kya).

There is a marked gap in the Eastern Beringian fossil record of brown bears between 35 and 25 kya (Fig. 2) as previously noted (Barnes et al., 2002), and after this point all samples belonged to either clade 3b or 3a. Clade 3b is the dominant group through MIS 2, comprising 13 samples, and appears to have arrived during the LGM with a TMRCA \sim 25 kya (95% HPD: 22.9–28.1 kya) (Fig. 1). The upper limit of this dispersal is constrained by a 39 kya estimate for the TMRCA with the closely related Eurasian clade 3b brown bears (95% HPD: 31.9–46.4 kya). In contrast, clade 3a is represented by only a single Holocene specimen and two previously published modern bears, and presumably constitutes a terminal-Pleistocene dispersal into North America as clade 3a bears arrive in Japan at a similar time (Hirata et al., 2013).

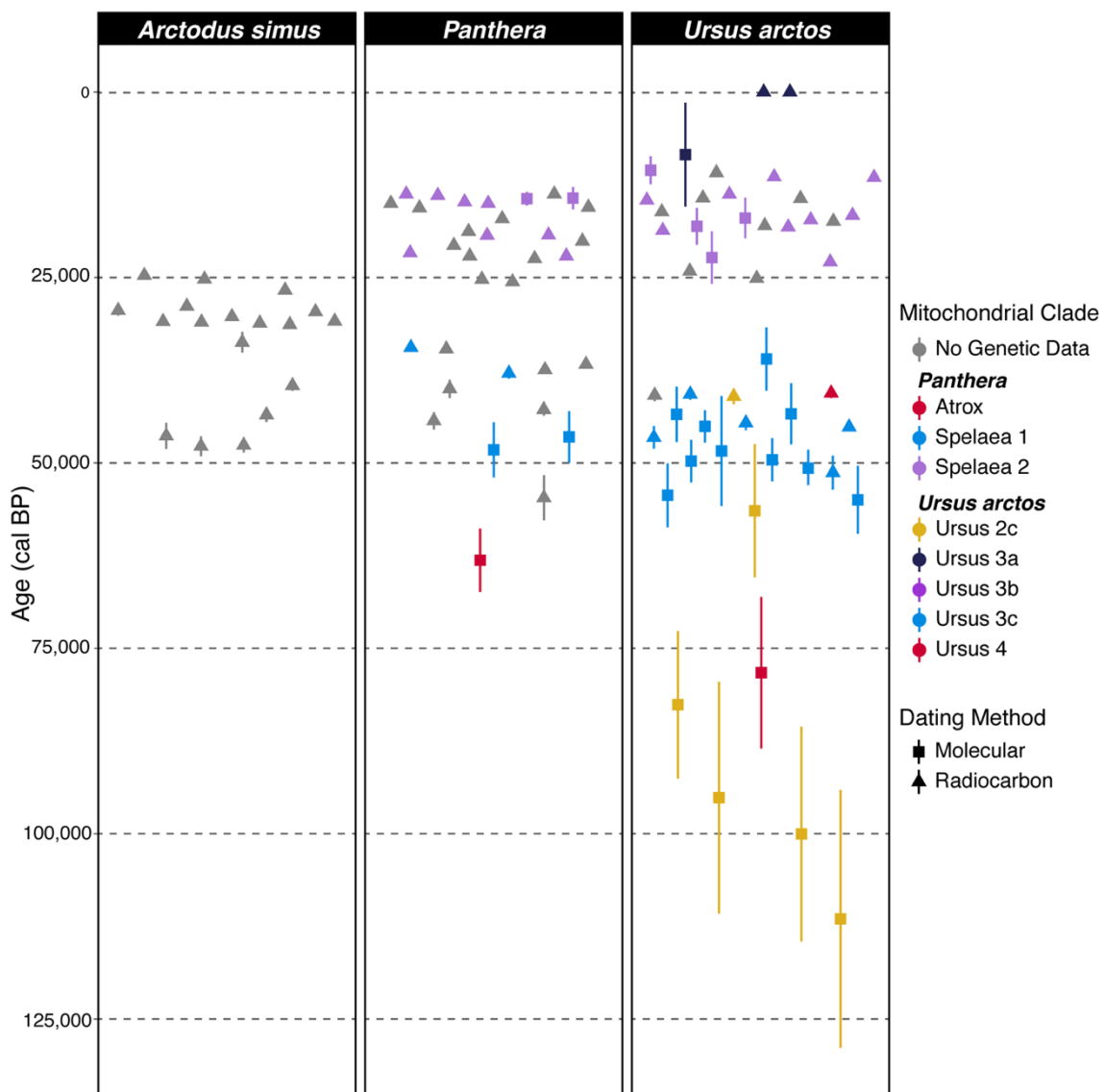


Fig. 2. Timeline of radiocarbon and molecular dates for Eastern Beringian giant short-faced bears (*Arctodus simus*), lions (*Panthera* spp.), and brown bears (*Ursus arctos*). Dates are shown with one standard error and are coloured by genetic clade. For additional radiocarbon dates used to produce this plot see Supplementary table S3.

Lastly, we recovered mitochondrial data from ten ancient clade 2a bears from Haida Gwaii and Prince of Wales Island (Alexander Archipelago). Clade 2a is closely related to the polar bear mitochondrial clade 2b, and a divergent clade 2a specimen (A308) was also recovered from Engineer Creek Mine near Fairbanks, Alaska dating to 23.3 kya, the first record of clade 2a in interior Alaska. This specimen was previously reported as belonging to clade 2b using control region sequences (Barnes et al., 2002; Davison et al., 2011), although doubts about species ID (polar bear versus brown bear) and provenance have been raised (Barnes et al., 2002; Edwards et al., 2011). In any case, the TMRCA of all Haida Gwaii and Alexander Archipelago specimens dates to ~20 kya (95% HPD: 17–24 kya), while the TMRCA between the Engineer Creek sample and all other clade 2a bears is 41 kya (95% HPD: 32.7–28.7 kya).

Lions

We produced 39 new near-complete mitogenomes from lion subfossil material from North America (n=24) and Eurasia (n=15), and analysed these along with two mitogenomes reconstructed from previously published data (Barnett et al., 2016), representing 35 unique haplotypes. The results of our phylogenetic analyses were in broad topological agreement with past studies, supporting the existence of two geographically restricted clades (Fig. 1B) corresponding to *Panthera (leo) spelaea* (Eastern Beringia and Eurasia) and *Panthera (leo) atrox* (all other North American specimens from Edmonton southwards). We observed one important exception to this pattern: a specimen from Sixtymile River in Yukon Territory (~64°N), A181, possessing an *atrox* (American lion) mitochondrial haplotype (Fig. 1; Supplementary Fig. S5), the first genetic *atrox* specimen ever recorded from any locality farther north than Edmonton (~53°N). Radiocarbon dating of this specimen yielded an infinite radiocarbon age (>51,500 uncal. yBP), but our Bayesian phylogenetic analyses suggested a median age for the specimen of 67 kya (95% HPD: 51.5–84.5 kya). The TMRCA of all *atrox* lions, representing the split between the two older *atrox* specimens (>50 kya, including A181) and the younger specimens (< 35 kya), dates to MIS 5 ~81 kya (95% HPD: 74.7–87.6 kya).

Our Bayesian analysis indicated a split date between *Panthera (leo) spelaea* and *Panthera (leo) atrox* of approximately 165 kya (95% HPD: 145.0–185.2 kya). This MIS 6 divergence date is substantially younger than the previous estimate of 340 kya based on short control region sequences (Barnett et al., 2009), which was likely an overestimate

2.2 MANUSCRIPT

resulting from application of a fossil-based node-age constraint and the time-dependency of mitochondrial substitution rates (Subramanian & Lambert, 2011). By relying on radiocarbon-dated tips to calibrate our analysis we have minimised the impact of rate time-dependency, allowing more accurate dating of population splits and sample ages, as demonstrated by the results of our leave-one-out cross-validation (Supplementary, Fig. S1).

Within Beringian lion diversity we were able to identify a genetically distinct pre-LGM mitochondrial clade of Eastern Beringian *Panthera (leo) spelaea* specimens with a TMRCA of 63 kya (95% HPD: 58.9–67.6 kya). These pre-LGM samples are genetically distinct from the two clades that include all younger Eastern Beringian lion specimens, which have TMRCA of 23 kya (95% HPD: 22.1–24.5 kya) and 22 kya (95% HPD: 18.9–25.5 kya), and a combined TMRCA of 33 kya (95% HPD: 29.2–37.0 kya). This suggests that in addition to the original dispersal of the ancestors of *Panthera (leo) atrox*, lions appear to have dispersed into North America on at least two other occasions during the Late Pleistocene. It is notable that the hiatus in the fossil record between the pre- and post-LGM lion clades falls between 33 and 22 kya, closely mirroring the pattern of local extinction observed in brown bears (Fig. 2).

Phylogeography: Testing the influence of the land bridge

The results of our separate phylogenetic analyses of brown bears and lions hinted at the existence of synchronous waves of dispersal and extinction tied to Pleistocene glacial cycles: in particular, most dispersal events seemed to occur during glacials, when the land bridge was present. To explicitly test whether the spatio-temporal distribution and parallel lineage turnover of lions and bears in Eastern Beringia was strongly affected by the presence or absence of the Bering Land Bridge, we performed a phylogeographic analysis in BEAST (Suchard et al., 2018). To overcome low power and over-parameterisation issues caused by the low number of dispersals in each clade, we used a novel approach uniting joint-tree (Sanmartin, Van der Mark, & Ronquist, 2008), and epoch-clock (Bielejec, Lemey, Baele, Rambaut, & Suchard, 2014) methods. We estimated both the bear and lion trees together in a single MCMC analysis (as separate unlinked trees); each tip in the trees (i.e., each specimen) was assigned an additional phylogeographical trait: Eurasia (Western Beringia) or North America (Eastern Beringia and South-of-the-Ice). We then estimated east-west dispersal rates (i.e., the rate of change of this

phylogeographic trait) simultaneously across both the bear and lion phylogenies, along with all other parameters associated with the previous two separate analyses (i.e., clock models, substitution models, topology, branch lengths). By using a single shared biogeographic model, data from both brown bears and lions are pooled to estimate dispersal patterns and drivers (Sanmartin et al., 2008). We compared two dispersal models using this method. (1) A simple null model, where a single dispersal rate across time was estimated, and (2) an epoch-based model where separate rates were estimated for two different groups of time slices: one rate for all periods when the Bering Land Bridge was likely emergent (i.e., glacials, even-numbered MISs) and another rate for all periods when the Bering Land Bridge was submerged (i.e., interglacials, odd-numbered MISs). Bayes factors (Kass & Raftery, 1995) provided moderate support for the epoch-based model over the single-rate null model (BF=3.038). The estimated dispersal rate for glacials was approximately 13 times higher than the dispersal rate during interglacials (1.56E-5 versus 1.22E-6 events per lineage per year). Supplementary Fig. S6 shows the pattern driving this difference: branches containing inferred dispersals are concentrated in glacials, yet the combined glacial epochs occupy less time and shorter tree length (compared to the combined interglacials).

Discussion:

Our results demonstrate that Pleistocene glacial cycles were an important driver of population dynamics in both Eastern Beringian brown bears and lions. In particular, dispersal between Western and Eastern Beringia was heavily influenced by presence of the Bering Land Bridge, with inferred dispersal rates across both species being over an order of magnitude higher during colder periods. This result strongly implicates geographical and environmental changes caused by glacial cycles as key drivers of carnivoran diversity, which is further supported by the remarkably parallel and synchronous response to these drivers observed in both brown bears and lions. For example, the respective origins of the American lion (*atrox*) mitochondrial lineage (~165 kya) and North American clade 4 brown bear lineage (~177 kya) — the earliest representatives of both species observed in North America (Fig. 2) — occurred during MIS 6, the Illinoian glaciation (Fig. 1), when the Bering Land Bridge was likely exposed (Fig. 3A). This is consistent with the first recorded lions occurring in Sangamonian (MIS 5) deposits in Kansas and Texas (Dalquest, 1962; Harington, 1969; Hibbard & Taylor,

1960). Notably, this also aligns with evidence that the steppe bison (*Bison priscus*) and red foxes (*Vulpes vulpes*) arrived in North America during MIS 6 (Froese et al., 2017), or immediately prior (Kutschera et al., 2013; Statham et al., 2014), respectively.

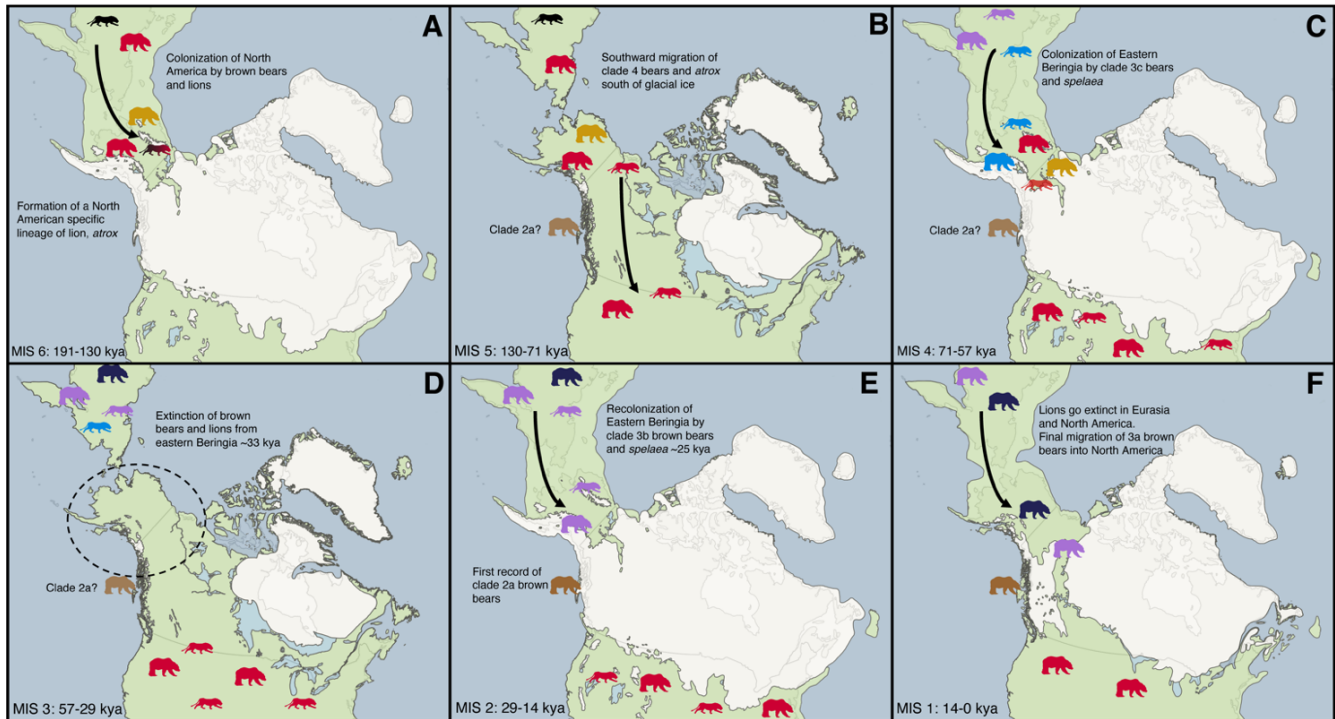


Fig. 3. Map of Late Quaternary phylogeography of North American brown bears and lions during six time periods. A) MIS 6, 191–130 kya, brown bears and lions first colonise North America via the Bering Land Bridge; B) MIS 5, 130–71 kya, Bering Land Bridge is flooded, dispersal of brown bears and lions south of continental ice sheets; C) MIS 4, 71–57 kya, dispersal of clade 3c bears and *spelaea* across the Bering Land Bridge; D) MIS 3, 57–29 kya, flooding of Bering Land Bridge and extinction of both carnivoran taxa in Eastern Beringia; E) MIS 2, Last Glacial Maximum, 29–14 kya, dispersal of clade 3b bears and second wave of *spelaea* lions; and F) MIS 1, Holocene, 14 kya to present, lions go extinct in North America and Eurasia, additionally clade 3a bears disperse into Eastern Beringia before the Bering Land Bridge is flooded for the last time. Different coloured silhouettes of brown bears and lions represent different genetic clades, corresponding to clade colouring in Figs 1 and 2. White area represents the approximate extent of glacial ice along with rough estimates of Bering Land Bridge extent during the different time periods using spatial data from Dyke, Moore, and Robertson (2003).

While our results suggest that clade 4 bears and *atrox* lions likely arrived in Eastern Beringia around 170 kya during MIS 6, they must have dispersed southwards soon afterwards, as individuals belonging to these lineages are never observed farther north than Edmonton (~53°N) following the end of MIS 3. The TMRCA of the North American clade 4 brown bear clade at 92 kya and *atrox* lion clade (including all North American samples) at 81 kya, both occurred during MIS 5, suggesting that both species dispersed southwards during this warmer period when ice sheets retreated and opened an ice-free

north-south corridor (Fig. 3B). This movement coincides with the first southward dispersal of the bison through the ice-free corridor between late MIS 6 and early MIS 5 (Froese et al., 2017; Heintzman et al., 2016; Shapiro et al., 2004). The dispersal and subsequent isolation of lions south of the ice was previously thought to have initiated the divergence between the American lion (*Panthera atrox*) and cave lion (*P. spelaea*) (Barnett et al., 2009). However, our discovery of a ~66.7 thousand-year-old *P. atrox* specimen north of the ice sheets in Yukon instead suggests that the formation of the endemic American lion lineage was more likely the result of their isolation in North America after the flooding of the Bering Land Bridge during MIS 5. Alternatively, this Yukon *atrox* sample could plausibly represent a migrant from south of the ice sheets, but we favour the former hypothesis as the timing of the split between *atrox* and *spelaea* coincides with the emergence of the Bering Land Bridge and there are no putative later examples of lions dispersing northwards.

Following MIS 6, the second wave of lion and brown bear dispersals into North America appears to have occurred during MIS 4 when lowered sea levels next exposed the Bering Land Bridge (Fig. 3C), corresponding with the respective TMRCAs of the North American endemic clade 3c bears and the clade comprising the four pre-LGM Eastern Beringian *spelaea* lions. However, during the interglacial period MIS 3, as the Bering Land Bridge was again submerged (Hu et al., 2010) (Fig. 3D), all lions (*atrox* and *spelaea*) and brown bears (clades 2c, 3c, and 4) appear to have become locally extinct in Eastern Beringia (Fig. 2), with *atrox* lions and clade 4 brown bears — descendants of the first wave of dispersal — surviving only in the contiguous USA and southern Canada. The absence of both brown bears and lions from the Eastern Beringian fossil record between 35 and 25 kya does not appear to be due to a taphonomic bias, as remains of the giant short-faced bear (*Arctodus simus*) are abundant during the same period (Fig. 2). Indeed, the reappearance of both lion and bear populations appears to be closely linked in time to the extinction of short-faced bears in the area, suggesting some form of competition (Barnes et al., 2002; Barnett et al., 2009; Davison et al., 2011; Ersmark et al., 2015; Leonard et al., 2000). Importantly, the timing of these carnivoran extinctions in Eastern Beringia coincides with evidence for widespread vegetation change in the region, namely expansion of peatlands caused by significant paludification (Mann et al., 2015; Reuther et al., 2020; Treat et al., 2019).

2.2 MANUSCRIPT

Populations of a number of megafaunal herbivores appear to have decreased during MIS 3, possibly related to the expansion of peatlands and restrictions on foraging and nutrition (Mann et al., 2015), which may have had reciprocal impacts on the megafaunal carnivores and omnivores that preyed upon them, plausibly causing the local extinction of both lions and brown bears. For example, musk-ox populations experienced a dramatic decrease in diversity and effective population size during MIS 3 (Campos et al., 2010), mammoth populations were steadily declining (Debruyne et al., 2008), and bison began to experience dramatic declines towards the end of MIS 3 into MIS 2 (Drummond, Rambaut, Shapiro, & Pybus, 2005; Lorenzen et al., 2011; Shapiro et al., 2004). In addition, it appears that non-caballine horses (i.e., *Haringtonhippus*) underwent a bottleneck during MIS 3 with only a single fossil specimen found in Eastern Beringia after ~31 kya (Guthrie, 2003; Heintzman et al., 2017) around the time that the brown bear and lion populations went extinct. In contrast, the giant short-faced bear appears to have persisted in Eastern Beringia throughout MIS 3. It is possible that the mobility, large home range, and solitary behaviour that has been proposed for the giant short-faced bear (Matheus, 1995; Schubert & Wallace, 2009) may have allowed them to exploit food resources that were less available to lions or brown bears. Grey wolves also appear to be present in eastern Beringia throughout MIS 3, with no evidence of genetic turnovers (Leonard et al., 2007; Loog et al., 2020). Isotope analyses have suggested Beringian wolves had similar diets to that of Pleistocene lions and brown bears, consisting largely of large herbivores (Fox-Dobbs, Leonard, & Koch, 2008; Leonard et al., 2007; Pilot et al., 2010). However, dietary analysis of a mummified MIS 3 Beringian wolf indicated a diet consisting a significant proportion of aquatic resources (Meachen et al., 2020), possibly indicating wolves may have utilised resources that may not have been available to lions or brown bears in Beringia during MIS 3.

Following MIS 3, lions and brown bears do not reappear in the fossil record of Eastern Beringia until after 27 kya, at the height of the LGM (MIS 2), when the Bering Land Bridge once again connected Eurasia and North America. This coincides with the invasion of North America from Eurasia by wapiti and moose (Hundertmark et al., 2002; Meiri et al., 2020; Meiri et al., 2014), and a secondary wave of bison dispersal across the Bering Land Bridge (Froese et al., 2017). The recolonizing populations were genetically distinct from those present in Eastern Beringia pre-MIS 2 as well as those south of the ice sheets, confirming that they likely comprised a new wave of dispersal from Western

Beringia (Fig. 3E). This wave of megafaunal dispersals associated with the re-emergence of the Bering Land Bridge in MIS 2 may also have included early Native American human populations, who are recorded shortly afterwards in the stratigraphic record of Chiquihuite Cave in Mexico, from approximately 26 kya (Ardelean et al., 2020).

The reappearance of lions and brown bears in Eastern Beringia during MIS 2 occurred at around the same time as the local extinction of *Arctodus*, which may relate to previously proposed competition between brown bears and *Arctodus* (Barnes et al., 2002; Steffen & Fulton, 2018). The apparent timing of the extinction of *Arctodus* in Eastern Beringia around 23 kya could be linked to the sharp climatic cooling associated with Heinrich Event 2 (24.3–23.3 ka BP), a period characterised by the collapse of the Northern Hemisphere ice sheets resulting in large discharges of ice into the North Atlantic causing drastic climatic changes (Heinrich, 1988; Hemming, 2004). In any case, the fact that Eastern Beringia was not instead recolonised by *atrox* lions and clade 4 bears from the contiguous USA may either reflect that conditions had not improved sufficiently to support lion and brown bear populations in Eastern Beringia before the ice-free corridor closed during the LGM or suggest that some other geographical or biogeographical barrier prevented dispersal from south of the ice sheets. Concordantly, in bison there is little evidence for northward dispersal through the ice-free corridor until after the LGM when a pulse of south to north dispersal is observed (Heintzman et al., 2016). Further, it is possible that clade 4 bears and *atrox* lions did contribute to the new populations of brown bears and lions in Eastern Beringia with the signal being lost either due to the maternal inheritance of mitochondrial DNA, or specimens harbouring these mitochondrial lineages yet to be sequenced.

All modern and ancient clade 2a brown bears from the Alexander and Haida Gwaii archipelagos coalesce at 20 kya (95% HPD: 17.0–24.0 kya), comparable to the TMRCA for Beringian clade 3b bears and *spelaea* lions. This supports the model proposed by Cahill *et al.* (Cahill et al., 2013) for the origin of clade 2a bears, under which the mitochondrial lineage was captured by brown bears following male-biased gene-flow into a population of polar bears stranded in the Alexander archipelago after the retraction of ice sheets post-LGM. Assuming all our ancient Alexander and Haida Gwaii archipelago samples represent brown bears (or at least brown-polar hybrids), and that mtDNA diversity in the stranded polar bear population was low, the coalescence of our samples can be considered

2.2 MANUSCRIPT

a proxy for the minimum age of hybridisation between polar and brown bears, and hence a minimum age for the arrival of brown bears in the Alexander and Haida Gwaii archipelagos post-LGM. If this is the case, then brown bears arrived in the islands no later than 17 kya (the lower bound of the 95% HPD). That timing is coincident with the first records of brown bears on the Haida Gwaii archipelago ~ 17.5 kya (Ramsey, Griffiths, Fedje, Wigen, & Mackie, 2004) and the existence of unglaciated western Alaskan coastline, which represents an alternative southward dispersal pathway into the continent that may also have been exploited by humans (Lesnek, Briner, Lindqvist, Baichtal, & Heaton, 2018; Shaw, Barrie, Conway, Lintern, & Kung, 2020).

Overall, our results highlight the key role of Pleistocene glacial cycles in driving the distribution and diversity of North American carnivorans. Glacial cycles may also have driven parallel waves of dispersal in other regions, such as across the Sakhalin land bridge that connected Japan with mainland Asia. Genetic evidence from modern Japanese brown bears suggests multiple waves of Pleistocene dispersal in a similar temporally staggered sequence, with present day Japanese mitochondrial diversity closely mirroring that observed in modern Eastern Beringia (i.e., clades 3a, 3b, and 4) and also exhibiting a marked phylogeographic structure (Hirata et al., 2013). Analysis of ancient Japanese brown bear specimens might allow determination of whether extinct Eastern Beringian clades such as 3c were also present in Japan during the late Pleistocene.

Conclusion:

Lions and brown bears display remarkably synchronous responses to Pleistocene glacial cycles, and combining phylogenetic data from these two Pleistocene carnivoran species in a shared common biogeographic model provides power to demonstrate a 13-fold increase in dispersal rate between Eastern and Western Beringia when the land bridge is present. By combining additional ancient DNA datasets from other species with trans-Beringian Pleistocene distributions (e.g., foxes), future studies may further refine the timing and magnitude of waves of dispersal across the Bering Land Bridge. A similar combined biogeographical approach may also be useful for exploring the timing of faunal dispersals through the ice-free corridor between the North American ice sheets, which available data suggests are biased southwards, with few observed northward dispersals. However, this apparent bias may be due to many ancient DNA studies focusing on recently

immigrated taxa (e.g., brown bears, bison, wapiti, humans) for which Eastern Beringia acts as a source, with the contiguous USA likely a sink. Endemic North American species may exhibit different patterns of phylogeography and dispersal, and large ancient DNA datasets from species like the giant short-faced bear or the western camel (*Camelops hesternus*) would be valuable in evaluating this possibility. Our densely-sampled study of rarer carnivorans contributes to the growing body of research suggesting remarkably concerted responses to Pleistocene geographical and environmental changes across many megafaunal taxa (e.g., Cooper et al., 2015).

Acknowledgements:

We would like to thank the following institutions for allowing access to specimens in their collections: University of Alaska Fairbanks Museum, University of Kansas Natural History Museum, University of Wyoming Geological Museum, Yukon Government, American Museum of Natural History, Cincinnati Museum, Bureau of Land Management Nevada-Elko District, St. Petersburg Institute of Zoology, Krakow Institute of Zoology, the Russian Academy of Sciences, Palaeontological Institute Moscow, Zoological Museum of Moscow University, The Institute of Plant and Animal Ecology of the Ural Branch of the Russian Academy of Sciences, Natural History Museum Stuttgart, University of Vienna, Museum of Natural History Vienna, Idaho Museum of Natural History, Royal Alberta Museum, Parks Canada, the Canadian Museum of Nature, Gwaii Haanas National Park Reserve and the Haida Nation. In addition, we are grateful to the following individuals who helped to collect and identify specimens and/or provided laboratory support during the early stages of the project: L. Orlando, T. Heaton, K. Chen, I. Barnes, A. Derevianko, E. Pankeyeva, I. Chernikov, M. Shunkov, A. Sher, N. Ovodov, C. Beard, D. Miao, D. Burnham, L. Vietti, M. Clementz, G. Zazula, P. Matheus, P. Wrinn, D. McLaren, and J. Austin. Gaadu Din Haida Gwaii fieldwork was funded by Social Science and Humanities Research Council of Canada Standard Grant awarded to DF (410-2005-0778). This research was funded by an Australian Research Council Laureate Fellowship awarded to AC (FL140100260) and U.S. National Science Foundation grant (EAR/SGP# 1425059) awarded to JM and AC.

References:

- Ardelean, C. F., Becerra-Valdivia, L., Pedersen, M. W., Schwenninger, J. L., Oviatt, C. G., Macias-Quintero, J. I., . . . Willerslev, E. (2020). Evidence of human occupation in Mexico around the Last Glacial Maximum. *Nature*, *584*, 87–92. doi:10.1038/s41586-020-2509-0
- Barnes, I., Matheus, P., Shapiro, B., Jensen, D., & Cooper, A. (2002). Dynamics of Pleistocene population extinctions in Beringian brown bears. *Science*, *295*(5563), 2267-2270. doi:10.1126/science.1067814
- Barnett, R., Lisandra, M., Zepeda Mendoza, M. L., Soares, A., Soares, R., Ho, S., . . . Gilbert, P. (2016). Mitogenomics of the extinct cave lion, *Panthera spelaea* (Goldfuss, 1810), resolve its position within the *Panthera* cats. *Open Quaternary*, *2*(4), 1-11. doi:10.5334/oq.24
- Barnett, R., Shapiro, B., Barnes, I., Ho, S. Y. W., Burger, J., Yamaguchi, N., . . . Cooper, A. (2009). Phylogeography of lions (*Panthera leo* ssp.) reveals three distinct taxa and a late Pleistocene reduction in genetic diversity. *Molecular Ecology*, *18*(8), 1668-1677. doi:10.1111/j.1365-294X.2009.04134.x
- Baryshnikov, G., & Boeskorov, G. (2001). The Pleistocene cave lion, *Panthera spelaea* (Carnivora, Felidae) from Yakutia, Russia. *Cranium*, *18*, 7-23.
- Bielejec, F., Lemey, P., Baele, G., Rambaut, A., & Suchard, M. A. (2014). Inferring heterogeneous evolutionary processes through time: from sequence substitution to phylogeography. *Systematic Biology*, *63*(4), 493-504. doi:10.1093/sysbio/syu015
- Bouckaert, R., Vaughan, T. G., Barido-Sottani, J., Duchene, S., Fourment, M., Gavryushkina, A., . . . Drummond, A. J. (2019). BEAST 2.5: An advanced software platform for Bayesian evolutionary analysis. *PLoS Computational Biology*, *15*(4), e1006650. doi:10.1371/journal.pcbi.1006650
- Bray, S. C. E., Austin, J. J., Metcalf, J. L., Østbye, K., Østbye, E., Lauritzen, S.-E., . . . Cooper, A. (2013). Ancient DNA identifies post-glacial recolonisation, not recent bottlenecks, as the primary driver of contemporary mtDNA phylogeography and diversity in Scandinavian brown bears. *Diversity and Distributions*, *19*(3), 245-256. doi:10.1111/j.1472-4642.2012.00923.x
- Cahill, J. A., Green, R. E., Fulton, T. L., Stiller, M., Jay, F., Ovsyanikov, N., . . . Shapiro, B. (2013). Genomic evidence for island population conversion resolves conflicting theories of polar bear evolution. *PLoS Genetics*, *9*(3), e1003345. doi:10.1371/journal.pgen.1003345
- Cahill, J. A., Heintzman, P. D., Harris, K., Teasdale, M. D., Kapp, J., Soares, A. E. R., . . . Shapiro, B. (2018). Genomic evidence of widespread admixture from polar bears into brown bears during the last ice age. *Molecular Biology and Evolution*, *35*(5), 1120-1129. doi:10.1093/molbev/msy018
- Cahill, J. A., Stirling, I., Kistler, L., Salamzade, R., Ersmark, E., Fulton, T. L., . . . Shapiro, B. (2015). Genomic evidence of geographically widespread effect of gene flow

- from polar bears into brown bears. *Molecular Ecology*, 24(6), 1205-1217. doi:10.1111/mec.13038
- Campos, P. F., Willerslev, E., Sher, A., Orlando, L., Axelsson, E., Tikhonov, A., . . . Gilbert, M. T. P. (2010). Ancient DNA analyses exclude humans as the driving force behind late Pleistocene musk ox (*Ovibos moschatus*) population dynamics. *Proceedings of the National Academy of Sciences of the United States of America*, 107(12), 5675-5680. doi:10.1073/pnas.0907189107
- Christiansen, P., & Harris, J. M. (2009). Craniomandibular Morphology and Phylogenetic Affinities of *Panthera Atrox*: Implications for the Evolution and Paleobiology of the Lion Lineage. *Journal of Vertebrate Paleontology*, 29(3), 934-945. doi:10.1671/039.029.0314
- Colleoni, F., Wekerle, C., Näslund, J.-O., Brandefelt, J., & Masina, S. (2016). Constraint on the penultimate glacial maximum Northern Hemisphere ice topography (≈ 140 kyrs BP). *Quaternary Science Reviews*, 137, 97-112. doi:10.1016/j.quascirev.2016.01.024
- Cooper, A., & Poinar, H. N. (2000). Ancient DNA: Do it right or not at all. *Science*, 289(5482), 1139. doi:10.1126/science.289.5482.1139b
- Cooper, A., Turney, C., Hughen, K. A., Brook, B. W., McDonald, H. G., & Bradshaw, C. J. A. (2015). Abrupt warming events drove Late Pleistocene Holarctic megafaunal turnover. *Science*, 349(6248), 602-606. doi:10.1126/science.aac4315
- Dabney, J., Knapp, M., Glocke, I., Gansauge, M.-T., Weihmann, A., Nickel, B., . . . Meyer, M. (2013). Complete mitochondrial genome sequence of a Middle Pleistocene cave bear reconstructed from ultrashort DNA fragments. *Proceedings of the National Academy of Sciences of the United States of America*, 110(39), 15758-15763.
- Dalquest, W. W. (1962). The Good Creek Formation, Pleistocene of Texas, and Its Fauna. *Journal of Paleontology*, 36(3), 568-582.
- Davison, J., Ho, S. Y. W., Bray, S. C., Korsten, M., Tammelleht, E., Hindrikson, M., . . . Saarna, U. (2011). Late-Quaternary biogeographic scenarios for the brown bear (*Ursus arctos*), a wild mammal model species. *Quaternary Science Reviews*, 30(3-4), 418-430. doi:10.1016/j.quascirev.2010.11.023
- Debruyne, R., Chu, G., King, C. E., Bos, K., Kuch, M., Schwarz, C., . . . Poinar, H. N. (2008). Out of America: Ancient DNA evidence for a New World origin of Late Quaternary woolly mammoths. *Current Biology*, 18(17), 1320-1326. doi:10.1016/j.cub.2008.07.061
- Drummond, A. J., Rambaut, A., Shapiro, B., & Pybus, O. G. (2005). Bayesian coalescent inference of past population dynamics from molecular sequences. *Molecular Biology and Evolution*, 22(5), 1185-1192. doi:10.1093/molbev/msi103
- Dyke, A., Moore, A., & Robertson, L. (2003). *Deglaciation of North America*. Ottawa, ON: Natural Resources Canada.

2.2 MANUSCRIPT

- Edgar, R. C. (2004). MUSCLE: multiple sequence alignment with high accuracy and high throughput. *Nucleic Acids Research*, *32*(5), 1792-1797. doi:10.1093/nar/gkh340
- Edwards, C. J., Suchard, M. A., Lemey, P., Welch, J. J., Barnes, I., Fulton, T. L., . . . Shapiro, B. (2011). Ancient hybridization and an Irish origin for the modern polar bear matriline. *Current Biology*, *21*(15), 1251-1258. doi:10.1016/j.cub.2011.05.058
- Elias, S. A., & Crocker, B. (2008). The Bering Land Bridge: a moisture barrier to the dispersal of steppe-tundra biota? *Quaternary Science Reviews*, *27*(27), 2473-2483. doi:10.1016/j.quascirev.2008.09.011
- Elias, S. A., Short, S. K., Nelson, C. H., & Birks, H. H. (1996). Life and times of the Bering land bridge. *Nature*, *382*(6586), 60-63. doi:10.1038/382060a0
- Enk, J., Devault, A., Widga, C., Saunders, J., Szpak, P., Southon, J., . . . Poinar, H. (2016). *Mammuthus* population dynamics in Late Pleistocene North America: Divergence, phylogeography, and introgression. *Frontiers in Ecology and Evolution*, *4*(42), 42. doi:10.3389/fevo.2016.00042
- Ersmark, E., Orlando, L., Sandoval-Castellanos, E., Barnes, I., Barnett, R., Stuart, A., . . . Dalén, L. (2015). Population demography and genetic diversity in the Pleistocene cave lion. *Open Quaternary*, *1*(4), 1-14. doi:10.5334/oq.aa
- Fox-Dobbs, K., Leonard, J. A., & Koch, P. L. (2008). Pleistocene megafauna from eastern Beringia: Paleoecological and paleoenvironmental interpretations of stable carbon and nitrogen isotope and radiocarbon records. *Palaeogeography, Palaeoclimatology, Palaeoecology*, *261*(1-2), 30-46. doi:10.1016/j.palaeo.2007.12.011
- Froese, D., Stiller, M., Heintzman, P. D., Reyes, A. V., Zazula, G. D., Soares, A. E., . . . Shapiro, B. (2017). Fossil and genomic evidence constrains the timing of bison arrival in North America. *Proceedings of the National Academy of Sciences of the United States of America*, *114*(13), 3457-3462. doi:10.1073/pnas.1620754114
- Guthrie, R. D. (2003). Rapid body size decline in Alaskan Pleistocene horses before extinction. *Nature*, *426*(6963), 169-171. doi:10.1038/nature02098
- Guthrie, R. D. (2006). New carbon dates link climatic change with human colonization and Pleistocene extinctions. *Nature*, *441*(7090), 207-209. doi:10.1038/nature04604
- Hailer, F. (2015). Introgressive hybridization: brown bears as vectors for polar bear alleles. *Molecular Ecology*, *24*(6), 1161-1163. doi:10.1111/mec.13101
- Hailer, F., & Welch, A. J. (2016). Evolutionary history of polar and brown bears. *eLS*, 1-8.
- Harington, C. R. (1969). Pleistocene Remains of the Lion-Like Cat (*Panthera atrox*) from Yukon Territory and Northern Alaska. *Canadian Journal of Earth Sciences*, *6*(5), 1277-1288. doi:10.1139/e69-127

- Harrington, C. R. (1996). American Lion. *Beringian Research Notes*, 5, 1-4.
- Harrington, C. R., Naughton, D., Dalby, A., Rose, M., & Dawson, J. (2003). *Annotated Bibliography of Quaternary Vertebrates of Northern North America*. Toronto: University of Toronto Press.
- Heinrich, H. (1988). Origin and Consequences of Cyclic Ice Rafting in the Northeast Atlantic-Ocean during the Past 130,000 Years. *Quaternary Research*, 29(2), 142-152. doi:10.1016/0033-5894(88)90057-9
- Heintzman, P. D., Froese, D., Ives, J. W., Soares, A. E., Zazula, G. D., Letts, B., . . . Shapiro, B. (2016). Bison phylogeography constrains dispersal and viability of the Ice Free Corridor in western Canada. *Proceedings of the National Academy of Sciences of the United States of America*, 113(29), 8057-8063. doi:10.1073/pnas.1601077113
- Heintzman, P. D., Zazula, G. D., Macphee, R. D. E., Scott, E., Cahill, J. A., McHorse, B. K., . . . Shapiro, B. (2017). A new genus of horse from Pleistocene North America. *Elife*, 6, e29944. doi:10.7554/eLife.29944
- Hemming, S. R. (2004). Heinrich events: Massive late pleistocene detritus layers of the North Atlantic and their global climate imprint. *Reviews of Geophysics*, 42(1), RG1005. doi:10.1029/2003rg000128
- Hibbard, C. W., & Taylor, D. W. (1960). Two late Pleistocene faunas from southwestern Kansas. *Contributions from the Museum of Paleontology, University of Michigan*, 16(1), 1-223.
- Hirata, D., Mano, T., Abramov, A. V., Baryshnikov, G. F., Kosintsev, P. A., Vorobiev, A. A., . . . Masuda, R. (2013). Molecular phylogeography of the brown bear (*Ursus arctos*) in Northeastern Asia based on analyses of complete mitochondrial DNA sequences. *Molecular Biology and Evolution*, 30(7), 1644-1652. doi:10.1093/molbev/mst077
- Hopkins, D. M. (1973). Sea level history in Beringia during the past 250,000 years. *Quaternary Research*, 3(4), 520-540. doi:10.1016/0033-5894(73)90029-X
- Hu, A. X., Meehl, G. A., Otto-Bliesner, B. L., Waelbroeck, C., Han, W. Q., Loutre, M. F., . . . Rosenbloom, N. (2010). Influence of Bering Strait flow and North Atlantic circulation on glacial sea-level changes. *Nature Geoscience*, 3(2), 118-121. doi:10.1038/Ngeo729
- Hundertmark, K. J., Shields, G. F., Udina, I. G., Bowyer, R. T., Danilkin, A. A., & Schwartz, C. C. (2002). Mitochondrial phylogeography of moose (*Alces alces*): Late Pleistocene divergence and population expansion. *Molecular Phylogenetics and Evolution*, 22(3), 375-387. doi:10.1006/mpev.2001.1058
- Hwang, D. S., Ki, J. S., Jeong, D. H., Kim, B. H., Lee, B. K., Han, S. H., & Lee, J. S. (2008). A comprehensive analysis of three Asiatic black bear mitochondrial genomes (subspecies *ussuricus*, *formosanus* and *mupinensis*), with emphasis on the complete mtDNA sequence of *Ursus thibetanus ussuricus* (Ursidae). *DNA Sequence*, 19(4), 418-429. doi:10.1080/19401730802389525

2.2 MANUSCRIPT

- Jakobsson, M., Pearce, C., Cronin, T. M., Backman, J., Anderson, L. G., Barrientos, N., . . . O'Regan, M. (2017). Post-glacial flooding of the Bering Land Bridge dated to 11 cal ka BP based on new geophysical and sediment records. *Climate of the Past*, *13*(8), 991-1005. doi:10.5194/cp-13-991-2017
- Kass, R. E., & Raftery, A. E. (1995). Bayes Factors. *Journal of the American Statistical Association*, *90*(430), 773-795. doi:10.1080/01621459.1995.10476572
- Kim, J. H., Antunes, A., Luo, S. J., Menninger, J., Nash, W. G., O'Brien, S. J., & Johnson, W. E. (2006). Evolutionary analysis of a large mtDNA translocation (numt) into the nuclear genome of the *Panthera* genus species. *Gene*, *366*(2), 292-302. doi:10.1016/j.gene.2005.08.023
- Kurtén, B. (1985). The Pleistocene Lion of Beringia. *Annales Zoologici Fennici*, *22*(1), 117-121.
- Kurtén, B., & Anderson, E. (1980). *Pleistocene Mammals of North America*. New York: Columbia University Press.
- Kutschera, V. E., Lecomte, N., Janke, A., Selva, N., Sokolov, A. A., Haun, T., . . . Hailer, F. (2013). A range-wide synthesis and timeline for phylogeographic events in the red fox (*Vulpes vulpes*). *BMC Evolutionary Biology*, *13*, 114. doi:10.1186/1471-2148-13-114
- Lanfear, R., Frandsen, P. B., Wright, A. M., Senfeld, T., & Calcott, B. (2016). PartitionFinder 2: New Methods for Selecting Partitioned Models of Evolution for Molecular and Morphological Phylogenetic Analyses. *Molecular Biology and Evolution*, *34*(3), 772-773. doi:10.1093/molbev/msw260
- Leonard, J. A., Vila, C., Fox-Dobbs, K., Koch, P. L., Wayne, R. K., & Van Valkenburgh, B. (2007). Megafaunal extinctions and the disappearance of a specialized wolf ecomorph. *Current Biology*, *17*(13), 1146-1150. doi:10.1016/j.cub.2007.05.072
- Leonard, J. A., Wayne, R. K., & Cooper, A. (2000). Population genetics of Ice age brown bears. *Proceedings of the National Academy of Sciences of the United States of America*, *97*(4), 1651-1654. doi:10.1073/pnas.040453097
- Lesnek, A. J., Briner, J. P., Lindqvist, C., Baichtal, J. F., & Heaton, T. H. (2018). Deglaciation of the Pacific coastal corridor directly preceded the human colonization of the Americas. *Science Advances*, *4*(5), eaar5040. doi:10.1126/sciadv.aar5040
- Li, H., & Durbin, R. (2009). Fast and accurate short read alignment with Burrows-Wheeler transform. *Bioinformatics*, *25*(14), 1754-1760. doi:10.1093/bioinformatics/btp324
- Li, H., Handsaker, B., Wysoker, A., Fennell, T., Ruan, J., Homer, N., . . . Genome Project Data Processing, S. (2009). The sequence alignment/map format and SAMtools. *Bioinformatics*, *25*(16), 2078-2079. doi:10.1093/bioinformatics/btp352
- Lindqvist, C., Schuster, S. C., Sun, Y. Z., Talbot, S. L., Qi, J., Ratan, A., . . . Wiig, O. (2010). Complete mitochondrial genome of a Pleistocene jawbone unveils the

- origin of polar bear. *Proceedings of the National Academy of Sciences of the United States of America*, 107(11), 5053-5057. doi:10.1073/pnas.0914266107
- Lister, A. M., & Sher, A. V. (2015). Evolution and dispersal of mammoths across the Northern Hemisphere. *Science*, 350(6262), 805. doi:10.1126/science.aac5660
- Liu, S. P., Lorenzen, E. D., Fumagalli, M., Li, B., Harris, K., Xiong, Z. J., . . . Wang, J. (2014). Population genomics reveal recent speciation and rapid evolutionary adaptation in polar bears. *Cell*, 157(4), 785-794. doi:10.1016/j.cell.2014.03.054
- Loog, L., Thalmann, O., Sinding, M. H. S., Schuenemann, V. J., Perri, A., Germonpré, M., . . . Manica, A. (2020). Ancient DNA suggests modern wolves trace their origin to a Late Pleistocene expansion from Beringia. *Molecular Ecology*, 29(9), 1596-1610. doi:10.1111/mec.15329
- Lorenzen, E. D., Nogues-Bravo, D., Orlando, L., Weinstock, J., Binladen, J., Marske, K. A., . . . Willerslev, E. (2011). Species-specific responses of Late Quaternary megafauna to climate and humans. *Nature*, 479(7373), 359-364. doi:10.1038/nature10574
- Mann, D. H., Groves, P., Reanier, R. E., Gaglioti, B. V., Kunz, M. L., & Shapiro, B. (2015). Life and extinction of megafauna in the ice-age Arctic. *Proceedings of the National Academy of Sciences of the United States of America*, 112(46), 14301-14306. doi:10.1073/pnas.1516573112
- Matheus, P. E. (1995). Diet and co-ecology of Pleistocene short-faced bears and brown bears in eastern Beringia. *Quaternary Research*, 44(3), 447-453. doi:10.1006/qres.1995.1090
- Meachen, J., Wooller, M. J., Barst, B. D., Funck, J., Crann, C., Heath, J., . . . Zazula, G. (2020). A mummified Pleistocene gray wolf pup. *Current Biology*, 30(24), R1467-R1468. doi:10.1016/j.cub.2020.11.011
- Meiri, M., Lister, A., Kosintsev, P., Zazula, G., & Barnes, I. (2020). Population dynamics and range shifts of moose (*Alces alces*) during the Late Quaternary. *Journal of Biogeography*, 00, 1-12. doi:10.1111/jbi.13935
- Meiri, M., Lister, A. M., Collins, M. J., Tuross, N., Goebel, T., Blockley, S., . . . Barnes, I. (2014). Faunal record identifies Bering isthmus conditions as constraint to end-Pleistocene migration to the New World. *Proceedings of the Royal Society B: Biological Sciences*, 281(1776). doi:10.1098/rspb.2013.2167
- Meyer, M., Kircher, M., Gansauge, M. T., Li, H., Racimo, F., Mallick, S., . . . Paabo, S. (2012). A high-coverage genome sequence from an archaic Denisovan individual. *Science*, 338(6104), 222-226. doi:10.1126/science.1224344
- Miller, W., Schuster, S. C., Welch, A. J., Ratan, A., Bedoya-Reina, O. C., Zhao, F. Q., . . . Lindqvist, C. (2012). Polar and brown bear genomes reveal ancient admixture and demographic footprints of past climate change. *Proceedings of the National Academy of Sciences of the United States of America*, 109(36), E2382-E2390. doi:10.1073/pnas.1210506109

- Mitchell, K. J., Bray, S. C., Bover, P., Soibelzon, L., Schubert, B. W., Prevosti, F., . . . Cooper, A. (2016). Ancient mitochondrial DNA reveals convergent evolution of giant short-faced bears (Tremarctinae) in North and South America. *Biology Letters*, *12*(4), 20160062. doi:10.1098/rsbl.2016.0062
- Pilot, M., Branicki, W., Jedrzejewski, W., Goszczynski, J., Jedrzejewska, B., Dyky, I., . . . Tsingarska, E. (2010). Phylogeographic history of grey wolves in Europe. *BMC Evolutionary Biology*, *10*:104. doi:10.1186/1471-2148-10-104
- Rambaut, A., Drummond, A. J., Xie, D., Baele, G., & Suchard, M. A. (2018). Posterior summarization in bayesian phylogenetics using Tracer 1.7. *Systematic Biology*, *67*(5), 901-904. doi:10.1093/sysbio/syy032
- Ramsden, C., Holmes, E. C., & Charleston, M. A. (2009). Hantavirus evolution in relation to its rodent and insectivore hosts: no evidence for codivergence. *Molecular Biology and Evolution*, *26*(1), 143-153. doi:10.1093/molbev/msn234
- Ramsey, C. B. (2009). Bayesian analysis of radiocarbon dates. *Radiocarbon*, *51*(1), 337-360. doi:10.1017/S0033822200033865
- Ramsey, C. L., Griffiths, P. A., Fedje, D. W., Wigen, R. J., & Mackie, Q. (2004). Preliminary investigation of a late Wisconsinan fauna from K1 cave, Queen Charlotte Islands (Haida Gwaii), Canada. *Quaternary Research*, *62*(1), 105-109. doi:10.1016/j.yqres.2004.05.003
- Reimer, P. J., Bard, E., Bayliss, A., Beck, J. W., Blackwell, P. G., Ramsey, C. B., . . . van der Plicht, J. (2013). Intcal13 and Marine13 radiocarbon age calibration curves 0-50,000 years cal BP. *Radiocarbon*, *55*(4), 1869-1887. doi:10.2458/azu_js_rc.55.16947
- Reuther, J. D., Rogers, J., Druckenmiller, P., Bundtzen, T. K., Wallace, K., Bowman, R., . . . Cherkinsky, A. (2020). Late Quaternary (\geq MIS 3 to MIS 1) stratigraphic transitions in a highland Beringian landscape along the Kuskokwim River, Alaska. *Quaternary Research*, *93*, 139-154. doi:10.1017/qua.2019.51
- Rey-Iglesia, A., Garcia-Vazquez, A., Treadaway, E. C., van der Plicht, J., Baryshnikov, G. F., Szpak, P., . . . Lorenzen, E. D. (2019). Evolutionary history and palaeoecology of brown bear in North-East Siberia re-examined using ancient DNA and stable isotopes from skeletal remains. *Scientific Reports*, *9*(1), 4462. doi:10.1038/s41598-019-40168-7
- Richards, S. M., Hovhannisyan, N., Gilliam, M., Ingram, J., Skadhauge, B., Heiniger, H., . . . Cooper, A. (2019). Low-cost cross-taxon enrichment of mitochondrial DNA using in-house synthesised RNA probes. *PLoS ONE*, *14*(2), e0209499. doi:10.1371/journal.pone.0209499
- Rohland, N., Harney, E., Mallick, S., Nordenfelt, S., & Reich, D. (2015). Partial uracil-DNA-glycosylase treatment for screening of ancient DNA. *Philosophical Transactions of the Royal Society of London B Biological Sciences*, *370*(1660), 20130624. doi:10.1098/rstb.2013.0624

- Sanmartin, I., Van der Mark, P., & Ronquist, F. (2008). Inferring dispersal: a Bayesian approach to phylogeny-based island biogeography, with special reference to the Canary Islands. *Journal of Biogeography*, 35(3), 428-449. doi:10.1111/j.1365-2699.2008.01885.x
- Schubert, B. W., & Wallace, S. C. (2009). Late Pleistocene giant short-faced bears, mammoths, and large carcass scavenging in the Saltville Valley of Virginia, USA. *Boreas*, 38(3), 482-492. doi:10.1111/j.1502-3885.2009.00090.x
- Schubert, M., Ermini, L., Sarkissian, C. D., Jonsson, H., Ginolhac, A., Schaefer, R., . . . Orlando, L. (2014). Characterization of ancient and modern genomes by SNP detection and phylogenomic and metagenomic analysis using PALEOMIX. *Nature Protocols*, 9(5), 1056-1082. doi:10.1038/nprot.2014.063
- Schubert, M., Lindgreen, S., & Orlando, L. (2016). AdapterRemoval v2: rapid adapter trimming, identification, and read merging. *BMC Research Notes*, 9, 88. doi:10.1186/s13104-016-1900-2
- Shapiro, B., Drummond, A. J., Rambaut, A., Wilson, M. C., Matheus, P. E., Sher, A. V., . . . Cooper, A. (2004). Rise and fall of the Beringian steppe bison. *Science*, 306(5701), 1561-1565. doi:10.1126/science.1101074
- Shaw, J., Barrie, J. V., Conway, K. W., Lintern, D. G., & Kung, R. (2020). Glaciation of the northern British Columbia continental shelf: the geomorphic evidence derived from multibeam bathymetric data. *Boreas*, 49(1), 17-37. doi:10.1111/bor.12411
- Sotnikova, M., & Nikolskiy, P. (2006). Systematic position of the cave lion *Panthera spelaea* (Goldfuss) based on cranial and dental characters. *Quaternary International*, 142, 218-228. doi:10.1016/j.quaint.2005.03.019
- Statham, M. J., Murdoch, J., Janecka, J., Aubry, K. B., Edwards, C. J., Soulsbury, C. D., . . . Sacks, B. N. (2014). Range-wide multilocus phylogeography of the red fox reveals ancient continental divergence, minimal genomic exchange and distinct demographic histories. *Molecular Ecology*, 23(19), 4813-4830. doi:10.1111/mec.12898
- Steffen, M. L., & Fulton, T. L. (2018). On the association of giant short-faced bear (*Arctodus simus*) and brown bear (*Ursus arctos*) in late Pleistocene North America. *Geobios*, 51(1), 61-74. doi:10.1016/j.geobios.2017.12.001
- Stiller, M., Molak, M., Prost, S., Rabeder, G., Baryshnikov, G., Rosendahl, W., . . . Knapp, M. (2014). Mitochondrial DNA diversity and evolution of the Pleistocene cave bear complex. *Quaternary International*, 339-340, 224-231. doi:10.1016/j.quaint.2013.09.023
- Stuart, A. J., & Lister, A. M. (2011). Extinction chronology of the cave lion *Panthera spelaea*. *Quaternary Science Reviews*, 30(17-18), 2329-2340. doi:10.1016/j.quascirev.2010.04.023
- Subramanian, S., & Lambert, D. M. (2011). Time dependency of molecular evolutionary rates? Yes and no. *Genome Biology and Evolution*, 3, 1324-1328. doi:10.1093/gbe/evr108

2.2 MANUSCRIPT

- Suchard, M. A., Lemey, P., Baele, G., Ayres, D. L., Drummond, A. J., & Rambaut, A. (2018). Bayesian phylogenetic and phylodynamic data integration using BEAST 1.10. *Virus Evolution*, *4*(1), vey016. doi:10.1093/ve/vey016
- Talbot, S. L., & Shields, G. F. (1996). Phylogeography of brown bears (*Ursus arctos*) of Alaska and paraphyly within the Ursidae. *Molecular Phylogenetics and Evolution*, *5*(3), 477-494. doi:DOI 10.1006/mpev.1996.0044
- Treat, C. C., Kleinen, T., Broothaerts, N., Dalton, A. S., Dommain, R., Douglas, T. A., . . . Brovkin, V. (2019). Widespread global peatland establishment and persistence over the last 130,000 y. *Proceedings of the National Academy of Sciences of the United States of America*, *116*(11), 4822-4827. doi:10.1073/pnas.1813305116
- Waits, L. P., Talbot, S. L., Ward, R. H., & Shields, G. F. (1998). Mitochondrial DNA phylogeography of the North American brown bear and implications for conservation. *Conservation Biology*, *12*(2), 408-417. doi:10.1046/j.1523-1739.1998.96351.x
- Whitmore, F. C., & Foster, H. L. (1967). *Panthera atrox* (Mammalia: Felidae) from Central Alaska. *Journal of Paleontology*, *41*(1), 247-251.

2.3 Supplementary Information

Lions and brown bears colonised North America in multiple synchronous waves of dispersal across the Bering Land Bridge

Alexander T Salis, Sarah C E Bray, Michael S Y Lee, Holly Heiniger, Ross Barnett, James A Burns, Vladimir Doronichev, Daryl Fedje, Liubov Golovanova, C Richard Harington, Bryan Hockett, Pavel Kosintsev, Xulong Lai, Quentin Mackie, Sergei Vasiliev, Jacobo Weinstock, Nobuyuki Yamaguchi, Julie Meachen, Alan Cooper, Kieren J Mitchell

Corresponding authors: A.T.S. (alexander.salis@adelaide.edu.au), A.C. (alanjcooper42@gmail.com), K.J.M. (kieren.mitchell@adelaide.edu.au)

This file includes:

- Supplementary text
- Tables S1 to S6
- Figures S1 to S6
- Supplementary References

Supplementary Information Text

Extended Material and Methods:

Sampling

We sampled 120 brown bear subfossil bone and tooth specimens from northern Asia and North America, and 47 lion subfossils from Europe, northern Asia, and North America (supplementary tables S1 and S2). Fourteen brown bear specimens, and 12 lion specimens were radiocarbon dated at the Oxford Radiocarbon Accelerator Unit of the University of Oxford. All radiocarbon dates were calibrated with the IntCal13 curve (Reimer et al., 2013) using OxCal 4.4 (Ramsey, 2009).

All pre-PCR steps (extraction, library preparation) were conducted in purpose-built aDNA clean-room facilities at the University of Adelaide's Australian Centre for Ancient DNA (ACAD) or the Henry Wellcome Ancient Biomolecules Centre at the University of Oxford, spatially separated and physically isolated from any other molecular laboratories. Strict protocols were followed and a number of precautions taken to minimize contamination of samples with exogenous DNA (Cooper & Poinar, 2000). Protective clothing was worn, including: hooded coveralls over ancient-DNA lab-dedicated clothing (clothes never previously worn in any other molecular laboratory), hairnets, facemasks, face shields, designated footwear for both transitional areas and the physical laboratory, and three pairs of gloves worn at all times to prevent skin exposure between frequent changes of the outer layer of gloves. Furthermore, the lab was designed with positive air pressure, flowing from the cleanest workrooms to the outside of the lab. Stringent decontamination procedures were also adhered to, including cleaning equipment and surfaces with bleach or disinfectant detergent before and after use as well as regular UV irradiation of surfaces. These precautions also included negative controls for both DNA extraction and PCR setup. PCR amplification and all downstream procedures (*e.g.*, quantification and hybridization enrichment) were carried out in independent DNA laboratories.

DNA extraction

Potential surface contamination on each sample was reduced by UV irradiation for 15 min each side, followed by abrasion of the exterior surface (*c.* 1 mm) using a Dremel tool and a disposable carborundum disk. The sample was then pulverized using either a metallic

mallet or a Mikro-Dismembrator S (Sartorius). Approximately 100 mg of powder was extracted using one of two protocols: 1) Phenol-chloroform-based extraction protocol from Bray et al. (Bray et al., 2013); or 2) an in-house silica-based extraction protocol adapted from Dabney et al. (Dabney et al., 2013). For the latter protocol, the powder was digested first in 1 mL 0.5 M EDTA for 60 min, followed by an overnight incubation in 970 μ L fresh 0.5 M EDTA and 30 μ L proteinase K (20 mg/ml) at 55°C. The samples were centrifuged and the supernatant mixed with 13 mL of a modified PB buffer (12.6 mL PB buffer (Qiagen), 6.5 μ L Tween-20, and 390 μ L of 3M Sodium Acetate) and bound to silicon dioxide particles, which were then washed two times with 80% ethanol. The DNA was eluted from silica particles with 100 μ L TE buffer.

Library preparation

Double-stranded Illumina libraries were constructed following the protocol of Meyer et al. (Meyer et al., 2012) from 25 μ L of DNA extract, with truncated Illumina adapters with unique dual 7-mer internal barcodes added to allow identification and exclusion of any downstream contamination. In addition, all samples underwent partial uracil-DNA glycosylase (UDG) treatment (Rohland, Harney, Mallick, Nordenfelt, & Reich, 2015) to restrict cytosine deamination, characteristic of ancient DNA, to terminal nucleotides, while eliminating damage in the centre of the molecules. A short round of PCR using PCR primers complementary to the adapter sequences was performed to increase the total amount of DNA. Cycle number was determined via real-time PCR and each library split into 8 separate PCR reactions to minimize PCR bias and maintain library complexity. Each PCR of 25 μ L contained 1 \times HiFi buffer, 2.5 mM MgSO₄, 1 mM dNTPs, 0.5 mM each primer, 0.1 U Invitrogen Platinum Taq Hi-Fi polymerase and 3 μ L DNA. The cycling conditions were 94 °C for 6 min, 9–31 cycles of 94 °C for 30 s, 60 °C for 30 s, and 68 °C for 40 s, followed by 68 °C for 10 min. PCR replicates were pooled and products were then purified using AxyPrep™ magnetic beads (Axygen™). DNA was eluted in 30 μ L EB buffer and quantified with a Qubit fluorometer (Thermo Fisher).

Mitochondrial enrichment

For lion libraries, commercially synthesized biotinylated 80-mer RNA baits (Arbor Biosciences, MI, USA) were used to enrich for mammalian mitochondrial DNA (Mitchell et al., 2016). DNA-RNA hybridization enrichment was performed according to

2.3 SUPPLEMENTARY INFORMATION

manufacturer's recommendations (MYbaits protocol v3) with the exception that 1.25 μ L of baits per reaction was used and the incubation step which was changed to 55 °C for 15 hr followed by 50 °C for 16 hrs. The beads were washed three times with 0.1 x SSC and 0.1% SDS (5 min 55 °C).

Brown bear libraries were enriched with home-made RNA baits following Richards et al. (Richards et al., 2019). DNA was extracted from two brown bear tissue samples obtained from the University of Alaska Fairbanks Museum (UAM 87948 and UAM 125917) using a Qiagen DNeasy Blood and Tissue kit following manufacturer's protocols. The mitochondrial genomes were then amplified from the two specimens in two long-range PCR fragments of 8-9 kb fragments using primers adapted from Hwang et al. (Hwang et al., 2008), ensuring a T7 promoter sequence was ligated to the 5' end of one primer of each pair. The primer sequences were as follows: fragment 1, S-LA-16S-L-T7: 5'-AATTGTAATACGACTCACTATAGGG GAT GTT GGA TCA GGA CAT CCT AAT GGT GCA-3', H-12193-Leu: 5'-AGT TGC ACC AAT TTT TTG GTT CCT AAG ACC-3', and fragment 2, L-12193-Leu-T7: 5'-AATTGTAATACGACTCACTATAGGG GGT CTT AGG AAC CAA AAA ATT GGT GCA ACT-3', S-LA-16S-H, 5'-TGC ACC ATT AGG ATG TCC TGA TCC AAC ATC-3'. The long-range PCR fragments from both samples were then pooled in equimolar amount and subjected to *in vitro* transcription. The resulting RNA was then fragmented and biotinylated to form completed RNA baits specific to the brown bear mitochondrial genome. Brown bear samples were then enriched for mitochondrial DNA following the same protocol as per the lions but using the homemade RNA baits instead of commercially synthesized baits.

Full-length Illumina sequencing adapters were then added to the enriched libraries via a final round of "off-bead" PCR split into 5 replicate PCRs (25 μ L) containing 1 \times Gold PCR buffer, 2.5 mM MgCl₂, 1 mM dNTPs, 0.5 mM each primer and 0.1 U AmpliTaq Gold. Cycling conditions were as follows: 94 °C for 6 min; 15 cycles of 94 °C for 30 s, 60 °C for 30 s, 72 °C for 45 s; and 72 °C for 10 min. Following PCR, replicates were pooled and purified using AxyPrep™ magnetic beads, eluted in 30 μ L H₂O, and quantified on TapeStation 2200 (Agilent Technologies), using a D1000 ScreenTape assay. Libraries were pooled and sequenced on an Illumina NextSeq using 2 x 75 bp PE (150 cycle) High Output chemistry.

Data processing

Sequenced reads were demultiplexed using SABRE (<https://github.com/najoshi/sabre>) using the unique 5' and 3' barcodes allowing one mismatch in the barcode sequence (-m 1). Demultiplexed reads were then processed through Paleomix v1.2.12 (Schubert et al., 2014). Within Paleomix, adapter sequences were removed and paired end reads merged using ADAPTER REMOVAL v2.1.7 (Schubert, Lindgreen, & Orlando, 2016), trimming low-quality bases (<Phred20 --minquality 4) and discarding merged reads shorter than 25 bp (--minlength 25). Read quality was visualized before and after adapter trimming using fastQC v0.11.5 (<http://www.bioinformatics.babraham.ac.uk/projects/fastqc/>) to ensure efficient adapter removal. Merged reads were mapped against the mitochondrial genome of *Panthera spelaea* (KX258452) and *Ursus arctos* (EU497665) using BWA v0.7.15 (Li & Durbin, 2009) (aln -l 1024 (seed inactivated), -n 0.01, -o 2). Reads with mapping Phred scores less than 25 were removed using SAMTOOLS 1.5 (Li et al., 2009) and PCR duplicates were removed using “paleomix rmdup_collapsed” and MARKDUPLICATES from the Picard package (<http://broadinstitute.github.io/picard/>).

Heterozygous sites were observed across a 7-kb region in multiple *Panthera* samples, presumably as the result of nuclear mitochondrial DNA segments (numts), which are known to be widespread in felids (Kim et al., 2006). To counteract this, we constructed a numt sequence reference by identifying runs of sequences that disagreed with flanking homozygous sequences of the “true” mitochondrial genome. This numt reference was included as an additional scaffold when mapping to the lion mitochondrial genome reference so that reads preferentially mapping to the numt reference could subsequently be excluded from downstream analyses.

Following mapping, reads for all samples were visualized in Geneious Prime v2019.0.4 (<https://www.geneious.com>) and we created a 75% majority consensus sequence, calling N at sites with less than 3x coverage. Subsequent analyses were restricted to specimens with greater than 70% of the mitochondrial genome covered, representing 103 and 39 of the brown bear and lion samples respectively. We also re-analysed published data from one modern brown bear (Liu et al., 2014) and two ancient cave lions (Barnett et al., 2016) through the pipeline described above to produce full mitochondrial genomes (table S4).

2.3 SUPPLEMENTARY INFORMATION

Phylogenetic analysis

Using MUSCLE v3.8.425 (Edgar, 2004) in Geneious Prime v2019.0.4, we aligned the 104 brown bear consensus sequences described above with an additional 46 brown bear and polar bear mitogenomes downloaded from GenBank (table S5). We aligned our lion consensus sequences the same way, thus creating a separate alignment for each taxon (*i.e.*, *Panthera* and *Ursus arctos*). Repetitive regions with poor read mapping were deleted from the control region in both alignments, representing 308 bp in brown bears and 245 bp in lions. The final alignment was 16451 bp for brown bears and 16694 in lions.

Bayesian tip-dating analyses were performed using BEAST 2.6.1 (Bouckaert et al., 2019) on each alignment to co-estimate the tree topology and divergence dates of our sequences. First, PartitionFinder 2.1.1 (Lanfear, Frandsen, Wright, Senfeld, & Calcott, 2016) was used to find the best-fitting partitioning scheme using the Bayesian information criterion, separating the data into 5 partitions for each alignment (table S6). We then evaluated the temporal signal in our dataset using leave-one-out cross-validation (e.g. Stiller et al., 2014), using only the finite-dated specimens (28 lions and 119 brown bears). In sequential analyses we left out and then attempted to estimate the age of each specimen. For all but two of the lion and two of the brown bear specimens, the “true” (radiocarbon) age was within the 95% credibility interval of the estimated age, suggesting that our dataset included sufficient temporal information to estimate the age of undated samples (fig. S1). Consequently, we performed sequential analyses where undated samples were added to the dataset one at a time, in order to estimate their ages (fig. S2). Runs were performed with a strict clock with a uniform prior on rate ($0-10^{-5}$ mutations per site per year), constant population coalescent tree prior with a $1/x$ distribution on population size, a uniform prior (0–500,000) on the age of the sequence being estimated, and run for 30 million steps with sampling every 3000 steps. Some chains were extended to ensure effective sampling sizes near or above 200 for all parameters. The first 10% of samples were discarded as burn-in and parameter values were monitored to check for convergence in Tracer v1.7.1 (Rambaut, Drummond, Xie, Baele, & Suchard, 2018). Once all samples were assigned an age (either based on radiocarbon dating or Bayesian date estimation), we conducted a date-randomization test (Ramsden, Holmes, & Charleston, 2009; Stiller et al., 2014). Runs were conducted as for date estimation but excluding a prior on sequence age. For both datasets the rate estimate of the original data did not overlap the credibility

intervals of the rate estimate from 20 randomized replicates (fig. S3), suggesting that our dataset could be used to reliably estimate evolutionary rate and divergence times.

For the final BEAST analysis, a strict clock was used with a uniform prior on rate ($0-10^{-5}$ mutations per site per year), and a Bayesian skyline coalescent tree prior. We ran three independent MCMC chains, each run for 50 million steps, sampling every 5,000 steps. We checked for convergence and sufficient sampling of parameters in Tracer v1.7.1 (Rambaut et al., 2018) and combined individual runs in LogCombiner, after discarding the first 10% of steps as burn-in. Maximum clade credibility consensus trees were generated in TreeAnnotator using the median node age.

Phylogeographic model testing

The joint-tree epoch analyses used BEAST (Suchard et al., 2018) and identical DNA substitution model settings as above. However, the analysis was set up so that two separate alignments (lions and bears) were encoded in a single common xml file, and two separate trees (lions and bears) were estimated simultaneously during the MCMC. Additionally, clade 2 bears were excluded from the analysis due to a lack of sufficient sampling and introgressed relationship with polar bears (*Ursus maritimus*). Each tip or taxon was coded with an additional binary phylogeographic character (Eastern vs Western Beringia), and the rate of evolution of this character was estimated directly from the data. Two models for the evolution of this character were tested: a strict clock, where rates of evolution were constant through time, and a two-epoch clock, which had two separate rates (interglacial and glacial periods). We ascertained Bayes Factors using both stepping-stone and AICM (Tracer) approaches, but the former values were very unstable across runs (possibly due to poor convergence during some steps), and the values reported in the main text are AICM.

We ran four independent MCMC chains, each run for 20 million steps, sampling every 2,000 steps. We checked for convergence and sufficient sampling of parameters in Tracer v1.7.1 (Rambaut et al., 2018) and combined individual runs using LogCombiner after discarding the first 20% of steps as burn-in. Maximum clade credibility consensus trees were generated in TreeAnnotator using the median node age (fig. S6).

2.3 SUPPLEMENTARY INFORMATION

Table S1 : Information on brown bear bone and tooth samples analysed. New radiocarbon dates are highlighted in red.

ICAD#	Genetic ID	Museum	Museum/Field Accession	Country	Site	Latitude	Longitude	Sample Type	Carbon Date	Reference	Calibrated Median	Calibrated Sigma	Estimated Age	Standard Deviation	Labeltype	Extraction Method	Reeds	Coverage	Depth of Coverage	
95	Ursus arctos	Institute of Plant and Animal Ecology of Plant and Animal	IPAE 719/44/9	Russia	Boduchingy cave	58.10	57.44	Phalange	5329±24	OxA-35018	537	29			3a	Prenol-dihorform	7605 ±0.99	0.99	331.45	
97	Ursus arctos	Institute of Plant and Animal Ecology	IPAE 871/1	Russia	Ukhu-Tsai cave	55.33	57.70	Humerus	8900±45	OxA-37456	10031	94			3a	Prenol-dihorform	36902 ±0.99	0.99	135.94	
99	Ursus arctos	Institute of Plant and Animal Ecology	IPAE 107/06	Russia	Shataniky cave	60.42	60.22	Tooth	798±25	OxA-35019	711	19			3a	Prenol-dihorform	9925 ±0.99	0.99	503.91	
102	Ursus arctos	Institute of Plant and Animal Ecology	IPAE 621/9	Russia	Shataniky cave	60.42	60.22	Tooth	809±25	OxA-35017	716	22			3a	Prenol-dihorform	82297 ±0.99	0.99	341.22	
131	Ursus arctos	Zoological Museum of Moscow University	MMZ S-66/59	Russia	Pechoro-Itych Nature Reserve, Female	62.40	58.93	Bone							3a	Prenol-dihorform	511021 ±0.99	0.99	2865	
132	Ursus arctos	Zoological Museum of Moscow University	MMZ S113733	Russia	Evenkia Vannara	60.33	102.27	Bone							3a	Prenol-dihorform	293378 ±0.99	0.99	1791.69	
133	Ursus arctos	Zoological Museum of Moscow University	MMZ S86/62	Russia	Pechora-Itych Nature Reserve, Ervons Poyntis, Bannov-Balte gural	62.40	58.93	Bone							3a	Prenol-dihorform	81079 ±0.99	0.99	423.05	
134	Ursus arctos	Zoological Museum of Moscow University	MMZ S34946	Russia	province Dagestan, Stavropol, Cherdnyy	42.84	34.84	Bone							3a	Prenol-dihorform	865643 ±0.99	0.99	20.33	
137	Ursus arctos	Zoological Museum of Moscow University	MMZ S22359	Russia	Caucasian Biosphere Nature Reserve, Pskakhi Mt., Kisha	43.84	40.40	Bone							3a	Prenol-dihorform	81228 ±0.99	0.99	438.26	
138	Ursus arctos	Zoological Museum of Moscow University	MMZ S23499	Russia	Krasnoyarsk region, Mana river, Targa forests	55.84	92.74	Bone							3b	Prenol-dihorform	10425 ±0.99	0.99	36.34	
139	Ursus arctos	Zoological Museum of Moscow University	MMZ S80149	Russia	Kurali lakes	46.50	151.50	Bone							3a	Prenol-dihorform	7765 ±0.99	0.99	42.81	
140	Ursus arctos	Zoological Museum of Moscow University	MMZ S2073	Russia	Volgula province, Velik district	61.06	42.12	Bone							3a	Prenol-dihorform	492693 ±0.99	0.99	3025.29	
141	Ursus arctos	Zoological Museum of Moscow University	MMZ S13195	Russia	Kamchatka	56.11	159.60	Bone							3a	Prenol-dihorform	135816 ±0.99	0.99	602.99	
142	Ursus arctos	Zoological Museum of Moscow University	MMZ S34945	Russia	Selenge, Kirovsk (Momonak), Mide	67.62	33.63	Bone							3a	Prenol-dihorform	90183 ±0.99	0.99	376.53	
144	Ursus arctos	Zoological Museum of Moscow University	MMZ S3007	Mongolia	Rusuan-Chinese border, upper Kosogol Lake	51.64	100.51	Bone							3a	Prenol-dihorform	2414	0.99	16.25	
145	Ursus arctos	Zoological Museum of Moscow University	MMZ S8039	Russia	Okhotsk region, Barguzina	60.00	142.00	Bone							3a	Prenol-dihorform	82063 ±0.99	0.99	478.93	
146	Ursus arctos	Zoological Museum of Moscow University	MMZ S1373	Russia	Kamchatka	56.11	159.60	Bone							3a	Prenol-dihorform	2975 ±0.99	0.99	12.27	
148	Ursus arctos	Zoological Museum of Moscow University	MMZ S14933	Russia	Bakala lake, Barguzin Nature Reserve	54.45	109.86	Bone							3a	Prenol-dihorform	3284 ±0.99	0.99	10.81	
149	Ursus arctos	Zoological Museum of Moscow University	MMZ S29248	Russia	Erisei River, Verkhnyy Inzhak River	62.97	88.55	Bone							3a	Prenol-dihorform	809144 ±0.99	0.99	5632.18	
150	Ursus arctos	Zoological Museum of Moscow University	MMZ S86341	Russia	Pechoro-Itych Nature Reserve	62.40	58.93	Bone							3a	Prenol-dihorform	477252 ±0.99	0.99	2954.12	
151	Ursus arctos	Zoological Museum of Moscow University	MMZ S84887	Russia	Yakutia, Elgyey settlement, Babloy Shamur Island, Radukhyi cape	67.55	134.63	Bone							3a	Prenol-dihorform	26672 ±0.99	0.99	140.07	
152	Ursus arctos	Zoological Museum of Moscow University	MMZ S34934	Russia	Yakutia, Elgyey settlement	54.93	137.50	Bone							3a	Prenol-dihorform	1275410 ±0.99	0.99	6975.11	
153	Ursus arctos	Zoological Museum of Moscow University	MMZ S84888	Russia	Yakutia, Elgyey settlement	67.55	134.63	Bone							3a	Prenol-dihorform	363100 ±0.99	0.99	2449.86	
154	Ursus arctos	Zoological Museum of Moscow University	MMZ S22367	Russia	Caucasian Biosphere Nature Reserve, Dugluge Mt., Kosoy meadow	43.84	40.40	Bone							3a	Prenol-dihorform	19051 ±0.99	0.99	106.04	
155	Ursus arctos	Zoological Museum of Moscow University	MMZ S34938	Russia	Usury Region	43.66	132.51	Bone							3b	Prenol-dihorform	90939 ±0.99	0.99	252.81	
156	Ursus arctos	Zoological Museum of Moscow University	MMZ S34972	Mongolia	Alai Mountains	48.00	99.00	Bone							3b	Prenol-dihorform	705894 ±0.99	0.99	3987.31	
164	Ursus arctos	Zoological Museum of Moscow University	MMZ S34955	Russia	Krasnoyarsk region, Ayinsk district	50.94	114.53	Bone							3a	Prenol-dihorform	5713 ±0.99	0.99	27.82	
165	Ursus arctos	Zoological Museum of Moscow University	MMZ S159009	Russia	Magadan province, upper stream of Anzhyr river, Baluganik river	64.93	168.58	Bone							3a	Prenol-dihorform	102099 ±0.99	0.99	607.19	
166	Ursus arctos	Zoological Museum of Moscow University	MMZ S14939	Russia	Nlt, Caucasus Chechya.	42.72	45.46	Bone							3a	Prenol-dihorform	4047 ±0.99	0.99	30.89	
167	Ursus arctos	Zoological Museum of Moscow University	MMZ S1396	Russia	Kamchatka	56.11	159.60	Bone							3a	Prenol-dihorform	653583 ±0.99	0.99	3816.37	
168	Ursus arctos	Zoological Museum of Moscow University	MMZ S34928	Russia	Shataniky cave	54.93	137.50	Bone							3a	Prenol-dihorform	503051 ±0.99	0.99	2720.40	
169	Ursus arctos	USFPA	AK-574-148	USA	Prince of Wales Island	55.65	-132.59	L. femur of juvenile	9929±59	AA-10451	11509	178			2a	Prenol-dihorform	29222 ±0.99	0.99	108.37	
171	Ursus arctos	Canadian Museum of Nature	CNMS 29005	Canada	Dawson area Loc. 1, Sulphur Creek	63.77	138.59	L. tibia distal end	9983±37	OxA-38823	11482	102			2b	Prenol-dihorform	15138 ±0.99	0.99	166.77	
172	Ursus arctos	Canadian Museum of Nature	HK-98-1005	USA (Alaska)	North Slope - Igloodah River	70.81	-154.44	Humerus	50310±80	?	40899	721			3b	Silica	48 ±0.1	0.19	60.19	
173	Ursus arctos	Canadian Museum of Nature	CNMS 38279	Canada	Skyprite, Loc. 3	63.99	-140.78	Humerus	50500±150	Bm-16162	41044	1046			2c	Low DNA Silica	76905 ±0.99	0.99	302.55	
174	Ursus arctos	University of Alaska Museum of Natural History	V-55-58	Canada	Skyprite, Loc. 3	63.99	-140.78	Phalange							2c	Silica	1830 ±0.2296485	7.84	7.84	
176	Ursus arctos	University of Alaska Museum of Natural History	F-AM 9534	USA (Alaska)	Goldstream	64.96	-141.62	R. humerus	41787±212	?	45182	236			3c	Silica	37401 ±0.99	0.99	146.18	
177	Ursus arctos	University of Alaska Museum of Natural History	?	Canada	Prince Edward Island	46.37	-63.36	Bone							3c	Prenol-dihorform	2109 ±0.7541431	9.55	9.55	
180	Ursus arctos	USA	FAM 9564 A-4393812	USA (Alaska)	Skyprite Creek	63.83	-141.99	Metatarsal III							Low DNA Silica		117 ±0.1	0.38		
182	Ursus arctos	USA	CNMS 42381, 582 UCCLA	USA	Skyprite, Loc. 4	64.93	-140.78	R. ulna	35970±660	CAMS 51808	40599	658			4	Silica	143149 ±0.99	0.99	550.88	
184	Ursus arctos	University of Kansas	KU 88497	USA	Kansas R. Bonner Springs	39.04	-94.89	Cranium							4	U. anstranum Silica	1206	0.48	5.49	
187	Ursus arctos	Canadian Museum of Nature	CNMS 28972	USA (Alaska)	Dawson area Loc. 17 Sulphur Creek	63.76	-138.83	R. radius	13760±50	CAMS 54128	16628	129			3b	Prenol-dihorform	124720 ±0.99	0.99	493.07	
189	Ursus arctos	University of Kansas	KU 27034	Canada	Bonneson	65.75	-113.88	R. tibia							3b	Silica	1885.23 ±0.99	0.99	154.1	
190	Ursus arctos	University of Kansas	AK-370A-30A-0	USA	Prince of Wales Island	55.65	-132.59	L. femur fragment	413 ± 22	OxA-38828	401	37			U. anstranum Silica	26100	0.83	103.09		
192	Ursus arctos	Canadian Museum of Nature	CNMS 46448	USA	Prince of Wales Island	55.65	-132.59	Tooth							4	Prenol-dihorform	312011 ±0.99	0.99	1499.64	
193	Ursus arctos	University of Kansas	KU 42725	Canada	Skyprite, Loc. 3	63.99	-140.78	R. ulna							3c	Silica	18261 ±0.99	0.99	102.88	
195	Ursus arctos	University of Kansas	CNMS 33965	USA	Northrup Top Cave, Wyoming	44.97	-108.19	Phalange							3c	Silica	95503 ±0.99	0.99	337.31	
198	Ursus arctos	Canadian Museum of Natural History	FAM 9599 A-6514222	Canada	Dawson area Loc. 16 Hunter Creek	63.95	-138.90	Mandible	41000 ± 1050	Bm-16159	44610	992			3c	Prenol-dihorform Silica	5840.32	0.99	52.17	
288	Ursus arctos	Canadian Museum of Natural History	FAM 9599 A-6514222	USA (Alaska)	Cold Hill	64.88	-147.98	R. ramus							3b	Silica	2477.53 ±0.99	0.99	45.88	
																				30.42

Table S1 cont.

NCAB#	Genetic ID	Museum	Museum Field Accession	Country	Site	Latitude	Longitude	Sample Type	Carbon Date	Reference	Calibrated Median	Calibrated Sigma	Estimated Age	Standard Deviation	Haplotype	Extraction Method	Reads	Coverage*	Depth of	
290	Ursus arctos	American Museum of Natural History	FAM 95641 A-203-8241	USA (Alaska)	Engineer Creek	64.92	-147.62	Ribula	11940±100	OXA-9798	13781	135	54367.78	4311.62	3b	Silica	7515	~0.99	33.07	
293	Ursus arctos	American Museum of Natural History	FAM 95640	USA (Alaska)	Cripple Ck	64.83	-147.99	bone	>53900	OXA-9861			54367.78	4311.62	3c	Silica	24387	~0.99	1053.21	
295	Ursus arctos	American Museum of Natural History	FAM 95666 A-340-2949	USA (Alaska)	Cripple Ck	64.83	-147.99	Ulna	47100±3100	OXA-9260	Out of bounds		51187.53	2381.63	3c	Silica	3034	0.98	11.95	
298	Ursus arctos	American Museum of Natural History	FAM 95602 A-576-3445	USA (Alaska)	Cripple Creek camp	64.83	-147.99	R. mandible					95146.10	15633.49	2c	Silica	3420	0.98	12.91	
299	Ursus arctos	American Museum of Natural History	FAM 95648 A-340-8835	USA (Alaska)	Engineer Creek	64.92	-147.62	metatarsal V					56453.99	8979.90	2c	Silica	1960	0.12	0.71	
300	Ursus arctos	American Museum of Natural History	FAM 95657 A-386-4550	USA (Alaska)	Cripple Creek	64.83	-147.99	ibula					54994.91	4570.22	3c	Silica	33637	1	127.96	
301	Ursus arctos	American Museum of Natural History	FAM 30770-F	USA (Alaska)	Goldstream	64.96	-147.62	radius	50800±1900	OXA-9767	51315	2293	49763.79	2875.13	3c	Silica	16073	~0.99	73.73	
302	Ursus arctos	American Museum of Natural History	FAM 95605	USA (Alaska)	Lower Goldstream	64.96	-147.62	r. manus	35295.40	35295.40	6268.65	3c	Silica	48390.55	7437.73	3c	Silica	7865	0.99	25.41
303	Ursus arctos	American Museum of Natural History	FAM 95607	USA (Alaska)	Cripple Creek	64.83	-147.99	ibula	48390.55	48390.55	7437.73	3c	Silica	48390.55	7437.73	3c	Silica	7865	0.99	25.41
304	Ursus arctos	American Museum of Natural History	FAM 95651 A-653-5316	USA (Alaska)	Gold Hill	64.85	-147.98	ibula					49763.79	2875.13	3c	Silica	433	0.33	1.23	
305	Ursus arctos	American Museum of Natural History	FAM 95603 A-439-3806	USA (Alaska)	Cripple Creek	64.83	-147.99	r. manus					54994.91	4570.22	3c	Silica	5271	0.99	21.49	
306	Ursus arctos	American Museum of Natural History	FAM 95671	USA (Alaska)	Goldstream, Banks near Fox	64.96	-147.62	ibula	50800±1900	OXA-9767	51315	2293	49763.79	2875.13	3c	Silica	114416	~0.99	444.6	
307	Ursus arctos	American Museum of Natural History	FAM 95670	USA (Alaska)	Cripple Creek	64.83	-147.99	bone					54994.91	4570.22	3c	Silica	5271	0.99	21.49	
308	Ursus arctos	American Museum of Natural History	FAM 95657	USA (Alaska)	Engineer Creek	64.92	-147.62	ibula	19360±140	OXA-10036	23313	194	22326.03	3532.23	3b	Silica	16966.83	~0.99	238.44	
309	Ursus arctos	American Museum of Natural History	FAM 30421	USA (Alaska)	Fairbanks area	65.00	-147.00	r. manus					22326.03	3532.23	3b	Silica	57280	~0.99	47.99	
310	Ursus arctos	American Museum of Natural History	FAM 95596 A-255-6946	USA (Alaska)	Goldstream	64.96	-147.62	r. manus					16966.83	2726.69	3b	Silica	13057	~0.99	779.87	
311	Ursus arctos	American Museum of Natural History	FAM 95601 A-528-4149	USA (Alaska)	Cripple Creek	64.83	-147.99	r. manus	36137±783	AA-17509	40742	741	43387.77	4123.84	3c	Silica	12491	0.99	399.46	
312	Ursus arctos	American Museum of Natural History	FAM 95612 A-199-8654	USA (Alaska)	Engineer Creek	64.84	-147.96	knob	10015±62	AA-17506	11512	141	43387.77	4123.84	3c	Silica	98774	~0.99	22.17	
314	Ursus arctos	American Museum of Natural History	FAM 95600 A-200-4347	USA (Alaska)	Lower Eldorado Creek	65.06	-147.53	r. manus					43387.77	4123.84	3c	Silica	5500	0.9718327	22.17	
316	Ursus arctos	American Museum of Natural History	FAM 95595 A-200-6671B	USA (Alaska)	Goldstream	64.96	-147.62	r. manus	12441±75	AA-17508	14571	219	49589.29	2930.01	3c	Silica	3032	0.97110423	13.56	
317	Ursus arctos	American Museum of Natural History	FAM 95602 A-386-4544	USA (Alaska)	Cripple Creek	64.83	-147.99	ibula	> 45600	OXA-38835			111490.00	17390.44	2c	Silica	1058	0.73232775	3.39	
318	Ursus arctos	American Museum of Natural History	FAM 95653	USA (Alaska)	Goldstream	64.96	-147.62	ibula					111490.00	17390.44	2c	Silica	148	0.11	0.53	
320	Ursus arctos	American Museum of Natural History	FAM 95642 A-425	USA (Alaska)	Esler Ck	64.84	-147.96	tearur	14150±90	OXA-9262	17224	148	91587	~0.99	3b	Silica	91587	~0.99	426.96	
322	Ursus arctos	American Museum of Natural History	FAM 95640 A-458-1545	USA (Alaska)	Gold Hill	64.85	-147.98	Ulna	15830±100	OXA-9263	18650	107	12552	~0.99	3b	Silica	12552	~0.99	75	
329	Ursus arctos	Canadian Museum of Nature	CN 97056	Canada	Caribou Ck, Dawson	63.83	-128.82	R. ulna	2296 ± 39	OXA-9288			161771	~0.99	3c	Silica	161771	~0.99	665.59	
328	Ursus arctos	American Museum of Natural History	FAM 95630	USA (Alaska)	Lower Goldstream	64.96	-147.62	R. manus	14980±60	CMMS-51805	18204	101	82616.42	9943.96	2c	Silica	101779	~0.99	382.79	
331	Ursus arctos	University of Alaska Museum of Natural History	AMNH 30422	USA (Alaska)	Edmonton	65.00	-147.00	r. manus	19027±132	AA-17507	22309	195	8076.72	9943.96	2c	Silica	101779	~0.99	382.79	
333	Ursus arctos	University of Alaska Museum of Natural History	V-55-583	USA (Alaska)	Edmonton	65.00	-147.00	r. manus	42900 ± 1700	OXA-38832	46566	1530	82616.42	9943.96	2c	Silica	101779	~0.99	382.79	
341	Ursus arctos	Clarendon Museum	CMCVP 8866 9001 932-20	USA (Alaska)	Shredan Cave	70.81	-154.41	Humans	> 52500	OXA-38831	31064	122	78288.60	10208.43	4	Silica	20247	0.8829685	83.98	
342	Ursus arctos	University of Alaska Museum of Natural History	IK-01-112	USA (Alaska)	North Slope - Iipipuk River	70.81	-154.41	Humans	27020 ± 190	OXA-38821	31064	122	78288.60	10208.43	4	Silica	20247	0.8829685	83.98	
407	Ursus arctos	PNM	3657-153	Canada	Indigarka area	70.38	-113.58	Mandible	30660±180	OXA-12912	34600	187	13393.18	3128.03	2a	Pheno-chloroform	1888	0.9718327	7.92	
1672	Ursus arctos	Philo Canada	GPD7D16-T10-A-259	Canada	Gaudi Don 1, Haida Gwaii	52.44	-141.77	vertebra	12.085±30	OXA-14944	13387	76	14708.50	2847.24	2a	Pheno-chloroform	37833	~0.99	200.25	
1673	Ursus arctos	Philo Canada	GPD8A6-61128	Canada	Gaudi Don 1, Haida Gwaii	52.44	-141.77	vertebra	12.085±30	OXA-14944	13387	76	14708.50	2847.24	2a	Pheno-chloroform	37833	~0.99	200.25	
1674	Ursus arctos	Philo Canada	72A15-83500_DBI	Canada	Gaudi Don 1, Haida Gwaii	52.44	-141.77	vertebra	12.250 ± 30	OXA-9288	14322	60	14708.50	2847.24	2a	Pheno-chloroform	49487	~0.99	228.71	
1675	Ursus arctos	Philo Canada	GDP786-471	Canada	Gaudi Don 1, Haida Gwaii	52.44	-141.77	bone	12.205±40	OXA-9288	14697	66	14708.50	2847.24	2a	Pheno-chloroform	41723	~0.99	207.50	
1676	Ursus arctos	Philo Canada	GDP786-471	Canada	Gaudi Don 1, Haida Gwaii	52.44	-141.77	bone	12.205±40	OXA-9288	14697	66	14708.50	2847.24	2a	Pheno-chloroform	41723	~0.99	207.50	
1677	Ursus arctos	Philo Canada	GDP786-471	Canada	Gaudi Don 1, Haida Gwaii	52.44	-141.77	bone	12.205±40	OXA-9288	14697	66	14708.50	2847.24	2a	Pheno-chloroform	41723	~0.99	207.50	
1678	Ursus arctos	Philo Canada	GDP786-471	Canada	Gaudi Don 1, Haida Gwaii	52.44	-141.77	bone	12.205±40	OXA-9288	14697	66	14708.50	2847.24	2a	Pheno-chloroform	41723	~0.99	207.50	
1679	Ursus arctos	Philo Canada	GDP786-471	Canada	Gaudi Don 1, Haida Gwaii	52.44	-141.77	bone	12.205±40	OXA-9288	14697	66	14708.50	2847.24	2a	Pheno-chloroform	41723	~0.99	207.50	
1680	Ursus arctos	Philo Canada	GDP786-471	Canada	Gaudi Don 1, Haida Gwaii	52.44	-141.77	bone	12.205±40	OXA-9288	14697	66	14708.50	2847.24	2a	Pheno-chloroform	41723	~0.99	207.50	
1681	Ursus arctos	Philo Canada	GDP786-471	Canada	Gaudi Don 1, Haida Gwaii	52.44	-141.77	bone	12.205±40	OXA-9288	14697	66	14708.50	2847.24	2a	Pheno-chloroform	41723	~0.99	207.50	
1682	Ursus arctos	Philo Canada	GDP786-471	Canada	Gaudi Don 1, Haida Gwaii	52.44	-141.77	bone	12.205±40	OXA-9288	14697	66	14708.50	2847.24	2a	Pheno-chloroform	41723	~0.99	207.50	
1683	Ursus arctos	Philo Canada	GDP786-471	Canada	Gaudi Don 1, Haida Gwaii	52.44	-141.77	bone	12.205±40	OXA-9288	14697	66	14708.50	2847.24	2a	Pheno-chloroform	41723	~0.99	207.50	
1684	Ursus arctos	Philo Canada	GDP786-471	Canada	Gaudi Don 1, Haida Gwaii	52.44	-141.77	bone	12.205±40	OXA-9288	14697	66	14708.50	2847.24	2a	Pheno-chloroform	41723	~0.99	207.50	
1685	Ursus arctos	Philo Canada	GDP786-471	Canada	Gaudi Don 1, Haida Gwaii	52.44	-141.77	bone	12.205±40	OXA-9288	14697	66	14708.50	2847.24	2a	Pheno-chloroform	41723	~0.99	207.50	
1686	Ursus arctos	Philo Canada	GDP786-471	Canada	Gaudi Don 1, Haida Gwaii	52.44	-141.77	bone	12.205±40	OXA-9288	14697	66	14708.50	2847.24	2a	Pheno-chloroform	41723	~0.99	207.50	
1687	Ursus arctos	Philo Canada	GDP786-471	Canada	Gaudi Don 1, Haida Gwaii	52.44	-141.77	bone	12.205±40	OXA-9288	14697	66	14708.50	2847.24	2a	Pheno-chloroform	41723	~0.99	207.50	
1688	Ursus arctos	Philo Canada	GDP786-471	Canada	Gaudi Don 1, Haida Gwaii	52.44	-141.77	bone	12.205±40	OXA-9288	14697	66	14708.50	2847.24	2a	Pheno-chloroform	41723	~0.99	207.50	
1689	Ursus arctos	Philo Canada	GDP786-471	Canada	Gaudi Don 1, Haida Gwaii	52.44	-141.77	bone	12.205±40	OXA-9288	14697	66	14708.50	2847.24	2a	Pheno-chloroform	41723	~0.99	207.50	
1690	Ursus arctos	Philo Canada	GDP786-471	Canada	Gaudi Don 1, Haida Gwaii	52.44	-141.77	bone	12.205±40	OXA-9288	14697	66	14708.50	2847.24	2a	Pheno-chloroform	41723	~0.99	207.50	
1691	Ursus arctos	Philo Canada	GDP786-471	Canada	Gaudi Don 1, Haida Gwaii	52.44	-141.77	bone	12.205±40	OXA-9288	14697	66	14708.50	2847.24	2a	Pheno-chloroform	41723	~0.99	207.50	
1692	Ursus arctos	Philo Canada	GDP786-471	Canada	Gaudi Don 1, Haida Gwaii	52.44	-141.77	bone	12.205±40	OXA-9288	14697	66	14708.50	2847.24	2a	Pheno-chloroform	41723	~0.99	207.50	
1693	Ursus arctos	Philo Canada	GDP786-471	Canada	Gaudi Don 1, Haida Gwaii	52.44	-141.77	bone	12.205±40	OXA-9288	14697	66	14708.50	2847.24	2a	Pheno-chloroform	41723	~0.99	207.50	
1694	Ursus arctos	Philo Canada	GDP786-471	Canada	Gaudi Don 1, Haida Gwaii	52.44	-141.77	bone												

Table S1 cont.

ACAD#	Genetic ID	Museum	Museum/Field Accession	Country	Site	Latitude	Longitude	Sample Type	Carbon Date	Reference	Calibrated Method	Calibrated Span	Estimated Age	Standard Deviation	Haplotype	Extension Method	Reads	Coverage ^a	Depth of Coverage
1944	Ursus arctos	Institute of Archaeology Russian Academy of Sciences		Russia	Altai, Razboyniyya Cave	51.30	84.47	Uina	13925±40	UCIAMS-56994	16886	112	102290.00	18882.00	3b	Phenol-chloroform	76173	<0.99	315.37
1945	Ursus arctos	Russian Academy of Sciences		Russia	Altai, Razboyniyya Cave	51.30	84.47	Uina	15370±100	UCIAMS-56995	18641	108			3b	Phenol-chloroform	375299	<0.99	1959.65
1946	Ursus arctos	Institute of Archaeology Russian Academy of Sciences		Russia	Altai, Razboyniyya Cave	51.30	84.47	Uina	13830±40	UCIAMS-56996	16738	118			3b	Phenol-chloroform	108549	<0.99	442.22
4098	Ursus arctos	Field collected	MMN N18	Russia	Caucasus Mountains	44.17	40.00	Long bone fragment	42,900±1600	CURL-10273	46549	1481			3a	Phenol-chloroform	16466	<0.99	60.92
5390	Ursus arctos	Museum of Natural History Vietnam	VNHN 40604	Russia	Kamchatka	56.11	159.60	top right incisor	Historic collected 1878-1883						3a	Phenol-chloroform	74827	<0.99	421.68
5391	Ursus arctos	Museum of Natural History Vietnam	VNHN 40648	Russia	Kamchatka	56.11	159.60	top right I3	Historic collected 1878-1883						3a	Phenol-chloroform	173669	<0.99	1209.16
5392	Ursus arctos	Museum of Natural History Vietnam	VNHN 40627	Russia	Kamchatka	56.11	159.60	bottom left 1st molar	Historic collected 1878-1883						3a	Phenol-chloroform	45993	<0.99	243.18
5393	Ursus arctos	Museum of Natural History Vietnam	VNHN 40601	Russia	Kamchatka	56.11	159.60	bottom right 1st molar	Historic collected 1878-1883						3a	Phenol-chloroform	101794	<0.99	450.65
5394	Ursus arctos	Field collected	VNHN 40626	Russia	Kamchatka	56.11	159.60	bottom left 1st incisor	Historic collected 1878-1883						3a	Phenol-chloroform	71664	<0.99	429.94
5568	Ursus arctos		OK-01719	USA	Wales Island	56.33	-133.59	Tooth							Low DNA	Phenol-chloroform	12	<0.1	0.06
5569	Ursus arctos		OK-01725	USA	Wales Island	56.33	-133.59	Tooth							U. americanus	Phenol-chloroform	14	<0.1	0.06
5570	Ursus arctos		OK-10826	USA	Wales Island	56.33	-133.59	Tooth							U. americanus	Phenol-chloroform	124		0.56
5571	Ursus arctos		OK-19677	USA	Wales Island	56.33	-133.59	Tooth							Low DNA	Phenol-chloroform	55	<0.1	0.28
5572	Ursus arctos		OK-19730	USA	Wales Island	56.33	-133.59	Tooth							U. americanus	Phenol-chloroform	19	<0.1	0.06
5573	Ursus arctos		OK-13482	USA	Wales Island	56.33	-133.59	Tooth							U. americanus	Phenol-chloroform	230		0.88
5883	Ursus arctos		DDR00371	China	Dananglong Cave	41.68	125.277	Tooth	< 47000	ONA-38854	48293	1247	102290.00	18882.00	4	Phenol-chloroform	3716	0.96539792	12.77
5889	Ursus arctos		07HGXC	China	Zhen, Luobing	40.38	122.971	Tooth	46100 ± 2600	ONA-38852	48293	1247	102290.00	18882.00	3b	Silica	10440	0.99	36.77

^aProportion of mtDNA regions covered in consensus sequence

Table S1: Information on brown bear bone and tooth samples analysed. New radiocarbon dates are highlighted in red.

Table S2: Information on lion bone and tooth samples analysed. New radiocarbon dates are highlighted in red.

ACAD#	Genetic ID	Museum	Museum/Field	Country	Site	Latitude	Longitude	Sample Type	Carbon Date	Reference	Calibrated median	Calibrated sigma	Estimated Age	Standard Deviation	Extraction Method	Reads	Coverage ^a	Depth of Coverage
1796	Parthena splenda	American Museum of Natural History	FAM 95666	USA (Alaska)	Franks Ave	63.00	-147.00	Radius	> 51500	OK-A-38851	22108	133	14726.0	1763.3	Silica	21847	0.99	65.38
1816	Parthena atrox	Canadian Museum of Nature	CMN 46739	Canada	St. Mary's	63.99	-140.78	R. radius	48000 ± 3200	OK-A-38819	13750	109	66680.3	8343.2	Silica	27310	0.99	76
3226	Parthena splenda	American Museum of Natural History	FAM 13754	Canada	Fox Gulch	63.62	-139.35	bone	OK-A-38819	Out of bounds	14815	215	47317.2	2672.2	Silica	42717	0.99	138.38
3326	Parthena splenda	Canadian Museum of Nature	CMN 44433	Canada	Dixon - Dominion Loc 50	64.84	-138.71	R. femur	33620 ± 530	OK-A-38820	19279	115	15601.4	1864.2	Silica	616	0.73	2.56
3326	Parthena splenda	Canadian Museum of Nature	CMN 44433	Canada	Big Delta D-6	64.84	-146.92	bone	20240 ± 110	OK-A-37750	24313	147	23340.6	1215.3	Silica	209274	0.99	611.4
3346	Parthena splenda	UAF/Philo	AK-326-Y-1	USA (Alaska)	LoonChien Creek	64.05	-141.88	R. tibia	OK-A-37750	24313	24313	157	157	157	Silica	4	<0.1	0.01
3083	Parthena atrox	University of New Mexico	UNM 41.62	USA	Islen Cave No.1, New Mexico	34.88	-106.88	Phalange	OK-A-37750	24313	24313	157	25340.6	1215.3	Phenol-chloroRf	21998	0.99	60.72
5178	Parthena atrox	University of Kansas	KU 38992	USA	Natural Trap Cave, Wyoming	44.97	-108.19	Humerus	18.240±90	OK-A-10084	22108	133	179675	1215.3	Phenol-chloroRf	375	0.99	1.12
5180	Parthena, low quality DNA	University of Kansas	KU 44000	USA	Natural Trap Cave, Wyoming	44.97	-108.19	Humerus	OK-A-10080	OK-A-10080	13750	109	179675	1215.3	Phenol-chloroRf	375	>0.99	509.49
5183	Parthena splenda	American Museum of Natural History	FAM 69016	USA	Gold Hill, Alaska	64.85	-147.96	Ramus	11.925±70	OK-A-10080	13750	109	179675	1215.3	Phenol-chloroRf	71690	>0.99	509.49
5186	Parthena splenda	American Museum of Natural History	FAM 69044	USA	Franks Creek, Alaska	64.96	-147.62	Humerus	12.540±75	OK-A-10081	14815	215	14815	5091.8	Silica	98051	0.99	193.89
5187	Parthena splenda	American Museum of Natural History	FAM 69094	USA	Lower Goldstream, Alaska	64.32	-146.35	Ramus	15.975±65	OK-A-13832	19279	115	19279	111	Phenol-chloroRf	31991	0.99	78.97
5191	Parthena splenda	American Museum of Natural History	FAM 30757	USA	Franks Creek, Alaska	64.84	-146.35	Ramus	12.090±80	OK-A-13451	19320	108	19320	111	Phenol-chloroRf	11138	0.98	26.89
5193	Parthena splenda	American Museum of Natural History	FAM 69167	USA	Franks Creek, Alaska	65.07	-147.17	Ulna	16.005±65	OK-A-13834	21675	147	21675	5418	Phenol-chloroRf	5418	0.97	14.19
5195	Parthena splenda	American Museum of Natural History	FAM 69139	USA	Franks Creek, Alaska	65.07	-147.17	Ulna	17.890±100	OK-A-13452	21675	147	21675	37210	Phenol-chloroRf	37210	0.99	100.42
5199	Parthena splenda	American Museum of Natural History	FAM 69138	USA	Franks Creek, Alaska	65.07	-147.17	Ulna	12.450±60	OK-A-12901	14857	203	14857	255928	Phenol-chloroRf	255928	>0.99	767.67
5216	Parthena splenda	St. Petersburg Institute of Zoology	29421 (2)	Russia	Lena River	72.50	127.50	Humerus	38.650±600	OK-A-10087	42677	445	42677	5525.0	Phenol-chloroRf	15310	0.97	36.51
5252	Parthena splenda	Kellogg Institute of Zoology	6857	Poland	Wrzeszowska Gorna	50.17	19.81	Tibia	12.525±50	OK-A-13833	14809	183	14809	4639.5	Silica	341964	>0.99	1027.38
5252	Parthena splenda	Russian Academy of Sciences	153-003	Russia	Arga-Y wekhi River	62.20	146.78	Ulna	27.950±140	OK-A-13833	31659	226	31659	38768	Phenol-chloroRf	38768	>0.99	100.29
5271	Parthena splenda	Phenological Institute Moscow	3020-073	Russia	Berzovinka River	68.00	156.00	Ulna	13.770±55	OK-A-13835	16646	133	16646	69638.1	Phenol-chloroRf	169323	>0.99	520.83
5272	Parthena splenda	Phenological Institute Moscow	3020-073	Russia	Alzeya River	70.85	153.70	Radius	>61,500	OK-A-13829	54556	2128	69638.1	5525.0	Phenol-chloroRf	95921	>0.99	257.58
5273	Parthena splenda	Phenological Institute Moscow	3752-024A	Russia	Dumany Yar	68.62	159.13	Femur	>80,600	OK-A-13023	54556	2128	82240.1	7270.5	Phenol-chloroRf	233765	>0.99	745.47
5274	Parthena splenda	Phenological Institute Moscow	3915-121	Russia	Khomsbaya G.Oba, Khapchubinsky	71.83	145.88	Femur	54.100±1800	OK-A-13023	54556	2128	82240.1	7270.5	Phenol-chloroRf	233765	>0.99	745.47
5275	Parthena splenda	Phenological Institute Moscow	3916-162	Russia	Kenshoia River, Loc. 6	60.08	139.90	Radius	46.200±1500	OK-A-13024	48860	901	66209.0	4639.5	Phenol-chloroRf	4719	0.98	13.54
5276	Parthena splenda	Moscow State University	772-095/1341	Russia	Dumany Yar, Loc. 1341	68.62	159.13	Calcaneus	>53,200	OK-A-13022	48860	901	66209.0	4639.5	Phenol-chloroRf	178970	0.99	486.68
5278	Parthena splenda	IPF	DX/62002	Russia	Dumany Yar	68.62	159.13	Mandibula	28.720±160	OK-A-12981	32859	295	28720	28260	Silica	28260	0.99	76.89
5283	Parthena splenda	Natural History Museum Stuttgart	99995-2_SIB01	Germany	Syltchenbach	48.65	9.05	Calcaneus	>48,100	OK-A-15354	54556	2128	82240.1	7270.5	Phenol-chloroRf	14434	0.98	33.44
5298	Parthena splenda	Russian Academy of Sciences	BI-0415-L	Russia	Radolny Lakhovskiy Island	73.32	141.37	Tibia	>62,100	OK-A-13837	33278	370	66686.3	5876.3	Phenol-chloroRf	14434	0.98	33.44
5310	Parthena atrox	Royal Alberta Museum	P94.1.672	Canada	Consolidated nr 48 Edmonton	53.64	-113.28	Right Metatarsal IV	29100 ± 310	OK-A-37876	33278	370	80908.1	7356.6	Phenol-chloroRf	21093	>0.99	52.95
5311	Parthena atrox	Royal Alberta Museum	P99.1.3.110	Canada	American Park, Idaho	53.64	-113.28	Left Humerus	28.940 ± 340	OK-A-37876	33278	370	64652.5	8279.1	Silica	33028	0.99	70.2
5312	Parthena atrox	Royal Alberta Museum	P98.3.404	Canada	Consolidated nr 48 Edmonton	53.64	-113.28	Right Mandible	>48,100	OK-A-13453	33134	330	80908.1	7356.6	Silica	54796	>0.99	149.08
5313	Parthena atrox	Royal Alberta Museum	P99.1.3.546	Canada	Consolidated nr 48 Edmonton	53.64	-113.28	Left metatarsal II	11.355 ± 55	OK-A-12900	13198	57	13198	59828	Phenol-chloroRf	59828	0.99	167.68
5326	Low quality DNA	Idaho Museum of Natural History	IMNH 7100523870	USA	American Park, Idaho	42.96	-112.83	Ulna	>50,300	OK-A-37879	33278	370	80908.1	7356.6	Phenol-chloroRf	132	<0.1	0.32
5326	Low quality DNA	Idaho Museum of Natural History	IMNH 470022544	USA	American Park, Idaho	42.96	-112.83	Right Ulna	>49,700	OK-A-37880	33278	370	80908.1	7356.6	Phenol-chloroRf	2	<0.1	0.01
5327	Equus caballus	Idaho Museum of Natural History	IMNH 5000117237	USA	American Park, Idaho	42.96	-112.83	Right Humerus	>49,000	OK-A-37893	33278	370	80908.1	7356.6	Phenol-chloroRf	283	0.1	0.67
5333	Low quality DNA	University of Kansas	127201	USA	Kew River, Kansas	39.08	-95.71	Right Humerus	11990 ± 50	OK-A-37751	13755	91	13755	17889	Phenol-chloroRf	7	<0.1	0.01
5343	Parthena splenda	University of Kansas	GS-27	Austria	Gamsstern	47.68	14.30	Tibia	49.900±1500	OK-A-13110	50204	1677	1677	17889	Phenol-chloroRf	17889	0.99	0.99
5353	Parthena splenda	University of Alaska	KU 38992	USA	North Slope, Alaska	70.81	-154.41	Phalange	12.630±60	OK-A-13473	15909	139	15909	80361	Phenol-chloroRf	>0.99	0.99	
5355	Parthena atrox	University of Kansas	KU 38992	USA	Natural Trap Cave, Wyoming	44.97	-108.19	Phalange	21090 ± 120	OK-A-37896	25385	152	25412.4	1276.9	Phenol-chloroRf	28559	0.99	77.02
5356	Parthena, low quality DNA	University of Kansas	KU 44000	USA	Natural Trap Cave, Wyoming	44.97	-108.19	Humerus	24.080 ± 170	OK-A-10078	28124	196	28124	2625.9	Phenol-chloroRf	316	0.29	0.88
5357	Parthena atrox	University of Kansas	KU 44009	USA	Natural Trap Cave, Wyoming	44.97	-108.19	Humerus	12.995±90	OK-A-10078	28124	196	28124	2625.9	Phenol-chloroRf	17740	0.99	49.39
5363	Parthena splenda	University of Bergen	1.S. 951	Russia	Pyrova Slon, Ural Mountains, Russia	67.10	60.51	bone	20020 ± 110	OK-A-37895	15544	157	17253.6	2625.9	Silica	40228	0.99	106.28
16196	Parthena, low quality DNA	Natural Trap Cave Collection	NTC14403	USA	Natural Trap Cave, Wyoming	44.97	-108.19	Prenatal Tooth	19840 ± 60	OK-A-37895	24084	147	24084	4222	Silica	477	0.48	1.38
16207	Parthena atrox	Natural Trap Cave Collection	NTC1412	USA	Natural Trap Cave, Wyoming	44.97	-108.19	Phalax	21080 ± 120	OK-A-37895	23883	113	23883	4222	Silica	4222	0.95	12.15
16214	Parthena atrox	Natural Trap Cave Collection	NTC1419	USA	Natural Trap Cave, Wyoming	44.97	-108.19	Phalax	21080 ± 120	OK-A-37895	23883	113	23883	4222	Silica	4222	0.95	12.15
18153	Parthena atrox	Natural Trap Cave Collection	No. #	USA	Natural Trap Cave, Wyoming	44.97	-108.19	Metatarsal	21080 ± 120	OK-A-37895	23431	146	23431	4222	Silica	11979	>0.99	38.26

^a These specimens were originally identified as *Ursus arctos* and were initially run through the brown bear pipeline. Re-sequencing was performed on NCB1 returning the highest hits against the cave lion mitochondrial reference. (this is how other misidentifications such as sample 5377 were identified). Consequently the samples were run through the lion pipeline.
^b Proportion of mitogenome covered in consensus sequence
^c Table S2: Information on lion bone and tooth samples analyzed. New radiocarbon dates are highlighted in red.

2.3 SUPPLEMENTARY INFORMATION

Table S3: Additional radiocarbon dates used to produce Figure 2.

Date ID	Species	Museum Accession	Locality	Country	Radiocarbon age	Radiocarbon error	Calibrated median	Calibrated error
ANUA-38615	<i>A. simus</i>	YT03/134	Quartz Creek, Yukon	Canada	26940	570	31029	576
OxA-37428	<i>A. simus</i>	YT03/288 Cat No 129.1	Hester Creek, Klondike, Dawson, Yukon	Canada	26800	240	30950	157
OxA-9259	<i>A. simus</i>	CMN 49874	Dawson area, Hester Creek Loc.57, Yukon	Canada	26720	270	30899	193
Wk20235	<i>A. simus</i>	CMN 37957	Dawson area Loc. 45, Eldorado Creek, Yukon	Canada	22417	452	26713	436
OxA-37426	<i>A. simus</i>	A-1828	Goldstream, Alaska	USA	20900	120	25233	188
TO-2699	<i>A. simus</i>	CMN 42388	Sixtymile, Yukon	Canada	44240	930	47621	984
OxA-37425	<i>A. simus</i>	A-203-2808	Cripple Creek, Alaska	USA	44600	2000	47763	1347
I-11037	<i>A. simus</i>	CMN 37577	Lower Hunker Creek, Yukon	Canada	29600	1200	33744	1384
Wk20236	<i>A. simus</i>	AMNH A-'Alaska' Bx 35	Alaska	USA	25264	650	29450	695
AA-17511	<i>A. simus</i>	NA	Fairbanks, Alaska	USA	20524	180	24727	262
AA-17512	<i>A. simus</i>	NA	Fairbanks, Alaska	USA	25496	224	29632	330
AA-17513	<i>A. simus</i>	NA	Upper Cleary Creek Fairbanks area, Alaska	USA	27511	279	31355	258
AA-17514	<i>A. simus</i>	NA	Fairbanks, Alaska	USA	39565	1126	43536	964
AA-17515	<i>A. simus</i>	NA	Birch Creek , Alaska	USA	34974	652	39576	714
CAMS-58092	<i>A. simus</i>	T99-033	Titaluk River, Alaska	USA	42600	2200	46368	1767
TO-2539	<i>A. simus</i>	ROM:VP 43646	Ikpikpuk River, Alaska	USA	27190	280	31158	183
TO-2696	<i>A. simus</i>	CMN 7438	Gold Run Creek (Dawson Loc. 31), Yukon	Canada	26040	270	30284	336
TO-3707	<i>A. simus</i>	CMN 50367	Hunker Creek (Dawson Loc. 37), Yukon	Canada	24850	150	28884	184
OxA-9261	<i>U. arctos</i>	FAM 30771	Lower Goldstream, Alaska	USA	20080	160	24149	200
OxA-9709	<i>U. arctos</i>	FAM 95659	Goldstream, Alaska	USA	13415	70	16141	115
OxA-9799	<i>U. arctos</i>	FAM 95598	Cripple Creek, Alaska	USA	12320	90	14347	216
OxA-9800	<i>U. arctos</i>	FAM 95653	Engineer Creek, Alaska	USA	9535	75	10883	144
OxA-9801	<i>U. arctos</i>	FAM 95599	Goldstream, Alaska	USA	14310	100	17430	153
OxA-9828	<i>U. arctos</i>	FAM 95628	Lower Goldstream, Alaska	USA	12310	65	14285	174
OxA-9829	<i>U. arctos</i>	FAM 95681	Fairbanks Creek, Alaska	USA	20820	120	25119	208
OxA-9830	<i>U. arctos</i>	FAM 95632	Rosie Creek, Alaska	USA	14810	80	18019	113
CAMS-131346	<i>P. spelaea</i>	FAM 69126	Fairbanks, Alaska	USA	16650	110	20094	157
CAMS-131347	<i>P. spelaea</i>	FAM 69173	Fairbanks, Alaska	USA	14050	80	17077	152
CAMS-131348	<i>P. spelaea</i>	FAM 69053	Fairbanks, Alaska	USA	13040	70	15616	142
CAMS-131349	<i>P. spelaea</i>	FAM 69078	Fairbanks, Alaska	USA	18270	130	22134	159
CAMS-131350	<i>P. spelaea</i>	FAM 69080	Fairbanks, Alaska	USA	12990	70	15536	136
CAMS-131361	<i>P. spelaea</i>	AMNH 69142	Fairbanks, Alaska	USA	18590	130	22462	153
CAMS-131362	<i>P. spelaea</i>	AMNH 69172	Fairbanks, Alaska	USA	17140	110	20678	152
CAMS-18421	<i>P. spelaea</i>	NA	Porcupine River, Yukon	Canada	39300	1000	43286	830
OxA-10085	<i>P. spelaea</i>	FAM 69158	Cripple Creek Sump, Alaska	USA	53900	2300	54706	3036

Date ID	Species	Museum Accession	Locality	Country	Radiocarbon age	Radiocarbon error	Calibrated median	Calibrated error
AA-48280	<i>P. spelaea</i>	IK01-409	Ikpikpuk River, Alaska	USA	12930	130	15466	201
Beta-117142	<i>P. spelaea</i>	IK97-1001	Ikpikpuk River, Alaska	USA	35710	1180	40335	1154
Beta-286419	<i>P. spelaea</i>	IK06-18	Ikpikpuk River, Alaska	USA	33260	230	37514	434
Beta-331881	<i>P. spelaea</i>	MAY12-24	Maybe Creek, Alaska	USA	15990	60	19301	109
Beta-339277	<i>P. spelaea</i>	TIT12-07	Titaluk River, Alaska	USA	30520	180	34483	185
CAMS-131360	<i>P. spelaea</i>	AMNH 69140	Fairbanks, Alaska	USA	20970	180	25303	243
CAMS-53909	<i>P. spelaea</i>	IK98-278	Ikpikpuk River, Alaska	USA	11290	50	13143	51
CAMS-53910	<i>P. spelaea</i>	IK98-436	Ikpikpuk River, Alaska	USA	40900	1140	44558	1085
SI-456	<i>P. spelaea</i>	NA	Upper Ester Creek, Alaska	USA	22680	300	26965	323
TO-7743	<i>P. spelaea</i>	NA	Thistle Creek, Yukon	Canada	32750	370	36838	552

Table S4: Information on read data downloaded from EMBL-EBI.

Sample	SRA number/ EBI run accession number	Age	Location	Species	Mitochondrial Clade	Reference
GP01	SRR935602, SRR935609, SRR935616, SRR935617, SRR941811, SRR941814	Modern	Glacier National Park, Montana, USA	<i>Ursus arctos</i>	Clade 4	Liu et al. 2014
F2678/70	SRR3591801, SRR3591802	28,690 ± 130, OZQ292	Malyi Anyui river, Chukotka, Russia	<i>Panthera spelaea</i>	<i>Spelaea</i>	Barnett et al. 2016
YG 401.410	SRR3630971	29,860 ± 210, UCIAMS-143525	Quartz Creek, Yukon, Canada	<i>Panthera spelaea</i>	<i>Spelaea</i>	Barnett et al. 2016

Table S5: Information on sequences downloaded from GenBank included as part of the brown bear dataset.

GenBank code	Age	Location	Species	Mitochondrial Clade	Reference
AF303110.1	Modern	Continental USA	<i>Ursus arctos</i>	4	Delisle & Strobeck 2002
AP012559.1	Modern	Central Hokkaido	<i>Ursus arctos</i>	3a	Hirata et al. 2013
AP012560.1	Modern	Central Hokkaido	<i>Ursus arctos</i>	3a	Hirata et al. 2013
AP012561.1	Modern	Central Hokkaido	<i>Ursus arctos</i>	3a	Hirata et al. 2013
AP012562.1	Modern	Central Hokkaido	<i>Ursus arctos</i>	3a	Hirata et al. 2013
AP012563.1	Modern	Central Hokkaido	<i>Ursus arctos</i>	3a	Hirata et al. 2013
AP012564.1	Modern	Central Hokkaido	<i>Ursus arctos</i>	3a	Hirata et al. 2013
AP012565.1	Modern	Central Hokkaido	<i>Ursus arctos</i>	3a	Hirata et al. 2013
AP012566.1	Modern	Central Hokkaido	<i>Ursus arctos</i>	3a	Hirata et al. 2013
AP012567.1	Modern	Central Hokkaido	<i>Ursus arctos</i>	3a	Hirata et al. 2013
AP012568.1	Modern	Central Hokkaido	<i>Ursus arctos</i>	3a	Hirata et al. 2013
AP012569.1	Modern	Central Hokkaido	<i>Ursus arctos</i>	3a	Hirata et al. 2013
AP012570.1	Modern	Eastern Hokkaido	<i>Ursus arctos</i>	3b	Hirata et al. 2013
AP012571.1	Modern	Eastern Hokkaido	<i>Ursus arctos</i>	3b	Hirata et al. 2013
AP012572.1	Modern	Eastern Hokkaido	<i>Ursus arctos</i>	3b	Hirata et al. 2013
AP012573	Modern	Eastern Hokkaido	<i>Ursus arctos</i>	3b	Hirata et al. 2013

2.3 SUPPLEMENTARY INFORMATION

GenBank code	Age	Location	Species	Mitochondrial Clade	Reference
AP012574	Modern	Southern Hokkaido	<i>Ursus arctos</i>	4	Hirata et al. 2013
AP012575	Modern	Southern Hokkaido	<i>Ursus arctos</i>	4	Hirata et al. 2013
AP012576	Modern	Southern Hokkaido	<i>Ursus arctos</i>	4	Hirata et al. 2013
AP012577	Modern	Southern Hokkaido	<i>Ursus arctos</i>	4	Hirata et al. 2013
AP012578	Modern	Southern Hokkaido	<i>Ursus arctos</i>	4	Hirata et al. 2013
AP012579	Modern	Sakhalin	<i>Ursus arctos</i>	3a	Hirata et al. 2013
AP012580.1	Modern	Kunashiri Island	<i>Ursus arctos</i>	3b	Hirata et al. 2013
AP012581.1	Modern	Etorofu Island	<i>Ursus arctos</i>	3b	Hirata et al. 2013
AP012582.1	Modern	Etorofu Island	<i>Ursus arctos</i>	3b	Hirata et al. 2013
AP012583.1	Modern	Etorofu Island	<i>Ursus arctos</i>	3b	Hirata et al. 2013
AP012584.1	Modern	Etorofu Island	<i>Ursus arctos</i>	3b	Hirata et al. 2013
AP012585	Modern	Ekaterinburg	<i>Ursus arctos</i>	3a	Hirata et al. 2013
AP012586	Modern	Ekaterinburg	<i>Ursus arctos</i>	3a	Hirata et al. 2013
AP012587	Modern	Ekaterinburg	<i>Ursus arctos</i>	3a	Hirata et al. 2013
AP012592.1	Modern	Tibet	<i>Ursus arctos</i>	5	Hirata et al. 2013
AP012593.1	Modern	Tibet	<i>Ursus arctos</i>	5	Hirata et al. 2013
AP012594.1	Modern	Asahikawa Municipal Asahiyama Zoo, Japan	<i>Ursus maritimus</i>	2b	Hirata et al. 2013
AP012595.1	Modern	Asahikawa Municipal Asahiyama Zoo, Japan	<i>Ursus maritimus</i>	2b	Hirata et al. 2013
AP012596.1	Modern	Asahikawa Municipal Asahiyama Zoo, Japan	<i>Ursus maritimus</i>	2b	Hirata et al. 2013
AP012597.1	Modern	Asahikawa Municipal Asahiyama Zoo, Japan	<i>Ursus maritimus</i>	2b	Hirata et al. 2013
GU573485.1	Modern	St Lawrence Island, Alaska, USA	<i>Ursus maritimus</i>	2b	Lindqvist et al. 2010
GU573486.1	Modern	Admiralty Island, Alaska, USA	<i>Ursus arctos</i>	2a	Lindqvist et al. 2010
GU573487.1	Modern	Admiralty Island, Alaska, USA	<i>Ursus arctos</i>	2a	Lindqvist et al. 2010
GU573489.1	Modern	Baranof Island, Alaska, USA	<i>Ursus arctos</i>	2a	Lindqvist et al. 2010
GU573490.2	Modern	Little Diomed Island, Alaska, USA	<i>Ursus maritimus</i>	2b	Lindqvist et al. 2010
GU573491.1	Modern	Kodiak Island	<i>Ursus arctos</i>	2a	Lindqvist et al. 2010
JX196367.1	Modern	Kenai Peninsula, Alaska, USA	<i>Ursus arctos</i>	3a	Miller et al. 2012
JX196368.1	Modern	Baranof Island, Alaska, USA	<i>Ursus arctos</i>	2a	Miller et al. 2012
JX196369.1	Modern	Admiralty Island, Alaska, USA	<i>Ursus arctos</i>	2a	Miller et al. 2012
MH255807.1	>48000	Indigirka river basin, Uyandina river, Yakutia, Russia	<i>Ursus arctos</i>	3b	Rey-Iglesia et al. 2019

Table S6: Best partition scheme according to BIC for BEAST analyses

Brown Bears			
Partition	Best Model	#sites	Positions
1	TRN+I	4227	Second codon position of ND6, tRNAs, and rRNAs
2	HKY+I	3603	First codon position of ATP6, ATP8, CO1, CO2, CO3, CYTB, ND1, ND2, ND3, ND4, ND4L, ND5, ND6
3	HKY+I	3603	Second codon position of ATP6, ATP8, CO1, CO2, CO3, CYTB, ND1, ND2, ND3, ND4, ND4L, ND5, ND6
4	TRN+G	3955	First and third codon position ND6, third codon position of ATP6, ATP8, CO1, CO2, CO3, CYTB, ND1, ND2, ND3, ND4, ND4L, ND5, ND6
5	TRN+I+G	1063	Non Coding
Lions			
Partition	Best Model	#sites	Positions
1	HKY	4229	Second codon position of ND6, tRNAs, and rRNAs
2	HKY+I	3602	First codon position of ATP6, ATP8, CO1, CO2, CO3, CYTB, ND1, ND2, ND3, ND4, ND4L, ND5, ND6
3	HKY+I	3602	Second codon position of ATP6, ATP8, CO1, CO2, CO3, CYTB, ND1, ND2, ND3, ND4, ND4L, ND5, ND6
4	TRN	3954	First and third codon position ND6, third codon position of ATP6, ATP8, CO1, CO2, CO3, CYTB, ND1, ND2, ND3, ND4, ND4L, ND5, ND6
5	TRN+I+G	1357	Non Coding

2.3 SUPPLEMENTARY INFORMATION

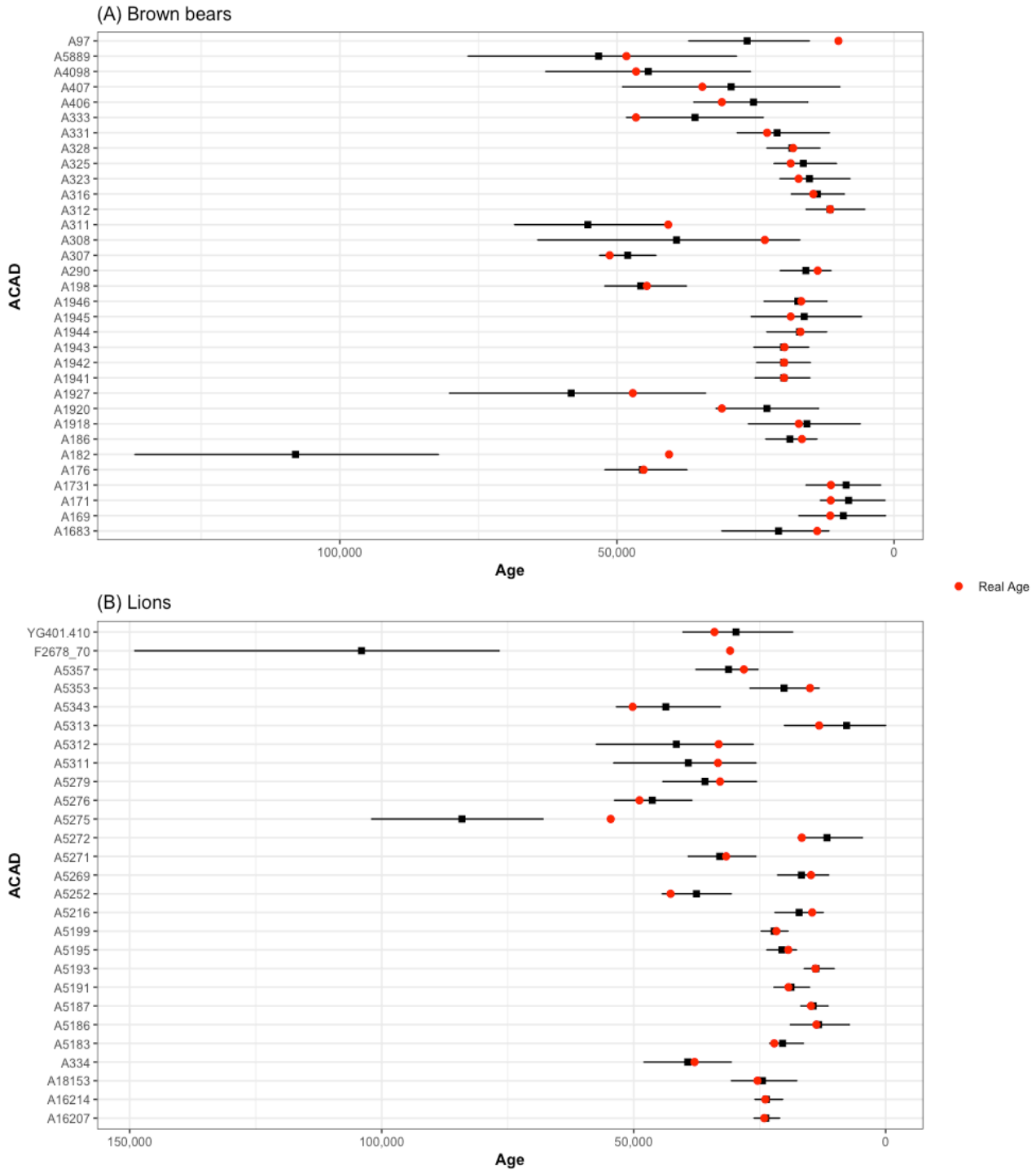


Fig. S1: Plots of median estimated ages from leave-one-out cross-validation in BEAST2 for (A) Brown bears and (B) Lions. Error-bars represent 95% higher posterior density (HPD). The real age of the specimen is within the 95% HPD of each estimate for all but 2 of each of the brown bears and lions. The specimens for which the real age is outside the 95% HPD were still included in subsequent analyses as they fall in under sampled regions of the tree.

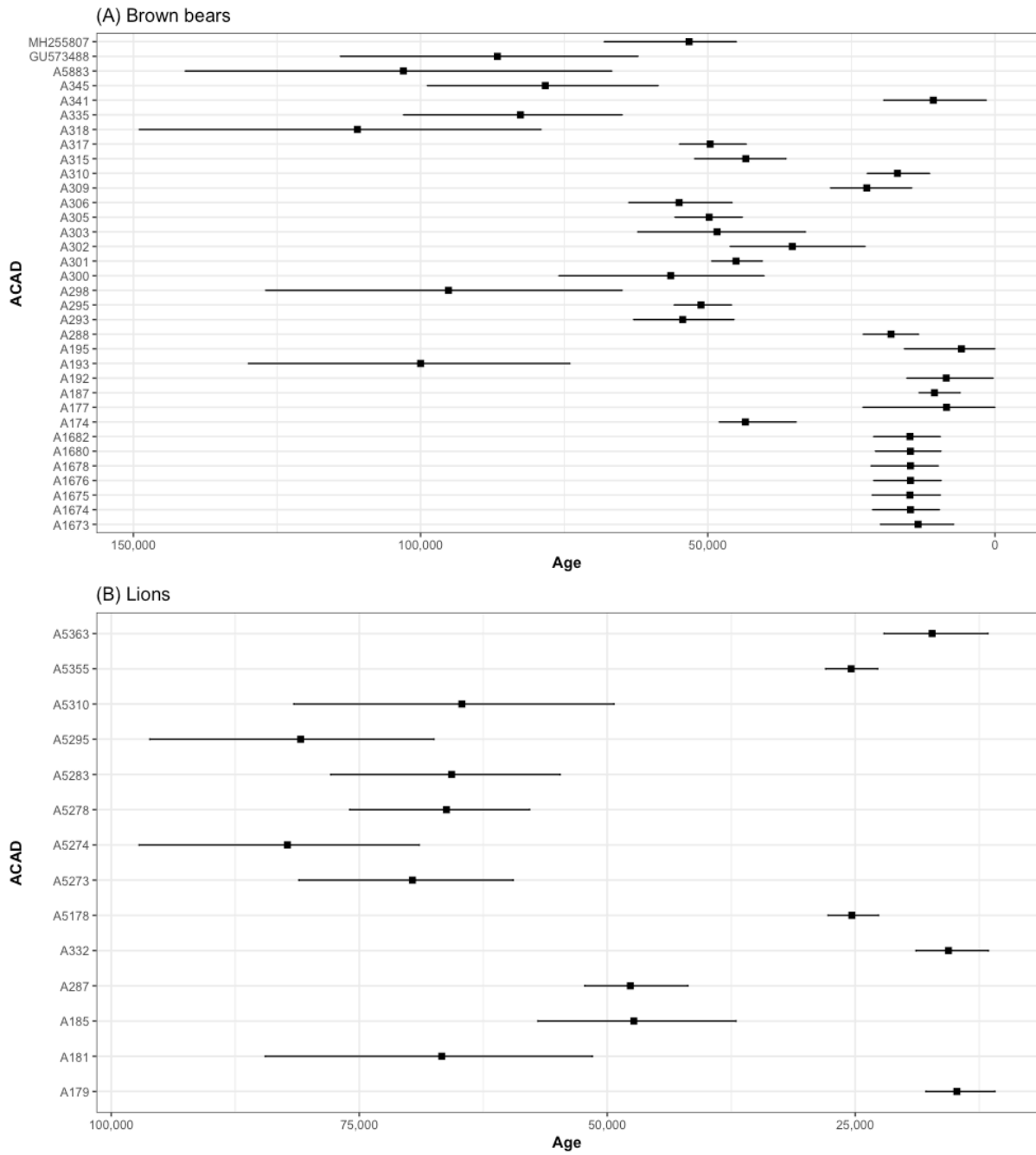


Fig. S2: Estimated ages from BEAST2 of specimens with no associated date or infinite radiocarbon dates. Error bars represent 95% higher posterior densities.

2.3 SUPPLEMENTARY INFORMATION

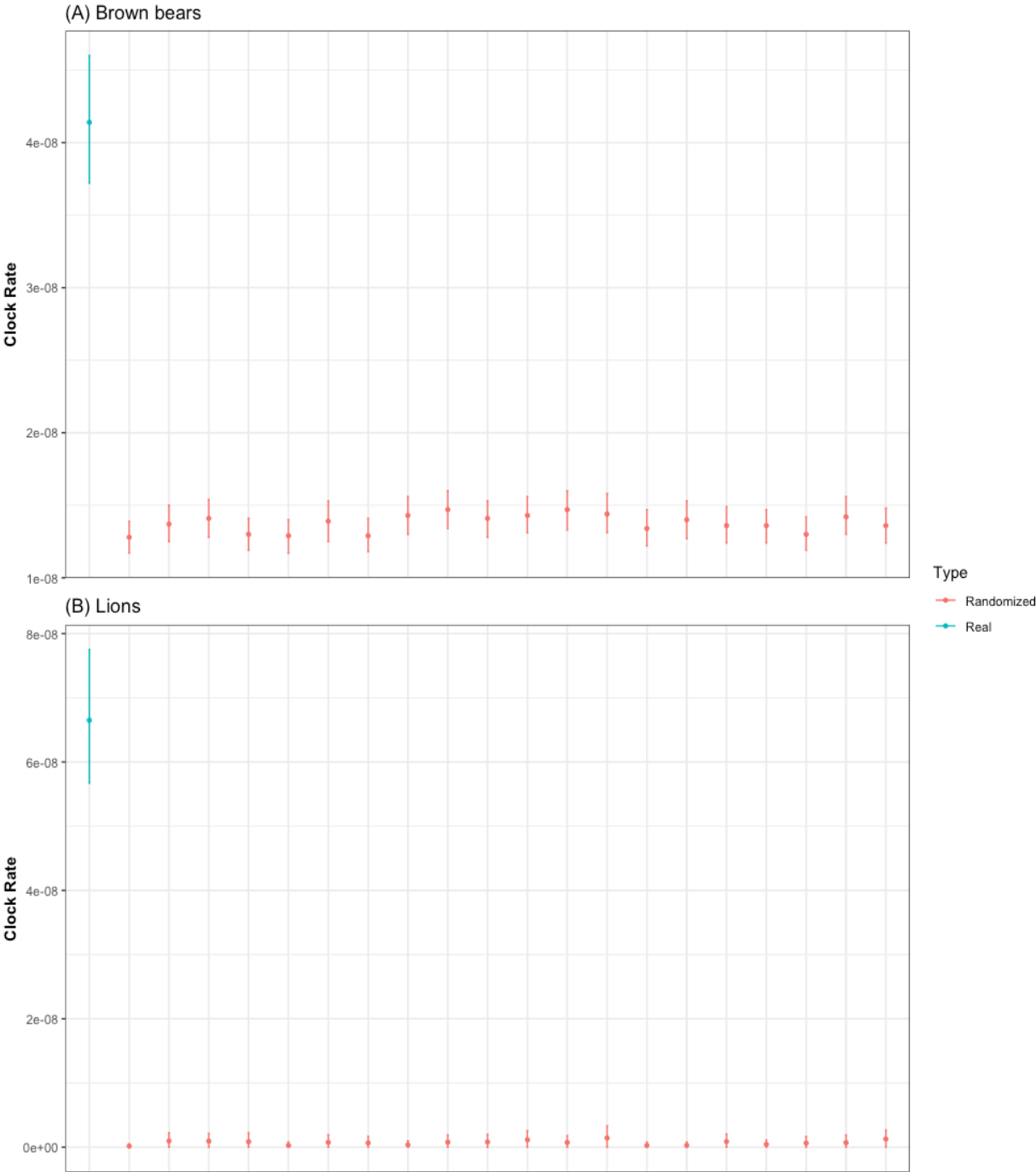


Fig. S3: Comparison of mean clock rate estimations with 95% higher posterior intervals from BEAST2 for the real data and the 20 date-randomized datasets from the date-randomization test (DRT).

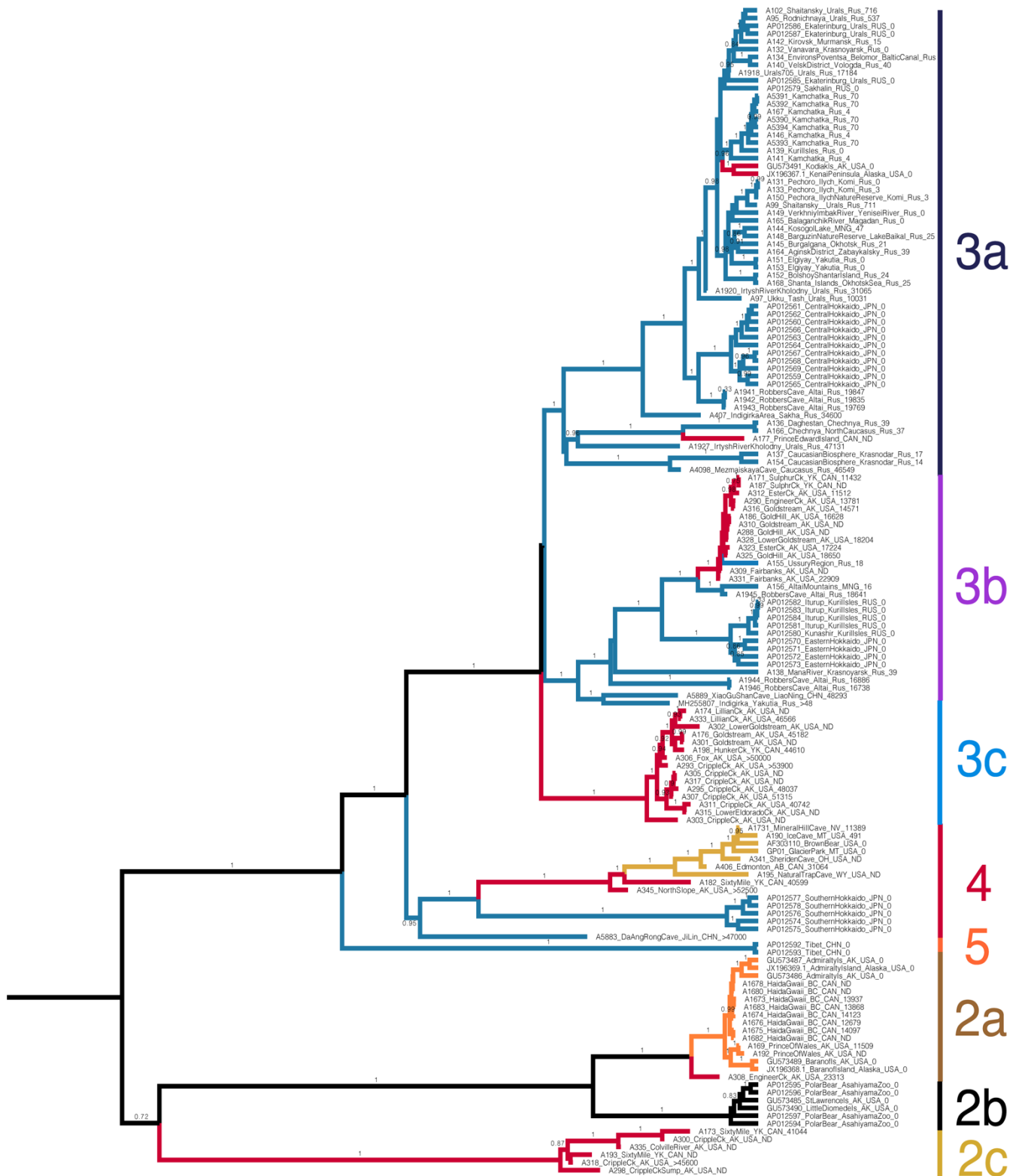


Fig. S4: Bayesian phylogenetic tree inferred from brown bear mitogenomes. Branch labels represent posterior support values above 0.75.

2.3 SUPPLEMENTARY INFORMATION

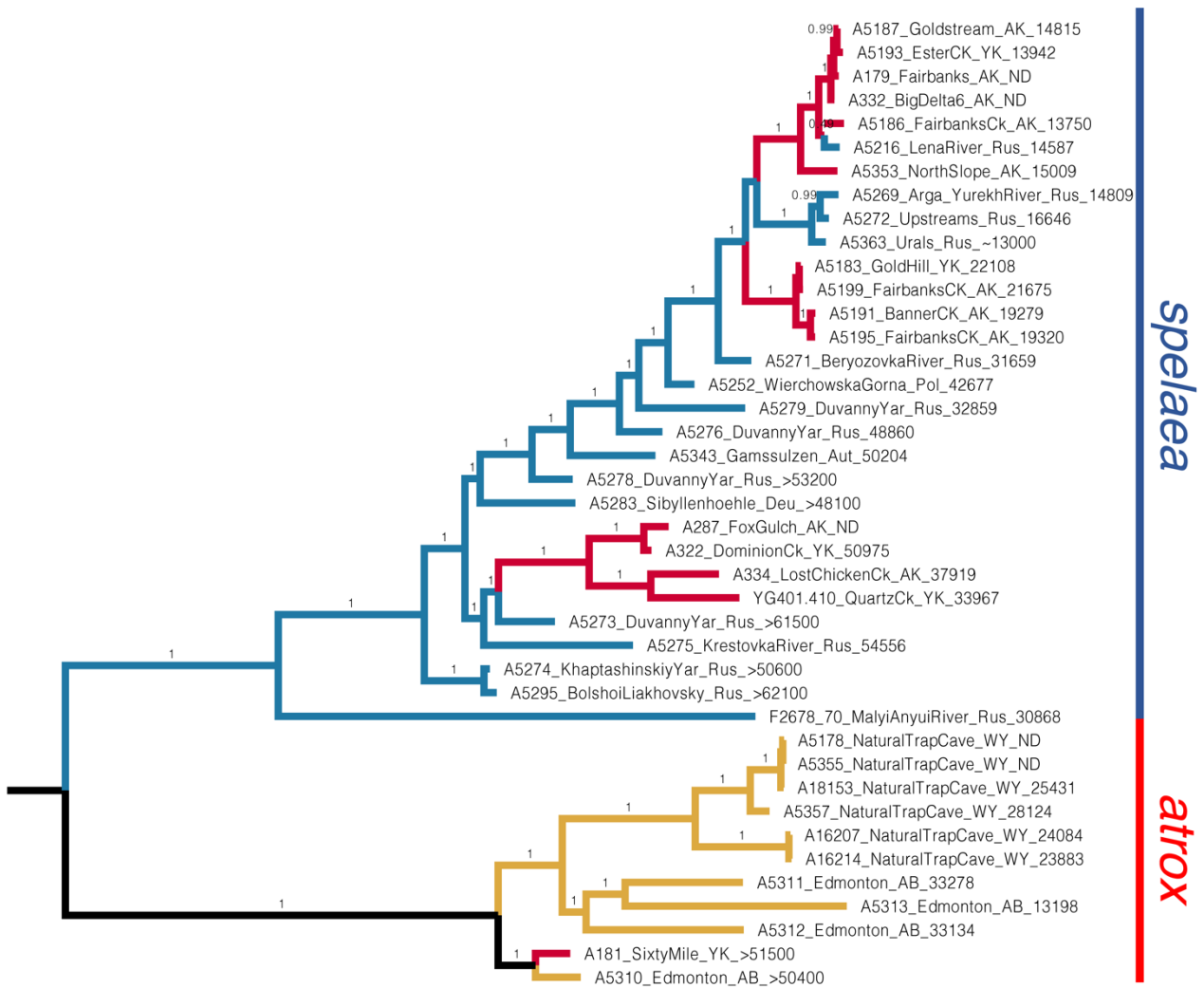


Fig. S5: Bayesian phylogenetic tree inferred from lion mitogenomes. Branch labels represent posterior support values above 0.75.

2.3 SUPPLEMENTARY INFORMATION

Fig. S6: Bayesian phylogenetic trees inferred from (A) brown bear and (B) lion mitogenomes under joint-tree epoch analyses in BEAST. The gray vertical columns represent odd-numbered MIS stages (interglacials) and white columns even-numbered MIS stages (glacials). Colours of branches correspond to geographic character in the joint-tree epoch analyses, where blue is Eurasia and red North America. Shifts from blue to red and vice versa are inferred migrations across the Bering Land Bridge. The white vertical columns even-numbered MIS stages (glacials) and grey vertical columns represent odd-numbered MIS stages (interglacials). The combined glacials occupy less time, and subtend less tree length, than combined interglacials, yet branches with inferred migration events tend to span glacials: of 11 such branches, 2 are entirely restricted to glacials and 2 are largely restricted to glacials, whereas none are restricted to interglacials and only 1 is largely restricted to interglacials (the other 6 broadly span both glacial and interglacial time slices).

Supplementary References:

- Barnett, R., Lisandra, M., Zepeda Mendoza, M. L., Soares, A., Soares, R., Ho, S., . . . Gilbert, P. (2016). Mitogenomics of the extinct cave lion, *Panthera spelaea* (Goldfuss, 1810), resolve its position within the *Panthera* cats. *Open Quaternary*, 2(4), 1-11. doi:10.5334/oq.24
- Bouckaert, R., Vaughan, T. G., Barido-Sottani, J., Duchene, S., Fourment, M., Gavryushkina, A., . . . Drummond, A. J. (2019). BEAST 2.5: An advanced software platform for Bayesian evolutionary analysis. *PLoS Computational Biology*, 15(4), e1006650. doi:10.1371/journal.pcbi.1006650
- Bray, S. C. E., Austin, J. J., Metcalf, J. L., Østbye, K., Østbye, E., Lauritzen, S.-E., . . . Cooper, A. (2013). Ancient DNA identifies post-glacial recolonisation, not recent bottlenecks, as the primary driver of contemporary mtDNA phylogeography and diversity in Scandinavian brown bears. *Diversity and Distributions*, 19(3), 245-256. doi:10.1111/j.1472-4642.2012.00923.x
- Cooper, A., & Poinar, H. N. (2000). Ancient DNA: Do it right or not at all. *Science*, 289(5482), 1139. doi:10.1126/science.289.5482.1139b
- Dabney, J., Knapp, M., Glocke, I., Gansauge, M.-T., Weihmann, A., Nickel, B., . . . Meyer, M. (2013). Complete mitochondrial genome sequence of a Middle Pleistocene cave bear reconstructed from ultrashort DNA fragments. *Proceedings of the National Academy of Sciences of the United States of America*, 110(39), 15758-15763.
- Edgar, R. C. (2004). MUSCLE: multiple sequence alignment with high accuracy and high throughput. *Nucleic Acids Research*, 32(5), 1792-1797. doi:10.1093/nar/gkh340
- Hwang, D. S., Ki, J. S., Jeong, D. H., Kim, B. H., Lee, B. K., Han, S. H., & Lee, J. S. (2008). A comprehensive analysis of three Asiatic black bear mitochondrial genomes (subspecies *ussuricus*, *formosanus* and *mupinensis*), with emphasis on the complete mtDNA sequence of *Ursus thibetanus ussuricus* (Ursidae). *DNA Sequence*, 19(4), 418-429. doi:10.1080/19401730802389525

- Kim, J. H., Antunes, A., Luo, S. J., Menninger, J., Nash, W. G., O'Brien, S. J., & Johnson, W. E. (2006). Evolutionary analysis of a large mtDNA translocation (numt) into the nuclear genome of the *Panthera* genus species. *Gene*, *366*(2), 292-302. doi:10.1016/j.gene.2005.08.023
- Lanfear, R., Frandsen, P. B., Wright, A. M., Senfeld, T., & Calcott, B. (2016). PartitionFinder 2: New Methods for Selecting Partitioned Models of Evolution for Molecular and Morphological Phylogenetic Analyses. *Molecular Biology and Evolution*, *34*(3), 772-773. doi:10.1093/molbev/msw260
- Li, H., & Durbin, R. (2009). Fast and accurate short read alignment with Burrows-Wheeler transform. *Bioinformatics*, *25*(14), 1754-1760. doi:10.1093/bioinformatics/btp324
- Li, H., Handsaker, B., Wysoker, A., Fennell, T., Ruan, J., Homer, N., . . . Genome Project Data Processing, S. (2009). The sequence alignment/map format and SAMtools. *Bioinformatics*, *25*(16), 2078-2079. doi:10.1093/bioinformatics/btp352
- Liu, S. P., Lorenzen, E. D., Fumagalli, M., Li, B., Harris, K., Xiong, Z. J., . . . Wang, J. (2014). Population genomics reveal recent speciation and rapid evolutionary adaptation in polar bears. *Cell*, *157*(4), 785-794. doi:10.1016/j.cell.2014.03.054
- Meyer, M., Kircher, M., Gansauge, M. T., Li, H., Racimo, F., Mallick, S., . . . Paabo, S. (2012). A high-coverage genome sequence from an archaic Denisovan individual. *Science*, *338*(6104), 222-226. doi:10.1126/science.1224344
- Mitchell, K. J., Bray, S. C., Bover, P., Soibelzon, L., Schubert, B. W., Prevosti, F., . . . Cooper, A. (2016). Ancient mitochondrial DNA reveals convergent evolution of giant short-faced bears (Tremarctinae) in North and South America. *Biology Letters*, *12*(4), 20160062. doi:10.1098/rsbl.2016.0062
- Rambaut, A., Drummond, A. J., Xie, D., Baele, G., & Suchard, M. A. (2018). Posterior summarization in bayesian phylogenetics using Tracer 1.7. *Systematic Biology*, *67*(5), 901-904. doi:10.1093/sysbio/syy032
- Ramsden, C., Holmes, E. C., & Charleston, M. A. (2009). Hantavirus evolution in relation to its rodent and insectivore hosts: no evidence for codivergence. *Molecular Biology and Evolution*, *26*(1), 143-153. doi:10.1093/molbev/msn234
- Ramsey, C. B. (2009). Bayesian analysis of radiocarbon dates. *Radiocarbon*, *51*(1), 337-360. doi:10.1017/S0033822200033865
- Reimer, P. J., Bard, E., Bayliss, A., Beck, J. W., Blackwell, P. G., Ramsey, C. B., . . . van der Plicht, J. (2013). Intcal13 and Marine13 radiocarbon age calibration curves 0-50,000 years cal BP. *Radiocarbon*, *55*(4), 1869-1887. doi:10.2458/azu_js_rc.55.16947
- Richards, S. M., Hovhannisyan, N., Gilliam, M., Ingram, J., Skadhauge, B., Heiniger, H., . . . Cooper, A. (2019). Low-cost cross-taxon enrichment of mitochondrial DNA using in-house synthesised RNA probes. *PLoS ONE*, *14*(2), e0209499. doi:10.1371/journal.pone.0209499

2.3 SUPPLEMENTARY INFORMATION

- Rohland, N., Harney, E., Mallick, S., Nordenfelt, S., & Reich, D. (2015). Partial uracil-DNA-glycosylase treatment for screening of ancient DNA. *Philosophical Transactions of the Royal Society of London B Biological Sciences*, 370(1660), 20130624. doi:10.1098/rstb.2013.0624
- Schubert, M., Ermini, L., Sarkissian, C. D., Jonsson, H., Ginolhac, A., Schaefer, R., . . . Orlando, L. (2014). Characterization of ancient and modern genomes by SNP detection and phylogenomic and metagenomic analysis using PALEOMIX. *Nature Protocols*, 9(5), 1056-1082. doi:10.1038/nprot.2014.063
- Schubert, M., Lindgreen, S., & Orlando, L. (2016). AdapterRemoval v2: rapid adapter trimming, identification, and read merging. *BMC Research Notes*, 9, 88. doi:10.1186/s13104-016-1900-2
- Stiller, M., Molak, M., Prost, S., Rabeder, G., Baryshnikov, G., Rosendahl, W., . . . Knapp, M. (2014). Mitochondrial DNA diversity and evolution of the Pleistocene cave bear complex. *Quaternary International*, 339-340, 224-231. doi:10.1016/j.quaint.2013.09.023
- Suchard, M. A., Lemey, P., Baele, G., Ayres, D. L., Drummond, A. J., & Rambaut, A. (2018). Bayesian phylogenetic and phylodynamic data integration using BEAST 1.10. *Virus Evolution*, 4(1), vey016. doi:10.1093/ve/vey016

Chapter 3

Phylogeography of the extinct North American giant short-faced bear (*Arctodus simus*), with comments on their palaeobiology

Manuscript written for submission to *Biology Letters*

3.1 Authorship Statement

Statement of Authorship

Title of Paper	Phylogeography of the extinct North American giant short-faced bear (<i>Arctodus simus</i>), with comments on their paleobiology
Publication Status	<input type="checkbox"/> Published <input type="checkbox"/> Accepted for Publication <input type="checkbox"/> Submitted for Publication <input checked="" type="checkbox"/> Unpublished and Unsubmitted work written in manuscript style
Publication Details	Unpublished and unsubmitted work written in manuscript style intended to be submitted to Biology Letters

Principal Author

Name of Principal Author (Candidate)	Alexander T Salis			
Contribution to the Paper	Performed DNA extractions, DNA library construction and amplification, hybridisation enrichment, preparation for sequencing, and bioinformatic processing of sequencing data. Performed phylogenetic analyses, interpreted results, created figures, wrote manuscript and edited manuscript.			
Overall percentage (%)	75			
Certification:	This paper reports on original research I conducted during the period of my Higher Degree by Research candidature and is not subject to any obligations or contractual agreements with a third party that would constrain its inclusion in this thesis. I am the primary author of this paper.			
Signature	<table border="1"> <tr> <td></td> <td>Date</td> <td>07/08/2020</td> </tr> </table>		Date	07/08/2020
	Date	07/08/2020		

Co-Author Contributions

By signing the Statement of Authorship, each author certifies that:

- i. the candidate's stated contribution to the publication is accurate (as detailed above);
- ii. permission is granted for the candidate to include the publication in the thesis; and
- iii. the sum of all co-author contributions is equal to 100% less the candidate's stated contribution.

Name of Co-Author	Blaine W Schubert			
Contribution to the Paper	Conception of project, provided access to samples, collated morphological information, interpreted results, wrote manuscript, edited and critically evaluated the manuscript.			
Signature	<table border="1"> <tr> <td></td> <td>Date</td> <td>15 August 2020</td> </tr> </table>		Date	15 August 2020
	Date	15 August 2020		

Name of Co-Author	Sarah C E Bray			
Contribution to the Paper	Performed DNA extractions, interpreted results, edited and critically evaluated the manuscript.			
Signature	<table border="1"> <tr> <td></td> <td>Date</td> <td>07/08/2020</td> </tr> </table>		Date	07/08/2020
	Date	07/08/2020		

Name of Co-Author	Holly Heiniger		
Contribution to the Paper	Performed DNA extractions, DNA library construction and amplification, and preparation for sequencing. Edited and critically evaluated the manuscript.		
Signature		Date	07/08/2020

Name of Co-Author	Julie Meachen		
Contribution to the Paper	Provided access to samples, conception of project, edited and critically evaluated the manuscript.		
Signature		Date	August 11, 2020

Name of Co-Author	Alan Cooper		
Contribution to the Paper	Supervised work, conception of project, edited and critically evaluated the manuscript.		
Signature		Date	10 Sep, 2020

Name of Co-Author	Kieren J Mitchell		
Contribution to the Paper	Supervised work, conception of project, interpreted results, wrote and edited the manuscript.		
Signature		Date	17/8/20

3.2 Manuscript

Phylogeography of the extinct North American giant short-faced bear (*Arctodus simus*), with comments on their palaeobiology

Alexander T Salis¹, Blaine W. Schubert², Sarah C. E. Bray^{1,3}, Holly Heiniger¹, Julie Meachen⁴, Alan Cooper⁵, Kieren J Mitchell¹

¹Australian Centre for Ancient DNA (ACAD), School of Biological Sciences, University of Adelaide, South Australia 5005, Australia

²Center of Excellence in Paleontology and Department of Geosciences, East Tennessee State University (ETSU), Johnson City, Tennessee 37614, USA

³Registry of Senior Australians (ROSA), South Australian Health and Medical Research Institute (SAHMRI), Adelaide, South Australia 5000, Australia

⁴South Australian Museum, Adelaide, South Australia 5000, Australia

⁵Anatomy Department, Des Moines University, Des Moines, IA, USA

Abstract:

Giant short-faced bears (*Arctodus simus*) represent the largest carnivoran of Pleistocene North America and are one of the most extensively studied extinct megafaunal species from the continent. Smaller and larger forms of the giant short-faced bear have previously been recognised across its wide range, which are sometimes considered subspecies (*A. s. simus* and *A. s. yukonensis*, respectively). However, researchers have also proposed that this size variation is the result of sexual dimorphism within a single species. We sequenced 31 mitogenomes of *A. simus* from locations ranging from Alaska to as far south as New Mexico. Our results revealed a striking lack of phylogeographic structure in *A. simus*, as well as low genetic diversity and relatively recent mitochondrial diversification. These observations may either represent population bottlenecks during the Late Pleistocene or simply a naturally low effective population size resulting from a wide-ranging lifestyle. We found no evidence for genetic differences among our samples that were compatible with the previously proposed *A. simus* subspecies. In contrast, by comparing the size of specimens to their sex, as determined using low-coverage shotgun data, we showed that all large specimens were male and all small specimens female, supporting the hypothesis that *A. simus* size variation is explained by significant sexual dimorphism. Finally, our sex determination results also revealed that only female specimens were associated with cave sites, backing the supposition that female short-faced bears used caves for denning.

Introduction:

The giant short-faced bear, *Arctodus simus*, represents one of the most iconic and thoroughly studied megafaunal species from Pleistocene North America [1-14], and also one of the largest ever terrestrial carnivorans [1]. Short-faced bears in general (Ursidae; Tremarctinae) are endemic to the Americas and are represented today by the spectacled or Andean bear (*Tremarctos ornatus*) from South America. Tremarctinae appears in the latest Miocene fossil record of North America represented by *Plionarctos* [15], which subsequently diversified into three genera: *Tremarctos*, *Arctotherium* (including several extinct species, primarily from South America), and *Arctodus*. *Arctodus* is known exclusively from North America and occurs as *A. pristinus* from the late Pliocene to middle Pleistocene [11, 16]. *Arctodus simus*, a larger and proportionally distinct taxon [17], appears in the middle Pleistocene, and became extinct at the Pleistocene–Holocene transition [10, 11]. While previous morphological research supported a close relationship between *Arctodus* and *Arctotherium* [18], recent ancient DNA (aDNA) analyses have suggested that *Arctotherium* and *Tremarctos* shared a more recent common ancestor [19]. However, while several studies have included aDNA from extinct short-faced bears [6, 19], including *A. simus*, sample sizes have generally been too small to draw conclusions about intra-species diversity, demography, and evolutionary history.

While *Arctodus simus* individuals could approach 1000 kg [1], the species exhibited a remarkable degree of size variation through time and space, which has been variously explained as sexual dimorphism (common in extant bears [17, 20]) and/or subspecific differentiation. Kurtén [17] recognised and discussed size dimorphism in *A. simus*, but he also supported separating the species into two subspecies based on size and (to some degree) geographical distribution. This subspecific separation was subsequently followed by other researchers, with the smaller morph referred to *A. s. simus* and the larger morph *A. s. yukonensis* [2, 5, 8, 9]. According to Richards, Churcher [8], *A. s. yukonensis* occupied western North America during the Irvingtonian (1.6–0.25 mya), persisted in Beringia, western Canada, and areas of the western and eastern United States during the Rancholabrean (250–11 kya), and survived up until the terminal Pleistocene in some areas. In contrast, by the Rancholabrean *A. s. simus* had apparently “differentiated south of the Wisconsinan glaciated area and was widespread throughout much of the United States and Mexico” [8]. However, some researchers have argued against the subspecific separation

3.2 MANUSCRIPT

of *A. simus* based on notable size differences observed in specimens from the same site [3, 13] and/or from analysing geographic, temporal, and size variation across the known range of the species [10, 11, 21]. In these cases, researchers suggested that sexual dimorphism could fully account for the recorded size variation in *A. simus*. Further, Schubert [10, 21] discovered that all specimens from cave deposits represent the smaller form (*i.e.* “*A. simus simus*”) and suggested that female *A. simus* utilized caves, perhaps for denning like other bears [10, 11, 21].

Ancient DNA can be used to test hypotheses about sexual dimorphism [22, 23], taxonomy, and phylogeography [24-33]. For example, genetic sex assignment was recently used to confirm that two extinct genera of North American muskoxen — *Symbos* and *Bootherium* — had originally been described based on size variation that actually represented sexual dimorphism within a single species [26]. In terms of phylogeography, the majority of studies in North America have focused on non-endemic megafaunal taxa (*i.e.* those also found outside of North America), including brown bears (*Ursus arctos*) [24, 34, 35], the woolly mammoth (*Mammuthus primigenius*) [27, 32, 33], bison (*Bison* sp.) [28, 30, 31], and lions (*Panthera* sp.) [25]. These studies have generally found that these taxa displayed strong phylogeographic structure, often with a separation between populations in Beringia (“North of the Ice”) and the contiguous USA (“South of the Ice”), as well as dynamic population histories with local extinction and replacement from Eurasia via the Bering Land Bridge (*e.g.* brown bears and bison) [24, 28, 31]. In contrast, very little work has been done on the ancient phylogeographic structure of endemic North American taxa like *A. simus*.

In the present study we investigate the evolutionary history of *Arctodus simus* through time and space, and test the hypothesis that intraspecific size variation represents distinct subspecies. We successfully obtained near complete mitochondrial genome sequences from 34 *A. simus* specimens, representing at least 31 individuals, from a number of deposits across North America. We also used chromosome-specific read-dosage from low-depth shotgun data to determine the sex of 31 individuals in order to test how much of the observed size variation in *A. simus* can be explained by sexual dimorphism.

Methods:***Sampling***

Analyses were performed on 49 bone samples putatively identified as *Arctodus simus* obtained from a range of museum and field collections (Table S1). The samples were broadly distributed across the range of *A. simus*, from Alaska and the Yukon Territory to the contiguous USA. Eight specimens were radiocarbon dated at the Oxford Radiocarbon Accelerator Unit of the University of Oxford. All radiocarbon dates were calibrated with the IntCal13 curve [36] using OxCal 4.4 [37]. Size estimates were collated from Richards, Churcher [8] for relevant specimens, an additional size estimate was obtained for specimen A17860 through measurements performed by author B.W.S.

All pre-PCR steps (*i.e.* extraction, library preparation) were conducted in purpose-built ancient DNA (aDNA) clean-room facilities at the University of Adelaide's Australian Centre for Ancient DNA (ACAD), Australia, spatially separated and physically isolated from any other molecular laboratories. Strict protocols were followed and a number of precautions taken to minimise contamination of samples with exogenous DNA [38]. Protective clothing was worn, including: hooded coveralls over ancient-DNA lab-dedicated clothing (clothes never previously worn in any other molecular laboratory), hairnets, facemasks, face shields, designated footwear for both transitional areas and the physical laboratory, and three pairs of gloves worn at all times to prevent skin exposure between frequent changes of the outer layer of gloves. Furthermore, the lab was designed with positive air pressure, flowing from the cleanest workrooms to the outside of the lab. Stringent decontamination procedures were also be adhered to, including cleaning equipment and surfaces with bleach or disinfectant detergent before and after use as well as regular UV irradiation of surfaces. These precautions also included the inclusion of negative controls for both DNA extraction and PCR setup, and the exclusion of modern positive controls. PCR amplification and all downstream procedures were carried out in independent, physically separated DNA laboratories at the University of Adelaide.

DNA extraction

Surface contamination on each sample was reduced by UV irradiation for 15 min each side followed by abrading the exterior surface (c. 1 mm) using a Dremel tool and a disposable carborundum disk. The sample was then pulverised with a metallic mallet and

3.2 MANUSCRIPT

approximately 100 mg of powder used for extraction using one of two protocols: 1) a phenol-chloroform based extraction protocol Bray, Austin [39]; or 2) an in-house silica-based extraction protocol adapted from Dabney, Knapp [40]. The latter method involved digesting the powder first in 1 mL 0.5 M EDTA for 60 min, followed by an overnight incubation in 970 μ L fresh 0.5 M EDTA and 30 μ L proteinase K (20 mg/ml) at 55 °C. The samples were centrifuged and the supernatant mixed with 13 mL of a modified PB buffer (12.6 mL PB buffer (Qiagen), 6.5 μ L Tween-20, and 390 μ L of 3M Sodium Acetate) and bound to silicon dioxide particles, which were then washed two times with 80% ethanol. The DNA was eluted from silica particles with 100 μ L TE buffer.

Library preparation

Double-stranded Illumina libraries were built following the protocol of Meyer, Kircher [41] using 25 μ L of DNA extract and truncated Illumina adapters with unique dual 7-mer internal barcodes to allow identification and exclusion of any downstream contamination. In addition, all samples underwent partial uracil-DNA glycosylase (UDG) treatment [42] to restrict cytosine deamination, characteristic of ancient DNA, to terminal nucleotides. A short round of PCR using PCR primers complementary to the adapter sequences was performed to increase the total amount of DNA. Cycle number was determined via rtPCR and each library split into 8 separate PCR reactions to minimise PCR bias and maintain library complexity. Each PCR of 25 μ L contained 1 \times HiFi buffer, 2.5 mM MgSO₄, 1 mM dNTPs, 0.5 mM each primer, 0.1 U Platinum Taq Hi-Fi polymerase and 2 μ L DNA. The cycling conditions were 94 °C for 12 min, 12–27 cycles of 94 °C for 30 s, 60 °C for 30 s, and 68 °C for 40 s, followed by 68 °C for 10 min. PCR replicates were pooled and products were then purified using AxyPrep™ magnetic beads (Axygen™). DNA was eluted in 30 μ L EB buffer and quantified with a Qubit fluorometer (Thermo Fisher).

Mitochondrial enrichment

Commercially synthesised biotinylated 80-mer RNA baits (Arbor Biosciences, MI, USA) were used to enrich the libraries for mammalian mitochondrial DNA [19]. DNA-RNA hybridisation enrichment was performed according to manufacturer's recommendations (MYbaits protocol v3) with the exception of 1.25 μ L of baits used per reaction and the incubation step which was changed to 55 °C for 15 hrs followed by 50 °C for 16 hrs. The beads were washed three times with 0.1 \times SSC and 0.1% SDS (5 min at 50 °C). Full-length Illumina sequencing adapters were then added to the enriched libraries via a final

round of “off-bead” PCR split into 5 replicate PCRs (25 µL) containing 1× Gold PCR buffer, 2.5 mM MgCl₂, 1 mM dNTPs, 0.5 mM each sequencing primer and 0.1 U AmpliTaq Gold. Cycling conditions were as follows: 94 °C for 12 min; 15 cycles of 94 °C for 30 s, 60 °C for 30 s, 72 °C for 40 s; and 72 °C for 10 min. Following PCR, replicates were pooled and purified using AxyPrep™ magnetic beads, eluted in 30 µL H₂O, and quantified using a TapeStation (Agilent Technologies). Enriched libraries were pooled and sequenced on an Illumina NextSeq 500 (2x 75 bp paired end).

Data processing

Sequenced reads were demultiplexed using SABRE (<https://github.com/najoshi/sabre>) using the unique 5’ and 3’ barcodes allowing one mismatch in the barcode sequence (-m 1). Demultiplexed reads were then processed through Paleomix v1.2.12 [43]. Within Paleomix adapter sequences were removed and paired end reads merged using ADAPTER REMOVAL 2.1.7 [44], trimming low quality bases (<Phred20 --minquality 4) and discarding merged reads shorter than 25 bp (--minlength: 25). Read quality was visualised before and after adapter trimming using fastQC v0.11.5 (<http://www.bioinformatics.babraham.ac.uk/projects/fastqc/>) to ensure efficient adapter removal.

Merged reads from the mitochondrially enriched libraries were mapped against the published mitochondrial genome sequence of *Arctodus simus* (FM177762) using BWA v0.7.15 (aln -l 1024, -n 0.01, -o 2; Li and Durbin [45]) as implemented in Paleomix. Reads with mapping a Phred score less than 25 were removed using SAMTOOLS v1.5 (Li et al., 2009) and PCR duplicates were removed using “paleomix rmdup_collapsed” and MARKDUPLICATES from the Picard package (<http://broadinstitute.github.io/picard/>). Damage profiles were assessed using MapDamage 2.0.8 [46] (Figure S1). We visualised mapped reads in Geneious Prime v2019.0.4 (<https://www.geneious.com>) and created a 75% majority consensus sequence, calling N at sites with depth of coverage <2X. Consensus sequences were aligned using MUSCLE v3.8.425 [47] as implemented in Geneious Prime v2019.0.4.

Genetic diversity

In order to compare mitogenomic diversity of *A. simus* to other mammalian species of varying life histories, a number of mitogenomes from various species were downloaded

3.2 MANUSCRIPT

from GenBank. The sequences for each species were aligned using MUSCLE v3.8.425 [47] as implemented in Geneious Prime v2019.0.4. The average pairwise distances (k) and nucleotide diversity (π) were calculated in DnaSP v6 [48] for *A. simus* and the downloaded datasets, only including sequences with at least 90% coverage.

Phylogenetic analyses

Population structure was investigated using median-joining haplotype networks [49] constructed in PopART [50]. Haplotype networks were constructed for all specimens with >60% coverage (n=34) and for a subset of specimens with >90% coverage (n=32) of the mitochondrial genome.

Bayesian tip-dating analyses were performed using BEAST 2.6.1 [51]. The dataset used for our Bayesian phylogenetic analyses consisted of 31 aligned sequences (excluding specimens that could be duplicates), 14 of which had finite radiocarbon dates (five new), three of which had infinite radiocarbon dates (all new), and 14 for which no age information was available (Table S1). Firstly, to check the power of the relatively few dated samples to estimate the ages of the undated specimens a leave-one-out cross-validation was performed using only the finite dated specimens [e.g. 29]. Sequentially, the age of each specimen was individually left out and estimated using the remaining sequences as calibration. This approach identified one specimen for which the age could not be recapitulated (Figure S2). The radiocarbon date of this specimen predated the routine utilization ultra-filtration methods of sample preparation for radioisotope analysis [52], and likely underwent an alkali extraction without ultrafiltration (Salvador Herrando-Pérez 2021, personal communication). Therefore, it was deemed that this radiocarbon date was likely unreliable as a result of contamination with modern carbon, resulting in a younger radiocarbon age than the actual age of the specimen [53]. The radiocarbon age for this sample was excluded, and analyses rerun. Subsequently, we sequentially estimated the age of undated specimens and those with infinite ages, using the dated specimens as calibrations. All specimens returned non-zero unimodal age estimates (Figure S3). Runs were performed with a strict clock with a uniform prior on rate ($0-10^{-5}$ mutations per site per year), constant population coalescent tree prior with a $1/X$ distribution on population size, a uniform prior ($0-500,000$) on the age of the sequence being estimated, and run for 15 million steps with sampling every 1500 steps. The substitution model was co-estimated and averaged throughout the analyses using bModelTest [54]. Some chains were extended

to ensure effective sampling sizes near or above 200 for all parameters. The first 10% of samples were discarded as burn-in and parameter values were monitored to check for convergence in Tracer v1.7.1 [55]. Once all specimens had an associated date (whether estimated or radiocarbon), a date-randomisation test was performed [29, 56]. This involved randomly reassigning the ages of the sequences 20 times and comparing the resulting rates. Runs were conducted as for date estimation but excluding a prior on sequence age. The credibility intervals of the rate estimates from the original data and the randomized replicates did not overlap (Figure S4), suggesting our dataset contained sufficient temporal information to estimate evolutionary rates and divergence times.

For the final BEAST analysis, a strict clock was used with a uniform prior on rate ($0-10^{-5}$ mutations per site per year), and a Bayesian skyline coalescent tree prior. We ran three independent MCMC chains, each run for 30 million steps, sampling every 3000 steps. We checked for convergence and sufficient sampling of parameters in Tracer v1.7.1 [55] and combined individual runs after discarding the first 10% of steps as burnin in logcombiner. MCC consensus trees were generated in TreeAnnotator using the median node age. A second BEAST analysis was performed excluding two basal samples with wide 95% higher posterior density (HPD) interval (A183 and A439).

Shotgun sequencing and genetic sex determination

Non-enriched libraries were pooled equimolarly and full-length Illumina sequencing adapters added in a final PCR containing $1\times$ Gold PCR buffer, 2.5 mM MgCl₂, 1 mM dNTPs, 0.5 mM of each sequencing primer and 0.1 U AmpliTaq Gold. Cycling conditions were as follows: 94 °C for 12 min; 15 cycles of 94 °C for 30 s, 60 °C for 30 s, 72 °C for 40 s; and 72 °C for 10 min. Following PCR, replicates were pooled and purified using AxyPrep™ magnetic beads, eluted in 30 uL H₂O, and quantified using a TapeStation (Agilent Technologies). Shotgun libraries were pooled and sequenced on an Illumina NextSeq 500 (2x 75 bp paired end).

Merged reads from the shotgun libraries were mapped to the polar bear reference genome UrsMar 1.0 (GCA_000687225) [57] using Paleomix v 1.2.2 as described above. SAMTOOLS was used to index and generate mapping statistics for the bam files of each sample. As the UrsMar1.0 reference genome is only assembled to the scaffold level, X-linked scaffolds were identified by mapping scaffolds longer than 1 Mb to the dog

3.2 MANUSCRIPT

reference genome, CanFam3.1 [58, 59], using minimap2 [60] with default mapping parameters. Scaffolds with more than 100 kb in total matches to the CanFam3.1 chrX were considered as being putatively X-linked. The genetic sex of each individual was determined by the ratio of reads mapping to the X-linked scaffolds versus those mapping to autosomal scaffolds, as implemented by Gower, Fenderson [22]. As the number of reads mapping to the X-chromosome is assumed to be the result of the length and copy number of the chromosome (i.e., one copy in males, two in females), it is expected that in males approximately half the number of reads will map to the X-chromosome as to an autosome of similar length. Therefore, sex was determined by counting the reads that mapped to the X chromosome and to the autosomes, with the ratio determined after taking into account the length of the respective chromosomes. A ratio-likelihood test was then used to determine whether one sex fit the data better, where the ratio of males clustered near 0.5 and females near 1.0 with a p-value <0.001. Samples that had a ratio that fell between 0.6 and 0.8 did not have a sex assigned.

Results:

Mitochondrial diversity

Of the 49 samples analysed, 36 produced sequencing reads identifiable as belonging to *Arctodus simus* (Table S1). Of these 36 specimens, only 34 produced mitochondrial genome sequences with a coverage of $\geq 60\%$. Network analyses collapsed these 34 sequences into 18 haplotypes (Figure 1B). When restricting to samples with at least 90% coverage ($n = 32$) the number of haplotypes increased to 20 (Figure S5). Three pairs of samples had matching haplotypes, provenance, and sex (where available) and could therefore conceivably be from the same individual (A1954 and A344; A421 and A436; A429 and A440). Consequently, only one sample from each of these pairs was used for subsequent analyses, resulting in a final dataset of 31 sequences (18 haplotypes) with coverage $\geq 60\%$ and 29 sequences (20 haplotypes) with $>90\%$ coverage. Diversity measures for the 29 unique sequences with $>90\%$ coverage showed an average of 27 pairwise mismatches (k) and an average of 0.00186 (± 0.0005) nucleotide differences per site (π). We compared these values to those obtained from a number of other extinct and extant mammalian species (Table 1). *Arctodus simus* exhibited low genetic diversity overall, with lower nucleotide diversity (π) and a lower average number of nucleotide differences between two sequences (k).

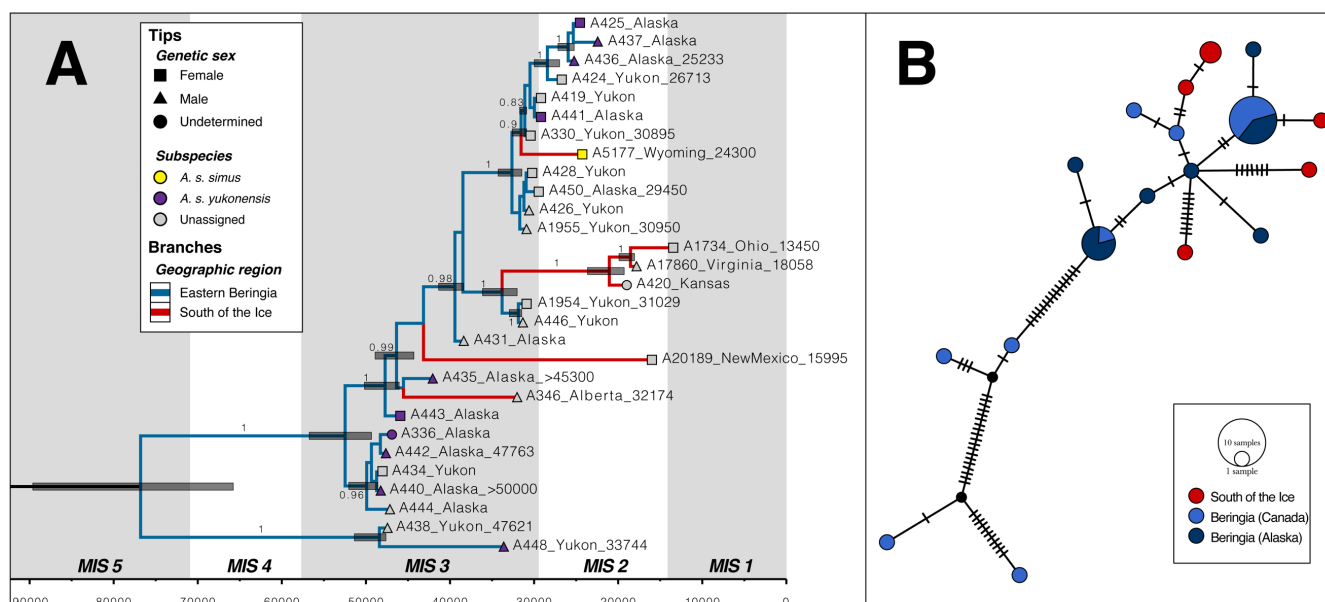


Figure 1: Phylogenetic analysis of *Arctodus simus* mitogenomes with >60% coverage. **A.** Bayesian tip-dated phylogenetic tree, excluding two basal specimens with wide 95% HPDs associated with their age estimates. The grey vertical columns represent odd-numbered MIS stages (interglacials) and white columns even-numbered MIS stages (glacials). See Figure S4 for tree with these samples included. **B.** Median-joining network of all samples. See Figure S5 for network restricted to specimens with >90% coverage.

Phylogenetics and molecular dating

Bayesian phylogenetic analyses allowed us to successfully estimate the age of 17 specimens for which direct radiocarbon dates were unavailable (Table S1, Figure S6). Notably, our analyses suggested ages >100 kya for two specimens from the Yukon Territory: A183 (mean: 125.2 kya, 95% Higher Posterior Density, HPD: 64.2–176.6 kya) and A439 (mean: 183.7 kya, 95% HPD: 97.8–256.8 kya) (Figure S3). Our phylogenetic analyses also suggested that the Time to Most Recent Common Ancestor (TMRCA) of all sampled *A. simus* mitochondrial lineages was 218.3 kya (95% HPD: 176.1–261.3 kya) (Figure S6). When the two older samples — A183 and A439 — were excluded the TMRCA was only 77.1 kya (95% HPD: 66.9–87.8 kya), with the root of the tree falling between a clade comprising two samples from the Yukon Territory (A438 and A448) and the remaining samples (Figure 1A). Samples from south of the North American icesheets (*i.e.* southern Canada and the contiguous USA) did not form a monophyletic clade, but instead belonged to four distinct lineages across five haplotypes intermingled with Eastern Beringian specimens (Figure 1). While *A. simus* did not become extinct in Beringia until ~21 kya, the youngest observed TMRCA between northern and southern *A. simus* samples was 31.7 kya (95% HPD: 30.9–32.6 kya) (Figure 1A).

Table 1: Population genetic diversity statistics for different mammalian taxa. The number of haplotypes (h), haplotype diversity (Hd) and standard deviation, nucleotide diversity (π) and standard deviation, the average number of pairwise differences, and IUCN red list classification.

Species	h	Hd (SD)	π (SD)	k	IUCN
New Zealand Fur Seal (<i>Arctocephalus forsteri</i>)	48	0.999 (0.004)	0.01373 (0.00117)	226.79	Least concern
Lion (<i>Panthera leo</i>)	25	0.992 (0.012)	0.01161 (0.00357)	177.72	Vulnerable
Brown Bear (<i>Ursus arctos</i>)	112	0.994 (0.0025)	0.00947 (0.00061)	138.78	Least concern
Leopard (<i>Panthera pardus</i>)	24	0.98 (0.017)	0.00857 (0.0006)	117.36	Vulnerable
Moose (<i>Alces alces</i>)	47	0.997 (0.005)	0.00809 (0.00479)	128.97	Least concern
Mammoth	50	0.997 (0.004)	0.00685 (0.00068)	95.01	Extinct
Cave bear (<i>Ingressus & Spelaea</i>)	38	0.959 (0.019)	0.00679 (0.00039)	66.99	Extinct
European Bison (<i>Bison bonasus</i>)	31	0.995 (0.009)	0.00611 (0.00029)	72.09	Vulnerable
Tiger (<i>Panthera tigris</i>)	27	0.97 (0.022)	0.00488 (0.00135)	71.71	Endangered
Grey Wolf (<i>Canis lupus</i>)	85	0.994 (0.002)	0.00387 (0.00028)	57.36	Least concern
Grey Fox (<i>Urocyon cinereoargenteus</i>)	22	0.983 (0.015)	0.00361 (0.00111)	59.39	Least concern
Tasmanian Devil (<i>Sarcophilus harrisi</i>)	30	0.986 (0.01)	0.00346 (0.00027)	53.96	Endangered
Polar Bear (<i>Ursus maritimus</i>)	23	0.973 (0.014)	0.00335 (0.00114)	54.85	Vulnerable
Orca (<i>Orcinus orca</i>)	29	0.998 (0.009)	0.00306 (0.00015)	50.07	Data deficient
Thylacine (<i>Thylacinus cynocephalus</i>)	23	0.932 (0.023)	0.00269 (0.00044)	40.61	Extinct
Ingressus (<i>Ursus ingressus</i>)	19	0.983 (0.021)	0.00249 (0.00035)	32.61	Extinct
Cougar (<i>Puma concolor</i>)	10	0.905 (0.035)	0.00219 (0.0006)	35.56	Least concern
<i>Arctodus simus</i>	20	0.954 (0.021)	0.00186 (0.0005)	27.05	Extinct
New World Stilt-Legged Horse (<i>Haringtonhippus francisci</i>)	20	0.984 (0.019)	0.00167 (0.00039)	23.58	Extinct
Steller Sealion (<i>Eumetopias jubatus</i>)	10	0.982 (0.046)	0.00161 (0.0003)	25.87	Near threatened
Spelaeus (<i>Ursus spelaeus</i>)	20	0.899 (0.045)	0.00137 (0.0002)	15.37	Extinct
Island Fox (<i>Urocyon littoralis</i>)	10	0.876 (0.015)	0.00101 (0.00008)	16.65	Near threatened
Eurasian Lynx (<i>Lynx lynx</i>)	24	0.927 (0.011)	0.001 (0.00007)	16.31	Least concern
Brown Hyena (<i>Hyaena brunnea</i>)	8	0.895 (0.053)	0.00021 (0.00002)	3.66	Near threatened

Subspecific assignment

The majority of the specimens assigned to a subspecies based on size data as per Richards, Churcher [8] were assigned to the larger *A. s. yukonensis* (Table 2). Only one specimen (A5177), from Natural Trap Cave in Wyoming, was assigned to *A. s. simus* [8] (Table 1). Reciprocal monophyly was not observed between the two hypothesised subspecies, with the phylogenetic position of A5177 nested within “*A. s. yukonensis*”, most closely related to specimens from Eastern Beringia (Figure 2). The specimen shared a common ancestor with specimens representing “*A. s. yukonensis*” 31.7 kya (95% HPD: 30.9–32.6 kya), much later than the split between the two putative subspecies proposed based on fossil data.

Genetic sex determination

We were able to determine the sex of 29 specimens belonging to unambiguously unique individuals (Table 2): 13 females and 16 males. However, only 11 specimens could be characterised as large or small based off Richards, Churcher [8] or by additional measurements. Of these 11, all large specimens were males ($n = 7$) and all smaller specimens females ($n = 4$), including the one specimen proposed to represent “*A. s. simus*” [8]. Three of the specimens that produced genetic results were associated with cave sites, all of which were female (Table 2). While one of these specimens was excavated from Natural Trap Cave, and likely represents an individual that fell into the cave, the other two specimens were found in caves that could represent denning sites.

3.2 MANUSCRIPT

Table 2: Genetic sex and morphological size of specimens with positive genetic ID for *Arctodus simus*. Samples that could not be confirmed to be from separate individuals were considered to be from the same individual. Superscript numbers in subspecies column refer to the reference number from Richards, Churcher [8]. Size estimates are taken from Richards, Churcher [8] unless indicated otherwise.

Sample number	Museum Accession	Genetic Sex	Richards 1996 subspecies	Size	Country	Specific Location
183	CMN 44730	F	none		Canada (Yukon)	Sixty Mile
330	CMN 49874	F	none		Canada (Yukon)	Hester Creek
336	AMNH F:AM 145914	U	<i>A. s. yukonensis</i> ⁹²	large	USA (Alaska)	Cripple Creek
346	P96.2.38	M	none		Canada (Alberta)	Consolidated pit 48
419	CMN 42335	F	none		Canada (Yukon)	Hunker Creek
420	KUVP 88869	U	none		USA (Kansas)	Kansas River, Leavenworth
424	CMN 37957	F	none		Canada (Yukon)	Eldorado Creek
425	AMNH F:AM 30493	F	<i>A. s. yukonensis</i> ⁹¹	small	USA (Alaska)	Cleary Creek
426	CMN 44566	M	none		Canada (Yukon)	Hunker Creek
428	CMN 34556	M	none		Canada (Yukon)	Gold Run
431	PM-97-001-100	M	none		USA (Alaska)	Eva Creek Mine
434	YG-24.1 CRH-95-3	F	none		Canada (Yukon)	Ophir Creek
435	AMNH F:AM 127693	M	<i>A. s. yukonensis</i> ⁹⁵	large	USA (Alaska)	Ester Creek
436; 421	AMNH F:AM 145917; AMNH F:AM 145915	M	<i>A. s. yukonensis</i> ⁹⁷	large	USA (Alaska)	Goldstream
437	AMNH F:AM 145920	M	<i>A. s. yukonensis</i> ⁹⁷	large	USA (Alaska)	Goldstream
438	CMN 42388	M	ssp? ⁸⁰	no measure	Canada (Yukon)	Sixtymile
439	CMN 26864	M	<i>A. s. yukonensis</i> ⁸⁴	no measure	Canada (Yukon)	Old Crow River
440; 429	AMNH F:AM 145560; AMNH F:AM 145561	M	<i>A. s. yukonensis</i> ⁹²	large	USA (Alaska)	Cripple Creek
441	AMNH F:AM 95656	F	<i>A. s. yukonensis</i> ⁹⁵	small	USA (Alaska)	Ester Creek
442	AMNH F:AM 145918	M	<i>A. s. yukonensis</i> ⁹²	large	USA (Alaska)	Cripple Creek
443	AMNH F:AM 127688	F	<i>A. s. yukonensis</i> ⁹⁸	small	USA (Alaska)	Cripple Creek
444	AMNH F:AM 145919	M	none		USA (Alaska)	Cripple Creek
446	CMN 36236	M	none		Canada (Yukon)	Dawson Area
448	CMN 37577	M	<i>A. s. yukonensis</i> ⁷⁷	no measure	Canada (Yukon)	Hunker Creek
450	AMNH F:AM 145921	F	none		USA (Alaska)	Alaska
1734	CMNHS VP8289	F	ssp? ²	no measure	USA (Ohio)	Sheriden Pit
1954	YT03/134	F	none		Canada (Yukon)	Quartz Creek
1955; 344	YT03/288 Cat No 129.1; YG 76.4	M	none		Canada (Yukon)	Hester Creek
5177	KU 31956	F	<i>A. s. simus</i> ⁴⁹	small	USA (Wyoming)	Natural Trap Cave
17859*	NSRL 276, CHEM 358, CHN-444, AAA-236	U	<i>A. s. yukonensis</i> ⁶⁶	large	USA (Utah)	Huntington Dam
17860	ETMNH 3429	M	none	large [#]	USA (Virginia)	Saltville
20189		F	spp? ²¹	unknown	USA (New Mexico)	Oso cave

* Specimen did not produce sufficient mitogenomic data

Size estimated by Blaine Schubert

Discussion:

Our genetic results are incompatible with the hypothesis that there were two subspecies of *Arctodus simus* (*A. s. simus* and *A. s. yukonensis*) in North America during the Late Pleistocene. Instead it appears all specimens in this study represent members of a single highly sexually dimorphic taxon, with males sometimes being twice as large as females [10]. This interpretation is supported by our observations that the only putative “*A. s. simus*” sample in our dataset fell within the mitochondrial diversity of “*A. s. yukonensis*”, and that the size of specimens we analysed closely reflected the sex of the individual. Further, the lack of deep phylogeographic structure between *A. simus* populations north and south of the North American ice sheets suggests that the ice sheets did not represent a severe barrier to dispersal, as they did for other megafaunal taxa during the Pleistocene, such as bison [28, 30], brown bears [24, 34, 61], and lions [25]. Alternatively, the ice sheets may have posed a geographic barrier to *Arctodus* while at their maximum extent, but the species was able to migrate freely soon after the icesheets retreated post-LGM. Definitively resolving the chronology and direction of *Arctodus* migration will require aDNA from additional southern specimens from before the LGM.

The lack of mitochondrial phylogeographic structure observed in *Arctodus simus* supports the hypothesis that it was wide-ranging and more vagile than other species of bear [1, 7, 62, 63]. This result also suggests that *Arctodus* may not have engaged in the same level of philopatry seen in other bear species such as brown bears, where strong maternal philopatry has resulted in striking phylogeographic structure [24, 35, 61] and perhaps contributed to an overrepresentation of males in the fossil record [22]. Indeed, while our sample size was smaller, the proportion of male *A. simus* individuals we detected in the present study (55%) was much lower than previously reported for brown bear subfossils (75% [22]). This result further supports the hypothesis that *A. simus* did not show strong maternal philopatry.

Overall *Arctodus simus* appears to have possessed relatively low genetic diversity, similar to species that have undergone bottlenecks, such as Steller’s sea lion, and solitary wide-ranging carnivores such as the cougar and Eurasian lynx (Table 2). The lowered genetic diversity and shallow mitogenomic structure in *A. simus* may therefore be a result of population bottlenecks leading up to their extinction, possibly with competition with

3.2 MANUSCRIPT

invading brown bears playing a role [24]. Alternatively, this lowered diversity could simply be a function of the ecological niche that *A. simus* filled, or a characteristic of tremarctine bears in general. Indeed, wide-ranging, solitary carnivores often possess lowered genetic diversity; for example, the cougar [64-66], cape vulture [67], snow leopard [68-70], and cheetah [71, 72]. Notably, brown hyenas and striped hyenas, wide-ranging scavengers, also lack clear phylogeographic signals and have lower mitochondrial diversity [73, 74], as do scavenging bird species with high dispersal capabilities, such as vultures [67, 75-77]. Overall, our findings agree with morphological evidence that *A. simus* was a wide-ranging carnivoran, with fossils possessing characters suggestive of a gait suited for long-range dispersal [7, 34, 63].

While not conclusive, our findings are also consistent with the hypothesis that *A. simus* females used caves for denning, as observed among extant spectacled bears [78] and suggested for the extinct *Arctotherium angustidens* [79]. Schubert and Kaufmann [21] noted that no large specimens of *A. simus* — which our genetic results suggest represent males — have been associated with cave sites. In contrast, the two samples we analysed that were from putative denning caves were small and female. Ultimately, our results further demonstrate the power of ancient DNA for resolving outstanding questions about behaviour and morphological variation of other Pleistocene species, particularly with respect to sex-linked differences. Application of similar genomic methods may be particularly useful for resolving the causes of conflict between mitochondrial DNA data and morphology-based taxonomy in groups like bison, where several morphologically divergent species have been described that do not appear to be genetically distinct [e.g. 30, 31].

Acknowledgements:

We would like to thank the following institutions for allowing access to specimens: Canadian Museum of Nature, University of Kansas Natural History Museum, Yukon Territorial Government, American Museum of Natural History, and the Royal Alberta Museum. In addition, we are grateful to the following individuals who helped in the collection and identification of specimens and/or provided laboratory support: Grant Zazula, Jeremy Austin, Sarah Bray, Jacobo Weinstock, Ian Barnes, Beth Shapiro, and Paul Matheus. We would like to thank the Wyoming BLM and permit number PA-13-WY-

207. This research was funded by an Australian Research Council Laureate Fellowship awarded to AC (FL140100260) and U.S. National Science Foundation grant (EAR/SGP#1425059) awarded to JM and AC.

References

- [1] Christiansen, P. 1999 What size were *Arctodus simus* and *Ursus spelaeus* (Carnivora: Ursidae)? *Ann. Zool. Fenn.* **36**, 93-102.
- [2] Churcher, C.S., Morgan, A.V. & Carter, L.D. 1993 *Arctodus simus* from the Alaskan Arctic Slope. *Can. J. Earth Sci.* **30**, 1007-1013. (doi:10.1139/e93-084).
- [3] Cox, S. 1991 Size range or sexual dimorphism in *Arctodus simus* from Rancho La Brea. *Annual Meeting of the Southern California Academy of Sciences*. Abstract 15.
- [4] Figueirido, B., Pérez-Claros, J.A., Torregrosa, V., Martín-Serra, A. & Palmqvist, P. 2010 Demythologizing *Arctodus simus*, the ‘short-faced’ long-legged and predaceous bear that never was. *J. Vertebr. Paleontol.* **30**, 262-275. (doi:10.1080/02724630903416027).
- [5] Gobetz, K. & Martin, L. 2001 An exceptionally large short faced bear (*Arctodus simus*) from the late Pleistocene (?)/early Holocene of Kansas. *Curr. Res. Pleistocene* **18**, 97-99.
- [6] Krause, J., Unger, T., Nocon, A., Malaspinas, A.S., Kolokotronis, S.O., Stiller, M., Soibelzon, L., Spriggs, H., Dear, P.H., Briggs, A.W., et al. 2008 Mitochondrial genomes reveal an explosive radiation of extinct and extant bears near the Miocene-Pliocene boundary. *BMC Evol. Biol.* **8**, 220. (doi:10.1186/1471-2148-8-220).
- [7] Matheus, P.E. 1995 Diet and co-ecology of Pleistocene short-faced bears and brown bears in eastern Beringia. *Quat. Res.* **44**, 447-453. (doi:10.1006/qres.1995.1090).
- [8] Richards, R.L., Churcher, C.S. & Turnbull, W.D. 1996 Distribution and size variation in North American short-faced bears, *Arctodus simus*. In *Palaeoecology and palaeoenvironments of late Cenozoic mammals: tributes to the career of C.S. (Rufus) Churcher* (eds. K.M. Stewart & K.L. Seymour), pp. 191-246. Toronto, University of Toronto Press.
- [9] Richards, R.L. & Turnbull, W.D. 1995 Giant short-faced bear (*Arctodus simus yukonensis*) remains from Fulton County, northern Indiana. *Fieldiana. Geol.* **30**, 1-34. (doi:10.5962/bhl.title.3480).
- [10] Schubert, B.W. 2010 Late Quaternary chronology and extinction of North American giant short-faced bears (*Arctodus simus*). *Quat. Int.* **217**, 188-194. (doi:10.1016/j.quaint.2009.11.010).

3.2 MANUSCRIPT

- [11] Schubert, B.W., Hulbert, R.C., MacFadden, B.J., Searle, M. & Searle, S. 2010 Giant Short-Faced Bears (*Arctodus simus*) in Pleistocene Florida USA; A Substantial Range Extension. *J. Paleontol.* **84**, 79-87. (doi:10.1666/09-113.1).
- [12] Schubert, B.W. & Wallace, S.C. 2009 Late Pleistocene giant short-faced bears, mammoths, and large carcass scavenging in the Saltville Valley of Virginia, USA. *Boreas* **38**, 482-492. (doi:10.1111/j.1502-3885.2009.00090.x).
- [13] Scott, E. & Cox, S.M. 1993 *Arctodus simus* (Cope, 1879) from Riverside County, California. *Paleobios* **15**, 27-36.
- [14] Steffen, M.L. & Fulton, T.L. 2018 On the association of giant short-faced bear (*Arctodus simus*) and brown bear (*Ursus arctos*) in late Pleistocene North America. *Geobios* **51**, 61-74. (doi:10.1016/j.geobios.2017.12.001).
- [15] Tedford, R.H. & Martin, J. 2001 *Plionarctos*, a tremarctine bear (Ursidae: Carnivora) from western North America. *J. Vertebr. Paleontol.* **21**, 311-321. (doi:10.1671/0272-4634(2001)021[0311:PATBUC]2.0.CO;2).
- [16] Emslie, S.D. 1995 The fossil record of *Arctodus pristinus* (Ursidae: Tremarctinae) in Florida. *Bull. Fla. Mus. Nat. Hist.* **37**, 501-514.
- [17] Kurtén, B. 1967 Pleistocene bears of North America. 2. Genus *Arctodus*, short-faced bears. *Acta Zool. Fenn.* **117**, 1-60.
- [18] Soibelzon, L.H. 2004 Revisión sistemática de los Tremarctinae (Carnivora, Ursidae) fósiles de América del Sur. *Rev. Mus. Argent. Cienc. Nat.* **6**, 107-133.
- [19] Mitchell, K.J., Bray, S.C., Bover, P., Soibelzon, L., Schubert, B.W., Prevosti, F., Prieto, A., Martin, F., Austin, J.J. & Cooper, A. 2016 Ancient mitochondrial DNA reveals convergent evolution of giant short-faced bears (Tremarctinae) in North and South America. *Biol. Lett.* **12**, 20160062. (doi:10.1098/rsbl.2016.0062).
- [20] Stirling, I. 1993 The living bears. In *Bears: Majestic Creatures of the Wild*. (ed. I. Stirling), pp. 36-49. Emmaus, Rodale Press.
- [21] Schubert, B.W. & Kaufmann, J.E. 2003 A partial short-faced bear skeleton from an Ozark cave with comments on the paleobiology of the species. *J. Cave Karst Stud.* **65**, 101-110.
- [22] Gower, G., Fenderson, L.E., Salis, A.T., Helgen, K.M., van Loenen, A.L., Heiniger, H., Hofman-Kaminska, E., Kowalczyk, R., Mitchell, K.J., Llamas, B., et al. 2019 Widespread male sex bias in mammal fossil and museum collections. *Proc. Natl. Acad. Sci. U. S. A.* **116**, 19019-19024. (doi:10.1073/pnas.1903275116).
- [23] Pecnerova, P., Diez-Del-Molino, D., Dussex, N., Feuerborn, T., von Seth, J., van der Plicht, J., Nikolskiy, P., Tikhonov, A., Vartanyan, S. & Dalen, L. 2017 Genome-Based Sexing Provides Clues about Behavior and Social Structure in the Woolly Mammoth. *Curr. Biol.* **27**, 3505-3510.e3503. (doi:10.1016/j.cub.2017.09.064).

- [24] Barnes, I., Matheus, P., Shapiro, B., Jensen, D. & Cooper, A. 2002 Dynamics of Pleistocene population extinctions in Beringian brown bears. *Science* **295**, 2267-2270. (doi:10.1126/science.1067814).
- [25] Barnett, R., Shapiro, B., Barnes, I., Ho, S.Y.W., Burger, J., Yamaguchi, N., Higham, T.F.G., Wheeler, H.T., Rosendahl, W., Sher, A.V., et al. 2009 Phylogeography of lions (*Panthera leo* ssp.) reveals three distinct taxa and a late Pleistocene reduction in genetic diversity. *Mol. Ecol.* **18**, 1668-1677. (doi:10.1111/j.1365-294X.2009.04134.x).
- [26] Bover, P., Llamas, B., Thomson, V.A., Pons, J., Cooper, A. & Mitchell, K.J. 2018 Molecular resolution to a morphological controversy: The case of North American fossil muskoxen *Bootherium* and *Symbos*. *Mol. Phylogenet. Evol.* **129**, 70-76. (doi:10.1016/j.ympev.2018.08.008).
- [27] Enk, J., Devault, A., Widga, C., Saunders, J., Szpak, P., Southon, J., Rouillard, J.-M., Shapiro, B., Golding, G.B., Zazula, G., et al. 2016 *Mammuthus* population dynamics in Late Pleistocene North America: Divergence, phylogeography, and introgression. *Front. Ecol. Evol.* **4**, 42. (doi:10.3389/fevo.2016.00042).
- [28] Heintzman, P.D., Froese, D., Ives, J.W., Soares, A.E., Zazula, G.D., Letts, B., Andrews, T.D., Driver, J.C., Hall, E., Hare, P.G., et al. 2016 Bison phylogeography constrains dispersal and viability of the Ice Free Corridor in western Canada. *Proc. Natl. Acad. Sci. U. S. A.* **113**, 8057-8063. (doi:10.1073/pnas.1601077113).
- [29] Stiller, M., Molak, M., Prost, S., Rabeder, G., Baryshnikov, G., Rosendahl, W., Münzel, S., Bocherens, H., Grandal-d'Anglade, A., Hilpert, B., et al. 2014 Mitochondrial DNA diversity and evolution of the Pleistocene cave bear complex. *Quat. Int.* **339-340**, 224-231. (doi:10.1016/j.quaint.2013.09.023).
- [30] Shapiro, B., Drummond, A.J., Rambaut, A., Wilson, M.C., Matheus, P.E., Sher, A.V., Pybus, O.G., Gilbert, M.T.P., Barnes, I., Binladen, J., et al. 2004 Rise and fall of the Beringian steppe bison. *Science* **306**, 1561-1565. (doi:10.1126/science.1101074).
- [31] Froese, D., Stiller, M., Heintzman, P.D., Reyes, A.V., Zazula, G.D., Soares, A.E., Meyer, M., Hall, E., Jensen, B.J., Arnold, L.J., et al. 2017 Fossil and genomic evidence constrains the timing of bison arrival in North America. *Proc. Natl. Acad. Sci. U. S. A.* **114**, 3457-3462. (doi:10.1073/pnas.1620754114).
- [32] Debruyne, R., Chu, G., King, C.E., Bos, K., Kuch, M., Schwarz, C., Szpak, P., Grocke, D.R., Matheus, P., Zazula, G., et al. 2008 Out of America: Ancient DNA evidence for a New World origin of Late Quaternary woolly mammoths. *Curr. Biol.* **18**, 1320-1326. (doi:10.1016/j.cub.2008.07.061).
- [33] Palkopoulou, E., Dalen, L., Lister, A.M., Vartanyan, S., Sablin, M., Sher, A., Edmark, V.N., Brandstrom, M.D., Germonpre, M., Barnes, I., et al. 2013 Holarctic genetic structure and range dynamics in the woolly mammoth. *Proc. R. Soc. B.* **280**, 20131910. (doi:10.1098/rspb.2013.1910).

3.2 MANUSCRIPT

- [34] Matheus, P., Burns, J., Weinstock, J. & Hofreiter, M. 2004 Pleistocene brown bears in the mid-continent of North America. *Science* **306**, 1150-1150. (doi:10.1126/science.1101495).
- [35] Leonard, J.A., Wayne, R.K. & Cooper, A. 2000 Population genetics of Ice age brown bears. *Proc. Natl. Acad. Sci. U. S. A.* **97**, 1651-1654. (doi:10.1073/pnas.040453097).
- [36] Reimer, P.J., Bard, E., Bayliss, A., Beck, J.W., Blackwell, P.G., Ramsey, C.B., Buck, C.E., Cheng, H., Edwards, R.L., Friedrich, M., et al. 2013 Intcal13 and Marine13 radiocarbon age calibration curves 0-50,000 years cal BP. *Radiocarbon* **55**, 1869-1887. (doi:10.2458/azu_js_rc.55.16947).
- [37] Ramsey, C.B. 2009 Bayesian analysis of radiocarbon dates. *Radiocarbon* **51**, 337-360. (doi:10.1017/S0033822200033865).
- [38] Cooper, A. & Poinar, H.N. 2000 Ancient DNA: Do it right or not at all. *Science* **289**, 1139. (doi:10.1126/science.289.5482.1139b).
- [39] Bray, S.C.E., Austin, J.J., Metcalf, J.L., Østbye, K., Østbye, E., Lauritzen, S.-E., Aaris-Sørensen, K., Valdiosera, C., Adler, C.J. & Cooper, A. 2013 Ancient DNA identifies post-glacial recolonisation, not recent bottlenecks, as the primary driver of contemporary mtDNA phylogeography and diversity in Scandinavian brown bears. *Divers. Distrib.* **19**, 245-256. (doi:10.1111/j.1472-4642.2012.00923.x).
- [40] Dabney, J., Knapp, M., Glocke, I., Gansauge, M.-T., Weihmann, A., Nickel, B., Valdiosera, C., García, N., Pääbo, S., Arsuaga, J.-L., et al. 2013 Complete mitochondrial genome sequence of a Middle Pleistocene cave bear reconstructed from ultrashort DNA fragments. *Proc. Natl. Acad. Sci. U. S. A.* **110**, 15758-15763.
- [41] Meyer, M., Kircher, M., Gansauge, M.T., Li, H., Racimo, F., Mallick, S., Schraiber, J.G., Jay, F., Prufer, K., de Filippo, C., et al. 2012 A high-coverage genome sequence from an archaic Denisovan individual. *Science* **338**, 222-226. (doi:10.1126/science.1224344).
- [42] Rohland, N., Harney, E., Mallick, S., Nordenfelt, S. & Reich, D. 2015 Partial uracil-DNA-glycosylase treatment for screening of ancient DNA. *Philos. Trans. R. Soc. Lond. B. Biol. Sci* **370**, 20130624. (doi:10.1098/rstb.2013.0624).
- [43] Schubert, M., Ermini, L., Sarkissian, C.D., Jonsson, H., Ginolhac, A., Schaefer, R., Martin, M.D., Fernandez, R., Kircher, M., McCue, M., et al. 2014 Characterization of ancient and modern genomes by SNP detection and phylogenomic and metagenomic analysis using PALEOMIX. *Nat. Protoc.* **9**, 1056-1082. (doi:10.1038/nprot.2014.063).
- [44] Schubert, M., Lindgreen, S. & Orlando, L. 2016 AdapterRemoval v2: rapid adapter trimming, identification, and read merging. *BMC Res. Notes* **9**, 88. (doi:10.1186/s13104-016-1900-2).
- [45] Li, H. & Durbin, R. 2009 Fast and accurate short read alignment with Burrows-Wheeler transform. *Bioinformatics* **25**, 1754-1760. (doi:10.1093/bioinformatics/btp324).

- [46] Jonsson, H., Ginolhac, A., Schubert, M., Johnson, P.L.F. & Orlando, L. 2013 mapDamage2.0: fast approximate Bayesian estimates of ancient DNA damage parameters. *Bioinformatics* **29**, 1682-1684. (doi:10.1093/bioinformatics/btt193).
- [47] Edgar, R.C. 2004 MUSCLE: multiple sequence alignment with high accuracy and high throughput. *Nucleic Acids Res.* **32**, 1792-1797. (doi:10.1093/nar/gkh340).
- [48] Rozas, J., Ferrer-Mata, A., Sanchez-DelBarrio, J.C., Guirao-Rico, S., Librado, P., Ramos-Onsins, S.E. & Sanchez-Gracia, A. 2017 DnaSP 6: DNA Sequence Polymorphism Analysis of Large Data Sets. *Mol. Biol. Evol.* **34**, 3299-3302. (doi:10.1093/molbev/msx248).
- [49] Bandelt, H.J., Forster, P. & Rohl, A. 1999 Median-joining networks for inferring intraspecific phylogenies. *Mol. Biol. Evol.* **16**, 37-48. (doi:10.1093/oxfordjournals.molbev.a026036).
- [50] Leigh, J.W. & Bryant, D. 2015 POPART: full-feature software for haplotype network construction. *Methods in Ecology and Evolution* **6**, 1110-1116. (doi:10.1111/2041-210x.12410).
- [51] Bouckaert, R., Vaughan, T.G., Barido-Sottani, J., Duchene, S., Fourment, M., Gavryushkina, A., Heled, J., Jones, G., Kuhnert, D., De Maio, N., et al. 2019 BEAST 2.5: An advanced software platform for Bayesian evolutionary analysis. *PLoS Comp. Biol.* **15**, e1006650. (doi:10.1371/journal.pcbi.1006650).
- [52] Matheus, P.E. 1997 Paleoeology and ecomorphology of the giant short-faced bear in Eastern Beringia. Fairbanks, Alaska, University of Alaska Fairbanks.
- [53] Higham, T.F.G., Jacobi, R.M. & Ramsey, C.B. 2006 AMS radiocarbon dating of ancient bone using ultrafiltration. *Radiocarbon* **48**, 179-195. (doi:10.1017/S0033822200066388).
- [54] Bouckaert, R.R. & Drummond, A.J. 2017 bModelTest: Bayesian phylogenetic site model averaging and model comparison. *BMC Evol. Biol.* **17**, 42. (doi:10.1186/s12862-017-0890-6).
- [55] Rambaut, A., Drummond, A.J., Xie, D., Baele, G. & Suchard, M.A. 2018 Posterior summarization in bayesian phylogenetics using Tracer 1.7. *Syst. Biol.* **67**, 901-904. (doi:10.1093/sysbio/syy032).
- [56] Ramsden, C., Holmes, E.C. & Charleston, M.A. 2009 Hantavirus evolution in relation to its rodent and insectivore hosts: no evidence for codivergence. *Mol. Biol. Evol.* **26**, 143-153. (doi:10.1093/molbev/msn234).
- [57] Liu, S.P., Lorenzen, E.D., Fumagalli, M., Li, B., Harris, K., Xiong, Z.J., Zhou, L., Korneliussen, T.S., Somel, M., Babbitt, C., et al. 2014 Population genomics reveal recent speciation and rapid evolutionary adaptation in polar bears. *Cell* **157**, 785-794. (doi:10.1016/j.cell.2014.03.054).
- [58] Hoepfner, M.P., Lundquist, A., Pirun, M., Meadows, J.R., Zamani, N., Johnson, J., Sundstrom, G., Cook, A., FitzGerald, M.G., Swofford, R., et al. 2014 An improved

3.2 MANUSCRIPT

- canine genome and a comprehensive catalogue of coding genes and non-coding transcripts. *PLoS ONE* **9**, e91172. (doi:10.1371/journal.pone.0091172).
- [59] Lindblad-Toh, K., Wade, C.M., Mikkelsen, T.S., Karlsson, E.K., Jaffe, D.B., Kamal, M., Clamp, M., Chang, J.L., Kulbokas, E.J., Zody, M.C., et al. 2005 Genome sequence, comparative analysis and haplotype structure of the domestic dog. *Nature* **438**, 803-819. (doi:10.1038/nature04338).
- [60] Li, H. 2018 Minimap2: pairwise alignment for nucleotide sequences. *Bioinformatics* **34**, 3094-3100. (doi:10.1093/bioinformatics/bty191).
- [61] Davison, J., Ho, S.Y.W., Bray, S.C., Korsten, M., Tammeleht, E., Hindrikson, M., Ostbye, K., Ostbye, E., Lauritzen, S.E., Austin, J., et al. 2011 Late-Quaternary biogeographic scenarios for the brown bear (*Ursus arctos*), a wild mammal model species. *Quat. Sci. Rev.* **30**, 418-430. (doi:10.1016/j.quascirev.2010.11.023).
- [62] Matheus, P.E. 2003 Locomotor adaptations and ecomorphology of short-faced bears (*Arctodus simus*) in eastern Beringia. In *Occasional Papers in Earth Science No. 7* (Whitehorse, Yukon Palaeontology Program, Department of Tourism and Culture).
- [63] Kurtén, B. & Anderson, E. 1980 *Pleistocene Mammals of North America*. New York, Columbia University Press; 442 p.
- [64] Caragiulo, A., Dias-Freedman, I., Clark, J.A., Rabinowitz, S. & Amato, G. 2014 Mitochondrial DNA sequence variation and phylogeography of Neotropic pumas (*Puma concolor*). *Mitochondrial DNA* **25**, 304-312. (doi:10.3109/19401736.2013.800486).
- [65] Mcrae, B.H., Beier, P., Dewald, L.E., Huynh, L.Y. & Keim, P. 2005 Habitat barriers limit gene flow and illuminate historical events in a wide-ranging carnivore, the American puma. *Mol. Ecol.* **14**, 1965-1977. (doi:10.1111/j.1365-294X.2005.02571.x).
- [66] Saremi, N.F., Supple, M.A., Byrne, A., Cahill, J.A., Coutinho, L.L., Dalen, L., Figueiro, H.V., Johnson, W.E., Milne, H.J., O'Brien, S.J., et al. 2019 Puma genomes from North and South America provide insights into the genomic consequences of inbreeding. *Nat. Commun.* **10**. (doi:10.1038/s41467-019-12741-1).
- [67] Kleinhans, C. & Willows-Munro, S. 2019 Low genetic diversity and shallow population structure in the endangered vulture, *Gyps coprotheres*. *Sci. Rep.* **9**, 5536. (doi:10.1038/s41598-019-41755-4).
- [68] Aruge, A., Batool, H., Khan, F.M., Fakhar-i-Abbas & Janjua, S. 2019 A pilot study-genetic diversity and population structure of snow leopards of Gilgit-Baltistan, Pakistan, using molecular techniques. *PeerJ* **7**, e7672. (doi:10.7717/peerj.7672).
- [69] Janecka, J.E., Jackson, R., Yuquang, Z., Diqiang, L., Munkhtsog, B., Buckley-Beason, V. & Murphy, W.J. 2008 Population monitoring of snow leopards using noninvasive collection of scat samples: a pilot study. *Anim. Conserv.* **11**, 401-411. (doi:10.1111/j.1469-1795.2008.00195.x).

- [70] Janecka, J.E., Zhang, Y.G., Li, D.Q., Munkhtsog, B., Bayaraa, M., Galsandorj, N., Wangchuk, T.R., Karmacharya, D., Li, J., Lu, Z., et al. 2017 Range-Wide Snow Leopard Phylogeography Supports Three Subspecies. *J. Hered.* **108**, 597-607. (doi:10.1093/jhered/esx044).
- [71] Dobrynin, P., Liu, S., Tamazian, G., Xiong, Z., Yurchenko, A.A., Krashennnikova, K., Kliver, S., Schmidt-Kuntzel, A., Koepfli, K.P., Johnson, W., et al. 2015 Genomic legacy of the African cheetah, *Acinonyx jubatus*. *Genome Biol.* **16**, 277. (doi:10.1186/s13059-015-0837-4).
- [72] Schmidt-Küntzel, A., Dalton, D.L., Menotti-Raymond, M., Fabiano, E., Charruau, P., Johnson, W.E., Sommer, S., Marker, L., Kotzé, A. & O'Brien, S.J. 2018 Conservation Genetics of the Cheetah: Genetic History and Implications for Conservation. In *Cheetahs: Biology and Conservation* (eds. L. Marker, L. Boast & A. Schmidt-Küntzel), pp. 71-92. San Diego, Elsevier.
- [73] Rohland, N., Pollack, J.L., Nagel, D., Beauval, C., Airvaux, J., Paabo, S. & Hofreiter, M. 2005 The population history of extant and extinct hyenas. *Mol. Biol. Evol.* **22**, 2435-2443. (doi:10.1093/molbev/msi244).
- [74] Westbury, M.V., Hartmann, S., Barlow, A., Wiesel, I., Leo, V., Welch, R., Parker, D.M., Sicks, F., Ludwig, A., Dalen, L., et al. 2018 Extended and Continuous Decline in Effective Population Size Results in Low Genomic Diversity in the World's Rarest Hyena Species, the Brown Hyena. *Mol. Biol. Evol.* **35**, 1225-1237. (doi:10.1093/molbev/msy037).
- [75] Arshad, M., Gonzalez, J., El-Sayed, A.A., Osborne, T. & Wink, M. 2009 Phylogeny and phylogeography of critically endangered *Gyps* species based on nuclear and mitochondrial markers. *J. Ornithol.* **150**, 419-430. (doi:10.1007/s10336-008-0359-x).
- [76] Kretzmann, M.B., Capote, N., Gautschi, B., Godoy, J.A., Donázar, J.A. & Negro, J.J. 2003 Genetically distinct island populations of the Egyptian vulture (*Neophron percnopterus*). *Conserv. Genet.* **4**, 697-706. (doi:10.1023/B:COGE.0000006123.67128.86).
- [77] Le Gouar, P., Rigal, F., Boisselier-Dubayle, M.C., Sarrazin, F., Arthur, C., Choisy, J.P., Hatzofe, O., Henriquet, S., Lécuyer, P., Tessier, C., et al. 2008 Genetic variation in a network of natural and reintroduced populations of Griffon vulture (*Gyps fulvus*) in Europe. *Conserv. Genet.* **9**, 349-359. (doi:10.1007/s10592-007-9347-6).
- [78] García-Rangel, S. 2012 Andean bear *Tremarctos ornatus* natural history and conservation. *Mammal Rev.* **42**, 85-119. (doi:10.1111/j.1365-2907.2011.00207.x).
- [79] Soibelzon, L.H., Pomi, L.H., Tonni, E.P., Rodriguez, S. & Dondas, A. 2009 First report of a South American short-faced bears' den (*Arctotherium angustidens*): palaeobiological and palaeoecological implications. *Alcheringa* **33**, 211-222. (doi:10.1080/03115510902844418).

3.3 Supplementary Information

Phylogeography of the extinct North American giant short-faced bear (*Arctodus simus*), with comments on their paleobiology

Alexander T Salis, Blaine W. Schubert, Sarah C. E. Bray, Holly Heiniger, Julie Meachen, Alan Cooper, Kieren J Mitchell

Supplementary Information

This file includes:

Tables S1 to S2
Figures S1 to S6

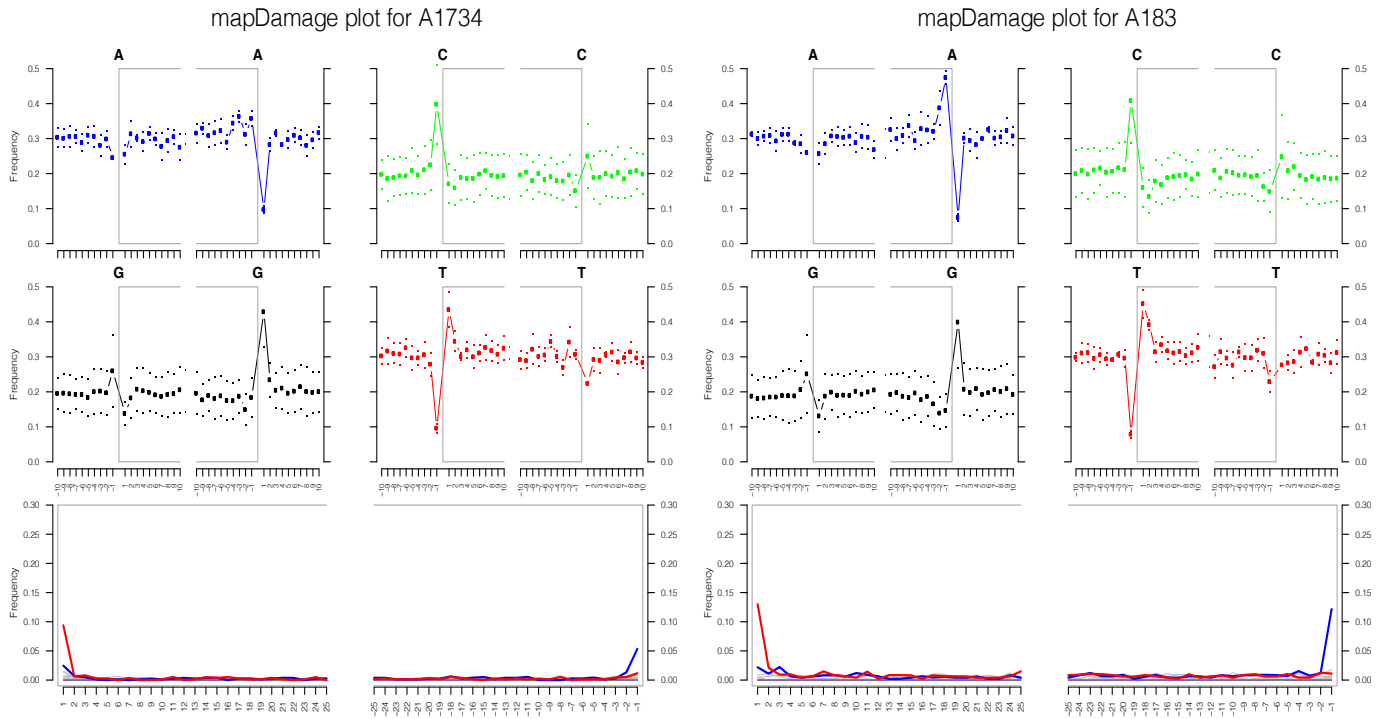
Table S1: Information on bone and teeth samples analysed. New radiocarbon dates are highlighted in red.

ACAD#	ID	Genetic ID	Museum	Country	Location	Sample Type	Carbon Date	Reference	Calibrated median	Calibrated sigma
183	Arctodus	Arctodus	CMNH 44730	Canada (Yukon)	Sixtymile	R. ulna	> 50500	OxA-37558		
299	Arctodus	Too few reads	AMNH F.:AM 95648	USA (Alaska)	Engineer Creek	metatarsal V				
330	Arctodus	Arctodus	CMNH 49874	Canada (Yukon)	Hester Creek	Ulna	26720 +/- 270	OxA-9259	30899	193
336	Arctodus	Arctodus	AMNH F.:AM 145914	USA (Alaska)	Cripple Creek	Tibia				
344	Arctodus	Arctodus	YG 76.4	Canada (Yukon)	Hester Ck.	R. radius	28270 +/- 280	OxA-35022	32174	418
346	Arctodus	Arctodus	CMN 42335	Canada (Alberta)	Consolidated pit	Radius				
419	Arctodus	Arctodus	KUVP 88869	USA (Kansas)	Kaw River bank	Bone				
420	Arctodus	Arctodus	AMNH F.:AM 145915	USA (Alaska)	Goldstream	Femur				
421	Arctodus	Arctodus	CMN 27831	Canada (Yukon)	Old Crow River	R. humerus				
422	Arctodus	Too few reads	AMNH F.:AM 145916	USA (Alaska)	Dawson Cut	Bone				
423	Arctodus	Too few reads	AMNH F.:AM 145916	Canada (Yukon)	Eldorado Creek	R. calcaneum	22417 +/- 452	WK20235	26713	436
424	Arctodus	Arctodus	AMNH F.:AM 30493	USA (Alaska)	Cleary Creek	Ramus				
425	Arctodus	Arctodus	CMN 44566	Canada (Yukon)	Hunker Creek	Bone				
426	Arctodus	Too few reads	UAF/Palco V.-55-524	USA (Alaska)	Lillian Creek	Humerus				
427	Arctodus	Arctodus	CMN 34556	Canada (Yukon)	Gold Run	Femur				
428	Arctodus	Arctodus	AMNH F.:AM 145561	USA (Alaska)	Cripple Creek	Ulna				
429	Arctodus	Arctodus	T-99-016	USA (Alaska)	North Slope	Phalange				
430	Arctodus	Cave Lion	PM-97-001-100	USA (Alaska)	Eva Creek Mine	Femur				
431	Arctodus	Arctodus	YG-24.1 CRH-95-3	Canada (Yukon)	Ophir Creek	Skull	20210 +/- 110	CAMS-18514	24280	151
432	Arctodus	Arctodus	AMNH F.:AM 127693	USA (Alaska)	Ester Creek	Ulna	> 45300	OxA-37427		
434	Arctodus	Arctodus	AMNH F.:AM 145917	USA (Alaska)	Goldstream	Ulna	20900 ± 120	OxA-37426	25233	188
436	Arctodus	Arctodus	AMNH F.:AM 145920	USA (Alaska)	Goldstream	Radius				
437	Arctodus	Arctodus	CMN 42388	Canada (Yukon)	Sixtymile	Metacarpal	44240 +/- 930	TO-2699	47621	984
438	Arctodus	Arctodus	CMN 26864	Canada (Yukon)	Old Crow River	L. radius				
439	Arctodus	Arctodus	AMNH F.:AM 145560	USA (Alaska)	Cripple Creek	radius	> 50000	OxA-37424		
440	Arctodus	Arctodus	AMNH F.:AM 95656	USA (Alaska)	Ester Creek	Humerus				
441	Arctodus	Arctodus	AMNH F.:AM 145918	USA (Alaska)	Cripple Creek	Humerus	44600 ± 2000	OxA-37425	47763	1347
442	Arctodus	Arctodus	AMNH F.:AM 127688	USA (Alaska)	Cripple Creek	Ramus				
443	Arctodus	Arctodus	AMNH F.:AM 145919	USA (Alaska)	Cripple Creek	Ulna				
444	Arctodus	Arctodus	KU 81230	USA (Kansas)	Kaw River bank	vertebrae				
445	Arctodus	Too few reads	CMN 36236	Canada (Yukon)	Dawson Area	r. tibia				
446	Arctodus	Too few reads	CMN 43461	Canada (Yukon)	Old Crow River	old. L.				
447	Arctodus	Arctodus	CMN 37577	Canada (Yukon)	Hunker Creek	R. humerus	29600 +/- 1200	I-11037	33744	1384
448	Arctodus	Arctodus	AMNH F.:AM 145921	USA (Alaska)	Alaska	Humerus	25264 +/- 650	WK20236	29450	695
450	Arctodus	Black	VP2045 9001/91-14	USA (Ohio)	Sheridan Pit	Fibula				
1732	Arctodus	Black	VP8291	USA (Ohio)	Sheridan Pit	Incisor				
1733	Arctodus	Pecary	CMNHNS VP8289	USA (Ohio)	Sheridan Pit	Phalange	11619 +/- 40	Weighted average of CAMS-12837, 12839 and 12845	13450	50
1734	Arctodus	Arctodus	CMNHNS VP8289	USA (Ohio)	Sheridan Pit	Incisor				
1735	Arctodus	Canid	P1737	USA (Ohio)	Sheridan Pit	Incisor				
1953	Arctodus	Arctodus	YT03/48	Canada (Yukon)	Irish Gulch	tibia	26940 +/- 570	ANUA-38615	31029	576
1954	Arctodus	Arctodus	YT03/134	Canada (Yukon)	Quartz Creek	Ulna	26800 ± 240	OxA-37428	30950	157
1955	Arctodus	Arctodus	YT03/288 Cat No 129.1	USA (Ontario)	Hester Ck	Ulna				
1956	Arctodus	Black	KU 31956	USA (Wyoming)	Ottawa	Coprolite	20220 +/- 150	OxA-37990	24300	208
5177	Lion	Arctodus	1770/13-13-01	USA (Ohio)	Natural Trap Cave	Tooth				
17395	Arctodus	Arctodus	NSRL 276, CHEM 358,	USA (Utah)	Sheridan Cave	Long Bone	10976 +/- 40	NZA-28855	12818	66
17859	Arctodus	Arctodus	ETMNH 3429	USA (Virginia)	Huntington	Bone	14853 +/- 55	NZA-21830	18058	93
17860	Arctodus	Arctodus	No #	USA (New Mexico)	Salvville	Tooth root	13300 +/- 60	CAMS-22029 NSRL-504	15995	107
20189	Arctodus	Arctodus	No #	USA (New Mexico)	Oso cave	Femur				

3.3 SUPPLEMENTARY INFORMATION

Table S2: GenBank accession numbers for mitogenomes used in the calculation of population genetic statistics for different mammalian taxa.

Species	Genbank accessions
New Zealand Fur Seal (<i>Arctocephalus forsteri</i>)	KT693333–KT693381
Lion (<i>Panthera leo</i>)	JQ904290, KC834784, KF776494, KF907306, KP001493–KP001507, KP202262, KR132589, KU234271, MG772937, MG792275–MG792277
Brown Bear (<i>Ursus arctos</i>)	Chapter 2 data, AF303110, AP012559–AP012587, AP012591–AP012597, GU573485–GU573491, JX196367–JX196369, MH255807
Leopard (<i>Panthera pardus</i>)	EF551002, KJ866876, KP001507, KP202265, KX655614, MG932393, MH588611–MH588632, MK043027
Moose (<i>Alces alces</i>)	JN632595, KP164854, KP405229, MF784597–MF784604, MK644889–MK644928
Mammoth	KX176750–KX176803, MF579931–MF579950, MG334264–MG334285
European Bison (<i>Bison bonasus</i>)	HM045017, HQ223450, JN632602, KX553930–KX553934, KX592176–KX592189, KX773459, KX898005–KX898017, KY055664
Tiger (<i>Panthera tigris</i>)	EF551003, HM185182, HM589214, HM589215, JF357967–JF357974, KF297576, KF892541, KJ508412, KJ508413, KP202268, KR132595, MH124079–MH124114, MH893763, MN624080
Grey Wolf (<i>Canis lupus</i>)	AB499818–AB499824, DQ480503–DQ480508, EU789787, EU789788, GQ374438, KC461238, KC89637, KF661038–KF661077, MK936995–MK937053, MN071185–MN071206
Grey Fox (<i>Urocyon cinereoargenteus</i>)	KP129083–KP129108
Tasmanian Devil (<i>Sarcophilus harrisi</i>)	JX475454–JX475467, MG957409–MG957430
Polar Bear (<i>Ursus maritimus</i>)	AF303111, AJ428577, GU573485–GU573491, JX196370–JX196392
Orca (<i>Orcinus orca</i>)	GU187156–GU187215
Thylacine (<i>Thylacinus cynocephalus</i>)	FJ515780, FJ515781, KY678342–KY678392
Ingressus (<i>Ursus ingressus</i>)	FM177760, FN390842–FN390846, FN390848, FN390853, FN390854, FN390855–FN390862, FN390869, FN390870, MN311249, MN311250, KX641330–KX641332
Cougar (<i>Puma concolor</i>)	JN999997, KP202261, KX808222–KX808231, MH807447, MH814703–MH814707, MH818219–MH818222
New World Stilt-Legged Horse (<i>Haringtonhippus francisci</i>)	JX312727, KT168317–KT168336, MF134655–MF134661
Steller Sealion (<i>Eumetopias jubatus</i>)	AB300601–AB300608, GU475464, NC_004030
Spelaeus (<i>Ursus spelaeus</i>)	EU327344, FN390847, FN390849–FN390852, FN390855, FN390865–FN390868, FN390871, FN390872, KX641289–KX641314, KX641333–KX641335, KX641337
Island Fox (<i>Urocyon littoralis</i>)	KP128924–KP129056
Eurasian Lynx (<i>Lynx lynx</i>)	MK229198–MK229293
Brown Hyena (<i>Hyaena brunnea</i>)	MF593938–MF593952



FigureS1: Example mapDamage2 plots for an older (A183) and younger (A1734) sample.

3.3 SUPPLEMENTARY INFORMATION

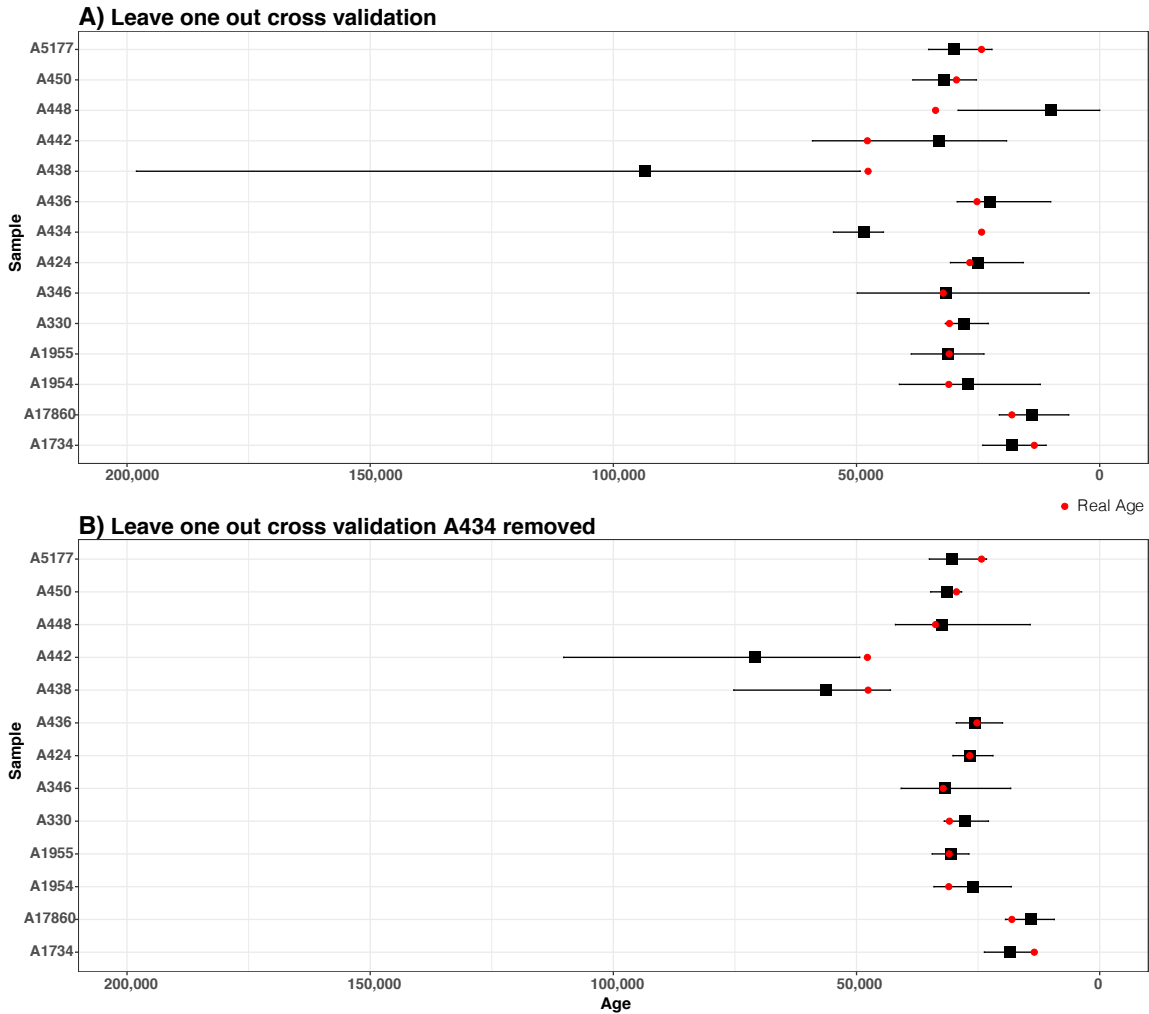


Figure S2: Plots of median estimated ages from leave-one-out cross-validation in BEAST2 for (A) all radiocarbon dated specimens and (B) all radiocarbon dated specimens but with but with A434 excluded due to an unreliable radiocarbon date. Error-bars represent 95% Higher Posterior Density (HPD). The real age of the specimen is within the 95% HPD of each estimate for all but 1 the specimens in the final analysis with A434 removed but was still included in subsequent analyses as it fell in an under sampled region of the tree.

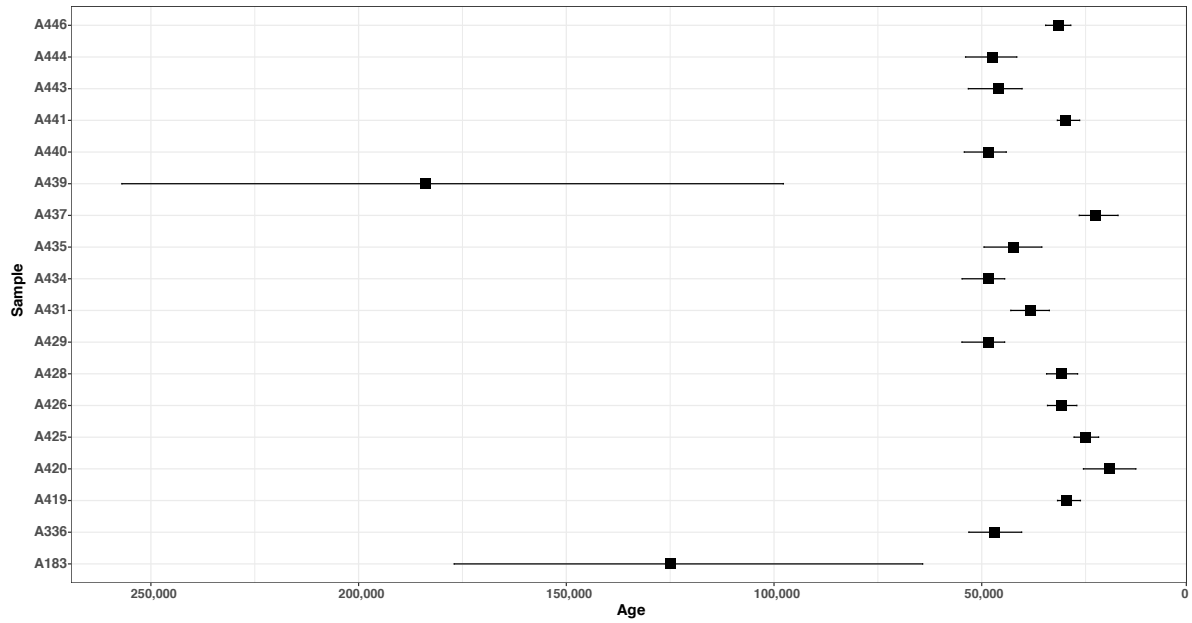


Figure S3: Estimated ages from BEAST2 of specimens with no associated date or infinite radiocarbon dates. Error bars represent 95% Higher Posterior Densities.

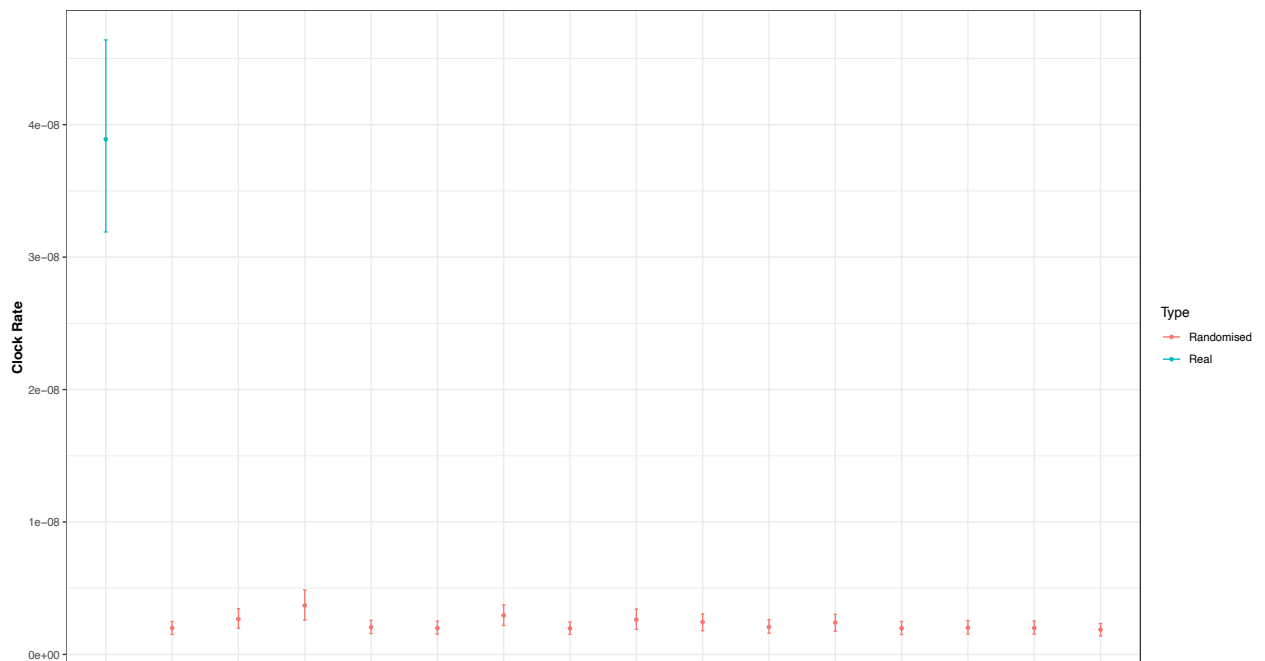


Figure S4: Comparison of mean clock rate estimations with 95% Higher Posterior Densities from BEAST2 for the real data and 15 date-randomised datasets from the date-randomisation test (DRT).

3.3 SUPPLEMENTARY INFORMATION

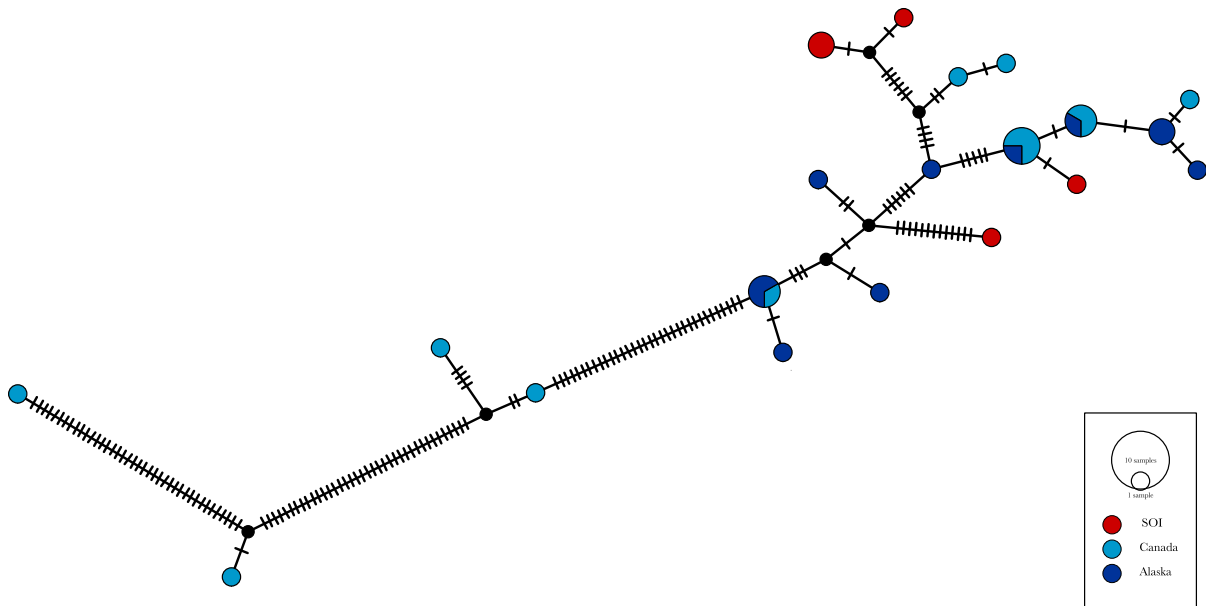


Figure S5: Median-joining network for samples with >90% mitochondrial coverage.

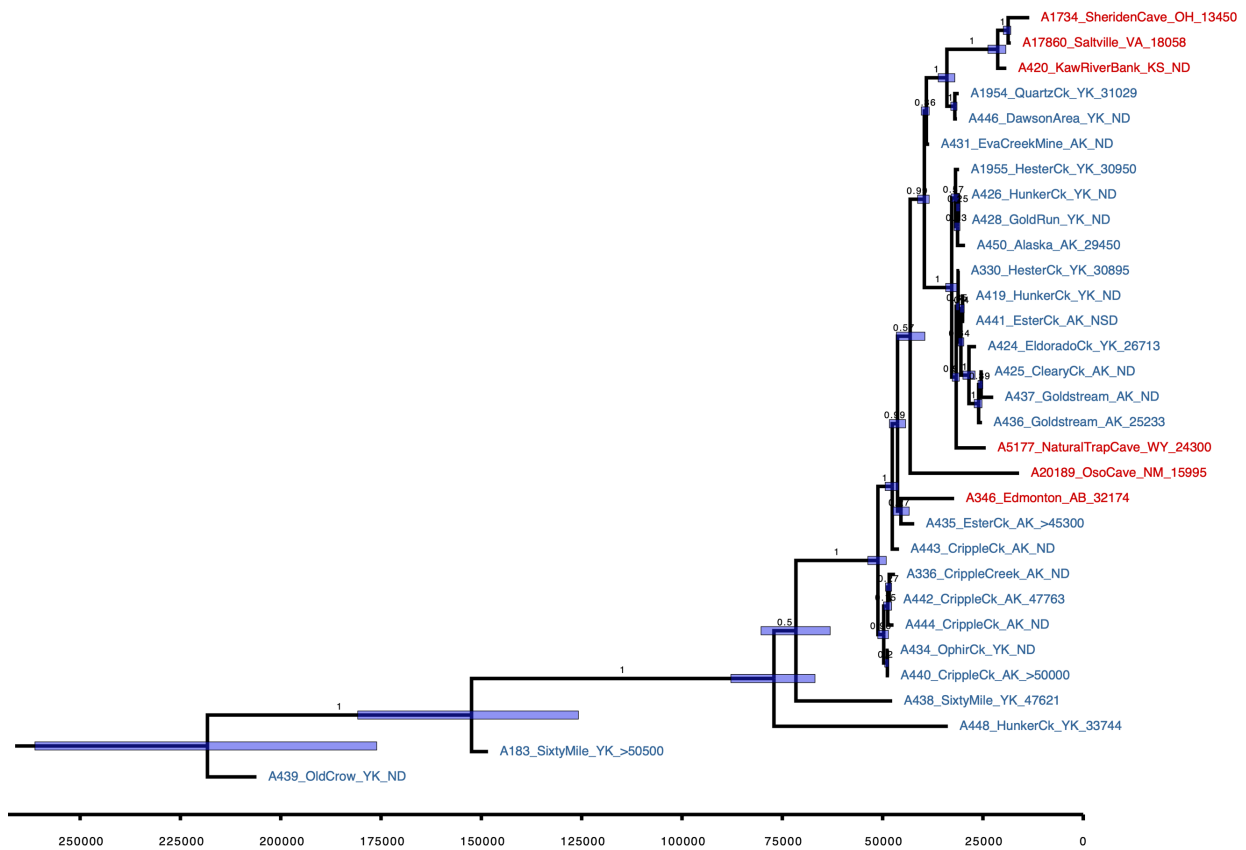


Figure S6: Bayesian phylogenetic trees inferred from *A. simus* mitogenomes with the divergent A183 and A439 included. Bars on nodes represent 95% Highest Posterior Densities for node age estimates. Branch labels represent posterior support values. Tips are coloured by geographic region: red — south of the ice, blue — Eastern Beringia.

Chapter 4

Ancient genomes reveal hybridisation between extinct short-faced bears and the extant spectacled bear (*Tremarctos ornatus*)

Manuscript written for submission to *Current Biology*

Submitted to *bioRxiv*

4.1 Authorship Statement

Statement of Authorship

Title of Paper	Ancient genomes reveal hybridisation between extinct short-faced bears and the extant spectacled bear (<i>Tremarctos ornatus</i>)
Publication Status	<input type="checkbox"/> Published <input type="checkbox"/> Accepted for Publication <input type="checkbox"/> Submitted for Publication <input checked="" type="checkbox"/> Unpublished and Unsubmitted work written in manuscript style
Publication Details	Unpublished and unsubmitted work written in manuscript style intended to be submitted to Current Biology

Principal Author

Name of Principal Author (Candidate)	Alexander T Salis			
Contribution to the Paper	Performed DNA extractions, DNA library construction and amplification, preparation for sequencing, and bioinformatic processing of sequencing data. Performed phylogenetic and gene flow analyses, interpreted results, created figures, wrote manuscript and edited manuscript.			
Overall percentage (%)	85			
Certification:	This paper reports on original research I conducted during the period of my Higher Degree by Research candidature and is not subject to any obligations or contractual agreements with a third party that would constrain its inclusion in this thesis. I am the primary author of this paper.			
Signature	<table border="1" style="width: 100%;"> <tr> <td style="width: 50%;"></td> <td style="width: 10%; text-align: center;">Date</td> <td style="width: 40%;">14/08/2020</td> </tr> </table>		Date	14/08/2020
	Date	14/08/2020		

Co-Author Contributions

By signing the Statement of Authorship, each author certifies that:

- i. the candidate's stated contribution to the publication is accurate (as detailed above);
- ii. permission is granted for the candidate to include the publication in the thesis; and
- iii. the sum of all co-author contributions is equal to 100% less the candidate's stated contribution.

Name of Co-Author	Graham Gower			
Contribution to the Paper	Development of bioinformatic pipeline, critically evaluated and edited the manuscript.			
Signature	<table border="1" style="width: 100%;"> <tr> <td style="width: 50%;"></td> <td style="width: 10%; text-align: center;">Date</td> <td style="width: 40%;">14/8/2020</td> </tr> </table>		Date	14/8/2020
	Date	14/8/2020		

Name of Co-Author	Blaine W Schubert			
Contribution to the Paper	Assisted with interpretation of results, critically evaluated and edited the manuscript.			
Signature	<table border="1" style="width: 100%;"> <tr> <td style="width: 50%;"></td> <td style="width: 10%; text-align: center;">Date</td> <td style="width: 40%;">15 August 2020</td> </tr> </table>		Date	15 August 2020
	Date	15 August 2020		

Name of Co-Author	Leopoldo Soibelzon		
Contribution to the Paper	Provided access to samples. Assisted with interpretation of results, critically evaluated and edited the manuscript.		
Signature		Date	15/8/2020

Name of Co-Author	Holly Heiniger		
Contribution to the Paper	Performed DNA extraction, DNA library construction and amplification (Sample A5177), preparation for sequencing, critically evaluated and edited the manuscript.		
Signature		Date	14/08/2020

Name of Co-Author	Julie Meachen		
Contribution to the Paper	Provided access to samples. Critically evaluated and edited the manuscript.		
Signature		Date	August 14, 2020

Name of Co-Author	Alan Cooper		
Contribution to the Paper	Supervised work, conception of project, critically evaluated and edited the manuscript.		
Signature		Date	10 Sep, 2020

Name of Co-Author	Kieren J Mitchell		
Contribution to the Paper	Supervised work, conception of project, interpreted results, wrote and edited the manuscript.		
Signature		Date	17/8/20

4.2 Manuscript

Ancient genomes reveal hybridisation between extinct short-faced bears and the extant spectacled bear (*Tremarctos ornatus*)

Alexander T Salis¹, Graham Gower^{1,2}, Blaine W. Schubert³, Leopoldo H. Soibelzon⁴, Holly Heiniger¹, Julie Meachen⁵, Alan Cooper⁶, Kieren J Mitchell¹

¹Australian Centre for Ancient DNA (ACAD), School of Biological Sciences, University of Adelaide, South Australia 5005, Australia

²Lundbeck GeoGenetics Centre, GLOBE Institute, University of Copenhagen, Copenhagen 1350, Denmark

³Center of Excellence in Paleontology and Department of Geosciences, East Tennessee State University (ETSU), Johnson City, Tennessee 37614, USA

⁴ División Paleontología de Vertebrados, Museo de La Plata, 1900 La Plata, Argentina

⁵Anatomy Department, Des Moines University, Des Moines, IA, USA

⁶ South Australian Museum, Adelaide, South Australia 5000, Australia

Lead contact

*Corresponding author(s): A.T.S. (alexander.t.salis@gmail.com), and K.J.M. (kieren.mitchell@adelaide.edu.au)

Summary:

Two genera and multiple species of short-faced bear from the Americas went extinct during or toward the end of the Pleistocene, and all belonged to the endemic New World subfamily Tremarctinae [1-7]. Two of these species were giants, growing in excess of 1,000 kg [6, 8, 9], but it remains uncertain how these extinct bears were related to the sole surviving short-faced bear: the spectacled bear (*Tremarctos ornatus*). Ancient mitochondrial DNA has recently suggested phylogenetic relationships among these lineages that conflict with interpretations based on morphology [1, 10-12]. However, widespread hybridisation and incomplete lineage sorting among extant bears mean that the mitochondrial phylogeny frequently does not reflect the true species tree [13, 14]. Here we present ancient nuclear genome sequences from representatives of the two extinct short-faced bear genera, *Arctotherium* and *Arctodus*. Our new data support a third hypothesis for the relationships among short-faced bears, which conflicts with existing mitochondrial and morphological data. Based on genome-wide D-statistics, we suggest that the extant spectacled bear derives substantial ancestry from Pleistocene hybridisation with an extinct short-faced bear lineage, resulting in a discordant phylogenetic signal between the mitochondrion and portions of the nuclear genome.

Results and Discussion:

The spectacled bear (*Tremarctos ornatus*) is the only extant species of short-faced bear (Tremarctinae), a once diverse subfamily endemic to the Americas. This subfamily also includes many species that became extinct during the Pleistocene, including the Florida cave bear (*Tremarctos floridanus*), two species of North American short-faced bears (*Arctodus* spp. [3, 4]), and as many as five species of South American short-faced bears (*Arctotherium* spp. [2, 6]), one of which (*Arctotherium wingei*) has recently been discovered as far north as the Yucatan of Mexico [5]. Notably, the genera *Arctodus* and *Arctotherium* both included giant (>1,000kg) forms [8, 9] — *Arctodus simus* and *Arctotherium angustidens*, respectively — and based on morphology it was hypothesised that these genera were closely related [1, 6, 10, 11]. However, recently published mitochondrial DNA data suggested that *Arctotherium* was most closely related to the extant spectacled bear, to the exclusion of North American *Arctodus* [12]. While this result supported the convergent evolution of giant bears in North and South America, the mitochondrial genome does not always reflect the true relationships among species [e.g. 15, 16-19]. Importantly, discordance between mitochondrial and nuclear loci has been previously noted in bears, and has been attributed to a combination of stochastic processes and the rapid evolution of bears [13], as well as hybridisation between species [13, 14, 20-25]. To further resolve the evolutionary history of short-faced bears, we applied ancient DNA techniques to retrieve and analyse whole genome data from both *Arctodus* and *Arctotherium*.

Ancient DNA (aDNA) was extracted and sequenced from three *Arctodus simus* specimens: one each from placer mines at Sixty Mile Creek (ACAD 438; Canadian Museum of Nature; CMN 42388) and Hester Creek (ACAD 344; Yukon Government; YG 76.4) in the Yukon Territory, Canada; and one from Natural Trap Cave in Wyoming, USA (ACAD 5177; University of Kansas; KU 31956). We also analysed one specimen of *Arctotherium* sp. from Cueva del Puma, Patagonia, Chile (ACAD 3599; complete right femur, no. 32104, Centro de Estudios del Hombre Austral, Instituto de la Patagonia, Universidad de Magallanes). The *Arctotherium* specimen was previously dated to $12,105 \pm 175$ cal yBP (Ua-21033) [26], while two of the *Arctodus* specimens have been dated: ACAD 438 at $47,621 \pm 984$ cal yBP (TO-2699) [27] and ACAD 5177 at $24,300 \pm 208$ cal yBP (OxA-37990) (Table S1). The *Arctotherium* specimen has yielded mitochondrial aDNA in a previous study [12], however, here we shotgun sequenced this specimen, along

4.2 MANUSCRIPT

with the three *A. simus* specimens, at much greater depth in order to reconstruct nuclear genome sequences. Mapping our new sequencing data from these specimens to the giant panda (*Ailuropoda melanoleuca*) reference genome (LATN01) yielded average depths of coverage between 0.12x to 5.9x for the *A. simus* specimens and 3.9x for the *Arctotherium* specimen (Table S3). We compared these new genomic data to previously published genomes from all extant species of bear (Table S2): spectacled bear, giant panda, brown bear (*Ursus arctos*), American black bear (*U. americanus*), Asian black bear (*U. thibetanus*), polar bear (*U. maritimus*), sloth bear (*U. ursinus*), and sun bear (*U. malayanus*).

Phylogenetic analyses on a concatenated dataset of genome-wide SNPs revealed relationships within Ursinae that were consistent with previous genomic studies: *U. americanus*, *U. maritimus*, and *U. arctos* formed a monophyletic clade sister to a clade consisting of *U. thibetanus*, *U. malayanus*, and *U. ursinus* [13, 14]. In contrast, within short-faced bears (Tremarctinae) we recovered strong support for a close relationship between the spectacled bear and the North American short-faced bear (*Arctodus simus*) to the exclusion of the South American *Arctotherium* (Figure 1A, Figure S2). This result conflicts with the mitochondrial tree, which instead supports a clade comprising *Arctotherium* and *Tremarctos ornatus* to the exclusion of *Arctodus simus* [12] (Figure 1B). As the radiation of bears is thought to have occurred rapidly during the Miocene - Pliocene transition, it is possible that this discordance could be explained by incomplete lineage sorting (ILS) [28], a process whereby pre-existing genetic variation in an ancestral species is randomly inherited and fixed in descendant species [29, 30]. Alternatively, given the observed propensity of bears for hybridisation [e.g. 13, 14, 20-22, 25, 31], mitochondrial/nuclear discordance within short-faced bears may instead result from gene flow between *Tremarctos* and either *Arctodus* or *Arctotherium*.

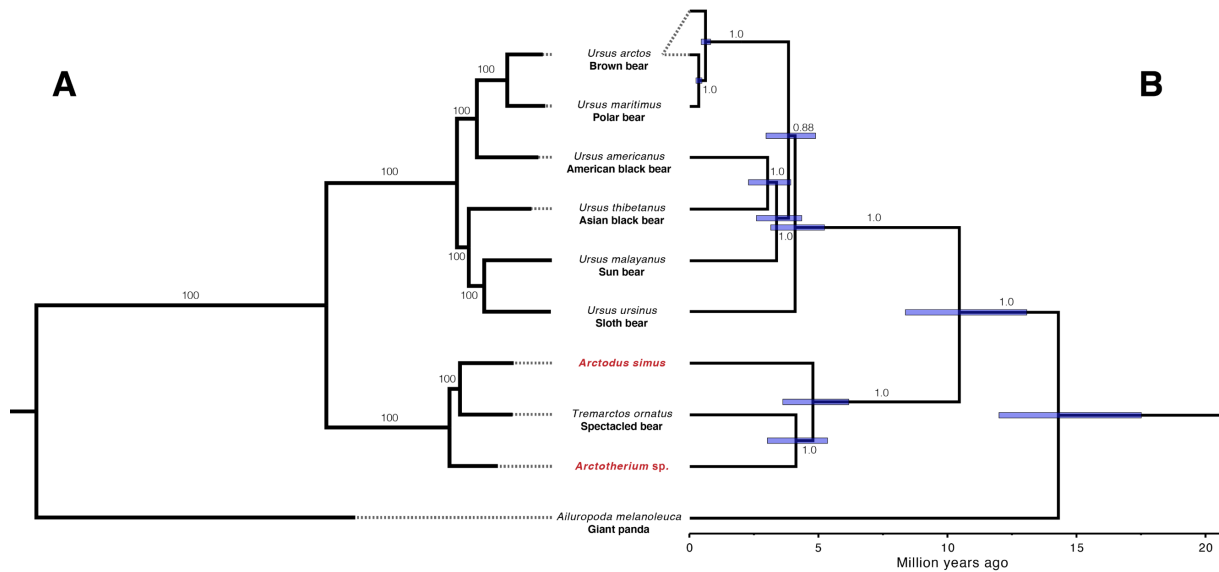


Figure 1: Phylogenetic relationships among ursids **A.** Maximum likelihood tree based on nuclear SNPs constructed in RAXML. Branch labels represent bootstrap support percentages. For RAXML tree with all individuals analysed see Figure S2. **B.** Bayesian phylogeny based on full mitochondrial genomes adapted from Mitchell, et al. [12]. Blue bars represent 95% highest posterior density interval on node ages. Branch labels represent BEAST posterior support values.

To test for potential phylogenetic discordance across our short-faced bear genomes, we constructed phylogenetic trees from 500 kb non-overlapping windows ($n = 2622$) across the 85 largest autosomal scaffolds of the giant panda reference genome (LATN01). Trees created from roughly 70% of windows agreed with the results from our genome-wide concatenated dataset (Topology 1; *i.e.* *Tremarctos* + *Arctodus*; Figure 2B & S3). However, approximately 30% of windows instead supported the mitochondrial tree topology (Topology 2; *i.e.* *Tremarctos* + *Arctotherium*; Figure 2B & S3), while the third possible topology where the two extinct genera form a clade — *Arctodus* + *Arctotherium* — was rejected for over 95% of windows. The frequencies of the three possible tree topologies are difficult to explain as a result of ILS, which we would expect to result in a more even representation of the two “minority” topologies (*i.e.* Topologies 2 and 3). Our results therefore suggest that introgression may be the most likely explanation for the observed phylogenetic discordance. Consequently, we calculated D-statistics [32, 33] using our concatenated genome-wide SNPs in order to identify signals of hybridisation between the bear species in our dataset.

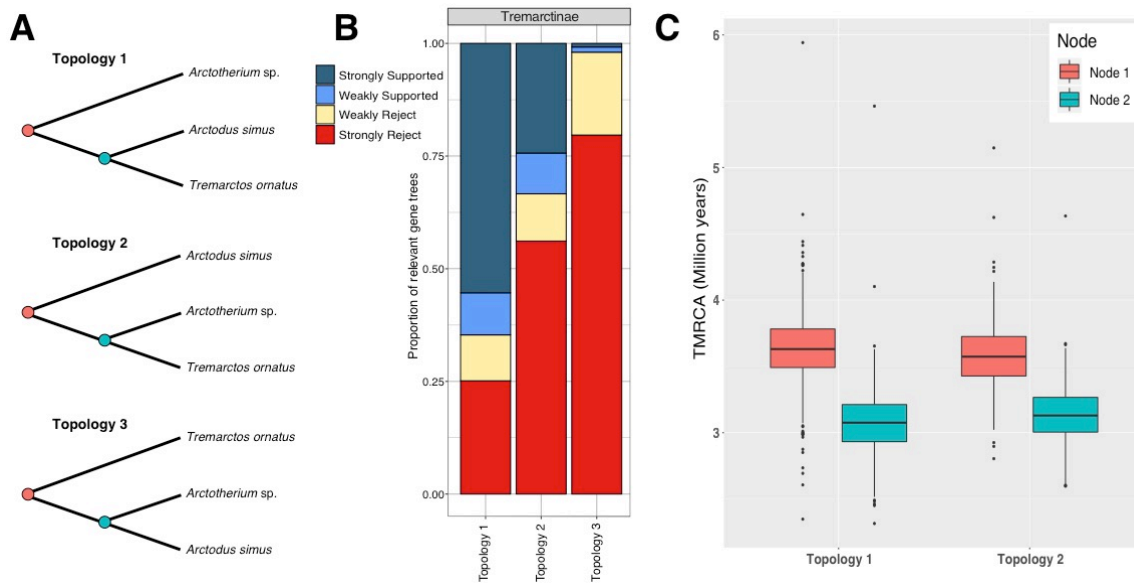


Figure 2: **A.** The three possible short-faced bear (*Tremarctinae*) tree topologies. **B.** Discordance visualisation using DiscoVista from 2622 500 kb genomic fragments. The x-axis represents topologies tested and the y-axis the proportion of fragments that support the topology, with >80% bootstrap support used to define strong support. For more comprehensive tests of phylogenetic placements see Figure S3. **C.** Divergence time estimates (TMRCA) of *Tremarctos*, *Arctodus*, and *Arctotherium* (Node 1) and for sister species (Node 2) of the two most common short-faced bear topologies.

Consistent with previous studies [i.e. 14], our D-statistics revealed compelling evidence for hybridisation between: Asian black bears and all North American ursine bears (including the polar bear); sun bears and North American ursine bears; and Asian black bear and sun bear (Table S4). In contrast, we did not obtain any significantly non-zero values for D-statistics calculated using our two extinct short-faced bear genomes, any member of Ursinae, and the panda outgroup (Table 1). This result suggests that no gene flow occurred between *Arctodus* or *Arctotherium* and the ancestors of any modern ursine bear, and also demonstrates a lack of any discernible reference bias in the ancient genomic data (which would result in asymmetrical allele sharing with the reference). Thus, it appears *Arctodus* and *Arctotherium* did not hybridise with brown and black bears in the Americas during the late Pleistocene, even though the distribution of *Arctodus* overlapped with both ursines, and *Arctotherium* may have encountered them in Mexico or Central America [5].

Contrary to previous studies, our D-statistics revealed signals consistent with gene flow between the spectacled bear and members of Ursinae (Table 1 & S5), suggesting the possibility that *Tremarctos* hybridised with ancestors of either the brown bear or American black bear during the Pleistocene. This signal is surprising given the deep divergence between ursine and short-faced bears, having split approximately 10 million years ago (mya) [12, 14, 28]. However, in support of this hypothesis, offspring between spectacled bear and Asiatic black bear have resulted from hybridisation in zoos, although whether these hybrids were fertile remains unknown [34]. Importantly, members of *Tremarctos* and the ancestors of modern American black bears had overlapping distributions throughout the Pleistocene in North America [4, 10], meaning that hybridisation may have occurred when the two lineages were less divergent and reproductive barriers had had less time to evolve.

In addition to evidence for hybridisation between *Tremarctos* and ursine bears, we also recovered convincing evidence for hybridisation between *Arctotherium* and *Tremarctos* (Table 1). These results are consistent with a model where the divergence between *Arctodus* and *Tremarctos* occurred in North America after the ancestors of *Arctotherium* dispersed southwards into South America, with subsequent hybridisation between *Tremarctos* and *Arctotherium*. This interpretation is supported by the presence of *Arctodus* and *Tremarctos* (and absence of *Arctotherium*) in the late Pliocene fossil record of North America [3, 4, 7, 10]. The fossil record further suggests that contact between *Tremarctos* and *Arctotherium* occurred during the late Pleistocene, when representatives of *Arctotherium* were distributed as far north as the Yucatan of Mexico [5], providing an opportunity for hybridisation.

4.2 MANUSCRIPT

Table 1: D-statistics for short-faced bears (Tremarctinae). D-statistics (D), standard error, and Z-Score (significant if $> |3|$) are displayed, with ABBA-BABA counts and the number of SNPs considered in the analysis. It is clear that there is an excess of allele sharing between the spectacled bears (*T. ornatus*) and *Arctotherium*. However, neither of the spectacled bear individuals show elevated D-statistics in relation to each other, meaning gene flow likely occurred in the ancestor of both individuals, or they carry similar proportions of hybridised DNA.

D-statistic: D(H1, H2, H3, Giant Panda)	D	Stderr	Z-Score	BABA	ABBA	nSNPs
D(<i>T. ornatus</i> (Chaparri), <i>Arctodus</i> , <i>Arctotherium</i>)	0.3116	0.009559	32.6*	41219	21633	6071021
D(<i>T. ornatus</i> (Nobody), <i>Arctodus</i> , <i>Arctotherium</i>)	0.3112	0.009462	32.889*	41187	21637	6070446
D(<i>T. ornatus</i> (Chaparri), <i>T. ornatus</i> (Nobody), <i>Arctodus</i>)	0.0206	0.022575	0.911	1375	1320	6393667
D(<i>T. ornatus</i> (Chaparri), <i>T. ornatus</i> (Nobody), <i>Arctotherium</i>)	0.0172	0.021533	0.801	1227	1186	6258343
D(<i>T. ornatus</i> (Nobody), <i>Arctotherium</i> sp., <i>Ursus arctos</i>)	0.2079	0.008878	23.418*	11177	7329	6184195
D(<i>T. ornatus</i> (Chaparri), <i>Arctotherium</i> sp., <i>Ursus arctos</i>)	0.2074	0.009242	22.442*	11185	7342	6185696
D(<i>T. ornatus</i> (Nobody), <i>Arctodus simus</i> , <i>Ursus arctos</i>)	0.2152	0.009651	22.302*	11172	7214	6317724
D(<i>T. ornatus</i> (Chaparri), <i>Arctodus simus</i> , <i>Ursus arctos</i>)	0.2131	0.010012	21.281*	11191	7260	6319318
D(<i>Arctodus simus</i> , <i>Arctotherium</i> sp., <i>Ursus malayanus</i> (Klaus))	0.0215	0.00854	2.523	9662	9254	6010428
D(<i>Arctodus simus</i> , <i>Arctotherium</i> sp., <i>Ursus americanus</i>)	0.0225	0.009168	2.453	9661	9236	6025070
D(<i>Arctodus simus</i> , <i>Arctotherium</i> sp., <i>Ursus malayanus</i> (Anabell))	0.0211	0.009128	2.308	9691	9291	6009103
D(<i>Arctodus simus</i> , <i>Arctotherium</i> sp., <i>Ursus maritimus</i> (PB1))	0.0187	0.009374	1.99	9677	9323	6019285
D(<i>Arctodus simus</i> , <i>Arctotherium</i> sp., <i>Ursus arctos</i>)	0.0167	0.009247	1.802	9717	9398	6033406
D(<i>Arctodus simus</i> , <i>Arctotherium</i> sp., <i>Ursus maritimus</i> (PB9))	0.016	0.009483	1.683	9752	9446	6044167
D(<i>Arctodus simus</i> , <i>Arctotherium</i> sp., <i>Ursus ursinus</i>)	0.016	0.009584	1.666	9608	9306	6012634
D(<i>Arctodus simus</i> , <i>Arctotherium</i> sp., <i>Ursus thibetanus</i>)	0.0157	0.009487	1.652	9644	9346	6019681

*Significantly positive d-statistic, denote deviations from a typical bifurcating tree with H1 and H3 being closer than expected

If the ancestors of the spectacled bear hybridised with *Arctotherium* somewhere in the American mid-latitudes during the migration of *Tremarctos* into South America, then signals of gene flow between members of these two genera could date to the latest Pleistocene or earliest Holocene, when spectacled bears are thought to have migrated into South America [6, 35, 36]. To test this hypothesis, we estimated divergence times among the three short-faced bear lineages for all 500 kb windows from the largest 40 scaffolds corresponding to either Topology 1 (n = 980) or Topology 2 (n = 413) and summarised the results (Figure 2c). The age of the most recent common ancestor (TMRCA) of *Tremarctos*, *Arctodus*, and *Arctotherium* was similar irrespective of topology (Topology 1: 3.6 mya; Topology 2: 3.6 mya), as was the subsequent divergence between the remaining two lineages (Topology 1: 3.1 mya; Topology 2: 3.1 mya). Assuming that members of *Tremarctos* migrated southward no earlier than the latest Pleistocene, our results superficially appear to be incompatible with late Pleistocene/Holocene hybridisation between *Tremarctos* and *Arctotherium*. The fossil record suggests two ways these observations may be explained.

Late Pleistocene fossil data indicate that the ancestors of the spectacled bear are likely to have encountered *Arctotherium* individuals from Mexico, Central America, and/or northern South America, which were comparable in size and diet to the spectacled bear [1, 5, 37] and which may have represented a different *Arctotherium* species from the Chilean specimen sequenced in the present study [1, 6, 12, 26]. Indeed, throughout the Pleistocene a number of *Arctotherium* species have been described across South and Central America, with putative species ranging from gigantic in the early-mid Pleistocene to relatively small in the late Pleistocene [1, 2, 6, 9]. If the ancestors of our sampled Patagonian *Arctotherium* specimen diverged from those of more northerly *Arctotherium* species during the Pliocene or early Pleistocene, then our molecular dating results remain consistent with hybridisation being the primary driver of phylogenetic discordance in our genomic data. Alternatively, hybridisation between *Tremarctos* and *Arctotherium* could have occurred in Central America during the Pleistocene. *Tremarctos* and *Arctotherium* have both been recorded in Central American cave deposits [5, 38], however, the extent of occupation by both genera in the region is unknown, and conceivably Central America represents a contact zone between the genera throughout the Pleistocene where hybridisation may have occurred.

An alternative interpretation of our phylogenetic results is that Topology 2 (*Tremarctos* + *Arctotherium*), which is supported by the mitochondrion and ~30% of our nuclear genome windows, is the pre-hybridisation tree. Recently, Li, et al. [39] suggested that under scenarios involving substantial gene flow the predominant phylogenetic signal across the genome may not reflect the pre-hybridisation tree. If this were the case for short-faced bears, the majority of support for Topology 1 would actually result from extensive hybridisation between *Arctodus* and *Tremarctos* in North America. Li, et al. [39] contend that the phylogenetic signal of the pre-hybridisation tree may be enriched in regions of low recombination, especially on the X-chromosome. In order to test this hypothesis, we identified panda scaffolds corresponding to the ~40 Mb recombination cold-spot on the X-chromosome highlighted by Li, et al. [39] and produced phylogenetic trees for each 500 kb window along this region (Figure S4). Interestingly, the majority of these fragments supported Topology 2 (*Tremarctos* + *Arctotherium*), the same topology as the mitochondrial phylogeny but contrasting with the majority of autosomal scaffolds.

4.2 MANUSCRIPT

Unlike felids [e.g. 40, 41, 42], a high-quality reference assembly and linkage map does not exist for any bear species, meaning scaffolds pertaining to high and low recombination areas of the genome could not be identified. Unfortunately, this currently makes it impossible to further explore the possibility that Topology 2 (*Tremarctos* + *Arctotherium*) may reflect the pre-hybridisation short-faced bear tree, rather than Topology 1 (*Tremarctos* + *Arctodus*). In the absence of a linkage map, sequencing aDNA from either the extinct *Tremarctos floridanus* or more northerly *Arctotherium* populations will be key to further resolving the evolutionary history of short-faced bears, though this will be challenging given that the core range of these species lies in the lower-latitudes where aDNA preservation is less reliable. For now, we conclude that the weight of evidence supports a closer relationship between the spectacled bear and the extinct short-faced bears from North America (*Arctodus*) rather than South America (*Arctotherium*). In any case, our genomic data imply extensive hybridisation occurred between the spectacled bear and one of the extinct short-faced bear lineages. These results contribute to the growing consensus that hybridisation is widespread among carnivoran groups generally [13, 14, 39, 43].

Acknowledgements:

We would like to thank the following institutions for allowing access to specimens: Canadian Museum of Nature, University of Kansas Natural History Museum, Yukon Government, Centro de Estudios del Hombre Austral, Instituto de la Patagonia, Universidad de Magallanes. In addition, we are grateful to the following individuals who helped in the collection and identification of specimens and/or provided laboratory support: Grant Zazula (Yukon Territorial Government, Palaeontology Program, Canada), Fabiana Martin (Universidad de Magallanes, Chile), Jeremy Austin (University of Adelaide, Australia) and Sarah Bray (University of Adelaide, Australia). We would like to thank the Wyoming BLM and permit number PA-13-WY-207. This research was funded by an Australian Research Council Laureate Fellowship awarded to AC (FL140100260), U.S. National Science Foundation grant (EAR/SGP#1425059) awarded to JM and AC, and Agencia Nacional de Promoción Científica y Técnica' (ANPCyT, Argentina) (PICT 2015–966) awarded to FJP.

Author Contributions:

Conceptualization, A.T.S., A.C. and K.J.M.; Methodology, A.T.S., G.G., A.C., and K.J.M.; Investigation, A.T.S., H.H., and K.J.M.; Writing – Original Draft, A.T.S. and K.J.M.; Writing – Review & Editing, G.G., B.W.S., L.H.S., H.H., A.P., F.J.P., J.M., and A.C.; Funding Acquisition, F.J.P., J.M., and A.C.; Resources, J.M., A.P., and F.J.P.; Supervision, A.C., and K.J.M.

Materials and Methods:***Sampling***

Analyses were performed on three bone samples identified as *Arctodus simus* and one sample identified as *Arctotherium* sp. (Table S1). The *Arctotherium* specimen ACAD 3599, had previously be radiocarbon dated, as well as one of the *A. simus* specimens (ACAD 438), a further *A. simus* specimen was radiocarbon dated at the Oxford Radiocarbon Accelerator Unit of the University of Oxford. All radiocarbon dates were calibrated with the either the IntCal13 curve [44] or the SHCal13 curve [45] using OxCal 4.4 [46] (Table S1).

Sample preparation and extraction

All pre-PCR steps (*i.e.*, extraction, library preparation) were conducted in purpose-built ancient DNA clean-room facilities at the University of Adelaide’s Australian Centre for Ancient DNA (ACAD). Potential surface contamination on each sample was reduced by UV irradiation for 15 min each side, followed by abrasion of the exterior surface (c. 1 mm) using a Dremel tool and a disposable carborundum disk. The sample was then pulverised using a metallic mallet. Approximately 100 mg of powder was extracted using an in-house silica-based extraction protocol adapted from Dabney, et al. [47] optimised for the recovery of small fragments. the powder was digested first in 1 mL 0.5 M EDTA for 60 min, followed by an overnight incubation in 970 μ L fresh 0.5 M EDTA and 30 μ L proteinase K (20 mg/ml) at 55°C. The samples were centrifuged and the supernatant mixed with 13 mL of a modified PB buffer (12.6 mL PB buffer (Qiagen), 6.5 μ L Tween-20, and 390 μ L of 3M Sodium Acetate) and bound to silicon dioxide particles, which were then washed two times with 80% ethanol. The DNA was eluted from silica particles with 100 μ L TE buffer.

4.2 MANUSCRIPT

Library preparation

Double-stranded Illumina libraries were constructed following the protocol of Meyer, et al. [48] from 25 μ L of DNA extract. In addition, all samples underwent partial uracil-DNA glycosylase (UDG) treatment [49] to restrict cytosine deamination, characteristic of ancient DNA, to terminal nucleotides. A short round of PCR using PCR primers complementary to the library adapter sequences was performed to increase the total amount of DNA and add full-length Illumina sequencing adapters. Cycle number was determined via rtPCR and each library split into 8 separate PCR reactions to minimise PCR bias and maintain library complexity. Each PCR of 25 μ L contained 1 \times HiFi buffer, 2.5 mM MgSO₄, 1 mM dNTPs, 0.5 mM each primer, 0.1 U Platinum Taq Hi-Fi polymerase and 3 μ L DNA. The cycling conditions were 94 °C for 6 min, 8–10 cycles of 94 °C for 30 s, 60 °C for 30 s, and 72 °C for 40 s, followed by 72 °C for 10 min. Following PCR, replicates were pooled and purified using AxyPrep™ magnetic beads, eluted in 30 μ L H₂O quantified on TapeStation (Agilent Technologies).

Sequencing

Libraries were initially pooled and sequenced on an Illumina NextSeq using 2 x 75 bp PE (150 cycle) High Output chemistry. For deeper sequencing, libraries were diluted to 1.5 nM and each was run on one lane of an Illumina HiSeq X Ten using 2 x 150 bp PE (300 cycle) chemistry, except for ACAD 438 which was run on two lanes of an Illumina HiSeq X Ten.

Data processing

Demultiplexed sequencing reads were processed through Paleomix v1.2.12 [50]. Within Paleomix, raw reads were filtered, adapter sequences removed, and pair-end reads merged using ADAPTER REMOVAL v2.1.7 [51], trimming low quality bases (<Phred20 --minquality 4) and discarding merged reads shorter than 25 bp (--minlength 25). Read quality was visualised before and after adapter trimming using fastQC v0.11.5 (<http://www.bioinformatics.babraham.ac.uk/projects/fastqc/>) to ensure efficient adapter removal. Reads were mapped to the Panda ASM200744v1 genome [52] with BWA v0.7.15 using the mem algorithm [53]. Reads with mapping Phred scores less than 25 were removed using SAMtools 1.5 [54] and PCR duplicates were removed using “paleomix rmdup_collapsed” and MARKDUPLICATES from the Picard package

(<http://broadinstitute.github.io/picard/>). Indel realignment was performed using GATK [55] and damage profiles assessed using MapDamage v2.0.8 [56] (Figure S1).

Sequencing reads were downloaded from the European Nucleotide Archive for all extant bear species (Table S2) [14, 21, 24, 57, 58] and processed using the same pipeline as for the ancient samples.

Phylogenetic analysis

Indexed VCF files were created for each BAM file using mpileup, part of the SAMtools package v0.1.19 [54], and the call and index functions as a part of the BCFtools package v0.1.19. Parallel v2010622 [59] was used to process each BAM file in parallel. BCFtools was then used to filter SNPs within 3 bp of an indel (--SnpGap 3). The 85 largest scaffolds of the Panda reference genome were renamed as chromosomes (chr1–85) in each VCF file using BCFtools annotate. Biallelic variants in VCF files were converted to random pseudohaploid variants in eigenstrat format for the 85 largest scaffolds using vcf2eig (part of eig-utils; <https://github.com/grahamgower/eig-utils>) including monomorphic (-m) and singleton (-s) sites, and excluding transitions (-t). Eigenstrat formatted files were then converted to PHYLIP files using eig2phylip (part of eig-utils; <https://github.com/grahamgower/eig-utils>). A supermatrix tree was then created in RAxML v8.2.4 [60] using the rapid bootstrapping algorithm (-f a) and using the GTRCAT model of substitution with ascertainment correction (-m ASC_GTRCAT) with 100 bootstrap replicates (-#100) and using the Felsenstein ascertainment correction (--asc-corr=felsenstein) based on the number of invariant sites (calculated from the total ungapped length of the largest 85 scaffolds of the Panda reference genome minus the length of the alignment).

Discordance analysis using DiscoVista

The eigenstrat files were broken down into non-overlapping 500kb sliding windows using eigreduce (part of eig-utils; <https://github.com/grahamgower/eig-utils>). We only used the higher coverage *A. simus* sample (ACAD 344) in these analyses. For each window a PHYLIP file and tree were created as described above. The frequency and support of different tree topologies was then summarised and visualised using DiscoVista [61], using bootstrap values of 80 as the cutoff for strong support. Topologies tested included: 1) the inclusion of *Arctotherium* with ursine bears; 2) the inclusion of *Arctodus* with ursine

4.2 MANUSCRIPT

bears; 3) the inclusion of *Tremarctos* with ursine bears; 4) any combination of tremarctine bears included with ursine bears; 5) the monophyly of Tremarctinae; 6) monophyly of *Tremarctos* and *Arctodus*; 7) monophyly of *Tremarctos* and *Arctotherium*; and 8) monophyly of *Arctotherium* and *Arctodus*.

***D*-statistics**

To test for signals of gene flow within Tremarctinae and between tremarctine and ursine lineages we used D-statistics as implemented by Admixtools [62] in admixr [63]. We only used the higher coverage *A. simus* sample (ACAD 344) in this analysis. The giant panda was used as outgroup and block jack-knife procedure used to test for significant departures from zero ($|Z| > 3$). D-statistics within Tremarctinae were calculated in the form $D(\textit{Arctodus}, \textit{Tremarctos}, \textit{Arctotherium}, \textit{panda})$ and for detecting gene flow between Tremarctinae and Ursinae in the form $D(U1, U2, T1, \textit{panda})$, where T1 is any short-faced bear and U1 and U2 any ursine individual. D-statistics were also performed to detect gene flow within Ursinae (as per Kumar, et al. [14]), using either the giant panda or spectacled bear as outgroup. To account for the possibility of a reference bias in ancient samples, within Tremarctinae D-statistics were recalculated using the Asiatic black bear as outgroup (Table S5).

Molecular dating

Divergence times were estimated for each 500kb fragment from the discordance analysis using MCMCtree, part of the PAML package v4.8a [64], using the topology from the ML tree produced in the discordance analysis as the input tree. Four calibrations were used to calibrate the phylogeny:

1. The crown-age of Ursidae (*i.e.* the divergence of the giant panda lineage) was constrained to between 11.6 and 23 million years ago (mya) based on the presence of *Kretzoiarctos* [65], a putative ailuropodine, in the middle Miocene and the assumption that early Miocene *Ursavus* representatives are likely ancestral to modern ursids [10].
2. The divergence of Tremarctinae and Ursinae was constrained to between 7 and 13 mya based on the presence of putative early tremarctine bears (*e.g.* *Plionarctos*) in the Late Miocene/Early Pliocene [66].
3. The common ancestor of all sampled ursine bears was constrained to between 4.3 and 6 mya based on the occurrence of *Ursus minimus* [14, 67].

4. The divergence of polar and brown bears was constrained to between 0.48 and 1.1 mya based on previous nuclear estimates [21, 24, 25].

The JC +G substitution model with 5 discrete gamma categories was used with autocorrelated-rates, also known as the geometric Brownian diffusion clock model. Uniform priors for node ages using the birth-death (BD) process were used [$\lambda_{BD} = 1$ (birth-rate), $\mu_{BD} = 1$ (death-rate), and $\rho_{BD} = 0.1$ (sampling fraction for extant species)]. A gamma-Dirichlet distribution was used for the prior on rate with an α shape parameter of 2 (diffuse prior). The σ_i^2 prior was defined as a diffuse gamma-Dirichlet distribution (2,2). MCMC tree runs were performed with a burn-in of 10000, and a sample size of 10000, sampling every ten iterations. Median node ages were then averaged for each tree topology.

Low-recombining region of X-chromosome

Scaffolds of the panda ASM200744v1 reference genome [52] corresponding to low recombination regions of the X chromosome were identified by mapping all scaffolds to the recombination cold-spot of the X chromosome of the domestic cat (FelCat9) using minimap2 [68]. Default parameters were used, meaning the alignment lacked base-level precision (to account to phylogenetic distance between giant panda and the domestic cat). Only scaffolds larger than 500kb and with greater than 100 kb of segments mapping to the low recombining region of the domestic cat X-chromosome were retained, resulting in 15 scaffolds linked to the low recombination region of the X-chromosome. A maximum-likelihood phylogenetic tree and gene-tree discordance analysis were performed on these 15 scaffolds as described above for the genome-wide dataset.

References:

1. Soibelzon, L.H., Tonni, E.P., and Bond, M. (2005). The fossil record of South American short-faced bears (Ursidae, Tremarctinae). *J. South Am. Earth Sci.* *20*, 105-113.
2. Soibelzon, L.H. (2004). Revisión sistemática de los Tremarctinae (Carnivora, Ursidae) fósiles de América del Sur. *Rev. Mus. Argent. Cienc. Nat.* *6*, 107-133.
3. Kurtén, B. (1966). Pleistocene bears of North America. 1. Genus *Trematctos*, spectacled bears. *Acta Zool. Fenn.* *115*, 1-120.
4. Kurtén, B., and Anderson, E. (1980). *Pleistocene Mammals of North America*, (New York: Columbia University Press).

4.3 REFERENCES

5. Schubert, B.W., Chatters, J.C., Arroyo-Cabrales, J., Samuels, J.X., Soibelzon, L.H., Prevosti, F.J., Widga, C., Nava, A., Rissolo, D., and Erreguerena, P.L. (2019). Yucatan carnivorans shed light on the Great American Biotic Interchange. *Biol. Lett.* *15*, 20190148.
6. Prevosti, F.J. (2018). Evolution of South American Mammalian Predators During the Cenozoic: Paleobiogeographic and Paleoenvironmental Contingencies, 1st ed. 2018. Edition, (Cham: Springer International Publishing).
7. Kurtén, B. (1967). Pleistocene bears of North America. 2. Genus *Arctodus*, short-faced bears. *Acta Zool. Fenn.* *117*, 1-60.
8. Christiansen, P. (1999). What size were *Arctodus simus* and *Ursus spelaeus* (Carnivora: Ursidae)? *Ann. Zool. Fenn.* *36*, 93-102.
9. Soibelzon, L.H., and Schubert, B.W. (2011). The largest known bear, *Arctotherium angustidens*, from the early Pleistocene Pampean region of Argentina: with a discussion of size and diet trends in bears. *J. Paleontol.* *85*, 69-75, 67.
10. McLellan, B., and Reiner, D.C. (1994). A review of bear evolution. *Bears Their Biol. Manag.* *9*, 85-96.
11. Trajano, E., and Ferrarezzi, H. (1995). A Fossil Bear from Northeastern Brazil, with a Phylogenetic Analysis of the South American Extinct Tremarctinae (Ursidae). *J. Vertebr. Paleontol.* *14*, 552-561.
12. Mitchell, K.J., Bray, S.C., Bover, P., Soibelzon, L., Schubert, B.W., Prevosti, F., Prieto, A., Martin, F., Austin, J.J., and Cooper, A. (2016). Ancient mitochondrial DNA reveals convergent evolution of giant short-faced bears (Tremarctinae) in North and South America. *Biol. Lett.* *12*, 20160062.
13. Kutschera, V.E., Bidon, T., Hailer, F., Rodi, J.L., Fain, S.R., and Janke, A. (2014). Bears in a forest of gene trees: Phylogenetic inference is complicated by incomplete lineage sorting and gene flow. *Mol. Biol. Evol.* *31*, 2004-2017.
14. Kumar, V., Lammers, F., Bidon, T., Pfenninger, M., Kolter, L., Nilsson, M.A., and Janke, A. (2017). The evolutionary history of bears is characterized by gene flow across species. *Sci. Rep.* *7*, 46487.
15. Funk, D.J., and Omland, K.E. (2003). Species-Level Paraphyly and Polyphyly: Frequency, Causes, and Consequences, with Insights from Animal Mitochondrial DNA. *Annu. Rev. Ecol. Evol. Syst.* *34*, 397-423.
16. Leache, A.D., and McGuire, J.A. (2006). Phylogenetic relationships of horned lizards (*Phrynosoma*) based on nuclear and mitochondrial data: evidence for a misleading mitochondrial gene tree. *Mol. Phylogenet. Evol.* *39*, 628-644.
17. Wallis, G.P., Cameron-Christie, S.R., Kennedy, H.L., Palmer, G., Sanders, T.R., and Winter, D.J. (2017). Interspecific hybridization causes long-term phylogenetic discordance between nuclear and mitochondrial genomes in freshwater fishes. *Mol. Ecol.* *26*, 3116-3127.

18. Toews, D.P., and Brelsford, A. (2012). The biogeography of mitochondrial and nuclear discordance in animals. *Mol. Ecol.* *21*, 3907-3930.
19. Gompert, Z., Forister, M.L., Fordyce, J.A., and Nice, C.C. (2008). Widespread mitonuclear discordance with evidence for introgressive hybridization and selective sweeps in *Lycaeides*. *Mol. Ecol.* *17*, 5231-5244.
20. Barlow, A., Cahill, J.A., Hartmann, S., Theunert, C., Xenikoudakis, G., Fortes, G.G., Paijmans, J.L.A., Rabeder, G., Frischauf, C., Grandal-d'Anglade, A., et al. (2018). Partial genomic survival of cave bears in living brown bears. *Nat. Ecol. Evol.* *2*, 1563-1570.
21. Cahill, J.A., Green, R.E., Fulton, T.L., Stiller, M., Jay, F., Ovshynikov, N., Salamzade, R., St. John, J., Stirling, I., Slatkin, M., et al. (2013). Genomic evidence for island population conversion resolves conflicting theories of polar bear evolution. *PLoS Genet.* *9*, e1003345.
22. Cahill, J.A., Stirling, I., Kistler, L., Salamzade, R., Ersmark, E., Fulton, T.L., Stiller, M., Green, R.E., and Shapiro, B. (2015). Genomic evidence of geographically widespread effect of gene flow from polar bears into brown bears. *Mol. Ecol.* *24*, 1205-1217.
23. Hailer, F. (2015). Introgressive hybridization: brown bears as vectors for polar bear alleles. *Mol. Ecol.* *24*, 1161-1163.
24. Liu, S.P., Lorenzen, E.D., Fumagalli, M., Li, B., Harris, K., Xiong, Z.J., Zhou, L., Korneliussen, T.S., Somel, M., Babbitt, C., et al. (2014). Population genomics reveal recent speciation and rapid evolutionary adaptation in polar bears. *Cell* *157*, 785-794.
25. Hailer, F., Kutschera, V.E., Hallstrom, B.M., Klassert, D., Fain, S.R., Leonard, J.A., Arnason, U., and Janke, A. (2012). Nuclear genomic sequences reveal that polar bears are an old and distinct bear lineage. *Science* *336*, 344-347.
26. Martin, F.M., Prieto, A., Morello, F., Prevosti, F., and Borrero, L. (2004). Late Pleistocene megafauna at Cueva del Puma, Pali-Aike Lava Field, Chile. *Curr. Res. Pleistocene* *21*, 101-103.
27. Harington, C.R., Naughton, D., Dalby, A., Rose, M., and Dawson, J. (2003). *Annotated Bibliography of Quaternary Vertebrates of Northern North America*, (Toronto: University of Toronto Press).
28. Krause, J., Unger, T., Nocon, A., Malaspinas, A.S., Kolokotronis, S.O., Stiller, M., Soibelzon, L., Spriggs, H., Dear, P.H., Briggs, A.W., et al. (2008). Mitochondrial genomes reveal an explosive radiation of extinct and extant bears near the Miocene-Pliocene boundary. *BMC Evol. Biol.* *8*, 220.
29. Nichols, R. (2001). Gene trees and species trees are not the same. *Trends Ecol. Evol.* *16*, 358-364.
30. Maddison, W.P. (1997). Gene trees in species trees. *Syst. Biol.* *46*, 523-536.

4.3 REFERENCES

31. Cahill, J.A., Heintzman, P.D., Harris, K., Teasdale, M.D., Kapp, J., Soares, A.E.R., Stirling, I., Bradley, D., Edwards, C.J., Graim, K., et al. (2018). Genomic evidence of widespread admixture from polar bears into brown bears during the last ice age. *Mol. Biol. Evol.* *35*, 1120-1129.
32. Green, R.E., Krause, J., Briggs, A.W., Maricic, T., Stenzel, U., Kircher, M., Patterson, N., Li, H., Zhai, W.W., Fritz, M.H.Y., et al. (2010). A Draft Sequence of the Neandertal Genome. *Science* *328*, 710-722.
33. Durand, E.Y., Patterson, N., Reich, D., and Slatkin, M. (2011). Testing for ancient admixture between closely related populations. *Mol. Biol. Evol.* *28*, 2239-2252.
34. Mondolfi, E., and Boede, E. (1981). A hybrid of a spectacled bear (*Tremarctos ornatus*) and an asiatic black bear (*Selenarctos thibetanus*) born at the Maracay zoological park, Venezuela. *Mem. Soc. Cienc. Nat. La Salle* *41*, 143-148.
35. Stucchi, M., Salas-Gismondi, R., Baby, P., Guyot, J.-L., and Shockey, B.J. (2009). A 6,000 year-old specimen of a spectacled bear from an Andean cave in Peru. *Ursus* *20*, 63-68.
36. García-Rangel, S. (2012). Andean bear *Tremarctos ornatus* natural history and conservation. *Mammal Rev.* *42*, 85-119.
37. Figueirido, B., and Soibelzon, L.H. (2010). Inferring palaeoecology in extinct tremarctine bears (Carnivora, Ursidae) using geometric morphometrics. *Lethaia* *43*, 209-222.
38. Czaplewski, N.J., Krejca, J., and Miller, T.E. (2003). Late quaternary bats from Cebada Cave, Chiquibul cave system, Belize. *Caribb. J. Sci.* *39*, 23-33.
39. Li, G., Figueiro, H.V., Eizirik, E., and Murphy, W.J. (2019). Recombination-aware phylogenomics reveals the structured genomic landscape of hybridizing cat species. *Mol. Biol. Evol.* *36*, 2111-2126.
40. Menotti-Raymond, M., David, V.A., Roelke, M.E., Chen, Z.Q., Menotti, K.A., Sun, S., Schaffer, A.A., Tomlin, J.F., Agarwala, R., O'Brien, S.J., et al. (2003). Second-generation integrated genetic linkage/radiation hybrid maps of the domestic cat (*Felis catus*). *J. Hered.* *94*, 95-106.
41. Menotti-Raymond, M., David, V.A., Lyons, L.A., Schaffer, A.A., Tomlin, J.F., Hutton, M.K., and O'Brien, S.J. (1999). A genetic linkage map of microsatellites in the domestic cat (*Felis catus*). *Genomics* *57*, 9-23.
42. Li, G., Hillier, L.W., Grahn, R.A., Zimin, A.V., David, V.A., Menotti-Raymond, M., Middleton, R., Hannah, S., Hendrickson, S., Makunin, A., et al. (2016). A high-resolution SNP array-based linkage map anchors a new domestic cat draft genome assembly and provides detailed patterns of recombination. *G3 (Bethesda)* *6*, 1607-1616.
43. Li, G., Davis, B.W., Eizirik, E., and Murphy, W.J. (2016). Phylogenomic evidence for ancient hybridization in the genomes of living cats (Felidae). *Genome Res.* *26*, 1-11.

44. Reimer, P.J., Bard, E., Bayliss, A., Beck, J.W., Blackwell, P.G., Ramsey, C.B., Buck, C.E., Cheng, H., Edwards, R.L., Friedrich, M., et al. (2013). Intcal13 and Marine13 radiocarbon age calibration curves 0-50,000 years cal BP. *Radiocarbon* 55, 1869-1887.
45. Hogg, A.G., Hua, Q., Blackwell, P.G., Niu, M., Buck, C.E., Guilderson, T.P., Heaton, T.J., Palmer, J.G., Reimer, P.J., Reimer, R.W., et al. (2013). Shcal13 Southern Hemisphere Calibration, 0-50,000 Years Cal Bp. *Radiocarbon* 55, 1889-1903.
46. Ramsey, C.B. (2009). Bayesian analysis of radiocarbon dates. *Radiocarbon* 51, 337-360.
47. Dabney, J., Knapp, M., Glocke, I., Gansauge, M.-T., Weihmann, A., Nickel, B., Valdiosera, C., García, N., Pääbo, S., Arsuaga, J.-L., et al. (2013). Complete mitochondrial genome sequence of a Middle Pleistocene cave bear reconstructed from ultrashort DNA fragments. *Proc. Natl. Acad. Sci. U. S. A.* 110, 15758-15763.
48. Meyer, M., Kircher, M., Gansauge, M.T., Li, H., Racimo, F., Mallick, S., Schraiber, J.G., Jay, F., Prufer, K., de Filippo, C., et al. (2012). A high-coverage genome sequence from an archaic Denisovan individual. *Science* 338, 222-226.
49. Rohland, N., Harney, E., Mallick, S., Nordenfelt, S., and Reich, D. (2015). Partial uracil-DNA-glycosylase treatment for screening of ancient DNA. *Philos. Trans. R. Soc. Lond. B. Biol. Sci* 370, 20130624.
50. Schubert, M., Ermini, L., Sarkissian, C.D., Jonsson, H., Ginolhac, A., Schaefer, R., Martin, M.D., Fernandez, R., Kircher, M., McCue, M., et al. (2014). Characterization of ancient and modern genomes by SNP detection and phylogenomic and metagenomic analysis using PALEOMIX. *Nat. Protoc.* 9, 1056-1082.
51. Schubert, M., Lindgreen, S., and Orlando, L. (2016). AdapterRemoval v2: rapid adapter trimming, identification, and read merging. *BMC Res. Notes* 9, 88.
52. Hu, Y., Wu, Q., Ma, S., Ma, T., Shan, L., Wang, X., Nie, Y., Ning, Z., Yan, L., Xiu, Y., et al. (2017). Comparative genomics reveals convergent evolution between the bamboo-eating giant and red pandas. *Proc. Natl. Acad. Sci. U. S. A.* 114, 1081-1086.
53. Li, H., and Durbin, R. (2009). Fast and accurate short read alignment with Burrows-Wheeler transform. *Bioinformatics* 25, 1754-1760.
54. Li, H., Handsaker, B., Wysoker, A., Fennell, T., Ruan, J., Homer, N., Marth, G., Abecasis, G., Durbin, R., and Genome Project Data Processing, S. (2009). The sequence alignment/map format and SAMtools. *Bioinformatics* 25, 2078-2079.
55. McKenna, A., Hanna, M., Banks, E., Sivachenko, A., Cibulskis, K., Kernytzky, A., Garimella, K., Altshuler, D., Gabriel, S., Daly, M., et al. (2010). The Genome Analysis Toolkit: a MapReduce framework for analyzing next-generation DNA sequencing data. *Genome Res.* 20, 1297-1303.

4.3 REFERENCES

56. Jonsson, H., Ginolhac, A., Schubert, M., Johnson, P.L.F., and Orlando, L. (2013). mapDamage2.0: fast approximate Bayesian estimates of ancient DNA damage parameters. *Bioinformatics* 29, 1682-1684.
57. Zhao, S.C., Zheng, P.P., Dong, S.S., Zhan, X.J., Wu, Q., Guo, X.S., Hu, Y.B., He, W.M., Zhang, S.N., Fan, W., et al. (2013). Whole-genome sequencing of giant pandas provides insights into demographic history and local adaptation. *Nat. Genet.* 45, 67-71.
58. Miller, W., Schuster, S.C., Welch, A.J., Ratan, A., Bedoya-Reina, O.C., Zhao, F.Q., Kim, H.L., Burhans, R.C., Drautz, D.I., Wittekindt, N.E., et al. (2012). Polar and brown bear genomes reveal ancient admixture and demographic footprints of past climate change. *Proc. Natl. Acad. Sci. U. S. A.* 109, E2382-E2390.
59. Tange, O. (2011). Gnu parallel-the command-line power tool. *The USENIX Magazine* 36, 42-47.
60. Stamatakis, A. (2014). RAxML version 8: a tool for phylogenetic analysis and post-analysis of large phylogenies. *Bioinformatics* 30, 1312-1313.
61. Sayyari, E., Whitfield, J.B., and Mirarab, S. (2018). DiscoVista: Interpretable visualizations of gene tree discordance. *Mol. Phylogenet. Evol.* 122, 110-115.
62. Patterson, N., Moorjani, P., Luo, Y., Mallick, S., Rohland, N., Zhan, Y., Genschoreck, T., Webster, T., and Reich, D. (2012). Ancient admixture in human history. *Genetics* 192, 1065-1093.
63. Petr, M., Vernot, B., and Kelso, J. (2019). admixr-R package for reproducible analyses using ADMIXTOOLS. *Bioinformatics* 35, 3194-3195.
64. Yang, Z. (2007). PAML 4: phylogenetic analysis by maximum likelihood. *Mol. Biol. Evol.* 24, 1586-1591.
65. Abella, J., Alba, D.M., Robles, J.M., Valenciano, A., Rotgers, C., Carmona, R., Montoya, P., and Morales, J. (2012). *Kretzoiarctos* gen. nov., the oldest member of the giant panda clade. *PLoS ONE* 7, e48985.
66. Tedford, R.H., and Martin, J. (2001). *Plionarctos*, a tremarctine bear (Ursidae: Carnivora) from western North America. *J. Vertebr. Paleontol.* 21, 311-321.
67. Vangengeim, E.A., Vislobokova, I., and Sotnikova, M. (1998). Large Ruscinian Mammalia in the territory of the former Soviet Union. *Stratigr. Geol. Correl* 6, 368-382.
68. Li, H. (2018). Minimap2: pairwise alignment for nucleotide sequences. *Bioinformatics* 34, 3094-3100.

4.3 Supplementary Information

Ancient genomes reveal hybridisation between extinct short-faced bears and the extant spectacled bear (*Tremarctos ornatus*)

Alexander T Salis, Graham Gower, Blaine W. Schubert, Leopoldo H. Soibelzon, Holly Heiniger, Julie Meachen, Alan Cooper, Kieren J Mitchell

Supplementary Information

This file includes:

Figures S1 to S4
Tables S1 to S4
Supplementary References

4.3 SUPPLEMENTARY INFORMATION

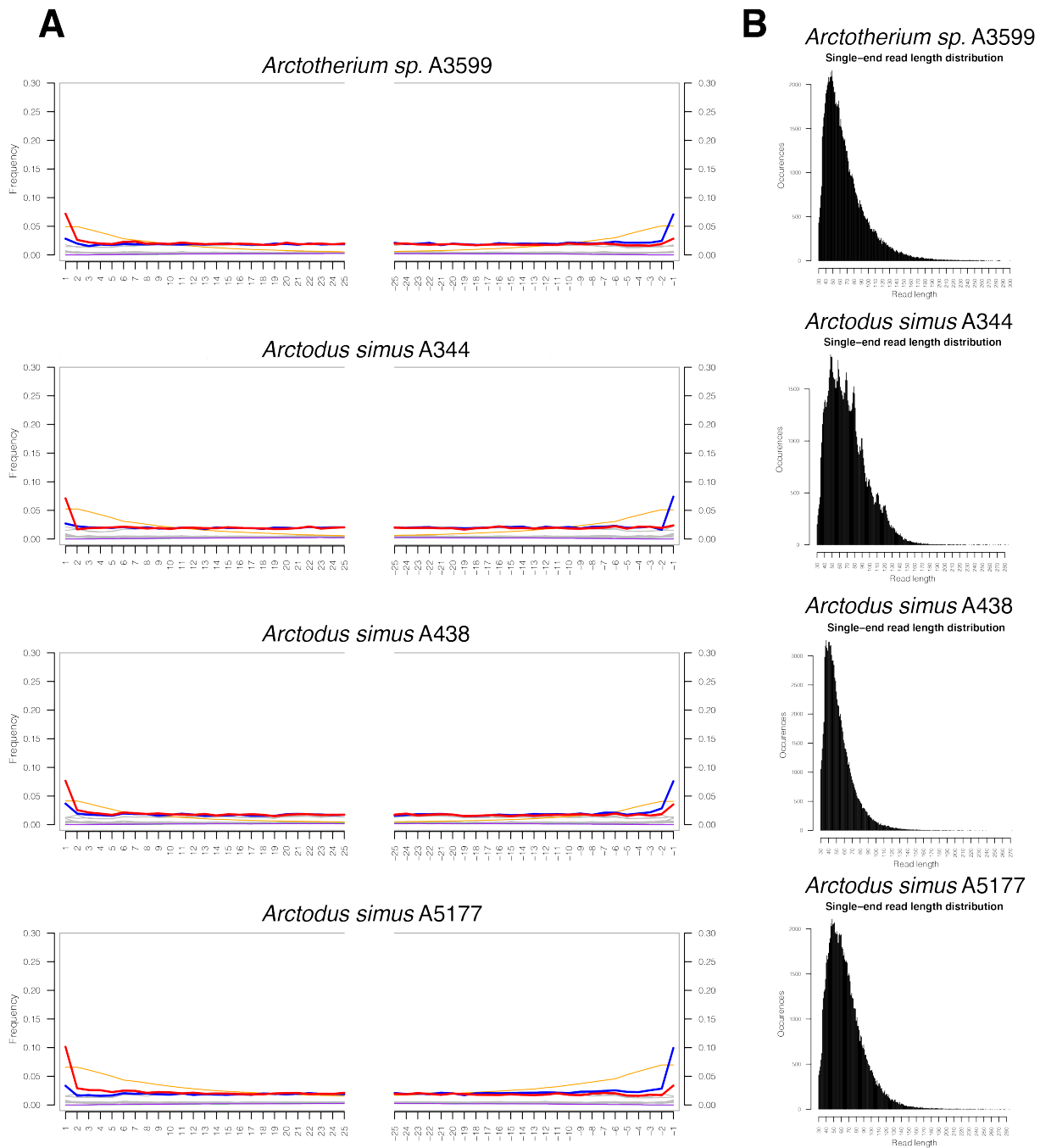


Figure S1: Authentication of ancient genomic data from the four extinct short-faced bears specimens. **A)** Cytosine deamination patterns where the x-axis represents the number of bases from the 5' or 3' end of a DNA fragment. The red lines represent cytosine (C) to thymine (T) transitions and blue lines guanine (G) to adenine (A) transitions compared to the giant panda reference genome. All samples show an accumulation of C-T transitions on the first base of DNA fragments, characteristic of aDNA that has undergone partial UDG treatment. The increase in G-A at terminal 3' base is an artefact of the double-stranded DNA library procedure and actually represents C-T transitions. **B)** Fragment length distributions of the length of reads mapping to the giant panda reference from each sample. The minimum read length used for mapping was 30 bp, resulting in a hard cut-off at this length. All samples show an abundance of small fragments (all centred around ~50 bp), characteristic of aDNA.

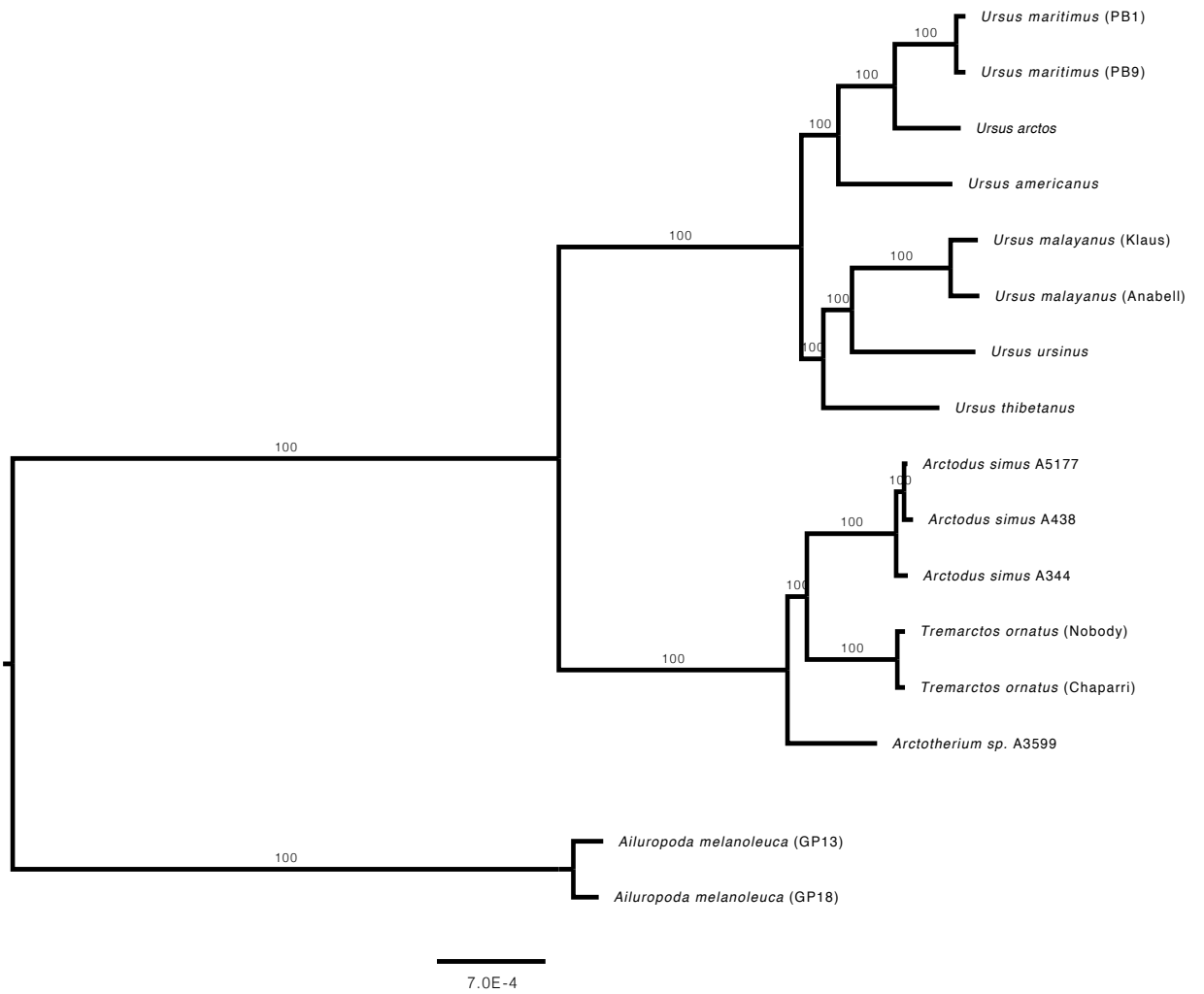


Figure S2: Maximum likelihood tree based on nuclear SNPs constructed in RAxML. Branch labels represent bootstrap support percentages.

4.3 SUPPLEMENTARY INFORMATION

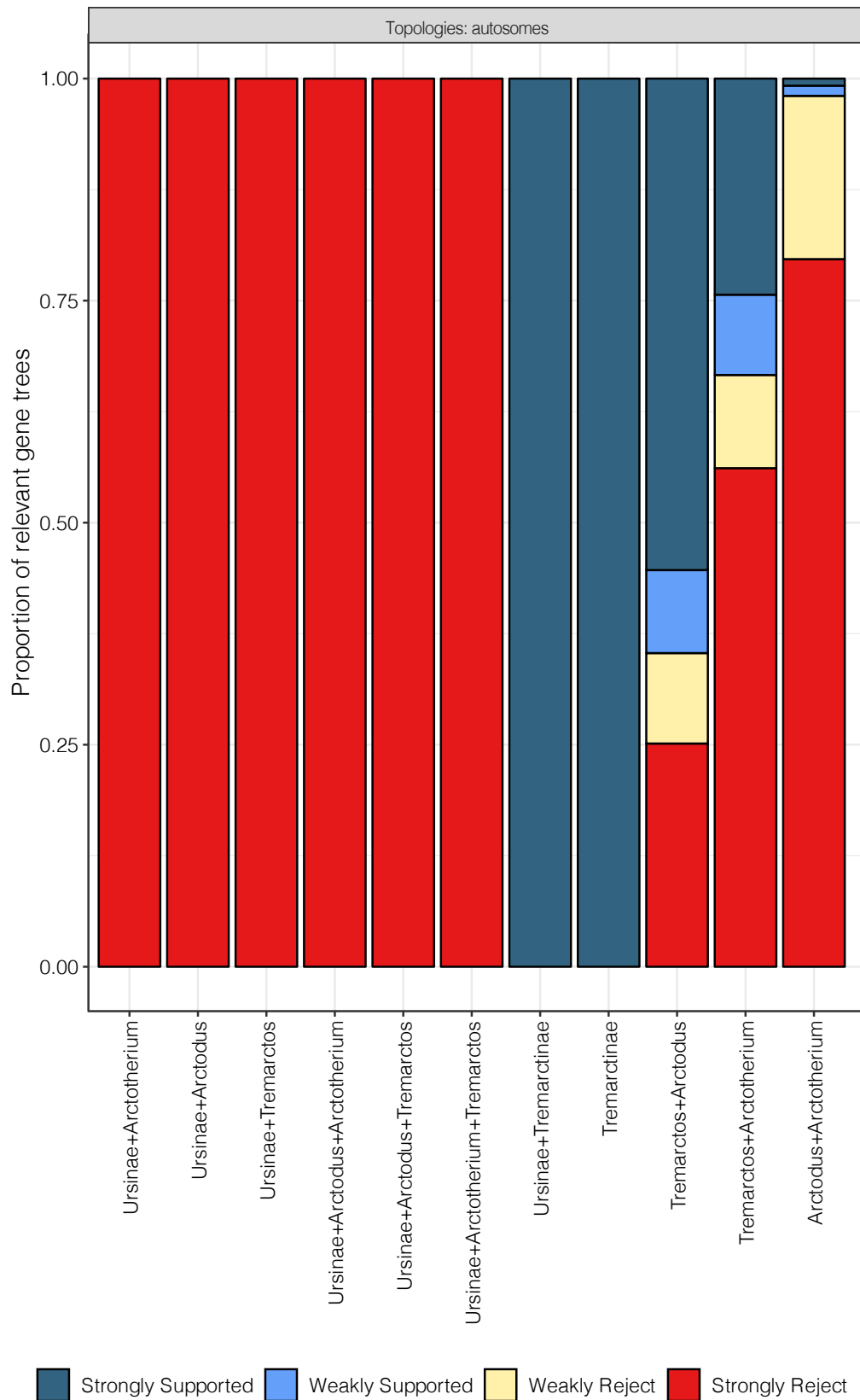


Figure S3: Discordance visualisation using DiscoVista from 2622 500 kb autosomal genomic fragments for all tested topologies involving tremarctine bears, with >80 bootstrap support used to define strong support. The x-axis represents topologies tested and the y-axis the proportion of fragments that support the topology.

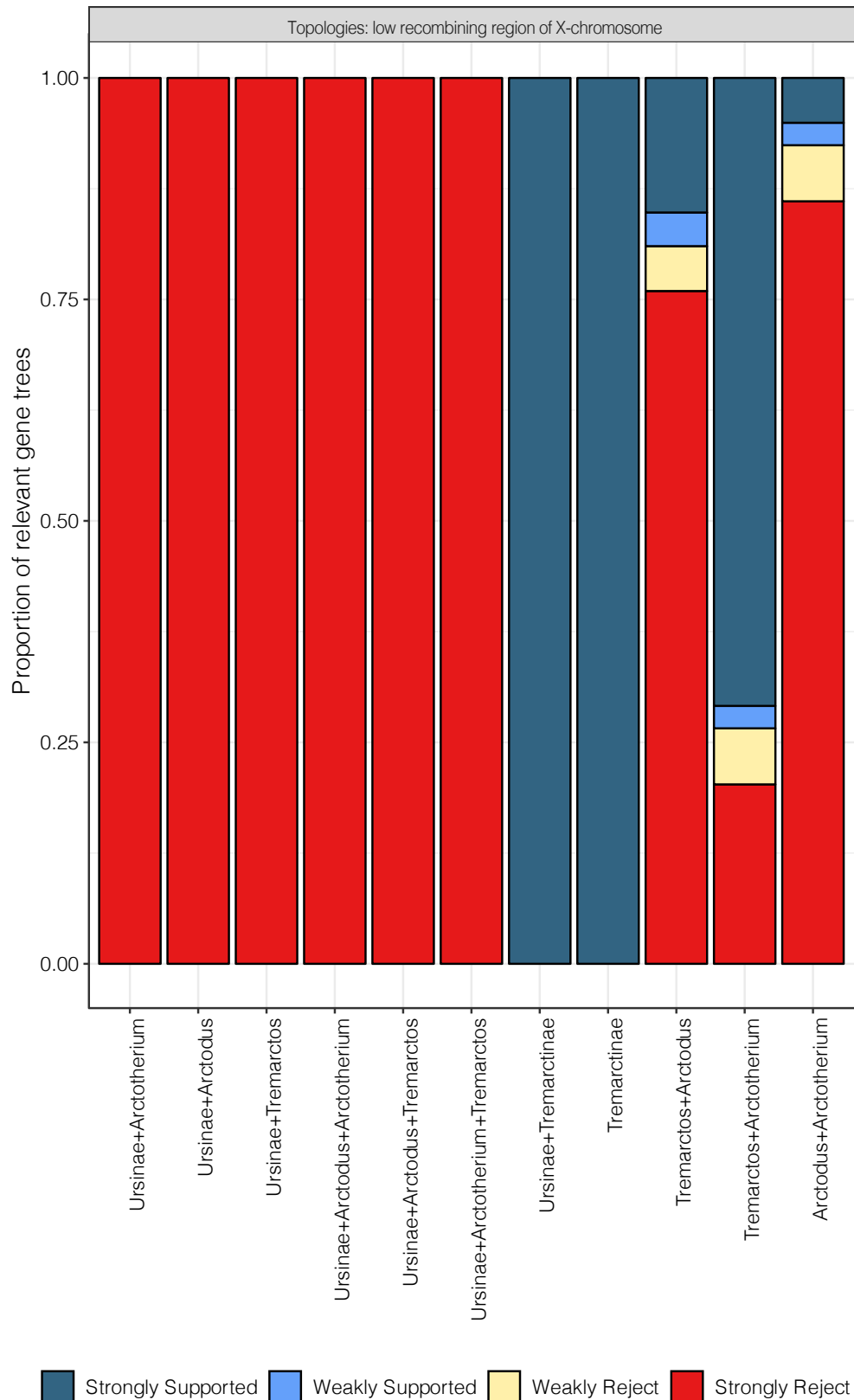


Figure S4: Discordance visualisation using DiscoVista from 80 500 kb genomic fragments pertaining to the ~40 Mb recombination cold-spot on the X chromosome, with >80 bootstrap support used to define strong support. The x-axis represents topologies tested and the y-axis the proportion of fragments that support the topology.

4.3 SUPPLEMENTARY INFORMATION

Table S1: Details of published and newly sequenced bears used in this study.

Binomial Name	Common Name	Sample Name	Location	EBI Sample Accession	EBI Read Accession	Study
* <i>Arctodus simus</i>	North American short-faced bear	ACAD 344/ YG 76.4	Hester Creek, Yukon	NA	NA	this study
* <i>Arctodus simus</i>	North American short-faced bear	ACAD 438/ CMN 42388	Sixty Mile Creek, Yukon	NA	NA	this study
* <i>Arctodus simus</i>	North American short-faced bear	ACAD 5177/ KU 31956	Natural Trap Cave, Wyoming	NA	NA	this study
* <i>Arctotherium sp.</i>	South American short-faced bear	ACAD 3599/ no. 32104	Cueva del Puma, Patagonia	NA	NA	this study
<i>Tremarctos ornatus</i>	Spectacled bear	Chaparrí	Zoo Basel	SAMEA3749107	ERR946788	Kumar, et al. [1]
<i>Tremarctos ornatus</i>	Spectacled bear	Nobody	Zoo Basel	SAMEA3749205	ERR946789	Kumar, et al. [1]
<i>Ursus maritimus</i>	Polar bear	PB1	Spitsbergen, Svalbard	SAMN01057636	SRR518661, SRR518662	Miller, et al. [2]
<i>Ursus maritimus</i>	Polar bear	PB9	Spitsbergen, Svalbard	SAMN01057666	SRR518686, SRR518687	Miller, et al. [2]
<i>Ursus arctos</i>	Brown bear	GP01	Glacier National Park, Montana	SAMN02256322	SRR935609, SRR935616, SRR935617, SRR941811, SRR941814	Liu, et al. [3]
<i>Ursus americanus</i>	American black bear	JC012	Pennsylvania	SAMN02045561	SRR830685	Cahill, et al. [4]
<i>Ursus thibetanus</i>	Asiatic black bear	Anorexica	Zoo Madrid	SAMEA3749106	ERR946787	Kumar, et al. [1]
<i>Ursus ursinus</i>	Sloth bear	Renate	Zoo Leipzig	SAMEA3749105	ERR946786	Kumar, et al. [1]
<i>Ursus malayanus</i>	Sun bear	Anabell	Zoo Munster	SAMEA3749104	ERR946784	Kumar, et al. [1]
<i>Ursus malayanus</i>	Sun bear	Klaus	Zoo Madrid	SAMEA3750870	ERR946785	Kumar, et al. [1]
<i>Ailuropoda melanoleuca</i>	Giant Panda	GP13	Baoxing, Sichuan	SAMN01040418	SRR504866	Zhao, et al. [5]
<i>Ailuropoda melanoleuca</i>	Giant Panda	GP18	Beichuan, Sichuan	SAMN01040423	SRR504871	Zhao, et al. [5]

*Newly sequenced samples

Table S2: Sequencing and mapping statistics for all bear samples analysed in this study. Columns show the number of filtered raw reads used in mapping, the number of successfully mapped reads to the giant panda reference genome, the number of unique reads that mapped after PCR duplicates were removed, the percentage of original reads that mapped, and the percentage of mapped reads that were PCR duplicates.

Binomial Name	Sample Name	Retained Reads	Raw Mapped Reads	Unique Mapped Reads	Mapped Reads %	Clonality	Coverage (X)
* <i>Arctodus simus</i>	ACAD 344	496403229	279086649	202678836	0.562217634	0.273778102	5.92566319
* <i>Arctotherium sp.</i>	ACAD 3599	402733914	192677824	140025115	0.478424631	0.273268132	3.892443033
* <i>Arctodus simus</i>	ACAD 438	800500649	33649637	23716909	0.04203574	0.295180837	0.519775289
* <i>Arctodus simus</i>	ACAD 5177	475874477	5166918	4488594	0.010857733	0.13128213	0.121626851
<i>Tremarctos ornatus</i>	Chaparrí	312051217	268627345	256263228	0.860843767	0.046027023	9.199861216
<i>Tremarctos ornatus</i>	Nobody	318173650	274620841	263660657	0.863116229	0.039910241	9.459313992
<i>Ursus maritimus</i>	PB1	346660533	298508499	289412061	0.861097444	0.030472962	11.58217001
<i>Ursus maritimus</i>	PB9	340345215	297785719	290239526	0.874951978	0.025341017	11.58504902
<i>Ursus arctos</i>	GP01	553954695	433336259	382711352	0.782259385	0.11682592	15.30793958
<i>Ursus americanus</i>	JC012	194019255	160004491	153521351	0.824683566	0.040518488	10.34896241
<i>Ursus thibetanus</i>	Anorexica	331174468	280801772	269428174	0.847896801	0.040504011	9.659247534
<i>Ursus ursinus</i>	Renate	295156761	254126145	240552726	0.860987037	0.053412131	8.639123446
<i>Ursus malayanus</i>	Anabell	294000644	250655873	243756105	0.852569129	0.027526856	8.753848913
<i>Ursus malayanus</i>	Klaus	319734539	271802375	260802737	0.850087625	0.040469249	9.370637783
<i>Ailuropoda melanoleuca</i>	GP13	137650116	119980120	111763758	0.871631085	0.068481028	3.765764372
<i>Ailuropoda melanoleuca</i>	GP18	138649930	124714455	112803002	0.899491655	0.095509803	4.014613177

*Newly sequenced samples

4.3 SUPPLEMENTARY INFORMATION

Table S3: D-statistics testing for Ursinae hybridisation within short-faced bears (Tremarctinae). D-statistics (D), standard error, and Z-Score (significant if $> |3|$) are displayed, with ABBA-BABA counts and the number of SNPs considered in the analysis

D-statistic	D	Stderr	Z-score	BABA	ABBA	nSNPs
D(T. ornatus (Nobody), Arctotherium sp., U. maritimus (PB1))	0.1922	0.007582	25.347	10828	7336	6158376
D(T. ornatus (Nobody), Arctotherium sp., U. malayanus (Klaus))	0.2057	0.008348	24.646	10960	7219	6157958
D(T. ornatus (Nobody), Arctotherium sp., U. thibetanus)	0.2043	0.008319	24.555	11051	7301	6171003
D(T. ornatus (Nobody), Arctotherium sp., U. malayanus (Anabell))	0.2024	0.008262	24.499	10921	7243	6158753
D(T. ornatus (Nobody), Arctotherium sp., U. ursinus)	0.2008	0.00824	24.367	10882	7242	6163089
D(T. ornatus (Nobody), Arctotherium sp., U. maritimus (PB9))	0.1932	0.008019	24.091	10935	7394	6184441
D(T. ornatus (Chaparri), Arctotherium sp., U. malayanus (Klaus))	0.2083	0.008725	23.875	10997	7205	6159057
D(T. ornatus (Chaparri), Arctotherium sp., U. maritimus (PB1))	0.1942	0.008137	23.86	10864	7331	6158997
D(T. ornatus (Chaparri), Arctotherium sp., U. malayanus (Anabell))	0.206	0.008636	23.851	10976	7227	6159872
D(T. ornatus (Nobody), Arctotherium sp., U. arctos)	0.2079	0.008878	23.418	11177	7329	6184195
D(T. ornatus (Chaparri), Arctotherium sp., U. thibetanus)	0.2052	0.008794	23.338	11072	7300	6172374
D(T. ornatus (Nobody), Arctotherium sp., U. americanus)	0.187	0.008062	23.191	10684	7318	6158065
D(T. ornatus (Chaparri), Arctotherium sp., U. ursinus)	0.2	0.00868	23.039	10885	7256	6164301
D(T. ornatus (Chaparri), Arctotherium sp., U. americanus)	0.188	0.008193	22.952	10727	7331	6158709
D(T. ornatus (Chaparri), Arctotherium sp., U. maritimus (PB9))	0.1962	0.008646	22.692	10978	7376	6184907
D(T. ornatus (Chaparri), Arctotherium sp., U. arctos)	0.2074	0.009242	22.442	11185	7342	6185696
D(T. ornatus (Nobody), Arctodus simus, U. arctos)	0.2152	0.009651	22.302	11172	7214	6317724
D(T. ornatus (Nobody), Arctodus simus, U. maritimus (PB1))	0.1958	0.009013	21.728	10753	7230	6290704
D(T. ornatus (Nobody), Arctodus simus, U. malayanus (Klaus))	0.2065	0.009668	21.36	10878	7154	6290343
D(T. ornatus (Chaparri), Arctodus simus, U. arctos)	0.2131	0.010012	21.281	11191	7260	6319318
D(T. ornatus (Nobody), Arctodus simus, U. thibetanus)	0.2091	0.009899	21.126	11026	7212	6302970
D(T. ornatus (Nobody), Arctodus simus, U. maritimus (PB9))	0.2003	0.009484	21.125	10898	7259	6317216
D(T. ornatus (Chaparri), Arctodus simus, U. thibetanus)	0.2104	0.010212	20.604	11076	7225	6304295
D(T. ornatus (Nobody), Arctodus simus, U. americanus)	0.1879	0.00916	20.512	10580	7233	6292779
D(T. ornatus (Chaparri), Arctodus simus, U. malayanus (Klaus))	0.2075	0.010129	20.487	10909	7159	6291437
D(T. ornatus (Nobody), Arctodus simus, U. malayanus (Anabell))	0.2029	0.009971	20.347	10862	7198	6290304
D(T. ornatus (Chaparri), Arctodus simus, U. maritimus (PB9))	0.1998	0.009847	20.287	10942	7298	6317882
D(T. ornatus (Nobody), Arctodus simus, U. ursinus)	0.206	0.010293	20.014	10868	7154	6294596
D(T. ornatus (Chaparri), Arctodus simus, U. maritimus (PB1))	0.196	0.01	19.604	10789	7252	6291256
D(T. ornatus (Chaparri), Arctodus simus, U. malayanus (Anabell))	0.2042	0.010502	19.444	10879	7189	6291443
D(T. ornatus (Chaparri), Arctodus simus, U. americanus)	0.188	0.009687	19.403	10609	7252	6293439
D(T. ornatus (Chaparri), Arctodus simus, U. ursinus)	0.2036	0.010578	19.246	10855	7182	6295812

Table S4: D-statistics testing for Tremarctinae hybridisation within Ursinae. D-statistics (D), standard error, and Z-Score (significant if $> |3|$) are displayed, with ABBA-BABA counts and the number of SNPs considered in the analysis

D-statistic	D	Stderr	Z-score	BABA	ABBA	nSNPs
D(U. arctos, U. americanus, T. ornatus (Nobody))	0.038	0.006774	5.615	10688	9904	6585424
D(U. arctos, U. maritimus (PB1), T. ornatus (Nobody))	0.0664	0.012707	5.222	6824	5974	6612645
D(U. arctos, U. maritimus (PB9), T. ornatus (Nobody))	0.0639	0.012328	5.181	6869	6043	6646165
D(U. arctos, U. maritimus (PB1), T. ornatus (Chaparri))	0.0639	0.012684	5.041	6867	6041	6614829
D(U. arctos, U. maritimus (PB9), T. ornatus (Chaparri))	0.061	0.012929	4.717	6847	6059	6648311
D(U. arctos, U. americanus, T. ornatus (Chaparri))	0.0309	0.006752	4.577	10651	10011	6587600
D(U. thibetanus, U. maritimus (PB1), T. ornatus (Chaparri))	0.0377	0.009127	4.136	12758	11829	6580987
D(U. thibetanus, U. maritimus (PB1), T. ornatus (Nobody))	0.0378	0.009426	4.013	12691	11764	6579114
D(U. ursinus, U. maritimus (PB1), T. ornatus (Chaparri))	0.0252	0.006652	3.794	14671	13948	6566596
D(U. ursinus, U. maritimus (PB1), T. ornatus (Nobody))	0.0253	0.006734	3.761	14617	13894	6565035
D(U. thibetanus, U. maritimus (PB9), T. ornatus (Chaparri))	0.0318	0.009213	3.447	12689	11907	6614426
D(U. thibetanus, U. americanus, T. ornatus (Nobody))	0.0315	0.009223	3.412	12659	11886	6562354
D(U. thibetanus, U. maritimus (PB9), T. ornatus (Nobody))	0.0309	0.009438	3.279	12628	11869	6612456
D(U. ursinus, U. maritimus (PB9), T. ornatus (Nobody))	0.0216	0.006665	3.242	14605	13986	6598187
D(U. thibetanus, U. americanus, T. ornatus (Chaparri))	0.0287	0.008944	3.214	12632	11925	6564284
D(U. ursinus, U. maritimus (PB9), T. ornatus (Chaparri))	0.0211	0.006599	3.199	14624	14018	6599795
D(U. ursinus, U. americanus, T. ornatus (Nobody))	0.02	0.00684	2.919	14280	13721	6549440
D(U. thibetanus, U. malayanus (Anabell), Arctotherium sp.)	0.0219	0.007818	2.807	9969	9540	6169185
D(U. thibetanus, U. malayanus (Klaus), Arctotherium sp.)	0.0208	0.007595	2.734	9997	9590	6166665
D(U. malayanus (Anabell), U. maritimus (PB1), T. ornatus (Chaparri))	0.0182	0.006915	2.639	14490	13970	6562190
D(U. thibetanus, U. malayanus (Klaus), Arctodus simus)	0.0219	0.008346	2.625	10302	9859	6298833
D(U. ursinus, U. americanus, T. ornatus (Chaparri))	0.0173	0.006651	2.597	14286	13801	6551084
D(U. thibetanus, U. malayanus (Anabell), Arctodus simus)	0.0219	0.008617	2.544	10267	9826	6300444
D(U. malayanus (Anabell), U. maritimus (PB1), T. ornatus (Nobody))	0.0171	0.006838	2.496	14405	13922	6560582
D(U. thibetanus, U. malayanus (Anabell), T. ornatus (Nobody))	0.0209	0.008549	2.439	11846	11361	6621261
D(U. malayanus (Klaus), U. maritimus (PB1), T. ornatus (Nobody))	0.0179	0.007362	2.426	14489	13981	6559995
D(U. arctos, U. malayanus (Anabell), T. ornatus (Nobody))	0.0159	0.006604	2.404	14306	13858	6630767
D(U. malayanus (Klaus), U. maritimus (PB1), T. ornatus (Chaparri))	0.017	0.007132	2.386	14515	14030	6561717
D(U. thibetanus, U. malayanus (Anabell), T. ornatus (Chaparri))	0.0198	0.008296	2.382	11879	11418	6623482
D(U. ursinus, U. malayanus (Anabell), Arctotherium sp.)	0.0172	0.007243	2.373	9061	8754	6162684
D(U. malayanus (Klaus), U. americanus, T. ornatus (Nobody))	0.0135	0.006132	2.197	14115	13740	6545186
D(U. americanus, U. malayanus (Anabell), Arctotherium sp.)	0.015	0.006894	2.17	12125	11766	6146174
D(U. thibetanus, U. malayanus (Klaus), T. ornatus (Chaparri))	0.0183	0.008645	2.119	11898	11469	6621804
D(U. americanus, U. malayanus (Klaus), Arctotherium sp.)	0.014	0.006638	2.109	12111	11776	6146598
D(U. ursinus, U. malayanus (Klaus), Arctotherium sp.)	0.0161	0.007726	2.084	9078	8790	6160076
D(U. arctos, U. malayanus (Anabell), T. ornatus (Chaparri))	0.0139	0.006701	2.075	14310	13917	6633179
D(U. arctos, U. malayanus (Klaus), T. ornatus (Chaparri))	0.0131	0.006487	2.017	14293	13923	6632784
D(U. arctos, U. malayanus (Klaus), T. ornatus (Nobody))	0.013	0.006487	1.999	14267	13901	6630244
D(U. thibetanus, U. malayanus (Klaus), T. ornatus (Nobody))	0.0182	0.009231	1.972	11827	11403	6619492
D(U. americanus, U. malayanus (Anabell), Arctodus simus)	0.0125	0.006756	1.854	12469	12159	6279339
D(U. malayanus (Anabell), U. maritimus (PB9), T. ornatus (Chaparri))	0.0129	0.006962	1.852	14438	14070	6595307
D(U. malayanus (Klaus), U. maritimus (PB9), T. ornatus (Nobody))	0.0131	0.007208	1.812	14448	14075	6593005
D(U. malayanus (Anabell), U. maritimus (PB9), T. ornatus (Nobody))	0.0123	0.006926	1.775	14403	14052	6593765
D(U. malayanus (Klaus), U. americanus, T. ornatus (Chaparri))	0.0107	0.00619	1.734	14152	13852	6546765
D(U. malayanus (Anabell), U. americanus, T. ornatus (Nobody))	0.0106	0.006177	1.712	14113	13817	6545768
D(U. americanus, U. malayanus (Klaus), Arctodus simus)	0.0115	0.006802	1.687	12471	12187	6280782
D(U. malayanus (Klaus), U. maritimus (PB9), T. ornatus (Chaparri))	0.0108	0.007032	1.538	14429	14120	6594752
D(U. thibetanus, U. maritimus (PB1), Arctotherium sp.)	0.0124	0.00808	1.536	10388	10133	6160785
D(U. ursinus, U. malayanus (Anabell), Arctodus simus)	0.012	0.008027	1.496	9221	9002	6293600
D(U. ursinus, U. malayanus (Klaus), Arctodus simus)	0.0119	0.008029	1.484	9238	9020	6291880
D(U. ursinus, U. malayanus (Klaus), T. ornatus (Chaparri))	0.0112	0.007567	1.481	10795	10556	6611944
D(U. ursinus, U. malayanus (Anabell), T. ornatus (Nobody))	0.0104	0.007157	1.45	10715	10495	6611714
D(U. malayanus (Anabell), U. americanus, T. ornatus (Chaparri))	0.0092	0.006374	1.447	14136	13877	6547286
D(U. maritimus (PB9), U. malayanus (Anabell), Arctodus simus)	0.0097	0.006692	1.442	12513	12274	6304388
D(U. arctos, U. malayanus (Klaus), Arctodus simus)	0.0084	0.005941	1.422	12439	12230	6306227

4.3 SUPPLEMENTARY INFORMATION

D-statistic	D	Stderr	Z-score	BABA	ABBA	nSNPs
D(U. maritimus (PB9), U. malayanus (Anabell), Arctotherium sp.)	0.0095	0.00683	1.396	12168	11938	6172713
D(U. americanus, U. maritimus (PB1), Arctotherium sp.)	0.0097	0.006981	1.383	8712	8545	6163675
D(U. maritimus (PB9), U. malayanus (Klaus), Arctodus simus)	0.0092	0.006852	1.348	12505	12275	6305556
D(U. arctos, U. malayanus (Anabell), Arctodus simus)	0.0081	0.006004	1.344	12435	12235	6306804
D(U. maritimus (PB9), U. malayanus (Klaus), Arctotherium sp.)	0.0088	0.006675	1.324	12157	11944	6172885
D(U. maritimus (PB1), U. maritimus (PB9), Arctotherium sp.)	0.0326	0.025583	1.276	816	764	6217830
D(U. ursinus, U. malayanus (Klaus), T. ornatus (Nobody))	0.0104	0.008174	1.272	10737	10515	6609836
D(U. arctos, U. malayanus (Anabell), Arctotherium sp.)	0.0093	0.007391	1.253	12077	11856	6174614
D(U. maritimus (PB1), U. maritimus (PB9), Arctodus simus)	0.0361	0.029276	1.234	850	790	6352025
D(U. arctos, U. malayanus (Klaus), Arctotherium sp.)	0.0089	0.007464	1.189	12073	11860	6173076
D(U. ursinus, U. malayanus (Anabell), T. ornatus (Chaparri))	0.009	0.007655	1.174	10700	10509	6613671
D(U. thibetanus, U. ursinus, T. ornatus (Chaparri))	0.0087	0.007445	1.169	12094	11885	6627699
D(U. thibetanus, U. maritimus (PB9), Arctotherium sp.)	0.0089	0.00805	1.108	10410	10225	6186620
D(U. thibetanus, U. arctos, Arctodus simus)	0.009	0.008333	1.075	10491	10303	6323067
D(U. thibetanus, U. arctos, Arctotherium sp.)	0.009	0.008403	1.075	10232	10048	6190143
D(U. thibetanus, U. maritimus (PB1), Arctodus simus)	0.0093	0.008807	1.051	10576	10381	6292413
D(U. thibetanus, U. ursinus, Arctodus simus)	0.0101	0.009698	1.044	10471	10260	6303292
D(U. thibetanus, U. ursinus, Arctotherium sp.)	0.0077	0.007388	1.043	10153	9997	6172199
D(U. thibetanus, U. ursinus, T. ornatus (Nobody))	0.0081	0.007806	1.039	12052	11858	6625682
D(U. thibetanus, U. maritimus (PB9), Arctodus simus)	0.0083	0.008649	0.956	10587	10412	6318797
D(U. maritimus (PB1), U. malayanus (Anabell), Arctodus simus)	0.0063	0.006685	0.946	12449	12292	6277891
D(U. ursinus, U. maritimus (PB1), Arctotherium sp.)	0.0061	0.006559	0.924	12233	12086	6149992
D(U. maritimus (PB1), U. malayanus (Anabell), Arctotherium sp.)	0.0059	0.006736	0.87	12080	11939	6147000
D(U. americanus, U. maritimus (PB1), Arctodus simus)	0.0065	0.007941	0.816	8965	8849	6298576
D(U. thibetanus, U. americanus, Arctotherium sp.)	0.0055	0.007927	0.689	10461	10347	6158742
D(U. americanus, U. maritimus (PB9), Arctotherium sp.)	0.005	0.007409	0.673	8722	8635	6189156
D(U. americanus, U. maritimus (PB1), T. ornatus (Chaparri))	0.0047	0.007502	0.626	10245	10149	6548802
D(U. ursinus, U. maritimus (PB9), Arctotherium sp.)	0.0041	0.006544	0.623	12225	12126	6175763
D(U. maritimus (PB1), U. malayanus (Klaus), Arctodus simus)	0.0044	0.007094	0.615	12432	12323	6279261
D(U. ursinus, U. arctos, Arctotherium sp.)	0.0044	0.007176	0.613	12135	12028	6178377
D(U. arctos, U. ursinus, T. ornatus (Nobody))	0.0045	0.007454	0.609	14264	14135	6635967
D(U. thibetanus, U. americanus, Arctodus simus)	0.005	0.008311	0.603	10769	10662	6292658
D(U. maritimus (PB1), U. malayanus (Klaus), Arctotherium sp.)	0.004	0.006962	0.576	12052	11954	6147130
D(U. americanus, U. arctos, Arctotherium sp.)	0.0041	0.007475	0.546	8699	8628	6176832
D(U. ursinus, U. maritimus (PB1), Arctodus simus)	0.0036	0.006714	0.542	12472	12382	6281231
D(U. arctos, U. ursinus, T. ornatus (Chaparri))	0.0037	0.00755	0.495	14265	14158	6638300
D(U. malayanus (Anabell), U. malayanus (Klaus), T. ornatus (Chaparri))	0.0072	0.015624	0.46	2495	2459	6638489
D(U. arctos, U. maritimus (PB9), Arctodus simus)	0.0049	0.011036	0.441	5348	5296	6347717
D(U. americanus, U. arctos, Arctodus simus)	0.0033	0.007697	0.431	8976	8917	6312319
D(U. arctos, U. maritimus (PB1), Arctodus simus)	0.0046	0.01109	0.412	5336	5287	6321140
D(U. americanus, U. maritimus (PB9), Arctodus simus)	0.003	0.008203	0.36	8960	8906	6324725
D(U. ursinus, U. arctos, Arctodus simus)	0.0023	0.006705	0.349	12408	12350	6310873
D(U. arctos, U. maritimus (PB1), Arctotherium sp.)	0.0037	0.01124	0.325	5117	5080	6187644
D(U. ursinus, U. maritimus (PB9), Arctodus simus)	0.002	0.006596	0.308	12441	12390	6307573
D(U. americanus, U. ursinus, Arctotherium sp.)	0.0016	0.00651	0.24	12034	11997	6148976
D(U. americanus, U. maritimus (PB1), T. ornatus (Nobody))	0.0017	0.007694	0.215	10165	10131	6547890
D(U. thibetanus, U. arctos, T. ornatus (Chaparri))	0.0021	0.010081	0.206	12079	12028	6654575
D(U. malayanus (Anabell), U. malayanus (Klaus), Arctodus simus)	0.0028	0.015051	0.189	1899	1888	6316094
D(U. maritimus (PB1), U. maritimus (PB9), T. ornatus (Nobody))	0.0044	0.023285	0.188	1242	1231	6631992
D(U. malayanus (Anabell), U. malayanus (Klaus), Arctotherium sp.)	0.0031	0.01673	0.187	1854	1842	6183689
D(U. arctos, U. maritimus (PB9), Arctotherium sp.)	0.0021	0.011285	0.187	5150	5128	6213415
D(U. americanus, U. ursinus, Arctodus simus)	0.0011	0.007109	0.159	12368	12339	6282149
D(U. arctos, U. thibetanus, T. ornatus (Nobody))	0.0016	0.010223	0.154	12068	12031	6651971
D(U. maritimus (PB9), U. americanus, T. ornatus (Nobody))	0.001	0.008065	0.13	10221	10201	6577928
D(U. maritimus (PB9), U. americanus, T. ornatus (Chaparri))	0.001	0.00799	0.126	10262	10242	6578875
D(U. maritimus (PB9), U. maritimus (PB1), T. ornatus (Chaparri))	0.0013	0.0221	0.058	1284	1281	6633124
D(U. malayanus (Klaus), U. malayanus (Anabell), T. ornatus (Nobody))	0.0001	0.014705	0.006	2451	2451	6636253

Supplementary References:

1. Kumar, V., Lammers, F., Bidon, T., Pfenninger, M., Kolter, L., Nilsson, M.A., and Janke, A. (2017). The evolutionary history of bears is characterized by gene flow across species. *Sci. Rep.* 7, 46487.
2. Miller, W., Schuster, S.C., Welch, A.J., Ratan, A., Bedoya-Reina, O.C., Zhao, F.Q., Kim, H.L., Burhans, R.C., Drautz, D.I., Wittekindt, N.E., et al. (2012). Polar and brown bear genomes reveal ancient admixture and demographic footprints of past climate change. *Proc. Natl. Acad. Sci. U. S. A.* 109, E2382-E2390.
3. Liu, S.P., Lorenzen, E.D., Fumagalli, M., Li, B., Harris, K., Xiong, Z.J., Zhou, L., Korneliussen, T.S., Somel, M., Babbitt, C., et al. (2014). Population genomics reveal recent speciation and rapid evolutionary adaptation in polar bears. *Cell* 157, 785-794.
4. Cahill, J.A., Green, R.E., Fulton, T.L., Stiller, M., Jay, F., Ovseyanikov, N., Salamzade, R., St. John, J., Stirling, I., Slatkin, M., et al. (2013). Genomic evidence for island population conversion resolves conflicting theories of polar bear evolution. *PLoS Genet.* 9, e1003345.
5. Zhao, S.C., Zheng, P.P., Dong, S.S., Zhan, X.J., Wu, Q., Guo, X.S., Hu, Y.B., He, W.M., Zhang, S.N., Fan, W., et al. (2013). Whole-genome sequencing of giant pandas provides insights into demographic history and local adaptation. *Nat. Genet.* 45, 67-71.

Chapter 5

From Iberia to Siberia: Phylogeography and evolutionary history of Eurasian brown bears

Manuscript written in the style of *Quaternary Science Reviews*

5.1 Authorship statement

Statement of Authorship

Title of Paper	From Iberia to Siberia: Phylogeography and evolutionary history of Eurasian brown bears
Publication Status	<input type="checkbox"/> Published <input type="checkbox"/> Accepted for Publication <input type="checkbox"/> Submitted for Publication <input checked="" type="checkbox"/> Unpublished and Unsubmitted work written in manuscript style
Publication Details	Unpublished and unsubmitted work written in manuscript style (Quaternary Science Reviews)

Principal Author

Name of Principal Author (Candidate)	Alexander T Salis			
Contribution to the Paper	Performed DNA extractions, DNA library construction and amplification, hybridisation enrichment, preparation for sequencing, and bioinformatic processing of sequencing data. Performed phylogenetic analyses, interpreted results, created figures, wrote manuscript and edited manuscript.			
Overall percentage (%)	85			
Certification:	This paper reports on original research I conducted during the period of my Higher Degree by Research candidature and is not subject to any obligations or contractual agreements with a third party that would constrain its inclusion in this thesis. I am the primary author of this paper.			
Signature	<table border="1" style="width: 100%;"> <tr> <td style="width: 60%;"></td> <td style="width: 20%;">Date</td> <td style="width: 20%;">03/09/2020</td> </tr> </table>		Date	03/09/2020
	Date	03/09/2020		

Co-Author Contributions

By signing the Statement of Authorship, each author certifies that:

- i. the candidate's stated contribution to the publication is accurate (as detailed above);
- ii. permission is granted for the candidate to include the publication in the thesis; and
- iii. the sum of all co-author contributions is equal to 100% less the candidate's stated contribution.

Name of Co-Author	Sarah C. E. Bray			
Contribution to the Paper	Performed DNA extractions, interpreted results, edited and critically evaluated the manuscript.			
Signature	<table border="1" style="width: 100%;"> <tr> <td style="width: 60%;"></td> <td style="width: 20%;">Date</td> <td style="width: 20%;">03-09-2020</td> </tr> </table>		Date	03-09-2020
	Date	03-09-2020		

Name of Co-Author	Jeremy J. Austin		
Contribution to the Paper	Conception of project, interpreted results, edited and critically evaluated the manuscript.		
Signature	(Date	07 Sep 2020

Name of Co-Author	Kieren J Mitchell		
Contribution to the Paper	Supervised work, conception of project, interpreted results, wrote and edited the manuscript.		
Signature		Date	3/9/20

5.2 Manuscript

From Iberia to Siberia: Phylogeography and evolutionary history of Eurasian brown bears

Alexander T Salis¹, Sarah C. E. Bray^{1,2}, Cristina E. Valdiosera^{3,4}, Jeremy J. Austin¹, Kieren J Mitchell¹

¹Australian Centre for Ancient DNA (ACAD), School of Biological Sciences, University of Adelaide, South Australia 5005, Australia

²Registry of Senior Australians (ROSA), South Australian Health and Medical Research Institute (SAHMRI), Adelaide, South Australia 5000, Australia

³Laboratorio de Evolución Humana, Departamento de Historia, Geografía y Comunicación, Universidad de Burgos, 09001. Burgos, Spain

⁴Department of Archaeology and History, La Trobe University, Melbourne, VIC 3086, Australia

Abstract:

Climatic changes during the Late Quaternary have had profound impacts on the biogeography and diversity of animal communities. Brown bears offer an excellent biogeographic model species during the Late Quaternary owing to their Holarctic distribution and abundant subfossil record. However, previous brown bear phylogeographic studies have either focused on short fragments of the mitochondrial genome or lacked large-scale sampling of ancient and historic specimens. To investigate the influence of the changing Quaternary environment on brown bears we sequenced mitogenomes from 114 ancient and historic brown bears from across Eurasia, ranging from Iberia in the West to western Beringia in the East. These were combined with published brown and polar bear mitogenomes (and unpublished data from Chapter 2) and analysed using Bayesian tip-dating analyses. Our results reiterate the profound impact the fluctuating climate of the Pleistocene had on animal species, with modern day European diversity dating back to the LGM. We further cast doubt on the existence of traditional southern Mediterranean refugia in brown bears. Furthermore, our results reveal a number of expansions and migrations across Eurasia apparently originating in northern Asia and coinciding with drastic changes in the paleoenvironment. We suggest the Altai-Sayan and Urals-Caucasus regions formed important refugia during the Pleistocene. These results

underpin Asia as the heartland for brown bear evolutionary history, being a source for the majority of brown bear mitochondrial diversity in North America, Japan and parts of Europe. Overall, brown bear biogeography and diversity has been strongly shaped by the changing environment of the Late Quaternary and the use of ancient DNA has proven fundamental in unravelling the evolutionary history of the species.

Introduction:

Fluctuations in the climate during the Late Quaternary (the past one million years) have greatly affected the diversity, phylogeographic structure, and distribution of modern-day species, and have been implicated in the extinction of a number of species (Barnosky et al., 2004; Campos et al., 2010; Cooper et al., 2015; Hofreiter and Stewart, 2009; Lorenzen et al., 2011; Mann et al., 2015; Metcalf et al., 2016; Mondanaro et al., 2019). The Late Quaternary is characterized by the cyclical growth and retraction of glaciers and polar ice caps driven by periods of cooler (glacial) and warmer global temperatures (interglacial) (Denton et al., 2010; Jansson and Dynesius, 2002), which impacted faunal population size and distribution, ultimately affecting species' evolutionary history. Models describing this mechanism have been proposed. For example, in Europe a model of expansion and contraction (E/C) has been proposed to explain the phylogeographic structure and modern distribution of several temperate species (Hewitt, 1999, 2000). Under this model, during glacial periods populations became isolated and genetically differentiated, while retraction of icesheets during interglacials facilitated the expansion and mixing of populations. Therefore, it has been proposed that the modern phylogeography of many European faunal populations date to the Last Glacial Maximum (LGM) and correspond to expansion out of several glacial refugia (Hewitt, 1999, 2000, 2001; Taberlet et al., 1998). Key to the development of this model has been the brown bear, *Ursus arctos*. However, outside of Europe and North America, the potential for brown bears as a model has not been fully realised.

Brown bears are one of the largest extant terrestrial carnivorans. With a Holarctic distribution, the brown bear is key to a number of Northern Hemisphere ecosystems. Brown bears have proven useful as an animal model for Quaternary biogeography (e.g. Davison et al., 2011), due to their wide distribution and relatively abundant subfossil remains from throughout the Holocene and Pleistocene (Sommer and Benecke, 2005).

5.2 MANUSCRIPT

Brown bears are believed to have evolved from the Etruscan bear (*Ursus etruscus*) in Asia (probably the Great Steppe region) (McLellan and Reiner, 1994), with the oldest brown bear fossils found in North China 0.5 million years ago (mya) (Kurtén, 1968; Pasitschniak-Arts, 1993). During historic times brown bears were common across Eurasia, but with habitat loss and human persecution populations have declined and their distribution has become increasingly fragmented (McLellan and Reiner, 1994; Servheen, 1999). Currently, brown bears in Eurasia are found across North Asia, while being restricted to forested areas of North and Eastern Europe, and extinct across most of their former Western European range, only surviving in small isolated populations (Servheen, 1999; Sørensen, 1990; Swenson et al., 1995; Zedrosser et al., 2001).

Understanding the mechanisms underlying the current distribution of brown bears, often with a focus on conservation, has been a driving force behind the myriad of phylogenetic studies on the species. Early phylogeographic studies based on DNA data from modern individuals found strong spatial structuring of mitochondrial diversity (Kohn et al., 1995; Korsten et al., 2009; Taberlet and Bouvet, 1994; Talbot and Shields, 1996; Waits et al., 2000; Waits et al., 1998), owing to the strong philopatry exhibited by female bears (Davison et al., 2011; Stoen et al., 2006; Zedrosser et al., 2007). These early studies identified two main lineages of brown bears, an eastern lineage (comprising clades 3, 4, and 5) and a western lineage (comprising clades 1 and 2). Studies of extinct and more enigmatic populations have revealed diversity outside of these two main lineages: an extinct North African clade, and clades 6 and 7, found in the Tibetan plateau and Middle East respectively. Ancient DNA studies have complicated the patterns observed, revealing turnovers and striking responses to climate and environmental change associated with the Quaternary Period (Barnes et al., 2002; Bray et al., 2013; Calvignac et al., 2009; Calvignac et al., 2008; Davison et al., 2011; Edwards et al., 2014; Edwards et al., 2011; Ersmark et al., 2019; Hofreiter et al., 2004; Leonard et al., 2000; Valdiosera et al., 2007; Valdiosera et al., 2008). This is best epitomized in North America, where four clades of bears are currently found (clades 2a, 3a, 3b, and 4) with strong phylogeographic structuring (Shields et al., 2000; Talbot and Shields, 1996; Waits et al., 1998), but ancient DNA has also revealed the past presence of extinct clades (clades 2c, and 3c), and temporal structuring, resulting from multiple waves of migration across the Bering Land Bridge at different times during the Late Pleistocene (Barnes et al., 2002; Leonard et al., 2000; Chapter 2).

In contrast to North America, modern European bears have been described as descending from two lineages: the eastern lineage (represented by clade 3a) and the western lineage (represented by clade 1) (Davison et al., 2011; Kohn et al., 1995; Taberlet and Bouvet, 1994). The western lineage has been further subdivided based on the proposed glacial refugia they are thought to have occupied under the E/C model of postglacial recolonization: clade 1a, representing the Iberian Peninsula; and clade 1b, representing the Italian and Balkan peninsulas. However, ancient DNA studies have identified extinct clades in Europe, clade 1e and 1c (Valdiosera et al., 2007; Valdiosera et al., 2008), and have purported the existence of clade 3c and 4 bears in northern Spain (Rey-Iglesia et al., 2019; Valdiosera et al., 2008). These ancient DNA studies have undermined the viability of the E/C model of postglacial recolonization, instead suggesting a lack of phylogeographic structure leading up to the LGM followed by a complex history of post-LGM turnovers and migration (Bray et al., 2013; Edwards et al., 2014; Ersmark et al., 2019; García-Vázquez et al., 2019; Hofreiter et al., 2004; Valdiosera et al., 2007; Valdiosera et al., 2008).

Modern brown bears across Eastern Europe and Siberia predominantly belong to clade 3a (Davison et al., 2011; Korsten et al., 2009; Murtskhvaladze et al., 2010; Saarma et al., 2007), but recent studies have uncovered increased clade 3 diversity, including clade 3b in eastern Russia (Gus'kov et al., 2013; Miller et al., 2006; Rey-Iglesia et al., 2019; Tumendemberel et al., 2019). However, the diversity observed in modern Siberian populations is less than would be expected considering the role the region likely played during the past in populating North America and Japan. Meanwhile, clades endemic to South, Central, and Western Asia have been described — clades 1d, 5, 6, and 7 (Calvignac et al., 2009; Calvignac et al., 2008; Çilingir et al., 2016; Lan et al., 2017; Tumendemberel et al., 2019) — while ancient DNA has revealed an extinct lineage of brown bears in North Africa that was subsequently replaced by clade 1a bears during historic times (Calvignac et al., 2008).

A major limitation of the majority of past phylogeographic studies is that they have focused only on small mitochondrial fragments (cytochrome *b* and control region), whereas studies using complete mitogenomes have tended to uncover finer scale patterns and better resolved phylogenies (Anijalg et al., 2018; Hirata et al., 2013; Keis et al., 2013; Rey-Iglesia et al., 2019). However, these mitogenomic studies have lacked extensive

5.2 MANUSCRIPT

sampling of ancient DNA, as well as modern representatives from clades 1c, 1d, 1e, 2c, 3c, 7, and the extinct North African clade. In this study we analyse 114 new mitogenomes from ancient and historic brown bears across Europe, Siberia, and North Africa, combined with an additional 103 mitogenomes from Chapter 2 and an additional 310 brown bear and polar bear mitogenomes downloaded from GenBank, in order to complete a comprehensive temporal and geographic mitogenomic phylogeny, and study past phylogeographic changes and the evolutionary history of brown bears in Eurasia and as a whole.

Methods:

We sampled 149 brown bear subfossil bone and tooth specimens from northern Asia, Europe, and North Africa (Table S1), which ranged in age from historic times to over 50 thousand years old, spanning the Holocene and Late Pleistocene. Thirteen brown bear specimens were radiocarbon dated at the Oxford Radiocarbon Accelerator Unit of the University of Oxford. All radiocarbon dates were calibrated with the IntCal13 curve (Reimer et al., 2013) using OxCal 4.4 (Ramsey, 2009).

All pre-PCR steps (extraction, library preparation) were conducted in purpose-built aDNA clean-room facilities at the University of Adelaide's Australian Centre for Ancient DNA (ACAD), spatially separated and physically isolated from any other molecular laboratories. Strict protocols were followed and a number of precautions taken to minimize contamination of samples with exogenous DNA (Cooper and Poinar, 2000). Protective clothing was worn, including: hooded coveralls over ancient-DNA lab-dedicated clothing (clothes never previously worn in any other molecular laboratory), hairnets, facemasks, face shields, designated footwear for both transitional areas and the physical laboratory, and three pairs of gloves worn at all times to prevent skin exposure between frequent changes of the outer layer of gloves. Furthermore, the lab was designed with positive air pressure, flowing from the cleanest workrooms to the outside of the lab. Stringent decontamination procedures were also adhered to, including cleaning equipment and surfaces with bleach or disinfectant detergent before and after use as well as regular UV irradiation of surfaces. These precautions also included the inclusion of negative controls for both DNA extraction and PCR setup. PCR amplification and all downstream

procedures (*e.g.* quantification, hybridization enrichment) were carried out in independent physically isolated DNA laboratories at the University of Adelaide.

DNA extraction, library preparation, and mitochondrial enrichment

DNA extraction and library preparation was performed as per brown bear samples in Chapter 2 using one of two extraction protocols: 1) Phenol-chloroform based extraction protocol from Bray et al. (2013); or 2) an in-house silica-based extraction protocol adapted from Dabney et al. (2013), followed by construction of double-stranded Illumina libraries following Meyer et al. (2012) from 25 μ L of DNA extract, with the addition of truncated Illumina adapters that had unique dual 7-mer internal barcodes added to allow identification and exclusion of any downstream contamination. A partial uracil-DNA glycosylase (UDG) treatment (Rohland et al., 2015) was performed to restrict cytosine deamination, characteristic of ancient DNA, to terminal nucleotides. Enrichment of mitochondrial sequences was performed as per Chapter 2, using the same brown bear specific baits constructed following Richards et al. (2019).

Sequencing

Full-length Illumina sequencing adapters were added to the enriched libraries via a final round of “off-bead” PCR split into 5 replicate reactions (25 μ L) containing 1 \times Gold PCR buffer, 2.5 mM MgCl₂, 1 mM dNTPs, 0.5 mM each primer, and 0.1 U AmpliTaq Gold. Cycling conditions were as follows: 94 °C for 6 min; 15 cycles of 94 °C for 30 s, 60 °C for 30 s, 72 °C for 45 s; and 72 °C for 10 min. Following PCR, replicates were pooled and purified using AxyPrep™ SPRI magnetic beads, eluted in 30 μ L H₂O quantified on TapeStation (Agilent Technologies). Libraries were pooled and sequenced on an Illumina NextSeq using 2 x 75 bp PE (150 cycle) High Output chemistry.

Data processing

Sequenced reads were demultiplexed using SABRE (<https://github.com/najoshi/sabre>) using the unique 5' and 3' barcodes allowing one mismatch in the barcode sequence (-m 1). Demultiplexed reads were then processed through Paleomix v1.2.12 (Schubert et al., 2014). Within Paleomix, adapter sequences were removed and paired end reads merged using ADAPTER REMOVAL v2.1.7 (Schubert et al., 2016), trimming low quality bases (<Phred20 --minquality 4) and discarding merged reads shorter than 25 bp (--minlength 25). Read quality was visualized before and after adapter trimming using fastQC v0.11.5

5.2 MANUSCRIPT

(<http://www.bioinformatics.babraham.ac.uk/projects/fastqc/>) to ensure efficient adapter removal. Merged reads were mapped against the mitochondrial genome of *Ursus arctos* (EU497665) using BWA v0.7.15 (Li and Durbin, 2009) (aln -l 1024 (seed inactivated), -n 0.01, -o 2). Reads with mapping Phred scores less than 25 were removed using SAMTOOLS 1.5 (Li et al., 2009) and PCR duplicates were removed using “paleomix rmdup_collapsed” and MARKDUPLICATES from the Picard package (<http://broadinstitute.github.io/picard/>).

Following mapping, reads for all samples were visualized in Geneious Prime v2019.0.4 (<https://www.geneious.com>) and a 75% majority consensus sequence created, calling N at sites with less than 3x coverage. We also downloaded reads from published ancient Irish brown bears (Cahill et al., 2018) and processed them through the pipeline described above to create full mitochondrial genomes (Table S2).

Phylogenetic analysis

Using MUSCLE v3.8.425 (Edgar, 2004) in Geneious Prime v2019.0.4, we aligned the 114 brown bear consensus sequences described above with the 103 mitogenomes produced in Chapter 2 and an additional 310 brown bear and polar bear mitogenomes downloaded from GenBank (Table S3).

We also created two additional datasets by aligning and trimming our full mitogenome sequences to match published control region (Table S4) and cytochrome *b* sequences (Table S5). A maximum of two ambiguous bases or cases of missing data in a sequence was allowed across the 177 bp control region fragment published by Valdiosera et al. (2008) and the 278 bp cytochrome *b* fragment published by Calvignac et al. (2008). Due to an excess of ambiguities or missingness across these fragments, 57 and 20 sequences were removed from the control region and cytochrome *b* alignments respectively. We aligned to control region sequences, which have been typically used in brown bear genetic studies, to compare how the two types of data compare in the accuracy of clade assignment and phylogenetic analysis. We aligned to cytochrome *b* to see whether our North African bears fall into the extinct North African clade identified in previous studies (Calvignac et al., 2009; Calvignac et al., 2008), as no North African clade bear mitogenomes have been sequenced and our North African samples had poor coverage across the control region.

We produced maximum-likelihood trees for each dataset (mitogenomes, control region, and cytochrome *b*) using RAxML v8.2.4 (Stamatakis, 2014) with 1000 bootstraps, and the GTRGAMMA model of substitution, using the American black bear as outgroup (MG772937). Two Median-joining networks for the control region and cytochrome *b* datasets were produced in PopART (Leigh and Bryant, 2015).

Due to poor resolution of the control region maximum-likelihood tree, a bayesian tip-dated tree was produced in BEAST v2.6.1 (Bouckaert et al., 2019), using only the finite-dated specimens. A strict clock with a uniform prior on rate ($0-10^{-3}$ mutations per site per year) was used with a Bayesian skyline coalescent tree prior. The substitution model was co-estimated and averaged throughout the analyses using bModelTest (Bouckaert and Drummond, 2017). Two independent chains were run for 20 million steps sampling every 2,000 steps. Convergence and sufficient sampling of parameters was checked in Tracer v1.7.1 (Rambaut et al., 2018) and individual runs combined in LogCombiner, after discarding the first 10% of steps as burn-in. MCC consensus trees were generated in TreeAnnotator using the median node age.

Bayesian tip-dating analyses were performed on mitogenomes with >85% coverage using BEAST v2.6.1 (Bouckaert et al., 2019) to co-estimate the tree topology and divergence dates of our sequences. We evaluated the temporal signal in our dataset using leave-one-out cross-validation (*e.g.* Stiller et al., 2014), using only the finite-dated specimens or samples with a specific age ($n=441$). In sequential analyses we left out and then attempted to estimate the age of each ancient specimen ($n=119$). Consequently, we performed sequential analyses where undated samples ($n=87$) were added to the dataset one at a time, in order to estimate their ages (Figure S3). Runs were performed with a strict clock with a uniform prior on rate ($0-10^{-5}$ mutations per site per year), constant population coalescent tree prior with a $1/x$ distribution on population size, a uniform prior ($0-500,000$) on the age of the sequence being estimated, and run for 30 million steps with sampling every 3000 steps. The substitution model was co-estimated and averaged throughout the analyses using bModelTest (Bouckaert and Drummond, 2017). Some chains were extended to ensure effective sampling sizes near or above 200 for all parameters. The first 10% of samples were discarded as burn-in and parameter values were monitored to check for convergence in Tracer v1.7.1 (Rambaut et al., 2018). Eight samples produced date estimates that were not unimodal or overlapped substantially with

5.2 MANUSCRIPT

zero and therefore were excluded from subsequent analyses. Once all samples were assigned an age (either based on radiocarbon dating or Bayesian date estimation), we conducted a date-randomization test (Ramsden et al., 2009; Stiller et al., 2014). Runs were conducted as for date estimation but excluding a prior on sequence age. For both datasets the rate estimate of the original data did not overlap the credibility intervals of the rate estimate from 20 randomized replicates (Supplementary Figure 3), suggesting that our dataset could be used to reliably estimate evolutionary rate and divergence times.

For the final BEAST analysis, a strict clock was used with a uniform prior on rate ($0-10^{-5}$ mutations per site per year), and a Bayesian skyline coalescent tree prior. The substitution model was co-estimated and averaged throughout the analyses using bModelTest (Bouckaert and Drummond, 2017). We ran three independent MCMC chains, each run for 100 million steps, sampling every 10,000 steps. We checked for convergence and sufficient sampling of parameters in Tracer v1.7.1 (Rambaut et al., 2018) and combined individual runs in LogCombiner, after discarding the first 10% of steps as burn-in. MCC consensus trees were generated in TreeAnnotator using the median node age.

Isotope analysis

Two brown specimens produced genetic results that cast doubt on their provenance and/or species identification (A308 and A1947). In order to contextualise isotopic data ($\delta^{13}\text{C}$ and $\delta^{15}\text{N}$) produced from these specimens, additional isotopic data was collected from published literature (Barnes et al., 2002; Bocherens et al., 2011; Fox-Dobbs et al., 2008; Horton et al., 2009; Kirillova et al., 2015; Leonard et al., 2007; Mann et al., 2013; Matheus, 1995; Rey-Iglesia et al., 2019; Richards et al., 2008; Terlato et al., 2019) representing brown bears, coastal brown bears (Alexander Archipelago), cave bears (*Ursus spelaeus*), polar bears (*Ursus maritimus*), short-faced bears (*Arctodus simus*), horses (*Equus* spp.), and cave lions (*Panthera spelaea*).

Results and Discussion:

Of the 149 samples we analysed, mitochondrial genomes with >60% coverage were obtained for 114, of which 110 had >85% coverage. Thirty-five samples either did not produce sufficient mitochondrial reads or were misidentified remains belonging to another species (*e.g.* cave bear, horse; Table S1). The 114 brown bear mitogenomes with >60% coverage were aligned with 103 mitogenomes produced in Chapter 2 and 310 published mitogenomes from brown and polar bears (total $n = 517$) (Table S2). However, only samples with >85% coverage were included in our Bayesian analysis (excluding nine undated samples that did not produce unimodal age estimate distributions; total $n = 509$). The age of samples included in our analyses ranged from modern day to beyond the limit of radiocarbon dating (including some with molecular age estimates >200 kya; Figure S2).

Brown bear phylogeny and distribution

Our Bayesian phylogenetic analyses revealed that all brown bear mitogenomic diversity coalesced 445.1 kya (95% HPD: 412–481.6 kya), representing the divergence of clade 6 from the remaining samples (Figure 1). Our estimate for this node falls within the wide credibility interval of 336 to 1258 kya obtained by a previous study (Lan et al., 2017), though our mean estimate is much younger: 445.1 versus 658 kya. Our more precise estimate for the divergence of clade 6 is coincident with MIS 12, the Anglian Glacial in Britain and the Elster glaciation in North America. MIS 12 is known as one of the strongest glacial periods of the Quaternary, occurring after a prolonged period without full glacial conditions (Lang and Wolff, 2011; McManus et al., 1999; Naafs et al., 2014; Oppo et al., 1998; Rodrigues et al., 2017; Stein et al., 2009). This divergence may therefore reflect the isolation of brown bears into separate glacial refugia during this severe glacial period (*i.e.* clade 6 may be representative of a Central Asian refugium, where the clade is currently found).

The divergence of clade 6 was followed by the eastern (clade 3, 4, and 5) and western (clade 1 and 2) lineages 376 kya (95% HPD: 344.4–409 kya) (Figure 1). Our estimate for the divergence of the eastern and western lineages is much younger than previously published mitogenomic estimates of 556 kya (Hirata et al., 2013), 505 kya (Lan et al., 2017), 514 kya (Anijalg et al., 2018), and ~420 kya (Rey-Iglesia et al., 2019). The discrepancies between these estimates are likely the result of the loci used (control region

5.2 MANUSCRIPT

versus mitogenome) and/or the type of calibration used (fossil calibration or tip-dating using a single ancient specimen versus tip-dating using multiple ancient specimens). In the present study, by relying on a large number of radiocarbon dated tips to calibrate our analysis we have minimised the impact of rate time-dependency (Subramanian and Lambert, 2011), therefore, allowing more accurate dating of population splits when compared to studies using only a few tip-dated specimens or fossil calibrations. In any case, within the western lineage, our results suggest that clade 2c subsequently diverged from the remaining lineages 361.6 kya (95% HPD: 328–391.7 kya), resulting in paraphyly of clade 2 with respect to clade 1, in conflict with control region studies that place 2c as sister to clade 2a (Davison et al., 2011). The divergence of the eastern and western lineages, and the subsequent divergence of clade 2c from the common ancestor of the remaining western lineages, occurred during late MIS 11 or early MIS 10. MIS 11 represents the longest and warmest of the interglacial periods (Lang and Wolff, 2011; McManus et al., 1999; Oppo et al., 1998; Rodrigues et al., 2017), with extreme reductions in sea ice and ice sheets resulting in areas such as Greenland being largely unglaciated (Raymo and Mitrovica, 2012; Robinson et al., 2017), as well as northerly expansion of forests (Kleinen et al., 2014). Therefore, the formation of the main lineages of brown bear and the establishment of their broad geographical distributions correlate with a period of warmer climate and forest expansion, when bears may have been able to expand out of glacial refugia following MIS 12 into a wide range of habitats across the Northern Hemisphere.

Our results suggest that clade 1 split from the common ancestor of the polar bear clades 2a and 2b 235.5 kya (95% HPD: 215.4–258.2 kya), more recently than suggested by other mitogenomic studies using fossil calibrations (Anijalg et al., 2018; Hirata et al., 2013), but comparable to previous estimates using tip-dating (Rey-Iglesia et al., 2019). This split has been purported to represent the initial introgression of a brown bear mitogenome into early polar bear populations (Hailer, 2015) and occurred during the transition from MIS 8 to MIS 7, a period of transition from cold to warm conditions. This transition likely caused the contraction of polar bear ranges and increasing terrestrial presence of polar bears as sea ice cover reduced in the arctic, likely resulting in interactions between polar and brown bears, as seen with current reductions in sea ice (Kelly et al., 2010; Post et al., 2013)

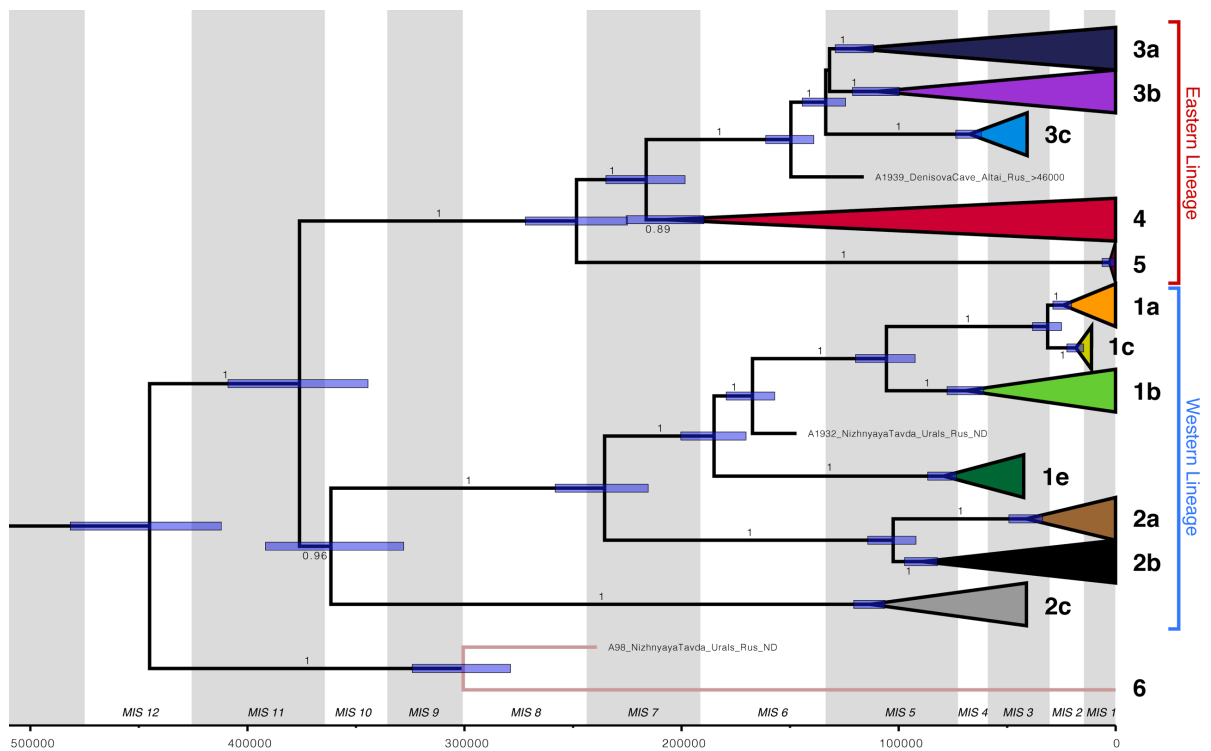


Figure 1: Bayesian phylogenetic tree inferred from full mitogenomes showing the divergence of the major brown bear mitochondrial. Bars on nodes represent 95% Highest Posterior Densities for node age estimates indicated for nodes with >0.7 posterior support. Previously published clades are collapsed and coloured corresponding to clade membership.

Comparison of short control region and cytochrome b sequences to full mitogenomes

To explore some of the differences observed between our results and those of previous studies, we created two additional datasets by trimming our new sequences to match published mitochondrial control region and cytochrome *b* alignments. Analysis of these additional datasets showed that full mitogenomes performed considerably better at resolving deeper branches compared to the control region and cytochrome *b* datasets, with many of the splits inferred using the control region dataset being especially problematic. Notably the relationship of clade 6 to the other lineages is uncertain and poorly supported by the results from both cytochrome *b* (Figure S6) and control region analyses (Figure S4), while analyses of full mitogenomes unequivocally place clade 6 as sister to all remaining brown bear diversity (with the exception of the North African clade). Furthermore, the results of control region analyses suggest that clade 2 is monophyletic (Figures S4), whereas analyses using full mitochondrial genomes strongly suggest that clade 2 is paraphyletic, with clade 2c the most basal in the western lineage, sister to the remainder of clade 2 and clade 1 (Figure 1).

5.2 MANUSCRIPT

When assigning clade membership to sequences, the use of the control region was again problematic. Rey-Iglesia et al. (2019) reported an ancient clade 3c bear in Yakutia, Russia, and while our control region analysis supports this grouping (Figure S4), our full mitogenome analysis unequivocally places this sample within clade 3b. Previous studies have also purported clade 4 haplotypes in Russian and Spanish bears based on control region sequences (Bray, 2010; García-Vázquez et al., 2019). The same Russian samples have been reanalysed in this study and instead possess haplotypes more closely related to clade 3a. When looking at the results of our control region analyses, these samples fall in a separate clade within clade 3 (Figure S4), or closely related to clades 3a, 4 and 5 (Figure S5). This highlights a consistent problem with using control region to assign mitochondrial clade membership: more divergent haplotypes within clades often appear to be more closely related to other clades or form unrelated clades.

The differences we observed between results obtained using full mitogenomes and the control region are likely in part the result of substitution saturation of the control region due to the depth of the brown bear mitochondrial tree (TMRCA: 445.1 kya) and the relatively high mutation rate and short length of the control region. Additionally, these control region based studies have generally used traditional PCR and Sanger sequencing methods, meaning that their results may be more susceptible to damage-induced nucleotide misincorporations (Brotherton et al., 2007). These findings call into question previous reports of clade 4 and 3c bears in Spain (García-Vázquez et al., 2019; Valdiosera et al., 2008), which is a somewhat surprising result given the distribution of these clades, and suggest they may instead represent clade 3a, which has been widely reported in Europe. Full mitogenome sequences will need to be generated from these samples to confirm their clade membership and phylogeographic implications.

Less common brown bear clades (North Africa and clade 6)

Unfortunately, no published full mitogenomes were available for the extinct North African brown bear clade, so to deduce the clade membership of our Moroccan samples we created a contracted cytochrome *b* dataset (as low coverage prevented us from using the control region). Analyses of this dataset unequivocally placed our Moroccan samples as close relatives of the previously published data from extinct North African bears (Figure S6 & S7), meaning that our new data represent the first full mitogenomes from members of this clade. These two samples unfortunately have no radiocarbon dates associated with them,

and due to their deep divergence and long branch lengths their age could not accurately be estimated using Bayesian analyses. However, as the North African clade forms the outgroup to all other brown bear lineages in the maximum-likelihood tree (Figure S8), we can assume that the origin of this clade predates 456 kya and possibly represents an early expansion of brown bears during the Middle Pleistocene following the origin of the species in Asia (McLellan and Reiner, 1994). This expansion into Africa from Eurasia could have occurred through Europe via the strait of Gibraltar during a glacial period when sea levels would have been lower, or alternatively through the Middle East. The latter route through the Middle East has been favoured on the basis of shared species assemblages (Dobson and Wright, 2000).

Of the other more obscure and less well-represented brown bear clades, we also identified a clade 6 bear from the Ural Mountains dating to 238.7 kya (95% HPD: 176.3–311.2 kya). Most previous evidence suggested that clade 6 was restricted to the Gobi Desert and Pakistan, meaning that this Urals specimen represents a substantial range expansion and suggests that this clade of brown bears was more widespread earlier during the Pleistocene. The observation that these more obscure, underrepresented, and often deeply-branching brown bear clades, such as clades 5, 6, and 7, are found nearly exclusively in Asia indicates that early migrations of brown bears occurred throughout Asia from their hypothesised source of speciation (McLellan and Reiner, 1994). Elsewhere, clades such as clade 6 in the Urals and the extinct North African clade were largely replaced by more common haplotypes seen in modern brown bears worldwide (Calvignac et al., 2008).

Another unexpected result is the recovery of a clade 2b haplotype from a specimen from the Altai Mountains (A1947), with an estimated age of 58.4 ky (95% HPD: 37.1–79.9 kya). Clade 2b is normally associated with polar bears (Cronin et al., 1991; Davison et al., 2011; Shields et al., 2000; Talbot and Shields, 1996), but has also been found in brown bears in Ireland as a result of hybridisation (Cahill et al., 2018; Edwards et al., 2011). To exclude the possibility that A1947 may have incorrect provenance data – as the Altai Mountains are far outside the range of polar bears (*e.g.* the Arctic Circle) – we compared the stable isotopic signature of the bone to those of other brown bears, polar bears, and a variety of other taxa (Figure 2). Similar approaches have identified an ancient North American *Ursus sp.* sample (A308) with incorrect provenance data (Barnes et al.,

5.2 MANUSCRIPT

2002), which has isotopic values closer to polar bears despite supposedly having been collected well inland. Conversely, the isotopic signature of A1947 was typical of terrestrial brown bear populations and distant from those of polar bears from the Arctic Circle. These results suggest that A1947 is indeed a brown bear with a clade 2b haplotype.

The clade 2b haplotype possessed by A1947 is only distantly related to those found in Irish brown bears, coalescing with the most closely related clade 2b haplotypes 75 kya (95% HPD: 64.3–85.1 kya), suggesting an independent and much more ancient hybridisation event between polar and brown bears than occurred in the Pacific Northwest and Ireland. This finding suggests the hybridisation of polar bears and brown bears was not isolated to the Pacific Northwest (Cahill et al., 2013; Cahill et al., 2015; Hailer, 2015; Hailer et al., 2012; Hassanin, 2015; Kutschera et al., 2014; Lindqvist et al., 2010; Liu et al., 2014; Miller et al., 2012) and Ireland (Cahill et al., 2018; Edwards et al., 2011), but was likely common across the northerly range of brown bears (where they overlapped with the range of polar bears). As A1947 was found thousands of kilometres inland, it likely represents a hybrid individual that either migrated from or descended from a migrant from the original hybridisation zone (likely the northern Siberian coast within the Arctic Circle). This would support the expectation proposed by Cahill et al. (2013) that brown bears carrying polar bear alleles would disperse polar bear ancestry widely across the brown bear range.

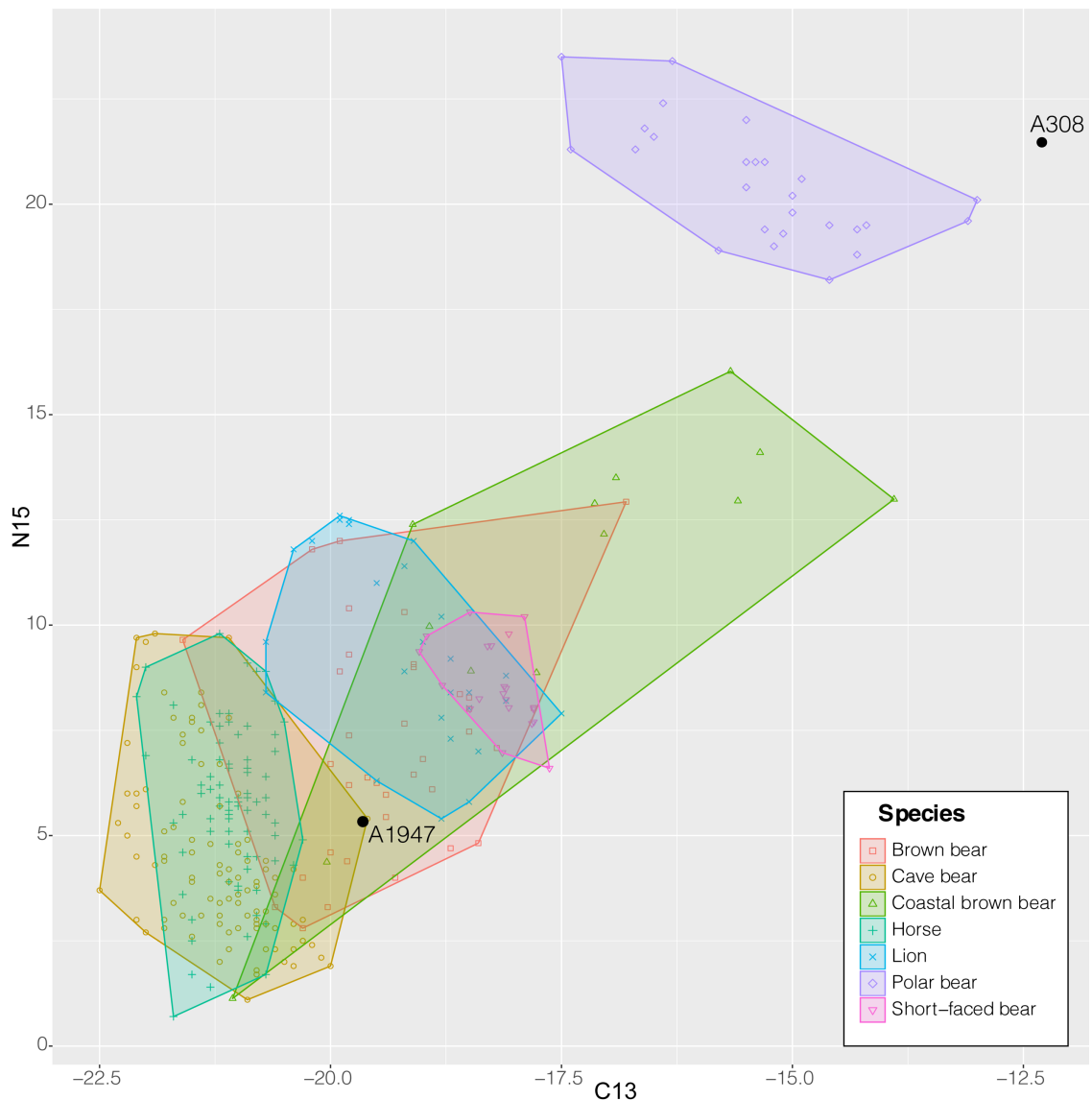


Figure 2: Bivariate plot of stable carbon and nitrogen isotope values for two bears with suspect species identity plotted against published values from brown bears (including coastal brown bears from the Alexander Archipelago), horses, cave lions, cave bears, polar bears, and short-faced bears (Table S6). Shaded areas represent convex hulls for each species, which are the minimum area required to encompass all points.

Asia as the heartland of brown bear matriline

Ancient brown bears in Asia (including the Ural and Caucasus mountains) fell into six clades: 2b, 3a, 3b, 4, 5, and 6, reflecting the diversity of brown bears that have been found in the region throughout prehistory. Previously, only clades 3a and 3b have been recovered from bears across North Asia, but results from Chapter 2 and the present study increase this to include clades 2b, 4, 6, and haplotypes basal to clade 1 and 3. In our dataset we found that clade 3 and clade 4 are closely associated with Siberia and the Russian Far East, while clade 5 and 6 have only been found in Asia. Clade 3 likely originated in Asia,

5.2 MANUSCRIPT

possibly in the Altai-Sayan region, before diversifying outwards to the Russian Far East and the Urals/Eastern Europe (Figure 6). The divergence of clade 5 and 6 at 248 and 445 kya respectively may represent early migrations of brown bears into central and southern Asia or possibly represent remnants of the original brown bear populations that first evolved in Asia.

Clade 3

The split of clade 3a, 3b, and 3c dates to 133.6 kya (95% HPD: 124.4–144.4 kya), just prior to or during the Eemian (MIS5e), a warm period that is often climatically likened to the Holocene (Lang and Wolff, 2011; Rodrigues et al., 2017). This is similar to the age of divergence of clade 3 estimated by Davison et al. (2011), but younger than that estimated by other full mitogenome analyses (Anijalg et al., 2018; Hirata et al., 2013), although these older estimates were associated with large credibility intervals. The discrepancies between these estimates are likely the result of the loci used (control region versus mitogenome) or the type of calibration used (fossil calibration or tip dating using a single ancient specimen versus tip dating using multiple ancient specimens). This divergence would have been associated with the rapid deglaciation of ice sheets and northerly expansion of forests (Kukla et al., 2002; Lozhkin and Anderson, 1995; Nikolova et al., 2013; Otto-Bliesner et al., 2006), potentially opening up available habitat for brown bears to expand into different areas resulting in the formation of the three subclades: 3a, 3b, and 3c. Each of these subclades appears to be primarily associated with different regions: the Urals-Caucasus, Altai-Sayan, and Russian Far East, respectively (Figure 6).

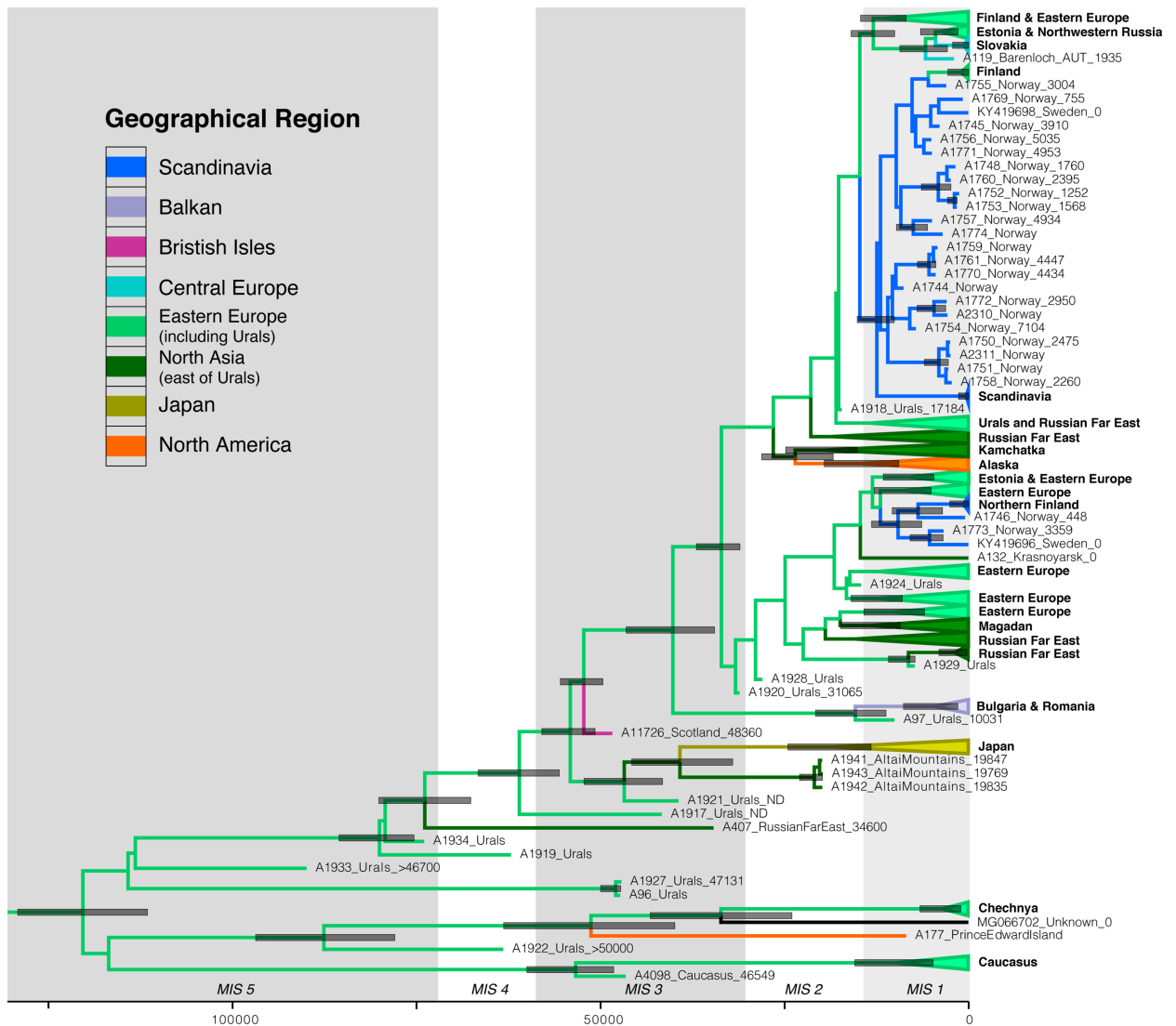


Figure 3: Bayesian phylogenetic tree of clade 3a lineages inferred from mitochondrial genomes. Bars on nodes represent 95% Highest Posterior Densities for node age estimates indicated for nodes with >0.7 posterior support. Branches are coloured by geographic region and clades consisting of largely modern samples from the same region have been collapsed. For the remainder of the eastern lineage see Figure S9.

Furthermore, we also present a specimen possessing a never before sampled haplotype sister to all clade 3 diversity, ACAD 1939, from Denisova Cave, in the Altai Mountains, dating to 116.1 kya (95% HPD: 89.6–141.1 kya). This specimen diverged from the rest of clade 3 149.6 kya (95% HPD: 139.1–161.2 kya). This could suggest that clade 3 as a whole originated in the Altai-Sayan region between MIS 7 and MIS 5, with an expansion during the Eemian during MIS 5 when climate conditions improved, with clade 3a representing the descendants of a westward migration into Eastern Europe and Caucasus, and clade 3c representing an eastward migration into Western Beringia. However, this hypothesis is highly speculative and is only based on one sample.

5.2 MANUSCRIPT

Clade 3a

Clade 3a is the most widespread and common clade among modern brown bears, being distributed from North America to Europe. Our results suggest clade 3a originated somewhere in the region comprising the Ural Mountains, the East European Plain, and the Caucasus. This contrasts with Anijalg et al. (2018), who presented the Altai-Sayan region as a refugium for clade 3a bears, with migrations westward to the Urals and Eastern Europe starting around 29 kya. We instead suggest that the Altai-Sayan region was a refugium for clade 3b bears, with clade 3b being present in a large proportion of our samples from the Altai Mountains (Figures 2 & 3), and with clade 3b remaining a prominent fixture in historic and modern populations of the region (Tumendemberel et al., 2019). In contrast, our ancient samples from the Ural Mountains largely possess basal clade 3a haplotypes, with some samples as old as ~90 kya, close to the divergence of clade 3a from the rest of clade 3, 130 kya. The Ural Mountains were hypothesised to provided glacial refuge for numerous animal and plant species (Bilton et al., 1998; Danukalova et al., 2009; Jaarola and Searle, 2002; Korsten et al., 2009; Ledevin et al., 2010; Markova et al., 2020; Schmitt and Varga, 2012; Skrede et al., 2006), while the Caucasus has been known as a biodiversity hotspot that likely hosted a number of refugia during the Pleistocene (Antonosyan et al., 2019; Belmaker et al., 2016; Drovetski et al., 2018; Myers et al., 2000; Neiber and Hausdorf, 2015; Orth et al., 2002; Parvizi et al., 2018). Previous studies have estimated the MRCA of clade 3a at around 50 kya (Anijalg et al., 2018; Davison et al., 2011; Hirata et al., 2013; Rey-Iglesia et al., 2019), the inclusion of ancient specimens from the Urals and Caucasus pushed this date back to 120.3 kya (95% HPD: 111.6–129.2 kya), over doubling the amount of time captured, bringing the MRCA very close to the divergence of clade 3a from the rest of clade 3.

Within clade 3a we observed what appears to be a large expansion of clade 3a bears at the end of MIS 3 and/or start of MIS2, around 33.3 kya (95% HPD: 31.1–37 kya) (Figures 3 & 6). This expansion is associated with previous reports of clade 3a1, which comprises the majority of extant clade 3a diversity (Anijalg et al., 2018; Hirata et al., 2013). However, we refrain from the subdivision of clade 3a due to the lack of truly monophyletic groups, especially more basally within the clade (Figure 3). Many of the more tipward branches of the clade 3a phylogenetic tree are poorly supported, suggesting a more star-like phylogeny, consistent with a rapid expansion. The timing of this expansion is associated with turnovers and extinctions of large mammals across Northern

Eurasia leading to the onset of the LGM: Neanderthal extinction, extinction of Eurasian spotted hyena (*Crocuta crocuta*), range reduction and extinction of cave bears (Bocherens et al., 2014; Mondanaro et al., 2019; Pacher and Stuart, 2009; Stiller et al., 2014), range reductions of woolly rhinoceros (*Coelodonta antiquitatis*) (Stuart and Lister, 2012), and turnovers of mammoth and bison (Cooper et al., 2015; Massilani et al., 2016; Palkopoulou et al., 2013; Soubrier et al., 2016). This period of faunal population change coincides with abrupt changes in the palaeoclimate. MIS 3 is associated with some of the most dramatic changes in climate, containing multiple Dansgaard-Oeschger (DO) events, which are abrupt changes from cold to mild-warm conditions, often with changes of up to 15°C within a few decades. Furthermore, there is evidence of a shift towards cold tundra-steppe across northern Eurasia and the breakup of grass and herb-dominated vegetation communities (Hubberten et al., 2004) and a loss of boreal forests in Eastern Europe during late MIS 3 (Obrecht et al., 2017).

Notably MIS 3 is associated with drastic declines in cave bears between 35 and 40 kya, before their extinction during the LGM (Gretzinger et al., 2019; Mondanaro et al., 2019; Stiller et al., 2010). The extinction of cave bears has been associated with the migration and expansion of anatomically modern humans in Europe and worsening climate during MIS 3/MIS 2 leading to vegetation changes, directly impacting the largely herbivorous cave bear (Mondanaro et al., 2019). Notably the extinction appears to have occurred in an east to west direction, with cave bears largely restricted to Western Europe after 30 kya (Bon et al., 2011; Mondanaro et al., 2019; Stiller et al., 2014). The last cave bears from the Urals date to between 30 and 37 kya (Pacher and Stuart, 2009), while the youngest sample from the Caucasus dates to 34 kya (Stiller et al., 2014). It appears that during MIS 3, cave bears were likely largely extirpated from the Urals, Caucasus, and Eastern European plain. Owing to a more herbivorous diet, the survival of cave bears would have been closely associated with vegetation changes, while the more omnivorous diet of brown bears possibly allowed them to survive drastic changes in palaeovegetation. The extinction of cave bears would have opened up territories and cave sites, allowing brown bear populations, which were likely clade 3a bears, to expand across Eurasia.

The expansion of clade 3a after 33kya is associated with migrations eastward toward North America, Kamchatka, and the Russian Far East. Notably this expansion leads to the majority of Kamchatka clade 3a diversity, and ultimately North American clade 3a bears,

which form a clade with Kamchatka that coalesces around 23.5 kya (95% HPD: 18.8–29.3 kya), suggesting a wave of migration into North America following the LGM (Figure 3). The MCRA of Eastern Beringian clade 3a brown bears dates to 14.4 kya (95% HPD: 9.5–19.6 kya), supporting the hypothesis that clade 3a bears crossed the Bering Land Bridge around the same time as humans and wapiti (Anijalg et al., 2018; Meiri et al., 2014).

Anijalg et al. (2018) found that clade 3a bears found elsewhere in the modern Russian Far East were not from the same migration into Kamchatka and Eastern Beringia. However, with our more comprehensive sampling of clade 3a bears, we could not confidently recover the split observed by Anijalg et al. (2018) between Kamchatka-Eastern Beringian bears and other clade 3a bears associated with clade 3a1, possibly due to the inclusion of ancient basal clade 3a bears with very short branch lengths (Figure 3). Therefore, we cannot exclude the possibility that bears from Eastern Beringia, Kamchatka and modern Russian Far East were from the same migration. However, it is noteworthy that Anijalg et al. (2018) hypothesised that a 30 ky-old clade 3a bear described from the Indigirka area of Western Beringia by Bray (2010) was possibly ancestral to the bears of Kamchatka and Eastern Beringia.

We produced a mitogenome from this clade 3a sample (A407) and found it was not directly related to modern bears from Kamchatka or Alaska, or any other Russian Far East bears, instead this specimen diverged more deeply within clade 3a, 73.8 kya (95% HPD: 67.6–80.1 kya), possibly indicating an earlier migration of clade 3a bears eastward. Furthermore, there also appears to have been an additional migration out of the Urals into the Russian Far East and eventually Japan (Figure 3). Japanese clade 3a bears diverged from clade 3a bears in the Altai-Sayan region 39.2 kya (95% HPD: 32.1–45.8 kya), while the TMRCA of all Japanese clade 3a bears dates to 18.5 kya (95% HPD: 13.3–24.5 kya). These Japanese and Altai bears further split from clade 3a bears from the Urals 46.8 kya (95% HPD: 41.6–52.2 kya), suggesting an eastward migration from the Urals, through Siberia and the Russia Far East during MIS 3 and ultimately into Japan, likely during the LGM before the land bridge connecting Sakhalin and Hokkaido was submerged 11 kya (Hirata et al., 2013; Ohshima, 1990). This scenario is similar to that proposed by Hirata et al. (2013) who also suggested that clade 3a bears from Japan and North America were the result of separate migrations, although we were able to refine the timing with the inclusion of closely related Altai brown bears.

Notably there are several cases of clade continuity in the Urals and Caucasus region, with highly similar haplotypes found in the same area thousands of years apart, such as a 46.5 cal kyBP basal clade 3a bear from the Caucasus (A4098) forming a monophyletic group with historic Caucasus bears, with a TMRCA of 53.4 kya (95% HPD: 48.2–60 kya), indicating this lineage has likely been in the region for at least 46.5 ky (Figure 3). Furthermore, ancient Urals specimens consistently fall in deeply diverging positions within subclades that encompass modern bears found in the Urals, the Caucasus, or Eastern European plain, further suggesting this region as a refuge for clade 3a.

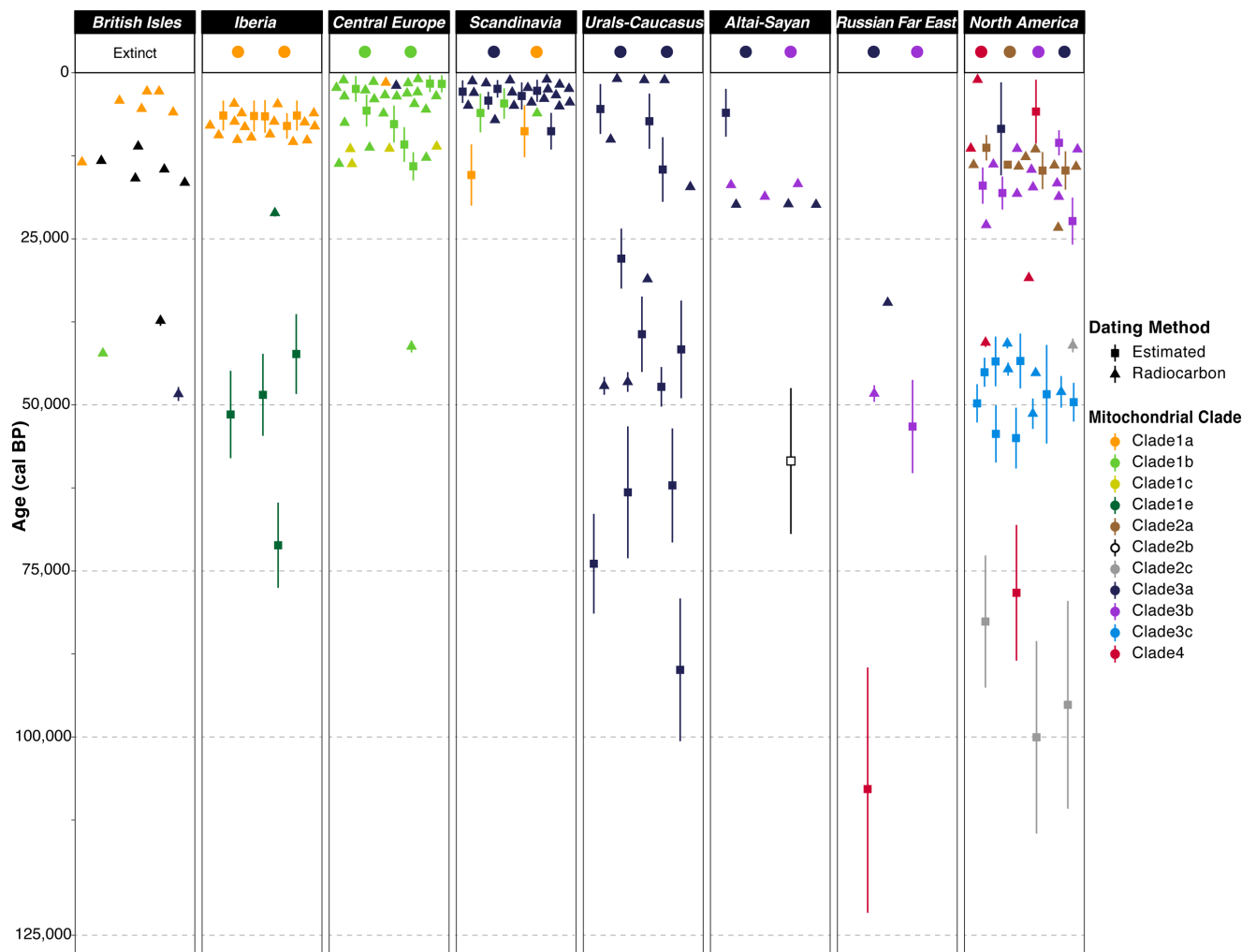


Figure 4: Timeline of radiocarbon and molecular dates for brown bears (*Ursus arctos*) from across their Holarctic range. Dates are shown with one standard error and are coloured by genetic clade.

5.2 MANUSCRIPT

Clade 3b

Clade 3b is primarily found in North America and Japan today; however, a few studies have found representatives in the Russian Far East and in the Altai-Sayan region (Tumendemberel et al., 2019). Our Bayesian analysis revealed that clade 3b is well represented in ancient and historic Siberian and Russian Far East samples, also including an ancient Chinese sample from the Manchurian Plain (Figures 3, 4, & 6), as well as being well represented in modern bears found in the Altai-Sayan region (Tumendemberel et al., 2019). Furthermore, it appears clade 3b likely arose in this broad area, more specifically the Altai-Sayan region, which has previously been hypothesised as a Pleistocene refugium for bears and other megafauna (Anijalg et al., 2018; Pavelkova Ricankova et al., 2014; Ricankova et al., 2015). From this population there appear to have been subsequent migrations into North America during the LGM (Chapter 2), as well as an earlier, separate migration to Japan and the Kuril Islands likely via Sakhalin (Hirata et al., 2013). Hirata et al. (2013) could not refine the timing of arrival of clade 3b into Japan beyond the divergence time from clade 3a due to a lack of published clade 3b mitogenomes from North America or Eurasia. We included 13 mitogenomes from North America and 8 mitogenomes from eastern Eurasia, which show that Japanese clade 3b bears split from Eurasian and North American bears 58 kya (95% HPD: 49–68.6 kya) while Japanese clade 3b bears coalesce 16 kya (95% HPD: 11.5–21.2 kya), suggesting that clade 3b bears migrated into Japan during MIS 3 or MIS 2.

Clade 3c

Clade 3c has currently only been found in ancient North American samples (Chapter 2, Barnes et al., 2002; Leonard et al., 2000); however, it is likely that this clade first arose in Asia, possibly western Beringia, and only entered North America after ~70 kya during the MIS 4 glacial, when the Bering Land Bridge would have been subaerial following a submerged state during MIS 5 (see Chapter 2). Despite likely arising in Asia, we found no evidence of clade 3c in Eurasia; however, this is likely to be an artefact of biased sampling. As clade 3c is the first of the clade 3 bears to enter North America, it is likely this clade's distribution was centred in western Beringia and/or the Russian Far East. Beringia and/or north-eastern Asia has been postulated as a refugium for grey wolves during the Pleistocene, with all extant diversity stemming from this region (Loog et al., 2020), as well as a refugium for collared lemmings (Fedorov et al., 2020). To date, only two brown bear specimens predating the LGM from western Beringia have been

genetically analysed (both from Yakutia, the western border of Western Beringia), representing clade 3b and clade 3a (Figures 3 & 4). Further sampling of ancient bears from more eastern Russian regions that make up Western Beringia (such as Magadan, Chukotka, and Kamchatka) may reveal the presence of clade 3c in the region.

Clade 4

Modern clade 4 bears are restricted to the contiguous USA, Southern Canada, and Hokkaido; however, ancient DNA has revealed clade 4 specimens in Eastern Beringia and mainland Eurasia (namely the Manchurian Plain of China) (Chapter 2, Barnes et al., 2002; Leonard et al., 2000). Clade 4 splits from clade 3 around 216.3 kya (95% HPD:198.4–234.8 kya), and the presence of a basal representative of clade 4 on the Manchurian Plain from north-eastern Russia indicates clade 4 may reflect an early movement of bears to the Russian Far East and/or Western Beringia during MIS 7, when the climate was warmer and wetter, eventually leading to migrations into Japan and North America (Chapter 2). Although clade 4 likely arose in mainland Asia during MIS 7, only one sample associated with clade 4 has been found outside of Japan or North America. As discussed in Chapter 2, this specimen is basal to the diversity of clade 4 bears from both North America and Japan, splitting 207.3 kya (95% HPD: 189.7–225.5 kya), with North American and Japanese bears diverging later during MIS 6 170.1 kya (95% HPD: 151.6–188.9 kya). Thus, it appears that Japanese and North American clade 4 bears may originate from the same population of mainland Eurasian bears and that clade 4 bears were the first to arrive in Hokkaido (Hirata et al., 2013). The original clade 4 Eurasian populations may have ultimately been replaced during the expansion of clade 3 across Eurasia ~130 kya. However, more extensive sampling of clade 4 bears from mainland Eurasia, especially during MIS 6 and 5 from the Russian Far East, would be required to fully investigate these hypotheses. As discussed for clade 3c, we lack sufficient sampling of ancient Russian Far East bears. Further sampling in this region may reveal greater diversity of clade 4 haplotypes in Eurasia. Further, sampling in this region may also reveal clade 2c haplotypes in Eurasia, which, along with clade 4, comprised the first wave of dispersal into North America, predating the waves of clade 3 dispersal (Chapter 2).

Colonisation of Europe and LGM range dynamics

Ancient and modern brown bears from Europe fell into six clades with differing patterns spatially and temporally, as reported by previous studies (Benazzo et al., 2017; Bray et

5.2 MANUSCRIPT

al., 2013; Davison et al., 2011; Edwards et al., 2014; Edwards et al., 2011; Ersmark et al., 2019; Fortes et al., 2016; García-Vázquez et al., 2019; Taberlet and Bouvet, 1994; Taberlet et al., 1997; Valdiosera et al., 2007; Valdiosera et al., 2008; Waits et al., 2000). Clade 3a was predominately found in eastern and central Europe, as well as Scandinavia, while clade 1a was detected in post-LGM specimens from the Iberian Peninsula, southern Scandinavia, and the British Isles. Clade 1b was found in modern bears from the Alps, Italy, and the Balkan Peninsula, and also ancient Scandinavian bears, while clade 1c was found exclusively in extinct bears from the Alps and clade 1e exclusively in pre-LGM bears from the Iberian Peninsula.

Clade 3

Clade 3 within Europe is largely restricted to Central and Eastern Europe and Scandinavia. However, we recovered one sample from pre-LGM Scotland bearing a clade 3a haplotype (Figure 3 & 4). This specimen shared a common ancestor with Russian brown bears around 52.3 kya (95% HPD: 49.7–55.5 kya) and appears to be unrelated to Holocene European clade 3a bears reported from Central Europe and Scandinavia. Therefore, it appears this specimen represents a pre-LGM migration of clade 3 into Europe, possibly associated with other reports of pre-LGM clade 3 bears in Western Europe (García-Vázquez et al., 2019; Valdiosera et al., 2008). Our results suggest that the current diversity of clade 3 in Europe arises from westward migration following the LGM, as has previously been hypothesised (Anijalg et al., 2018; Korsten et al., 2009).

Clade 3a bears appear to have entered the Scandinavian Peninsula from Eastern Europe during the Pleistocene/Holocene transition. There appear to be two groups of Scandinavian clade 3a bears: the more common group has a TMRCA of 12.3 kya (95% HPD: 10.1–15.1 kya), while the less common group coalesces 9.6 kya (95% HPD: 6.4–13.2 kya). These dates coincide with the receding of the Fennoscandian ice sheet. The Fennoscandian icesheet starting to recede by 17 kya, with much of Sweden, Finland, and the Baltic states ice-free by the Younger Dryas (12.8–11.5 kya), and the ice sheet isolated to northerly mountains on the Scandinavian Peninsula by 9.7 kya (Stroeven et al., 2016), allowing the migration of fauna into the region. Interestingly, within the more common clade 3a Scandinavia group there appears to have been a back migration into Southern and Central Finland. This group of Finnish bears coalesces 1,030 years ago (95% HPD: 30–2182 years ago) indicating a very recent arrival, possibly associated with human activity.

Keis et al. (2013) noted that modern Finnish brown bears showed greater heterogeneity than other Baltic states and western Russian oblasts, where this was attributed to migrations from Russian Karelia. Instead, we propose that the back migration from Scandinavia is likely the source of this increased heterogeneity, supplementing a population closely associated with Eastern European populations (Keis et al., 2013). This migration was likely facilitated by strong population declines leading to extirpation during the 19th Century predator extermination programs in southern and western regions of Finland (Saarma and Kojola, 2007).

Modern clade 3a bears from Slovakia and ancient clade 3a bears from Austria appear to descend from bears that migrated from Eastern Europe during the Holocene, around 5.8 kya (95% HPD: 2.9–9.4 kya). There also appears to be second group of clade 3a bears associated with the Balkan region. While, Anijalg et al. (2018) suggested that Bulgarian and Romanian brown bears may descend from bears in the Carpathian Mountains — which has been proposed as a refugium for the species — we find that these bears are most closely related to a bear from the Ural mountains dating to 10 kya. These clade 3a bears share a TMRCA 15.3 kya (95% HPD: 11.2–20.8 kya), indicating a post-LGM migration from the Urals region. However, we note that this could equally represent a migration eastward from the Carpathian Mountains into the Urals.

The complicated history of clade 3a bears in Eastern, Central, and Northern Europe suggest that these populations have been shaped by numerous migrations following the LGM from more westerly regions (for example the Urals, and Western Russia) (Anijalg et al., 2018; Korsten et al., 2009). It also appears that predator extermination programs in historic times have resulted in changes to the phylogeography of the clade (Keis et al., 2013; Xenikoudakis et al., 2015). An interesting observation is that the Caucasus did not appear to contribute to European clade 3a populations. Historic samples from the Caucasus were not associated with European clade 3a bears, falling in more deeply divergent positions within clade 3a more closely associated with ancient Urals and Caucasus brown bears. Basal clade 3a haplotypes have previously been reported in modern brown bears from the Caucasus (Murtskhvaladze et al., 2010). These findings may indicate that Caucasus is a remnant of the Pleistocene clade 3a populations.

5.2 MANUSCRIPT

Clade 1

Clade 1 is the most common clade found among ancient samples in Europe falling into four subclades: clades 1a, 1b, 1c, and 1e (Figure 5). The MRCA of clade 1, representing the split of Clade 1e from the rest of clade 1, dates to around 185 kya (95% HPD: 170.3–200.4 kya). Potentially, clade 1e may represent the original migration of brown bears into Europe. This migration may have originated from the Caucasus and/or Middle East, owing to the relatively greater diversity of haplotypes in that region (*i.e.* clades 7, 3a, 1b, and 1d) (Ashrafzadeh et al., 2016; Calvignac et al., 2009; Çilingir et al., 2016). Sequencing of full mitogenomes of bears from the Middle East, and from clades 7 and 1d in particular, would allow this hypothesis to be tested.

We identified a previously unsampled clade 1 haplotype from the Ural Mountains (ACAD 1932) (Figure 1 & 5), which our molecular age estimation suggested is approximately 147 thousand years old (95% HPD: 118.1–178.7 kya). This sample appears to be sister to clades 1a and 1b, splitting around 168.1 kya (95% HPD: 157.1–179.4 kya). Control region analyses show that this sample is not closely related to clade 1d and instead forms its own lineage (Figure S4 & S5). This result could indicate that ancestor of clades 1a and 1b originated in the Urals region, or bears from the original distribution of clade 1 migrated to the Urals during MIS 6. Further sampling of pre-LGM Urals brown bears would help deduce whether this clade was more common in the region, or an exception. This finding combined with the presence of a clade 6 specimen dated to 238.7 kya indicates that the past mitogenomic structure of Urals populations was vastly different prior to the proliferation of clade 3 bears. Clade 1a and 1b coalesce, during MIS5, this MRCA may represent the original wave of bears migrating into Europe that eventually gave rise to clades 1a, 1b, and 1c, separating into unglaciated refuges as glacial conditions increased towards the end of MIS5 (Kukla et al., 2002; Lang and Wolff, 2011; Rodrigues et al., 2017). However, the regions where these refugia were located remain unknown, as does the source of these clade 1 bears.

Clade 1a

Clade 1a in our mitogenomic dataset is largely represented by post-LGM specimens from Spain and Northern Europe (Figure 5). However, there appear to be two main lineages within clade 1a, one represented by Iberia, and the other northern Europe (Scandinavia and the British Isles), which share a common ancestor during MIS 3, around 24.2 kya

(95% HPD: 20.3–28.9 kya). The northern European lineage coalesces 21.7 kya (95% HPD: 18.2–25.7 kya), but has relatively low posterior support, possibly indicating a more star-like rapid expansion of clade 1a during the LGM. We recovered two ancient clade 1a haplotypes from bears from Denmark in the northern lineage with a TMRCA of 18.3 kya (95% HPD: 15.9–21.3 kya). A modern clade 1a specimen from Sweden fell more closely related to Irish brown bears, but could not be excluded as being more closely related to these Danish specimens due to low posterior support. This may indicate the expansion of clade 1a in northern Europe was rapid, expanding into Scandinavia and the British Isles as the ice sheets in Northern Europe began to recede after 22 kya (Stroeven et al., 2016).

Within the Iberian lineage, there appears to be a further split 19 kya (95% HPD: 15.6–22.7 kya) between the Cantabrian Mountains and Pyrenees through to the French Alps (Figure 5). Notably there appears to be over 10,000 years of continuity of this lineage in the Cantabrian Mountains. Therefore, it appears that clade 1a structuring and expansion coincides with the LGM, which could be argued to be consistent with the E/C model of postglacial recolonization. The clade is relatively young, with all diversity coalescing 24.2 kya. However, it remains difficult to estimate where clade 1a originated. Our data indicate it may have originated in Iberia, with a migration into northern Europe during the LGM. Alternatively, early arrival of clade 1a post-LGM in the British-Isles, as well as the presence of clade 1a in France and Belgium during the LGM, suggest a more northerly refugium (Edwards et al., 2014; Ersmark et al., 2019). Yet others have suggested that a cryptic Atlantic refugium may be the origin of clade 1a, as Iberia lacks brown bear fossils dating to the LGM (García-Vázquez et al., 2019). However, our estimates for the TMRCA of Iberian clade 1a bears indicate clade 1a brown bears were present on the peninsula during the LGM. Thus, it is likely that clade 1a originated somewhere in Western Europe and, leading up to the LGM, dispersed into Iberia and Northern Europe (in areas that remained ice-free during the LGM). To fully untangle the origin of clade 1a, mitogenomes from clade 1a bears from LGM France and Belgium, as well as the British Isles will be key.

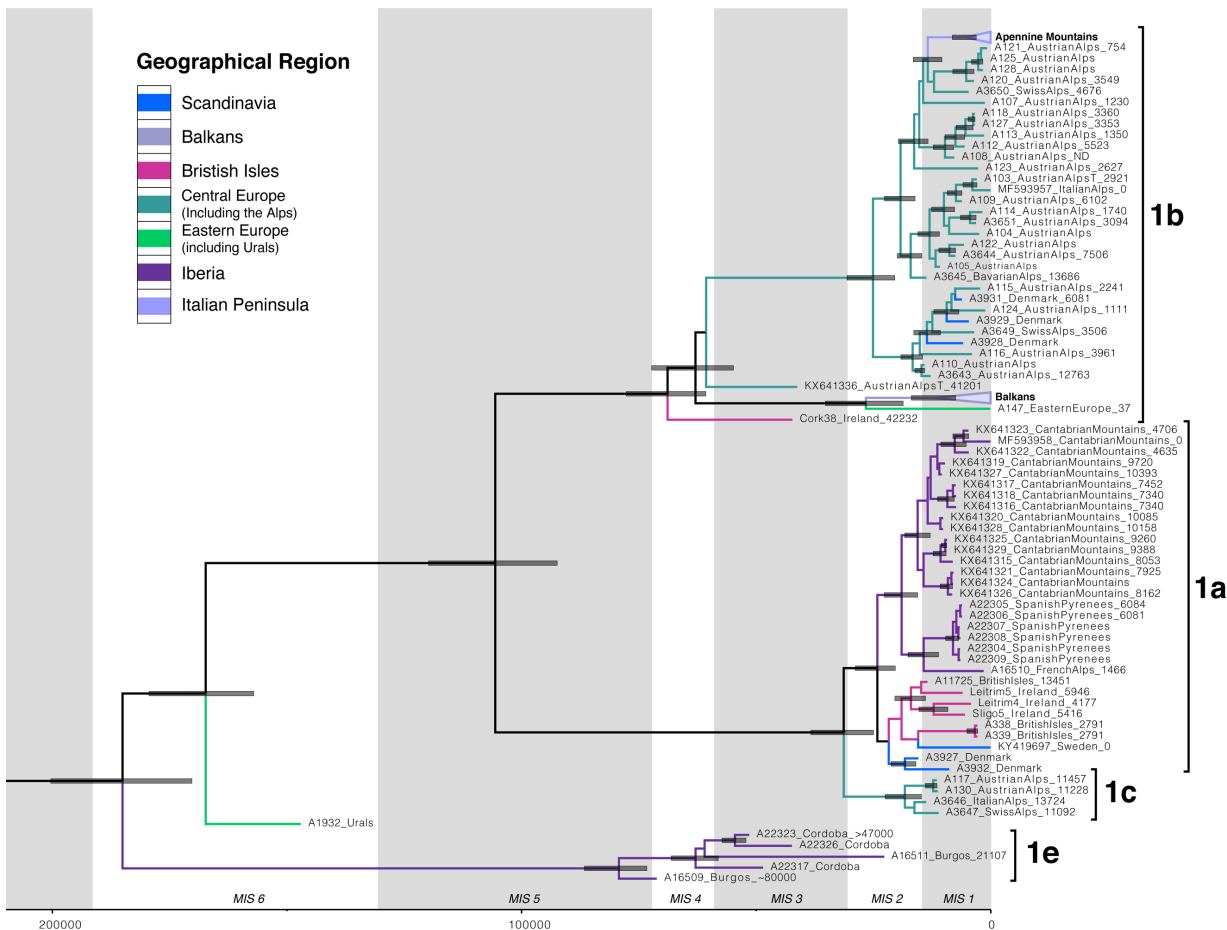


Figure 5: Bayesian phylogenetic tree of clade 1 brown bears inferred from mitochondrial genomes. Bars on nodes represent 95% Highest Posterior Densities for node age estimates indicated for nodes with >0.7 posterior support. Branches are coloured by geographic region.

Clade 1b

In our dataset clade 1b is predominately represented by samples from the Alps, Italy, and the Balkans (Figure 5). Clade 1b coalesces around 68.9 kya (95% HPD: 60.7–77.7 kya) during MIS4, representing the divergence of the lineage leading to the haplotype possessed by a 42.2 thousand-year-old Irish bear. Clade 1b subsequently split into two lineages around 62.9 kya (95% HPD: 54.8–72.3 kya), seemingly corresponding to the Italian peninsula and the Balkan Peninsula as previously described. One pre-LGM Alps sample (KX641336) fell within the Italian lineage; however, posterior support for this branch is low, perhaps indicating a trichotomy between this sample, the Balkan lineage, and the Italian lineage. The TMRCA of both the Italian and Balkan lineages date to the LGM — 25.1 kya (95% HPD: 20.5–30.6 kya) and 26.6 kya (95% HPD: 18.7–35.3 kya), respectively — indicating both these lineages expanded following the LGM, consistent with E/C model of postglacial recolonization (Hewitt, 1999, 2000, 2001; Taberlet et al., 1998).

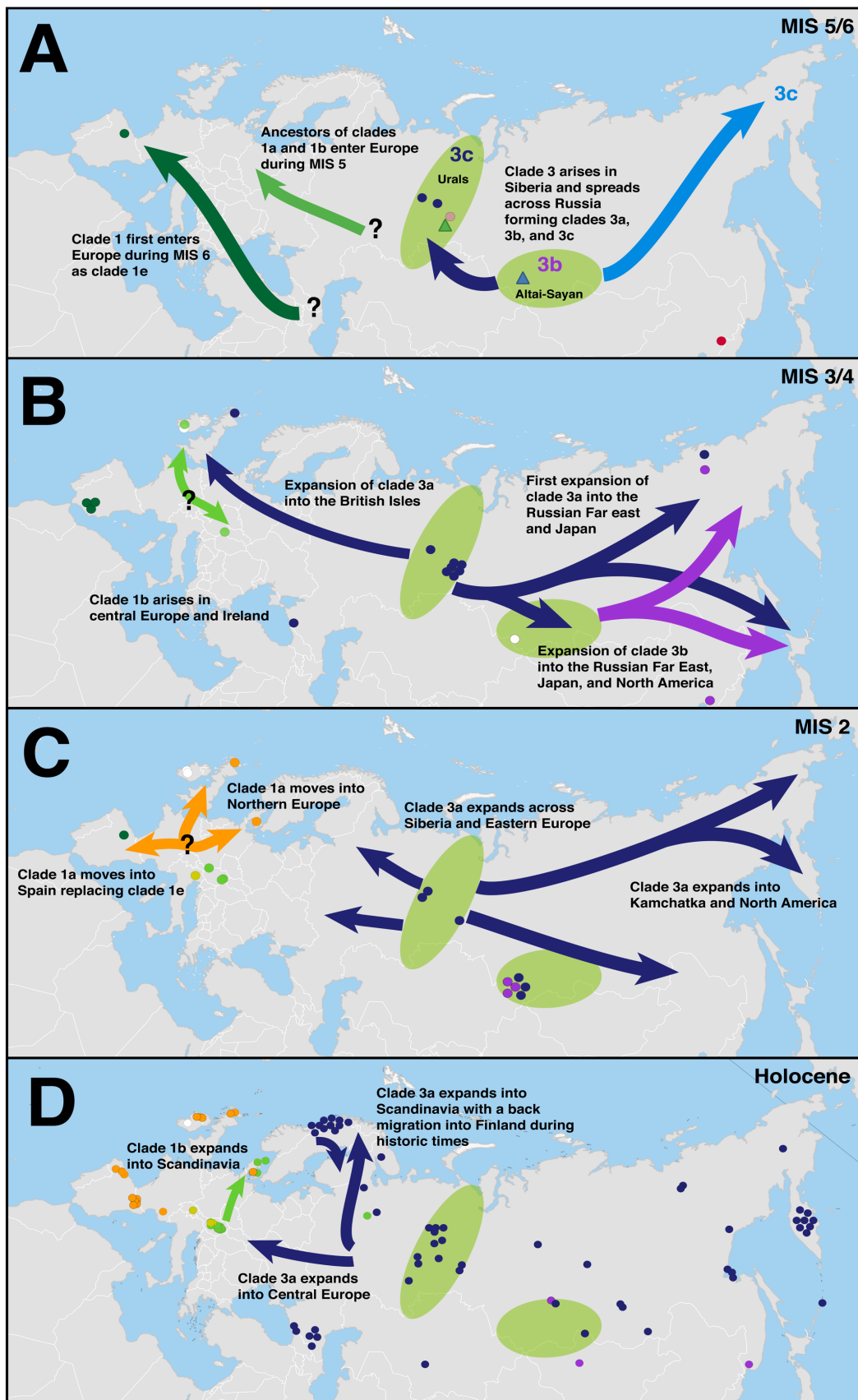


Figure 6: Map of Late Quaternary phylogeography of Eurasian brown bears during four time periods: **A**) MIS 5 and MIS 6 (191–71 kya); **B**) MIS 3 and MIS 4 (71–29 kya); **C**) MIS 2 (29–11.7 kya); and **D**) the Holocene (11.7 kya to historic times). Different coloured circles represent ancient and historic subfossil brown bears of different mtDNA clades, corresponding to clade colouring in Figures 1 and 4.

5.2 MANUSCRIPT

Of our newly sequenced mitogenomes, only one clade 1b specimen from the Balkan lineage was identified, ACAD 147, a historic sample from Vologoda Oblast of Russia, extending the range of this clade further east (Figure 5). The rest of our newly sequenced mitogenomes grouped with published data from Italian Apennine and Alpine bears. These new sequences included 27 Holocene Alpine bears and three Holocene Danish bears (Figure 5). The published modern Alpine bear (MF593957) was nested within the ancient Holocene diversity of Alpine bears, suggesting the extant small alpine bear populations are a descendent of the larger Holocene populations. Bray et al. (2013) identified clade 1b of the Italian lineage in mid-Holocene southern Scandinavia (this sample is represented by A3931), which is supported by our results, including the detection of two additional specimens from Denmark possessing clade 1b. Notably, clade 1b Scandinavian bears are not monophyletic and are associated with those from the Alps. All clade 1b Scandinavian bears coalesce around 13.6 kya (95% HPD: 10.8–16.4 kya), consistent with the hypothesis that these bears represent an early Holocene migration from the Italian peninsula and/or Alps (Bray et al., 2013). Clade 1b bears have not been found in modern Scandinavian populations. These findings are in contrast to clade 1a bears in Scandinavia, which appear to have arrived earlier and have had a more permanent presence in the region (Ersmark et al., 2019).

Clade 1c

We further discovered a clade of bears from the Alps closely related to clade 1a, splitting from clade 1a 31.3 kya (95% HPD: 25–38.4 kya) during MIS 3 (Figure 5). Analysis with published control region sequences revealed this clade to be clade 1c, first described from ancient specimens from France (Valdiosera et al., 2007). Our tip-dating analysis reveals that this clade/subclade likely formed as a separation of clade 1a bears into a separate refugium prior to the LGM (possibly in the Alps or elsewhere in mid-latitude Europe). The TMRCA of the clade 1c bears in this study of 18.3 kya (95% HPD: 14.8–22.5 kya) coincides with a range expansion of the Alpine bear population following the LGM. After ~11 kya clade 1c does not appear to be present in Alpine bears (Figure 4), indicating this clade may have gone extinct in the region following the end of the Pleistocene, while clade 1b appears to expand across in the region. However, clade 1c has been reported to survive in France until historic times (Ersmark et al., 2019; Valdiosera et al., 2007)

Clade 1e

As has previously been reported, pre-LGM Iberian brown bear samples fell into the extinct clade 1e (Figure 4 & 5). Previously published examples were exclusively from the northern regions of Spain (Fortes et al., 2016; Valdiosera et al., 2007; Valdiosera et al., 2008); however, in the present study we include ancient mitogenomes from Cordoba, in the south of Spain, which also belong to clade 1e. This finding suggests that clade 1e was found throughout Spain during the Pleistocene and went extinct leading up to and/or during the LGM. Clade 1e from pre-LGM Iberia perhaps represent remnants of one of the original migrations of brown bears into Europe, while after the LGM clade 1a is found in Spain (Figure 4). Conceivably, the extinction of clade 1e may have allowed the subsequent expansion of clade 1a into Iberia, refuting the idea that clade 1a was repeatedly restricted to Iberia during glacial periods (Davison et al., 2011; Hewitt, 1999, 2000; Taberlet and Bouvet, 1994).

Postglacial recolonisation

Although it appears the traditional E/C model of postglacial recolonisation is far too simple to explain brown bear phylogeography and evolutionary history in Europe, our results suggest that it cannot be completely rejected. Indeed, expansions of clade 1a and 1b, as well as migrations of clade 3a bears into Europe, date to during or just after the LGM. Indeed, clade 3a was present in Western Europe prior to the LGM, but these bears do not appear to contribute to post-LGM bears in Northern and Eastern Europe, while the LGM appears to have caused the extinction of clades 1c and 1e, with the latter being replaced by clade 1a on the Iberian Peninsula. Despite the population processes leading to current phylogeographic patterns in European brown bears being more complex than those of Hewitt's E/C model of postglacial recolonization, it is evident the LGM, and presumably previous glacial periods, had a profound impact on the phylogeography and evolutionary history of brown bears in Europe.

Conclusion:

This study underscores the importance of ancient DNA for understanding phylogeography and the evolutionary history of species. The diversity and phylogeography of Eurasian bears east of the Urals was especially poorly understood and lacked extensive ancient sampling. We extensively sampled subfossil material across Eurasia, increasing the mitogenomic representation of bears from across this area. Our results highlight Asia as the heartland for Late Pleistocene brown bear evolution. Further we find that extant brown bear diversity in Europe stems from the LGM, emphasising the prominent role that past glacial fluctuations had on European fauna. The evolutionary history of brown bears across the Eurasian continent is characterised by migrations, expansions, and turnovers, strongly associated with climatic and environmental changes during the Late Pleistocene.

Acknowledgements:

We would like to thank the following institutions for allowing access to specimens in their collections: St. Petersburg Institute of Zoology, Krakow Institute of Zoology, the Russian Academy of Sciences, Palaeontological Institute Moscow, Zoological Museum of Moscow University, The Institute of Plant and Animal Ecology of the Ural Branch of the Russian Academy of Sciences, Natural History Museum Stuttgart, University of Vienna, Museum of Natural History Vienna, the Canadian Museum of Nature, Institute of Zoology Almaty, Smithsonian, National Museum of Scotland, University of Oslo, Australian National University, Zoological Museum Copenhagen, and the Geological Survey Sweden. In addition, we are grateful to the following individuals who helped to collect and identify specimens and/or provided laboratory support during the early stages of the project: L. Orlando, I. Barnes, A. Derevianko, E. Pankeyeva, I. Chernikov, M. Shunkov, A. Sher, N. Ovodov, A. Vorobiev, V. Doronichev, L. Golovanova, P. Kosintsev, S. Vasiliev, J. Weinstock, N. Yamaguchi, R. Grun, C. Beard, D. Miao, D. Burnham, L. Vietti, M. Clementz, P. Wrinn, D. Döppes, M. Pacher, D. Nagel, A. Kitchener, K. Østbye, E. Østbye, S. Lauritzen, and K. Aaris-Sørensen This research was funded by an Australian Research Council Laureate Fellowship awarded to A. Cooper (FL140100260).

References:

- Anijalg, P., Ho, S.Y.W., Davison, J., Keis, M., Tammeleht, E., Bobowik, K., Tumanov, I.L., Saveljev, A.P., Lyapunova, E.A., Vorobiev, A.A., Markov, N.I., Kryukov, A.P., Kojola, I., Swenson, J.E., Hagen, S.B., Eiken, H.G., Paule, L., Saarma, U., 2018. Large-scale migrations of brown bears in Eurasia and to North America during the Late Pleistocene. *J. Biogeogr.* 45, 394-405.
- Antonosyan, M., Seersholm, F.V., Grealy, A.C., Barham, M., Werndly, D., Margaryan, A., Cieslik, A., Stafford, T.W., Allentoft, M.E., Bunce, M., Yepiskoposyan, L., 2019. Ancient DNA shows high faunal diversity in the Lesser Caucasus during the Late Pleistocene. *Quat. Sci. Rev.* 219, 102-111.
- Ashrafzadeh, M.R., Kaboli, M., Naghavi, M.R., 2016. Mitochondrial DNA analysis of Iranian brown bears (*Ursus arctos*) reveals new phylogeographic lineage. *Mamm. Biol.* 81, 1-9.
- Barnes, I., Matheus, P., Shapiro, B., Jensen, D., Cooper, A., 2002. Dynamics of Pleistocene population extinctions in Beringian brown bears. *Science* 295, 2267-2270.
- Barnosky, A.D., Koch, P.L., Feranec, R.S., Wing, S.L., Shabel, A.B., 2004. Assessing the causes of late Pleistocene extinctions on the continents. *Science* 306, 70-75.
- Belmaker, M., Bar-Yosef, O., Belfer-Cohen, A., Meshveliani, T., Jakeli, N., 2016. The environment in the Caucasus in the Upper Paleolithic (Late Pleistocene): Evidence from the small mammals from Dzudzuana cave, Georgia. *Quat. Int.* 425, 4-15.
- Benazzo, A., Trucchi, E., Cahill, J.A., Delser, P.M., Mona, S., Fumagalli, M., Bunnefeld, L., Cornetti, L., Ghirotto, S., Girardi, M., Ometto, L., Panziera, A., Rota-Stabelli, O., Zanetti, E., Karamanlidis, A., Groff, C., Paule, L., Gentile, L., Vila, C., Vicario, S., Boitani, L., Orlando, L., Fuselli, S., Vernesi, C., Shapiro, B., Ciucci, P., Bertorelle, G., 2017. Survival and divergence in a small group: The extraordinary genomic history of the endangered Apennine brown bear stragglers. *Proc. Natl. Acad. Sci. U. S. A.* 114, E9589-E9597.
- Bilton, D.T., Mirol, P.M., Mascheretti, S., Fredga, K., Zima, J., Searle, J.B., 1998. Mediterranean Europe as an area of endemism for small mammals rather than a source for northwards postglacial colonization. *Proc. R. Soc. B.* 265, 1219-1226.
- Bocherens, H., Bridault, A., Drucker, D.G., Hofreiter, M., Munzel, S.C., Stiller, M., van der Plicht, J., 2014. The last of its kind? Radiocarbon, ancient DNA and stable isotope evidence from a late cave bear (*Ursus spelaeus* ROSENMÜLLER, 1794) from Rochedane (France). *Quat. Int.* 339, 179-188.
- Bocherens, H., Drucker, D.G., Bonjean, D., Bridault, A., Conard, N.J., Cupillard, C., Germonpre, M., Honeisen, M., Munzel, S.C., Napierala, H., Patou-Mathis, M., Stephan, E., Uerpmann, H.P., Ziegler, R., 2011. Isotopic evidence for dietary ecology of cave lion (*Panthera spelaea*) in North-Western Europe: Prey choice, competition and implications for extinction. *Quat. Int.* 245, 249-261.

- Bon, C., Berthonaud, V., Fosse, P., Gely, B., Maksud, F., Vitalis, R., Philippe, M., van der Plicht, J., Elalouf, J.M., 2011. Low regional diversity of late cave bears mitochondrial DNA at the time of Chauvet Aurignacian paintings. *J. Archaeol. Sci.* 38, 1886-1895.
- Bouckaert, R., Vaughan, T.G., Barido-Sottani, J., Duchene, S., Fourment, M., Gavryushkina, A., Heled, J., Jones, G., Kuhnert, D., De Maio, N., Matschiner, M., Mendes, F.K., Muller, N.F., Ogilvie, H.A., du Plessis, L., Poppinga, A., Rambaut, A., Rasmussen, D., Siveroni, I., Suchard, M.A., Wu, C.H., Xie, D., Zhang, C., Stadler, T., Drummond, A.J., 2019. BEAST 2.5: An advanced software platform for Bayesian evolutionary analysis. *PLoS Comp. Biol.* 15, e1006650.
- Bouckaert, R.R., Drummond, A.J., 2017. bModelTest: Bayesian phylogenetic site model averaging and model comparison. *BMC Evol. Biol.* 17, 42.
- Bray, S.C., 2010. Mitochondrial DNA analysis of the evolution and genetic diversity of ancient and extinct bears, School of Earth and Environmental Sciences. University of Adelaide.
- Bray, S.C.E., Austin, J.J., Metcalf, J.L., Østbye, K., Østbye, E., Lauritzen, S.-E., Aaris-Sørensen, K., Valdiosera, C., Adler, C.J., Cooper, A., 2013. Ancient DNA identifies post-glacial recolonisation, not recent bottlenecks, as the primary driver of contemporary mtDNA phylogeography and diversity in Scandinavian brown bears. *Divers. Distrib.* 19, 245-256.
- Brotherton, P., Endicott, P., Sanchez, J.J., Beaumont, M., Barnett, R., Austin, J., Cooper, A., 2007. Novel high-resolution characterization of ancient DNA reveals C > U-type base modification events as the sole cause of post mortem miscoding lesions. *Nucleic Acids Res.* 35, 5717-5728.
- Cahill, J.A., Green, R.E., Fulton, T.L., Stiller, M., Jay, F., Ovseyanikov, N., Salamzade, R., St. John, J., Stirling, I., Slatkin, M., Shapiro, B., 2013. Genomic Evidence for Island Population Conversion Resolves Conflicting Theories of Polar Bear Evolution. *PLoS Genet* 9, e1003345.
- Cahill, J.A., Heintzman, P.D., Harris, K., Teasdale, M.D., Kapp, J., Soares, A.E.R., Stirling, I., Bradley, D., Edwards, C.J., Graim, K., Kisleika, A.A., Malev, A.V., Monaghan, N., Green, R.E., Shapiro, B., 2018. Genomic evidence of widespread admixture from polar bears into brown bears during the last ice age. *Mol. Biol. Evol.* 35, 1120-1129.
- Cahill, J.A., Stirling, I., Kistler, L., Salamzade, R., Ersmark, E., Fulton, T.L., Stiller, M., Green, R.E., Shapiro, B., 2015. Genomic evidence of geographically widespread effect of gene flow from polar bears into brown bears. *Mol. Ecol.* 24, 1205-1217.
- Calvignac, S., Hughes, S., Hanni, C., 2009. Genetic diversity of endangered brown bear (*Ursus arctos*) populations at the crossroads of Europe, Asia and Africa. *Divers. Distrib.* 15, 742-750.
- Calvignac, S., Hughes, S., Tougaard, C., Michaux, J., Thevenot, M., Philippe, M., Hamdine, W., Hanni, C., 2008. Ancient DNA evidence for the loss of a highly divergent brown bear clade during historical times. *Mol. Ecol.* 17, 1962-1970.

- Campos, P.F., Willerslev, E., Sher, A., Orlando, L., Axelsson, E., Tikhonov, A., Aaris-Sorensen, K., Greenwood, A.D., Kahlke, R.D., Kosintsev, P., Krakhmalnaya, T., Kuznetsova, T., Lemey, P., MacPhee, R., Norris, C.A., Shepherd, K., Suchard, M.A., Zazula, G.D., Shapiro, B., Gilbert, M.T.P., 2010. Ancient DNA analyses exclude humans as the driving force behind late Pleistocene musk ox (*Ovibos moschatus*) population dynamics. *Proc. Natl. Acad. Sci. U. S. A.* 107, 5675-5680.
- Çilingir, F.G., Akin Pekşen, Ç., Ambarlı, H., Beerli, P., Bilgin, C.C., 2016. Exceptional maternal lineage diversity in brown bears (*Ursus arctos*) from Turkey. *Zool. J. Linn. Soc.* 176, 463-477.
- Cooper, A., Poinar, H.N., 2000. Ancient DNA: Do it right or not at all. *Science* 289, 1139.
- Cooper, A., Turney, C., Hughen, K.A., Brook, B.W., McDonald, H.G., Bradshaw, C.J.A., 2015. Abrupt warming events drove Late Pleistocene Holarctic megafaunal turnover. *Science* 349, 602-606.
- Cronin, M.A., Amstrup, S.C., Garner, G.W., Vyse, E.R., 1991. Interspecific and intraspecific Mitochondrial DNA variation in North American bears (*Ursus*). *Can. J. Zool.* 69, 2985-2992.
- Dabney, J., Knapp, M., Glocke, I., Gansauge, M.-T., Weihmann, A., Nickel, B., Valdiosera, C., García, N., Pääbo, S., Arsuaga, J.-L., Meyer, M., 2013. Complete mitochondrial genome sequence of a Middle Pleistocene cave bear reconstructed from ultrashort DNA fragments. *Proc. Natl. Acad. Sci. U. S. A.* 110, 15758-15763.
- Danukalova, G., Yakovlev, A., Kosintsev, P., Agadjanian, A., Alimbekova, L., Eremeev, A., Morozova, E., 2009. Quaternary fauna and flora of the Southern Urals region (Bashkortostan Republic). *Quat. Int.* 201, 13-24.
- Davison, J., Ho, S.Y.W., Bray, S.C., Korsten, M., Tammelleht, E., Hindrikson, M., Ostbye, K., Ostbye, E., Lauritzen, S.E., Austin, J., Cooper, A., Saarma, U., 2011. Late-Quaternary biogeographic scenarios for the brown bear (*Ursus arctos*), a wild mammal model species. *Quat. Sci. Rev.* 30, 418-430.
- Denton, G.H., Anderson, R.F., Toggweiler, J.R., Edwards, R.L., Schaefer, J.M., Putnam, A.E., 2010. The last glacial termination. *Science* 328, 1652-1656.
- Drovetski, S.V., Fadeev, I.V., Prime, M.R., Lopes, R.J., Boano, G., Pavia, M., Koblik, E.A., Lohman, Y.V., Red'kin, Y.A., Aghayan, S.A., Reis, S., Drovetskaya, S.S., Voelker, G., 2018. A test of the European Pleistocene refugial paradigm, using a Western Palaearctic endemic bird species. *Proc. R. Soc. B.* 285.
- Edgar, R.C., 2004. MUSCLE: a multiple sequence alignment method with reduced time and space complexity. *BMC Bioinform.* 5, 113.
- Edwards, C.J., Ho, S.Y.W., Barnett, R., Coxon, P., Bradley, D.G., Lord, T.C., O'Connor, T., 2014. Continuity of brown bear maternal lineages in northern England through the Last-glacial period. *Quat. Sci. Rev.* 96, 131-139.
- Edwards, C.J., Suchard, M.A., Lemey, P., Welch, J.J., Barnes, I., Fulton, T.L., Barnett, R., O'Connell, T.C., Coxon, P., Monaghan, N., Valdiosera, C.E., Lorenzen, E.D.,

- Willerslev, E., Baryshnikov, G.F., Rambaut, A., Thomas, M.G., Bradley, D.G., Shapiro, B., 2011. Ancient hybridization and an Irish origin for the modern polar bear matriline. *Curr. Biol.* 21, 1251-1258.
- Ersmark, E., Baryshnikov, G., Higham, T., Argant, A., Castanos, P., Doppes, D., Gasparik, M., Germonpre, M., Liden, K., Lipecki, G., Marciszak, A., Miller, R., Moreno-Garcia, M., Pacher, M., Robu, M., Rodriguez-Varela, R., Rojo Guerra, M., Sabol, M., Spassov, N., Stora, J., Valdiosera, C., Villaluenga, A., Stewart, J.R., Dalen, L., 2019. Genetic turnovers and northern survival during the last glacial maximum in European brown bears. *Ecol. Evol.* 9, 5891-5905.
- Fedorov, V.B., Trucchi, E., Goropashnaya, A.V., Waltari, E., Whidden, S.E., Stenseth, N.C., 2020. Impact of past climate warming on genomic diversity and demographic history of collared lemmings across the Eurasian Arctic. *Proc. Natl. Acad. Sci. U. S. A.* 117, 3026-3033.
- Fortes, G.G., Grandal-d'Anglade, A., Kolbe, B., Fernandes, D., Meleg, I.N., Garcia-Vazquez, A., Pinto-Llona, A.C., Constantin, S., de Torres, T.J., Ortiz, J.E., Frischauf, C., Rabeder, G., Hofreiter, M., Barlow, A., 2016. Ancient DNA reveals differences in behaviour and sociality between brown bears and extinct cave bears. *Mol. Ecol.* 25, 4907-4918.
- Fox-Dobbs, K., Leonard, J.A., Koch, P.L., 2008. Pleistocene megafauna from eastern Beringia: Paleocological and paleoenvironmental interpretations of stable carbon and nitrogen isotope and radiocarbon records. *Palaeogeogr., Palaeoclimatol., Palaeoecol.* 261, 30-46.
- García-Vázquez, A., Pinto Llona, A.C., Grandal-d'Anglade, A., 2019. Post-glacial colonization of Western Europe brown bears from a cryptic Atlantic refugium out of the Iberian Peninsula. *Hist. Biol.* 31, 618-630.
- Gretzinger, J., Molak, M., Reiter, E., Pfrenge, S., Urban, C., Neukamm, J., Blant, M., Conard, N.J., Cupillard, C., Dimitrijevic, V., Drucker, D.G., Hofman-Kaminska, E., Kowalczyk, R., Krajcarz, M.T., Krajcarz, M., Munzel, S.C., Peresani, M., Romandini, M., Rufi, I., Soler, J., Terlato, G., Krause, J., Bocherens, H., Schuenemann, V.J., 2019. Large-scale mitogenomic analysis of the phylogeography of the Late Pleistocene cave bear. *Sci. Rep.* 9.
- Gus'kov, V.Y., Sheremet'eva, I.N., Serebkin, I.V., Kryukov, A.P., 2013. Mitochondrial cytochrome *b* gene variation in brown bear (*Ursus arctos* Linnaeus, 1758) from southern part of Russian Far East. *Russ. J. Genet.* 49, 1213–1218.
- Hailer, F., 2015. Introgressive hybridization: brown bears as vectors for polar bear alleles. *Mol. Ecol.* 24, 1161-1163.
- Hailer, F., Kutschera, V.E., Hallstrom, B.M., Klassert, D., Fain, S.R., Leonard, J.A., Arnason, U., Janke, A., 2012. Nuclear genomic sequences reveal that polar bears are an old and distinct bear lineage. *Science* 336, 344-347.
- Hassanin, A., 2015. The role of Pleistocene glaciations in shaping the evolution of polar and brown bears. Evidence from a critical review of mitochondrial and nuclear genome analyses. *C. R. Biol.* 338, 494-501.

- Hewitt, G.M., 1999. Post-glacial re-colonization of European biota. *Biol. J. Linn. Soc.* 68, 87-112.
- Hewitt, G.M., 2000. The genetic legacy of the Quaternary ice ages. *Nature* 405, 907-913.
- Hewitt, G.M., 2001. Speciation, hybrid zones and phylogeography - or seeing genes in space and time. *Mol. Ecol.* 10, 537-549.
- Hirata, D., Mano, T., Abramov, A.V., Baryshnikov, G.F., Kosintsev, P.A., Vorobiev, A.A., Raichev, E.G., Tsunoda, H., Kaneko, Y., Murata, K., Fukui, D., Masuda, R., 2013. Molecular phylogeography of the brown bear (*Ursus arctos*) in Northeastern Asia based on analyses of complete mitochondrial DNA sequences. *Mol. Biol. Evol.* 30, 1644-1652.
- Hofreiter, M., Serre, D., Rohland, N., Rabeder, G., Nagel, D., Conard, N., Munzel, S., Paabo, S., 2004. Lack of phylogeography in European mammals before the last glaciation. *Proc. Natl. Acad. Sci. U. S. A.* 101, 12963-12968.
- Hofreiter, M., Stewart, J., 2009. Ecological change, range fluctuations and population dynamics during the Pleistocene. *Curr. Biol.* 19, R584-R594.
- Horton, T.W., Blum, J.D., Xie, Z.Q., Hren, M., Chamberlain, C.P., 2009. Stable isotope food-web analysis and mercury biomagnification in polar bears (*Ursus maritimus*). *Polar Res.* 28, 443-454.
- Hubberten, H.W., Andreev, A., Astakhov, V.I., Demidov, I., Dowdeswell, J.A., Henriksen, M., Hjort, C., Houmark-Nielsen, M., Jakobsson, M., Kuzmina, S., Larsen, E., Lunkka, J.P., Lysa, A., Mangerud, J., Moller, P., Saarnisto, M., Schirmer, L., Sher, A.V., Siegert, C., Siegert, M.J., Svendsen, J.I., 2004. The periglacial climate and environment in northern Eurasia during the Last Glaciation. *Quat. Sci. Rev.* 23, 1333-1357.
- Jaarola, M., Searle, J.B., 2002. Phylogeography of field voles (*Microtus agrestis*) in Eurasia inferred from mitochondrial DNA sequences. *Mol. Ecol.* 11, 2613-2621.
- Jansson, R., Dynesius, M., 2002. The fate of clades in a world of recurrent climatic change: Milankovitch oscillations and evolution. *Annu. Rev. Ecol. Syst.* 33, 741-777.
- Keis, M., Remm, J., Ho, S.Y.W., Davison, J., Tammeleht, E., Tumanov, I.L., Saveljev, A.P., Mannil, P., Kojola, I., Abramov, A.V., Margus, T., Saarma, U., 2013. Complete mitochondrial genomes and a novel spatial genetic method reveal cryptic phylogeographical structure and migration patterns among brown bears in north-western Eurasia. *J. Biogeogr.* 40, 915-927.
- Kelly, B.P., Whiteley, A., Tallmon, D., 2010. The Arctic melting pot. *Nature* 468, 891.
- Kirillova, I.V., Tiunov, A.V., Levchenko, V.A., Chernova, O.F., Yudin, V.G., Bertuch, F., Shidlovskiy, F.K., 2015. On the discovery of a cave lion from the Malyy Anyui River (Chukotka, Russia). *Quat. Sci. Rev.* 117, 135-151.

- Kleinen, T., Hildebrandt, S., Prange, M., Rachmayani, R., Müller, S., Bezrukova, E., Brovkin, V., Tarasov, P.E., 2014. The climate and vegetation of Marine Isotope Stage 11 – Model results and proxy-based reconstructions at global and regional scale. *Quat. Int.* 348, 247-265.
- Kohn, M., Knauer, F., Stoffella, A., Schroder, W., Paabo, S., 1995. Conservation genetics of the European brown bear - a study using excremental PCR of nuclear and mitochondrial sequences. *Mol. Ecol.* 4, 95-103.
- Korsten, M., Ho, S.Y.W., Davison, J., Pahn, B., Vulla, E., Roht, M., Tumanov, I.L., Kojola, I., Andersone-Lilley, Z., Ozolins, J., Pilot, M., Mertzanis, Y., Giannakopoulos, A., Vorobiev, A.A., Markov, N.I., Saveljev, A.P., Lyapunova, E.A., Abramov, A.V., Mannil, P., Valdmann, H., Pazetnov, S.V., Pazetnov, V.S., Rokov, A.M., Saarma, U., 2009. Sudden expansion of a single brown bear maternal lineage across northern continental Eurasia after the last ice age: a general demographic model for mammals? *Mol. Ecol.* 18, 1963-1979.
- Kukla, G.J., Bender, M.L., de Beaulieu, J.L., Bond, G., Broecker, W.S., Cleveringa, P., Gavin, J.E., Herbert, T.D., Imbrie, J., Jouzel, J., Keigwin, L.D., Knudsen, K.L., McManus, J.F., Merkt, J., Muhs, D.R., Muller, H., Poore, R.Z., Porter, S.C., Seret, G., Shackleton, N.J., Turner, C., Tzedakis, P.C., Winograd, I.J., 2002. Last interglacial climates. *Quat. Res.* 58, 2-13.
- Kurtén, B., 1968. Pleistocene mammals of Europe. Addine Publishing Co., Chicago.
- Kutschera, V.E., Bidon, T., Hailer, F., Rodi, J.L., Fain, S.R., Janke, A., 2014. Bears in a forest of gene trees: Phylogenetic inference is complicated by incomplete lineage sorting and gene flow. *Mol. Biol. Evol.* 31, 2004-2017.
- Lan, T.Y., Gill, S., Bellemain, E., Bischof, R., Nawaz, M.A., Lindqvist, C., 2017. Evolutionary history of enigmatic bears in the Tibetan Plateau - Himalaya region and the identity of the yeti. *Proc. R. Soc. B.* 284.
- Lang, N., Wolff, E.W., 2011. Interglacial and glacial variability from the last 800 ka in marine, ice and terrestrial archives. *Clim. Past* 7, 361-380.
- Ledevin, R., Michaux, J.R., Deffontaine, V., Henttonen, H., Renaud, S., 2010. Evolutionary history of the bank vole *Myodes glareolus*: a morphometric perspective. *Biol. J. Linn. Soc.* 100, 681-694.
- Leigh, J.W., Bryant, D., 2015. POPART: full-feature software for haplotype network construction. *Methods in Ecology and Evolution* 6, 1110-1116.
- Leonard, J.A., Vila, C., Fox-Dobbs, K., Koch, P.L., Wayne, R.K., Van Valkenburgh, B., 2007. Megafaunal extinctions and the disappearance of a specialized wolf ecomorph. *Curr. Biol.* 17, 1146-1150.
- Leonard, J.A., Wayne, R.K., Cooper, A., 2000. Population genetics of Ice age brown bears. *Proc. Natl. Acad. Sci. U. S. A.* 97, 1651-1654.
- Li, H., Durbin, R., 2009. Fast and accurate short read alignment with Burrows-Wheeler transform. *Bioinformatics* 25, 1754-1760.

- Li, H., Handsaker, B., Wysoker, A., Fennell, T., Ruan, J., Homer, N., Marth, G., Abecasis, G., Durbin, R., Genome Project Data Processing, S., 2009. The sequence alignment/map format and SAMtools. *Bioinformatics* 25, 2078-2079.
- Lindqvist, C., Schuster, S.C., Sun, Y.Z., Talbot, S.L., Qi, J., Ratan, A., Tomsho, L.P., Kasson, L., Zeyl, E., Aars, J., Miller, W., Ingolfsson, O., Bachmann, L., Wiig, O., 2010. Complete mitochondrial genome of a Pleistocene jawbone unveils the origin of polar bear. *Proc. Natl. Acad. Sci. U. S. A.* 107, 5053-5057.
- Liu, S.P., Lorenzen, E.D., Fumagalli, M., Li, B., Harris, K., Xiong, Z.J., Zhou, L., Korneliussen, T.S., Somel, M., Babbitt, C., Wray, G., Li, J.W., He, W.M., Wang, Z., Fu, W.J., Xiang, X.Y., Morgan, C.C., Doherty, A., O'Connell, M.J., McInerney, J.O., Born, E.W., Dalen, L., Dietz, R., Orlando, L., Sonne, C., Zhang, G.J., Nielsen, R., Willerslev, E., Wang, J., 2014. Population genomics reveal recent speciation and rapid evolutionary adaptation in polar bears. *Cell* 157, 785-794.
- Loog, L., Thalmann, O., Sinding, M.H.S., Schuenemann, V.J., Perri, A., Germonpré, M., Bocherens, H., Witt, K.E., Castruita, J.A.S., Velasco, M.S., Lundstrom, I.K.C., Wales, N., Sonet, G., Frantz, L., Schroeder, H., Budd, J., Jimenez, E.L., Fedorov, S., Gasparyan, B., Kandel, A.W., L'znyi-kov-Galetov, M., Napierala, H., Uerpmann, H.P., Nikolskiy, P.A., Pavlova, E.Y., Pitulko, V.V., Herzig, K.H., Malhi, R.S., Willerslev, E., Hansen, A.J., Dobney, K., Gilbert, M.T.P., Krause, J., Larson, G., Eriksson, A., Manica, A., 2020. Ancient DNA suggests modern wolves trace their origin to a Late Pleistocene expansion from Beringia. *Mol. Ecol.* 29, 1596-1610.
- Lorenzen, E.D., Nogues-Bravo, D., Orlando, L., Weinstock, J., Binladen, J., Marske, K.A., Ugan, A., Borregaard, M.K., Gilbert, M.T., Nielsen, R., Ho, S.Y., Goebel, T., Graf, K.E., Byers, D., Stenderup, J.T., Rasmussen, M., Campos, P.F., Leonard, J.A., Koepfli, K.P., Froese, D., Zazula, G., Stafford, T.W., Jr., Aaris-Sorensen, K., Batra, P., Haywood, A.M., Singarayer, J.S., Valdes, P.J., Boeskorov, G., Burns, J.A., Davydov, S.P., Haile, J., Jenkins, D.L., Kosintsev, P., Kuznetsova, T., Lai, X., Martin, L.D., McDonald, H.G., Mol, D., Meldgaard, M., Munch, K., Stephan, E., Sablin, M., Sommer, R.S., Sipko, T., Scott, E., Suchard, M.A., Tikhonov, A., Willerslev, R., Wayne, R.K., Cooper, A., Hofreiter, M., Sher, A., Shapiro, B., Rahbek, C., Willerslev, E., 2011. Species-specific responses of Late Quaternary megafauna to climate and humans. *Nature* 479, 359-364.
- Lozhkin, A.V., Anderson, P.M., 1995. The Last Interglaciation in Northeast Siberia. *Quat. Res.* 43, 147-158.
- Mann, D.H., Groves, P., Kunz, M.L., Reanier, R.E., Gaglioti, B.V., 2013. Ice-age megafauna in Arctic Alaska: extinction, invasion, survival. *Quat. Sci. Rev.* 70, 91-108.
- Mann, D.H., Groves, P., Reanier, R.E., Gaglioti, B.V., Kunz, M.L., Shapiro, B., 2015. Life and extinction of megafauna in the ice-age Arctic. *Proc. Natl. Acad. Sci. U. S. A.* 112, 14301-14306.
- Markova, S., Hornikova, M., Lanier, H.C., Henttonen, H., Searle, J.B., Weider, L.J., Kotlik, P., 2020. High genomic diversity in the bank vole at the northern apex of a

- range expansion: The role of multiple colonizations and end-glacial refugia. *Mol. Ecol.* 29, 1730-1744.
- Massilani, D., Guimaraes, S., Brugal, J.P., Bennett, E.A., Tokarska, M., Arbogast, R.M., Baryshnikov, G., Boeskorov, G., Castel, J.C., Davydov, S., Madelaine, S., Putelat, O., Spasskaya, N.N., Uerpmann, H.P., Grange, T., Geigl, E.M., 2016. Past climate changes, population dynamics and the origin of Bison in Europe. *BMC Biol.* 14, 93.
- Matheus, P.E., 1995. Diet and co-ecology of Pleistocene short-faced bears and brown bears in eastern Beringia. *Quat. Res.* 44, 447-453.
- McLellan, B., Reiner, D.C., 1994. A review of bear evolution. *Bears Their Biol. Manag.* 9, 85-96.
- McManus, J.F., Oppo, D.W., Cullen, J.L., 1999. A 0.5-million-year record of millennial-scale climate variability in the North Atlantic. *Science* 283, 971-975.
- Meiri, M., Lister, A.M., Collins, M.J., Tuross, N., Goebel, T., Blockley, S., Zazula, G.D., van Doorn, N., Guthrie, R.D., Boeskorov, G.G., Baryshnikov, G.F., Sher, A., Barnes, I., 2014. Faunal record identifies Bering isthmus conditions as constraint to end-Pleistocene migration to the New World. *Proc. R. Soc. B.* 281.
- Metcalf, J.L., Turney, C., Barnett, R., Martin, F., Bray, S.C., Vilstrup, J.T., Orlando, L., Salas-Gismondi, R., Loponte, D., Medina, M., De Nigris, M., Civalero, T., Fernandez, P.M., Gasco, A., Duran, V., Seymour, K.L., Otaola, C., Gil, A., Paunero, R., Prevosti, F.J., Bradshaw, C.J., Wheeler, J.C., Borrero, L., Austin, J.J., Cooper, A., 2016. Synergistic roles of climate warming and human occupation in Patagonian megafaunal extinctions during the Last Deglaciation. *Sci. Adv.* 2, e1501682.
- Meyer, M., Kircher, M., Gansauge, M.T., Li, H., Racimo, F., Mallick, S., Schraiber, J.G., Jay, F., Prufer, K., de Filippo, C., Sudmant, P.H., Alkan, C., Fu, Q.M., Do, R., Rohland, N., Tandon, A., Siebauer, M., Green, R.E., Bryc, K., Briggs, A.W., Stenzel, U., Dabney, J., Shendure, J., Kitzman, J., Hammer, M.F., Shunkov, M.V., Derevianko, A.P., Patterson, N., Andres, A.M., Eichler, E.E., Slatkin, M., Reich, D., Kelso, J., Paabo, S., 2012. A high-coverage genome sequence from an archaic Denisovan individual. *Science* 338, 222-226.
- Miller, C.R., Waits, L.P., Joyce, P., 2006. Phylogeography and mitochondrial diversity of extirpated brown bear (*Ursus arctos*) populations in the contiguous United States and Mexico. *Mol. Ecol.* 15, 4477-4485.
- Miller, W., Schuster, S.C., Welch, A.J., Ratan, A., Bedoya-Reina, O.C., Zhao, F.Q., Kim, H.L., Burhans, R.C., Drautz, D.I., Wittekindt, N.E., Tomsho, L.P., Ibarra-Laclette, E., Herrera-Estrella, L., Peacock, E., Farley, S., Sage, G.K., Rode, K., Obbard, M., Montiel, R., Bachmann, L., Ingolfsson, O., Aars, J., Mailund, T., Wiig, O., Talbot, S.L., Lindqvist, C., 2012. Polar and brown bear genomes reveal ancient admixture and demographic footprints of past climate change. *Proc. Natl. Acad. Sci. U. S. A.* 109, E2382-E2390.

- Mondanaro, A., Di Febbraro, M., Melchionna, M., Carotenuto, F., Castiglione, S., Serio, C., Danisi, S., Rook, L., Diniz, J.A.F., Raia, P., 2019. Additive effects of climate change and human hunting explain population decline and extinction in cave bears. *Boreas* 48, 605-615.
- Murtskhvaladze, M., Gavashelishvili, A., Tarkhnishvili, D., 2010. Geographic and genetic boundaries of brown bear (*Ursus arctos*) population in the Caucasus. *Mol. Ecol.* 19, 1829-1841.
- Myers, N., Mittermeier, R.A., Mittermeier, C.G., da Fonseca, G.A.B., Kent, J., 2000. Biodiversity hotspots for conservation priorities. *Nature* 403, 853-858.
- Naafs, B.D.A., Hefter, J., Stein, R., 2014. Dansgaard-Oeschger forcing of sea surface temperature variability in the midlatitude North Atlantic between 500 and 400ka (MIS 12). *Paleoceanography* 29, 1024-1030.
- Neiber, M.T., Hausdorf, B., 2015. Phylogeography of the land snail genus *Circassina* (Gastropoda: Hygromiidae) implies multiple Pleistocene refugia in the western Caucasus region. *Mol. Phylogenet. Evol.* 93, 129-142.
- Nikolova, I., Yin, Q., Berger, A., Singh, U.K., Karami, M.P., 2013. The last interglacial (Eemian) climate simulated by LOVECLIM and CCSM3. *Clim. Past* 9, 1789-1806.
- Obrecht, I., Hambach, U., Veres, D., Zeeden, C., Bosken, J., Stevens, T., Markovic, S.B., Klasen, N., Brill, D., Burow, C., Lehmkuhl, F., 2017. Shift of large-scale atmospheric systems over Europe during late MIS 3 and implications for Modern Human dispersal. *Sci. Rep.* 7, 5848.
- Ohshima, K., 1990. The history of straits around the Japanese islands in the Late-Quaternary. *Quaternary Res.* 29, 193-208.
- Oppo, D.W., McManus, J.F., Cullen, J.L., 1998. Abrupt climate events 500,000 to 340,000 years ago: Evidence from subpolar north Atlantic sediments. *Science* 279, 1335-1338.
- Orth, A., Auffray, J.C., Bonhomme, F., 2002. Two deeply divergent mitochondrial clades in the wild mouse *Mus macedonicus* reveal multiple glacial refuges south of Caucasus. *Heredity* 89, 353-357.
- Otto-Bliesner, B.L., Marsha, S.J., Overpeck, J.T., Miller, G.H., Hu, A.X., Mem, C.L.I.P., 2006. Simulating arctic climate warmth and icefield retreat in the last interglaciation. *Science* 311, 1751-1753.
- Pacher, M., Stuart, A.J., 2009. Extinction chronology and palaeobiology of the cave bear (*Ursus spelaeus*). *Boreas* 38, 189-206.
- Palkopoulou, E., Dalen, L., Lister, A.M., Vartanyan, S., Sablin, M., Sher, A., Edmark, V.N., Brandstrom, M.D., Germonpre, M., Barnes, I., Thomas, J.A., 2013. Holarctic genetic structure and range dynamics in the woolly mammoth. *Proc. R. Soc. B.* 280, 20131910.

5.2 MANUSCRIPT

- Parvizi, E., Naderloo, R., Keikhosravi, A., Solhjoui-Fard, S., Schubart, C.D., 2018. Multiple Pleistocene refugia and repeated phylogeographic breaks in the southern Caspian Sea region: Insights from the freshwater crab *Potamon ibericum*. *J. Biogeogr.* 45, 1234-1245.
- Pasitschniak-Arts, M., 1993. *Ursus arctos*. *Mamm. Species* 439, 1-10.
- Pavelkova Ricankova, V., Robovsky, J., Riegert, J., 2014. Ecological structure of recent and last glacial mammalian faunas in northern Eurasia: the case of Altai-Sayan refugium. *PLoS ONE* 9, e85056.
- Post, E., Bhatt, U.S., Bitz, C.M., Brodie, J.F., Fulton, T.L., Hebblewhite, M., Kerby, J., Kutz, S.J., Stirling, I., Walker, D.A., 2013. Ecological consequences of sea-ice decline. *Science* 341, 519-524.
- Rambaut, A., Drummond, A.J., Xie, D., Baele, G., Suchard, M.A., 2018. Posterior summarization in bayesian phylogenetics using Tracer 1.7. *Syst. Biol.* 67, 901-904.
- Ramsden, C., Holmes, E.C., Charleston, M.A., 2009. Hantavirus evolution in relation to its rodent and insectivore hosts: no evidence for codivergence. *Mol. Biol. Evol.* 26, 143-153.
- Ramsey, C.B., 2009. Bayesian analysis of radiocarbon dates. *Radiocarbon* 51, 337-360.
- Raymo, M.E., Mitrovica, J.X., 2012. Collapse of polar ice sheets during the stage 11 interglacial. *Nature* 483, 453-456.
- Reimer, P.J., Bard, E., Bayliss, A., Beck, J.W., Blackwell, P.G., Ramsey, C.B., Buck, C.E., Cheng, H., Edwards, R.L., Friedrich, M., Grootes, P.M., Guilderson, T.P., Hafliadason, H., Hajdas, I., Hatte, C., Heaton, T.J., Hoffmann, D.L., Hogg, A.G., Hughen, K.A., Kaiser, K.F., Kromer, B., Manning, S.W., Niu, M., Reimer, R.W., Richards, D.A., Scott, E.M., Southon, J.R., Staff, R.A., Turney, C.S.M., van der Plicht, J., 2013. Intcal13 and Marine13 radiocarbon age calibration curves 0-50,000 years cal BP. *Radiocarbon* 55, 1869-1887.
- Rey-Iglesia, A., Garcia-Vazquez, A., Treadaway, E.C., van der Plicht, J., Baryshnikov, G.F., Szpak, P., Bocherens, H., Boeskorov, G.G., Lorenzen, E.D., 2019. Evolutionary history and palaeoecology of brown bear in North-East Siberia re-examined using ancient DNA and stable isotopes from skeletal remains. *Sci. Rep.* 9, 4462.
- Ricankova, V.P., Robovsky, J., Riegert, J., Zrzavy, J., 2015. Regional patterns of postglacial changes in the Palearctic mammalian diversity indicate retreat to Siberian steppes rather than extinction. *Sci. Rep.* 5, 12682.
- Richards, M.P., Pacher, M., Stiller, M., Quiles, J., Hofreiter, M., Constantin, S., Zilhao, J., Trinkaus, E., 2008. Isotopic evidence for omnivory among European cave bears: Late Pleistocene *Ursus spelaeus* from the Pestera Cu Oase, Romania. *Proc. Natl. Acad. Sci. U. S. A.* 105, 600-604.
- Richards, S.M., Hovhannisyanyan, N., Gilliam, M., Ingram, J., Skadhauge, B., Heiniger, H., Llamas, B., Mitchell, K.J., Meachen, J., Fincher, G.B., Austin, J.J., Cooper, A.,

2019. Low-cost cross-taxon enrichment of mitochondrial DNA using in-house synthesised RNA probes. PLoS ONE 14, e0209499.
- Robinson, A., Alvarez-Solas, J., Calov, R., Ganopolski, A., Montoya, M., 2017. MIS-11 duration key to disappearance of the Greenland ice sheet. Nat. Commun. 8, 16008.
- Rodrigues, T., Alonso-Garcia, M., Hodell, D.A., Rufino, M., Naughton, F., Grimalt, J.O., Voelker, A.H.L., Abrantes, F., 2017. A 1-Ma record of sea surface temperature and extreme cooling events in the North Atlantic: A perspective from the Iberian Margin. Quat. Sci. Rev. 172, 118-130.
- Rohland, N., Harney, E., Mallick, S., Nordenfelt, S., Reich, D., 2015. Partial uracil-DNA-glycosylase treatment for screening of ancient DNA. Philos. Trans. R. Soc. Lond. B. Biol. Sci 370, 20130624.
- Saarma, U., Ho, S.Y.W., Pybus, O.G., Kaljuste, M., Tumanov, I.L., Kojola, I., Vorobiev, A.A., Markov, N.I., Saveljev, A.P., Valdmann, H., Lyapunova, E.A., Abramov, A.V., Mannil, P., Korsten, M., Vulla, E., Pazetnov, S.V., Pazetnov, V.S., Putschkovskiy, S.V., Rokov, A.M., 2007. Mitogenetic structure of brown bears (*Ursus arctos* L.) in northeastern Europe and a new time frame for the formation of European brown bear lineages. Mol. Ecol. 16, 401-413.
- Saarma, U., Kojola, I., 2007. Matrilinial genetic structure of the brown bear population in Finland. Ursus 18, 30-37, 38.
- Schmitt, T., Varga, Z., 2012. Extra-Mediterranean refugia: The rule and not the exception? Front. Zool. 9.
- Schubert, M., Ermini, L., Sarkissian, C.D., Jonsson, H., Ginolhac, A., Schaefer, R., Martin, M.D., Fernandez, R., Kircher, M., McCue, M., Willerslev, E., Orlando, L., 2014. Characterization of ancient and modern genomes by SNP detection and phylogenomic and metagenomic analysis using PALEOMIX. Nat. Protoc. 9, 1056-1082.
- Schubert, M., Lindgreen, S., Orlando, L., 2016. AdapterRemoval v2: rapid adapter trimming, identification, and read merging. BMC Res. Notes 9, 88.
- Servheen, C., 1999. Bears: status survey and conservation action plan. IUCN.
- Shields, G.F., Adams, D., Garner, G., Labelle, M., Pietsch, J., Ramsay, M., Schwartz, C., Titus, K., Williamson, S., 2000. Phylogeography of mitochondrial DNA variation in brown bears and polar bears. Mol. Phylogenet. Evol. 15, 319-326.
- Skrede, I., Eidesen, P.B., Portela, R.P., Brochmann, C., 2006. Refugia, differentiation and postglacial migration in arctic-alpine Eurasia, exemplified by the mountain avens (*Dryas octopetala* L.). Mol. Ecol. 15, 1827-1840.
- Sommer, R.S., Benecke, N., 2005. The recolonization of Europe by brown bears *Ursus arctos* Linnaeus, 1758 after the Last Glacial Maximum. Mammal Rev. 35, 156-164.

5.2 MANUSCRIPT

- Sørensen, O., 1990. The brown bear in Europe in the mid 1980's. *Aquilo*, Ser. Zool. 27, 3-16.
- Soubrier, J., Gower, G., Chen, K., Richards, S.M., Llamas, B., Mitchell, K.J., Ho, S.Y.W., Kosintsev, P., Lee, M.S.Y., Baryshnikov, G., Bollongino, R., Bover, P., Burger, J., Chivall, D., Cregut-Bonnoure, E., Decker, J.E., Doronichev, V.B., Douka, K., Fordham, D.A., Fontana, F., Fritz, C., Glimmerveen, J., Golovanova, L.V., Groves, C., Guerreschi, A., Haak, W., Higham, T., Hofman-Kaminska, E., Immel, A., Julien, M.A., Krause, J., Krotova, O., Langbein, F., Larson, G., Rohrlach, A., Scheu, A., Schnabel, R.D., Taylor, J.F., Tokarska, M., Tosello, G., van der Plicht, J., van Loenen, A., Vigne, J.D., Wooley, O., Orlando, L., Kowalczyk, R., Shapiro, B., Cooper, A., 2016. Early cave art and ancient DNA record the origin of European bison. *Nat. Commun.* 7, 13158.
- Stamatakis, A., 2014. RAxML version 8: a tool for phylogenetic analysis and post-analysis of large phylogenies. *Bioinformatics* 30, 1312-1313.
- Stein, R., Hefter, J., Grutzner, J., Voelker, A., Naafs, B.D.A., 2009. Variability of surface water characteristics and Heinrich-like events in the Pleistocene midlatitude North Atlantic Ocean: Biomarker and XRD records from IODP Site U1313 (MIS 16-9). *Paleoceanography* 24, PA2203.
- Stiller, M., Baryshnikov, G., Bocherens, H., Grandal-d'Anglade, A., Hilpert, B., Munzel, S.C., Pinhasi, R., Rabeder, G., Rosendahl, W., Trinkaus, E., Hofreiter, M., Knapp, M., 2010. Withering Away-25,000 Years of Genetic Decline Preceded Cave Bear Extinction. *Mol. Biol. Evol.* 27, 975-978.
- Stiller, M., Molak, M., Prost, S., Rabeder, G., Baryshnikov, G., Rosendahl, W., Münzel, S., Bocherens, H., Grandal-d'Anglade, A., Hilpert, B., Germonpré, M., Stasyk, O., Pinhasi, R., Tintori, A., Rohland, N., Mohandesan, E., Ho, S.Y.W., Hofreiter, M., Knapp, M., 2014. Mitochondrial DNA diversity and evolution of the Pleistocene cave bear complex. *Quat. Int.* 339-340, 224-231.
- Stoen, O.G., Zedrosser, A., Saebo, S., Swenson, J.E., 2006. Inversely density-dependent natal dispersal in brown bears *Ursus arctos*. *Oecologia* 148, 356-364.
- Stroeven, A.P., Hättestrand, C., Kleman, J., Heyman, J., Fabel, D., Fredin, O., Goodfellow, B.W., Harbor, J.M., Jansen, J.D., Olsen, L., Caffee, M.W., Fink, D., Lundqvist, J., Rosqvist, G.C., Strömberg, B., Jansson, K.N., 2016. Deglaciation of Fennoscandia. *Quat. Sci. Rev.* 147, 91-121.
- Stuart, A.J., Lister, A.M., 2012. Extinction chronology of the woolly rhinoceros *Coelodonta antiquitatis* in the context of late Quaternary megafaunal extinctions in northern Eurasia. *Quat. Sci. Rev.* 51, 1-17.
- Subramanian, S., Lambert, D.M., 2011. Time dependency of molecular evolutionary rates? Yes and no. *Genome Biol. Evol.* 3, 1324-1328.
- Swenson, J.E., Wabakken, P., Sandegren, F., Bjärvall, A., Franzén, R., Söderberg, A., 1995. The near extinction and recovery of brown bears in Scandinavia in relation to the bear management policies of Norway and Sweden. *Wildl. Biol.* 1, 11-25, 15.

- Taberlet, P., Bouvet, J., 1994. Mitochondrial DNA Polymorphism, Phylogeography, and Conservation Genetics of the Brown Bear *Ursus arctos* in Europe. *Proc. R. Soc. B.* 255, 195-200.
- Taberlet, P., Camarra, J.J., Griffin, S., Uhres, E., Hanotte, O., Waits, L.P., DuboisPaganon, C., Burke, T., Bouvet, J., 1997. Noninvasive genetic tracking of the endangered Pyrenean brown bear population. *Mol. Ecol.* 6, 869-876.
- Taberlet, P., Fumagalli, L., Wust-Saucy, A.G., Cosson, J.F., 1998. Comparative phylogeography and postglacial colonization routes in Europe. *Mol. Ecol.* 7, 453-464.
- Talbot, S.L., Shields, G.F., 1996. Phylogeography of brown bears (*Ursus arctos*) of Alaska and paraphyly within the Ursidae. *Mol. Phylogenet. Evol.* 5, 477-494.
- Terlato, G., Bocherens, H., Romandini, M., Nannini, N., Hobson, K.A., Peresani, M., 2019. Chronological and isotopic data support a revision for the timing of cave bear extinction in Mediterranean Europe. *Hist. Biol.* 31, 474-484.
- Tumendemberel, O., Zedrosser, A., Proctor, M.F., Reynolds, H.V., Adams, J.R., Sullivan, J.M., Jacobs, S.J., Khorloojav, T., Tserenbataa, T., Batmunkh, M., Swenson, J.E., Waits, L.P., 2019. Phylogeography, genetic diversity, and connectivity of brown bear populations in Central Asia. *PLoS ONE* 14.
- Valdiosera, C.E., Garcia, N., Anderung, C., Dalen, L., Cregut-Bonnoure, E., Kahlke, R.D., Stiller, M., Brandstrom, M., Thomas, M.G., Arsuaga, J.L., Gotherstrom, A., Barnes, I., 2007. Staying out in the cold: glacial refugia and mitochondrial DNA phylogeography in ancient European brown bears. *Mol. Ecol.* 16, 5140-5148.
- Valdiosera, C.E., Garcia-Garitagoitia, J.L., Garcia, N., Doadrio, I., Thomas, M.G., Hanni, C., Arsuaga, J.L., Barnes, I., Hofreiter, M., Orlando, L., Gotherstorm, A., 2008. Surprising migration and population size dynamics in ancient Iberian brown bears (*Ursus arctos*). *Proc. Natl. Acad. Sci. U. S. A.* 105, 5123-5128.
- Waits, L., Taberlet, P., Swenson, J.E., Sandegren, F., Franzen, R., 2000. Nuclear DNA microsatellite analysis of genetic diversity and gene flow in the Scandinavian brown bear (*Ursus arctos*). *Mol. Ecol.* 9, 421-431.
- Waits, L.P., Talbot, S.L., Ward, R.H., Shields, G.F., 1998. Mitochondrial DNA phylogeography of the North American brown bear and implications for conservation. *Conserv. Biol.* 12, 408-417.
- Xenikoudakis, G., Ersmark, E., Tison, J.L., Waits, L., Kindberg, J., Swenson, J.E., Dalen, L., 2015. Consequences of a demographic bottleneck on genetic structure and variation in the Scandinavian brown bear. *Mol. Ecol.* 24, 3441-3454.
- Zedrosser, A., Dahle, B., Swenson, J.E., Gerstl, N., 2001. Status and management of the brown bear in Europe. *Ursus* 12, 9-20.
- Zedrosser, A., Stoen, O.G., Saebo, S., Swenson, J.E., 2007. Should I stay or should I go? Natal dispersal in the brown bear. *Anim. Behav.* 74, 369-376.

5.3 Supplementary Information

From Iberia to Siberia: Phylogeography and evolutionary history of Eurasian brown bears

Alexander T. Salis, Sarah C. E. Bray, Cristina E. Valdiosera, Jeremy J. Austin, Kieren J. Mitchell

Supplementary Information

This file includes:

Figures S1 to S10
Tables S1 to S6
Supplementary References

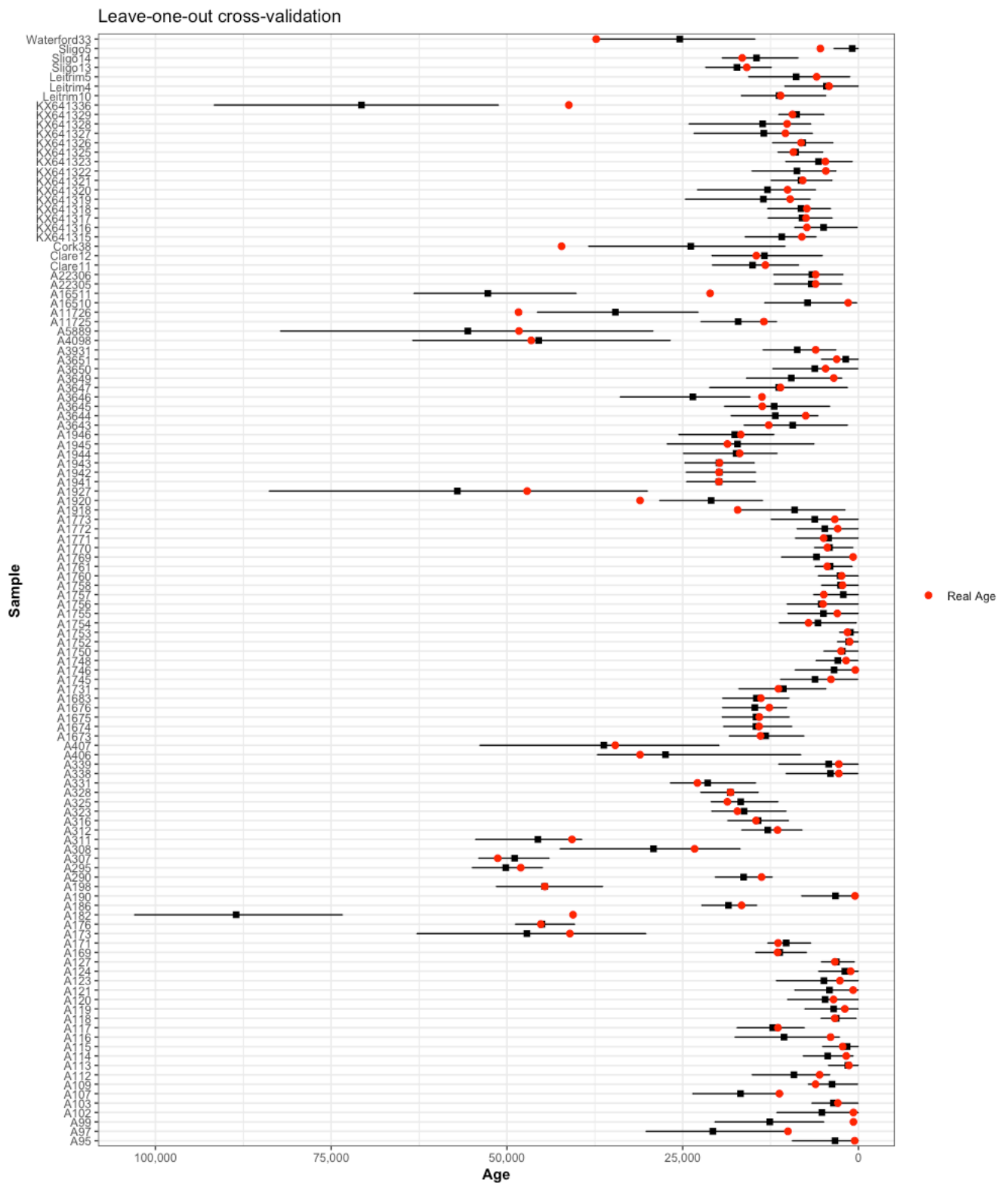


Figure S1: Plots of median estimated ages from leave-one-out cross-validation in BEAST2 for brown bears mitogenomes. Error-bars represent 95% Highest Posterior Density (HPD). The real age of the specimen is within the 95% HPD of each estimate for all but ten of the specimens. The specimens for which the real age is outside the 95% HPD were still included in subsequent analyses as they fall in under-sampled regions of the tree.

5.3 SUPPLEMENTARY INFORMATION

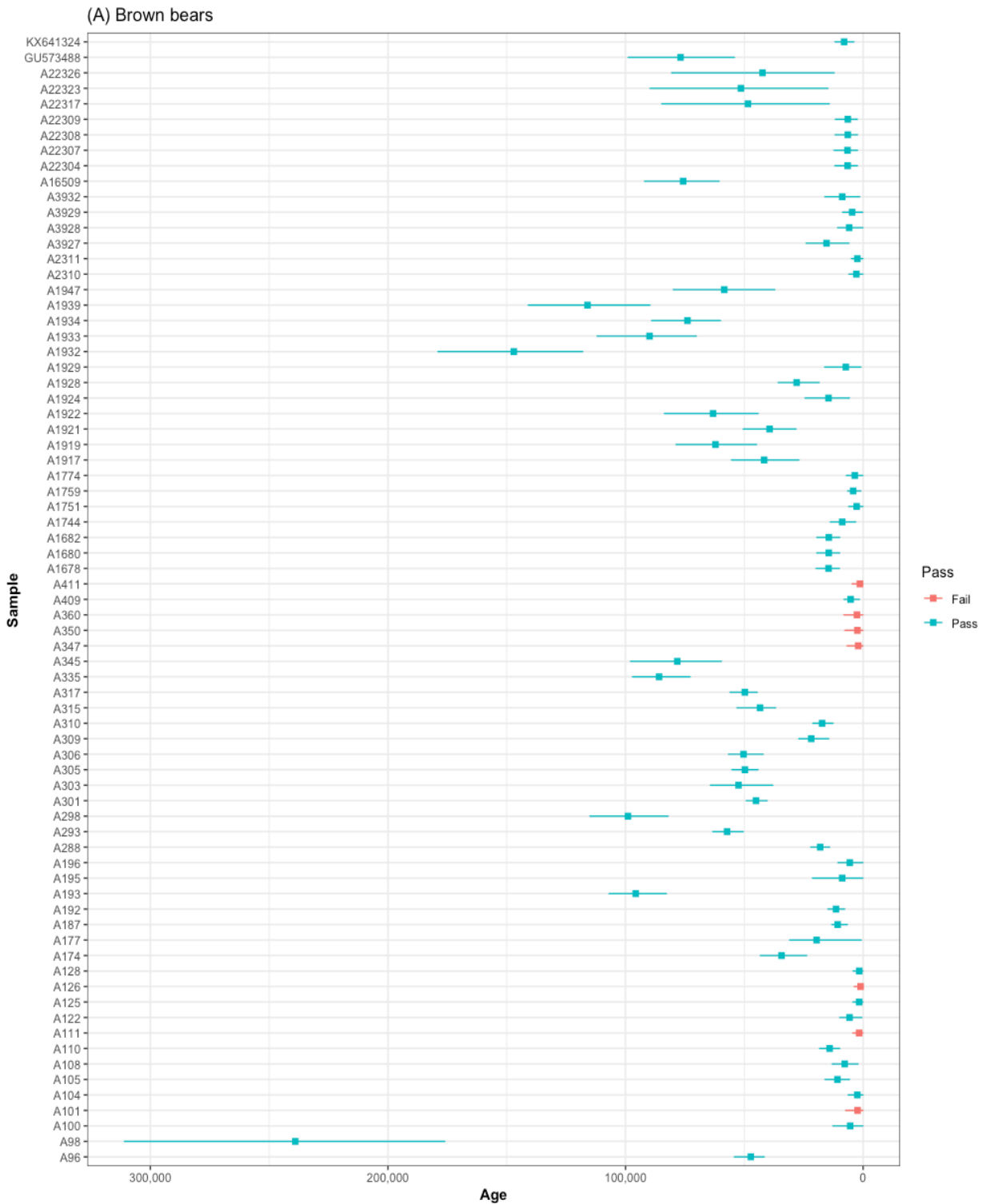


Figure S2: Estimated ages from BEAST2 of specimens with no associated date or infinite radiocarbon dates. Error bars represent 95% higher posterior densities. Specimens are coloured according to whether they produced unimodal estimates that were not skewed to zero (pass = blue, fail = red). Specimens that failed were excluded from further analyses.

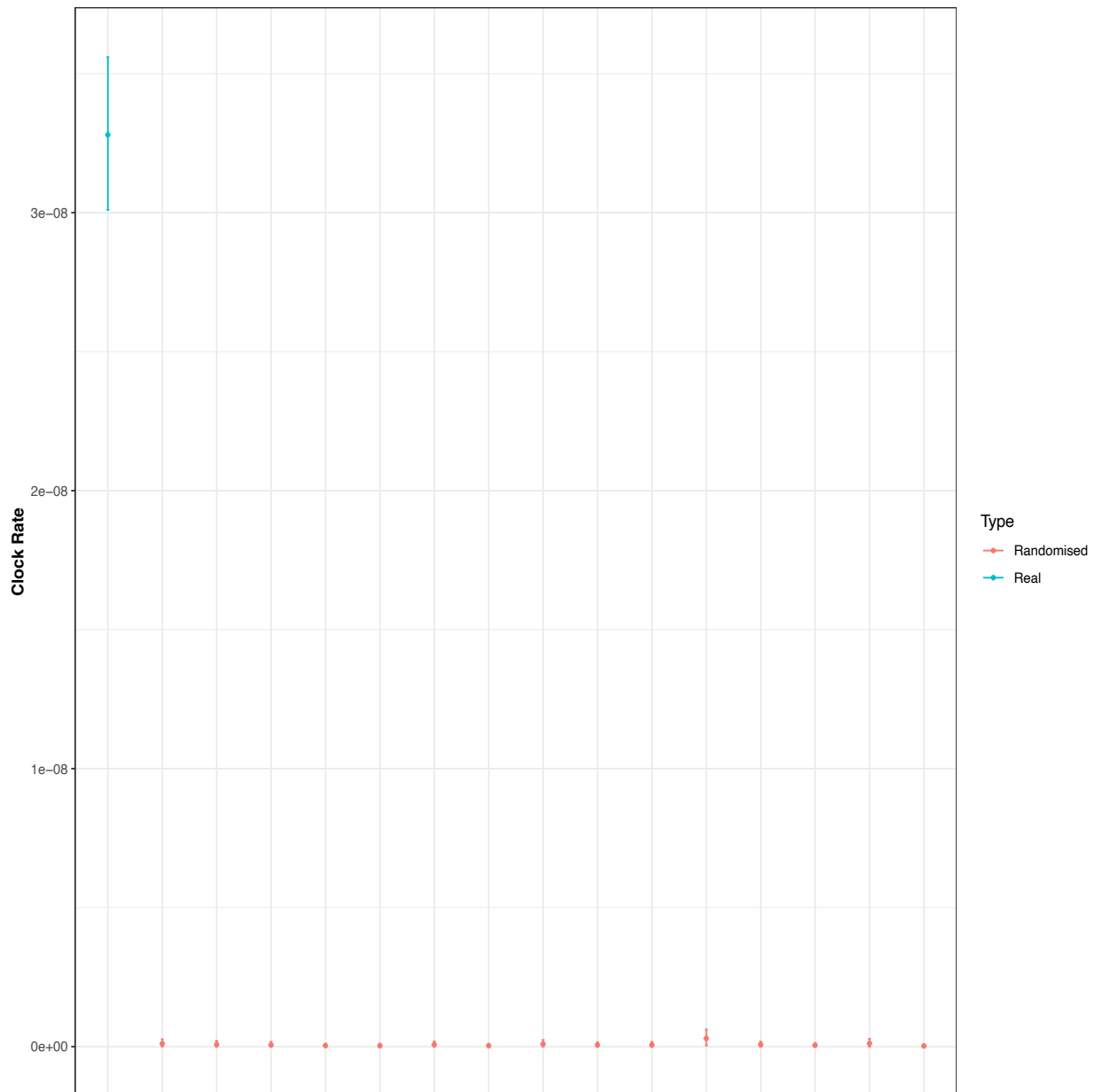


Figure S3: Comparison of mean clock rate estimations with 95% Highest Posterior Densities (HPD) from BEAST2 for the real data and the 15 date-randomized datasets from the date-randomization test (DRT). The 95% HPD of the true clock rate does not overlap with the 95% HPD of each randomization test.

5.3 SUPPLEMENTARY INFORMATION

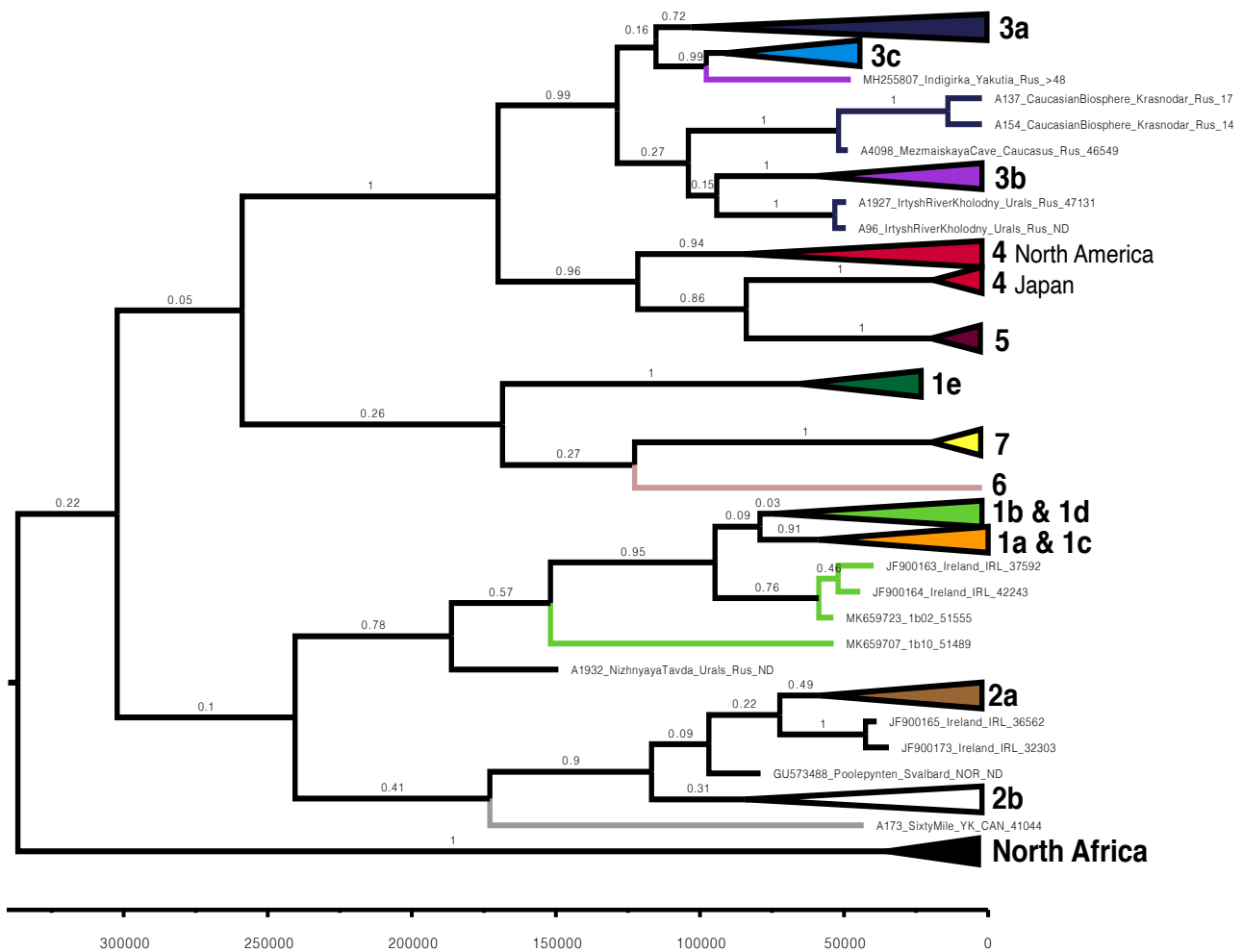


Figure S4: Bayesian phylogenetic tree based on 158 bp of the mitochondrial control region from brown and polar bears. Branch labels represent posterior support for branches with greater than 0.5 posterior support. The time scale is in years before present. Note the placement of A96, A137, A154, A1927, and A4098, which are erroneously placed outside of clade 3a (compared to results obtained from full mitochondrial genomes). In addition, MH255807 appears to be closely related to clade 3c. Further, clade 1b and 2b both appear to be paraphyletic.

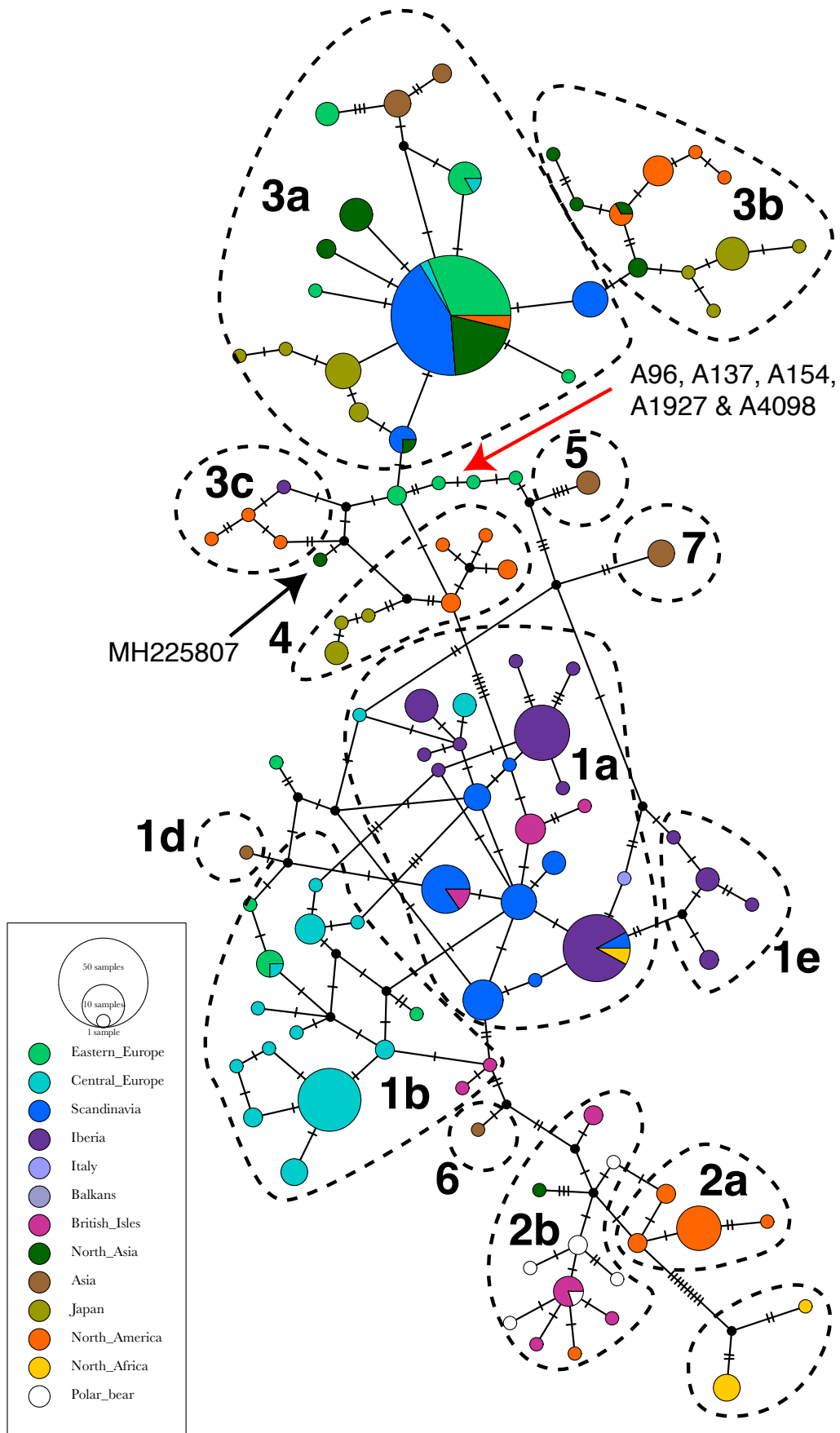


Figure S5: Median-joining haplotype network for brown and polar bear 158bp mitochondrial control region sequence. The placements of A22313, A22315, and MH255807 are indicated with arrows.

5.3 SUPPLEMENTARY INFORMATION

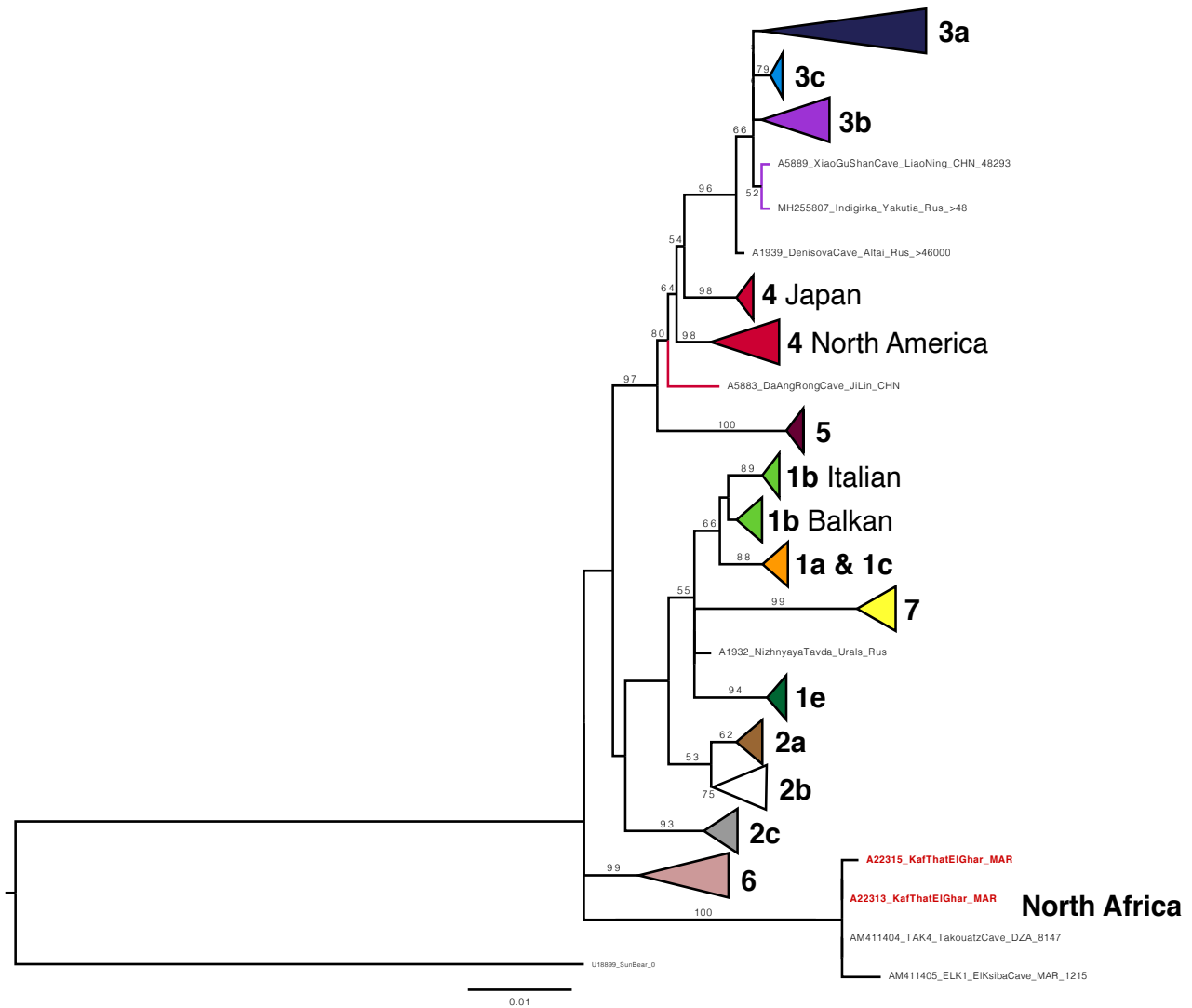


Figure S6: Maximum likelihood phylogenetic tree based on 278 bp of the cytochrome *b* mitochondrial gene from brown and polar bears. Branch labels represent bootstrap support for branches with greater than 50% support. Note the placement of A22313 and A22315 with ancient Atlas bear sequences from North Africa (from which no published mitogenomes are available). Further, clade 3 is poorly resolved

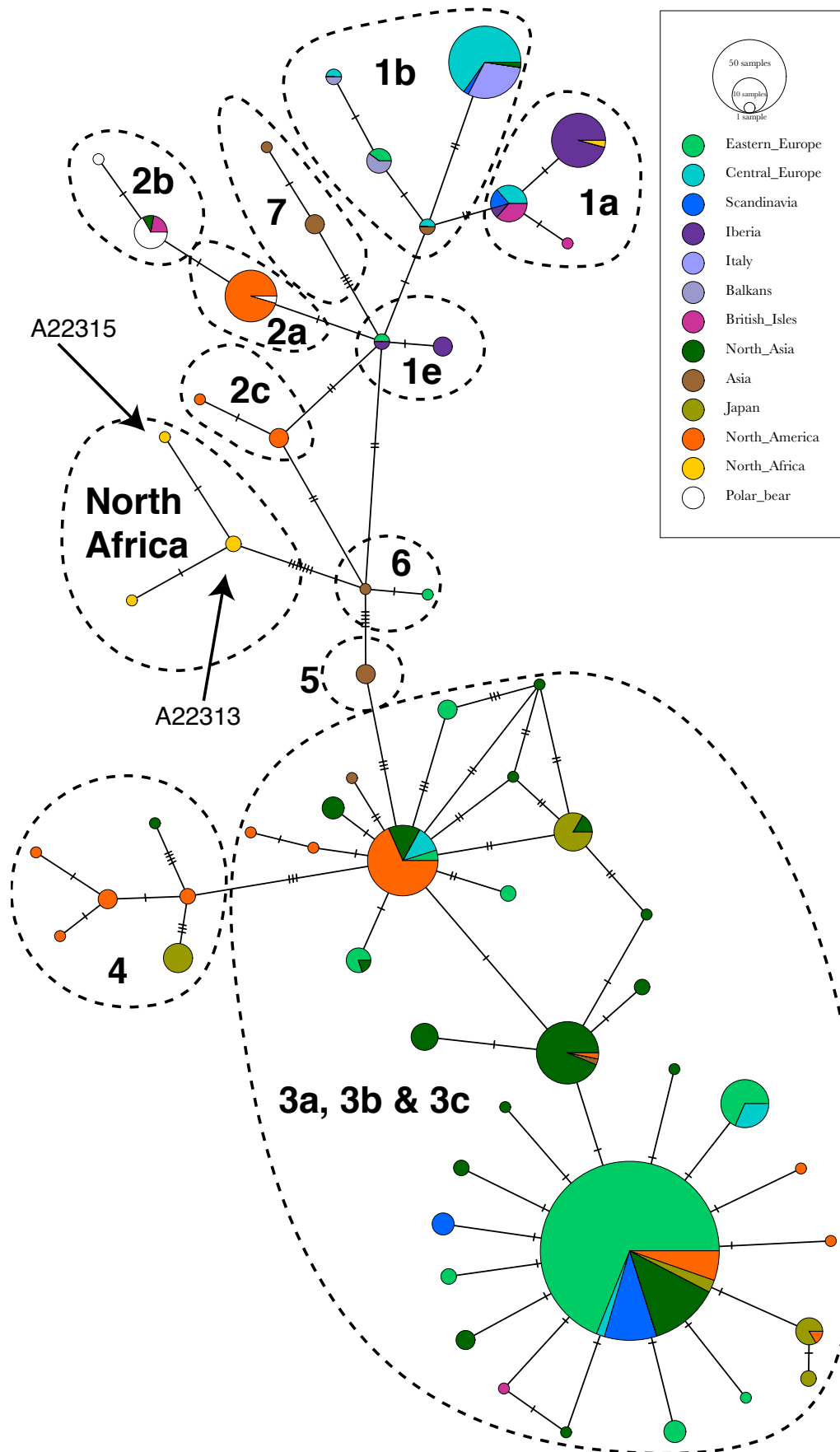


Figure S7: Median-joining haplotype network for brown and polar bear 278bp cytochrome *b* mitochondrial gene fragment. The placement of A22313 and A22315 is indicated with arrows.

5.3 SUPPLEMENTARY INFORMATION

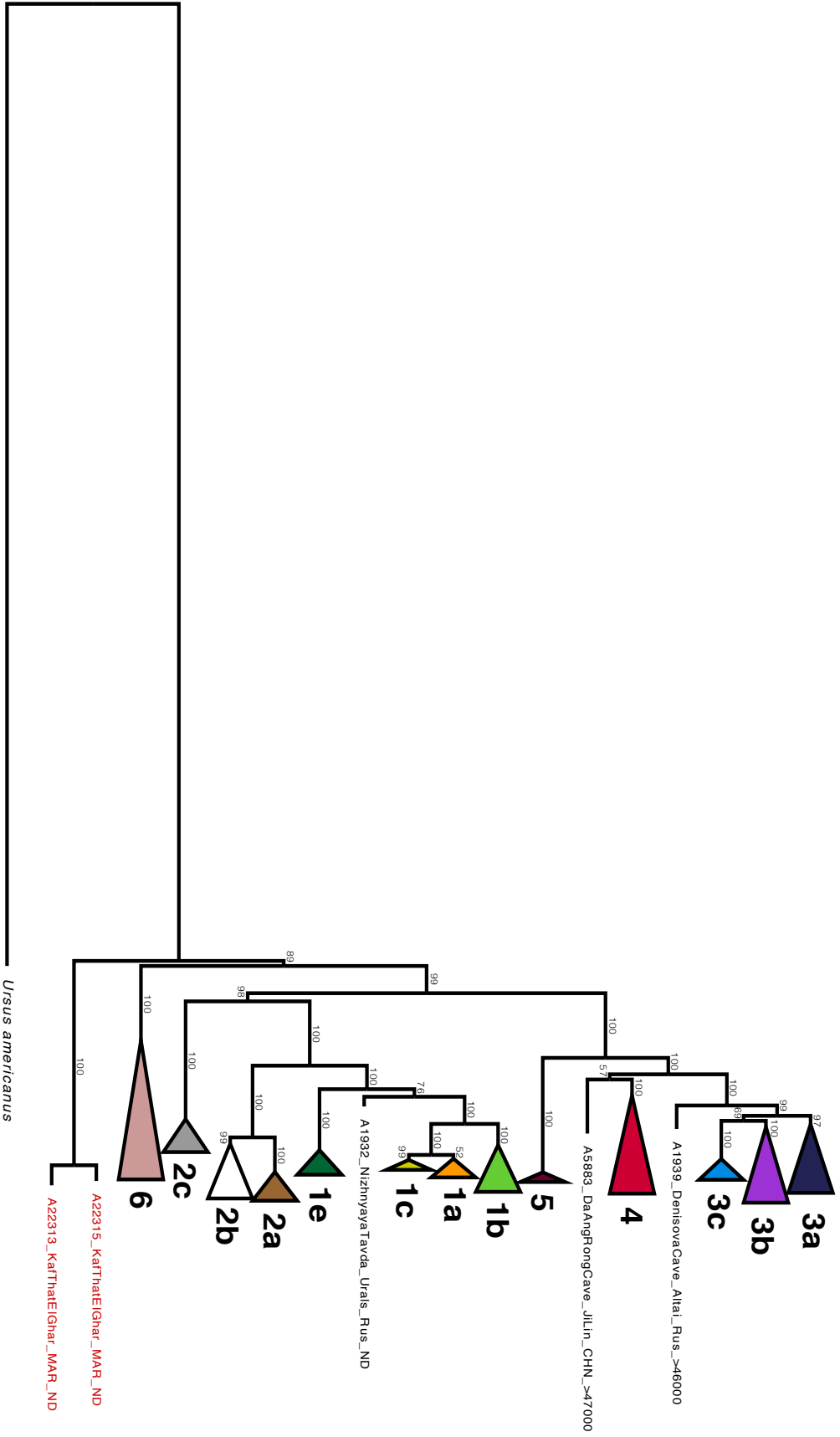


Figure S8: Maximum likelihood tree based on 527 near-complete brown and polar bear mitogenomes constructed in RAXML using the American black bear (*Ursus americanus*) as outgroup. Branch labels represent bootstrap support percentages. The two North African samples that were not included in final BEAST analyses are highlighted in red, showing their basal position within the tree.

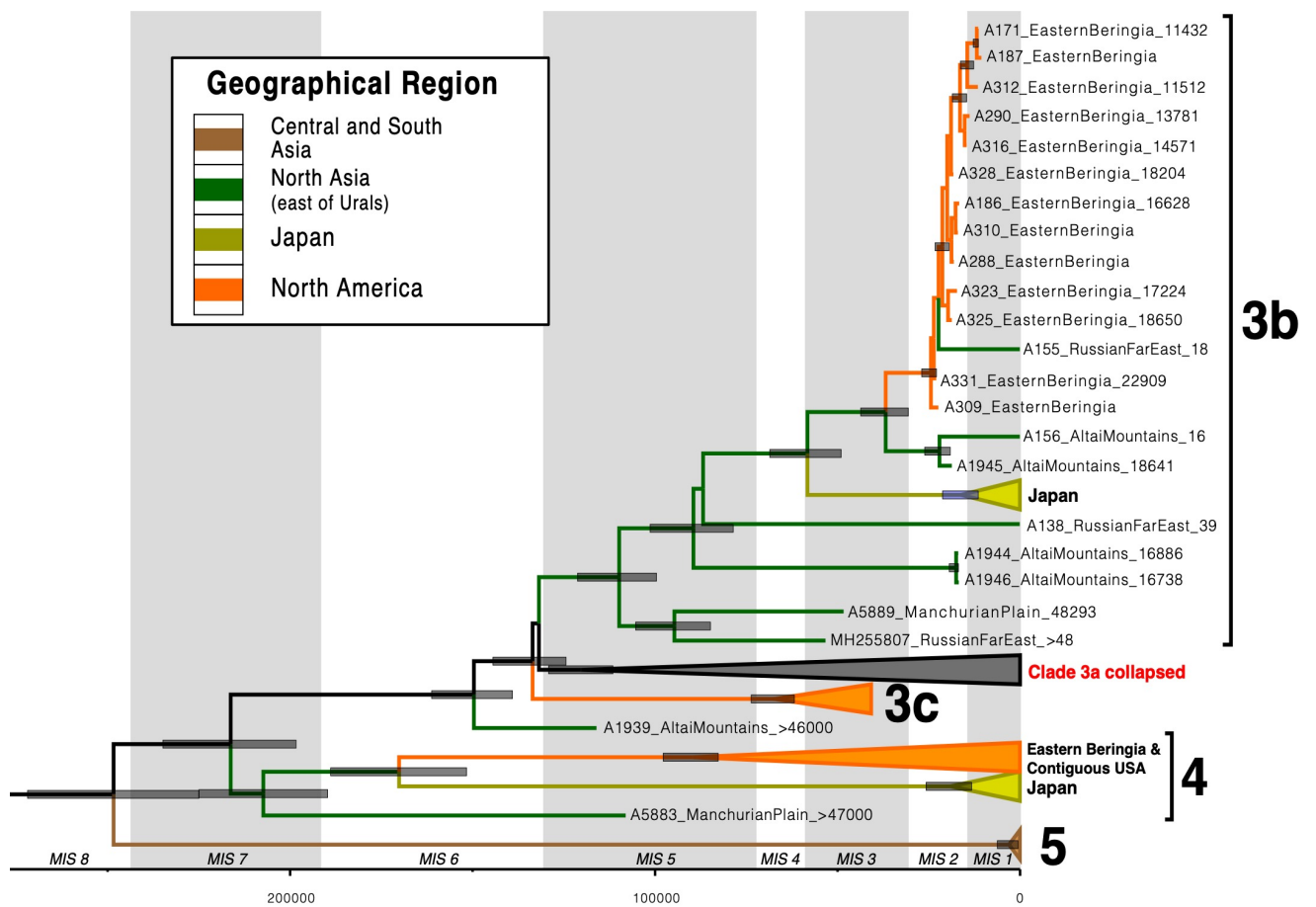


Figure S9: Bayesian phylogenetic tree of eastern lineage brown bears inferred from mitochondrial genomes. Clade 3a has been collapsed for ease of view. Mitochondrial clade is indicated on the right. Bars on nodes represent 95% Highest Posterior Densities for node age estimates indicated for nodes with >0.7 posterior support. Branches are coloured by geographic region.

5.3 SUPPLEMENTARY INFORMATION

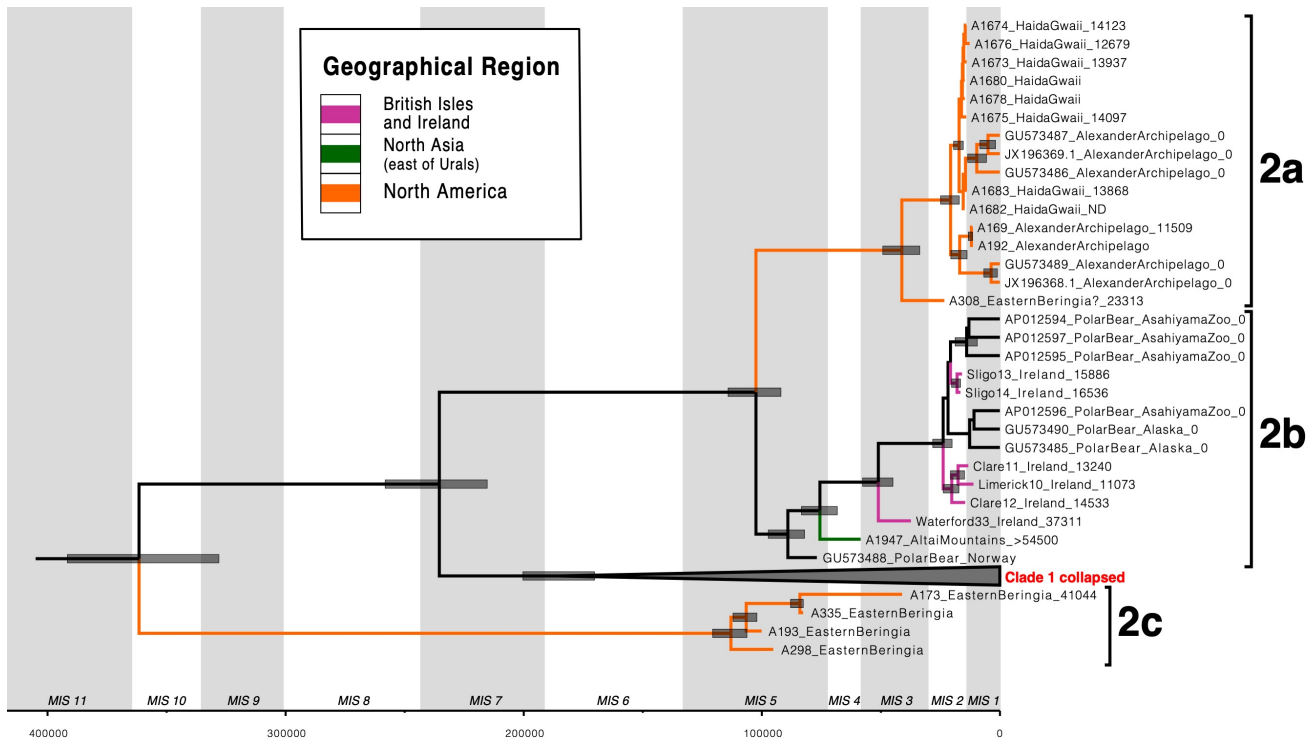


Figure S10: Bayesian phylogenetic tree of western lineage brown bears inferred from mitochondrial genomes. Clade 1 has been collapsed for ease of view. Mitochondrial clade is indicated on the right. Bars on nodes represent 95% Highest Posterior Densities for node age estimates indicated for nodes with >0.7 posterior support. Branches are coloured by geographic region.

Table S1: Information on brown bear bone and tooth samples analysed.

ACAD #	Museum/Institute	Museum/Field Accession	Country	Site	Carbon Date	Reference	Calibrated median	Calibrated sigma	Estimated Age	Standard Deviation	Haplotype
96	Institute of Plant and Animal Ecology	IPAE 915/869	Russia	Irtysh River	No Date				47279.42	2979.4276	3a
98	Institute of Plant and Animal Ecology	IPAE 178/440	Russia	Nizhnaya Taida	> 49700	OxA-39246			239000.00	33928.527	6
100	Institute of Plant and Animal Ecology	IPAE 253/843	Russia	Ignodivskaya	No Date				5451.85	3747.8171	3a
101*	Institute of Plant and Animal Ecology	IPAE 86/297	Russia	Lakseiskaya	No Date				2325.91	2289.7333	3a
103	Museum of Natural History Vienna	VNMH H1977-18-2	Austria	Brunnenschacht	2821 +/- -28	OxA 35021	2921	38			1b
104	Museum of Natural History Vienna	VNMH H-90-64	Austria	Flunkerhöhle	No Date				2431.19	1930.2422	1b
105	Museum of Natural History Vienna	VNMH H-1988-62b	Austria	Bärenhöhle in den Arzmauern	No Date				10794.48	2603.8873	1b
106	Museum of Natural History Vienna	VNMH H1975-43-1	Austria	Schwabenreithöhle	No Date						Cave bear
107	Museum of Natural History Vienna	VNMH H-1990-62-1	Austria	Seckarhöhle	9845 +/- 45	OxA-35023	11245	41			1b
108	Museum of Natural History Vienna	VNMH H1978-15-1	Austria	Felis-schacht	No Date				7727.49	2770.9528	1b
109	Museum of Natural History Vienna	VNMH H-1977-21-2	Austria	Notentalhöhle	5325 +/- 40	VERA-4523	6102	69			1b
110	Museum of Natural History Vienna	VNMH H1976-7	Austria	Dixlücke	No Date				14083.23	2125.3334	1b
111*	Museum of Natural History Vienna	VNMH H83-1-4	Austria	Turkenloch	No Date				1668.68	1320.4476	1b
112	Museum of Natural History Vienna	VNMH no #	Austria	Burianhöhle	4744 +/- 25	Hd-29330	5523	72			1b
113	Museum of Natural History Vienna	VNMH H-1983-47-1	Austria	Bärenkammer	1466 +/- 22	Hd-29305	1350	23			1b
114	Museum of Natural History Vienna	VNMH 3724	Austria	Gruberlocher	1805 +/- 35	VERA-4524	1740	56			1b
115	Museum of Natural History Vienna	VNMH H-74-13-1	Austria	Bärenhöhle in den Arzmauern	2264 +/- 40	Erl-13095	2241	60			1b
116	Museum of Natural History Vienna	VNMH H-1974-10-3	Austria	Rabenmaurhöhle	3643 +/- 41	Erl-13092	3961	64			1b
117	Museum of Natural History Vienna	VNMH H-1964-9	Austria	Napflücke	9985 +/- 57	Erl-13094	11457	128			1c
118	Museum of Natural History Vienna	VNMH H93-12	Austria	Gemshöhle	3135 +/- 33	OxA-35020	3360	50			1b
119	Museum of Natural History Vienna	VNMH H-86-178-1	Austria	Bärenloch	1985 +/- 35	VERA-4522	1935	39			3a
120	Museum of Natural History Vienna	VNMH H90-7-3	Austria	Windorgel	3321 +/- 40	Erl-13093	3549	52			1b
121	Museum of Natural History Vienna	VNMH H89-27-1	Austria	Schoberbergsschacht	848 +/- 21	Hd-29303	754	26			1b
122	Museum of Natural History Vienna	VNMH H1964-29-5	Austria	Kohlerwandhöhle	No Date				5696.53	2397.1701	1b
123	Museum of Natural History Vienna	VNMH H-1985-98-1	Austria	Bärenloch	2530 +/- 20	CURL-10276	2627	80			1b
124	Museum of Natural History Vienna	VNMH H1973-19-3	Austria	Sinterkamin	1176 +/- 23	Hd-29304	1111	45			1b
125	Museum of Natural History Vienna	VNMH H1983-6-3	Austria	Turkenloch	No Date				1663.85	1300.6221	1b
126*	Museum of Natural History Vienna	VNMH H90-103-11	Austria	Knochenrohre	No Date				1066.34	1216.3643	1b
127	Museum of Natural History Vienna	VNMH H-93-12a	Austria	Gemshöhle	3130 +/- 35	VERA-4525	3353	52			1b
128	Museum of Natural History Vienna	VNMH H1985-19-6	Austria	Turkenloch	No Date				1628.31	1268.3574	1b
130	Museum of Natural History Vienna	VNMH 2842-7	Austria	Laufenberg	9810 +/- 70	GrN-22339	11228	91			1c
135	Zoological Museum of Moscow Uni	MMZ S51937	Russia	Turkmenia, Ashkhabad - Zoo	Historic 1935						low/noDNA
143	Zoological Museum of Moscow Uni	MMZ S60146	Russia	Kuril isles, Iturup island	Historic 1955						low/noDNA
147	Zoological Museum of Moscow Uni	MMZ S3077	Russia	Vologda province	Historic 1913						1b
158	Zoological Museum of Moscow Uni	MMZ S66352	Russia	Pechoro-Ilych Nature Reserve	Historic 1954						3a
159	Zoological Museum of Moscow Uni	MMZ S580867	Russia	Sakhalin island	Historic 1967						3a
160	Zoological Museum of Moscow Uni	MMZ S34951	Russia	Krasnoyarsk region, Mana river	Historic 1911						3a
161	Zoological Museum of Moscow Uni	MMZ S14938	Russia	Stavropol, Chechnya	Historic 1912						3a
162	Zoological Museum of Moscow Uni	MMZ S20651	Russia	Baikal lake, Barguzin Nature Reserve, Sosnovka	Historic 1934						3a
163	Zoological Museum of Moscow Uni	MMZ S14896	Russia	Stavropol, Chechnya	Historic 1913						3a
178	Canadian Museum of Nature	NMC 7760a	Italy	Sardinia	No Date						low/noDNA
191	Institute of Zoology, Almaty	2814	Kazakhstan	Cave Pobeda	No Date						Cave bear
196	Institute of Zoology, Almaty	2699	Kazakhstan	South Central Kazakhstan	No Date				6020.19	3594.6708	3a
199	Smithsonian	no #	Italy	Cavern De Ualo	No Date						low/noDNA
338	National Museum of Scotland	NMS.Z.1962.63 (juvenile)	Scotland	Bear Cave	2673 ± 54	BM-724	2791	46			1a
339	National Museum of Scotland	NMS.Z.1962.63 (adult)	Scotland	Bear Cave	2673 ± 54	BM-724	2791	46			1a
347*	Institute of Plant and Animal Ecology	IPAE 250/13	Russia	Ekaterinberg	No Date				2074.51	2165.7802	3a
350*	Institute of Plant and Animal Ecology	IPAE 86/297	Russia	Ekaterinberg	No Date				2406.54	2431.1847	3a
360*	Institute of Plant and Animal Ecology	IPAE 88/1419	Russia	Ekaterinberg	No Date				2595.86	2488.7006	3a
409	Institute of Plant and Animal Ecology	No #	Russia	Ekaterinberg	No Date				5286.63	3788.1801	3a
410	Institute of Plant and Animal Ecology	No #	Russia	Ekaterinberg	2816 +/- 35	OxA-12910	2918	47			low/noDNA
411*	Institute of Plant and Animal Ecology	No #	Russia	Ekaterinberg	No Date				1336.42	1475.2461	3a
1744	University of Oslo	Bu-1982-2	Norway	Undisclosed cave	No Date				8790.46	2752.9571	3a
1745	University of Oslo	Bu-1982-1	Norway	Undisclosed cave	3600 +/- 80	T-6264	3910	115			3a
1746	University of Oslo		Norway	Undisclosed cave	420 +/- 90	T-8088	448	91			3a
1747	University of Oslo	JS-455	Norway	Undisclosed cave	2550 +/- 100	T-8087	2603	128			low/noDNA
1748	University of Oslo	HM 50	Norway	Undisclosed cave	1839 +/- 90	Ua-1925	1760	105			3a
1750	University of Oslo	RM-2392	Norway	Undisclosed cave	2440 +/- 20	Ua-1920	2475	105			3a
1751	University of Oslo	RM-418 B	Norway	Undisclosed cave	No Date				2711.06	1655.0567	3a
1752	University of Oslo	B-77-N-9-4	Norway	Undisclosed cave	1310 +/- 30		1252	35			3a
1753	University of Oslo	B-77-N-8-1	Norway	Undisclosed cave	1660 +/- 100	Ua-1926	1568	117			3a
1754	University of Oslo	RS-030986	Norway	Undisclosed cave	6210 +/- 100	T-7024	7104	124			3a
1755	University of Oslo	B-78-B-1	Norway	Undisclosed cave	2870 +/- 80	T-4155	3004	109			3a
1756	University of Oslo	B-77-G-5-7	Norway	Undisclosed cave	4420 +/- 70	T-4157	5035	128			3a
1757	University of Oslo	RM-1858	Norway	Undisclosed cave	4370 +/- 40	T-4654	4934	67			3a
1758	University of Oslo	RM-903	Norway	Undisclosed cave	2240 +/- 190	Ua-1924	2260	243			3a
1759	University of Oslo	B-81-S-1 A	Norway	Undisclosed cave	No Date				4188.91	1329.4132	3a
1760	University of Oslo	RM-418 A	Norway	Undisclosed cave	2340 +/- 200	Ua-1918	2395	247			3a
1761	University of Oslo	RM-3188 A	Norway	Undisclosed cave	3980 +/- 180	Ua-1923	4447	254			3a
1769	University of Oslo	B-80-G-1-A	Norway	Undisclosed cave	820 +/- 80	T-4156	755	75			3a
1770	University of Oslo	B-81-S-1-B	Norway	Undisclosed cave	3970 +/- 60	T-4655	4434	100			3a
1771	University of Oslo	BU-1982-3	Norway	Undisclosed cave	4340 +/- 200	Ua-1919	4953	279			3a
1772	University of Oslo	B1979-N-320	Norway	Undisclosed cave	2800 +/- 160	Ua-1927	2950	199			3a
1773	University of Oslo	82-9-11-5a	Norway	Undisclosed cave	3150 +/- 120	T-4901	3359	152			3a
1774	University of Oslo	HA-88-2	Norway	Undisclosed cave	No Date				3487.09	2041.3449	3a
1916	Institute of Plant and Animal Ecology	IPAE 802/699	Russia	Zylische Sokola	>50000						Asian Black bear
1917	Institute of Plant and Animal Ecology	IPAE 915/393	Russia	Irtysh River, Kholotny	No Date				41642.00	7347.3371	3a
1919	Institute of Plant and Animal Ecology	IPAE No #	Russia	Jalutazouk	No Date				62121.52	8582.6229	3a
1921	Institute of Plant and Animal Ecology	IPAE 915/1015	Russia	Irtysh River, Kholotny	37900 +/- 900	OxA-35016	42208	715	39357.33	5674.4189	3a
1922	Institute of Plant and Animal Ecology	IPAE No #	Russia	Urals, Zylische Sokola	>50000				63161.96	9921.1489	3a
1923	Institute of Plant and Animal Ecology	IPAE 915/1471	Russia	Irtysh River, Kholotny	No Date						Cave bear

5.3 SUPPLEMENTARY INFORMATION

Table S1 cont.

ACAD #	Museum/Institute	Museum/Field Accession	Country	Site	Carbon Date	Reference	Calibrated median	Calibrated sigma	Estimated Age	Standard Deviation	Haplotype
1924	Institute of Plant and Animal Ecology	IPAE 705/517	Russia	Urals, Tain Cave	14995±65	OxA-35068	18221	105	14559.11	4856.0528	3a
1925	Institute of Plant and Animal Ecology	IPAE No #.	Russia	Urals, Usolevskaya Cave	>50000						Cave bear
1928	Institute of Plant and Animal Ecology	IPAE 915/1185	Russia	Irtys River, Kholotny	No Date				27969.36	4516.7369	3a
1929	Institute of Plant and Animal Ecology	IPAE 915/1014	Russia	Irtys River, Kholotny	No Date				7285.44	4146.7797	3a
1930	Institute of Plant and Animal Ecology	IPAE No #.	Russia	Usolevskaya Cave	>50000						Cave bear
1931	Institute of Plant and Animal Ecology	IPAE No #.	Russia	Usolevskaya Cave	No Date						Cave bear Clade 1
1932	Institute of Plant and Animal Ecology	IPAE 178/316	Russia	NizhnayaTavda	> 54900	OxA-39368			147000.00	15696.729	Basal
1933	Institute of Plant and Animal Ecology	IPAE 705/517	Russia	Urals, Tain Cave	>46700				89886.89	10743.317	3a
1934	Institute of Plant and Animal Ecology	IPAE No #.	Russia	Usolevskaya Cave	> 55300	OxA-39367			73911.56	7494.4783	3a
1935	Institute of Plant and Animal Ecology	IPAE No #.	Russia	Urals, Zylische Sokola	>50000						low/noDNA
1936	Institute of Plant and Animal Ecology	IPAE 178/604	Russia	Nizhnaya Tavda	No Date						low/noDNA
1937	Institute of Archaeology Russian Academy of Sciences	No #	Russia	Altai, Denisova Cave	No Date						Hyena
1938	Institute of Archaeology Russian Academy of Sciences	No #	Russia	Altai, Denisova Cave	No Date						Hyena Clade 3
1939	Institute of Archaeology Russian Academy of Sciences	No #	Russia	Altai, Denisova Cave	>46000				116000.00	13091.286	Basal
1940	Institute of Archaeology Russian Academy of Sciences	No #	Russia	Altai, Denisova Cave	No Date						Hyena
1947	Institute of Archaeology Russian Academy of Sciences	No #	Russia	Altai, Razboinichya Cave	> 54500	OxA-39369			58444.94	10976.619	2b
2199	Australian National University		France	Payre cave	No Date						Low/noDNA
2204	Australian National University		France	Payre cave	No Date						Low/noDNA
2206	Australian National University		France	Payre cave	No Date						Low/noDNA
2309	University of Oslo	KJ91-2a	Norway	Undisclosed cave	No Date						Low/noDNA
2310	University of Oslo	B-197?-N- 1a	Norway	Undisclosed cave	No Date				2840.74	1695.6471	3a
2311	University of Oslo	FAU-05	Norway	Undisclosed cave	No Date				2410.37	1310.8774	3a
3643	Museum of Natural History Vienna	No #	Austria	Allander Tropfsteinhöhle	10870±/-80	?	12763	74			1b
3644	Museum of Natural History Vienna	No #	Austria	Wolfhöhle	6615±/-45	VERA-0836	7506	39			1b
3645	Museum of Natural History Vienna	No #	Germany	Neue Laubenstein-Barenhöhle	11872±/-92	Erl-7851	13686	114			1b
3646	Museum of Natural History Vienna	No #	Italy	Grotta d'Ernesto	11900±/-33	Gd-6182	13724	61			1c
3647	Museum of Natural History Vienna	No #	Switzerland	Höhle 92/2 Barenloch	9700±/-80	ETH-12785	11092	141			1c
3648 [#]	Museum of Natural History Vienna	No #	Switzerland	Höhle 92/2	9700±/-80	ETH-12785	11092	141			1c
3649	Museum of Natural History Vienna	No #	Switzerland	Barengaben hintersilberen	3275±/-50	ETH-31380	3506	57			1b
3650	Museum of Natural History Vienna	No #	Switzerland	Barengaben Hintersilberen	4135±/-50	ETH-31320	4676	89			1b
3651	Museum of Natural History Vienna	No #	Austria	Feistritzgrotte	2935±/-25	VERA-2193	3094	48			1b
3927	Zoological Museum Copenhagen	ZMK 52/1942	Denmark	Dyrhojgards Mose	No Date				15385.02	4611.8503	1a
3928	Zoological Museum Copenhagen	ZMK 170/1980	Denmark	Fauro Knold	No Date				5859.46	2914.8065	1b
3929	Zoological Museum Copenhagen	ZMK 1/1846	Denmark	Homsted Sogn	No Date				4617.98	2296.3192	1b
3930	Zoological Museum Copenhagen	ZMK 2/1918	Denmark	Svaerdborg I.	No Date						Brown bear (low DNA)
3931	Zoological Museum Copenhagen	ZMK 9/1861	Denmark	Virksund	5310±/-20	NSRL-15954	6081	54			1b
3932	Zoological Museum Copenhagen	ZMK 17/1980	Denmark	Oreso Molle	No Date				8788.62	3909.1114	1a
5872 [#]	Geological Survey of Sweden	SGU7712	Sweden	Ugglap	No Date						1a
11725	National Museum of Scotland		UK	Claonaite, Sutherland	11625±/-40	SUERC-26400					1a
11726	National Museum of Scotland		UK	Claonaite, Sutherland	45000±/-1000	SUERC-26399					3a
11727	National Museum of Scotland		UK	Claonaite, Sutherland	No Date						Low/noDNA
16509		Vb87 L13	Spain	Valdegoba Burgos	~ 80,000				75751.72	8093.9662	1c
16510		MV4 K399	France	Mont Ventoux	1570 ± 35		1466	43			1a
16511		CM-GE SI(?)31	Spain	Cueva mayor	17 440 ± 425		21107	535			1e
22304		UE14 Cuadro 620 Sector 1.4,5,7,8 SMTLL10 Metatarso 2. Neolithic	Spain	Els Trocs	No Date				6504.52	2320.7526	1a
22305		UE10 Cuadro 526 Sector 1.4,7,8 SMTLL7 Metatarso 3. Neolithic	Spain	Els Trocs	5314 ± 23	OxA-39365	6084	55			1a
22306		UE10 Cuadro 556 Sector 1-6 SMTLL8 Metatarso 4. Neolithic	Spain	Els Trocs	5288 ± 23	OxA-39248	6081	59			1a
22307		UE10 Cuadro 586 Sector 2 SMTLL9 Metatarso 5. Neolithic	Spain	Els Trocs	No Date				6560.52	2455.3919	1a
22308		UE1 Cuadro 1A SMTLL4 Astragalo. Neolithic	Spain	Els Trocs	No Date				6432.01	2258.4199	1a
22309		UE1 Cuadro 586 Sector 1-6,9 SMTLL8 Calcaneo. Neolithic	Spain	Els Trocs	No Date				6431.12	2238.8371	1a
22310		Nivel 2, Corte- Ecsultura, Escalon II, Metatarso 4. Edad del hierro (Iron Age)	Spain	Cerro de la Mesa	No Date						Low/noDNA
22311		-	Spain	Las Cogotas	No Date						Low/noDNA
22312		-	Spain	Cueva de Alkerdi (alckerdi Cave)	No Date						Low/noDNA
22313*		UE1029 Falange 1	Morocco	Kaf That El Ghar	No Date						North African Clade
22314		Campaña 2012 Corte 26G UE 1024 Falange 1	Morocco	Kaf That El Ghar	No Date						Low/noDNA
22315*		Campaña 2012 Corte 26G UE 1024 Canino Inferior	Morocco	Kaf That El Ghar	No Date						North African Clade
22316		MZ91 UE68 Nivel 6 Cuadrícula B2 Metatarso 4, Neolítico B (Intrusion Pleistoceno)	Spain	Cueva de los Murcielagos	No Date						Low/noDNA
22317		MZ91 UE93 Nivel 8N Marrón Cuadrícula A0-1 Falange 2, Paleolítico Superior	Spain	Cueva de los Murcielagos	No Date				48482.04	18519.356	1c
22318		MZ91 UE96 Nivel 10B Cuadrícula A0-1 Falange 3, Paleolítico Superior	Spain	Cueva de los Murcielagos	No Date						Low/noDNA
22319		MZ93 UE127 Nivel 6 Cuadrícula B3 Costillas, Neolítico B (Intrusion Pleistoceno)	Spain	Cueva de los Murcielagos	No Date						Low/noDNA
22320		MZ93 UE173 Nivel 8F Cuadrícula At Menapolo Metatarso 4, Neolítico A (Intrusion Pleistoceno)	Spain	Cueva de los Murcielagos	No Date						Low/noDNA
22321		MZ93 UE204 Nivel 8 Cuadrícula B5 Ulna, Neolítico A (Intrusion Pleistoceno)	Spain	Cueva de los Murcielagos	No Date						Brown bear (low DNA)
22322 [#]		MZ93 UE229 Nivel 9 Gravas Cuadrícula B5 Costilla, Paleolítico superior	Spain	Cueva de los Murcielagos	No Date						1e

Table S1 cont.

ACAD #	Museum/Institute	Museum/Field Accession	Country	Site	Carbon Date	Reference	Calibrated median	Calibrated sigma	Estimated Age	Standard Deviation	Haplotype
22323		MZ93 UE244 Nivel 10 Cuadrícula A2 Molar 1	Spain	Cueva de los Murcielagos	> 47100	OxA-39247			51440.00	19722.91	1e
22324		MZ93 UE245 Nivel 9C Cuadrícula B4-5 Mentarso 1, Paleolítico superior?	Spain	Cueva de los Murcielagos	No Date						Low/noDNA
22325 ^f		MZ93 UE250 Nivel 10 Cuadrícula B4-5 Molar 3, Paleolítico medio	Spain	Cueva de los Murcielagos	No Date						1e
22326		MZ93 UE255 Nivel 10 Cuadrícula A1-B3 Molar 2 superior, Paleolítico medio	Spain	Cueva de los Murcielagos	No Date				42337.91	18019.033	1e
22327		MZ93 UE263 Nivel 10E Cuadrícula A3 Canino superior, Paleolítico medio	Spain	Cueva de los Murcielagos	No Date						Low/noDNA

* Samples were excluded from final BEAST analyses due to failing date estimation requirements

Samples were excluded from BEAST analyses due to have mitochondrial coverage <85%

Table S2: Information on published read data downloaded from EMBL-EBI

Sample	SRA number/ EBI run accession number	Age	Location	mtDNA Clade	Reference
GP01	SRR935602, SRR935609, SRR935616, SRR935617, SRR941811, SRR941814	Modern	Glacier National Park, Montana, USA	Clade 4	Liu et al. (2014)
Kunashir1	SRR7408266, SRR7408267, SRR7408268	Modern	Kunashir Island, Russia	Clade 3b	Cahill et al. (2018)
Kunashir2	SRR7408269, SRR7408270	Modern	Kunashir Island, Russia	Clade 3b	Cahill et al. (2018)
Clare11	SRR7408246, SRR7408247, SRR7408248, SRR7408249	13240+/-116	Newhall Cave, Ireland	Clade 2b	Cahill et al. (2018)
Clare12	SRR7408250, SRR7408251, SRR7408258, SRR7408257	14533+/-355	Newhall Cave, Ireland	Clade 2b	Cahill et al. (2018)
Cork38	SRR7408288, SRR7408289, SRR7408290, SRR7408291	42232+/-431	Mammoth Cave, Ireland	Clade 1b	Cahill et al. (2018)
Leitrim4	SRR7408275, SRR7408277	4177+/-89	Pollnam Bear Cave, Ireland	Clade 1a	Cahill et al. (2018)
Leitrim5	SRR7408273, SRR7408274, SRR7408280	5946+/-130	Pollnam Bear Cave, Ireland	Clade 1a	Cahill et al. (2018)
Limerick10	SRR7408242, SRR7408243, SRR7408244, SRR7408245	11073+/-154	Red Cellar Cave, Ireland	Clade 2b	Cahill et al. (2018)
Sligo5	SRR7408276, SRR7408278, SRR7408279, SRR7408281	5416+/-128	Polldownin Cave, Ireland	Clade 1a	Cahill et al. (2018)
Sligo13	SRR7408255, SRR7408256, SRR7408261, SRR7408262	15886+/-166	Plunkett Cave, Ireland	Clade 2b	Cahill et al. (2018)
Sligo14	SRR7408254, SRR7408253, SRR7408259, SRR7408260	16536+/-275	Plunkett Cave, Ireland	Clade 2b	Cahill et al. (2018)
Waterford33	SRR7408284, SRR7408285, SRR7408286, SRR7408287	37311+/-780	Shandon Cave, Ireland	Clade 2b	Cahill et al. (2018)

5.3 SUPPLEMENTARY INFORMATION

Table S3: Information on mitogenomic sequences downloaded from GenBank.

GenBank Codes	Details	Reference
AP012559-AP012597	35 Modern brown bears from Japan, Kuril Islands, Sakhalin, Tibet, Russia, and Bulgaria as well as 4 polar bears.	Hirata et al. (2013)
GU573485-GU573491	Four Modern brown bears from Alexander Archipelago, two modern polar bears and one ancient polar bear from Svalbard	Lindqvist et al. (2010)
HQ685901-HQ685964	95 brown bears from European Russia, Estonia, and Finland. Note: some sequences were duplicated to match samples with identical sequences in the original study.	Keis et al. (2013)
JX196367-JX196369	Three modern Alaskan brown bears	Miller et al. (2012)
KX641315-KX641329, KX641336	15 mid-Holocene brown bears from northwestern Spain. One Pleistocene Austrian brown bear.	Fortes et al. (2016)
KY419593-KY419702	110 modern Eurasian brown bears	Anijalg et al. (2018)
MF593957-MF593979	Twelve modern Appenine brown bears, four brown bears from Greece, five from Slovakia, one from the Alps, and one from western Spain.	Benazzo et al. (2017)
MG066702, MG066702, MG066705	Three historic brown bears from the Tibetan Plateau–Himalaya region	Lan et al. (2017)
MH255807	Ancient brown bear (>48000) from Yakutia, Russia	Rey-Iglesia et al. (2019)

Table S4: Information on brown bear control region sequences downloaded from GenBank.

GenBank Codes	Details	Reference
AM411397-AM411403	Seven ancient North African and European brown bears	Calvignac et al. (2008)
EF488487-EF488505	Sixteen ancient European brown bears	Valdiosera et al. (2007)
EU400211-EU400176	Thirty-six Iberian brown bears	Valdiosera et al. (2008)
FN292971, FN292974, FN292976-FN292982	Nine historic and modern Middle Eastern brown bears	Calvignac et al. (2009)
HE657199-HE657216	Four North American brown bears and 14 European brown bears	Hailer et al. (2012)
HQ602651-HQ602653	Three modern Greek brown bears	Kocijan et al. (2011)
JF900158-JF900175	Fifteen ancient Irish brown bears	Edwards et al. (2011)
KJ638591-KJ638597	Seven modern Bulgarian brown bears	Frosch et al. (2014)
KM886400-KM886457	Fifty-eight historic Scandinavian brown bears	Xenikoudakis et al. (2015)
MK659705-MK659764	Sixty ancient European brown bear sequences	Ersmark et al. (2019)

Table S5: Information on brown bear cytochrome *b* sequences downloaded from GenBank.

GenBank Codes	Details	Reference
FJ792646	North American brown bear	Unpublished
FN292983-FN292993	Eleven modern and historic Middle Eastern brown bears	Calvignac et al. (2009)
EU567098-EU567120	Twenty-three modern Eurasian brown bears	Korsten et al. (2009)
AB020905-AB020909	Five modern Japanese brown bears	Matsushashi et al. (1999)
AM411404-AM411406, AM944505	Three North African brown bears and a European brown bear	Calvignac et al. (2008)
HG008039-HG008044	Six modern brown bears from the Russian Far East	Gus'kov et al. (2013)
L21879	Modern brown bear	Zhang and Ryder (1993)
U12855	Modern brown bear	Lento et al. (1995)
U18870-U18899	Thirty modern North American brown bears	Talbot and Shields (1996)
X82308	Modern brown bear	Arnason et al. (1995)

5.3 SUPPLEMENTARY INFORMATION

Table S6: Information on published carbon and nitrogen isotope sequences used in isotope analysis. In bold are the two bear specimens with uncertain provenance/species identification.

Lab. #	Field/Museum Accession	Species	d15N (‰)	d13C (‰)	Reference
OxA-9261	AMNH F:AM 30771	Brown bear	7.38	-19.8	Barnes et al. (2002)
OxA-9799	AMNH F:AM 95598	Brown bear	7.08	-18.2	Barnes et al. (2002)
OxA-9801	AMNH F:AM 95599	Brown bear	6.45	-19.1	Barnes et al. (2002)
AA-17509	AMNH F:AM 95601	Brown bear	3.3	-20.03	Barnes et al. (2002)
OxA-9767	AMNH F:AM 95609	Brown bear	7.66	-19.2	Barnes et al. (2002)
AA-17506	AMNH F:AM 95612	Brown bear	12.93	-16.8	Barnes et al. (2002)
OxA-9828	AMNH F:AM 95628	Brown bear	7.47	-18.5	Barnes et al. (2002)
OxA-9830	AMNH F:AM 95632	Brown bear	8.36	-18.6	Barnes et al. (2002)
OxA-9797	AMNH F:AM 95639	Brown bear	6.82	-19.0	Barnes et al. (2002)
OxA-9861	AMNH F:AM 95640	Brown bear	6.38	-19.6	Barnes et al. (2002)
OxA-9798	AMNH F:AM 95641	Brown bear	4.82	-18.4	Barnes et al. (2002)
OxA-9262	AMNH F:AM 95642	Brown bear	8.28	-18.5	Barnes et al. (2002)
OxA-9800	AMNH F:AM 95653	Brown bear	8.03	-17.8	Barnes et al. (2002)
OxA-9709	AMNH F:AM 95659	Brown bear	8.01	-18.5	Barnes et al. (2002)
OxA-9260	AMNH F:AM 95666	Brown bear	6.25	-19.5	Barnes et al. (2002)
OxA-9263	AMNH F:AM 95670	Brown bear	5.44	-19.4	Barnes et al. (2002)
OxA-9796	AMNH F:AM 95671	Brown bear	6.1	-18.9	Barnes et al. (2002)
OxA-9829	AMNH F:AM 95681	Brown bear	5.97	-19.4	Barnes et al. (2002)
AA-17507	AMNH 30422	Brown bear	10.31	-19.2	Barnes et al. (2002)
NA	CMN 35965	Brown bear	4.39	-19.82	Barnes et al. (2002)
NA	CMN 38279	Brown bear	6.70	-20.0	Barnes et al. (2002)
AA-17510	PM collected	Brown bear	9.07	-19.1	Barnes et al. (2002)
OxA-10036	A308/FAM 95657	Brown bear	21.47	-12.3	Barnes et al. (2002)
SCH-8	NA	Brown bear	3.3	-20.6	Bocherens et al. (2011)
SCH-9	NA	Brown bear	2.8	-20.3	Bocherens et al. (2011)
TUB-82	NA	Brown bear	4.0	-19.3	Bocherens et al. (2011)
TUB-56	NA	Brown bear	4.7	-18.7	Bocherens et al. (2011)
Goyet-A3-29	NA	Brown bear	9.0	-19.1	Bocherens et al. (2011)
Goyet-B4-33	NA	Brown bear	8.9	-19.9	Bocherens et al. (2011)
Goyet-B4-35	NA	Brown bear	4.6	-20.0	Bocherens et al. (2011)
Goyet-B4-36	NA	Brown bear	4.0	-20.3	Bocherens et al. (2011)
Goyet-B4-37	NA	Brown bear	6.2	-19.8	Bocherens et al. (2011)
NA	DGI-1	Brown bear	11.8	-20.2	Rey-Iglesia et al. (2019)
NA	CGG 1_0200005 / DGI-2	Brown bear	12	-19.9	Rey-Iglesia et al. (2019)
NA	CGG 1_0200006 / DGI-3	Brown bear	10.4	-19.8	Rey-Iglesia et al. (2019)
NA	DGI-4	Brown bear	9.3	-19.8	Rey-Iglesia et al. (2019)
NA	CGG 1_0200007 /DGI-5	Brown bear	9.65	-21.6	Rey-Iglesia et al. (2019)
OxA-39369	A1947/	Brown bear	5.33	-19.65	This Study
TUB-1	NA	Cave bear	4.0	-21.0	Bocherens et al. (2011)
TUB-2	NA	Cave bear	1.7	-20.8	Bocherens et al. (2011)
TUB-3	NA	Cave bear	2.9	-20.8	Bocherens et al. (2011)
TUB-4	NA	Cave bear	3.4	-21.0	Bocherens et al. (2011)
TUB-5	NA	Cave bear	2.5	-20.3	Bocherens et al. (2011)
TUB-6	NA	Cave bear	1.8	-20.8	Bocherens et al. (2011)
TUB-7	NA	Cave bear	3.0	-20.3	Bocherens et al. (2011)
TUB-9	NA	Cave bear	2.8	-21.0	Bocherens et al. (2011)
TUB-55	NA	Cave bear	3.9	-21.1	Bocherens et al. (2011)
TUB-10	NA	Cave bear	2.0	-21.2	Bocherens et al. (2011)
TUB-12	NA	Cave bear	2.3	-20.6	Bocherens et al. (2011)
TUB-13	NA	Cave bear	2.3	-21.1	Bocherens et al. (2011)
TUB-15	NA	Cave bear	2.3	-20.7	Bocherens et al. (2011)
TUB-16	NA	Cave bear	1.1	-20.9	Bocherens et al. (2011)
TUB-17	NA	Cave bear	3.0	-20.8	Bocherens et al. (2011)
TUB-18	NA	Cave bear	3.1	-21.2	Bocherens et al. (2011)
TUB-19	NA	Cave bear	2.8	-20.8	Bocherens et al. (2011)
TUB-54	NA	Cave bear	4.0	-21.5	Bocherens et al. (2011)
TUB-21	NA	Cave bear	4.2	-21.1	Bocherens et al. (2011)
TUB-22	NA	Cave bear	4.8	-21.3	Bocherens et al. (2011)
TUB-85	NA	Cave bear	2.8	-20.6	Bocherens et al. (2011)
TUB-86	NA	Cave bear	2.0	-20.5	Bocherens et al. (2011)
TUB-87	NA	Cave bear	2.9	-20.4	Bocherens et al. (2011)
TUB-89	NA	Cave bear	3.1	-20.9	Bocherens et al. (2011)
TUB-59	NA	Cave bear	3.2	-20.7	Bocherens et al. (2011)
TUB-62	NA	Cave bear	2.7	-21.1	Bocherens et al. (2011)
TUB-65	NA	Cave bear	4.2	-20.7	Bocherens et al. (2011)
TUB-67	NA	Cave bear	4.9	-20.9	Bocherens et al. (2011)
TUB-69	NA	Cave bear	3.2	-20.8	Bocherens et al. (2011)
TUB-70	NA	Cave bear	3.7	-20.9	Bocherens et al. (2011)
TUB-72	NA	Cave bear	4.0	-20.6	Bocherens et al. (2011)

Lab. #	Field/Museum Accession	Species	d15N (‰)	d13C (‰)	Reference
TUB-60	NA	Cave bear	2.9	-21.2	Bocherens et al. (2011)
TUB-61	NA	Cave bear	3.8	-20.8	Bocherens et al. (2011)
TUB-63	NA	Cave bear	3.6	-21.0	Bocherens et al. (2011)
TUB-66	NA	Cave bear	4.2	-21.1	Bocherens et al. (2011)
TUB-68	NA	Cave bear	4.4	-20.7	Bocherens et al. (2011)
TUB-88	NA	Cave bear	3.9	-20.8	Bocherens et al. (2011)
TUB-90	NA	Cave bear	4.1	-21.2	Bocherens et al. (2011)
TUB-64	NA	Cave bear	3.5	-21.1	Bocherens et al. (2011)
TUB-71	NA	Cave bear	4.3	-21.2	Bocherens et al. (2011)
Goyet-A2-3	NA	Cave bear	4.5	-22.1	Bocherens et al. (2011)
Goyet-A2-4	NA	Cave bear	3.4	-21.7	Bocherens et al. (2011)
Goyet-A2-5	NA	Cave bear	3.1	-21.6	Bocherens et al. (2011)
Goyet-A2-6	NA	Cave bear	3.0	-22.1	Bocherens et al. (2011)
Goyet-A3-20	NA	Cave bear	2.8	-21.8	Bocherens et al. (2011)
Goyet-A3-22	NA	Cave bear	2.6	-21.5	Bocherens et al. (2011)
Goyet-A3-23	NA	Cave bear	4.3	-21.9	Bocherens et al. (2011)
Goyet-A3-24	NA	Cave bear	4.9	-21.5	Bocherens et al. (2011)
Goyet-A3-25	NA	Cave bear	3.1	-21.4	Bocherens et al. (2011)
Goyet-A3-26	NA	Cave bear	5.8	-21.6	Bocherens et al. (2011)
Goyet-A3-27	NA	Cave bear	4.6	-21.5	Bocherens et al. (2011)
Goyet-A3-28	NA	Cave bear	5.3	-22.3	Bocherens et al. (2011)
Goyet-B4-9	NA	Cave bear	3.5	-21.3	Bocherens et al. (2011)
Goyet-B4-10	NA	Cave bear	4.4	-21.8	Bocherens et al. (2011)
Goyet-B4-11	NA	Cave bear	4.4	-20.9	Bocherens et al. (2011)
Goyet-B4-12	NA	Cave bear	3.7	-20.9	Bocherens et al. (2011)
Goyet-B4-13	NA	Cave bear	4.8	-21.0	Bocherens et al. (2011)
Goyet-B4-14	NA	Cave bear	4.5	-21.8	Bocherens et al. (2011)
Goyet-B4-15	NA	Cave bear	4.6	-21.0	Bocherens et al. (2011)
Goyet-B4-16	NA	Cave bear	6.0	-21.0	Bocherens et al. (2011)
Goyet-B4-17	NA	Cave bear	3.9	-20.8	Bocherens et al. (2011)
Goyet-B4-32	NA	Cave bear	5.2	-21.7	Bocherens et al. (2011)
Goyet-B4-34	NA	Cave bear	2.7	-22.0	Bocherens et al. (2011)
SC3100	NA	Cave bear	3.7	-22.5	Bocherens et al. (2011)
SC3200	NA	Cave bear	5.7	-22.1	Bocherens et al. (2011)
SC3300	NA	Cave bear	6.0	-22.2	Bocherens et al. (2011)
SC3500	NA	Cave bear	5.1	-21.8	Bocherens et al. (2011)
SC3600	NA	Cave bear	3.0	-21.8	Bocherens et al. (2011)
SC3700	NA	Cave bear	6.1	-22.0	Bocherens et al. (2011)
SC3800	NA	Cave bear	5.0	-22.2	Bocherens et al. (2011)
S-EVA-113	N34.157	Cave bear	7.8	-21.1	Richards et al. (2008)
S-EVA-114	N34.158	Cave bear	6.7	-21.4	Richards et al. (2008)
S-EVA-115	N32.30	Cave bear	6.7	-21.2	Richards et al. (2008)
S-EVA-116	N32.383	Cave bear	7.4	-21.6	Richards et al. (2008)
S-EVA-117	N33.271	Cave bear	7.8	-21.5	Richards et al. (2008)
S-EVA-121	O34.21	Cave bear	5.7	-21.2	Richards et al. (2008)
S-EVA-122	N32.401	Cave bear	9.6	-22	Richards et al. (2008)
S-EVA-123	N32.402	Cave bear	7.7	-21.5	Richards et al. (2008)
S-EVA-127	O33.79	Cave bear	8.1	-21.4	Richards et al. (2008)
S-EVA-128	O33.80	Cave bear	8.4	-21.4	Richards et al. (2008)
S-EVA-1514	GC	Cave bear	7.8	-21.7	Richards et al. (2008)
S-EVA-1517	GC	Cave bear	7.2	-21.6	Richards et al. (2008)
S-EVA-1520	GC-nest 6	Cave bear	3.6	-20.6	Richards et al. (2008)
S-EVA-1526	GC-nest 8	Cave bear	7.5	-21.4	Richards et al. (2008)
S-EVA-1530	M36.1	Cave bear	9.7	-22.1	Richards et al. (2008)
S-EVA-1534	M36.2	Cave bear	9	-22.1	Richards et al. (2008)
S-EVA-1537	SM-nest	Cave bear	8.4	-21.8	Richards et al. (2008)
S-EVA-1543	GL	Cave bear	8.1	-21.4	Richards et al. (2008)
S-EVA-1546	GL	Cave bear	9.8	-21.9	Richards et al. (2008)
OxA-15189	N37.147	Cave bear	7.8	-21.1	Richards et al. (2008)
OxA-15814	O35.28	Cave bear	9.7	-21.1	Richards et al. (2008)
CBV1	314	Cave bear	3.9	-21.5	Terlato et al. (2019)
CBV2	374	Cave bear	2.3	-20.4	Terlato et al. (2019)
CBV4	60	Cave bear	1.9	-20.4	Terlato et al. (2019)
CBV6	156	Cave bear	1.9	-20	Terlato et al. (2019)
CBV11	547	Cave bear	7.2	-22.2	Terlato et al. (2019)
CBV14	561	Cave bear	6	-22.1	Terlato et al. (2019)
CBV37	TR288	Cave bear	3.4	-21.2	Terlato et al. (2019)
CBV40	TR692	Cave bear	2.9	-20.7	Terlato et al. (2019)
CBV41	TR37	Cave bear	2.4	-20.2	Terlato et al. (2019)
CBV43	TR1166	Cave bear	2.1	-20.1	Terlato et al. (2019)
CBV47	TR387	Cave bear	5.4	-19.6	Terlato et al. (2019)
CBV52	TR439	Cave bear	4.2	-20.4	Terlato et al. (2019)
NA	UAM13789	Coastal brown bear	9.97	-18.93	Matheus (1995)
NA	UAM13791	Coastal brown bear	12.16	-17.04	Matheus (1995)

5.3 SUPPLEMENTARY INFORMATION

Lab. #	Field/Museum Accession	Species	d15N (‰)	d13C (‰)	Reference
NA	UAM13793	Coastal brown bear	13.5	-16.91	Matheus (1995)
NA	UAM13794	Coastal brown bear	4.37	-20.04	Matheus (1995)
NA	UAM13795	Coastal brown bear	8.87	-17.77	Matheus (1995)
NA	ADFG60	Coastal brown bear	1.13	-21.06	Matheus (1995)
NA	UAM13943	Coastal brown bear	12.39	-19.11	Matheus (1995)
NA	UAM13947	Coastal brown bear	16.03	-15.67	Matheus (1995)
NA	UAM13948	Coastal brown bear	8.91	-18.48	Matheus (1995)
NA	UAM13949	Coastal brown bear	12.95	-15.59	Matheus (1995)
NA	UAM13950	Coastal brown bear	14.1	-15.35	Matheus (1995)
NA	UAM13953	Coastal brown bear	12.99	-13.9	Matheus (1995)
NA	UAM13961	Coastal brown bear	12.89	-17.14	Matheus (1995)
NA	F-2967	Horse	5.5	-21.1	Kirillova et al. (2015)
NA	F-2968	Horse	5.6	-21.1	Kirillova et al. (2015)
NA	F-2969	Horse	7.7	-20.5	Kirillova et al. (2015)
NA	F-2970	Horse	8.9	-20.7	Kirillova et al. (2015)
NA	F-2971	Horse	6.6	-21.1	Kirillova et al. (2015)
NA	F-2972	Horse	5.9	-21	Kirillova et al. (2015)
NA	F-2974	Horse	5.9	-20.9	Kirillova et al. (2015)
NA	F-2976	Horse	9	-22	Kirillova et al. (2015)
NA	F-2977	Horse	5.5	-20.7	Kirillova et al. (2015)
NA	F-2979	Horse	5.4	-21.3	Kirillova et al. (2015)
NA	F-2982	Horse	5.8	-21	Kirillova et al. (2015)
NA	F-2987	Horse	6.2	-21.2	Kirillova et al. (2015)
NA	F-2988	Horse	6.6	-20.9	Kirillova et al. (2015)
NA	F-2989	Horse	6.1	-21.3	Kirillova et al. (2015)
NA	F-2990	Horse	3.7	-21	Kirillova et al. (2015)
NA	F-2993	Horse	6.7	-21.1	Kirillova et al. (2015)
NA	F-3002	Horse	7.7	-21.1	Kirillova et al. (2015)
NA	F-3058	Horse	6.9	-22	Kirillova et al. (2015)
NA	F-3059	Horse	8.9	-20.8	Kirillova et al. (2015)
CAMS119975	AMNH F:AM 142422	Horse	3	-21.5	Leonard et al. (2007)
CAMS119985	AMNH F:AM 142431	Horse	3.9	-21.1	Leonard et al. (2007)
CAMS119986	AMNH F:AM 142432	Horse	2.5	-21.5	Leonard et al. (2007)
CAMS119987	AMNH F:AM 142433	Horse	2.9	-20.7	Leonard et al. (2007)
CAMS119988	AMNH F:AM 142434	Horse	3.8	-21	Leonard et al. (2007)
CAMS120077	AMNH F:AM 60003	Horse	1.4	-21.3	Leonard et al. (2007)
CAMS119972	AMNH F:AM 60017	Horse	3.6	-21.6	Leonard et al. (2007)
CAMS119984	AMNH F:AM 60019	Horse	1.7	-21.5	Leonard et al. (2007)
CAMS120064	AMNH F:AM 60028	Horse	4.4	-20.6	Leonard et al. (2007)
CAMS120069	AMNH F:AM 60033	Horse	2.6	-20.9	Leonard et al. (2007)
CAMS120067	AMNH F:AM 60221	Horse	0.7	-21.7	Leonard et al. (2007)
CAMS-92078	IK01-080	Horse	5.4	-21.1	Mann et al. (2013)
CAMS-92079	IK01-121	Horse	6.8	-21.2	Mann et al. (2013)
CAMS-92081	IK01-150	Horse	7.2	-21.2	Mann et al. (2013)
CAMS-92083	IK01-183	Horse	5.3	-21.7	Mann et al. (2013)
CAMS-120717	IK01-218	Horse	6	-20.9	Mann et al. (2013)
CAMS-92089	IK01-282	Horse	4.5	-20.9	Mann et al. (2013)
CAMS-120646	IK01-320	Horse	5.6	-20.9	Mann et al. (2013)
CAMS-121733	IK01-320	Horse	5.6	-20.9	Mann et al. (2013)
CAMS-121736	IK01-368	Horse	7.6	-21.2	Mann et al. (2013)
CAMS-92093	IK01-369	Horse	5.9	-21.2	Mann et al. (2013)
CAMS-91957	IK01-459	Horse	7.6	-20.9	Mann et al. (2013)
CAMS-91959	IK02-026	Horse	1.7	-20.7	Mann et al. (2013)
CAMS-120650	IK02-072	Horse	7.7	-21.3	Mann et al. (2013)
Beta-331863	IK06-17	Horse	6.5	-20.9	Mann et al. (2013)
Beta-331865	IK07-06	Horse	5.8	-21.1	Mann et al. (2013)
Beta-331867	IK08-078	Horse	7	-20.6	Mann et al. (2013)
Beta-331868	IK08-079	Horse	5.7	-21.2	Mann et al. (2013)
Beta-331870	IK08-080	Horse	4.8	-21.1	Mann et al. (2013)
Beta-331869	IK08-082	Horse	7.4	-21	Mann et al. (2013)
Beta-331871	IK09-51	Horse	5.5	-21.6	Mann et al. (2013)
Beta-331873	IK10-074	Horse	5	-20.6	Mann et al. (2013)
Beta-331874	IK11-001	Horse	4.5	-20.8	Mann et al. (2013)
Beta-331875	IK12-010	Horse	4.3	-20.4	Mann et al. (2013)
Beta-331876	IK12-011	Horse	4.2	-20.9	Mann et al. (2013)
Beta-331877	IK12-015	Horse	6.4	-20.7	Mann et al. (2013)
Beta-339273	IK12-063	Horse	7.7	-20.5	Mann et al. (2013)
CAMS-91789	IK98-0009	Horse	5.9	-21	Mann et al. (2013)
CAMS-91790	IK98-0112	Horse	7.9	-21.1	Mann et al. (2013)
CAMS-120721	IK98-0288	Horse	6.8	-21.5	Mann et al. (2013)
CAMS-91791	IK98-0394	Horse	6	-21.4	Mann et al. (2013)
CAMS-91793	IK98-0539	Horse	7.9	-21.2	Mann et al. (2013)
CAMS-91796	IK98-1142	Horse	5.1	-21.1	Mann et al. (2013)
CAMS-91797	IK98-1176	Horse	5.1	-20.9	Mann et al. (2013)

Lab. #	Field/Museum Accession	Species	d15N (‰)	d13C (‰)	Reference
CAMS-91799	IK99-111	Horse	3.1	-20.8	Mann et al. (2013)
CAMS-91801	IK99-129	Horse	4.9	-20.3	Mann et al. (2013)
CAMS-120675	IK99-244	Horse	8.2	-20.6	Mann et al. (2013)
CAMS-91806	IK99-254	Horse	9.8	-21.2	Mann et al. (2013)
CAMS-120679	IK99-367	Horse	5.3	-20.6	Mann et al. (2013)
CAMS-120680	IK99-383	Horse	6.4	-21.3	Mann et al. (2013)
CAMS-120681	IK99-404	Horse	8.3	-22.1	Mann et al. (2013)
CAMS-92074	IK99-790	Horse	5.9	-20.7	Mann et al. (2013)
CAMS-92075	IK99-806	Horse	5.8	-20.8	Mann et al. (2013)
Beta-331879	KIK08-01	Horse	4.6	-21.6	Mann et al. (2013)
Beta-331880	KIK12-02	Horse	5.7	-21	Mann et al. (2013)
CAMS-91958	T02-001	Horse	3.7	-20.8	Mann et al. (2013)
CAMS-120712	T04-004	Horse	6.1	-21.3	Mann et al. (2013)
Beta-331884	TIT10-36	Horse	6.2	-21.4	Mann et al. (2013)
Beta-331885	TIT10-37	Horse	9.1	-20.9	Mann et al. (2013)
Beta-331886	TIT10-38	Horse	5.1	-21.3	Mann et al. (2013)
Beta-331888	TIT11-070	Horse	7.4	-20.6	Mann et al. (2013)
Beta-331889	TIT11-071	Horse	6.8	-20.9	Mann et al. (2013)
Beta-331890	TIT11-072	Horse	8.1	-21.7	Mann et al. (2013)
KSL-8	NA	Lion	5.4	-18.8	Bocherens et al. (2011)
KSL-9	NA	Lion	5.8	-18.5	Bocherens et al. (2011)
RAN-32lion	NA	Lion	7.0	-18.4	Bocherens et al. (2011)
TUB-73	NA	Lion	10.2	-18.8	Bocherens et al. (2011)
TUB-74	NA	Lion	8.4	-20.7	Bocherens et al. (2011)
TUB-75	NA	Lion	8.2	-18.1	Bocherens et al. (2011)
TUB-76	NA	Lion	7.9	-17.5	Bocherens et al. (2011)
Goyet-A2-7	NA	Lion	8.4	-18.5	Bocherens et al. (2011)
Goyet-A3-1	NA	Lion	8.4	-18.7	Bocherens et al. (2011)
Goyet-B5-1	NA	Lion	7.3	-18.7	Bocherens et al. (2011)
Goyet-B5-2	NA	Lion	9.6	-20.7	Bocherens et al. (2011)
Goyet-B5-3	NA	Lion	8.9	-19.2	Bocherens et al. (2011)
Goyet-B5-4	NA	Lion	6.3	-19.5	Bocherens et al. (2011)
NA	F-150	Lion	12.4	-19.8	Kirillova et al. (2015)
NA	F-2450	Lion	9.6	-19	Kirillova et al. (2015)
NA	F-2651	Lion	11.8	-20.4	Kirillova et al. (2015)
NA	F-2671	Lion	12	-19.1	Kirillova et al. (2015)
NA	F-2678/118	Lion	12.5	-19.8	Kirillova et al. (2015)
NA	F-2678/119	Lion	12.5	-19.9	Kirillova et al. (2015)
NA	F-2678/120	Lion	12.5	-19.9	Kirillova et al. (2015)
NA	F-2678/48	Lion	12.6	-19.9	Kirillova et al. (2015)
NA	F-2678/69	Lion	11.4	-19.2	Kirillova et al. (2015)
NA	F-278	Lion	12	-20.2	Kirillova et al. (2015)
AA-48271	IK01-112	Lion	7.8	-18.8	Mann et al. (2013)
CAMS-91784	IK02-164	Lion	11	-19.5	Mann et al. (2013)
CAMS-53910	IK98-436	Lion	8.8	-18.1	Mann et al. (2013)
Beta-339277	TIT12-07	Lion	9.2	-18.7	Mann et al. (2013)
OxA-13473 [#]	IK01-409	Lion	8.03	-18.5	Mann et al. (2013)
AMNH 42067	NA	Polar bear	21	-15.3	Horton et al. (2009)
AMNH 42068	NA	Polar bear	21	-15.5	Horton et al. (2009)
AMNH 15600	NA	Polar bear	18.8	-14.3	Horton et al. (2009)
AMNH 28105	NA	Polar bear	19.4	-15.3	Horton et al. (2009)
AMNH 22997	NA	Polar bear	18.9	-15.8	Horton et al. (2009)
AMNH 28104	NA	Polar bear	18.2	-14.6	Horton et al. (2009)
AMNH 34424	NA	Polar bear	21.8	-16.6	Horton et al. (2009)
AMNH 15601	NA	Polar bear	19.5	-14.6	Horton et al. (2009)
AMNH 80118	NA	Polar bear	19	-15.2	Horton et al. (2009)
AMNH 42081	NA	Polar bear	20.6	-14.9	Horton et al. (2009)
NMNH 275124	NA	Polar bear	20.4	-15.5	Horton et al. (2009)
NMNH 448769	NA	Polar bear	20.1	-13	Horton et al. (2009)
AMNH 34422	NA	Polar bear	21.3	-17.4	Horton et al. (2009)
NMNH 200770	NA	Polar bear	22.4	-16.4	Horton et al. (2009)
AMNH 14886	NA	Polar bear	19.4	-14.3	Horton et al. (2009)
NMNH 275117	NA	Polar bear	20.2	-15	Horton et al. (2009)
AMNH 42082	NA	Polar bear	19.5	-14.2	Horton et al. (2009)
MCZ 5792	NA	Polar bear	19.8	-15	Horton et al. (2009)
AMNH 42080	NA	Polar bear	21	-15.4	Horton et al. (2009)
AMNH 34423	NA	Polar bear	21.3	-16.7	Horton et al. (2009)
AmNH 34421	NA	Polar bear	21.6	-16.5	Horton et al. (2009)
NMNH 154207	NA	Polar bear	23.4	-16.3	Horton et al. (2009)
NMNH 154206	NA	Polar bear	23.5	-17.5	Horton et al. (2009)
AMNH 19255	NA	Polar bear	19.3	-15.1	Horton et al. (2009)
NMNH 13999	NA	Polar bear	22	-15.5	Horton et al. (2009)
NMNH 13361	NA	Polar bear	19.6	-13.1	Horton et al. (2009)
OxA-9259	CMN 49874	Short-faced bear	10.2	-17.9	Barnes et al. (2002)

5.3 SUPPLEMENTARY INFORMATION

Lab. #	Field/Museum Accession	Species	d15N (‰)	d13C (‰)	Reference
AA17511	AMNH F:AM 30492	Short-faced bear	8	-17.8	Fox-Dobbs et al. (2008)
AA17512	AMNH F:AM 30494	Short-faced bear	7.7	-17.8	Fox-Dobbs et al. (2008)
AA17513	AMNH A-37-10	Short-faced bear	9.5	-18.3	Fox-Dobbs et al. (2008)
AA17514	AMNH 99209	Short-faced bear	8.5	-18.1	Fox-Dobbs et al. (2008)
NA	NMC 7438	Short-faced bear	10.31	-18.49	Matheus (1995)
NA	NMC 36236	Short-faced bear	9.79	-18.07	Matheus (1995)
NA	NMC 37577	Short-faced bear	9.74	-18.96	Matheus (1995)
NA	FAM 30492	Short-faced bear	8.04	-17.80	Matheus (1995)
NA	FAM 30494	Short-faced bear	6.97	-18.14	Matheus (1995)
NA	FAM 95607	Short-faced bear	8.23	-18.10	Matheus (1995)
NA	FAM 99209	Short-faced bear	8.54	-18.12	Matheus (1995)
NA	FAM 127688	Short-faced bear	6.60	-17.63	Matheus (1995)
NA	FAM 127691	Short-faced bear	9.37	-19.04	Matheus (1995)
NA	FAM 127699	Short-faced bear	8.57	-18.79	Matheus (1995)
NA	AMNH30494	Short-faced bear	7.66	-17.82	Matheus (1995)
NA	A-37-10	Short-faced bear	9.51	-18.26	Matheus (1995)
NA	A-197-2972	Short-faced bear	8.37	-18.13	Matheus (1995)
NA	A-556	Short-faced bear	8.01	-18.49	Matheus (1995)
NA	L-gs-33	Short-faced bear	8.25	-18.39	Matheus (1995)
NA	"Birch"	Short-faced bear	8.04	-18.07	Matheus (1995)

References:

- Anijalg, P., Ho, S.Y.W., Davison, J., Keis, M., Tammeleht, E., Bobowik, K., Tumanov, I.L., Saveljev, A.P., Lyapunova, E.A., Vorobiev, A.A., Markov, N.I., Kryukov, A.P., Kojola, I., Swenson, J.E., Hagen, S.B., Eiken, H.G., Paule, L., Saarma, U., 2018. Large-scale migrations of brown bears in Eurasia and to North America during the Late Pleistocene. *J. Biogeogr.* 45, 394-405.
- Arnason, U., Bodin, K., Gullberg, A., Ledje, C., Mouchaty, S., 1995. A molecular view of pinniped relationships with particular emphasis on the true seals. *J. Mol. Evol.* 40, 78-85.
- Barnes, I., Matheus, P., Shapiro, B., Jensen, D., Cooper, A., 2002. Dynamics of Pleistocene population extinctions in Beringian brown bears. *Science* 295, 2267-2270.
- Benazzo, A., Trucchi, E., Cahill, J.A., Delsler, P.M., Mona, S., Fumagalli, M., Bunnefeld, L., Cornetti, L., Ghirotto, S., Girardi, M., Ometto, L., Panziera, A., Rota-Stabelli, O., Zanetti, E., Karamanlidis, A., Groff, C., Paule, L., Gentile, L., Vila, C., Vicario, S., Boitani, L., Orlando, L., Fuselli, S., Vernesi, C., Shapiro, B., Ciucci, P., Bertorelle, G., 2017. Survival and divergence in a small group: The extraordinary genomic history of the endangered Apennine brown bear stragglers. *Proc. Natl. Acad. Sci. U. S. A.* 114, E9589-E9597.
- Bocherens, H., Drucker, D.G., Bonjean, D., Bridault, A., Conard, N.J., Cupillard, C., Germonpre, M., Honeisen, M., Munzel, S.C., Napierala, H., Patou-Mathis, M., Stephan, E., Uerpmann, H.P., Ziegler, R., 2011. Isotopic evidence for dietary ecology of cave lion (*Panthera spelaea*) in North-Western Europe: Prey choice, competition and implications for extinction. *Quat. Int.* 245, 249-261.
- Cahill, J.A., Heintzman, P.D., Harris, K., Teasdale, M.D., Kapp, J., Soares, A.E.R., Stirling, I., Bradley, D., Edwards, C.J., Graim, K., Kisleika, A.A., Malev, A.V., Monaghan, N., Green, R.E., Shapiro, B., 2018. Genomic evidence of widespread

- admixture from polar bears into brown bears during the last ice age. *Mol. Biol. Evol.* 35, 1120-1129.
- Calvignac, S., Hughes, S., Hanni, C., 2009. Genetic diversity of endangered brown bear (*Ursus arctos*) populations at the crossroads of Europe, Asia and Africa. *Divers. Distrib.* 15, 742-750.
- Calvignac, S., Hughes, S., Tougard, C., Michaux, J., Thevenot, M., Philippe, M., Hamdine, W., Hanni, C., 2008. Ancient DNA evidence for the loss of a highly divergent brown bear clade during historical times. *Mol. Ecol.* 17, 1962-1970.
- Edwards, C.J., Suchard, M.A., Lemey, P., Welch, J.J., Barnes, I., Fulton, T.L., Barnett, R., O'Connell, T.C., Coxon, P., Monaghan, N., Valdiosera, C.E., Lorenzen, E.D., Willerslev, E., Baryshnikov, G.F., Rambaut, A., Thomas, M.G., Bradley, D.G., Shapiro, B., 2011. Ancient hybridization and an Irish origin for the modern polar bear matriline. *Curr. Biol.* 21, 1251-1258.
- Ersmark, E., Baryshnikov, G., Higham, T., Argant, A., Castanos, P., Doppes, D., Gasparik, M., Germonpre, M., Liden, K., Lipecki, G., Marciszak, A., Miller, R., Moreno-Garcia, M., Pacher, M., Robu, M., Rodriguez-Varela, R., Rojo Guerra, M., Sabol, M., Spassov, N., Stora, J., Valdiosera, C., Villaluenga, A., Stewart, J.R., Dalen, L., 2019. Genetic turnovers and northern survival during the last glacial maximum in European brown bears. *Ecol. Evol.* 9, 5891-5905.
- Fortes, G.G., Grandal-d'Anglade, A., Kolbe, B., Fernandes, D., Meleg, I.N., Garcia-Vazquez, A., Pinto-Llona, A.C., Constantin, S., de Torres, T.J., Ortiz, J.E., Frischauf, C., Rabeder, G., Hofreiter, M., Barlow, A., 2016. Ancient DNA reveals differences in behaviour and sociality between brown bears and extinct cave bears. *Mol. Ecol.* 25, 4907-4918.
- Fox-Dobbs, K., Leonard, J.A., Koch, P.L., 2008. Pleistocene megafauna from eastern Beringia: Paleoeological and paleoenvironmental interpretations of stable carbon and nitrogen isotope and radiocarbon records. *Palaeogeogr., Palaeoclimatol., Palaeoecol.* 261, 30-46.
- Frosch, C., Dutsov, A., Zlatanova, D., Valchev, K., Reiners, T.E., Steyer, K., Pfenninger, M., Nowak, C., 2014. Noninvasive genetic assessment of brown bear population structure in Bulgarian mountain regions. *Mamm. Biol.* 79, 268-276.
- Gus'kov, V.Y., Sheremet'eva, I.N., Seredkin, I.V., Kryukov, A.P., 2013. Mitochondrial cytochrome *b* gene variation in brown bear (*Ursus arctos* Linnaeus, 1758) from southern part of Russian Far East. *Russ. J. Genet.* 49, 1213-1218.
- Hailer, F., Kutschera, V.E., Hallstrom, B.M., Klassert, D., Fain, S.R., Leonard, J.A., Arnason, U., Janke, A., 2012. Nuclear genomic sequences reveal that polar bears are an old and distinct bear lineage. *Science* 336, 344-347.
- Hirata, D., Mano, T., Abramov, A.V., Baryshnikov, G.F., Kosintsev, P.A., Vorobiev, A.A., Raichev, E.G., Tsunoda, H., Kaneko, Y., Murata, K., Fukui, D., Masuda, R., 2013. Molecular phylogeography of the brown bear (*Ursus arctos*) in Northeastern Asia based on analyses of complete mitochondrial DNA sequences. *Mol. Biol. Evol.* 30, 1644-1652.

5.3 SUPPLEMENTARY INFORMATION

- Horton, T.W., Blum, J.D., Xie, Z.Q., Hren, M., Chamberlain, C.P., 2009. Stable isotope food-web analysis and mercury biomagnification in polar bears (*Ursus maritimus*). *Polar Res.* 28, 443-454.
- Keis, M., Remm, J., Ho, S.Y.W., Davison, J., Tammelaht, E., Tumanov, I.L., Saveljev, A.P., Mannil, P., Kojola, I., Abramov, A.V., Margus, T., Saarma, U., 2013. Complete mitochondrial genomes and a novel spatial genetic method reveal cryptic phylogeographical structure and migration patterns among brown bears in north-western Eurasia. *J. Biogeogr.* 40, 915-927.
- Kirillova, I.V., Tiunov, A.V., Levchenko, V.A., Chernova, O.F., Yudin, V.G., Bertuch, F., Shidlovskiy, F.K., 2015. On the discovery of a cave lion from the Malyy Anyui River (Chukotka, Russia). *Quat. Sci. Rev.* 117, 135-151.
- Kocijan, I., Galov, A., Cetkovic, H., Kusak, J., Gomercic, T., Huber, D., 2011. Genetic diversity of Dinaric brown bears (*Ursus arctos*) in Croatia with implications for bear conservation in Europe. *Mamm. Biol.* 76, 615-621.
- Korsten, M., Ho, S.Y.W., Davison, J., Pahn, B., Vulla, E., Roht, M., Tumanov, I.L., Kojola, I., Anderson-Lilley, Z., Ozolins, J., Pilot, M., Mertzanis, Y., Giannakopoulos, A., Vorobiev, A.A., Markov, N.I., Saveljev, A.P., Lyapunova, E.A., Abramov, A.V., Mannil, P., Valdmann, H., Pazetnov, S.V., Pazetnov, V.S., Rokov, A.M., Saarma, U., 2009. Sudden expansion of a single brown bear maternal lineage across northern continental Eurasia after the last ice age: a general demographic model for mammals? *Mol. Ecol.* 18, 1963-1979.
- Lan, T.Y., Gill, S., Bellemain, E., Bischof, R., Nawaz, M.A., Lindqvist, C., 2017. Evolutionary history of enigmatic bears in the Tibetan Plateau - Himalaya region and the identity of the yeti. *Proc. R. Soc. B.* 284.
- Lento, G.M., Hickson, R.E., Chambers, G.K., Penny, D., 1995. Use of spectral-analysis to test hypotheses on the origin of pinnipeds. *Mol. Biol. Evol.* 12, 28-52.
- Leonard, J.A., Vila, C., Fox-Dobbs, K., Koch, P.L., Wayne, R.K., Van Valkenburgh, B., 2007. Megafaunal extinctions and the disappearance of a specialized wolf ecomorph. *Curr. Biol.* 17, 1146-1150.
- Lindqvist, C., Schuster, S.C., Sun, Y.Z., Talbot, S.L., Qi, J., Ratan, A., Tomsho, L.P., Kasson, L., Zeyl, E., Aars, J., Miller, W., Ingolfsson, O., Bachmann, L., Wiig, O., 2010. Complete mitochondrial genome of a Pleistocene jawbone unveils the origin of polar bear. *Proc. Natl. Acad. Sci. U. S. A.* 107, 5053-5057.
- Liu, S.P., Lorenzen, E.D., Fumagalli, M., Li, B., Harris, K., Xiong, Z.J., Zhou, L., Korneliussen, T.S., Somel, M., Babbitt, C., Wray, G., Li, J.W., He, W.M., Wang, Z., Fu, W.J., Xiang, X.Y., Morgan, C.C., Doherty, A., O'Connell, M.J., McInerney, J.O., Born, E.W., Dalen, L., Dietz, R., Orlando, L., Sonne, C., Zhang, G.J., Nielsen, R., Willerslev, E., Wang, J., 2014. Population genomics reveal recent speciation and rapid evolutionary adaptation in polar bears. *Cell* 157, 785-794.
- Mann, D.H., Groves, P., Kunz, M.L., Reanier, R.E., Gaglioti, B.V., 2013. Ice-age megafauna in Arctic Alaska: extinction, invasion, survival. *Quat. Sci. Rev.* 70, 91-108.

- Matheus, P.E., 1995. Diet and co-ecology of Pleistocene short-faced bears and brown bears in eastern Beringia. *Quat. Res.* 44, 447-453.
- Matsuhashi, T., Masuda, R., Mano, T., Yoshida, M.C., 1999. Microevolution of the mitochondrial DNA control region in the Japanese brown bear (*Ursus arctos*) population. *Mol. Biol. Evol.* 16, 676-684.
- Miller, W., Schuster, S.C., Welch, A.J., Ratan, A., Bedoya-Reina, O.C., Zhao, F.Q., Kim, H.L., Burhans, R.C., Drautz, D.I., Wittekindt, N.E., Tomsho, L.P., Ibarra-Laclette, E., Herrera-Estrella, L., Peacock, E., Farley, S., Sage, G.K., Rode, K., Obbard, M., Montiel, R., Bachmann, L., Ingolfsson, O., Aars, J., Mailund, T., Wiig, O., Talbot, S.L., Lindqvist, C., 2012. Polar and brown bear genomes reveal ancient admixture and demographic footprints of past climate change. *Proc. Natl. Acad. Sci. U. S. A.* 109, E2382-E2390.
- Rey-Iglesia, A., Garcia-Vazquez, A., Treadaway, E.C., van der Plicht, J., Baryshnikov, G.F., Szpak, P., Bocherens, H., Boeskorov, G.G., Lorenzen, E.D., 2019. Evolutionary history and palaeoecology of brown bear in North-East Siberia re-examined using ancient DNA and stable isotopes from skeletal remains. *Sci. Rep.* 9, 4462.
- Richards, M.P., Pacher, M., Stiller, M., Quiles, J., Hofreiter, M., Constantin, S., Zilhao, J., Trinkaus, E., 2008. Isotopic evidence for omnivory among European cave bears: Late Pleistocene *Ursus spelaeus* from the Pesteră Cu Oase, Romania. *Proc. Natl. Acad. Sci. U. S. A.* 105, 600-604.
- Talbot, S.L., Shields, G.F., 1996. Phylogeography of brown bears (*Ursus arctos*) of Alaska and parapatry within the Ursidae. *Mol. Phylogenet. Evol.* 5, 477-494.
- Terlato, G., Bocherens, H., Romandini, M., Nannini, N., Hobson, K.A., Peresani, M., 2019. Chronological and isotopic data support a revision for the timing of cave bear extinction in Mediterranean Europe. *Hist. Biol.* 31, 474-484.
- Valdiosera, C.E., Garcia, N., Anderung, C., Dalen, L., Cregut-Bonnoure, E., Kahlke, R.D., Stiller, M., Brandstrom, M., Thomas, M.G., Arsuaga, J.L., Gotherstrom, A., Barnes, I., 2007. Staying out in the cold: glacial refugia and mitochondrial DNA phylogeography in ancient European brown bears. *Mol. Ecol.* 16, 5140-5148.
- Valdiosera, C.E., Garcia-Garitagoitia, J.L., Garcia, N., Doadrio, I., Thomas, M.G., Hanni, C., Arsuaga, J.L., Barnes, I., Hofreiter, M., Orlando, L., Gotherstrom, A., 2008. Surprising migration and population size dynamics in ancient Iberian brown bears (*Ursus arctos*). *Proc. Natl. Acad. Sci. U. S. A.* 105, 5123-5128.
- Xenikoudakis, G., Ersmark, E., Tison, J.L., Waits, L., Kindberg, J., Swenson, J.E., Dalen, L., 2015. Consequences of a demographic bottleneck on genetic structure and variation in the Scandinavian brown bear. *Mol. Ecol.* 24, 3441-3454.
- Zhang, Y.P., Ryder, O.A., 1993. Mitochondrial DNA sequence evolution in the Arctoidea. *Proc. Natl. Acad. Sci. U. S. A.* 90, 9557-9561.

Chapter 6

General Discussion

6.1 Thesis summary

6.1.1 Research summary

The use of ancient DNA (aDNA) has already contributed greatly to our understanding of faunal responses to climate and environmental change during the Late Quaternary, which would otherwise remain obscure. In my thesis I used phylogenetic, phylogeographic, and population genetic analyses to investigate a number of outstanding questions pertaining to the evolutionary history of bears. My results revealed pronounced responses to changes in the Pleistocene climate and environment and further add to the growing body of evidence suggesting hybridisation played a major role in the evolutionary history of bears. I further extended the methods I used to another non-model carnivoran, the lion (*Panthera (leo) spp.*), revealing analogous phylogeographic patterns to those observed in brown bears. Below I have summarised the findings of each of my chapters and discussed my findings in reference to the larger field of Quaternary biogeography.

6.1.2 Chapter 2: Lions and brown bears colonised North America in multiple synchronous waves of dispersal across the Bering Land Bridge

In Chapter 2, using phylogenetic analyses based on whole mitochondrial genomes, I identified multiple, synchronous waves of migration and extinction in Eastern Beringian brown bears (*Ursus arctos*) and lions (*Panthera spp.*). Phylogenetic model testing revealed that these migrations from Eurasia into North America were biased towards even-numbered marine isotope stages (MIS) — colder glacial periods — when the Bering Land Bridge was likely subaerial. The rate of migration was 13 times higher during these cold periods compared to that during odd-numbered MISs, when the Bering Land Bridge was likely submerged or highly erratic. Additionally, both taxa went extinct in Eastern Beringia during MIS 3, before subsequently reinvading during MIS 2 (the LGM), hinting at larger ecosystem changes during this warmer and wetter period before the LGM. Notably many endemic North American taxa, such as *Arctodus simus* and New World stilt-legged horses, survived this period. My results indicate that the Bering Land Bridge played a pivotal biogeographic role in the formation and maintenance of North America Pleistocene megafauna guilds. Further, my results also refined the timing of arrival of brown bears and lions in North America, pushing back the time of colonisation for brown

bears (from ~70 kya to ~177 kya), and nearly halving the inferred time of colonisation by lions (from ~340 kya to ~165 kya). The synchronicity of the patterns observed in both taxa suggest that my results are not a singular oddity but may reflect a wider pattern followed by taxa that invaded North America during the Pleistocene, with suggestions of similar patterns in other taxa such as foxes. These findings demonstrate the merit of using ancient DNA to investigate the response of megafauna to the ever-changing environment of the Pleistocene.

6.1.3 Chapter 3: Phylogeography of the extinct North American giant short-faced bear (*Arctodus simus*), with comments on their paleobiology

In Chapter 3 I investigated the phylogeography and taxonomy of the giant short-faced bear, *Arctodus simus*. Within *A. simus* two subspecies have been described, largely based on morphological size (Richards et al., 1996): the smaller *A. s. simus* and the larger *A. s. yukonensis*. However, the size variation on which these subspecies were described has also been argued to represent sexual dimorphism in a single taxon (Schubert, 2010; Schubert and Kaufmann, 2003). I produced mitochondrial genomes from 31 Late Pleistocene *A. simus* specimens representing both putative subspecies (or size morphs) and combine the data with size estimates and genetic sex estimation. I found no evidence for the existence of distinct subspecies of *A. simus* during the Late Pleistocene, with the sole *A. s. simus* specimen sampled nested within the mitochondrial phylogeny. I also found that, without exception, large specimens were males and small specimens were females. Notably, only females were found associated with cave sites, suggesting that this species may have used caves for denning. Further, *A. simus* lacked any clear phylogeographic signal in the Late Pleistocene and harboured relatively low mitogenomic diversity, comparable to diversity observed in severely bottlenecked species and long-ranging carnivores. These findings suggest that *A. simus* had experienced severe bottlenecks leading up to its extinction during the Pleistocene/Holocene transition or that its low genetic diversity was a result of its paleoecology: likely a long-ranging, solitary carnivore.

6.1.4 Chapter 4: Ancient genomes reveal hybridisation between extinct short-faced bears and the extant spectacled bear (*Tremarctos ornatus*)

Ursid phylogenetics has long been problematic, with studies showing discordance between mitochondrial and nuclear loci (Kumar et al., 2017; Kutschera et al., 2014; Pages

6.1 THESIS SUMMARY

et al., 2008). With the increasing use of whole genome data, much of the ursid phylogenetic tree has now been resolved, revealing an evolutionary history characterised by rapid speciation and hybridisation (Barlow et al., 2018; Kumar et al., 2017; Kutschera et al., 2014). However, research has largely focused on extant species, in particular ursine bears. In Chapter 4 I expanded our knowledge of ursid phylogenetics by focusing on the short-faced bears (Tremarctinae), sequencing whole genome data from two extinct taxa: *Arctodus simus* and *Arctotherium* sp. My results revealed further discordance between nuclear and mitochondrial data, with *A. simus* and the extant spectacled bear (*Tremarctos ornatus*) being more closely related according to most nuclear loci, whereas mitochondrial data suggests that the spectacled bear and *Arctotherium* are more closely related. I found that approximately one third of the genome data supported the mitochondrial topology, which combined with the results of genome-wide D-statistics, suggests extensive hybridisation. My findings suggest that mitochondrial-nuclear discordance among tremarctine bears likely stems from extensive hybridisation between the spectacled bear and one of the extinct short-faced bear lineages.

Additionally, I found support for hybridisation between the extant spectacled bear and ursine bears, while the extinct lineages did not show this pattern. This suggests that during the Pleistocene, spectacled bears hybridised with ursine bears — likely brown or American black bears (*Ursus americanus*) — despite their phylogenetic distance. This finding in addition to the extensive hybridisation revealed within short-faced bears adds to the growing evidence that hybridisation in the animal kingdom is common across deeply divergent taxa and suggests that widely accepted species concepts requiring reproductive isolation may need to be revisited.

6.1.5 Chapter 5: From Iberia to Siberia: Phylogeography and evolutionary history of Eurasian brown bears

In Chapter 5 I produced mitogenomes from subfossil brown bears across the Eurasian range of the species — from Western Beringia, the greatest extent of Siberia, to Iberia — and used these new data to refine the evolutionary history of brown bears. Using Bayesian phylogenetic analyses I resolved many of the deeper nodes within the brown bear phylogenetic tree and revealed finer scale population dynamics. This is the first study with extensive sampling of ancient and historic brown bear mitogenomes from Siberia, and

greatly increases the number of ancient and historic mitogenomes available, not only in terms of geography, but also phylogenetic representation. My results further support Asia (largely northern Asia) as a hotspot for the evolution of the brown bear. Brown bears are believed to have evolved in Asia from the Etruscan bear, with the oldest fossils being found in China (Kurtén, 1968; McLellan and Reiner, 1994; Pasitschniak-Arts, 1993). Clade 3 appears to have arisen in Siberia, splitting into three subclades during late MIS 6 or early MIS 5: clades 3a, 3b, and 3c, centred around the Urals/Caucasus region, Altai-Sayan region, and likely the Russian Far East respectively. Within these clades there were pronounced migrations out of their respective regions coinciding with drastic changes in environment, leading to migrations into North America and Europe. Compared to Russian bears, the evolutionary history of European bears is more recent, with a lot of pre-LGM diversity being replaced during the Pleistocene/Holocene transition. Although the patterns I observed do not strictly follow the traditional expansion/contraction (E/C) model of post-glacial colonisation, the hypothesis cannot be entirely rejected. Most of recent European brown bear diversity coalesces during the LGM or immediately post-LGM, indicative of expansions associated with the retreat of ice sheets and warming climate, emphasising the important role glacial fluctuations had on the biogeography of temperate species.

There has been a tendency in brown bear phylogeographic studies (this thesis included) to subdivide populations by mitochondrial clade membership (e.g., Clade 3a, Clade 4, Clade 1b, etc). This is likely an oversimplification of brown bear population dynamics and could be viewed as reductive. Although this would be a fatal practice in the study of many species, brown bears exhibit a strong degree of philopatry, and therefore, mitochondrial clades are often geographically structured and appear to reflect genuine demographic events (bottlenecks, migrations, etc.), as demonstrated in Chapter 2 and research investigating mitochondrial phylogeography in North American and Japanese brown bears (Barnes et al., 2002; Hirata et al., 2013; Leonard et al., 2000; Masuda et al., 1998; Waits et al., 1998). Ultimately, to ascertain whether the assumptions required to refer to populations by their mitochondrial clade membership are reasonable in brown bears, the population structure would need to be tested using nuclear markers. The addition of nuclear markers could potentially hint at vastly different population dynamics to those inferred from mitochondrial studies or reiterate and support the findings of mtDNA studies. However, even if nuclear markers conflict mtDNA evidence, it does not render past findings incorrect or obsolete, merely suggesting the maternal and paternal

6.2 SYNTHESIS AND GENERAL DISCUSSION

lineages underwent different demographic histories. Small-scale modern phylogeography studies utilising nuclear markers have found patterns both supporting (Norman et al., 2013; Xenikoudakis et al., 2015) and conflicting (Hirata et al., 2017; Tumendemberel et al., 2019) mitochondrial studies, with conflicts being interpreted as male-specific gene flow. However, no studies have used nuclear markers to test widespread phylogeographic patterns with the incorporation of ancient specimens from across the historic brown bear range (akin to the ancient sampling in Chapter 5).

6.2 Synthesis and General Discussion

6.2.1 Carnivore guilds of the Pleistocene: Diversity and niche partitioning

The role and importance of carnivores during the Pleistocene is often underestimated based off inferences drawn by comparison to the diversity of modern carnivore guilds, which are relatively depleted in both size and diversity (Dalerum et al., 2009; Van Valkenburgh et al., 2016). Today only two hypercarnivores (*i.e.* diet consisting of >80% animal protein) exist that exceed 100kg, the lion (*Panthera leo*) and tiger (*Panthera tigris*), the geographical ranges of which do not overlap. However, during the Pleistocene multiple hypercarnivores coexisted in the same ecosystems. For example, in North America, lions, dire wolves, sabre-toothed cats (*Smilodon*), scimitar-toothed cats (*Homotherium*), and giant short-faced bears (*Arctodus simus*) co-existed. Meanwhile in Eurasia, lions, scimitar-toothed cats, and massive spotted hyenas (or cave hyenas; *Crocota crocuta spelaea*) all coexisted. In addition to these hypercarnivores there were also more large omnivorous taxa such as brown bear and cave bears, and smaller predators such as wolves, lynx, wolverines, and foxes. Many of these extinct species, or extinct forms of extant species, were much larger than modern counterparts, and therefore could likely predate on much larger prey species. Intuitively, these large and diverse carnivore guilds were supported by a greater diversity of megaherbivores, with the estimated prey size ranges of many of these large Pleistocene hypercarnivores including infant and juvenile proboscideans (elephants and their extinct relatives such as mammoths and mastodons) (Van Valkenburgh et al., 2016).

In Chapter 2 I showed synchronous waves of migration into North America by two large carnivorans, lions (*Panthera spelaea*) and brown bear (*Ursus arctos*). These species were invading an area with an already diverse carnivore guild, which included *Smilodon*, *Homotherium*, dire wolves, and *Arctodus simus*. Notably, the association and interactions between *A. simus* and brown bears has been discussed previously, with some evidence indicating competition between the two taxa (Barnes et al., 2002; Steffen and Fulton, 2018). Comparing *A. simus* to lions and brown bears it is evident that *A. simus* does not show the same temporal phylogeographic patterns (see Chapter 3). This possibly indicates that *A. simus* populations were more established and stable in North America during the Late Pleistocene. Interestingly, when brown bears and lions went locally extinct in eastern Beringia during MIS 3, *A. simus* survived. This discrepancy may indicate that the ecological changes that caused the extirpation of brown bears and lions did not affect *A. simus* in the same way. Possibly *A. simus* was able to utilise prey species which did not experience the same population declines as other herbivores that lions and brown bears were not as efficient in hunting (for example, horses, which exhibit a more browsing lifestyle compared to other megaherbivores, which may be better supported by peatland type biomes).

In Chapter 2 I revealed that not only did brown bears and lions appear to go extinct during MIS 3 in eastern Beringia, not reinvading the region until MIS 2, but that *A. simus* appeared to be unaffected. In Chapter 3 I investigated *A. simus* phylogeography and notably found a relative lack of diversity, which I interpreted as either being the result of bottlenecks or a function of their ecological niche. Notably, within the *A. simus* dataset, most samples dated to less than 50 thousand years old (kya), with most diversity coalescing 77 kya. However, two specimens returned estimated ages greater than 100 kya. Indeed, these older specimens (ACAD 183 and ACAD 439) show more divergent haplotypes, suggesting genetic and haplotypic diversity may have been greater earlier in the Pleistocene. Furthermore, there does appear to be a temporal grouping of samples in Eastern Beringia, with samples younger than ~33 kya falling more tipward in the tree and with older samples falling more basal. Indeed, all Eastern Beringia samples younger than 33 kya coalesce 38 kya. This could indicate a haplotypic shift at this time, similar to that seen in brown bears (and lions) (Barnes et al., 2002), or a reduction in diversity leading up to the extinction of *A. simus* in Eastern Beringia by 20 kya. However, this observation could also be driven by five of the six samples from Cripple Creek in Alaska — all dating

6.2 SYNTHESIS AND GENERAL DISCUSSION

to older than 45 kya — grouping together in a more basal clade. The fact that these five samples are of similar age and are all closely genetically related may be suggestive of finer scale population structure at certain times during the Pleistocene.

It may be possible that *A. simus* experienced temporary local extinction during MIS 3 as well but was able to quickly recolonise from South of the Ice. This would be difficult to detect as I have demonstrated that *A. simus* lacks clear phylogeographic patterns, although there does appear to be a haplotypic shift in the Eastern Beringian population of *A. simus* around 33 kya, as described above. Alternatively, this situation could reflect competition between *A. simus* and both lions and brown bears in Eastern Beringia, where the niche of *A. simus* overlaps the niches of both lions and brown bears. With the ecological changes in Eastern Beringia, the environment may have switched to one where the landscape could no longer support a large number of megacarnivore populations, and as *A. simus* populations may have been more established (due to *A. simus* possibly having been exposed to glacial cycles *in situ* throughout its evolution) it was possibly able to outcompete both brown bears and lions. It has been previously suggested that *A. simus* likely dominated meat resources over brown bears in North America during the Pleistocene, supported by differences in dietary isotopes, which suggest that brown bears filled a less carnivorous niche when *A. simus* was present (Barnes et al., 2002; Bocherens et al., 1995; Matheus, 1995). If *A. simus* filled a more carnivorous niche, it is highly likely it would have competed for meat resources with lions, potentially stealing kills from lions in North America, a tactic that has been proposed for *A. simus* previously (Matheus, 1995; Matheus, 2003; Sorkin, 2006).

During MIS 2, as sea level fell and Bering Land Bridge once again connected Eurasia and North America, the landscape of Eastern Beringia cooled and dried, and peatlands were replaced with steppe environments, which supported larger megaherbivore communities (Mann et al., 2015), presumably allowing the reinvasion of brown bears and lions back into the region (Chapter 2). However, as these taxa were reinvading, *A. simus* went locally extinct. It is possible that the environmental conditions were unfavourable for *A. simus* populations at this time, although it might be expected that *A. simus* would have been exposed to similar environmental fluctuations throughout its evolution without being extirpated from the region. Competition with brown bears and/or lions may have played a part in the extirpation of *A. simus* from Eastern Beringia at this time. Lions and

brown bears had been coexisting in Eurasia for most of their evolutionary history, so it may be expected that the two taxa displayed sufficient niche partitioning to allow coexistence, where lions occupied a more active hypercarnivorous niche and brown bears occupied a more omnivorous, opportunistic niche. On the other hand, *A. simus* only coexisted with lions and brown bears when they first entered North America during MIS 6, with most of their evolutionary history being separate. The niche of *A. simus* is somewhat less clear, although much evidence points towards a more hypercarnivorous, potentially scavenger niche, likely with overlapping the niches of both lions and brown bears (Barnes et al., 2002; Matheus, 1995). Isotopes have also shown that the brown bears migrating into North America during MIS 2 had elevated N15 signal, indicative of a more carnivorous diet that may overlap with that of *A. simus*, resulting in more direct competition between the species (Barnes et al., 2002).

It must be noted that *A. simus* coexisted with brown bears and lions in Eastern Beringia for over 100 kya, beginning when the lions and brown bears invaded North America, likely during MIS 6 (Chapter 2). There has also been evidence for coexistence at sites across North America, with *A. simus* and brown bears found at the same sites at very similar times (Kurtén and Anderson, 1974; Steffen and Fulton, 2018). This suggests that there was likely at least some degree of niche partitioning between these taxa, which has been supported by isotopes (Barnes et al., 2002; Matheus, 1995). However, it may be that the changes in the palaeoenvironment during MIS 2 forced these taxa to become more direct competitors. One major factor that distinguishes MIS 2 from other glacial periods is that during this time humans arrived into Eastern Beringia likely for the first time (Ardelean et al., 2020; Hoffecker et al., 2016; Lesnek et al., 2018; Moreno-Mayar et al., 2018; Vachula et al., 2019; Waters, 2019). Human presence in the region may have been the defining factor in tipping the balance for human-naïve *A. simus* populations, causing them to be extirpated while brown bear and lion populations — that had been exposed to humans in Eurasia for thousands of years — were able to coexist. Undoubtedly, one of the key factors in the extinction of *A. simus* is the lack of a Holarctic distribution, without Eurasian populations as a source for replenishment, as seen in lions and brown bears (Chapter 2), bison (Froese et al., 2017; Shapiro et al., 2011), foxes (Kutschera et al., 2013; Statham et al., 2014), and potentially wolves (Loog et al., 2020) throughout the Late Pleistocene.

6.2 SYNTHESIS AND GENERAL DISCUSSION

Another widespread carnivore during the Pleistocene was the scimitar-toothed cat (*Homotherium*). It has been argued that scimitar-toothed cats went extinct in Eurasia during the Middle Pleistocene (Antón, 2013; Serangeli et al., 2015; Turner, 1997). However, a single Late Pleistocene specimen has been uncovered from the North Sea in Europe, dating to around 30 kya (Reumer et al., 2003). This Late Pleistocene sample was included in a recent study with samples from North America, which suggested they likely represented members of the same species (Paijmans et al., 2017). It has been argued that this specimen could represent a very small relict population surviving in Europe (Paijmans et al., 2017; Reumer et al., 2003), however, there is a temporal gap of over 200,000 years in the fossil record between this specimen and the next youngest, reliably dated specimens on the continent (Serangeli et al., 2015). Alternatively, it is possible the European specimen may have represented a migration from North America or Asia during the Late Pleistocene between 77–216 kya, replacing populations that went extinct during the Middle Pleistocene (Paijmans et al., 2017). This interval spans two major glacial stages corresponding to MIS 4 and 6, both of which were associated with migrations of brown bears and lions across the Bering Land Bridge into North America (Chapter 2). Although more Late Pleistocene *Homotherium* specimens from Eurasia and North America would need to be sampled to analyse the demographic scenario responsible for the observed pattern, it putatively appears that while brown bears and lions were invading North America from Eurasia, scimitar-toothed cats were reinvading Europe, possibly across the Bering Land Bridge in the opposite direction.

Population replacements have been further uncovered in grey wolves (*Canis lupus*), another carnivoran with a Holarctic distribution. Mitogenomic studies have revealed that extant grey wolves descend from a single Pleistocene population (Fan et al., 2016; Freedman et al., 2014; Skoglund et al., 2015), with Loog et al. (2020) suggesting that an expansion occurred ~25 kya from a Beringian or Northeast Asian population. This expansion appears to have replaced earlier Pleistocene populations throughout Eurasia and North America (Loog et al., 2020). Although it is possible this population may have originated in Eastern Beringia/North America, when interpreted alongside my data from brown bears and lions (Chapter 2), Western Beringia/Northeast Asia may be the more likely source. It appears that as brown bears and lions were reinvading Eastern Beringia during the LGM, grey wolves were likely doing the same. However, sampling of North American ancient specimens has been biased towards the end of the Pleistocene/Holocene,

meaning the possibility of earlier waves of migrations into North America analogous to brown bears and lions could not be investigated (Loog et al., 2020).

Chapter 2 may give the impression that Beringia was a form of a biotic highway, allowing the ubiquitous exchange of fauna between the old and new world. However, it is noteworthy that a number of otherwise widespread taxa never migrated across the Bering Land Bridge. Notably, within Carnivora, *A. simus* never migrated into Eurasia despite being a key member of the Eastern Beringian carnivore guild. While cave bears and cave hyenas never migrated into North America, despite being found in the Russian Far East (Baryshnikov, 2014; Boeskorov et al., 2012; Sher et al., 2011; Werdelin, 1991). This begs the question of why taxa such as brown bears, lions, wolves, foxes, wolverines, and (presumably) scimitar-toothed cats all crossed the Bering Land Bridge while the likes of *A. simus*, cave hyenas, and cave bears did not. The answer may lie in the ecological niches these taxa occupied. It may be that *A. simus* could never colonise Eurasia due to competitive exclusion. Two main theories on the ecological niche of *A. simus* have been proposed: 1) *A. simus* was a wide-ranging hypercarnivore (Barnes et al., 2002; Bocherens et al., 1995; Kurtén, 1967; Kurtén and Anderson, 1980; Matheus, 1995; Matheus, 2003), possibly with a high degree of scavenging (Matheus, 1995; Matheus, 2003; Sorkin, 2006), or 2) Some authors have argued that *A. simus* occupied a niche similar to cave bears of Eurasia, being relatively herbivorous (Emslie and Czaplewski, 1985; Figueirido et al., 2009; Figueirido et al., 2010; Sorkin, 2006). The latter hypothesis has been supported by a lack of tooth wear patterns that would otherwise be expected if the diet of *A. simus* included a large proportion of scavenging (Donohue et al., 2013; Emslie and Czaplewski, 1985; Figueirido et al., 2017). If *A. simus* did occupy a more herbivorous niche than has been previously assumed this could explain why neither cave bears nor *A. simus* migrated across the Bering Land Bridge: cave bears and *A. simus* may have been direct competitors. If the former hypothesis for the niche of *A. simus* is true, the niche of *A. simus* would potentially overlap largely with cave hyena (Stuart and Lister, 2014) and therefore may explain why cave hyenas never colonised North America. Although it currently appears cave hyenas did not occupy latitudes as far north as would be required to cross the Bering Land Bridge (Stuart and Lister, 2014; Werdelin, 1991), this may still explain why *A. simus* did not seem to establish populations in Eurasia.

6.2.2 Brown bear-polar bear relationship

Brown bears are mitochondrially paraphyletic, with polar bears nested within the diversity of brown bears (Cronin et al., 1991; Shields et al., 2000; Talbot and Shields, 1996). The extant polar bear clade 2b is sister to clade 2a brown bears from the ABC islands, a relationship that has been concluded to result from capture of a polar bear mitochondrial genome by brown bears (Cahill et al., 2013; Cahill et al., 2015; Edwards et al., 2011; Hailer et al., 2012; Miller et al., 2012). However, assuming clade 2a is of polar bear origin, polar bears still remain paraphyletic. This has been described as possibly the result of the original ancestral polar bear mtDNA lineage being replaced by that of brown bears (Hailer, 2015; Hailer et al., 2012; Hailer and Welch, 2016). In this case, the TMRCA of the split between clade 1 and clade 2a plus 2b would represent the timing of this initial introgression of a brown bear mitogenome into polar bears, here 240.2 kya (95% HPD: 218.7–263.6 kya; Chapter 5). It has also been suggested that the entirety of the western brown bear clade (clades 1 and 2) is of polar bear origin (*i.e.* clade 1 also represents an additional earlier major introgression of a polar bear mitochondrial clade into brown bears). In that case, clade 2a and clade 1 would represent separate introgression events of polar bear mitochondrial clades into brown bears, with the split between 2a and 2b representing the more recent introgression in North America (TMRCA: 102.2 kya, 95% HPD: 91.6–114.6 kya; Chapter 5), and the split between clade 1 and 2 representing the earlier introgression at 240.2 kya.

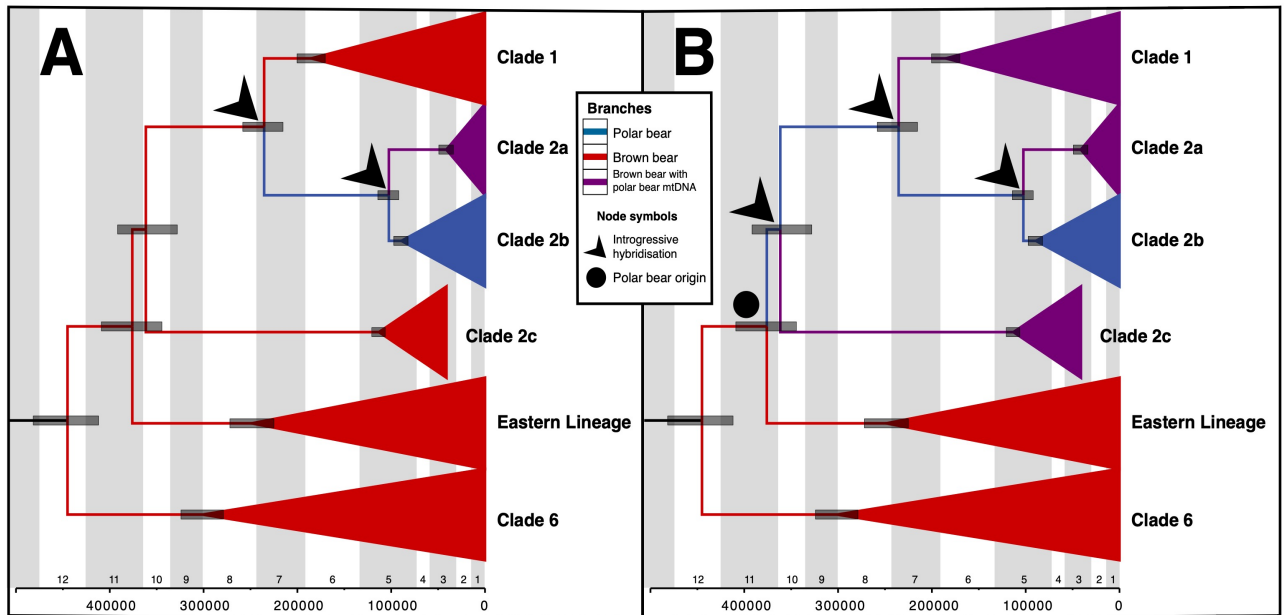


Figure 1: Mitochondrial phylogenies of brown and polar bears representing two hypotheses regarding the origin of western lineage clades. **(A)** The original polar bear mtDNA has not been sampled and the split of clade 1 with clade 2a and 2b represents introgressive hybridisation of brown bear mtDNA into polar bears, with subsequent capture of this clade 2a back into brown bears on the Alexander Archipelago. **(B)** As per Hassanin (2015) the split of the eastern and western lineages represents the speciation of polar bears from brown bears. Subsequently, clade 2c, 1 and 2a are captured by brown bears throughout the Pleistocene.

It is of note that clade 2 is not monophyletic (see Chapter 5), with clade 2c falling basal within the western lineage, sister to clade 1 and the rest of clade 2. Thus, under the hypothesis that the western brown bear clade is of polar bear origin we would expect clade 2c to represent another introgression of a polar bear mitochondrial genome into brown bears. Furthermore, under this hypothesis the split of eastern and western lineages would represent the divergence of brown and polar bears. In Chapter 5 we estimated this split at 376 kya (95% HPD: 344.4–409 kya), which lies within the credibility interval of more widely accepted population split estimates 343–479 kya (Hailer and Welch, 2016; Hassanin, 2015; Liu et al., 2014), but is considerably younger than other genomic estimates of the divergence of brown and polar bears (Kumar et al., 2017; Miller et al., 2012). Under this hypothesis, the original polar bear mtDNA lineage would still be nested within brown bears, due to the presence of Clade 6 in Asia and the extinct North African clade. However, this paraphyly is not necessarily surprising considering that these basal clades likely diverged before the evolution of polar bears from Eurasian brown bears isolated in the eastern Siberian arctic during a glacial period (Kurtén, 1964; McLellan and Reiner, 1994).

6.2 SYNTHESIS AND GENERAL DISCUSSION

Irrespective of the scenario that led to the patterns above, what is clear from both Chapter 2 and 5, as well as published data (Cahill et al., 2013; Cahill et al., 2018; Cahill et al., 2015; Edwards et al., 2011; Hailer, 2015; Hailer and Welch, 2016; Miller et al., 2012), is that the capture of polar bear mitogenomes appears to be ubiquitous across the northerly range of brown bears. During the Pleistocene, clade 2a was not only restricted to the ABC islands of Alaska as today but appears to have been found across the Alexander Archipelago, the Haida Gwaii archipelago, and possibly onto mainland Alaska (Chapter 2). Notably in Chapter 5 we recovered a clade 2b bear in the Altai Mountains. To eliminate the possibility that this Altai sample may actually be from a polar bear with incorrect provenance information, I compared the isotopic signature of the specimen to those of brown bears and polar bears (as well as other taxa). The isotopic signature of this specimen was typical of terrestrial brown bears, similar to other brown bears in the Altai region, and completely separate from those of polar bears, indicating this specimen is from a brown bear. Clade 2b has previously been found in ancient brown bears from Ireland, the result of hybridisation with polar bears (Cahill et al., 2018; Edwards et al., 2011). This Altai Clade 2b specimen indicates that brown bears likely hybridised with polar bears in other regions across their range, here likely in the Russian Arctic Circle where polar and brown bear ranges would have overlapped at different times during the Pleistocene. Hybrids dispersing out of the region likely carried this haplotype to the Altai Mountains, similar to hypotheses on how polar bear ancestry was dispersed from other hybridisation hotspots (Cahill et al., 2013; Cahill et al., 2018; Cahill et al., 2015).

For admixture studies, the use of a non-admixed “control” genotype is essential for accurate estimation of admixture rates and direction, and in many recent studies Swedish brown bear genomes have been used as a baseline (Cahill et al., 2018; Cahill et al., 2015; Schaefer et al., 2017). The implications of additional brown-polar bear admixture hotspots and the possibility of widespread hybridisation across the northerly range of brown bears means that these Swedish brown bears are unlikely to be unadmixed. Consequently, many estimates of admixture proportions are likely inaccurate and require adjustment. The use of a more reliable baseline would produce more accurate results concerning the nature and degree of admixture. Ancient individuals, or individuals from more southerly extents of the brown bear range (*e.g.*, Tibetan Plateau, Middle East) may provide a more reliable unadmixed baseline than currently available genomic data.

In Chapter 2, the addition of ancient clade 2a sequences from Haida Gwaii and Alexander Archipelagos allowed me to refine age of this brown bear clade in the Pacific Northwest, indicating that clade 2a brown bears have likely been present in the region for at least 20 thousand years (ky). Notably, I also recovered a clade 2a specimen from the LGM of the interior of Alaska (specifically the Fairbanks area). The provenance of this Fairbanks sample has been previously questioned, and stable isotopes suggest a marine origin of this specimen, therefore it seems likely that this specimen originates from the coast (Barnes et al., 2002). What remains unknown regarding this specimen is whether it represents a brown bear, polar bear, or a hybrid. Cahill et al. (2013)'s hypothesis was that clade 2a resulted from a conversion of a polar bear population into brown bears after being isolated in the Pacific Northwest at the end of the Pleistocene. Consequently, if this Fairbanks specimen is from a brown bear, or a hybrid, the capture of clade 2a in brown bear would be moved back to at least the LGM. If this sample is genetically a polar bear, then this could represent the original polar bear population of the Pacific Northwest that was eventually converted to predominantly brown bear ancestry by extensive migration of male brown bears into the region. Isotopic data I analysed in Chapter 5 placed this Fairbanks specimen well outside the isotopic range for brown bears and closer to that of modern polar bears, suggesting this sample likely represents a polar bear. Therefore, based on the current evidence, I favour the hypothesis that this specimen represents the original polar bear population.

6.2.3 Ancient DNA benefits museum collections

Throughout my thesis, I have demonstrated that ancient DNA is useful for revealing unknown information about samples, including the true species identification. In Chapters 2, 4, and 5, I revealed a number of specimens with incorrect species identification. This included misidentification of closely related species, such as putative brown bear samples that were actually cave bears, American black bears, or Asiatic Black bears, and putative *A. simus* specimens that were actually brown bears or American black bears. However, I also uncovered more surprising misidentifications. For example, when screening samples for Chapter 3, I found that several putative *A. simus* specimens were actually from lions, horses, and peccaries. Most notably in Chapter 3, one of the *A. simus* specimens analysed was actually from the enigmatic dire wolf (*Canis dirus*; Perri et al. (2021)), which had not previously been recorded from the site. Such misidentifications can have drastic impacts

6.2 SYNTHESIS AND GENERAL DISCUSSION

on the understanding of faunal assemblages from sites as these identifications involve species from completely different ecological niches.

Another noteworthy case of sample misidentification, which may have ecological explanations, was revealed in Chapter 2. Of the lion specimens that I extracted and sequenced, all the specimens that fell within the earlier, pre-LGM Eastern Beringian *Panthera spelaea* clade had been misidentified as brown bears. This finding is noteworthy as it may reflect morphological and ecological differences between the two different clades of *P. spelaea* that occupied Eastern Beringia during the Late Pleistocene. These earlier lions may have been larger, which resulted in their remains being misidentified as brown bears, a considerably more massive species. Measurement of these misidentified specimens, combined with isotopic analyses, may reveal whether these lions were larger on average, or the pattern of misidentification is purely coincidental. Differences in ecology between these temporally and genetically distinct populations of *spelaea* lions may not be entirely surprising. Isotopic analyses have revealed ecological difference between brown bears occupying pre-LGM Eastern Beringia and those from the LGM to present day (Barnes et al., 2002).

The advent of high-throughput sequencing has undoubtedly been essential in genetically identifying misidentified specimens. Traditional PCR and Sanger sequencing methods are likely to fail on misidentified specimens depending on the phylogenetic distance of misidentification and specificity of the primers used. High-throughput sequencing can also reveal other information about samples that may benefit museum collections. For example, genetic sexing was used by Gower et al. (2019) (see Appendix 1), revealing extensive biases in the sex ratios of mammalian fossil and museum collections. In both brown bears and bison, up to 75% of fossil specimens were male. Skewed sex ratios towards males have also been reported in mammoth collections (Pecnerova et al., 2017). In Appendix 1 we further showed that this deviation from a 1:1 sex ratio is pervasive across mammalian museum collections, with the majority of collections across all mammalian orders showing a bias towards males. We attributed this bias to the general characteristic in mammals that males have wider geographic ranges, increasing the geographic spread of remains and therefore chance of detection when randomly sampling across a landscape. Further sexual dimorphic behaviours and appearance were argued as possible further drivers of biased sex ratios. In Chapter 3 I

extended the examination of sex ratios to *A. simus* specimens, finding 55% of the specimens were male. This is much lower than the 75% observed in brown bear collections (Appendix 1) and suggests no discernible sex bias in collections from this species. The observation of no clear sex bias in the *A. simus* dataset further supports the idea discussed in Chapter 3 that female *A. simus* did not show strong philopatry, with females possibly dispersing equal distances to males. However, the sample size of *A. simus* (n=29) was much lower than those in Appendix 1, meaning that further sampling across the range of *A. simus* may be necessary to gain more accurate estimates of sex ratios.

I used Bayesian tip-dating analyses in three of my chapters, which involved both cross-validation methods and age estimation for specimens with no date information (or infinite radiocarbon dates). Cross-validation is done in order to determine whether a dataset has sufficient temporal information to estimate the age of undated specimens, however, it can also identify problematic radiocarbon dates. In Chapter 3, cross-validation allowed the identification of a likely incorrect radiocarbon date. In this case, the radiocarbon date of the specimen did not overlap with the credibility interval of the date estimation from the cross-validation procedure. This is likely an erroneous radiocarbon date rather than a failure of the cross-validation procedure, as radiocarbon dates from all other specimens were successfully recapitulated, and this specimen was very closely related to other specimens (radiocarbon dated to over 20 kya older) from the same site. Furthermore, the radiocarbon date was from 1999 (Harington et al., 2003), predating wide usage of ultrafiltration pre-treatment methods for radiocarbon dating, which drastically increase the accuracy of radiocarbon dating. Possibly, one of the most advantageous uses of Bayesian tip-dating analyses is the ability to estimate the ages of specimens that exceed the limit of radiocarbon dating (~50 kya). Under some circumstances (*i.e.* where comparative datasets exists), this method therefore represents a cheap and accurate alternative to direct date estimation (especially if genetic information is going to be generated anyway).

6.3 Limitations and Future Directions

6.3.1 Choice of loci

Mitochondrial data are widely used in ancient DNA (aDNA) research, as due to degradation of DNA over time, the high copy number of the mitochondrial genome increases the chance of recovery from ancient specimens when compared to nuclear DNA (Ho and Gilbert, 2010). Furthermore, while the characteristics of mtDNA make it suitable for ancient genetic analysis, the mitochondrion's maternal inheritance, lack of recombination, and high mutation rate make it ideal in evolutionary studies. However, due to these same characteristics of mitochondria, inferences based on mitochondrial data are biased towards the maternal line, lacking information from the paternal line, and only represent the evolutionary history of a single locus. As a result, demographic and evolutionary scenarios constructed from mtDNA are biased and come associated with considerable error, and therefore can be vastly different from those constructed using nuclear data (Heled and Drummond, 2008).

The majority of ancient DNA research and phylogeographic research pertaining to brown bears has focused on small fragments of the mitochondrial genome (generally cytochrome b or control region). More recent adoptions of mitogenomics — the use of the full mitochondrial genome (or mitogenome) — have revealed more well resolved brown bear phylogenies and refined evolutionary scenarios (Anijalg et al., 2018; Benazzo et al., 2017; Fortes et al., 2016; Hirata et al., 2013; Keis et al., 2013; Lan et al., 2017; Rey-Iglesia et al., 2019). Of these, only three studies utilised mitogenomes from ancient brown bear specimens (Anijalg et al., 2018; Fortes et al., 2016; Rey-Iglesia et al., 2019), a total of 17 published ancient mitogenomes: 15 from Spain, one from Austria, and one from the Russian Far East. Between Chapter 2 and Chapter 5, I have produced 217 ancient/historic brown bear mitogenomes, representing a 13-fold increase in the number of ancient brown bear mitogenomes available. These included the first mitogenomes from a number of clades: clade 1c, 1e, 3c, 2c, and the extinct North African clade. My adoption of large-scale ancient mitogenomics resulted in a refined branching order of the clades, revealing discordance between reconstructions based on the control region and the whole mitogenome.

For example, the phylogenetic placement of clade 2c as basal within the western lineage, resulting in the paraphyly of clade 2 (see Chapter 5). Furthermore, my full mitogenome approach identified problems with haplotyping more basal members of clades. Notably, Russian samples that had previously been haplotyped to clade 4 were found to actually represent basal clade 3a lineages, while a published putative clade 3c bear instead fell out as basal within clade 3b. These findings cast doubt on reports of clade 3c and 4 bears in Iberia (García-Vázquez et al., 2019; Valdiosera et al., 2008), which mitogenomics will be able to verify. Together, my results suggest that inferences on deep phylogenetics and surprising haplogroup assignments based on small mitochondrial fragments need to be approached sceptically. One of the major limitations of Chapters 2, 4, and 5, was my reliance on mitochondrial DNA (mtDNA) alone for testing phylogeography and forming hypotheses on the evolutionary history of bears.

Despite the mitogenome's high information content and utility in phylogeographic studies, it is not without its pitfalls. The mitogenome technically represents a single locus and therefore may not be an accurate reflection of the true species phylogeny. The mitogenome is often plagued by two phenomena: Incomplete Lineage Sorting (ILS) and introgression through hybridisation. Chapter 4 highlighted issues with building species phylogenies based on mitochondrial data alone, where the phylogeny based on mitogenomes and nuclear data were highly discordant: mitochondrial genomes suggest that extant spectacled bears and *Arctotherium* spp. are more closely related, while whole genome data suggested the extant spectacled bear and *Arctodus simus* are more closely related. In light of recent findings on how hybridisation can impact the genome of a species (Li et al., 2019), there remains a reasonable possibility that the mitochondrial phylogeny more closely represents the true species phylogeny. However, even if this is true, the reliance on mitochondrial data alone does not reveal the extensive hybridisation that would be required to result in approximately 70% of the genome supporting an alternative topology. Either way, the growing evidence of wide-scale hybridisation across the animal kingdom suggests that strict trees may not be the best representation of true species relationships.

Phylogenetic trees are often used to describe the evolutionary history of taxa, although it is becoming increasingly evident that trees often fail to accurately describe more complex evolutionary histories involving phenomena such as hybridisation,

6.3 LIMITATIONS AND FUTURE DIRECTIONS

introgression, horizontal gene transfer, where discordance among different loci is common. In order to address situations plagued by phylogenetic discordance, some authors have used phylogenetic clouds, such as those implemented in DensiTree, which overlay all trees on top of one another instead of forming a single consensus tree (Bouckaert, 2010). In other cases phylogenetic networks have been implemented, which still retain some of the tree like structure (Huson and Bryant, 2006). Network analyses have even been produced that take into account ILS, resulting in networks focused on detecting phenomena such as hybridisation (Than et al., 2008). These methods create clear indications of phylogenetic discordance, however, it is often difficult to quantify and interpret the output of such analyses when compared to traditional phylogenetic methods. Other, more easily interpreted approaches have been produced, such as the DiscoVista analyses I used in Chapter 4, which quantify gene tree discordance using simple summary statistics (Sayyari et al., 2018). Although this method does not produce a consensus tree and is far more user-driven (*i.e.*, requires user to input hypothetical topologies to be tested), it creates simple, easy to interpret results for focal branches, which were sufficient for the hypotheses I tested in Chapter 4.

6.3.2 Limitations of different loci

Increasing the number of loci in analyses greatly reduces the amount of error associated with demographic and evolutionary inferences (Gill et al., 2013; Heled and Drummond, 2008). Therefore, adoption of nuclear SNP assays or whole genome data can greatly improve inferences of demographic and evolutionary history and allow more complex analyses such as explicit tests of admixture (Durand et al., 2011), PSMC (Li and Durbin, 2011), and MSMC (Schiffels and Durbin, 2014), while also providing a more holistic reconstruction (including both the maternal and paternal lines). However, the recovery of nuclear DNA from ancient specimens is much more challenging and expensive than for mtDNA, due to the lower copy number and greater sequence length of the former. After an organism dies, cellular repair mechanisms no longer function and the DNA is exposed to numerous factors that threaten its stability (Dabney et al., 2013; Hofreiter et al., 2001; Paabo et al., 1989; Paabo et al., 2004), including digestion by intracellular nucleases and microorganisms. Under certain conditions (*e.g.*, extreme cold, anoxia) the impact of these digestive mechanisms may be inhibited, however, even then the DNA is still exposed to hydrolytic and oxidative damage (Dabney et al., 2013; Hofreiter et al., 2001; Paabo et al.,

1989; Paabo et al., 2004). As a result, aDNA is highly fragmented (average fragment length often <100 bp), contains lesions that block DNA replication, and contains miscoding lesions primarily resulting from cytosine deamination (Hofreiter et al., 2001; Paabo et al., 1989; Paabo et al., 2004). Therefore, endogenous molecules frequently make up less than 1% of the total DNA extracted from many ancient specimens.

Despite challenges involved with obtaining nuclear data from ancient samples, advances in sequencing technologies and the development of hybridisation enrichment techniques have resulted in the sequencing of ancient nuclear DNA becoming more common (Briggs et al., 2009; Carpenter et al., 2013; Knapp and Hofreiter, 2010; Lan and Lindqvist, 2019; Orlando et al., 2015). Although, shotgun sequencing (as implemented in Chapter 4) is only cost effective for the best-preserved samples, hybridisation enrichment can potentially overcome many of the technical downfalls and expenses associated with shotgun sequencing. Hybridisation enrichment involves enriching the relative proportion of preselected loci in an aDNA library, lowering the sequencing effort required to obtain useful genetic information from a specimen (Briggs et al., 2009; Carpenter et al., 2013; Knapp and Hofreiter, 2010; Lan and Lindqvist, 2019; Orlando et al., 2015). However, the pre-selection of loci can result in ascertainment bias which can make inferences of hybridisation, demographic history, and natural selection erroneous when compared to whole genome data (Lachance and Tishkoff, 2013). This is especially important for brown bears where polar bear ancestry is widespread (Cahill et al., 2013; Cahill et al., 2018; Cahill et al., 2015). The development of methods to produce panels of unascertained SNPs will be crucial to overcome this problem and allow reliable use of nuclear SNP panels for ancient ursid specimens (potentially in combination with whole genome data).

The degradation of DNA is correlated with temperature (Hofreiter et al., 2015), with DNA surviving longer in colder conditions (Figure 2). Therefore, the geographic distribution of well-preserved specimens is biased towards colder regions (such as permafrost regions of Russia and North America). While older specimens in warmer regions such as the contiguous USA, Middle East, North Africa, much of South America, and Southern Europe are much less likely to harbour well preserved DNA molecules. In these cases, mitogenomics is more practical due to the higher copy number of mitochondria, though even targeting mitogenomes does not guarantee sufficient DNA for molecular analyses. Therefore, although samples from colder regions may be sufficient

6.3 LIMITATIONS AND FUTURE DIRECTIONS

for nuclear analyses, it is unlikely that samples from warmer regions will have sufficient DNA preservation for many nuclear analyses, even when using hybridisation enrichment methods. Therefore, for large portions of brown bears range and that of many other bear species, which include large regions in the lower latitudes, where the preservation of nuclear DNA is limited. Other taxa are exclusively found in the mid to lower latitudes, meaning the retrieval of nuclear DNA is unlikely, let alone on a large-scale required for investigations of phylogeography. This ultimately means that mitochondrial DNA will continue to be an important locus in ancient DNA research as it's the only DNA that will likely be amplified from subfossils in many regions across the world. This is epitomised in Chapter 4, where the preservation of the sample from Natural Trap Cave (South of the Ice) was considerably lower than the samples from Eastern Beringia. As the purpose of Chapters 2, 3, and 5 was to investigate phylogeography and evolutionary history across large geographic regions — where DNA from lower latitudes was required — I used mitogenomes as nuclear DNA would likely be nearly impossible or cost ineffective to amplify from many of the samples.

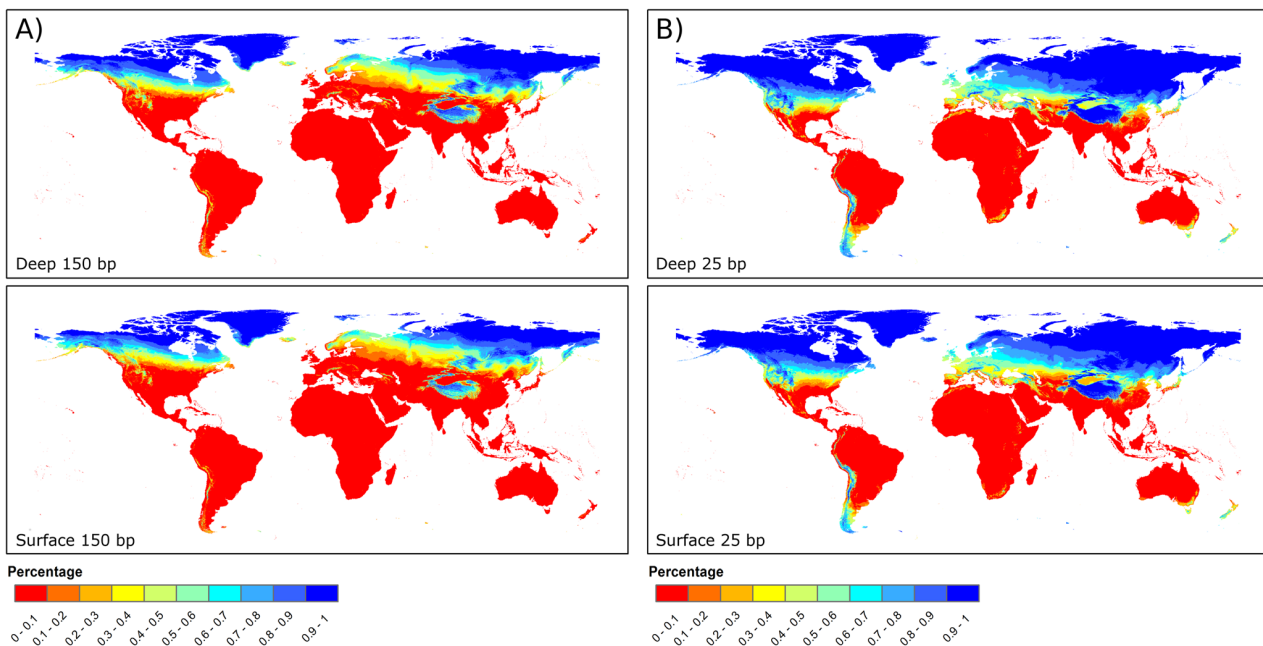


Figure 2: Estimations of the survival of DNA fragments of 150 bp (A) and 25 bp (B) after 10,000 years based on long-term environmental temperature fluctuations for open (surface) and cave (deep) sites. Figure reproduced from Hofreiter et al. (2015).

6.3.3 Evolutionary history of tremarctine bears

Although the sequencing of the first whole genome data from extinct short-faced bears in Chapter 4 greatly increased our understanding of evolution of Tremarctinae, my study was limited by a number of factors. Firstly, bears are non-model organisms, and the reference genomes available do not have the necessary associated information available to disentangle which of the two dominant topologies definitively reflects the species tree. For example, currently there is no linkage map for either the polar bear or giant panda reference genomes. If a linkage map were to be produced it could be used to determine which tremarctine bear topology was enriched in autosomal low recombining regions, likely representing the species tree (Li et al., 2019). The sequencing of genomic material from other extinct short-faced bears could also help disentangle the relationships within Tremarctinae. For example, sequencing DNA from the Florida spectacled bear (*Tremarctos floridanus*) — hypothesised to be the ancestor of the modern spectacled bear (*Tremarctos ornatus*) (Kurtén, 1966) — would provide considerable information about the evolutionary history of these bears. If the Florida spectacled bear showed similar levels of hybridisation with *Arctotherium* as the modern spectacled bear, we might then favour the hypothesis that *Tremarctos* and *Arctotherium* are sister taxa with extensive hybridisation with *Arctodus* in North America. While if the Florida spectacled bear genome supported the dominant topology (*Arctodus* and *Tremarctos* as sister taxa) and showed an absence of hybridisation with *Arctotherium* this would almost certainly suggest the results of Chapter 3 are the result of extensive hybridisation between *Arctotherium* and the spectacled bear. A Florida spectacled bear genome would also allow the hybridisation of tremarctine bears with ursine bears to be scrutinised with more accuracy.

In addition to the Florida spectacled bear, the sequencing of genomic data from more northerly *Arctotherium* populations would help in further understanding the timing and degree of hybridisation with the spectacled bear (assuming the dominant topology represents the species tree). Although the sequencing of genomic data from other extinct short-faced bears would be highly beneficial to disentangling the evolutionary history of Tremarctinae, the likelihood of obtaining genomic data from crucial specimens is extremely low. Because this hybridisation likely occurred in tropical or subtropical regions of the Americas, poor DNA preservation will likely hamper any efforts to recover

6.3 LIMITATIONS AND FUTURE DIRECTIONS

usable DNA (as discussed in 6.3.2). It may be that producing linkage maps for extant bears represents the best avenue for disentangling the evolutionary history of Tremarctinae.

6.3.4 Future directions for brown bear mitogenomics

Although in this thesis I undertook an extensive investigation of brown bear mitogenomics, there are still many questions that remain to be answered. More extensive sampling of LGM and pre-LGM samples from Europe will offer a more complete picture of the how European brown bears responded to the changing climate and extent of the European ice sheets, reveal how European brown bears are related to bears from the west, and provide more evidence about the existence and location of potential European glacial refugia. More extensive sampling of ancient bears from the Middle east, North Africa, and Central Asia would help deduce the origin and spread of the less well represented brown bear clades (Clade 5, 6, 7, and the extinct North African Clade), while dates from extinct North African clade specimens would help refine the brown bear mitochondrial phylogeny as a whole. More extensive sampling of Pleistocene Russian Far East (Western Beringian) brown bears will be pivotal for understanding the origin and spread of clade 2c and clade 3c bears into North America, while sampling of ancient individuals from Japan would clarify the timing and number of waves of migration of brown bears into Japan. With respect to Japan, of particular interest is whether the extinct clade 2c and clade 3c bears dispersed to Japan as they did to North America, and whether the timing of arrival of extant clades in Japan matches that seen in North America. Finally, extensive sampling of ancient polar bears, although difficult due to the marine niche occupied by the species, would help refine the mitochondrial relationship between brown bears and polar bears. In particular, it would reveal whether the entire eastern brown bear lineage is polar bear in origin, as hypothesised by Hassanin (2015), or whether the original polar bear mitogenome was replaced by one of brown bear origin, as hypothesised by others (Hailer, 2015; Hailer et al., 2012; Hailer and Welch, 2016).

6.3.5 Extending ancient mitogenomics to other animal taxa

One of the major strengths of Chapters 2 and 5 is my use of large aDNA datasets from a Holarctic species (brown bear) to investigate how megafauna respond to climate and environmental change. In Chapter 2 I extended this approach to include lions, revealing a strikingly similar evolutionary history and responses to the changing Late Quaternary

environment of North America to those observed in brown bears. This approach could be further extended to include more extensive sampling of European cave lions, as well as other Holarctic species. Molecular analyses of modern red foxes have alluded to waves of migration from Eurasia into North America analogous to Chapter 2. Similar ancient DNA analyses of red foxes could potentially therefore reveal similar evolutionary scenarios to brown bears and lions, but in a smaller carnivore (*i.e.* these patterns may not be restricted to large taxa). Other Holarctic taxa that these analyses could be extended to include: moose, scimitar-toothed cats (*Homotherium*), caribou, and wolverine. Large aDNA datasets from such taxa could further support common paradigms in the evolutionary history of Pleistocene megafauna or provide contrasting patterns. Ancient DNA datasets from extant and extinct taxa could identify contrasting responses to changing environments that could further help explain the survival or extinction of some taxa over others.

Although in Chapter 5 I could not provide definitive answers on the suitability of Hewitt's E/C model of postglacial recolonisation, which has long been debated, it is important to note that this model was not solely built upon evidence from brown bears. Grasshoppers and hedgehogs were central to the formation of this evolutionary model. While large-scale aDNA datasets from grasshoppers are unlikely, hedgehogs represent a natural progression in the investigation of the suitability of this model in temperate European fauna. Modern European hedgehog phylogeography has been extensively studied and there is a relative wealth of subfossil material that may be suitable for aDNA analysis. The analysis of ancient hedgehog material would allow the comparison of molecular data and Late Quaternary climate changes to better understand the responses of fauna to climate and environmental change. Furthermore, this would add evidence from less studied smaller species to understand how non-megafaunal taxa responded to changes in environment.

6.4 Conclusion

Ancient DNA provides a unique opportunity to genetically look back in time to help investigate how species respond to climate and environmental change and help explain the origin and current status of populations and species. In this thesis I predominantly used ancient DNA techniques to investigate questions relating to the evolutionary history of bears. In Chapters 2 and 5 I investigated the phylogeographic structure of brown bears across North America and Eurasia respectively, finding pronounced responses to changes in climate and environmental change throughout the Late Quaternary. In Chapter 2 this was extended to lions, revealing analogous patterns in North America. Chapters 3 and 4 investigated the evolutionary history of *Arctodus simus* and the short-faced bear subfamily respectively. Notably, in Chapter 4 I used whole genome data, which with improving sequencing technology and ancient DNA techniques is becoming a key tool in understanding of Late Quaternary biogeography and evolutionary history. My research greatly increases our understanding of the evolutionary history of bears and carnivores, and the understanding of the Late Quaternary biogeography and population dynamics of brown bears.

The world is currently experiencing an unprecedented rapid decline in biodiversity intertwined with anthropogenic encroachment and climate change. It is imperative that we act to preserve as many taxa as possible, as even with intervention many taxa will be lost. Taxa that survive will likely experience massive changes in biogeography and diversity. By studying species that went extinct during the Quaternary (such as *Arctodus*, *Arctotherium*, and extinct lions) and investigating the responses of species that survived through to the Holocene (such as brown bears), factors may be identified that help explain the differential survival of species. These results can then inform the allocation of conservation spending to better protect and manage current biodiversity. I hope the findings from my thesis can contribute to the essential understanding of faunal responses to climatic and environmental change and further stimulate research and efforts to better understand our rapidly changing world and how we can act to preserve the natural world.

6.5 References

- Anijalg, P., Ho, S.Y.W., Davison, J., Keis, M., Tammelaht, E., Bobowik, K., Tumanov, I.L., Saveljev, A.P., Lyapunova, E.A., Vorobiev, A.A., Markov, N.I., Kryukov, A.P., Kojola, I., Swenson, J.E., Hagen, S.B., Eiken, H.G., Paule, L., Saarma, U., 2018. Large-scale migrations of brown bears in Eurasia and to North America during the Late Pleistocene. *J. Biogeogr.* 45, 394-405.
- Antón, M., 2013. *Sabertooth*. Indiana University Press, Bloomington.
- Ardelean, C.F., Becerra-Valdivia, L., Pedersen, M.W., Schwenninger, J.L., Oviatt, C.G., Macias-Quintero, J.I., Arroyo-Cabrales, J., Sikora, M., Ocampo-Diaz, Y.Z.E., Rubio-Cisneros, I.I., Watling, J.G., de Medeiros, V.B., De Oliveira, P.E., Barba-Pingaron, L., Ortiz-Butron, A., Blancas-Vazquez, J., Rivera-Gonzalez, I., Solis-Rosales, C., Rodriguez-Ceja, M., Gandy, D.A., Navarro-Gutierrez, Z., De La Rosa-Diaz, J.J., Huerta-Arellano, V., Marroquin-Fernandez, M.B., Martinez-Riojas, L.M., Lopez-Jimenez, A., Higham, T., Willerslev, E., 2020. Evidence of human occupation in Mexico around the Last Glacial Maximum. *Nature* 584, 87–92.
- Barlow, A., Cahill, J.A., Hartmann, S., Theunert, C., Xenikoudakis, G., Fortes, G.G., Paijmans, J.L.A., Rabeder, G., Frischauf, C., Grandal-d'Anglade, A., Garcia-Vazquez, A., Murtskhvaladze, M., Saarma, U., Anijalg, P., Skrbinek, T., Bertorelle, G., Gasparian, B., Bar-Oz, G., Pinhasi, R., Slatkin, M., Dalen, L., Shapiro, B., Hofreiter, M., 2018. Partial genomic survival of cave bears in living brown bears. *Nat. Ecol. Evol.* 2, 1563-1570.
- Barnes, I., Matheus, P., Shapiro, B., Jensen, D., Cooper, A., 2002. Dynamics of Pleistocene population extinctions in Beringian brown bears. *Science* 295, 2267-2270.
- Baryshnikov, G., 2014. Late Pleistocene hyena *Crocuta ultima ussurica* (Mammalia, Carnivora, Hyaenidae) from the Paleolithic site in Geographical Society Cave in the Russian Far East. *Proc. Zool. Inst. RAS* 318, 197-225.
- Benazzo, A., Trucchi, E., Cahill, J.A., Delser, P.M., Mona, S., Fumagalli, M., Bunnefeld, L., Cornetti, L., Ghirotto, S., Girardi, M., Ometto, L., Panziera, A., Rota-Stabelli, O., Zanetti, E., Karamanlidis, A., Groff, C., Paule, L., Gentile, L., Vila, C., Vicario, S., Boitani, L., Orlando, L., Fuselli, S., Vernesi, C., Shapiro, B., Ciucci, P., Bertorelle, G., 2017. Survival and divergence in a small group: The extraordinary genomic history of the endangered Apennine brown bear stragglers. *Proc. Natl. Acad. Sci. U. S. A.* 114, E9589-E9597.
- Bocherens, H., Emslie, S.D., Billiou, D., Mariotti, A., 1995. Stable isotopes (C-13, N-15) and paleodiet of the giant short-faced bear (*Arctodus simus*). *Cr Acad Sci Ii* 320, 779-784.
- Boeskorov, G.G., Grigoriev, S.E., Baryshnikov, G.F., 2012. New evidence for the existence of pleistocene cave bears in Arctic Siberia. *Dokl. Biol. Sci.* 445, 239-243.
- Bouckaert, R.R., 2010. DensiTree: making sense of sets of phylogenetic trees. *Bioinformatics* 26, 1372-1373.

6.5 REFERENCES

- Briggs, A.W., Good, J.M., Green, R.E., Krause, J., Maricic, T., Stenzel, U., Lalueza-Fox, C., Rudan, P., Brajkovic, D., Kucan, Z., Gusic, I., Schmitz, R., Doronichev, V.B., Golovanova, L.V., de la Rasilla, M., Fortea, J., Rosas, A., Paabo, S., 2009. Targeted retrieval and analysis of five Neandertal mtDNA genomes. *Science* 325, 318-321.
- Cahill, J.A., Green, R.E., Fulton, T.L., Stiller, M., Jay, F., Ovseyanikov, N., Salamzade, R., St. John, J., Stirling, I., Slatkin, M., Shapiro, B., 2013. Genomic evidence for island population conversion resolves conflicting theories of polar bear evolution. *PLoS Genet.* 9, e1003345.
- Cahill, J.A., Heintzman, P.D., Harris, K., Teasdale, M.D., Kapp, J., Soares, A.E.R., Stirling, I., Bradley, D., Edwards, C.J., Graim, K., Kisleika, A.A., Malev, A.V., Monaghan, N., Green, R.E., Shapiro, B., 2018. Genomic evidence of widespread admixture from polar bears into brown bears during the last ice age. *Mol. Biol. Evol.* 35, 1120-1129.
- Cahill, J.A., Stirling, I., Kistler, L., Salamzade, R., Ersmark, E., Fulton, T.L., Stiller, M., Green, R.E., Shapiro, B., 2015. Genomic evidence of geographically widespread effect of gene flow from polar bears into brown bears. *Mol. Ecol.* 24, 1205-1217.
- Carpenter, M.L., Buenrostro, J.D., Valdiosera, C., Schroeder, H., Allentoft, M.E., Sikora, M., Rasmussen, M., Gravel, S., Guillen, S., Nekhrizov, G., Leshtakov, K., Dimitrova, D., Theodossiev, N., Pettener, D., Luiselli, D., Sandoval, K., Moreno-Estrada, A., Li, Y.R., Wang, J., Gilbert, M.T.P., Willerslev, E., Greenleaf, W.J., Bustamante, C.D., 2013. Pulling out the 1%: Whole-Genome Capture for the Targeted Enrichment of Ancient DNA Sequencing Libraries. *Am. J. Hum. Genet.* 93, 852-864.
- Cronin, M.A., Amstrup, S.C., Garner, G.W., Vyse, E.R., 1991. Interspecific and intraspecific Mitochondrial DNA variation in North American bears (*Ursus*). *Can. J. Zool.* 69, 2985-2992.
- Dabney, J., Meyer, M., Paabo, S., 2013. Ancient DNA damage. *Cold Spring Harb. Perspect. Biol.* 5, a012567.
- Dalerum, F., Cameron, E.Z., Kunkel, K., Somers, M.J., 2009. Diversity and depletions in continental carnivore guilds: implications for prioritizing global carnivore conservation. *Biol. Lett.* 5, 35-38.
- Donohue, S.L., DeSantis, L.R.G., Schubert, B.W., Ungar, P.S., 2013. Was the giant short-faced Bear a hyper-scavenger? A new approach to the dietary study of ursids using dental microwear textures. *PLoS ONE* 8, e77531.
- Durand, E.Y., Patterson, N., Reich, D., Slatkin, M., 2011. Testing for ancient admixture between closely related populations. *Mol. Biol. Evol.* 28, 2239-2252.
- Edwards, C.J., Suchard, M.A., Lemey, P., Welch, J.J., Barnes, I., Fulton, T.L., Barnett, R., O'Connell, T.C., Coxon, P., Monaghan, N., Valdiosera, C.E., Lorenzen, E.D., Willerslev, E., Baryshnikov, G.F., Rambaut, A., Thomas, M.G., Bradley, D.G., Shapiro, B., 2011. Ancient hybridization and an Irish origin for the modern polar bear matriline. *Curr. Biol.* 21, 1251-1258.

- Emslie, S.D., Czaplewski, N.J., 1985. A new record of giant short-faced bear, *Arctodus simus*, from western North America with a re-evaluation of its paleobiology. *Contrib. Sci. (Los. Angel.)* 371, 1-12.
- Fan, Z.X., Silva, P., Gronau, I., Wang, S.G., Armero, A.S., Schweizer, R.M., Ramirez, O., Pollinger, J., Galaverni, M., Del-Vecchio, D.O., Du, L.M., Zhang, W.P., Zhang, Z.H., Xing, J.C., Vila, C., Marques-Bonet, T., Godinho, R., Yue, B.S., Wayne, R.K., 2016. Worldwide patterns of genomic variation and admixture in gray wolves. *Genome Res.* 26, 163-173.
- Figueirido, B., Palmqvist, P., Perez-Claros, J.A., 2009. Ecomorphological correlates of craniodental variation in bears and paleobiological implications for extinct taxa: an approach based on geometric morphometrics. *J. Zool.* 277, 70-80.
- Figueirido, B., Pérez-Claros, J.A., Torregrosa, V., Martín-Serra, A., Palmqvist, P., 2010. Demythologizing *Arctodus simus*, the 'short-faced' long-legged and predaceous bear that never was. *J. Vertebr. Paleontol.* 30, 262-275.
- Figueirido, B., Perez-Ramos, A., Schubert, B.W., Serrano, F., Farrell, A.B., Pastor, F.J., Neves, A.A., Romero, A., 2017. Dental caries in the fossil record: a window to the evolution of dietary plasticity in an extinct bear. *Sci. Rep.* 7.
- Fortes, G.G., Grandal-d'Anglade, A., Kolbe, B., Fernandes, D., Meleg, I.N., Garcia-Vazquez, A., Pinto-Llona, A.C., Constantin, S., de Torres, T.J., Ortiz, J.E., Frischauf, C., Rabeder, G., Hofreiter, M., Barlow, A., 2016. Ancient DNA reveals differences in behaviour and sociality between brown bears and extinct cave bears. *Mol. Ecol.* 25, 4907-4918.
- Freedman, A.H., Gronau, I., Schweizer, R.M., Ortega-Del Vecchio, D., Han, E.J., Silva, P.M., Galaverni, M., Fan, Z.X., Marx, P., Lorente-Galdos, B., Beale, H., Ramirez, O., Hormozdiari, F., Alkan, C., Vila, C., Squire, K., Geffen, E., Kusak, J., Boyko, A.R., Parker, H.G., Lee, C., Tadiotla, V., Siepel, A., Bustamante, C.D., Harkins, T.T., Nelson, S.F., Ostrander, E.A., Marques-Bonet, T., Wayne, R.K., Novembre, J., 2014. Genome sequencing highlights the dynamic early history of dogs. *PLoS Genet.* 10, e1004016.
- Froese, D., Stiller, M., Heintzman, P.D., Reyes, A.V., Zazula, G.D., Soares, A.E., Meyer, M., Hall, E., Jensen, B.J., Arnold, L.J., MacPhee, R.D., Shapiro, B., 2017. Fossil and genomic evidence constrains the timing of bison arrival in North America. *Proc. Natl. Acad. Sci. U. S. A.* 114, 3457-3462.
- García-Vázquez, A., Pinto Llona, A.C., Grandal-d'Anglade, A., 2019. Post-glacial colonization of Western Europe brown bears from a cryptic Atlantic refugium out of the Iberian Peninsula. *Hist. Biol.* 31, 618-630.
- Gill, M.S., Lemey, P., Faria, N.R., Rambaut, A., Shapiro, B., Suchard, M.A., 2013. Improving bayesian population dynamics inference: a coalescent-based model for multiple loci. *Mol. Biol. Evol.* 30, 713-724.
- Gower, G., Fenderson, L.E., Salis, A.T., Helgen, K.M., van Loenen, A.L., Heiniger, H., Hofman-Kaminska, E., Kowalczyk, R., Mitchell, K.J., Llamas, B., Cooper, A.,

6.5 REFERENCES

2019. Widespread male sex bias in mammal fossil and museum collections. *Proc. Natl. Acad. Sci. U. S. A.* 116, 19019-19024.
- Hailer, F., 2015. Introgressive hybridization: brown bears as vectors for polar bear alleles. *Mol. Ecol.* 24, 1161-1163.
- Hailer, F., Kutschera, V.E., Hallstrom, B.M., Klassert, D., Fain, S.R., Leonard, J.A., Arnason, U., Janke, A., 2012. Nuclear genomic sequences reveal that polar bears are an old and distinct bear lineage. *Science* 336, 344-347.
- Hailer, F., Welch, A.J., 2016. Evolutionary history of polar and brown bears. *eLS*, 1-8.
- Harington, C.R., Naughton, D., Dalby, A., Rose, M., Dawson, J., 2003. *Annotated Bibliography of Quaternary Vertebrates of Northern North America*. University of Toronto Press, Toronto.
- Hassanin, A., 2015. The role of Pleistocene glaciations in shaping the evolution of polar and brown bears. Evidence from a critical review of mitochondrial and nuclear genome analyses. *C. R. Biol.* 338, 494-501.
- Heled, J., Drummond, A.J., 2008. Bayesian inference of population size history from multiple loci. *BMC Evol. Biol.* 8, 289.
- Hirata, D., Mano, T., Abramov, A.V., Baryshnikov, G.F., Kosintsev, P.A., Murata, K., Masuda, R., 2017. Paternal phylogeographic structure of the brown bear (*Ursus arctos*) in northeastern Asia and the effect of male-mediated gene flow to insular populations. *Zoological Lett* 3, 21.
- Hirata, D., Mano, T., Abramov, A.V., Baryshnikov, G.F., Kosintsev, P.A., Vorobiev, A.A., Raichev, E.G., Tsunoda, H., Kaneko, Y., Murata, K., Fukui, D., Masuda, R., 2013. Molecular phylogeography of the brown bear (*Ursus arctos*) in Northeastern Asia based on analyses of complete mitochondrial DNA sequences. *Mol. Biol. Evol.* 30, 1644-1652.
- Ho, S.Y.W., Gilbert, M.T.P., 2010. Ancient mitogenomics. *Mitochondrion* 10, 1-11.
- Hoffecker, J.F., Elias, S.A., O'Rourke, D.H., Scott, G.R., Bigelow, N.H., 2016. Beringia and the global dispersal of modern humans. *Evol. Anthropol.* 25, 64-78.
- Hofreiter, M., Pajmans, J.L., Goodchild, H., Speller, C.F., Barlow, A., Fortes, G.G., Thomas, J.A., Ludwig, A., Collins, M.J., 2015. The future of ancient DNA: Technical advances and conceptual shifts. *Bioessays* 37, 284-293.
- Hofreiter, M., Serre, D., Poinar, H.N., Kuch, M., Paabo, S., 2001. Ancient DNA. *Nat. Rev. Genet.* 2, 353-359.
- Huson, D.H., Bryant, D., 2006. Application of phylogenetic networks in evolutionary studies. *Mol. Biol. Evol.* 23, 254-267.
- Keis, M., Remm, J., Ho, S.Y.W., Davison, J., Tammeleht, E., Tumanov, I.L., Saveljev, A.P., Mannil, P., Kojola, I., Abramov, A.V., Margus, T., Saarma, U., 2013. Complete mitochondrial genomes and a novel spatial genetic method reveal cryptic

- phylogeographical structure and migration patterns among brown bears in north-western Eurasia. *J. Biogeogr.* 40, 915-927.
- Knapp, M., Hofreiter, M., 2010. Next generation sequencing of ancient DNA: Requirements, strategies and perspectives. *Genes* 1, 227-243.
- Kumar, V., Lammers, F., Bidon, T., Pfenninger, M., Kolter, L., Nilsson, M.A., Janke, A., 2017. The evolutionary history of bears is characterized by gene flow across species. *Sci. Rep.* 7, 46487.
- Kurtén, B., 1964. The evolution of the polar bear, *Ursus maritimus* Phipps. *Acta Zool. Fenn.* 108, 1-30.
- Kurtén, B., 1966. Pleistocene bears of North America. 1. Genus *Trematctos*, spectacled bears. *Acta Zool. Fenn.* 115, 1-120.
- Kurtén, B., 1967. Pleistocene bears of North America. 2. Genus *Arctodus*, short-faced bears. *Acta Zool. Fenn.* 117, 1-60.
- Kurtén, B., 1968. Pleistocene mammals of Europe. Addison Publishing Co., Chicago.
- Kurtén, B., Anderson, E., 1974. Association of *Ursus arctos* and *Arctodus simus* (Mammalia: Ursidae) in the late Pleistocene of Wyoming. *Breviora* 426, 1-6.
- Kurtén, B., Anderson, E., 1980. Pleistocene Mammals of North America. Columbia University Press, New York.
- Kutschera, V.E., Bidon, T., Hailer, F., Rodi, J.L., Fain, S.R., Janke, A., 2014. Bears in a forest of gene trees: Phylogenetic inference is complicated by incomplete lineage sorting and gene flow. *Mol. Biol. Evol.* 31, 2004-2017.
- Kutschera, V.E., Lecomte, N., Janke, A., Selva, N., Sokolov, A.A., Haun, T., Steyer, K., Nowak, C., Hailer, F., 2013. A range-wide synthesis and timeline for phylogeographic events in the red fox (*Vulpes vulpes*). *BMC Evol. Biol.* 13, 114.
- Lachance, J., Tishkoff, S.A., 2013. SNP ascertainment bias in population genetic analyses: why it is important, and how to correct it. *Bioessays* 35, 780-786.
- Lan, T., Lindqvist, C., 2019. Paleogenomics: Genome-Scale Analysis of Ancient DNA and Population and Evolutionary Genomic Inferences, in: Rajora, O.P. (Ed.), *Population Genomics: Concepts, Approaches and Applications*. Springer International Publishing, Cham, pp. 323-360.
- Lan, T.Y., Gill, S., Bellemain, E., Bischof, R., Nawaz, M.A., Lindqvist, C., 2017. Evolutionary history of enigmatic bears in the Tibetan Plateau - Himalaya region and the identity of the yeti. *Proc. R. Soc. B.* 284.
- Leonard, J.A., Wayne, R.K., Cooper, A., 2000. Population genetics of Ice age brown bears. *Proc. Natl. Acad. Sci. U. S. A.* 97, 1651-1654.
- Lesnek, A.J., Briner, J.P., Lindqvist, C., Baichtal, J.F., Heaton, T.H., 2018. Deglaciation of the Pacific coastal corridor directly preceded the human colonization of the Americas. *Sci. Adv.* 4, eaar5040.

6.5 REFERENCES

- Li, G., Figueiro, H.V., Eizirik, E., Murphy, W.J., 2019. Recombination-aware phylogenomics reveals the structured genomic landscape of hybridizing cat species. *Mol. Biol. Evol.* 36, 2111-2126.
- Li, H., Durbin, R., 2011. Inference of human population history from individual whole-genome sequences. *Nature* 475, 493-496.
- Liu, S.P., Lorenzen, E.D., Fumagalli, M., Li, B., Harris, K., Xiong, Z.J., Zhou, L., Korneliussen, T.S., Somel, M., Babbitt, C., Wray, G., Li, J.W., He, W.M., Wang, Z., Fu, W.J., Xiang, X.Y., Morgan, C.C., Doherty, A., O'Connell, M.J., McInerney, J.O., Born, E.W., Dalen, L., Dietz, R., Orlando, L., Sonne, C., Zhang, G.J., Nielsen, R., Willerslev, E., Wang, J., 2014. Population genomics reveal recent speciation and rapid evolutionary adaptation in polar bears. *Cell* 157, 785-794.
- Loog, L., Thalmann, O., Sinding, M.H.S., Schuenemann, V.J., Perri, A., Germonpré, M., Bocherens, H., Witt, K.E., Castruita, J.A.S., Velasco, M.S., Lundstrom, I.K.C., Wales, N., Sonet, G., Frantz, L., Schroeder, H., Budd, J., Jimenez, E.L., Fedorov, S., Gasparyan, B., Kandel, A.W., L'zni-kov?-Galetov, M., Napierala, H., Uerpman, H.P., Nikolskiy, P.A., Pavlova, E.Y., Pitulko, V.V., Herzig, K.H., Malhi, R.S., Willerslev, E., Hansen, A.J., Dobney, K., Gilbert, M.T.P., Krause, J., Larson, G., Eriksson, A., Manica, A., 2020. Ancient DNA suggests modern wolves trace their origin to a Late Pleistocene expansion from Beringia. *Mol. Ecol.* 29, 1596-1610.
- Mann, D.H., Groves, P., Reanier, R.E., Gaglioti, B.V., Kunz, M.L., Shapiro, B., 2015. Life and extinction of megafauna in the ice-age Arctic. *Proc. Natl. Acad. Sci. U. S. A.* 112, 14301-14306.
- Masuda, R., Murata, K., Aiurzaniin, A., Yoshida, M.C., 1998. Phylogenetic status of brown bears *Ursus arctos* of Asia: A preliminary result inferred from mitochondrial DNA control region sequences. *Hereditas* 128, 277-280.
- Matheus, P.E., 1995. Diet and co-ecology of Pleistocene short-faced bears and brown bears in eastern Beringia. *Quat. Res.* 44, 447-453.
- Matheus, P.E., 2003. Locomotor adaptations and ecomorphology of short-faced bears (*Arctodus simus*) in eastern Beringia, Occasional Papers in Earth Science No. 7. Yukon Palaeontology Program, Department of Tourism and Culture, Whitehorse.
- McLellan, B., Reiner, D.C., 1994. A review of bear evolution. *Bears Their Biol. Manag.* 9, 85-96.
- Miller, W., Schuster, S.C., Welch, A.J., Ratan, A., Bedoya-Reina, O.C., Zhao, F.Q., Kim, H.L., Burhans, R.C., Drautz, D.I., Wittekindt, N.E., Tomsho, L.P., Ibarra-Laclette, E., Herrera-Estrella, L., Peacock, E., Farley, S., Sage, G.K., Rode, K., Obbard, M., Montiel, R., Bachmann, L., Ingolfsson, O., Aars, J., Mailund, T., Wiig, O., Talbot, S.L., Lindqvist, C., 2012. Polar and brown bear genomes reveal ancient admixture and demographic footprints of past climate change. *Proc. Natl. Acad. Sci. U. S. A.* 109, E2382-E2390.
- Moreno-Mayar, J.V., Potter, B.A., Vinner, L., Steinrucken, M., Rasmussen, S., Terhorst, J., Kamm, J.A., Albrechtsen, A., Malaspinas, A.S., Sikora, M., Reuther, J.D., Irish,

- J.D., Malhi, R.S., Orlando, L., Song, Y.S., Nielsen, R., Meltzer, D.J., Willerslev, E., 2018. Terminal Pleistocene Alaskan genome reveals first founding population of Native Americans. *Nature* 553, 203-207.
- Norman, A.J., Street, N.R., Spong, G., 2013. De Novo SNP Discovery in the Scandinavian Brown Bear (*Ursus arctos*). *PLoS ONE* 8, e81012.
- Orlando, L., Gilbert, M.T., Willerslev, E., 2015. Reconstructing ancient genomes and epigenomes. *Nat. Rev. Genet.* 16, 395-408.
- Paabo, S., Higuchi, R.G., Wilson, A.C., 1989. Ancient DNA and the Polymerase Chain-Reaction - the Emerging Field of Molecular Archaeology. *J. Biol. Chem.* 264, 9709-9712.
- Paabo, S., Poinar, H., Serre, D., Jaenicke-Despres, V., Hebler, J., Rohland, N., Kuch, M., Krause, J., Vigilant, L., Hofreiter, M., 2004. Genetic analyses from ancient DNA. *Annu. Rev. Genet.* 38, 645-679.
- Pages, M., Calvignac, S., Klein, C., Paris, M., Hughes, S., Hanni, C., 2008. Combined analysis of fourteen nuclear genes refines the Ursidae phylogeny. *Mol. Phylogenet. Evol.* 47, 73-83.
- Pajmans, J.L.A., Barnett, R., Gilbert, M.T.P., Zepeda-Mendoza, M.L., Reumer, J.W.F., de Vos, J., Zazula, G., Nagel, D., Baryshnikov, G.F., Leonard, J.A., Rohland, N., Westbury, M.V., Barlow, A., Hofreiter, M., 2017. Evolutionary history of saber-toothed cats based on ancient mitogenomics. *Curr. Biol.* 27, 3330-3336.
- Pasitschniak-Arts, M., 1993. *Ursus arctos*. *Mamm. Species* 439, 1-10.
- Pecnerova, P., Diez-Del-Molino, D., Dussex, N., Feuerborn, T., von Seth, J., van der Plicht, J., Nikolskiy, P., Tikhonov, A., Vartanyan, S., Dalen, L., 2017. Genome-Based Sexing Provides Clues about Behavior and Social Structure in the Woolly Mammoth. *Curr. Biol.* 27, 3505-3510.e3503.
- Perri, A.R., Mitchell, K.J., Mouton, A., Alvarez-Carretero, S., Hulme-Beaman, A., Haile, J., Jamieson, A., Meachen, J., Lin, A.T., Schubert, B.W., Ameen, C., Antipina, E.E., Bover, P., Brace, S., Carmagnini, A., Caroe, C., Samaniego Castruita, J.A., Chatters, J.C., Dobney, K., Dos Reis, M., Evin, A., Gaubert, P., Gopalakrishnan, S., Gower, G., Heiniger, H., Helgen, K.M., Kapp, J., Kosintsev, P.A., Linderholm, A., Ozga, A.T., Presslee, S., Salis, A.T., Saremi, N.F., Shew, C., Skerry, K., Taranenko, D.E., Thompson, M., Sablin, M.V., Kuzmin, Y.V., Collins, M.J., Sinding, M.S., Gilbert, M.T.P., Stone, A.C., Shapiro, B., Van Valkenburgh, B., Wayne, R.K., Larson, G., Cooper, A., Frantz, L.A.F., 2021. Dire wolves were the last of an ancient New World canid lineage. *Nature* 591, 87-91.
- Reumer, J.W.F., Rook, L., van der Borg, K., Post, K., Mol, D., de Vos, J., 2003. Late Pleistocene survival of the saber-toothed cat *Homotherium* in northwestern Europe. *J. Vertebr. Paleontol.* 23, 260-262.
- Rey-Iglesia, A., Garcia-Vazquez, A., Treadaway, E.C., van der Plicht, J., Baryshnikov, G.F., Szpak, P., Bocherens, H., Boeskorov, G.G., Lorenzen, E.D., 2019. Evolutionary history and palaeoecology of brown bear in North-East Siberia re-

6.5 REFERENCES

- examined using ancient DNA and stable isotopes from skeletal remains. *Sci. Rep.* 9, 4462.
- Richards, R.L., Churcher, C.S., Turnbull, W.D., 1996. Distribution and size variation in North American short-faced bears, *Arctodus simus*, in: Stewart, K.M., Seymour, K.L. (Eds.), *Palaeoecology and palaeoenvironments of late Cenozoic mammals: tributes to the career of C.S. (Rufus) Churcher*. University of Toronto Press, Toronto, pp. 191-246.
- Sayyari, E., Whitfield, J.B., Mirarab, S., 2018. DiscoVista: Interpretable visualizations of gene tree discordance. *Mol. Phylogenet. Evol.* 122, 110-115.
- Schaefer, N.K., Shapiro, B., Green, R.E., 2017. AD-LIBS: inferring ancestry across hybrid genomes using low-coverage sequence data. *BMC Bioinform.* 18, 203.
- Schiffels, S., Durbin, R., 2014. Inferring human population size and separation history from multiple genome sequences. *Nat. Genet.* 46, 919-925.
- Schubert, B.W., 2010. Late Quaternary chronology and extinction of North American giant short-faced bears (*Arctodus simus*). *Quat. Int.* 217, 188-194.
- Schubert, B.W., Kaufmann, J.E., 2003. A partial short-faced bear skeleton from an Ozark cave with comments on the paleobiology of the species. *J. Cave Karst Stud.* 65, 101-110.
- Serangeli, J., Van Kolfschoten, T., Starkovich, B.M., Verheijen, I., 2015. The European saber-toothed cat (*Homotherium latidens*) found in the "Spear Horizon" at Schöningen (Germany). *J. Hum. Evol.* 89, 172-180.
- Shapiro, B., Ho, S.Y., Drummond, A.J., Suchard, M.A., Pybus, O.G., Rambaut, A., 2011. A Bayesian phylogenetic method to estimate unknown sequence ages. *Mol. Biol. Evol.* 28, 879-887.
- Sher, A.V., Weinstock, J., Baryshnikov, G.E., Davydov, S.P., Boeskorov, G.G., Zazhigin, V.S., Nikolskiy, P.A., 2011. The first record of "spelaeoid" bears in Arctic Siberia. *Quat. Sci. Rev.* 30, 2238-2249.
- Shields, G.F., Adams, D., Garner, G., Labelle, M., Pietsch, J., Ramsay, M., Schwartz, C., Titus, K., Williamson, S., 2000. Phylogeography of mitochondrial DNA variation in brown bears and polar bears. *Mol. Phylogenet. Evol.* 15, 319-326.
- Skoglund, P., Ersmark, E., Palkopoulou, E., Dalen, L., 2015. Ancient Wolf Genome Reveals an Early Divergence of Domestic Dog Ancestors and Admixture into High-Latitude Breeds. *Curr. Biol.* 25, 1515-1519.
- Sorkin, B., 2006. Ecomorphology of the giant short-faced bears *Agriotherium* and *Arctodus*. *Hist. Biol.* 18, 1-20.
- Statham, M.J., Murdoch, J., Janecka, J., Aubry, K.B., Edwards, C.J., Soulsbury, C.D., Berry, O., Wang, Z., Harrison, D., Pearch, M., Tomsett, L., Chupasko, J., Sacks, B.N., 2014. Range-wide multilocus phylogeography of the red fox reveals ancient

- continental divergence, minimal genomic exchange and distinct demographic histories. *Mol. Ecol.* 23, 4813-4830.
- Steffen, M.L., Fulton, T.L., 2018. On the association of giant short-faced bear (*Arctodus simus*) and brown bear (*Ursus arctos*) in late Pleistocene North America. *Geobios* 51, 61-74.
- Stuart, A.J., Lister, A.M., 2014. New radiocarbon evidence on the extirpation of the spotted hyaena (*Crocuta crocuta* (Erx1.)) in northern Eurasia. *Quat. Sci. Rev.* 96, 108-116.
- Talbot, S.L., Shields, G.F., 1996. Phylogeography of brown bears (*Ursus arctos*) of Alaska and paraphyly within the Ursidae. *Mol. Phylogenet. Evol.* 5, 477-494.
- Than, C., Ruths, D., Nakhleh, L., 2008. PhyloNet: a software package for analyzing and reconstructing reticulate evolutionary relationships. *BMC Bioinform.* 9, 322.
- Tumendemberel, O., Zedrosser, A., Proctor, M.F., Reynolds, H.V., Adams, J.R., Sullivan, J.M., Jacobs, S.J., Khorloojav, T., Tserenbataa, T., Batmunkh, M., Swenson, J.E., Waits, L.P., 2019. Phylogeography, genetic diversity, and connectivity of brown bear populations in Central Asia. *PLoS ONE* 14.
- Turner, A., 1997. *The Big Cats and Their Fossil Relatives: An Illustrated Guide to Their Evolution and Natural History*. Columbia University Press, New York.
- Vachula, R.S., Huang, Y., Longo, W.M., Dee, S.G., Daniels, W.C., Russell, J.M., 2019. Evidence of Ice Age humans in eastern Beringia suggests early migration to North America. *Quat. Sci. Rev.* 205, 35-44.
- Valdiosera, C.E., Garcia-Garitagoitia, J.L., Garcia, N., Doadrio, I., Thomas, M.G., Hanni, C., Arsuaga, J.L., Barnes, I., Hofreiter, M., Orlando, L., Gotherstrom, A., 2008. Surprising migration and population size dynamics in ancient Iberian brown bears (*Ursus arctos*). *Proc. Natl. Acad. Sci. U. S. A.* 105, 5123-5128.
- Van Valkenburgh, B., Hayward, M.W., Ripple, W.J., Meloro, C., Roth, V.L., 2016. The impact of large terrestrial carnivores on Pleistocene ecosystems. *Proc. Natl. Acad. Sci. U. S. A.* 113, 862-867.
- Waits, L.P., Talbot, S.L., Ward, R.H., Shields, G.F., 1998. Mitochondrial DNA phylogeography of the North American brown bear and implications for conservation. *Conserv. Biol.* 12, 408-417.
- Waters, M.R., 2019. Late Pleistocene exploration and settlement of the Americas by modern humans. *Science* 365.
- Werdelin, L., 1991. The Hyaenidae: taxonomy, systematics and evolution. *Fossils. Strata* 30, 1-104.
- Xenikoudakis, G., Ersmark, E., Tison, J.L., Waits, L., Kindberg, J., Swenson, J.E., Dalen, L., 2015. Consequences of a demographic bottleneck on genetic structure and variation in the Scandinavian brown bear. *Mol. Ecol.* 24, 3441-3454.

Appendix

Widespread male sex bias in mammal fossil and museum collections

This appendix contains published research investigating sex ratios in mammalian fossil and museum collections. I contributed the brown bear data in this study — extraction, DNA library preparation, shotgun sequencing, bioinformatic processing of sequencing data, and genetic sexing of specimens.

Gower, G., Fenderson, L.E., **Salis, A.T.**, Helgen, K.M., van Loenen, A.L., Heiniger, H., Hofman-Kaminska, E., Kowalczyk, R., Mitchell, K.J., Llamas, B., Cooper, A., 2019. Widespread male sex bias in mammal fossil and museum collections. *Proc. Natl. Acad. Sci. U. S. A.* 116, 19019-19024.



Widespread male sex bias in mammal fossil and museum collections

Graham Gower^{a,1,2}, Lindsey E. Fenderson^{a,3}, Alexander T. Salis^a, Kristofer M. Helgen^b, Ayla L. van Loenen^a, Holly Heiniger^a, Emilia Hofman-Kamińska^c, Rafał Kowalczyk^c, Kieren J. Mitchell^a, Bastien Llamas^a, and Alan Cooper^{a,1}

^aAustralian Centre for Ancient DNA, The University of Adelaide, Adelaide, SA 5005, Australia; ^bSchool of Biological Sciences, The University of Adelaide, Adelaide, SA 5005, Australia; and ^cMammal Research Institute, Polish Academy of Sciences, 17-230 Białowieża, Poland

Edited by Neil H. Shubin, The University of Chicago, Chicago, IL, and approved July 18, 2019 (received for review February 25, 2019)

A recent study of mammoth subfossil remains has demonstrated the potential of using relatively low-coverage high-throughput DNA sequencing to genetically sex specimens, revealing a strong male-biased sex ratio [P. Pečnerová et al., *Curr. Biol.* 27, 3505–3510.e3 (2017)]. Similar patterns were predicted for steppe bison, based on their analogous female herd-based structure. We genetically sexed subfossil remains of 186 Holarctic bison (*Bison* spp.), and also 91 brown bears (*Ursus arctos*), which are not female herd-based, and found that ~75% of both groups were male, very close to the ratio observed in mammoths (72%). This large deviation from a 1:1 ratio was unexpected, but we found no evidence for sex differences with respect to DNA preservation, sample age, material type, or overall spatial distribution. We further examined ratios of male and female specimens from 4 large museum mammal collections and found a strong male bias, observable in almost all mammalian orders. We suggest that, in mammals at least, 1) wider male geographic ranges can lead to considerably increased chances of detection in fossil studies, and 2) sexual dimorphic behavior or appearance can facilitate a considerable sex bias in fossil and modern collections, on a previously unacknowledged scale. This finding has major implications for a wide range of studies of fossil and museum material.

sex ratio | sex bias | bison | brown bears | ancient DNA

Most mammal species have a sex ratio of 1:1 at birth (1), but this may shift demographically according to differential patterns of mortality between the sexes across various life stages. A variety of factors have been identified that may affect sex ratios in mammal populations from birth to adulthood, including competition for mates and local resources, or the physiological condition of mothers (1–3). The sex ratios in natural populations are helpful in evaluating the impact of these and other factors, and to illuminate aspects of life history and comparative demographics within and across species. However, it is important that field-based studies of sex ratios capture real, rather than biased, information for both sexes. Pečnerová et al. (4) recently demonstrated that males are overrepresented in the fossil record of mammoths, and suggested that this also may be the case for the fossil record of other female herd-based mammal species, such as bison. To explore the extent of this problem, we examined the relative representation of males and females in the fossil record of 2 Late Pleistocene and Holocene megafauna, bison (*Bison* spp.) and brown bears (*Ursus arctos*), as well as in museum collections of a range of extant mammals.

Morphological sex determination of fossil and subfossil remains is generally reliable only where sexual dimorphism is apparent, but has been widely used despite this limitation (5, 6). However, it is also possible to genetically sex subfossil specimens using ancient DNA, either by direct PCR of a sex-linked gene or, more powerfully, via shotgun sequencing data (7, 8). In the latter approach, mammalian sex may be inferred by calculating the ratio of the number of reads that map to the Y versus X chromosomes (7), although, because many genome reference assemblies lack a Y chromosome, it is often better to calculate the ratio of

reads mapping to the X versus nonsex chromosomes (8). The 2 X chromosomes in female mammals result in approximately double X chromosomal “read dosage” compared with males. Read dosage for both X and Y has also been evaluated using ancient DNA nuclear single-nucleotide polymorphism capture data (9). The use of read dosage is very convenient for ancient DNA studies, as the method requires relatively little sequencing effort, and is typically generated as part of routine DNA quality screening.

The read dosage approach was recently used to show that male specimens are overrepresented (72%) in Holarctic mammoth remains (4). This was suggested to result from the “lone-male model,” originally proposed to explain the excess of young adult males in the Hot Springs mammoth assemblage (10). This model proposes that, after subadult males are expelled from their familial group, they lose the protection of a large herd and experienced group leaders, and consequently engage in riskier behavior or enter more dangerous territory. As a result, the excess of males in the fossil record is caused by segregation of sexes due to their social behavior leading to differential mortality, including at taphonomically favorable sites which preserve fossils (such as bogs and tarpits). Morphological age profiling has provided support for this model at specific mammoth mass death sites (reviewed by ref. 11), but it has not previously been suggested to be a more widespread pattern across the fossil record.

Significance

The extent to which the fossil record provides an accurate picture of past life is an important issue that is often difficult to assess. We genetically sexed 277 mammalian subfossils using high-throughput sequencing of ancient DNA, and found a strong male bias (~75%) in Pleistocene bison ($n = 186$) and brown bears ($n = 91$), matching signals previously reported for mammoth. Similarly, a male bias was also found in species of nearly all mammal orders in 4 large museum collections. For mammals, we suggest both male behavior and appearance can lead to increased chances of representation in fossil and museum collections, and this previously unrecognized sex bias could have substantial implications for views of past population and ecological processes.

Author contributions: G.G. and A.C. designed research; G.G., L.E.F., A.T.S., K.M.H., A.L.V.L., H.H., E.H.-K., R.K., K.J.M., and B.L. performed research; G.G., L.E.F., and A.T.S. analyzed data; and G.G., K.M.H., K.J.M., and A.C. wrote the paper.

The authors declare no conflict of interest.

This article is a PNAS Direct Submission.

Published under the PNAS license.

¹To whom correspondence may be addressed. Email: graham.gower@gmail.com or alan.cooper@adelaide.edu.au.

²Present address: Lundbeck GeoGenetics Centre, GLOBE Institute, University of Copenhagen, 1350 Copenhagen, Denmark.

³Present address: Department of Natural Resources and the Environment, University of New Hampshire, Durham, NH 03824.

This article contains supporting information online at www.pnas.org/lookup/suppl/doi:10.1073/pnas.1903275116/-/DCSupplemental.

Published online September 3, 2019.

Furthermore, the model is not readily falsifiable without the ability to profile age at death, and other possible causes for a male bias also remain untested.

To investigate this issue further, we examined large collections of several other Late Quaternary Holarctic megafauna, bison (*Bison* spp.) and brown bears (*U. arctos*) from across Europe, Beringia, and North America (SI Appendix, Fig. S1), along with the original mammoth dataset (4) and a small dataset of the extinct Balearic bovid *Myotragus balearicus*. Most of the specimens were collected by the authors either directly from the field (most of the North American samples) or from existing museum collections (the majority of the European and Russian samples), providing some level of control against collection biases. We used these datasets to investigate a number of aspects of sample taphonomy and collection activities that might influence their observed sex ratios.

Late Pleistocene bison thrived on the vast mammoth steppe, leaving a substantial fossil record across Eurasia and North America. Modern bison are polygynous and gregarious, forming large herds comprising mostly female adults and young of both sexes. Adult males are solitary or form small bachelor groups, joining with the female groups for only 1 to 2 mo of the year. Similar structures have been implied for Pleistocene steppe bison (12), and this has led to predictions that, like mammoth, steppe bison remains would also exhibit a pronounced male bias (4). We examined this by genetically sexing 188 subfossil bison specimens from across Europe, Beringia, and North America, mostly recovered from alluvial sediments.

Both modern and Late Pleistocene brown bears have a Holarctic distribution, and individuals are typically either solitary or form small family groups, only congregating in large numbers under atypical circumstances of highly abundant food. Dispersal of extant brown bears is density-dependent (13), with more than one-third of females and 80 to 90% of males dispersing before adulthood (13, 14). As a result, while the lone-male model doesn't apply to brown bears as there is no female-herd structure, the more generic model that greater landscape ranging in males might produce a male sex bias in fossil records can be examined. Given that brown bears are facultative carnivores, both their ecology and social structure are clearly different than mammoths and bison and provide a strong comparison to examine biased sex ratios. We genetically sexed 91 brown bear subfossils from Europe, Russia, and North America, recovered from caves and alluvial sediments.

Results

Shotgun sequencing data were used to confidently assign sex to 186 of the 188 subfossil bison and all of the 91 brown bear specimens, using the ratio of reads mapping to the X chromosome versus nonsex chromosomes (*Materials and Methods* and Table 1). A pronounced male sex bias close in size to that of mammoths (72%) was observed across all bison (75%) and the vast majority of the brown bear specimens (75%) (Table 1). Interestingly, in the more limited sets of cave-preserved bones, a contradictory signal of female bias was observed for bison

(4 males, 8 females), and for brown bears from the Alps region (8 males, 16 females). However, the dominance of female brown bears has previously been noted for Austrian caves (15), and is thought to relate to behavioral differences in the Alps region, where female bears hibernate in caves, whereas males do not. Outside of the Alps, both male and female brown bears hibernate, and a strong male sex bias was observed in cave sites (50 males, 26 females), while open sites showed a more equal ratio (8 males, 7 females).

To test whether additional information about the samples might explain the excess male ratio, we used an intercept-only logistic regression, as a null model, for comparison with logistic regression models containing explanatory variables. Intuitively, this null model can be interpreted as “there is a fixed ratio of males to females,” while the alternative models that we construct should be interpreted as “the sex ratio changes as the explanatory variable changes.” Alternative models were compared with the null using a likelihood ratio test (LRT). Logistic regression models with univariate predictors of sex were constructed for a variety of explanatory variables.

Bison. For the bison, only the type of site (cave vs. noncave) was found to be significantly better than the intercept-only model, due to the female bias in the 12 cave specimens noted above (Table 2). We searched for site-specific factors that might contribute to differential mortality of males and females, but we rejected univariate models with the following explanatory variables: latitude, longitude, and altitude. Univariate models may not reveal differences that arise only when jointly considering latitude and longitude, so we implemented a Gaussian kernel 2-sample test (16), for more-complex spatial differences between the sexes. This multivariate test has good sensitivity to detect such differences (SI Appendix), but was unable to reveal any sex-specific patterns for bison remains ($T = -0.0073311$, $p = 0.766$).

To examine whether larger bison might generate a “trophy” collection bias, we searched for an increase in the proportion of male bone samples where sexual dimorphism is more apparent (e.g., skulls). Due to the small sample size of many types of bone used for DNA extraction, we also collapsed the categories into either “crania” or “postcrania,” with teeth placed into the crania category, as they are regularly taken from full or partial skulls. Neither the model containing all bone categories nor that containing collapsed categories was significantly better than the null.

Brown Bears. While several variables (^{14}C age, longitude, and altitude) explained the brown bear male sex bias better than an intercept-only model (Table 2), these are all related to the strong female bias in the Alps cave samples ($p = 0.000363$). Outside of the Alps region, the only variables significantly better than an intercept-only model were latitude and cave/noncave (Table 2). Importantly, the male bias was less extreme at higher latitudes, where female home ranges are larger due to food scarcity, particularly after emerging from dens (17). This suggests the ratio of male to female landscape ranging may be

Table 1. Male and female sample counts

Variable	Bison			Brown bears			
	All	Postcrania	Noncave	All	Alps	Non-Alps	Mammoths*
Males	139	72	135	58	8	50	67
Females	47	31	39	33	16	17	26
Total	186	103	174	91	24	67	93
% male	74.73	69.90	77.59	63.74	33.33	74.63	72.04
Unassigned	2	0	2	0	0	0	5

*Mammoth data are from ref. 4.

Table 2. Logistic regression models with sex as the dependent variable

Explanatory variable	Bison			Brown bears			Mammoths*
	All	Postcrania	Noncave	All	Alps	Non-Alps	
Intercept-only	<i>1.31E-10</i>	<i>8.80E-05</i>	<i>8.51E-12</i>	<i>0.00973</i>	0.110	<i>0.000122</i>	<i>4.21E-05</i>
Cave/noncave	<i>0.00176</i>	<i>0.00646</i>		0.367		<i>0.0399</i>	
Material1	0.618	0.634	0.716	0.264	0.758	0.0695	0.132
Material2	0.227		0.245	0.594	0.671	0.590	
¹⁴ C age	0.768	0.534	0.614	<i>0.0122</i>	0.133	0.174	0.992
Latitude	0.954	0.657	0.682	0.619	0.494	<i>0.0244</i>	
Longitude	0.490	0.527	0.965	<i>0.0171</i>	0.708	0.417	
Altitude	0.676	0.802	0.847	<i>0.0157</i>	0.158	0.911	
Alps/non-Alps				<i>0.000363</i>			
Endogenous	0.707	0.790	0.941	0.137	0.521	0.439	
GC ratio	0.312	0.625	0.468	0.723	0.386	0.168	
DNA fragment length	0.237	0.343	0.705	0.352	0.717	0.514	
5' deamination (C→T)	0.558	0.681	0.644	0.162	0.446	0.148	

The row corresponding to an intercept-only model shows *P* values for the intercept term, which tests the null hypothesis that there is a 1:1 male to female ratio. All other cells contain *P* values from LRTs, comparing a logistic regression model of the form "sex ~ X," where X is a single explanatory variable, to the intercept-only model above it. *P*s < 0.05 are shown in boldface italics. Material1 consists of factors such as tooth, leg, astragalus, foot, petrous, other skull, vertebrae, flat bone, and horn. Material2 collapses factors from Material1 into crania and noncrania. Full model fitting results can be found in [SI Appendix, Tables S1 and S2](#).

*Mammoth data are from ref. 4.

an important factor. Brown bear bones found in caves outside the Alps showed a male bias, suggesting the female hibernation behavior in the Alps may indeed be producing the female sex bias, while, elsewhere, males dominated caves as preferred denning sites.

The kernel 2-sample test was also applied to brown bears, and identified the sex-specific spatial distribution caused by female-dominated sites in the Alps ($T = 0.13709$, $p = 0.001$). However, when applied to only brown bear remains outside the Alps, no spatial differences between the sexes could be identified ($T = 0.037225$, $p = 0.157$).

Mammoth. We also reanalyzed the mammoth samples from the previous study (4) for comparison, using our methods for consistency. Of 98 samples, 93 were unambiguously assigned to a sex (Table 1). We evaluated the 2 variables that were provided, material type and ¹⁴C date, as possible explanations for the sex ratio. Neither was significantly better than an intercept-only model (Table 2).

Myotragus. We sexed 9 bones of the fossil dwarf bovid *M. balearicus* from several different Mallorcan deposits (Balearic Islands, Spain) that were part of another study (18). Larger bones were deliberately chosen from available collections in an effort to identify specimens with good DNA preservation. All 9 bones were found to be male, suggesting that the deliberate choice of large bones in medium-small size species can result in a substantial male bias for taxa that have obvious sexual size dimorphism.

Modern Mammal Collections. To further explore the potential for biases in museum collections, we counted male and female samples in the online databases of large mammalogy collections from the American Museum of Natural History (AMNH), New York; the Natural History Museum (NHM), London; the Smithsonian Institution National Museum of Natural History (USNM), Washington; and the Royal Ontario Museum (ROM), Ontario. These specimens of modern and historical mammal samples were obtained during the past few hundred years, largely from hunted or trapped individuals. Many were sexed at the time of collection, or subsequently, based on preserved genitalia, or clearly distinguishing secondary sexual characters (such

as antlers, for most deer species). The ratio of males was calculated for each species represented by more than 100 individuals (Fig. 1). The male ratio, averaged across species, was greater than 1:1 in most mammalian orders, with notable exceptions for Chiroptera (bats) and Pilosa (sloths and anteaters). However, there was extreme variability across taxa, which may result from the method of collection (hunting vs. trapping), or the source of the samples (zoo vs. wild).

Discussion

A bias toward males appears to be a pervasive feature in both subfossil and live-collected mammal collections, and could be due to a range of plausible factors. Perhaps the simplest explanation in the subfossil datasets is a taphonomic artifact, where male bones in sexually dimorphic species such as bison are larger or denser and more likely to be better preserved or identified as likely to contain DNA. If this was the case, male bias might be expected to correlate with factors associated with postmortem DNA preservation, such as sample age, average DNA fragment length, and cytosine deamination rate. Greater bone density might also be expected to inhibit microbial intrusion, and thus increase the proportion of endogenous DNA (host species vs. microbial DNA). However, no such trends were observed here (Table 2), and it is reasonable to conclude that DNA preservation is equal between the sexes.

Given the evidence of equivalent postmortem preservation, the observed male bias could relate to differences in either deposition rates or collection activities. Regarding the latter, we found no evidence of a decreased male sex bias in smaller skeletal elements where sexual dimorphism is less apparent, suggesting that size-biased sampling is unlikely to be a major driver of the observed sex ratios in bison or brown bears. Consequently, our data would appear to support a biased male deposition rate in both bison and brown bears, consistent with the male landscape-ranging hypothesis proposed for mammoth (4), where male deaths are more broadly distributed. This bias is expected to be particularly strong for female-herding taxa, where female ranges are potentially clustered geographically ([SI Appendix, Fig. S2](#)). While the latter is likely to change in geographic distribution over time, random sampling across the landscape is still more likely to locate male remains.

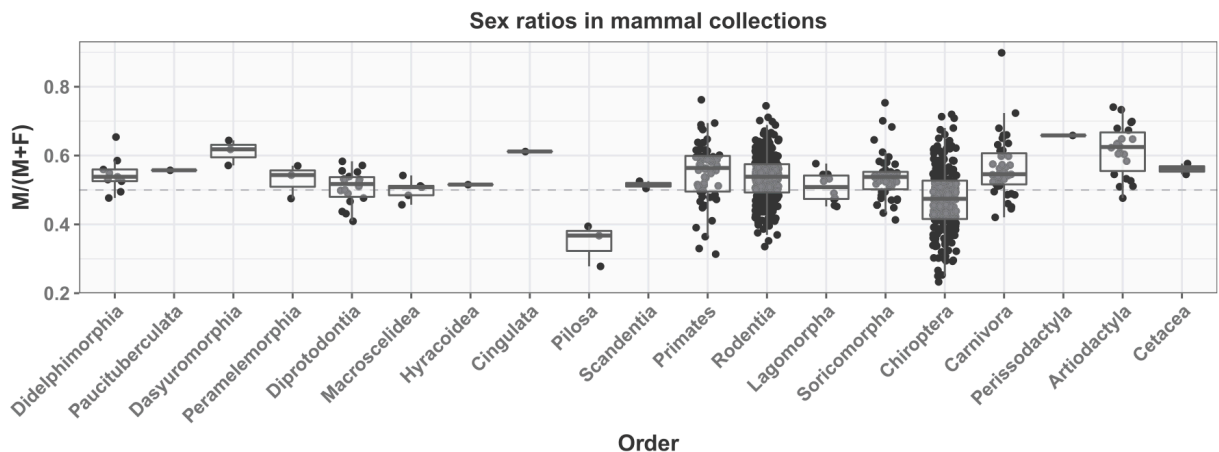


Fig. 1. Box plot summarizing the proportion of male samples for distinct species in modern mammal collections, grouped by order. Black dots represent the proportion of males for a single species, and are jittered horizontally. Boxes show the 25th, 50th (median), and 75th percentiles. Only species with more than 100 sexed samples were included.

A corollary of this model is that locations dominated by large female groups should be encountered occasionally, yielding female-biased ratios for such sites. Our dataset contains very few sites for which we have multiple samples, but we observed one such female-biased region with Alpine brown bears (for which a behavioral explanation is available). In addition, the overall female bias observed in bison cave specimens appears to be driven by 3 Canadian sites, accounting for half our total bison cave specimens ($n = 6$ out of 12), from which we obtained no male individuals (Extinction Cave and China Bowl Cave, Manitoba; Bison Cave, Yukon Territory), and may therefore represent sites within the core range of female herds. However, while this observation is consistent with the landscape-ranging hypothesis, the low number of cave sites from which we obtained bison remains ($n = 6$) prevents us from drawing strong conclusions. Finally, the female-biased sex ratios observed for bats may derive from collections dominated by sampling of single roosts, which, at certain times of the year, may be inhabited only by one sex, particularly maternity colonies (19).

Cave sites appear to provide different sex biases from open alluvial systems, possibly related to behavioral traits such as the differential denning activities for bears in the Alps and elsewhere. For example, the dominance of male brown bears in cave sites outside the Alps may reflect the ability of males to drive off females from preferred denning locations such as caves. Since the lone-male model technically only applies to herd animals, the brown bear data support a more generic model where greater landscape ranging in males results in higher average chances of fossil finds. This is supported by the finding that the male bias decreases at higher latitudes where female bear ranges are larger. It would be possible to further investigate specific predictions of the lone-male model by examining the age at death, which should be younger for males than for females, due to lack of experience and herd protection. Age at death can be measured morphologically from factors such as tooth eruption and wear, and, in mammoths, by dating the enamel layers of tusks. However, large collections of subfossil teeth preserving ancient DNA have not, so far, been analyzed. Certain methylomic loci can be used to indicate age in humans (20), so cytosine methylation in ancient DNA (21) could potentially also be used to age subfossil specimens.

Collection Bias. Where we deliberately sampled thicker and larger *M. balearicus* bones to maximize DNA preservation in a warm cli-

mate, all were found to be male ($n = 9$), indicating that this bias can potentially affect subfossil collections. It is highly likely that a similar collection bias affects modern mammalian collections arising from predominantly hunted and trapped individuals. For modern mammals, this bias need not only be driven by deliberate selection of large “impressive” male specimens, but also due to other factors such as hunters or trappers avoiding females tending young because of legislation or other motivation. At the same time, museum collections do not only represent the choices of collectors and hunters. Museum curators may act judiciously to select materials for accession with a goal of representing both sexes (as well as representing different localities, times, or ages) for species in their collections, a factor that may, in fact, counteract, to some extent, any tendency for extreme male bias in some collections. Whatever the cause, the pervasiveness of male overrepresentation in mammal collections requires attention. The use of museum specimens as the major platform for comparative anatomy, morphological variability, ontogenetic development, parasitology, stable isotope chemistry, stomach contents, and many other aspects of biology in mammalian species (22) raises the question of the extent that previous studies may be impacted by an unrecognized male bias.

While we have not examined the extent of male bias in modern bird collections, we suspect that the remarkable sexual dimorphism in color in many bird species may lead to similar male bias, as males typically exhibit more visually striking plumage. However, data available for the extinct moas of New Zealand suggest a different pattern for ratite birds, where sex roles are reversed. Moa exhibit pronounced reverse sexual size dimorphism, with females 2 or more times heavier than males (23). Fossil remains of 4 different moa species show heavily female-dominated sex ratios across 2 different deposits, with suggestions that female territoriality led to their abundance near watering holes or other prime sites (24). Importantly, this provides a further indication that differential sexual morphology and behavioral ecology of large vertebrates, rather than being male specifically, may be important drivers of sex ratios observed in the fossil record.

Conclusion

We observed a substantial excess of male bison and brown bear subfossils across a range of Late Quaternary Holarctic deposits, consistent with a model of greater landscape ranging in males. The female-herd structure of bison, like mammoths, explains the high ratio of male subfossils, as females are expected to be

clustered geographically, and therefore more heterogeneous on the landscape. In the case of brown bears, the lack of a herd structure leads to a more equal distribution of subfossil remains in alluvial sites, but a notably lower male ratio at higher latitudes where female ranges are larger.

Regardless of the actual mechanisms, a substantial male sex bias exists in both the subfossil record and modern mammalian collections. The biases are highly taxon-specific, and are likely to differ between collections. This has major implications for studies that assume their samples are representative of the whole population under consideration, such as comparisons of taxa or studies of factors such as bone dietary isotopes where sexes differ in their behavior or distribution. Our results suggest that sex biases are ubiquitous in collections, and should not be ignored. The routine application of genetic sexing will allow the possible confounding effects of cryptic sexual dimorphism to be identified when working with subfossils or museum collections.

Materials and Methods

Laboratory Procedures. All ancient DNA work was performed in the purpose-built isolated ancient DNA facility at the University of Adelaide's Australian Centre for Ancient DNA, or the Henry Wellcome Ancient Biomolecules Centre at Oxford University, following previously published guidelines (25, 26). DNA was extracted from bison samples using either a phenol–chloroform (27) or in-house silica-based method (28). Brown bear samples were extracted using a phenol–chloroform-based extraction protocol (29) or an in-house silica-based protocol (30). Double-stranded Illumina sequencing libraries were built from 25 μ L of DNA extract following the partial uracil–DNA–glycosylase treatment protocol (31), modified to include the use of dual 7-mer internal barcode sequences as per ref. 28. The libraries were pooled and sequenced using paired-end reactions on an Illumina MiSeq, NextSeq, or HiSeq.

Alignment and Filtering. Demultiplexed reads were mapped using the Paleomix pipeline (32) configured to use BWA-aln (33) with typical ancient DNA parameters (-l 16384 -o 2 -n 0.01). Alignments were subsequently filtered to exclude those with mapping quality lower than 30, and fragments longer than 100 base pairs (bp). We considered only samples with at least 5,000 reads mapped to the nuclear genome, and subsampled down to ~20,000 reads for sex determination.

Bison. Bison reads were mapped to a composite cattle reference assembly formed by concatenating the assembly UMD3.1 (34), with the Y chromosomal sequence from Btau4.6.1 (35). As very few reads map to this Y sequence, we were unable to do genetic sexing using counts of reads mapping to the Y chromosome vs. counts of those mapping to the X chromosome as in ref. 7. We instead counted reads mapping to the X chromosome vs. the autosome, in an approach similar to ref. 8.

We counted the reads that mapped to the X chromosome, N_X , and the reads that mapped to the autosome, N_A , using samtools idxstats (36). Assuming reads are drawn from the genome uniformly along its length, the observed ratio $R_X = N_X / (N_X + N_A)$ can be predicted from the length of the X chromosome, L_X , and the length of the autosome, L_A . Conditional on the sex, the expected ratios are

$$p_{XY} = \mathbb{E}[R_X | \text{sex} = XY] = L_X / (L_X + 2L_A) \quad \text{or} \\ p_{XX} = \mathbb{E}[R_X | \text{sex} = XX] = L_X / (L_X + L_A).$$

The likelihood of the male ratio p_{XY} given the observed counts N_X and N_A can thus be described using the Binomial probability mass function,

$$\mathcal{L}(p_{XY} | N_X, N_A) = \frac{(N_X + N_A)!}{N_X! N_A!} p_{XY}^{N_X} (1 - p_{XY})^{N_A},$$

and similarly for the female ratio. We determined whether one sex fit the data best using an LRT, requiring that the LRT result in a P value < 0.001 for one or the other sex, in order that a sex be assigned. Further, we considered

$$M_X = \begin{cases} 0.5 R_X / p_{XY} & \text{for males,} \\ 1.0 R_X / p_{XX} & \text{for females,} \end{cases}$$

depending on the result of the LRT, to cluster males near 0.5 and females near 1.0. We did not assign a sex to samples that had $0.6 < M_X < 0.8$,

under the assumption that they violated both male and female models. Our Python code implementation for the sex assignment is available from <https://github.com/grahamgower/sexassign>.

Mammoths. Mammoth sexing was done using the same method as for bison. Read counts N_X and N_A were taken from supplementary table 1 of ref. 4, which also lists material type and ^{14}C age for each sample. L_X and L_A were derived from the African elephant reference loxAfr4. A total of 398,360 mapped reads were reported for sample L285, which is likely missing a digit. We appended a zero, placing this sample into the male range, which matches the inferred sex from ref. 4.

Bears. Brown bear reads were mapped to the polar bear reference UrsMar1.0 (37), a scaffold-level reference assembly. For sex determination, we counted reads that mapped to X-linked scaffolds as N_X , and applied the same method as for bison. Only scaffolds longer than 1 Mbp were used in calculations of N_X , N_A , L_X , and L_A .

A list of X-linked scaffolds (SI Appendix, Table S3) was obtained by mapping all UrsMar1.0 scaffolds to the dog reference CanFam3.1 (38), with minimap2 (39). The default mapping parameters were used (minimap2 CanFam3.1.fasta UrsMar1.0.fasta > aln.paf), which provides an approximate alignment lacking base-level precision. We retained only UrsMar1.0 scaffolds having more than 100 kbp cumulative matches to the CanFam3.1 chrX, resulting in 28 putatively X-linked scaffolds comprising 102 Mbp of sequence.

Model Violations. While care was taken to minimize contamination from exogenous sources, such model violations may yet occur due to sample cross-contamination. Other factors that may contribute to sample-specific model violations include chromosome translocations, aneuploidy, and unanticipated postmortem preservation artifacts that (dis)favor one chromosome over another.

Systematic model violations may also be present, such as due to reference assembly errors, or postmortem preservation artifacts. Inactivated copies of chromosome X are heavily methylated, which may lead to additional postmortem DNA fragmentation compared with the active copy and hence fewer reads mapping from the inactivated chromosome. Conversely, an inactivated chromosome is condensed into heterochromatin, which may facilitate greater postmortem preservation than the active copy.

We note that the UrsMar1.0 assembly was derived by sequencing a male, and thus Y-linked scaffolds may be present, while the CanFam3.1 assembly was derived by sequencing a female and thus lacks a chrY. This leaves open the possibility that the pseudoautosomal region (PAR) on Y-linked UrsMar1.0 scaffolds could have mapped to CanFam1.0 chrX. The dog PAR region is ~6.6 Mbp (40), small compared with the size of chrX, but this could yet artificially inflate R_X values for males. Nonetheless, we observed a clear separation of R_X values into 2 cohorts, with few intermediate values, suggesting model violations are rare, or do not notably influence sex determination.

GLM. Logistic regression models were implemented in R (41) using the bayesglm function with default parameters, from the arm package (42). For categorical variables with 3 or more levels, we constructed multiple models, each with different reference levels, to verify this did not have a notable influence on the outcome.

Testing Spatial Distribution. We implemented the 2-sample kernel test described by ref. 16 with a Gaussian kernel, and obtained a P value by comparing the test statistic to 1,000 permutations. The Gaussian kernel $k(x, y) = \exp(-d(x, y)/\sigma)$, where $d(x, y)$ is the great circle distance between x and y , has a scaling parameter σ , which was chosen to maximize the test statistic in each permutation. More details regarding the test statistic, and validation of its performance for spatial data, can be found in SI Appendix. Our R code implementation for the kernel test is available from <https://github.com/grahamgower/kernel-test>.

Mammalian Databases. For mammalian species listed in the PanTHERIA WR05 database (43), we downloaded sample information from 3 museum databases: AMNH (44), NHM (45), and ROM v1.1.5 (46). In addition, samples for 38 species were manually downloaded from USNM (47). We excluded juveniles and hybrids, and sex ratios were calculated only for species represented by more than 100 samples.

Data Availability. Mapped reads and sample-associated metadata are available from https://figshare.com/projects/Widespread_male_sex_bias_in_mammal_fossil_and_museum_collections/60446.

ACKNOWLEDGMENTS. We thank P. Bover, J. Soubrier, S. Bray, J. Austin, J. Metcalf, B. Shapiro, C. Valdiosera, M. Wilson, D. Makowiecki, I. Barnes, and M. T. Rabanus-Wallace for assistance with sample collection and lab work. In addition, we are grateful for the assistance of the many institutions and curators who provided samples for this study: K. Østbye and E. Østbye (University of Oslo); S-E. Lauritzen (University of Bergen); K. Aaris-Sørense (Zoological Museum, University of Copenhagen); M. Pacher (Institute of Palaeontology, University of Vienna); P. Kosintsev (Institute of Plant and Animal Ecology, Russian Academy of Sciences); D. Fedje (Parks Canada); D. Guthrie, R. Gangloff, and R. Stephenson (University of Alaska Fairbanks); D. Harington (Canadian Museum of Nature); J. Storer, P. Matheus, and G. Zazula (Yukon Paleontology Program); A. Kitchener (National Museums Scotland); B. Hockett (Bureau of Land Management); D. Tedford (AMNH); P. Wrinn and S. Vasil'ev (Institute of Archaeology and Ethnography, Russian Academy of Sciences); L. Martin (University of Kansas); G. Storr (Museum of Natural History & Science, Cincinnati Museum); A. Sher (Paleontological Institute, Russian Academy of Sciences); S. Zimov and S. Davidoff (North-east Science Station); N. Vereshchagin (Zoological Institute, St. Petersburg); J. Burns (Provincial Museum Alberta); J. Driver (Simon Fraser University);

K. Rogers (Bell Museum Natural History); M. Arakelyan (Yerevan State University); M. Križnar (Slovenian Museum of Natural History); N. Spassov (National Museum of Natural History, Sofia); L. Bartosiewicz (Institute of Archeological Science, Hungary); A. Archacka (Nature Museum in Drozdowo); V. Gedminas (Tadas Ivanauskas Zoological Museum in Kaunas); M. Szymkiewicz (Nature Museum in Olsztyn); E. Keczyńska-Moroz (Białowieża National Park); J. Jastrzębski and J. Deptuła (Northern-Mazovian Museum in Łomża); N. Czeremnyh (State Museum of Natural History in Lviv, old Museum Dzieduszyckich); K. Wysocka (Vinnitsia Regional Local History Museum); M. Czarniański (Institute of History NAS of Belarus in Minsk); B. Studencka (Museum of the Earth PAS, Poland); U. Göhlich, F. Zachos, and E. Pucher (Vienna Natural History Museum); D. Nagel and D. Doeppes (University of Vienna); and staff at the Lietuvos Nacionalinis Muziejus and Universidad de Burgos. This work was supported by Australian Government Research Training Program Scholarships (to G.G., L.F., A.T.S., and A.L.v.L.), University of Adelaide Research Fellowship (to B.L.), Australian Research Council grant and Fellowship support (to A.C., B.L., H.H., and K.J.M.), and Polish National Science Centre grants (nos. 2013/11/B/NZ8/00914 and N N304 301940 [to R.K.] and 2015/17/N/ST10/01707 [to E.H.]).

1. S. Karlin, S. Lessard, *Theoretical Studies on Sex Ratio Evolution* (Princeton University Press, Princeton, NJ, 1986).
2. R. L. Trivers, D. E. Willard, Natural selection of parental ability to vary the sex ratio of offspring. *Science* **179**, 90–92 (1973).
3. E. L. Charnov, Sex ratio selection in an age-structured population. *Evolution* **29**, 366–368 (1975).
4. P. Pečnerová *et al.*, Genome-based sexing provides clues about behavior and social structure in the woolly mammoth. *Curr. Biol.* **27**, 3505–3510.e3 (2017).
5. D. W. Frayer, M. H. Wolpoff, Sexual dimorphism. *Annu. Rev. Anthropol.* **14**, 429–473 (1985).
6. J. A. Rehg, S. R. Leigh, Estimating sexual dimorphism and size differences in the fossil record: A test of methods. *Am. J. Phys. Anthropol.* **110**, 95–104 (1999).
7. P. Skoglund, J. Storå, A. Götherström, M. Jakobsson, Accurate sex identification of ancient human remains using DNA shotgun sequencing. *J. Archaeol. Sci.* **40**, 4477–4482 (2013).
8. A. Mittnik, C. C. Wang, J. Svoboda, J. Krause, A molecular approach to the sexing of the triple burial at the upper paleolithic site of Dolní Věstonice. *PLoS One* **11**, e0163019 (2016).
9. Q. Fu *et al.*, The genetic history of Ice Age Europe. *Nature* **534**, 200–205 (2016).
10. L. Agenbroad, J. Mead, Age structure analyses of *Mammuthus columbi*, Hot Springs mammoth site, South Dakota. *Curr. Res. Pleistocene* **4**, 101–102 (1987).
11. G. Haynes, Finding meaning in mammoth age profiles. *Quat. Int.* **443**, 65–78 (2017).
12. R. D. Guthrie, *Frozen Fauna of the Mammoth Steppe: The Story of Blue Babe* (University of Chicago Press, Chicago, IL, 1989).
13. O. G. Støen, A. Zedrosser, S. Sæbø, J. E. Swenson, Inversely density-dependent natal dispersal in brown bears *Ursus arctos*. *Oecologia* **148**, 356–364 (2006).
14. A. Zedrosser, O. G. Støen, S. Sæbø, J. E. Swenson, Should I stay or should I go? Natal dispersal in the brown bear. *Anim. Behav.* **74**, 369–376 (2007).
15. D. Döppes, M. Pacher, 10,000 years of *Ursus arctos* in the Alps – A success story? Analyses of the Late Glacial and Early Holocene brown bear remains from alpine caves in Austria. *Quat. Int.* **339–340**, 266–274 (2014).
16. A. Gretton, K. M. Borgwardt, M. J. Rasch, B. Schölkopf, A. Smola, A kernel two-sample test. *J. Mach. Learn. Res.* **13**, 723–773 (2012).
17. F. L. Bunnell, D. E. N. Tait, "Population dynamics of bears – implications" in *Dynamics of Large Mammal Populations*, C. W. Fowler, T. D. Smith, Eds. (John Wiley, 1981), pp. 75–98.
18. P. Bover *et al.*, Unraveling the phylogenetic relationships of the extinct bovid *Myotragus balearicus* Bate 1909 from the Balearic Islands. *Quat. Sci. Rev.* **215**, 185–195 (2019).
19. T. H. Kunz, Ed. *Ecology of Bats* (Plenum Press, New York, NY, 1982).
20. S. Horvath, K. Raj, DNA methylation-based biomarkers and the epigenetic clock theory of ageing. *Nat. Rev. Genet.* **19**, 371–384 (2018).
21. B. Llamas *et al.*, High-resolution analysis of cytosine methylation in ancient DNA. *PLoS One* **7**, e30226 (2012).
22. B. S. McLean *et al.*, Natural history collections-based research: Progress, promise, and best practices. *J. Mammal.* **97**, 287–297 (2016).
23. M. Bunce *et al.*, Extreme reversed sexual size dimorphism in the extinct New Zealand moa *Dinornis*. *Nature* **425**, 172–175 (2003).
24. M. E. Allentoft, M. Bunce, R. P. Scofield, M. L. Hale, R. N. Holdaway, Highly skewed sex ratios and biased fossil deposition of moa: Ancient DNA provides new insight on New Zealand's extinct megafauna. *Quat. Sci. Rev.* **29**, 753–762 (2010).
25. A. Cooper, H. N. Poinar, Ancient DNA: Do it right or not at all. *Science* **289**, 1139–1139 (2000).
26. B. Shapiro, M. Hofreiter, Eds. *Ancient DNA: Methods and Protocols (Methods in Molecular Biology, Humana Press, 2012)*.
27. B. Shapiro *et al.*, Rise and fall of the Beringian steppe bison. *Science* **306**, 1561–1565 (2004).
28. J. Soubrier *et al.*, Early cave art and ancient DNA record the origin of European bison. *Nat. Commun.* **7**, 13158 (2016).
29. S. C. E. Bray *et al.*, Ancient DNA identifies post-glacial recolonisation, not recent bottlenecks, as the primary driver of contemporary mtDNA phylogeography and diversity in Scandinavian brown bears. *Divers. Distrib.* **19**, 245–256 (2013).
30. J. Dabney *et al.*, Complete mitochondrial genome sequence of a Middle Pleistocene cave bear reconstructed from ultrashort DNA fragments. *Proc. Natl. Acad. Sci. U.S.A.* **110**, 15758–15763 (2013).
31. N. Rohland, E. Harney, S. Mallick, S. Nordenfelt, D. Reich, Partial uracil-DNA-glycosylase treatment for screening of ancient DNA. *Philos. Trans. R. Soc. Lond. B Biol. Sci.* **370**, 20130624 (2015).
32. M. Schubert *et al.*, Characterization of ancient and modern genomes by SNP detection and phylogenomic and metagenomic analysis using PALEOMIX. *Nat. Protoc.* **9**, 1056–1082 (2014).
33. H. Li, R. Durbin, Fast and accurate short read alignment with Burrows-Wheeler transform. *Bioinformatics* **25**, 1754–1760 (2009).
34. A. V. Zimin *et al.*, A whole-genome assembly of the domestic cow, *Bos taurus*. *Genome Biol.* **10**, R42 (2009).
35. C. G. Elsik, R. L. Tellam, K. C. Worley, The genome sequence of taurine cattle: A window to ruminant biology and evolution. *Science* **324**, 522–528 (2009).
36. H. Li, A statistical framework for SNP calling, mutation discovery, association mapping and population genetical parameter estimation from sequencing data. *Bioinformatics* **27**, 2987–2993 (2011).
37. S. Liu *et al.*, Population genomics reveal recent speciation and rapid evolutionary adaptation in polar bears. *Cell* **157**, 785–794 (2014).
38. K. Lindblad-Toh *et al.*, Genome sequence, comparative analysis and haplotype structure of the domestic dog. *Nature* **438**, 803–819 (2005).
39. H. Li, Minimap2: Pairwise alignment for nucleotide sequences. *Bioinformatics* **34**, 3094–3100 (2018).
40. A. C. Young, E. F. Kirkness, M. Breen, Tackling the characterization of canine chromosomal breakpoints with an integrated in-situ/in-silico approach: The canine PAR and PAB. *Chromosome Res.* **16**, 1193–1202 (2008).
41. R Core Team, *R: A Language and Environment for Statistical Computing* (R Foundation for Statistical Computing, Vienna, Austria, 2017).
42. A. Gelman, A. Jakulin, M. G. Pittau, Y. S. Su, A weakly informative default prior distribution for logistic and other regression models. *Ann. Appl. Stat.* **2**, 1360–1383 (2008).
43. K. E. Jones *et al.*, PanTHERIA: A species-level database of life history, ecology, and geography of extant and recently extinct mammals. *Ecology* **90**, 2648–2648 (2009).
44. American Museum of Natural History, AMNH vertebrate zoology database. <http://sci-web-001.amnh.org/db/emuwebamnh/index.php>. Accessed 29 May 2018.
45. London Natural History Museum, Dataset: Collection specimens. Resource: Specimens. Natural History Museum Data Portal. <http://data.nhm.ac.uk>. Accessed 29 May 2018.
46. Royal Ontario Museum, Mammalogy collection - Royal Ontario Museum. <http://gbif.rom.on.ca/ipt/resource.do?r=mamm>. Accessed 29 May 2018.
47. Smithsonian National Museum of Natural History, Mammals collections search. <https://collections.nmnh.si.edu/search/mammals/>. Accessed 30 May 2018.